ISSUED

DOE/WIPP-17-3560
Volume 1

Waste Isolation Pilot Plant

Geotechnical Analysis Report For July 2015 – June 2016

U.S. Department of Energy

October 2017

This page was intentionally left blank.

This document has been submitted as required to:

U.S. Department of Energy
Office of Scientific and Technical Information
PO Box 62
Oak Ridge, TN 37831
(865) 576-8401

Additional information about this document may be obtained by calling 1-800-336-9477

Unlimited, publicly available full-text scientific and technical reports produced since 1991 are available online at Information Bridge (www.osti.gov/bridge).

U.S Department of Energy and its contractors may obtain full-text reports produced prior to 1991 in paper form for a processing fee from:

U.S. Department of Energy
Office of Scientific and Technical Information
P.O. Box 62
Oak Ridge, TN 37831-0062
Telephone: (865) 576-8401
Facsimile: (865) 576-5728
E-mail: reports@osti.gov

Available for sale to the public from:

U.S. Department of Commerce
National Technical Information Service
5301 Shawnee Rd
Alexandra, VA 22312
Phone: (800) 553-6847 or (703) 605-6000
Fax: (703) 605-6900
Email: info@ntis.gov

This page was intentionally left blank.

FOREWORD AND ACKNOWLEDGMENTS

This report contains an assessment of the geotechnical status of the Waste Isolation Pilot Plant (WIPP). During the excavation of the principal underground access and experimental areas, the status was reported quarterly. Since 1987, when the initial construction phase was completed, reports have been published annually. This report presents and analyzes data collected from July 1, 2015, to June 30, 2016.

This Geotechnical Analysis Report (GAR) was written to meet the needs of several audiences. It satisfies requirements contained in the WIPP Hazardous Waste Facility Permit[1] (HWFP) and the Certification of Compliance[2] with Subparts B and C, Title 40 *Code of Federal Regulations* (CFR) Part 191, "Environmental Radiation Protection Standards for Management and Disposal of Spent Nuclear Fuel, High-Level and Transuranic Radioactive Wastes." It focuses on the geotechnical performance of the various components of the underground facility, including the shafts, shaft stations, access drifts, and waste disposal areas. The results of investigations of excavation effects and other geotechnical studies are also included.

The report compares the geotechnical performance of the repository to the design criteria. It describes the techniques that were used to acquire the data. The depth and breadth of the evaluation of the different components of the underground facility vary according to the types and quantities of data available and the complexity of the recorded geotechnical responses. Graphic documentation of data and tabular documentation of instrument history can be provided upon request.

This GAR was prepared by Nuclear Waste Partnership LLC (NWP) for the U.S. Department of Energy (DOE), Carlsbad Field Office (CBFO), in Carlsbad, New Mexico. Work was supported by the DOE under Contract No. DE-EM0001971.

[1] New Mexico Environment Department (NMED), 2016, Waste Isolation Pilot Plant Hazardous Waste Facility Permit, NM4890139088-TSDF, Santa Fe, NM

[2] U.S. Environmental Protection Agency, 1998, "Criteria for the Certification and Recertification of the Waste Isolation Pilot Plant's Compliance with the Disposal Regulations: Certification Decision," Federal Register, Vol. 63, No. 95, pp. 27354, May 18, 1998, Washington, DC

This page was intentionally left blank.

TABLE OF CONTENTS

TABLE OF CONTENTS (Continued)

LIST OF TABLES

LIST OF FIGURES

This page was intentionally left blank.

ACRONYMS AND ABBREVIATIONS

ASTM	American Society for Testing and Materials
bp	before present
bsc	below shaft collar
CAO	Carlsbad Area Office
CBFO	Carlsbad Field Office
CFR	Code of Federal Regulations
CH	contact-handled
cm	centimeter(s)
DOE	U.S. Department of Energy
EPA	U.S. Environmental Protection Agency
ft	foot (feet)
GAR	Geotechnical Analysis Report
GIS	geomechanical instrumentation system
HWFP	Hazardous Waste Facility Permit
in	inch(es)
km	kilometer(s)
kPa	kilopascal(s)
kVA	kilovolt ampere(s)
LANL	Los Alamos National Laboratory
lb(s)	pound(s)
m	meter(s)
Ma	million years
MB	marker bed
NMED	New Mexico Environment Department
NWP	Nuclear Waste Partnership LLC
OMB	orange marker bed
psi	pound(s) per square inch
RH	remote-handled

SDI	Salt Disposal Investigation
SDDI	Salt Defense Disposal Investigation
SPDV	Site and Preliminary Design Validation
TRU	transuranic
WIPP	Waste Isolation Pilot Plant
VOC	volatile organic compound
yr(s)	year(s)

1.0 INTRODUCTION

This Geotechnical Analysis Report presents and interprets geotechnical data from the underground excavations at the Waste Isolation Pilot Plant (WIPP). The data, which are obtained as part of a regular monitoring program, are used to characterize conditions, to compare actual performance to the design criteria and to evaluate and forecast the performance of the underground excavations.

Geotechnical Analysis Reports have been available to the public since 1983. During the Site and Preliminary Design Validation (SPDV) Program, the architect/engineer for the project produced these reports quarterly to document the geomechanical performance during and immediately after early excavations of the underground facility. Since completion of the construction phase of the project in 1987, the management and operating contractor for the facility has prepared these reports annually. This report describes the performance and condition of selected areas from July 1, 2015, to June 30, 2016. It is divided into nine sections.

Section 1 provides background information on WIPP, its mission, and the purpose and scope of the geomechanical monitoring program. Section 2 describes the local and regional geology of the WIPP site. Sections 3 and 4 describe the geomechanical instrumentation in the shafts and shaft stations, present the data collected by that instrumentation, and provide interpretation of these data. Sections 5 and 6 present the results of geomechanical monitoring in the two main portions of the WIPP underground (the access drifts and the waste disposal area). Section 7 introduces the Salt Disposal Investigation (SDI) and Salt Defense Disposal Investigation (SDDI) areas. Section 8 discusses the results of the Geoscience Program, which include fracture mapping and observation borehole information. Section 9 summarizes the results of geomechanical monitoring and compares the current excavation performance to the design requirements. Section 10 lists references.

1.1 Location and Description

The WIPP facility is located in southeastern New Mexico, 26 miles (42 kilometers [km]) east of Carlsbad (Figure 1-1). The surface facilities were built on the flat to gently rolling terrain that is characteristic of the Los Medaños area. The underground facility is being excavated approximately 2,150 feet (ft) (655 meters [m]) beneath the surface in the Salado Formation. Figure 1-2 shows a plan view of the underground configuration of WIPP as of June 30, 2016.

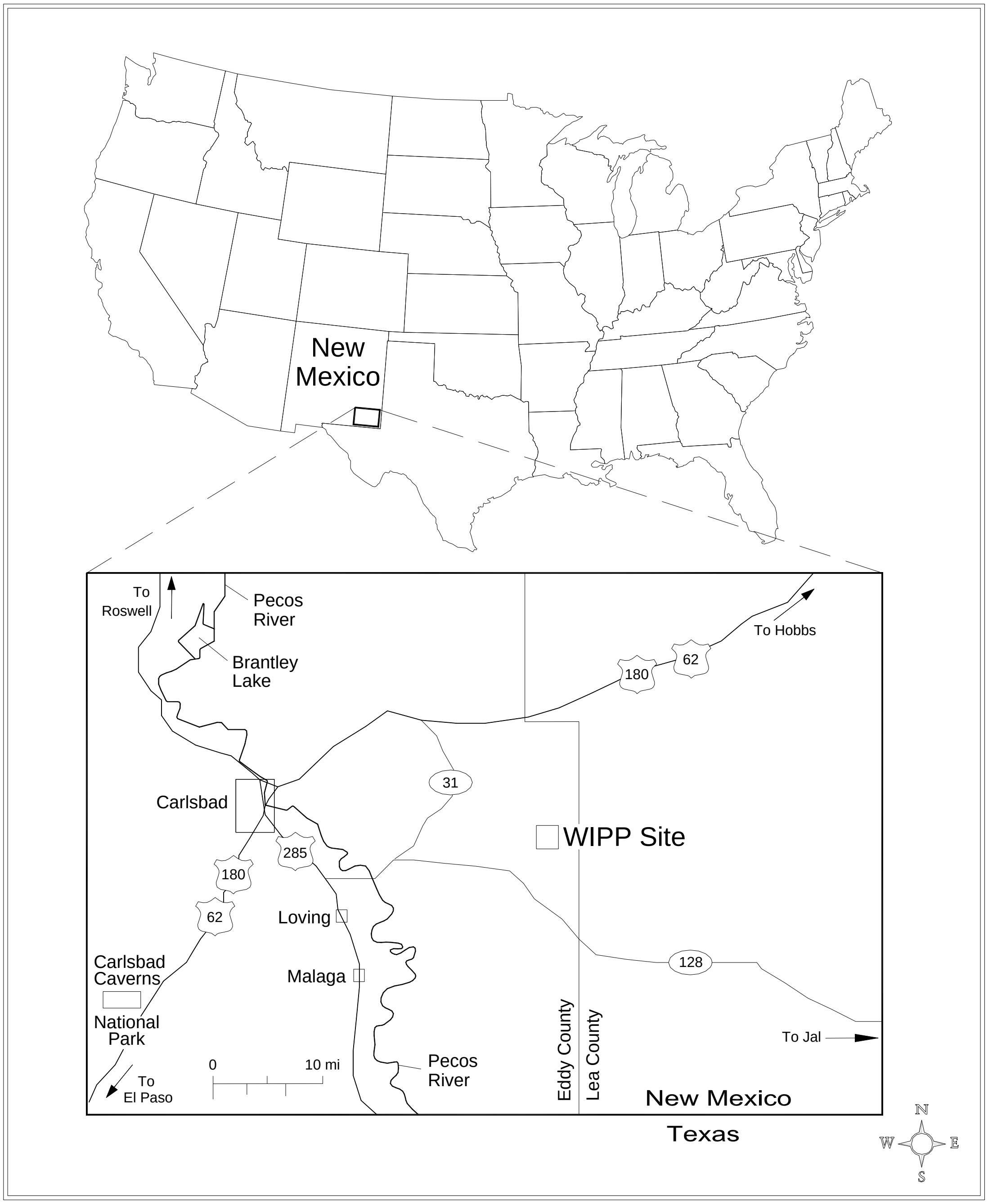

Figure 1-1 WIPP Location

ISSUED

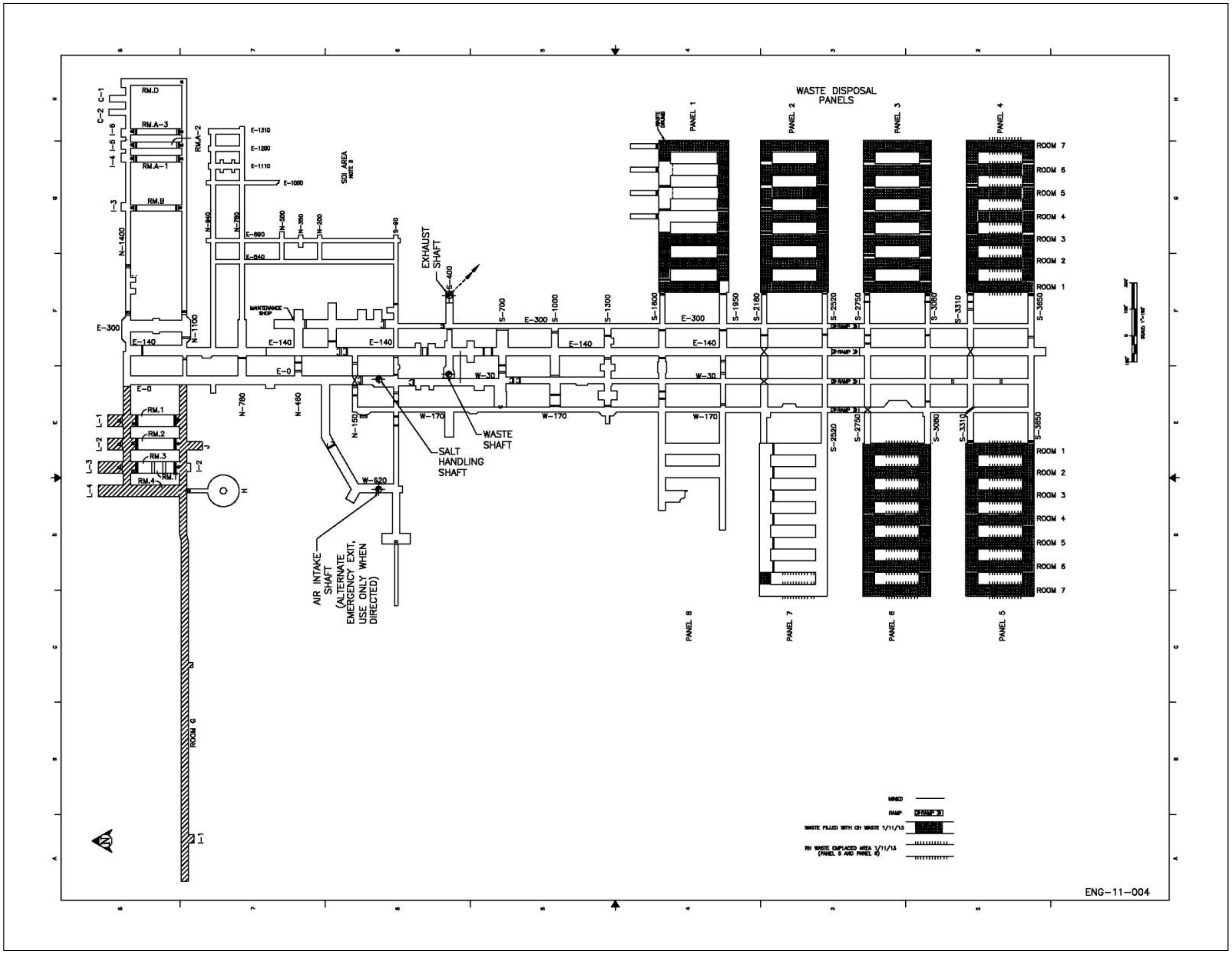

Figure 1-2 Underground Mining and Waste Disposal Configuration as of June 30, 2016

1.2 Mission

In 1979 Congress authorized WIPP (Public Law 96-164, National Security and Military Applications of Nuclear Energy Authorization Act of 1980) to provide ". . . a research and development facility to demonstrate the safe disposal of radioactive wastes resulting from the defense activities and programs of the United States exempted from regulation by the Nuclear Regulatory Commission." To fulfill this mission, the DOE constructed a full-scale facility to demonstrate both technical and operational principles of the permanent disposal of transuranic (TRU) and TRU mixed wastes. Technical aspects are those concerned with the design, construction, and performance of the subsurface excavations. Operational aspects refer to the receiving, handling, and emplacement of TRU wastes in the facility. The facility was first used for *in situ* studies and experiments without the use of radioactive waste. WIPP now receives, handles, and permanently disposes of TRU waste and TRU mixed waste.

1.3 Development Status

To fulfill its mission, the DOE developed WIPP in a phased manner. The goal of the SPDV phase, begun in 1980, was to characterize the site and obtain *in situ* geotechnical data from underground excavations to determine whether site characteristics and *in situ* conditions were suitable for permanent disposal. During this phase, the Salt Shaft, a ventilation shaft, a drift to the southernmost extent of the proposed waste disposal area, a four-room experimental panel, and access drifts were excavated. Surface-based geological and hydrological investigations were also conducted. The data obtained from the SPDV investigations were reported in the "Summary of the Results of the Evaluation of the WIPP Site and Preliminary Design Validation Program" (DOE, 1983).

Based upon the favorable results of the SPDV investigations, additional activities were initiated in 1983. These included the construction of surface structures, conversion of the ventilation shaft for use as the Waste Shaft, excavation of the Exhaust Shaft, development of additional access drifts to the waste disposal area, excavation of the Air Intake Shaft, and excavation of additional experimental rooms to support research and development. Geotechnical data acquired during this phase were used to evaluate the performance of the excavations in the context of established design criteria (DOE, 1984). Results of these evaluations were reported in *Geotechnical Field Data Reports* (DOE, 1985; DOE, 1986a) and were summarized in the *Design Validation Final Report* (DOE, 1986b).

The *Design Validation Final Report* concluded that the facility, including waste disposal areas, could be developed and operated to fulfill the long-term mission of WIPP (DOE, 1986b). All available information validated the design of underground openings to safely accommodate the permanent disposal of waste under routine operating conditions.

Panel 1 mining began in 1986 and was completed in 1988. Panel 1 was intended to receive waste for an initial operations demonstration and pilot plant phase that was scheduled to start in October 1988; however, the demonstration and pilot plant phase was not put into effect because waste could not be emplaced until permits were acquired.

In October 1996, the DOE submitted to the U.S. Environmental Protection Agency (EPA) a compliance certification application in accordance with 40 CFR Parts 191 and 194, which addressed the long-term (10,000-year) performance criteria for the disposal system. On May 18, 1998, the EPA published the final certification that allowed for the receipt of TRU waste at WIPP. Immediately before this certification, the DOE Carlsbad Area Office (CAO) completed an Operational Readiness Review, which is required by the DOE before the start-up or a process change of any nuclear facility. As a result of the review, the CAO notified the Energy Secretary on April 1, 1998, that WIPP was operationally ready to receive waste. On March 26, 1999, the first shipment of TRU waste was received from Los Alamos National Laboratory (LANL). By the end of June 2013, many additional generator sites had shipped waste to WIPP. The cleanup of several small-quantity generator sites, as well as one large-quantity site (Rocky Flats Environmental Technology Site) is now complete.

Waste disposal in Panels 1, 2, 3, 4, 5 and 6 is complete. Panels 1, 2, and 3 contain only CH waste. The first RH waste shipment arrived January 24, 2007. Panel 4 was the first to receive both CH and RH waste. CH and RH waste emplacement had commenced in Panel 7 but was halted initially by a truck fire in the underground and remained halted due to the radiological release.

1.4 Purpose and Scope of Geomechanical Monitoring Program

As specified in the WIPP HWFP (NMED, 2016), the purpose of the geomechanical monitoring program is to obtain *in situ* data to support the continuous assessment of the design for underground facilities.

Specifically, the program provides for:

- Early detection of conditions that could affect operational safety.
- Evaluation of disposal room closure that ensures adequate access.
- Guidance for design modifications and remedial actions.
- Data for interpreting the behavior of underground openings, in comparison with the established design criteria.

Data taken by or input into the geomechanical instrumentation system (GIS) are evaluated and reported in this GAR. This annual report fulfills the requirements set forth in Part 4.6.1.2, Attachment A2, Section A2-5b (2) of the WIPP HWFP (NMED,2016), and 40 CFR §191.14, "Assurance Requirements," implemented through the certification criteria, 40 CFR Part 194.

The Geomechanical Monitoring Program generates the data for four of the compliance monitoring parameters:

- Creep closure and stresses
- Extent of deformation
- Initiation of brittle deformation
- Displacement of deformation features

The instrumentation system for geomechanical monitoring provides data for routine evaluations of safety, stability, and performance of underground openings. *In situ* data are also used to model long-term disposal system performance. Changes resulting from excavations are monitored by routine inspections of selected observation hole arrays and fracture mapping to detect and quantify occurrences of discontinuities such as fractures and bed separations. Analysis of data indicating areas of potential instability allows timely corrective action before they could become safety issues. Other geoscience activities include geologic mapping and sampling, and seismic monitoring.

The GIS provides data that are collected, processed, and stored for analysis. The following subsections briefly describe the major components of the GIS.

1.4.1 Instrumentation

Instrumentation installed for measuring the geomechanical response of the shafts, drifts, and other underground openings includes convergence points, convergence meters, extensometers, rock bolt load cells, pressure cells, strain gauges, piezometers, and joint meters. Table 1-1 lists a summary of the specifications for geomechanical instrumentation.

Table 1-1 Geomechanical Instrumentation System

Instrument Type	Measures	Range[1]	Resolution[1]
Sonic probe extensometer	Cumulative deformation	0–2 in	0.001 in
Convergence point (tape extensometer)	Cumulative deformation	2–50 ft	0.001 in
Wire convergence meter	Cumulative deformation	0–3.5 ft	0.001 in
Embedded strain gauge	Cumulative strain	0–3000 µin/in	1 µin/in
Spot-welded strain gauge	Cumulative strain	0–2500 µin/in	1 µin/in
Rock bolt load cell	Load	0–50 tons	40 lb
Earth pressure cell	Pressure	0–1000 psi	1 psi
Piezometer	Fluid pressure	0–500 psi	0.5 psi
Joint meter	Cumulative deformation	0–4 in	0.001 in
Vibrating wire extensometer	Cumulative deformation	0–4 in	0.001 in
Wire extensometer	Cumulative deformation	0–20 in	0.001 in
Linear potentiometric extensometer	Cumulative deformation	0–6 in	0.001 in

[1] Manual readout boxes for the instruments were manufactured to render measurements in U.S. customary units. Range and resolution measurement units have not been converted to metric units. Measurements from these instruments have been converted for presentation elsewhere in this report.

1.1.2 Data Acquisition

Geomechanical instruments are read either manually, using portable devices, or remotely by electronically polling the stations from the surface in accordance with approved operating procedures. Remotely read instruments are connected to one of the underground data loggers, and readings are collected by initiating the appropriate polling routine. Upon completion of a verification process, data are transferred to a computer database. Manual readout devices are taken to instrument locations underground. Data are recorded on data sheets and later entered into an electronic database.

The underground data acquisition system consists of instruments, polling devices, and a communications network. Instruments are connected to polling devices that are installed in electrical enclosures near the instrument locations. Polling devices are connected by a data link to a surface computer.

Whether acquired manually or remotely, geomechanical data are entered into the database files of the GIS data processing system. The data processing system consists of computer programs that are used to enter, reduce, and transfer the data to permanent storage files. Additional routines allow access to the permanent storage files for numerical analysis, tabular reporting, and graphical plotting. Copies of the instrumentation database and data plots are available upon request.[3]

1.1.3 Data Evaluation

Rounding and significant digits are used in the data tables of this document. The reference document is American Society for Testing and Materials (ASTM) document ASTM D 6026-06, "Standard Practice for Using Significant Digits in Geotechnical Data."

Closure measurements are acquired manually from convergence point anchors and remotely from convergence meters. Data are presented in plots of closure versus time. Closure rate data are calculated and presented as part of the data analysis. Extensometers provide displacement data from instrumented rods or wires anchored at various depths. Plots show displacement versus time for individual anchors.

Displacement rate data from the hole (collar) to the deepest anchor are presented in the data analysis.

The annual closure rate is calculated as follows:

$$Rate\ \left(\frac{inches}{year}\right) = \left[\frac{reading2 - reading1}{date2 - date1}\right] * 365.25\frac{days}{year}$$

reading = the change from the initial reading (inches)

reading1 = reading closest to the beginning of the reporting period

reading2 = reading closest to the end of the reporting period

Comparisons between closure rates of the previous and current reporting periods are presented as percent changes in rate and are calculated as follows:

$$percent\ change\ in\ rate = (Rate_{Current\ Period} - Rate_{PreviousPeriod}) / (Rate_{PreviousPeriod}) \times 100\%$$

Rock bolt load cells are used to determine bolt support performance. Plots show load versus time for each instrumented bolt.

Earth pressure cells and strain gauges are used to determine the stresses and deformation in and around the shaft liners. Data are depicted in time-based plots.

[3] Instrumentation data and data plots are presented in "Geotechnical Analysis Report for July 2015 - June 2016 Supporting Data" (DOE/WIPP-16-3560 Volume 2).
The document is available upon request from the National Technical Information Service. See page 3 for details and addresses.

Piezometers are used to measure the gauge pressure of groundwater and are installed in the shafts at varying elevations to monitor the hydraulic head acting on the shaft liners. Data are plotted as pressure versus time.

Joint meters, installed perpendicular to a crack, monitor the dilation of the crack with time. Data are presented as displacement versus time.

1.1.4 Data Errors

GIS data are processed through a comprehensive database management system. Whether acquired manually or remotely, GIS data are processed and permanently stored according to approved procedures. On occasion, erroneous readings can occur. There are several possible explanations for erroneous readings, including the following:

- The measuring device was misread.
- The reading was recorded incorrectly.
- The measuring device was not functioning within specifications.

When a reading is believed to be erroneous, the suspect reading is evaluated, and, if necessary, a second reading is collected. If the second reading falls in line with the instrument trend, the first reading is discarded and the second reading is entered in the database. If the second reading and subsequent readings remain out of the instrument trend, the ground conditions in the vicinity of the instrument are assessed to determine the reason for the discrepancy. In addition, the reading frequency may be increased.

2.0 GEOLOGY

This section provides a summary of the stratigraphy of the WIPP region and the site. Readers desiring further geologic information may consult the "Geological Characterization Report, WIPP Site, Southeastern New Mexico" (Powers et al., 1978). This report was developed as a source document on the geology of the WIPP site for individuals, groups, or agencies seeking basic information on geologic history, hydrology, geochemistry, or detailed information, such as physical and chemical properties of repository rocks. A more recent survey of WIPP stratigraphy is included in Holt and Powers (1990).

2.1 Regional Stratigraphy

The stratigraphy in the vicinity of the WIPP site includes rocks of Permian (295 to 250 million years [Ma] before present [bp]), Triassic (250 to 203 Ma), and Quaternary (1.75 Ma to present) ages. The descriptions of formations provided in this section are given in order of deposition (oldest to youngest), beginning with the Castile Formation (Figure 2-1).

2.1.1 Permian

The Permian system in southwestern North America is divided into four series. The last of these, the Ochoan Series, contains the host rock in which the WIPP repository is located.

The Ochoan Series is of mostly marine origin and consists of four formations: three evaporite formations (the Castile, the Salado, and the Rustler) and one redbeds formation (the Dewey Lake). The Ochoan evaporites overlie marine limestones and sandstones of the Guadalupian Series (Delaware Mountain Group). The younger redbeds represent a transition from the lower evaporite deposition to fluvial deposition on a broad, low-relief, fluvial plain. The Permian rocks are overlain by fluvial deposits of the Triassic and Quaternary periods.

2.1.1.1 Castile Formation

The Castile Formation, lowermost of the four Ochoan formations, is approximately 1,250 ft (380 m) thick in the WIPP vicinity. Lithologically, the Castile is the least complex of the evaporite formations and is composed chiefly of interbedded anhydrite and halite, with limestone present in minor amounts.

2.1.1.2 Salado Formation

The Salado Formation comprises nearly 2,000 ft (610 m) of evaporites, primarily halite. The formation is subdivided into three informal members: the unnamed lower member, the McNutt potash zone, and the unnamed upper member. Each member contains similar amounts of halite, anhydrite, and polyhalite and is differentiated on the basis of soluble potassium- and magnesium-bearing minerals. The WIPP disposal horizon is located within the unnamed lower member, 2,150 ft (655 m) below the surface.

2.1.1.3 Rustler Formation

The Rustler Formation is subdivided into five members, starting from its base: the Los Medaños Member, the Culebra Dolomite Member, the Tamarisk Member, the Magenta Dolomite Member, and the Forty-niner Member.

In the vicinity of the WIPP site, the Rustler is approximately 310 ft (95 m) thick and thickens to the east. The lower portion (Los Medaños Member) contains primarily fine sandstone to mudstone with lesser amounts of anhydrite, polyhalite, and halite. Bedded and burrowed siliciclastic sedimentary rocks with cross-bedding and fossil remains signify the transition from the strongly evaporitic environments of the Salado to the brackish lagoonal environments of the Rustler (Holt and Powers, 1990).

The upper portion of the Rustler contains interbeds of anhydrite, dolomite, and mudstone. The Culebra Dolomite member is generally brown, finely crystalline, and locally argillaceous. The Culebra contains rare to abundant vugs with variable gypsum and anhydrite filling and is the most transmissive hydrologic unit within the Rustler. The Tamarisk Member consists of lower and upper sulfate units separated by a unit that varies laterally from mudstone to mainly halite. The Magenta Dolomite Member is a gypsiferous dolomite with abundant primary sedimentary structures and well-developed algal features. The Forty-niner Member consists of lower and upper sulfate units separated by a mudstone that displays sedimentary features and bedding. East of the site area, halite correlates with the mudstone. The Culebra and Magenta Dolomite members are persistent and serve as important marker units.

2.1.1.4 Dewey Lake Redbeds

The Dewey Lake Redbeds is the uppermost of the Ochoan Series formations. Within the series, the Dewey Lake represents a transition from the lower marine evaporite deposition to fluvial deposition on a broad, low-relief, fluvial plain. The redbeds, approximately 475 ft (145 m) thick, consist of predominantly reddish-brown interbedded fine-grained sandstone, siltstone, and claystone. This formation is differentiated from others by its lithology and distinctive color (both of which are remarkably uniform), and by sedimentary structures, including horizontal- and cross-laminae and ripple marks. The redbeds also contain locally abundant greenish-gray reduction spots and gypsum filled fractures. The formation thickens from west to east due to eastward dips and erosion to the west.

2.1.2 Triassic

The only Triassic rocks present in the WIPP region belong to the Dockum Group.

2.1.2.1 Dockum Group

The Dockum Group consists of fine-grained floodplain sediments and coarse alluvial debris of Triassic age. From a pinch-out near the center of the WIPP site it thickens eastward, forming an erosional wedge. Local subdivisions of the Dockum Group are the Santa Rosa Sandstone and the Chinle Formation; however, only the Santa Rosa occurs in the vicinity of the site. It consists primarily of poorly sorted sandstone with conglomerate lenses and thin mudstone partings and contains impressions and remnants of fossils. These rocks have more variegated hues than the underlying uniformly colored Dewey Lake.

2.1.3 Quaternary

Quaternary Period deposits include the Gatuña Formation, Mescalero Caliche, and surficial sediments.

2.1.3.1 Gatuña Formation, Mescalero Caliche, and Surficial Sediments

The Gatuña Formation (ranging in age from approximately 1.3 million to 600,000 years bp) (Powers and Holt, 1993) is a stream-laid deposit overlying the Dockum Group in the WIPP vicinity. At the site center, the formation consists of approximately 13 ft (4 m) of poorly consolidated sand, gravel, and silty clay. The Gatuña Formation is light red and mottled with dark stains. The unit contains abundant calcium carbonate, but is poorly cemented. Sedimentary structures are abundant (Powers and Holt, 1993, 1995).

The Mescalero Caliche (approximately 500,000 years bp) is approximately 4 ft (1.2 m) thick in the WIPP vicinity. The Mescalero is a hard, resistant soil horizon that lies beneath a cover of wind-blown sand. The horizon is petrocalcic (i.e., very strongly cemented with calcium carbonate). Petrocalcic horizons form slowly beneath a stable landscape at the average depth of infiltration of soil moisture and indicate stability and integrity of the land surface. Many of the surface buildings at WIPP are founded on top of the Mescalero Caliche.

Surficial sediments include sandy soils developed from eolian material and active dune areas. The Berino Series (a soil type) covers about 50 percent of the site and consists of deep sandy soils that developed from wind-worked material of mixed origin. Based on sample analyses, the Berino soil from the WIPP site formed 330,000 ± 75,000 years bp.

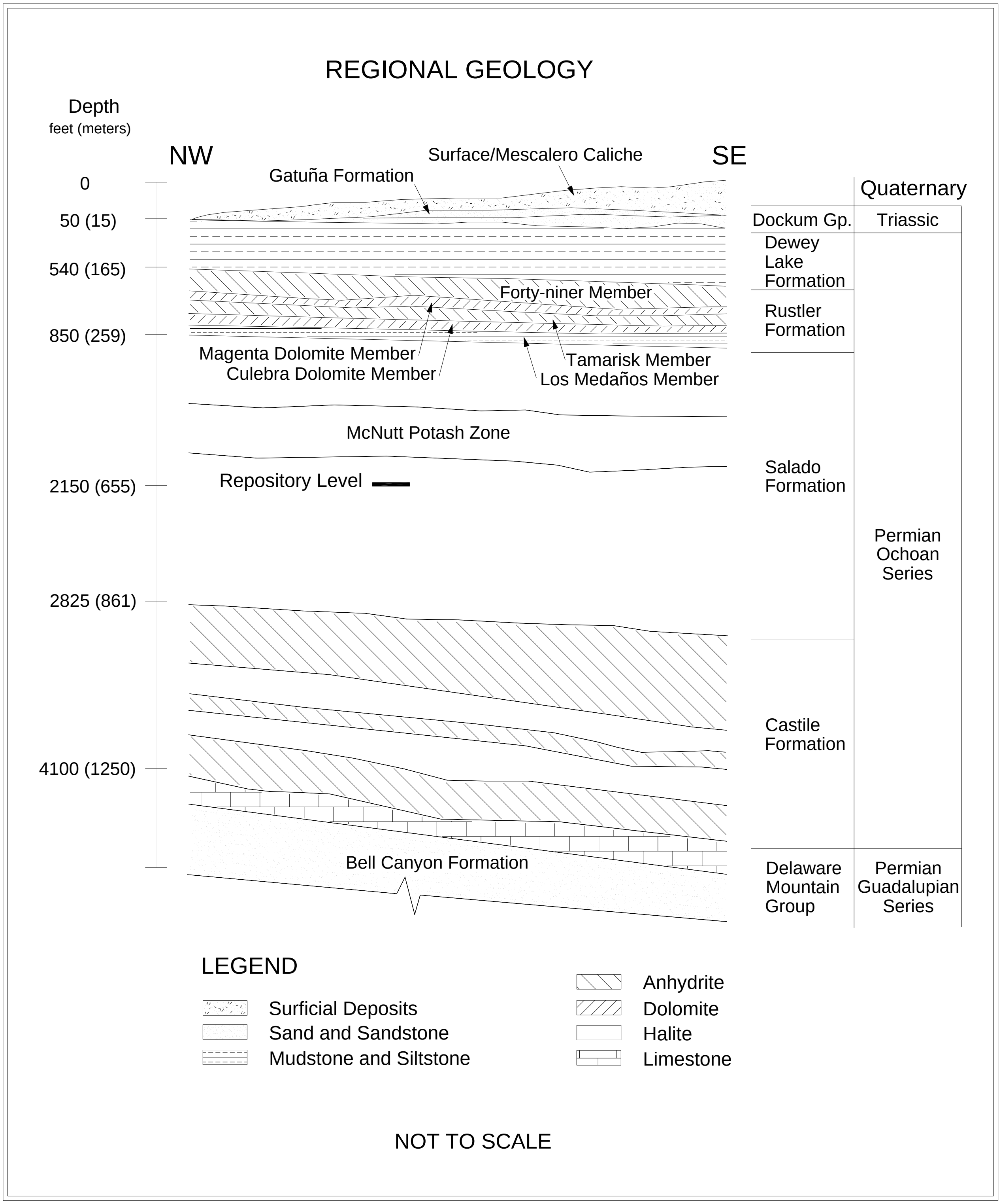

Figure 2-1 Regional Geology

2.2 Underground Facility Stratigraphy

The WIPP disposal horizon lies near the midpoint of the Salado Formation. The Salado was deposited in a shallow saline lagoon environment, which progressed through numerous inundation and desiccation cycles that are reflected in the formation. An "ideal" cycle progresses upward as follows: a basal layer consisting predominantly of claystone, followed by a layer of sulfate, which is in turn followed by a layer of halite. The entire sequence is capped by a bed of argillaceous (clay-rich) halite accumulated during a period of mainly subaerial exposure.

A regional system used for numbering the more significant sulfate beds within the Salado designates these beds as marker beds (MBs), counted from MB100 near the top of the formation to MB144 near the base. The repository is located between MB138 and MB139 within a sequence of laterally continuous depositional cycles as described above. Within this sequence, layers of clay and anhydrite that are locally designated (as shown) can have a significant impact on the geomechanical performance of the excavations. Clay layers provide surfaces along which slip and separation can occur, whereas anhydrites form brittle layers that do not deform plastically.

In the vicinity of WIPP, the stratigraphy is fairly continuous and uniform. Beds generally dip toward the south-southeast at a slope of approximately 3 percent.

2.2.1 Disposal Horizon Stratigraphy of Panels 1, 2, 7, and 8

This disposal horizon contains Panels 1, 2, 7, and 8, all the shaft areas, the shop areas, the SPDV areas (which are now closed), and all the access drifts north of S-2620. Farther south, the four main entries rise in a ramp that starts at S-2620 and ends at S-2740. Panel 7 excavation was completed in January of 2013. Panel 8 has not yet been excavated.

Most underground excavations are located within this disposal horizon (Figure 2-2). In it, the Orange Marker Bed (OMB) lies near the middle of the rib (i.e., the excavation wall). The OMB is a laterally consistent unit of moderate to light reddish-orange translucent halite about 6 inches (in) (15 centimeters [cm]) thick that is used as a point of reference during excavation.

MB139 lies approximately 11.5 ft (3.5 m) below the OMB. MB139 is a 20 to 32 in (50 to-80 cm) thick layer of polyhalitic anhydrite. The top of the anhydrite undulates up to 15 in (38 cm), while the bottom is sub-horizontal and is underlain by Clay E.

Above MB139 is a unit of halite that terminates at the base of the OMB. Within this unit, polyhalite is locally abundant and decreases upward, while argillaceous material increases upward.

Above the OMB, a thin band of argillaceous halite gives way to a thick sequence of clear halite that becomes increasingly argillaceous upward and is capped by Clay F. This constitutes a thin layer occasionally interrupted by partings and breaks and is readily visible in the upper ribs. Above Clay F, another sequence of halite begins that, as in lower sequences, becomes increasingly argillaceous upward. This sequence terminates at the Clay G/Anhydrite "b" interface, approximately 6.5 ft (2 m) above the roof of most disposal horizon excavations, forming a roof beam that typically acts as a structural unit.

The roof of some disposal horizon excavations (e.g., the E-140 drift between S-1000 and S-1950), has been excavated to the upper contact of Anhydrite "b." In this case, a roof beam is formed by the next depositional sequence beginning with Anhydrite "b" and progressing upward to the Clay H/Anhydrite "a" interface, approximately 6.5 ft (2 m) above the upper contact of Anhydrite "b."

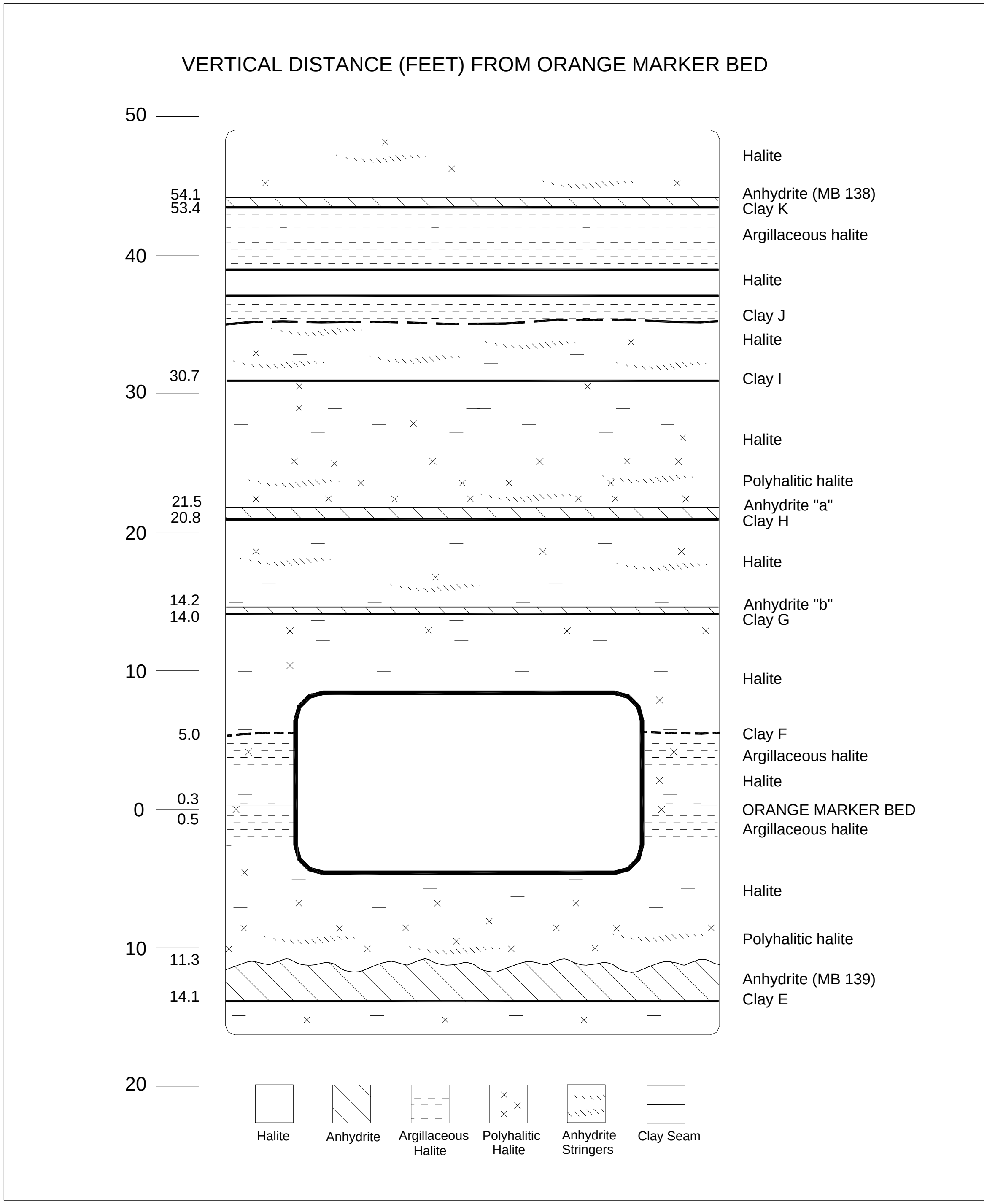

Figure 2-2 Repository Level Stratigraphy of Panels 1, 2, 7, and 8

2.2.2 Disposal Horizon Stratigraphy of Panels 3, 4, 5, and 6

Field observations and computer modeling indicated that moving the disposal horizon stratigraphically upward (so that the roof was located at Clay G) would improve long term ground conditions and provide a more stable roof configuration without significantly impacting repository performance. In 2000, the decision was made to implement this change by moving the mining horizon up approximately six feet. Subsequently, in 2000 and 2001, ramps were mined in the W-170, W-30, E-140, and E 300 drifts between S-2620 and S-2750 (Figure 1-2). As a result, the disposal horizon for Panels 3, 4, 5, and 6, and the associated connecting drifts lies above the horizon for the other panels (Figure 2-3).

In this horizon, the OMB lies at or below the floor. MB139 lies about 12 ft (3.7 m) below the floor. The roof lies at or slightly above Anhydrite "b." Clay G/ Anhydrite "b" is used as the mining reference during excavation of this disposal horizon. Locally continuous anhydrite stringers are found within this that extends to Clay H at Anhydrite “a”, generally concentrated in the lower portion toward Anhydrite "b". These effectively divide the roof beam itself into a series of thinner, independent beams thereby weakening the overall beam strength.

2.2.3 Northeast Area Stratigraphy

All of the Northeast Area, a former experimental area, is now deactivated and closed to access. These excavations lie at a higher stratigraphic level than the disposal excavations. Floors are at Anhydrite "b." As in the lower units, the halite intervals between the clay seams/anhydrite beds contain relatively pure halite that becomes increasingly argillaceous upward. Above clay I, two more halite intervals complete the underground facility stratigraphy. Clay J, at the top of the first of these intervals, may consist of a distinct seam or merely an argillaceous zone. Clay K tops the second interval and is overlain by MB138.

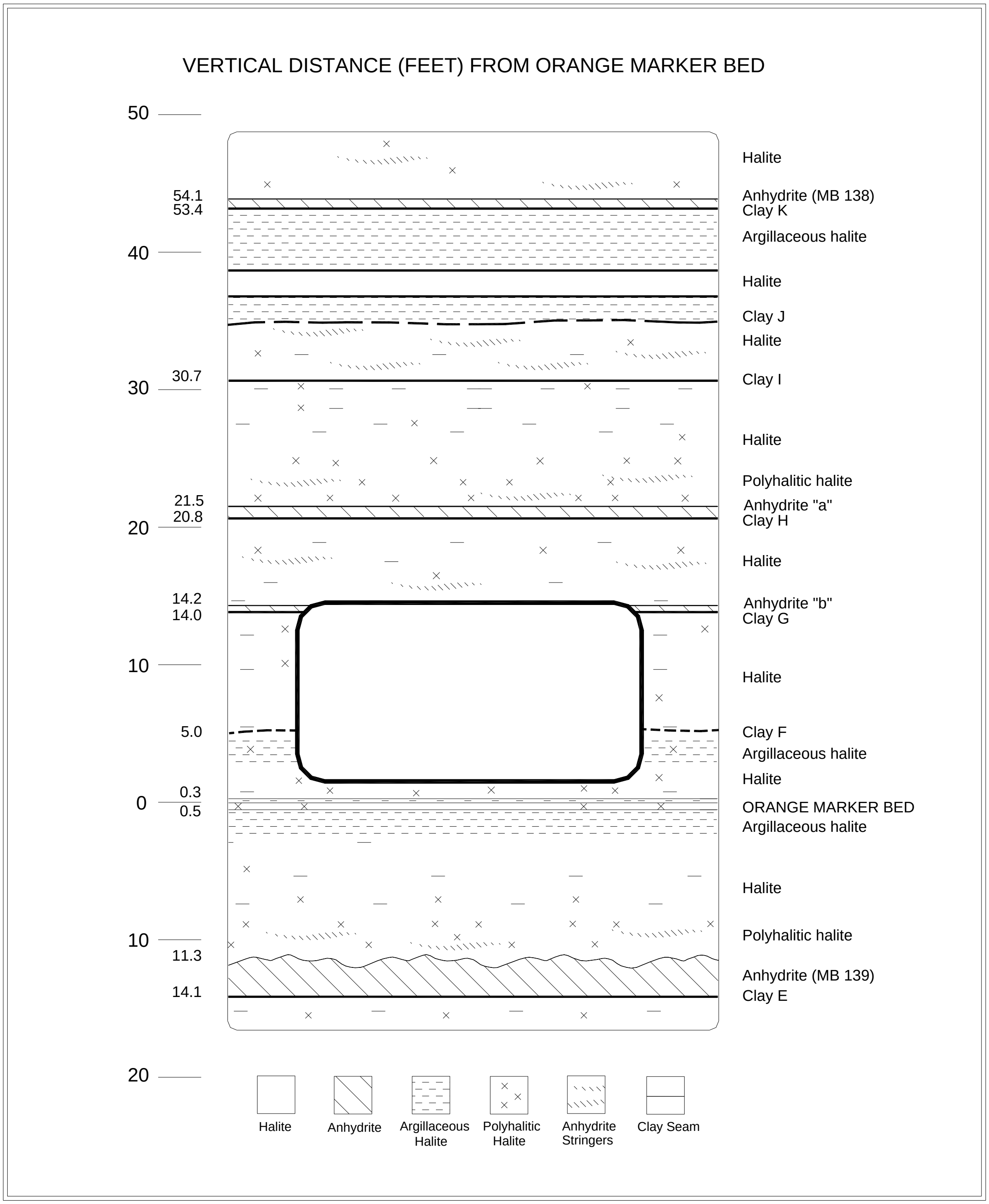

Figure 2-3 Repository Level Stratigraphy of Panels 3, 4, 5, and 6

3.0 PERFORMANCE OF SHAFTS AND KEYS

Four shafts connect the surface with the underground. They are the Salt Shaft, which is used primarily for removing excavated salt from the underground and for transporting personnel and material; the Waste Shaft, which is used primarily for transporting TRU waste to the underground and for transporting personnel and materials; the Exhaust Shaft, which is used to exhaust the ventilation air from the underground; and the Air Intake Shaft, which is the primary source of fresh air ventilation to the underground. This section describes the geomechanical performance of these shafts.

Although through the years much of the instrumentation installed in the shafts has failed, there are no plans to replace it. The project has a good understanding of the expected movements in the shafts. Monitoring results up to the point of instrument failure did not indicate unusual shaft movements or displacements. Continued periodic visual inspections confirm the expected shaft performance and provide necessary observations to evaluate shaft performance. Replacement of failed instrumentation will not provide significant additional information.

3.1 Salt Shaft

The first construction activity undertaken during the SPDV Program was the excavation of the Exploratory Shaft. This shaft was subsequently referred to as the Construction and Salt Shaft and is currently designated the Salt Shaft (see Figure 1-2). The shaft was drilled from July 4 to October 24, 1981, and geologically mapped in the spring of 1982 (DOE, 1983). Figure 3-1 presents the stratigraphy in the shaft.

The Salt Shaft is lined from the surface to 846 ft (258 m) with steel casing having an inside diameter of 10 ft (3 m). The thickness of the steel liner (including external stiffener rings) increases from 0.62 in (1.6 cm) at the top to 1.5 in (3.8 cm) at the key. Cement grout was placed between the liner and the rock face. The 10 ft (3 m) diameter extends through the concrete shaft key to 880 ft (268 m). The shaft key is a 37.5 ft (11.4 m) long, reinforced-concrete structure that begins 3.5 ft (1.07 m) above the bottom of the steel liner. From the key to the bottom at 2,298 ft (700 m), the shaft has a nominal diameter of 12 ft (4 m).

Wire mesh anchored by rock bolts is installed in sections of the lower shaft as a safety screen to contain rock fragments that may become detached. The shaft extends approximately 140 ft (43 m) below the repository horizon in order to accommodate the skip loading equipment and a sump.

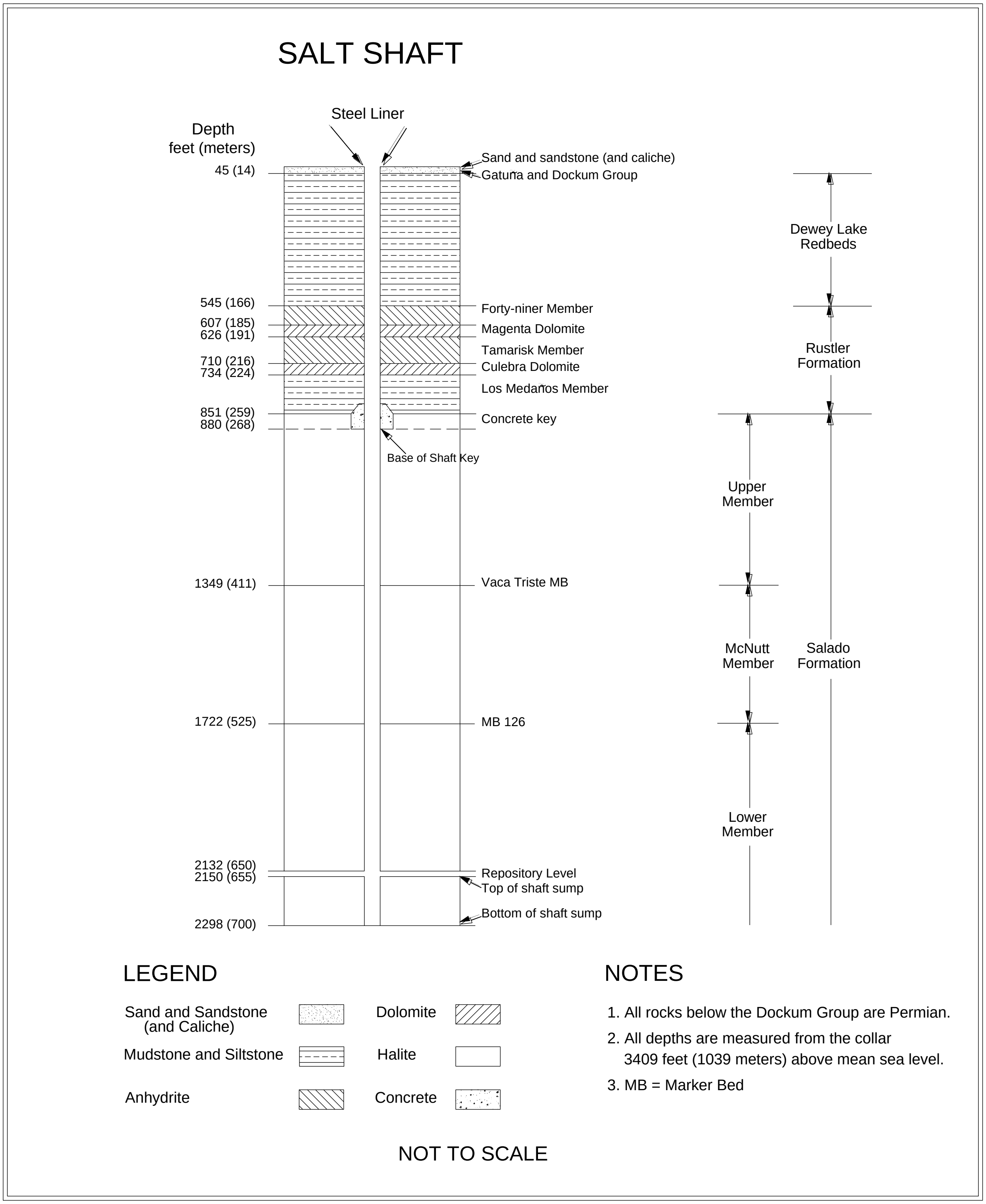

Figure 3-1 Salt Shaft Stratigraphy

3.1.1 Shaft Observations

Underground operations personnel conduct weekly visual inspections. These inspections are performed principally to assess the condition of the hoisting and mechanical systems, but they also include examining the shaft walls for water seepage, loose rock, or sloughing. Visual inspections during this reporting period found that the shaft remained in satisfactory condition. Only routine ground control activities were required.

3.1.2 Instrumentation

Geomechanical instruments (radial convergence points, extensometers, and piezometers) were installed at various levels in the shaft from April through July of 1982 (Figures 3-2 and 3-3). In the shaft key, instruments included strain gauges, pressure cells, and piezometers. Radial convergence points were installed prior to outfitting. Upon completion of shaft outfitting, no more readings were taken.

Ten of the 12 piezometers continue to provide data. The fluid pressures recorded at the end of this reporting period range from approximately 42 pounds per square inch (psi) (290 kilopascals [kPa]) at the 850-ft (259-m) level (upper section of the shaft key) to 160 psi (1103 kPa) at the 691-ft (211-m) level in the Tamarisk Member. The recorded pressures for this reporting period are generally consistent with the readings from the previous reporting period. The fluid pressure on the shaft liner will continue to be monitored on a regular basis.

Four earth pressure cells were installed in the key section during concrete emplacement at the 860-ft (262-m) level. These instruments measure the normal stress between the concrete key and the Salado Formation as salt creep loads up the key structure. Three of the four earth pressure cells continue to provide data. These instruments have indicated essentially no contact pressure since their installation (readings resemble instrument drift at a zero pressure). The maximum contact pressure recorded by the instruments for this reporting period is 5.0 psi (34 kPa).

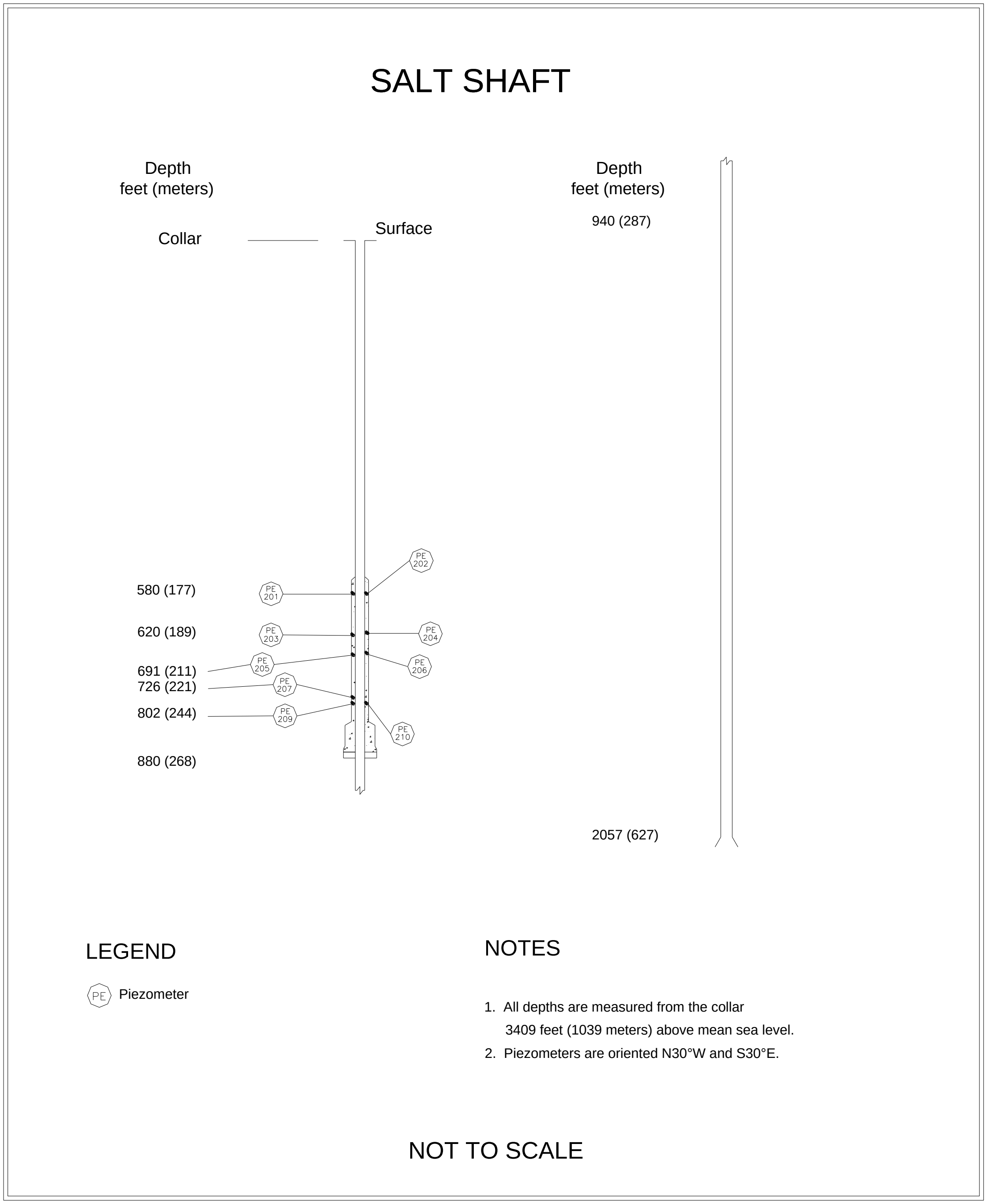

Figure 3-2 Salt Shaft Instrumentation

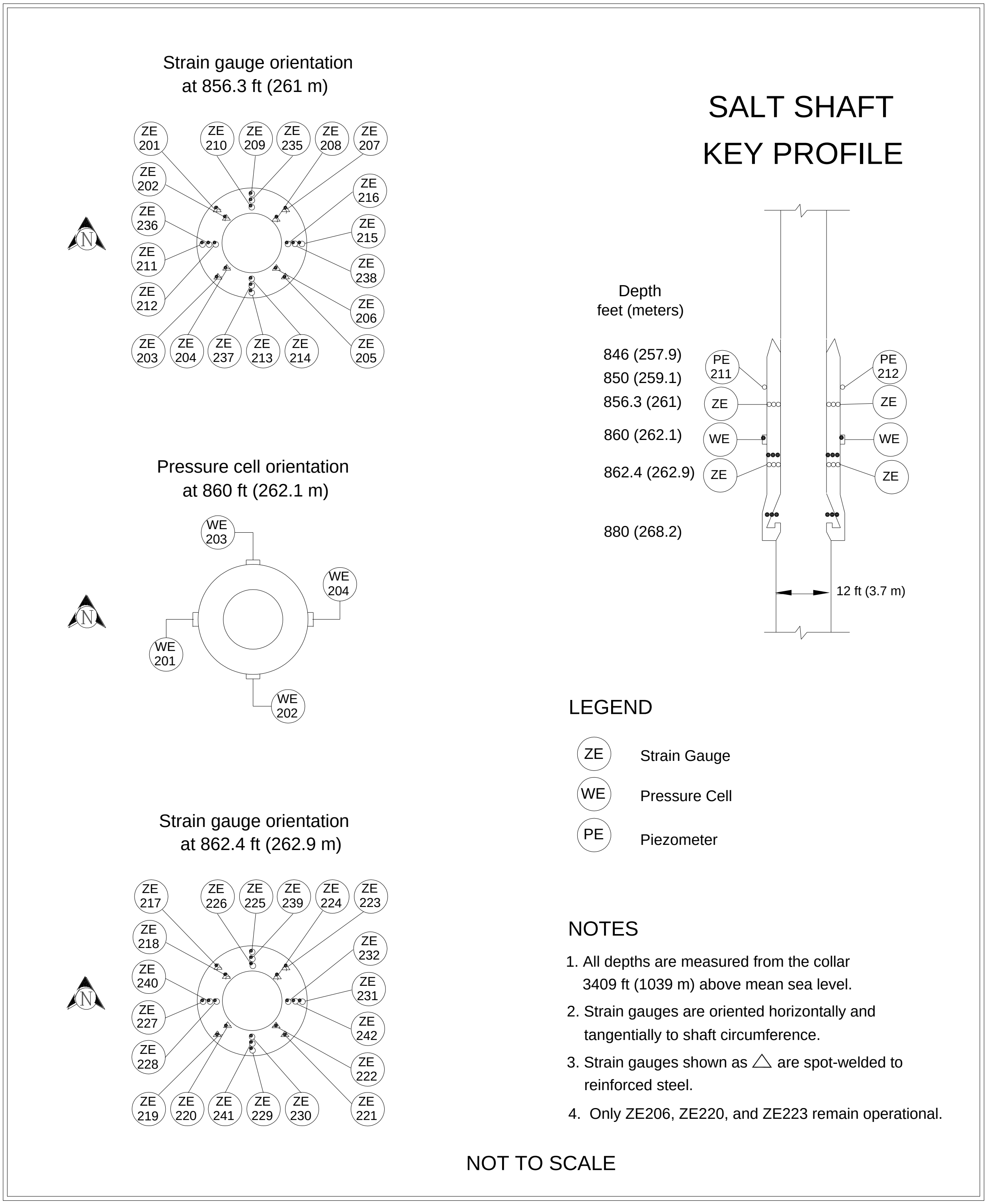

Figure 3-3 Salt Shaft Key Instrumentation

Sixteen spot-welded and twenty-four embedment strain gauges were installed on and in the shaft key concrete at both the 856.3 ft (261 m) level and at the 862.4 ft (263 m) level. Three spot-welded strain gauges are still functioning at these levels. Strains at the 856.3 ft (261 m) level recorded a maximum strain of 634 microstrain. Strains at the 862.4 ft (263 m) level were 921 and -1930 microstrain.

Fourteen embedment strain gauges are still functioning. The strains at the 856.3-ft (261-m) level ranged from -595 to 1005 microstrain. The strains from the two embedment strain gauges at the 862.4 ft (263-m) level were 299 to 407 microstrain. The strains recorded by the spot-welded strain gauges and the embedment strain gauges during this reporting period are similar to the strains recorded by these instruments at the end of the previous reporting period.

3.2 Waste Shaft

As part of the SPDV Program, a 6-ft (2-m) diameter ventilation shaft, now referred to as the Waste Shaft, was excavated from December 1981 through February 1982 (see Figure 1-2). This shaft, in combination with the Salt Shaft, provided a two-shaft underground air circulation system. From October 11, 1983, to June 11, 1984, the shaft was enlarged to a diameter of 20 to 23 ft (6 to 7 m) and lined above the key. Stratigraphic mapping (Figure 3-4) was conducted during shaft enlargement from December 9, 1983, to June 5, 1984 (Holt and Powers, 1984).

The Waste Shaft is lined with non-reinforced concrete having a 19 ft (6 m) inside diameter from the surface to the top of the key at 837 ft (255 m). Liner thickness increases from 10 in (25 cm) at the surface to 20 in (51 cm) at the key. The key is 63 ft (19 m) long and 4.25 ft (1.3 m) thick and is constructed of reinforced concrete. The bottom of the key is 900 ft (274 m) below the surface. The diameter of the shaft is 20 ft (6 m) at the bottom of the key and increases to 23 ft (7 m) just above the shaft station. The shaft below the key is lined with wire mesh anchored by rock bolts. The diameter of 23 ft (7 m) extends to a depth of approximately 2,286 ft (697 m), with the shaft sump comprising the lower 119 ft (36 m) of that interval.

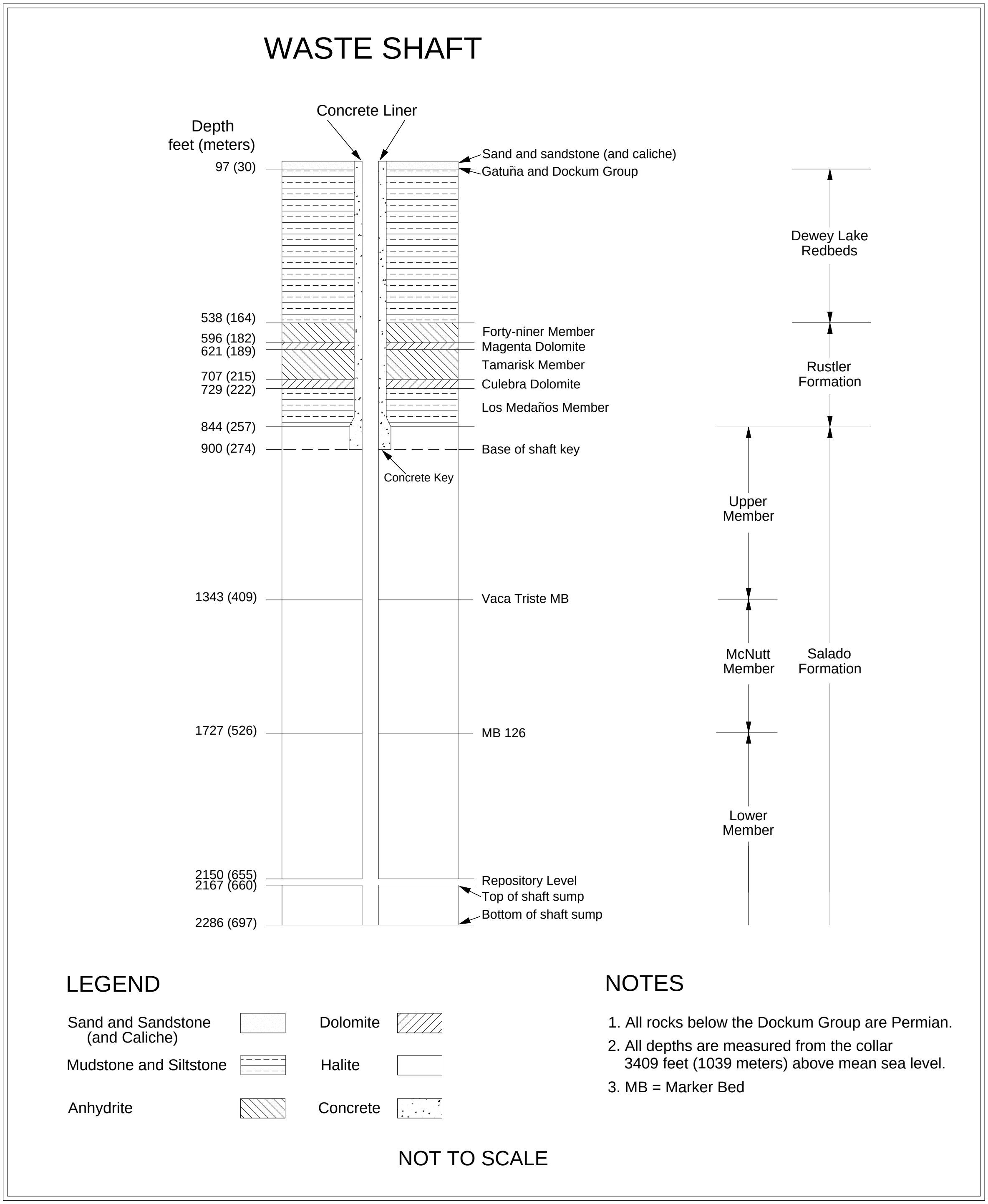

Figure 3-4 Waste Shaft Stratigraphy

3.2.1 Shaft Observations

Underground operations personnel conduct weekly visual inspections, principally to assess the condition of the hoisting and mechanical systems, but also include observation of the shaft walls for water seepage, loose rock, or sloughing. The visual inspections found that the shaft was in satisfactory condition. No ground control activities other than routine maintenance were required.

3.2.2 Instrumentation

Radial convergence points, extensometers, piezometers, and earth pressure cells were installed in the Waste Shaft between August 27 and September 10, 1984. Radial convergence points were installed prior to the outfitting. Upon completion of shaft outfitting, no more radial convergence readings were taken. Figure 3-5 and Figure 3-6 show the instrument locations.

Nine multi-position extensometers were installed in arrays 1,071 ft (326 m), 1,566 ft (477 m), and 2,059 ft (628 m) below the surface as shown in Figure 3-5. Each array consists of three extensometers. No extensometer data have been collected in recent years due to the malfunction of the data acquisition equipment. Since the type of extensometers installed in the shaft over 30 years ago is no longer manufactured, remote data acquisition equipment for these extensometers is also unavailable.

Twelve piezometers were installed in the lined section of the Waste Shaft on September 7 and 8, 1984, to monitor fluid pressure behind the shaft liner and the key section. As of this reporting period, data is no longer being received from any of the piezometers.

Four earth pressure cells were installed in the key section of the Waste Shaft during concrete emplacement between March 23 and April 3, 1984. Earth pressure cells measure the normal stress between the concrete key and the Salado Formation as salt creep loads the key structure. As of this reporting period, data is no longer being received from any of the earth pressure cells.

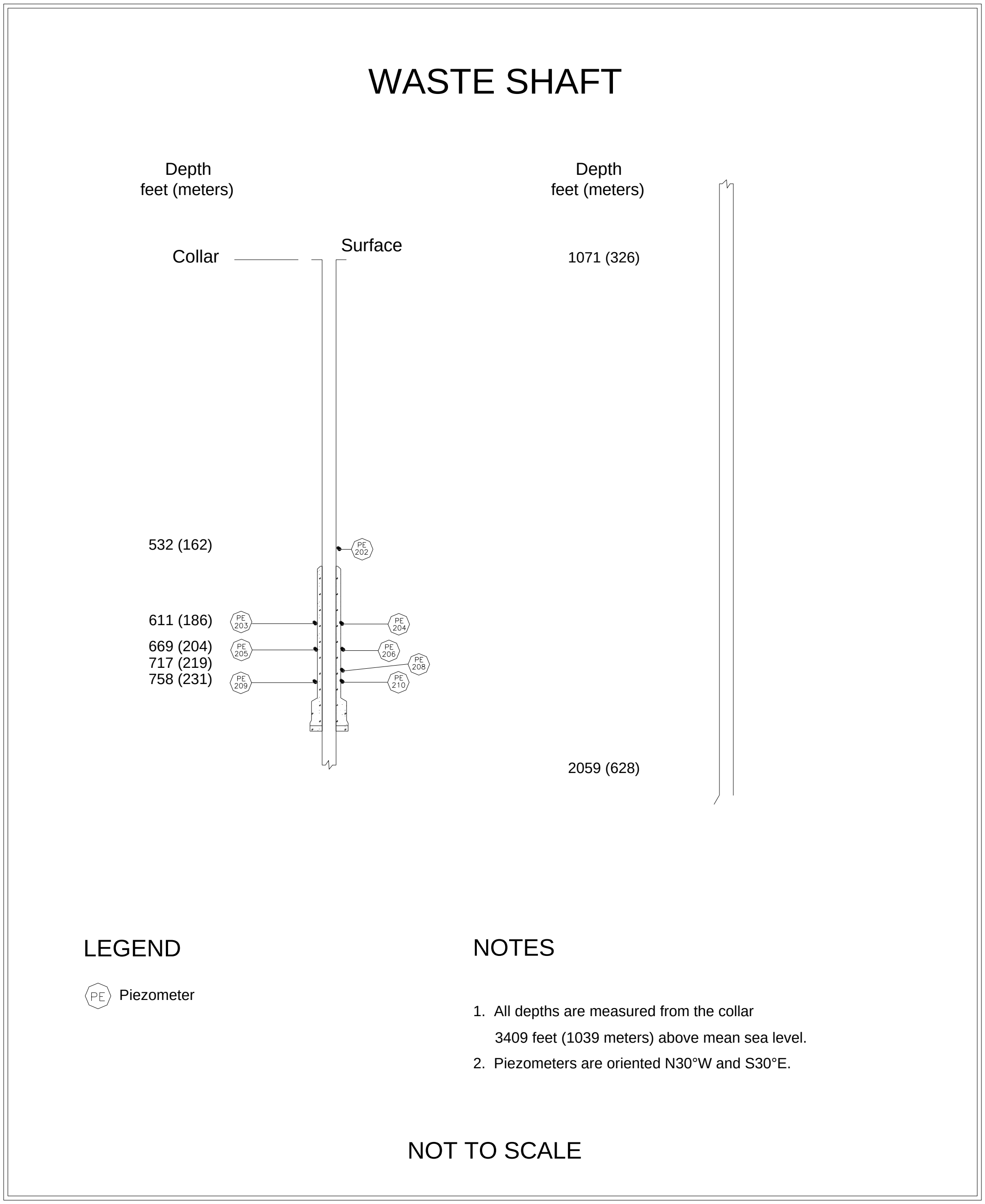

Figure 3-5 Waste Shaft Instrumentation

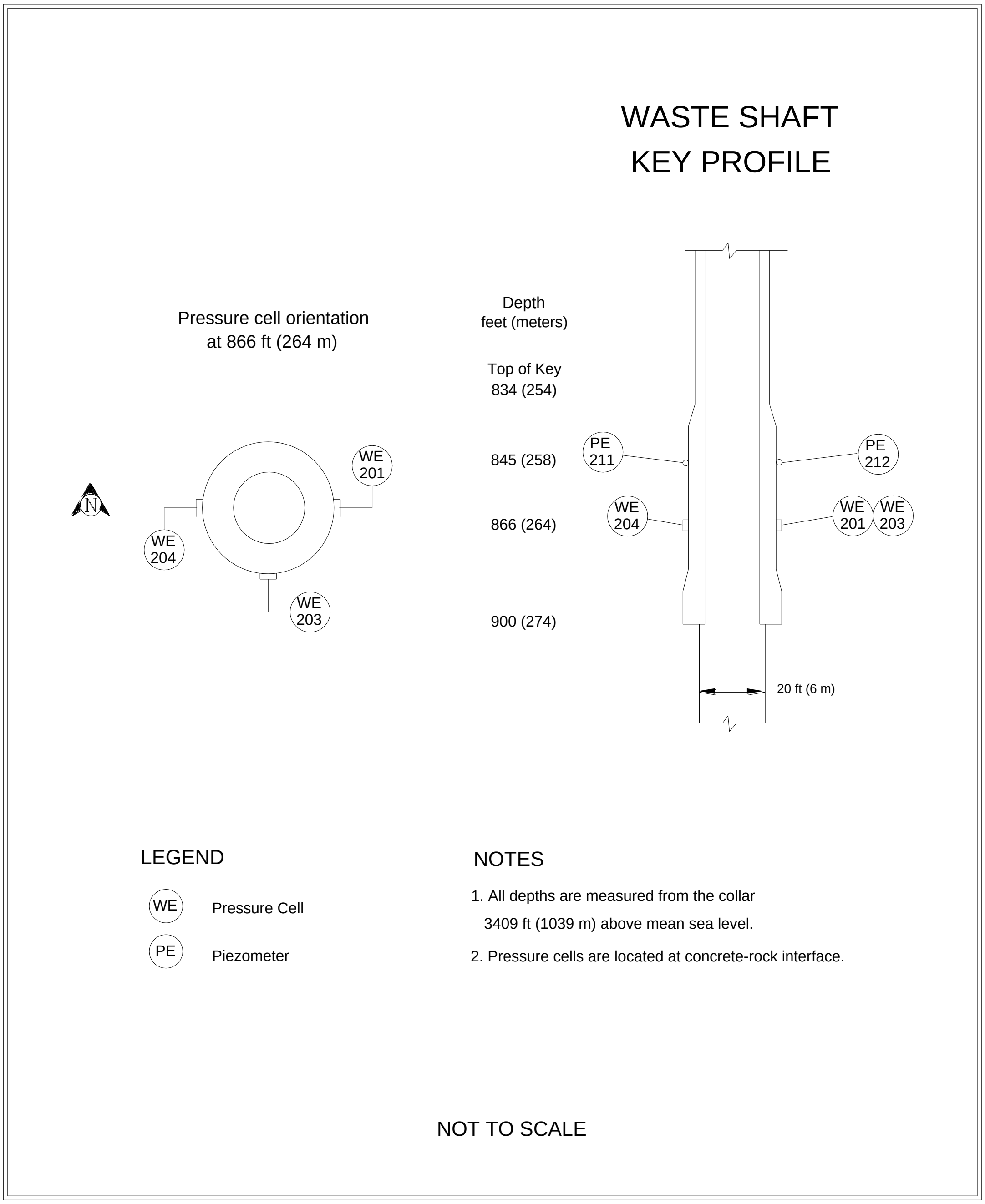

Figure 3-6 Waste Shaft Key Instrumentation

3.3 Exhaust Shaft

The Exhaust Shaft was drilled from September 22, 1983, to November 29, 1984, to establish a route from the underground to the surface for exhaust air (Figure 1-2). Stratigraphic mapping was conducted from July 16, 1984, to January 18, 1985 (DOE, 1986c). Figure 3-7 illustrates the shaft stratigraphy.

The Exhaust Shaft is lined with non-reinforced concrete from the surface to the top of the shaft key at 844 ft (257 m). The liner thickness increases from 10 to 16 in (25 to 41 cm) over that interval. The key is 63 ft (19 m) long and 3.5 ft (1 m) thick. The shaft diameter below the key is 15 ft (5 m), and the interval below the key is lined with wire mesh anchored by rock bolts. The shaft terminates at the facility horizon, approximately 2,150 ft (655 m) deep. This shaft has no sump.

3.3.1 Quarterly Shaft Inspection

Quarterly video inspections are conducted according to approved WIPP procedures. Inspections are performed to evaluate the condition and to verify the integrity of the shaft. The shaft is examined for cracks, corrosion, salt buildup, seeps, and debris. In addition, inspections examine the condition of anchors, brackets, and down-hole equipment. Three inspections were performed between July 1, 2015 and June 30, 2016 on September 14, 2015, February 3, 2016 and May 17, 2016.

3.3.1.1 Video Camera

Video inspections use a custom-designed vertical-drop color camera in an aerodynamic housing, suspended by a dual-armored cable, with pan, tilt, and zoom capability. The cable contains five copper conductors and two multi-mode optical fibers. It is reeled out by a winch mounted in a control trailer. Inspections are recorded electronically.

3.3.1.2 Shaft Inspection Observations

Quarterly video inspection observations concentrate on four major areas: air monitoring components, shaft liner, shaft walls, and equipment support and cabling. The air monitoring components consist of one air-velocity and three air-monitoring devices as shown in Figure 3-8. The video inspection includes examination of each device, including the transport assembly, guide tubes, the sample intake, and the support brackets that extend from Station "A" above the shaft to the shaft collar. Air monitoring components extend from the collar 21 ft into the shaft. Video inspections indicate that the air-sampling components can accumulate salt buildup of up to several inches thick.

The Exhaust Shaft liner is examined for cracks, seepage, and general shaft stability. Currently, there are three principal zones of seepage in the shaft. The first is about 50 to 55 ft below the shaft collar (bsc). The second is about 60 to 65 ft bsc. The third is about 80 to 85 ft bsc, as shown in Figure 3-9. Monitoring of seepage horizons started before 1995. Water entering the shaft through these cracks is believed to originate from a perched –shallow water-bearing horizon at the base of the Santa Rosa Formation that is being recharged as the result of surface modifications at the site. The fluid level in the Santa Rosa near the shaft is about 48 to 49 ft below the surface. Based on examination of inspection videos, the flow rate into the shaft during this reporting period is estimated at about 1 to 1 ½ gallons per minute. Seepage cracks are confined primarily to the eastern side of the shaft wall.

When fluid was detected seeping into the shaft, a catch basin was designed and installed at the base of the Exhaust Shaft to intercept water and prevent it from draining into the Waste Shaft Sump. Fluid was removed from the catch basin from March 1996 through October 2005 as needed. The catch basin was damaged in 2004 by fallen debris, either salt or instrumentation cables or both. A new catch basin was fabricated and installed in December 2004. This basin was damaged in August 2005, most likely the result of fallen debris. An interception well system was installed between November 2005 and March 2006 to replace the catch basin. Interception wells were drilled down gradient in S-400 between E-140 and E 300 (Figure 3-10). The interception well system initially consisted of four 30-ft deep 9-7/8-in diameter fluid collection holes with a submersible pump and pressure transducer in each. Fluid is pumped from each hole to a series of storage containers in S-550. A data-acquisition system monitors the fluid level in each hole, turning the pump on and off between set limits as needed.

Between February 2 and 6, 2008, two additional fluid collection holes, OH631 and OH632, were drilled in S-400 to improve the total volume of fluid recovered by the interception well system. They replaced OH613 and OH614 which generated little fluid. As with the previous four holes, the additional holes were drilled at 9-7/8-inch diameter to a total depth of 30 feet. Pumps were pulled from OH613 and OH614 and installed in OH631 and OH632. Figure 3-10 shows the location of the interception wells system and the 500-gallon storage containers.

It was noted during the Exhaust Shaft video inspections performed in September 2015, February 2016, and May 2016 that shaft conditions were generally good. There were no significant changes in the thickness of the salt in the shaft plenum ranging from zero to several feet thick. The principle cracks and seepage horizons in the shaft liner were located at about 63-65 feet and 82-84 feet below the shaft collar. Based on examination of the fluid flow from the shaft liner and evaluation of previous shaft inspections the estimated average flow rate of fluid seeping through the shaft liner into the shaft was 1.1 gallons per minute. The thickness of the salt has significantly thinned in the upper portion of the shaft between the shaft collar and 600 feet below ground surface. At the same time there appears to be an increase in the buildup of salt along the shaft walls in the form of stalactites in the lower portion of the shaft.

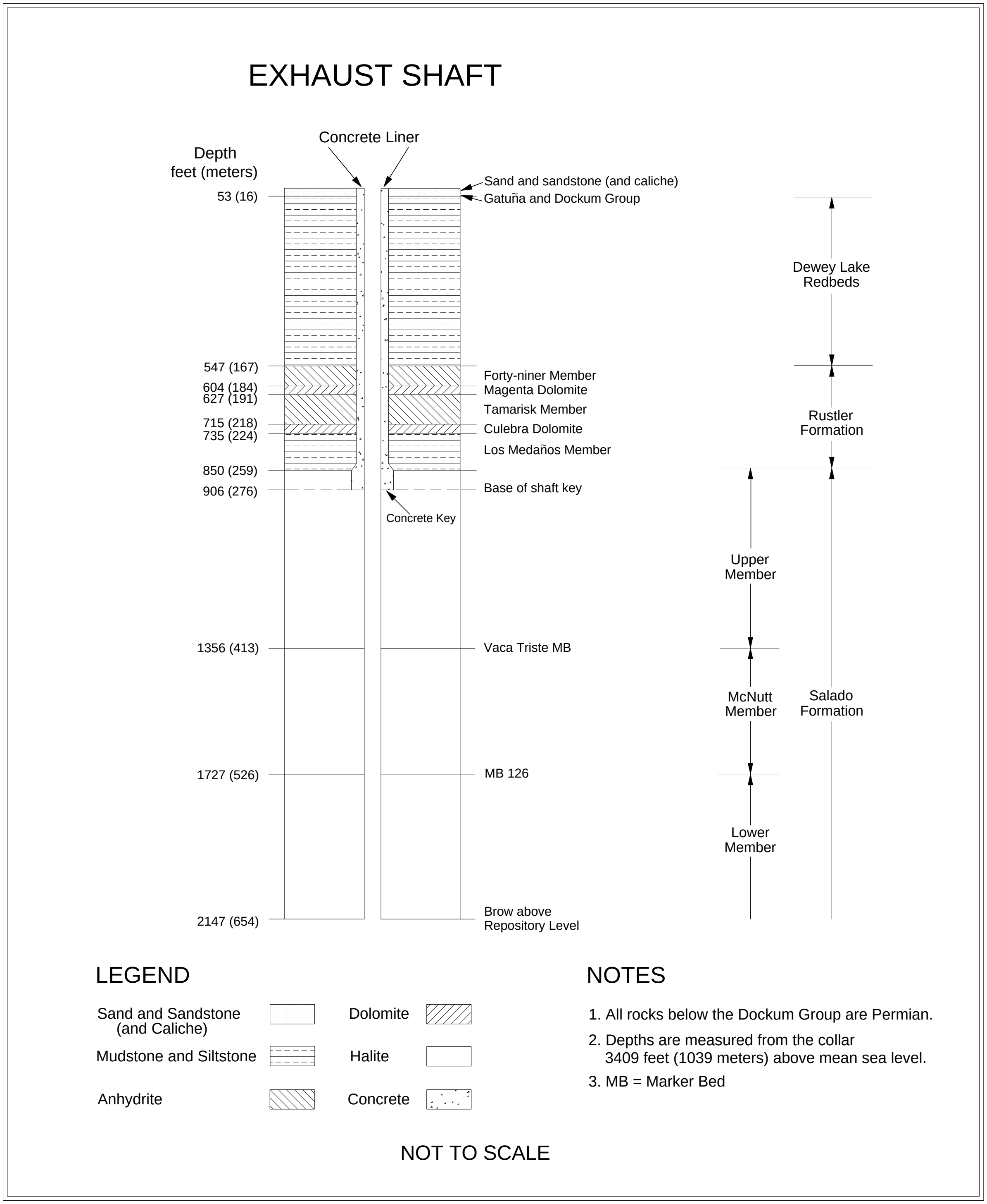

Figure 3-7 Exhaust Shaft Stratigraphy

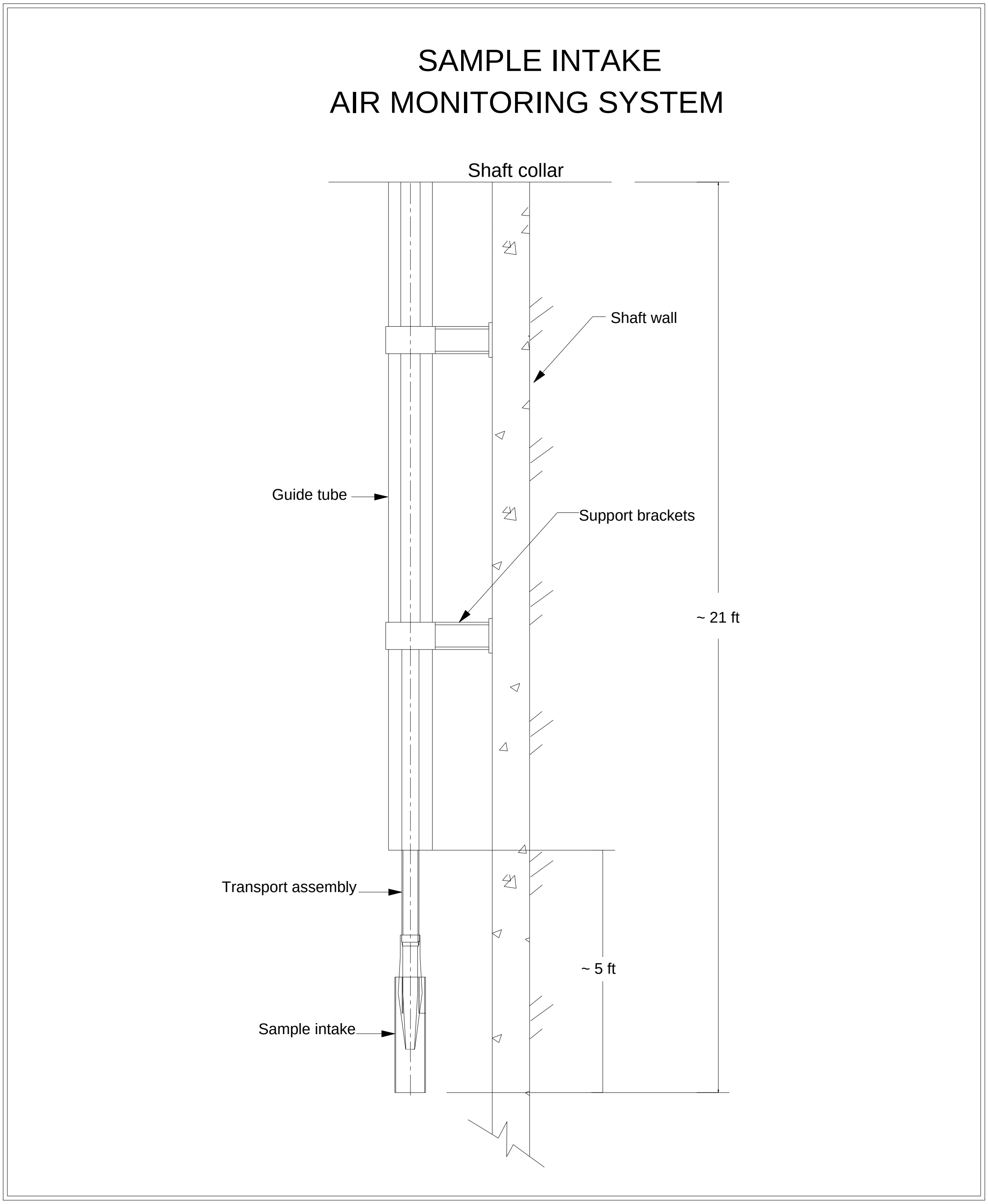

Figure 3-8 Sample Intake of Exhaust Shaft Air Monitoring System

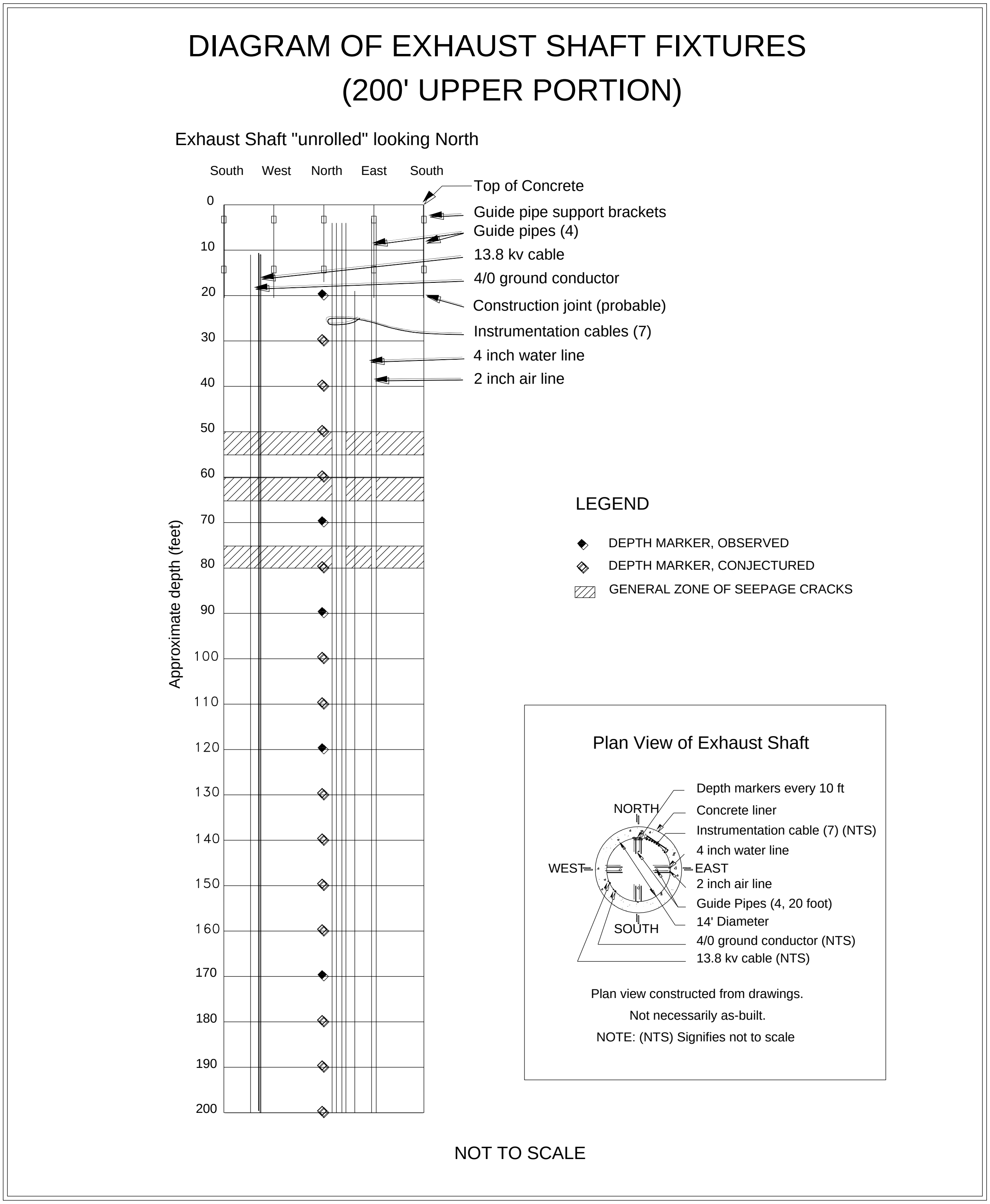

Figure 3-9 Diagram of Exhaust Shaft Fixtures and Seepage Zones (Upper 200 ft)

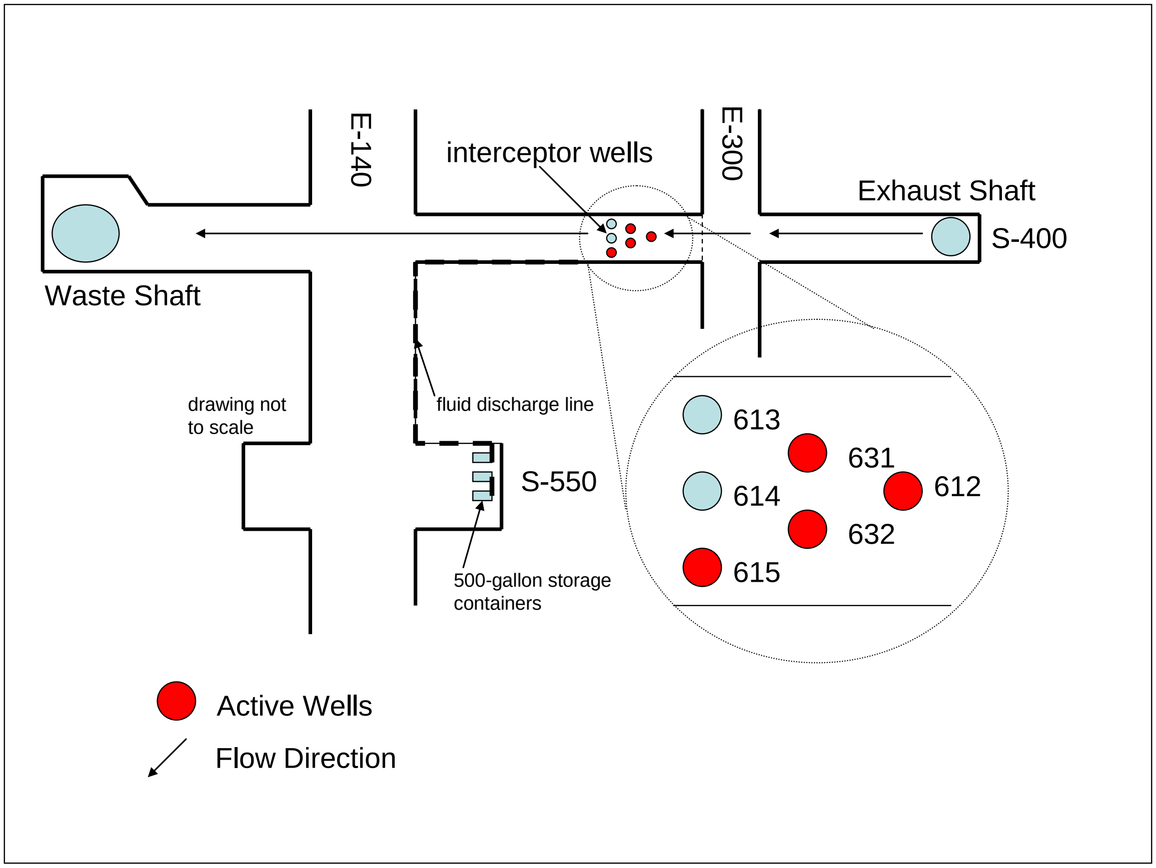

Figure 3-10 Location of Interception Wells and Storage Containers

Figure 3-11 presents the volume of fluid removed from the catch basin from July 1997 through June 2006, and by the interception well system from July 2006 through June 2016. The largest reported volumes are typically associated with periods of reduced ventilation and increased humidity. For a discussion of the factors affecting the quantity of fluid produced in the Exhaust Shaft, refer to DOE/WIPP-00-2000, *Brine Generation Study*.

The shaft walls were examined for salt buildup, cracks, moisture, and encrustations, with particular attention paid to power cables, instrument cables, air lines and water-lines, and the three water rings at the base of the Magenta and Culebra members of the Rustler Formation and the bottom of the shaft key. The condition of the shaft wall varies depending on airflow, humidity, temperature, and underground mining activities. The principal areas in the shaft with significant salt buildup were the three water rings at the Magenta, the Culebra, and the key, and along upper portions of the shaft generally associated with power cables, support brackets, instrument cables, and the air lines and water-lines.

Though the Magenta and Culebra water rings are encrusted with salt buildup, no water appears to originate from the liner or water rings. Most of the seepage was observed along the east face of the shaft wall near the instrumentation cables and the air-lines and water-lines in the upper section of the shaft. Though the presence of water is an inconvenience requiring periodic disposal, at this time it does not appear to have created any hazard or affected the structural integrity of the shaft. However, brine increases the probability of corrosion and deterioration of utility hangers and brackets. There are no visible signs of dissolution of the salt below the key.

The video inspections also focused on the installed utilities and support brackets. These include a 13.8 kVA power cable that is no longer active and the grounding cable on the west wall of the shaft, the instrumentation cables on the northeast wall of the shaft, and the 4 in. air-line and the 2-in. water-line on the east wall of the shaft.

Sporadic salt buildup continues on remaining cables in the shaft. The long-term implication of salt buildup is increased loading on cables and cable hangers, accompanied by intermittent falls of debris. The 4-in. compressed air-line and the 2-in. water-line extend from the surface to the bottom of the shaft. At present, neither line is being used. The integrity of the brackets holding the air-line and water-line was difficult to assess because of salt buildup; however, there was no indication that the brackets were broken. Many instrumentation cables and most of the 138kVA power cable have broken off and fallen to the base of the shaft.

3.1.3 Instrumentation

The Exhaust Shaft was equipped with geomechanical instrumentation in two stages. Earth pressure cells were installed behind the liner key in November 1984. Piezometers and nine multi-position extensometers were installed during November and December 1985. Figure 3-12 and Figure 3-13 show the instrument locations. None of these instruments continues to provide data.

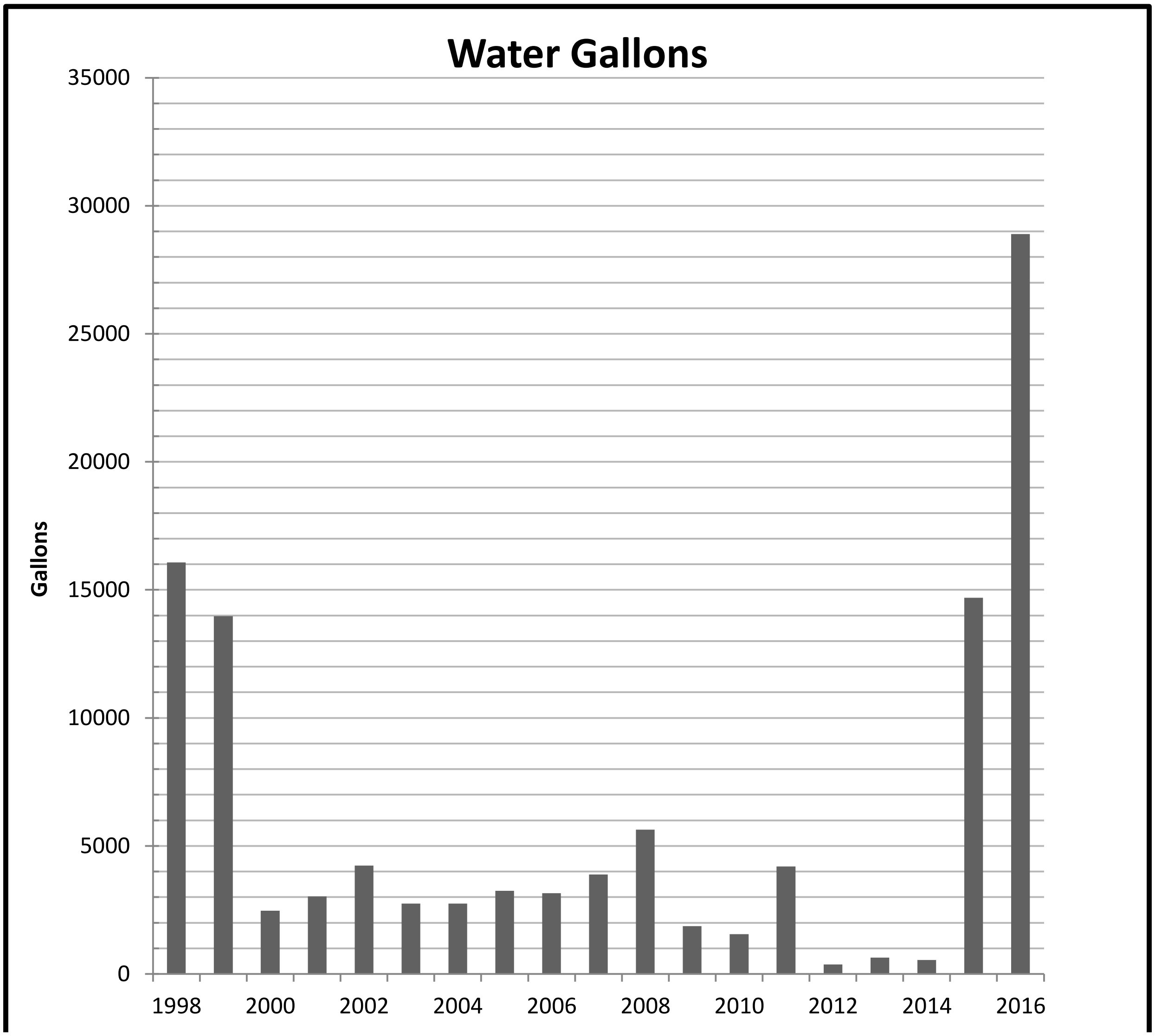

Figure 3-11 Water Removed from the Exhaust Shaft Catch Basin and the Interception Well System

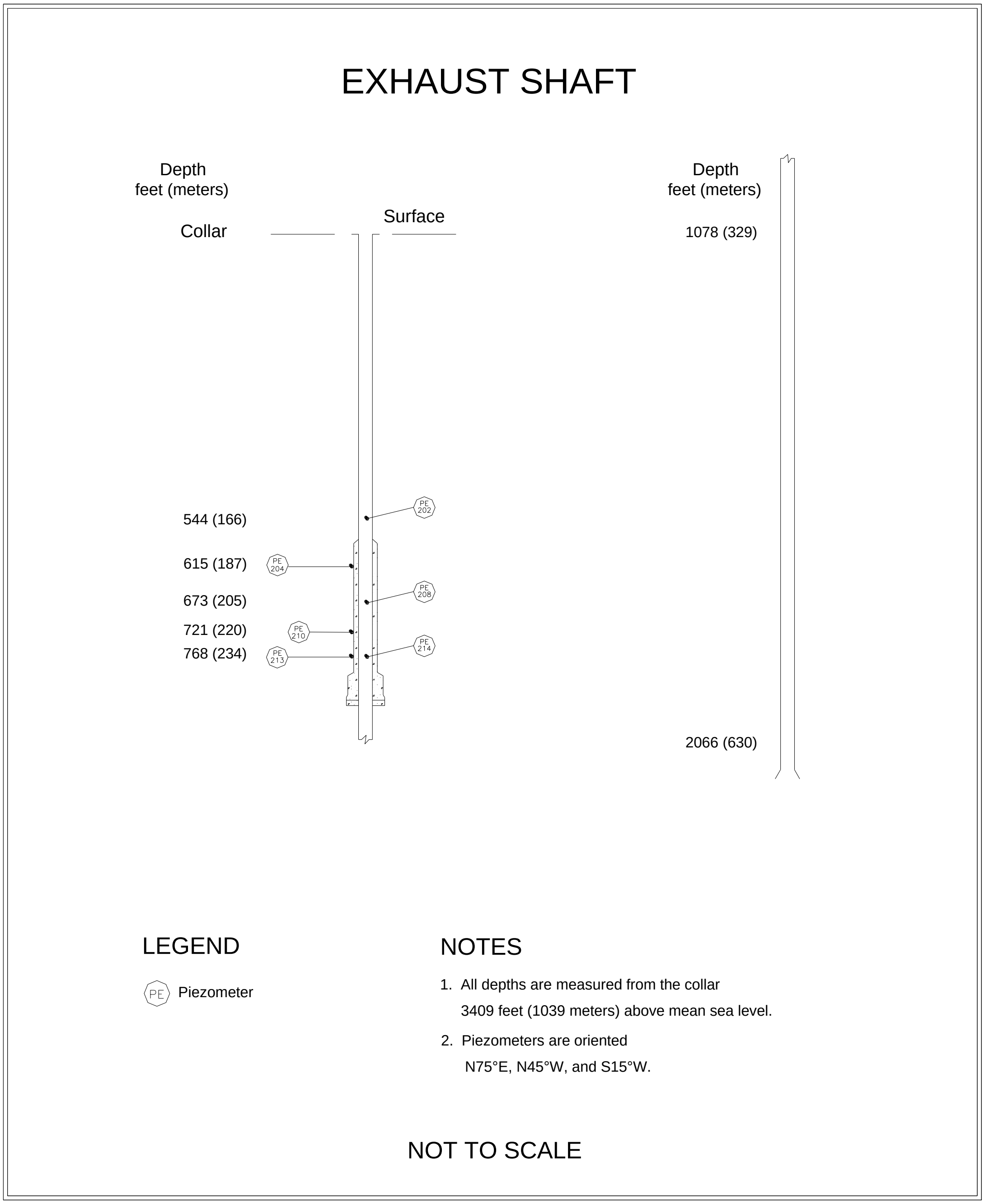

Figure 3-12 Exhaust Shaft Instrumentation

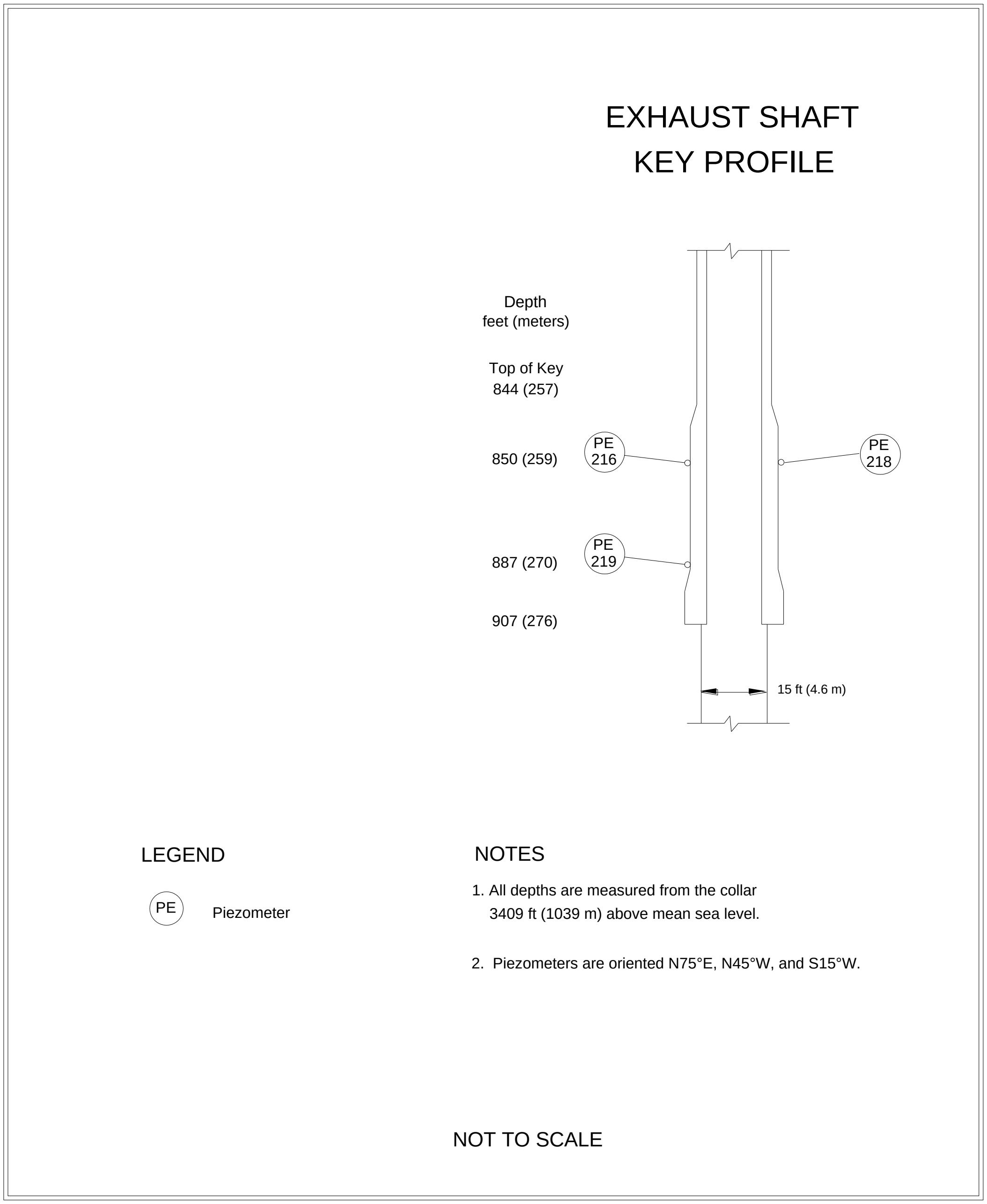

Figure 3-13 Exhaust Shaft Key Instrumentation

3.4 Air Intake Shaft

The Air Intake Shaft was drilled from December 4, 1987, to August 31, 1988, to establish a primary route for surface air to enter the repository (see Figure 1-2). The stratigraphy was mapped from September 14, 1988, to November 14, 1989 (Holt and Powers, 1990). Figure 3-14 summarizes the shaft stratigraphy.

The Air Intake Shaft is lined with non-reinforced concrete from the surface to the bottom of the shaft key at 903 ft (275 m). The key is 81 ft (25 m) long with an inside diameter of 16 ft (5 m). The shaft diameter below the key is 20 ft (6 m), and the shaft below the key is unlined to the facility horizon at 2,150 ft (655 m). The shaft walls are bolted and meshed from just below the key all the way down to the shaft station. This shaft has no sump.

3.4.1 Shaft Performance

Weekly visual inspections were performed on the Air Intake Shaft (except for a brief period following the radiological release) during this reporting period, and the shaft was found to be in satisfactory condition. No ground control activities other than routine maintenance were required during this reporting period.

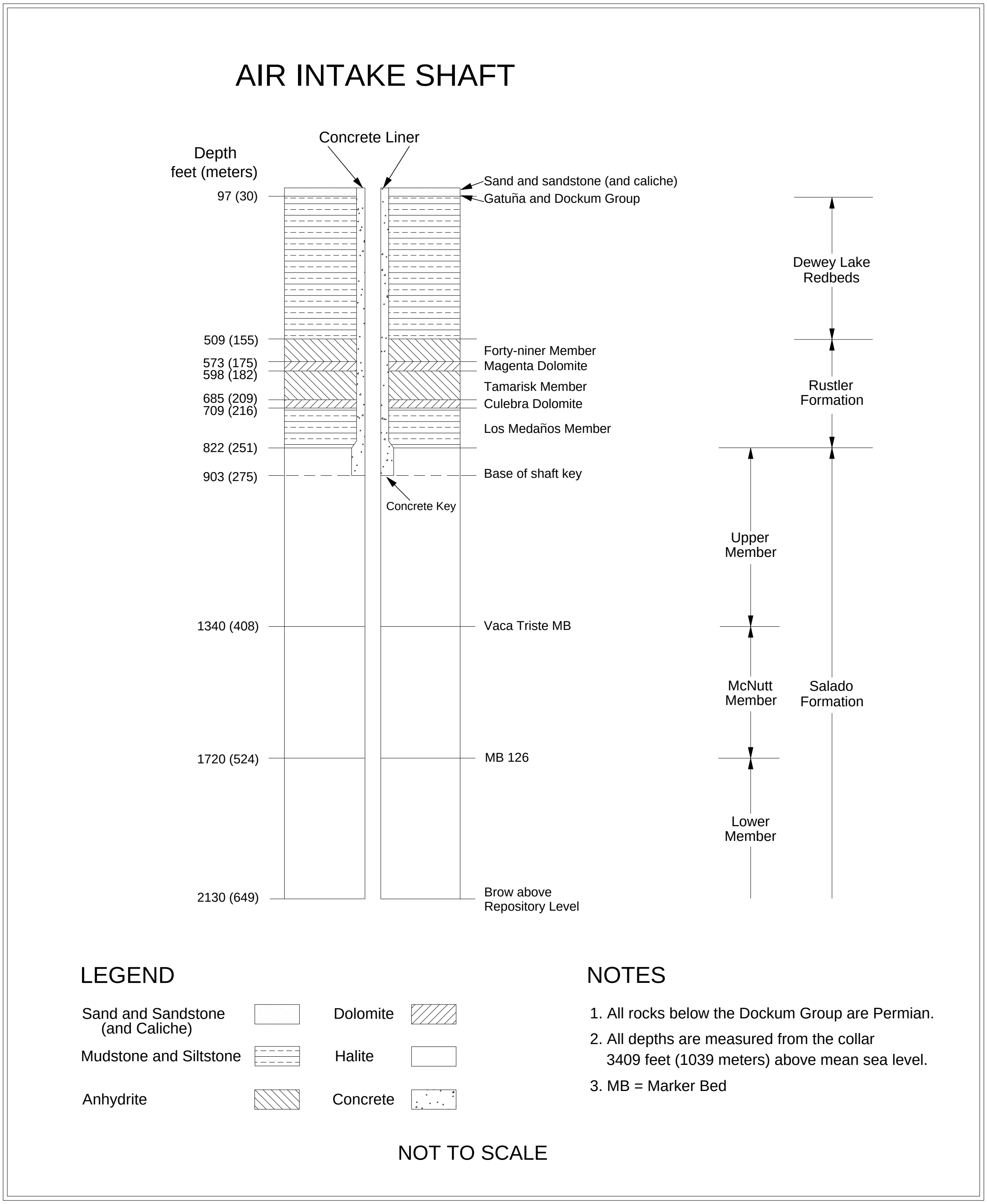

Figure 3-14 Air Intake Shaft Stratigraphy

4.0 PERFORMANCE OF SHAFT STATIONS

This section describes the instrumentation and geomechanical performance of the shaft stations at the base of the Salt Shaft, the Waste Shaft, and the Air Intake Shaft. The Exhaust Shaft does not have an enlarged shaft station; therefore, it is not included in this section.

4.1 Salt Shaft Station

The Salt Shaft Station was excavated by drilling and blasting between May 2 and June 3, 1982. In 1987 the station was enlarged by removing the roof beam up to Anhydrite "b" between S-90 and N-20 using a mechanical scaler. In 1995, the remaining roof beam at the north end of the station was also removed up to Anhydrite "b." The station area south of the shaft is 90 ft (27.5 m) long and 32 to 38 ft (10 to 12 m) wide. The height of the station south of the shaft is 18 ft (5.5 m). The station dimensions north of the shaft are approximately 30 ft (9 m) long, 32 to 35 ft (10 to 11 m) wide, and 18 ft (5.5 m) high. The shaft extends approximately 140 ft (43 m) below the facility horizon to accommodate the skip loading equipment and a sump. Figure 4-1 shows a cross section of the station.

4.1.1 Modifications to Excavation and Ground Control Activities

The Salt Shaft Station was not modified during this reporting period. Ground control activities were limited to routine maintenance.

4.1.2 Instrumentation

Geomechanical instrumentation was installed in the Salt Shaft Station between June 1982 and February 1983, with subsequent re-installation of extensometers and convergence points as necessary. Figure 4-2 shows the instrument locations after the roof beam was taken down.

Five vertical convergence points are currently monitored. Table 4-1 summarizes the vertical closure rates in the Salt Shaft Station from July 2015 through June 2016. Salt Shaft Station vertical closure rates indicate that the rates are lower than during the previous reporting period.

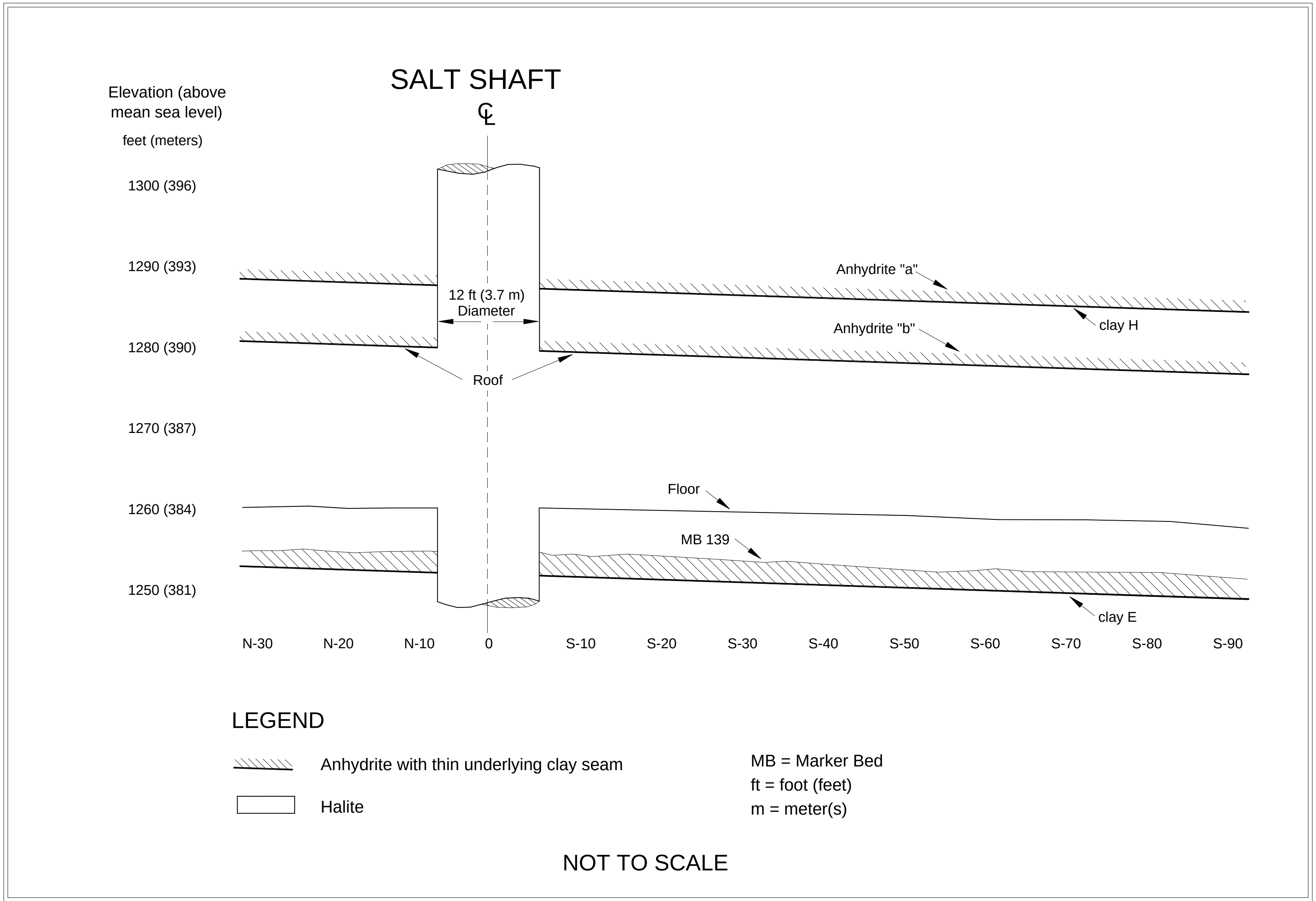

Figure 4-1 Salt Shaft Station Stratigraphy

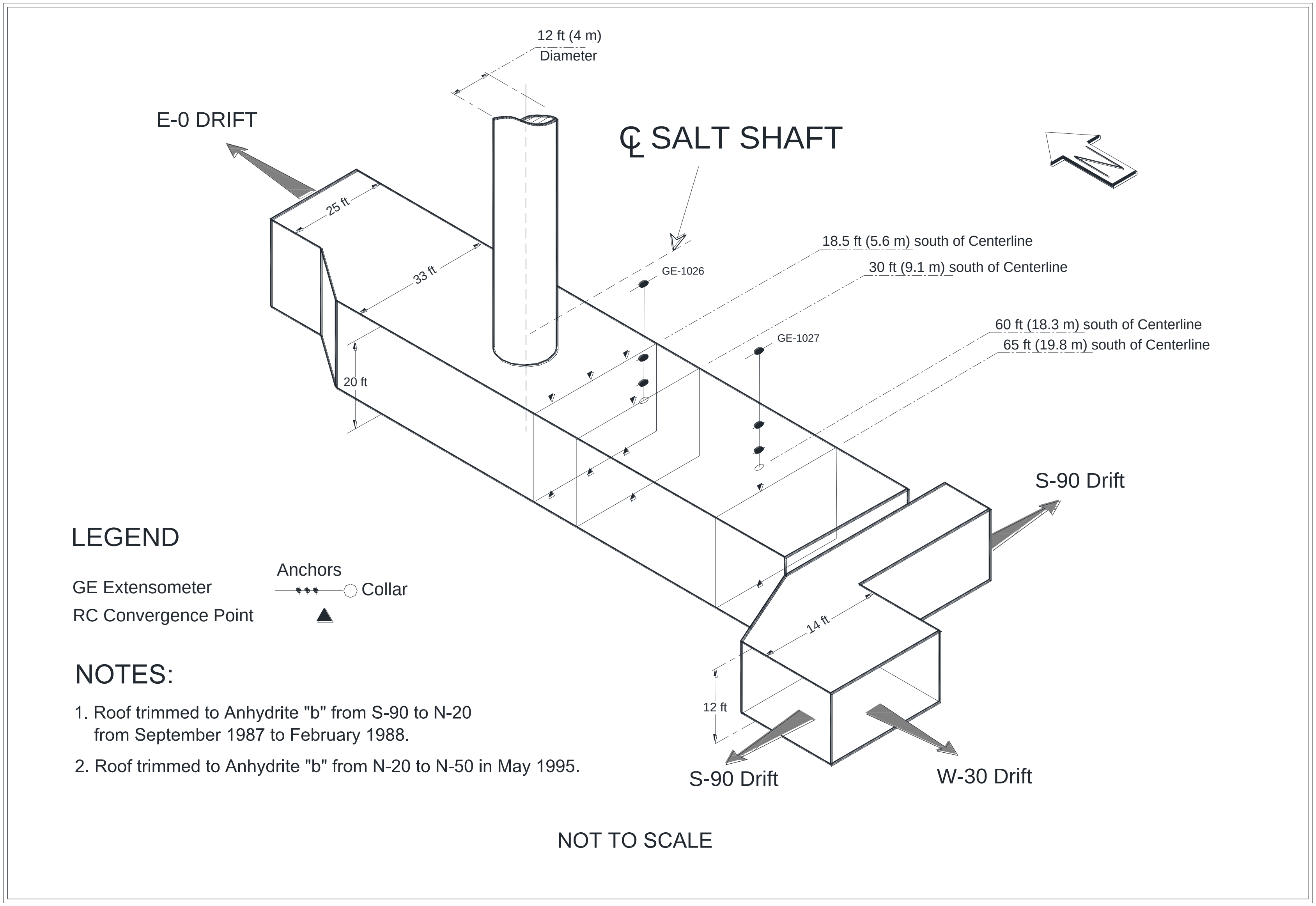

Figure 4-2 Salt Shaft Station Instrumentation after Roof Beam Excavation

Table 4-1 Closure Rates in the Salt Shaft Station

Location	Chord[1]	Last Reading	Total Cumulative Displacement in (cm)	Closure Rate 2015-2016 in/yr (cm/yr)	Closure Rate 2014-2015 in/yr (cm/yr)	Rate Percent Change
E0-S18	A-E	04/06/16	7.749 (19.682)	2.6 (6.6)	1.2 (3.0)	117%
E0-S18	B-D	04/06/16	8.626 (21.910)	2.7 (6.8)	1.3 (3.3)	108%
E0-S18	H-F	04/06/16	5.139 (13.053)	2.1 (5.3)	0.7 (1.8)	200%
E0-S30	A-C	04/06/16	7.769 (19.733)	2.6 (6.6)	1.2 (3.0)	117%
E0-S65	A-C	04/06/16	5.641 (14.328)	2.3 (5.8)	0.8 (2.0)	188%

[1] Chord is defined in Section 5.2.2

4.2 Waste Shaft Station

The Waste Shaft Station was initially excavated with a continuous miner as a ventilation connection to a 6-ft (2-m) diameter exhaust shaft in November 1982. In 1984, the station was enlarged to a height of 15 to 20 ft (4.5 to 6 m) and a width of 20 to 30 ft (6 to 9 m). The station is approximately 150 ft (46 m) long. In 1988, the station walls were trimmed, and concrete was placed on the floor. Since 1988, the Waste Shaft Station has undergone five major floor renovations. A 53-ft (16-m)-long section of the reinforced concrete was removed in February 1991, in 1995 an additional 30-ft (9-m) section was removed, and in 2000 floor maintenance included trimming of the floor and reinstallation of the rails supported by segmented concrete panels on a crushed rock backfill. The roof of the Waste Shaft Station was mined up to Clay G in December 2008 to assure adequate operational clearance. 12-ft resin-anchored roof bolts and chain link were installed for ground support. Figure 4-3 shows a cross-section of the Waste Shaft Station stratigraphy.

4.2.1 Modifications to Excavation and Ground Control Activities

No modifications to the Waste Shaft Station were made during this reporting period. Ground control activities were limited to routine maintenance.

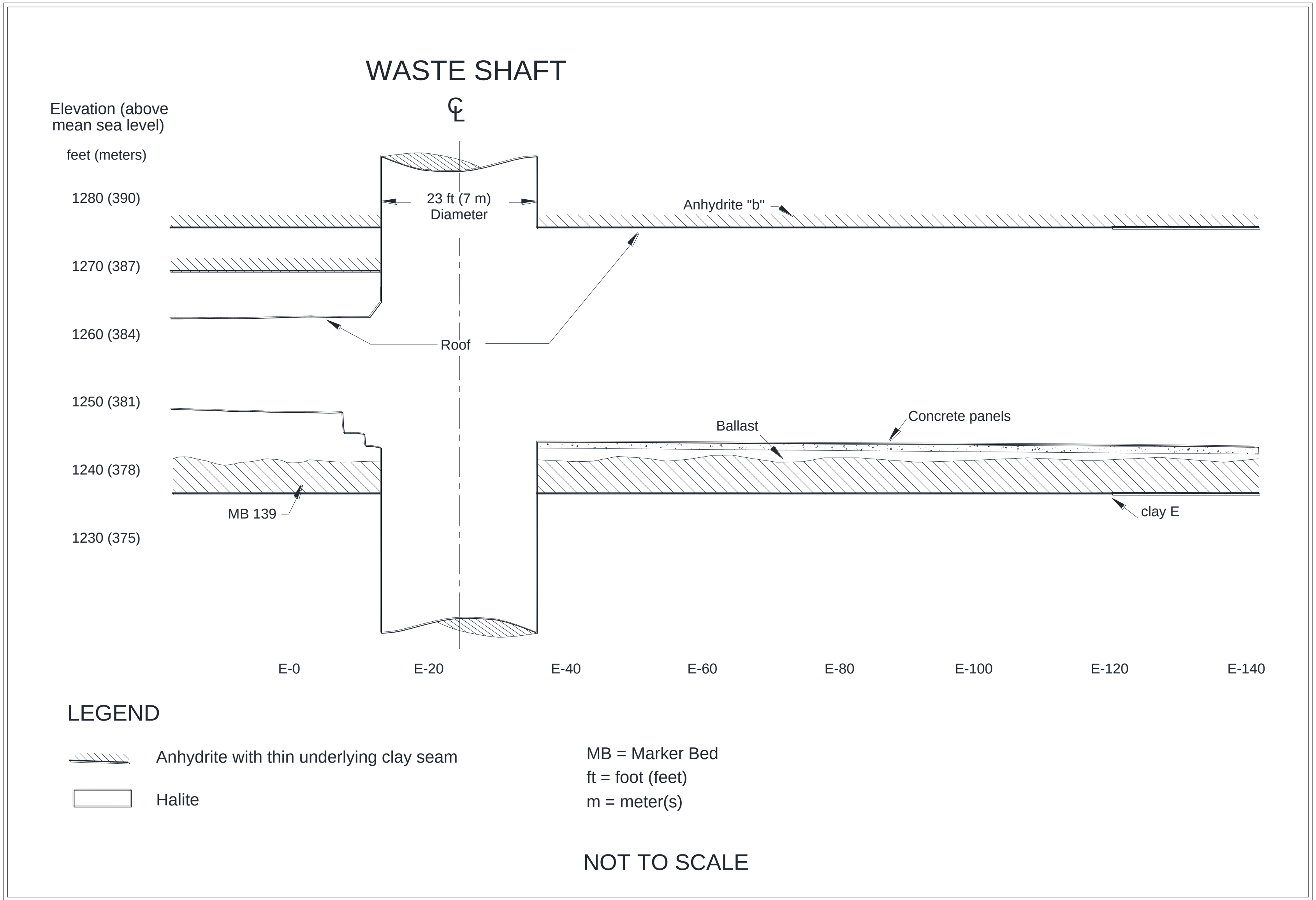

Figure 4-3 Waste Shaft Station Stratigraphy

4.2.2 Instrumentation

Instruments were initially installed in the Waste Shaft Station between November 12 and December 2, 1982. Figure 4-4 illustrates the locations after enlargement. Two extensometers in the Waste Shaft Station are currently being monitored. In addition, horizontal convergence is being monitored at E-32 and E-85.

Table 4-2 summarizes the recent history of the roof extensometers in the Waste Shaft Station.

Table 4-3 summarizes the annual horizontal closure rates calculated from convergence point data for this reporting period.

Table 4-2 Summary of Roof Extensometers in Waste Shaft Station

Instrument	Location	Last Reading	Displacement Relative to Deepest Anchor in (cm)	Displacement Rate 2015 to 2016 in/yr (cm/yr)	Displacement Rate 2014 to 2015 in/yr (cm/yr)	Rate Change Percent
51X-GE-00268	S400-W30	02/04/16	7.333 (18.626)	0.0 (0.0)	0.1 (0.3)	-100%
51X-GE-00404-2	S400-E35	10/05/15	1.579 (4.011)	0.3 (0.8)	0.3 (0.8)	0%

Table 4-3 Closure Rates in the Waste Shaft Station

Location	Chord[1]	Last Reading[2]	Cumulative Displacement in (cm)	Closure Rate 2013 to 2014 in/yr (cm/yr)	Closure Rate 2012 to 2013 in/yr (cm/yr)	Rate Change Percent
S400-E32	B-D	02/05/14	6.435 (16.345)	1.1 (2.8)	1.4 (3.6)	-21%
S400-E85	B-D	02/05/14	6.590 (16.739)	1.2 (3.0)	1.4 (3.6)	-14%

[1] Chord is defined in Section 5.2.2.
[2] The horizontal chords were not read this period due to the unavailability of a lifting vehicle. Based on the 2013 to 2014 closure rate the estimated 2015 cumulative displacement is 6.435" + 1.1" = 7.535 inches at S400-E32 and 6.590" + 1.2 = 7.790 inches at S400-E85.

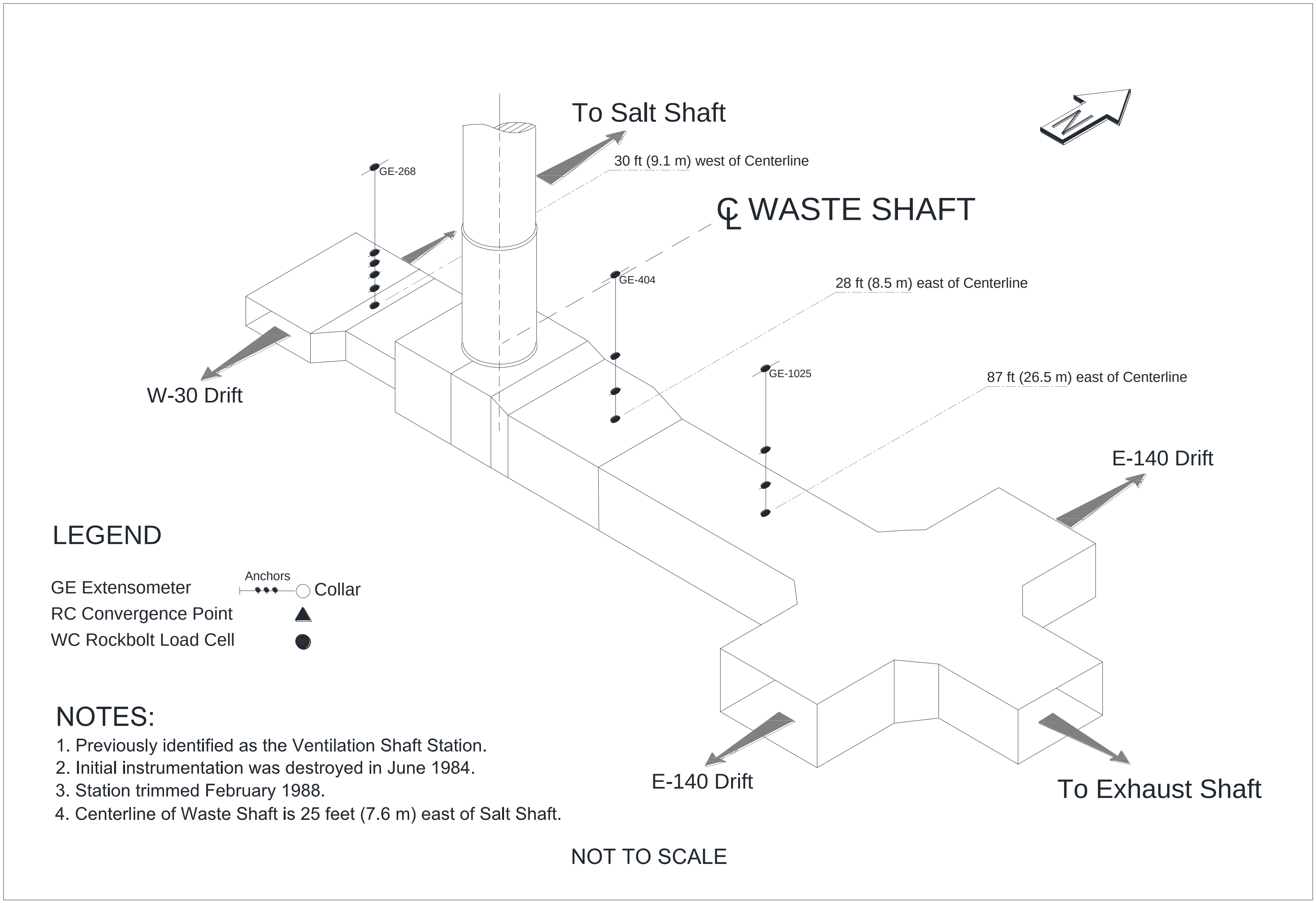

Figure 4-4 Waste Shaft Station Instrumentation after Roof Beam Excavation

4.3 Air Intake Shaft Station

The Air Intake Shaft Station was excavated in late 1987 and early 1988, using a continuous miner. The Air Intake Shaft is furnished with a work platform and a small cage that can be raised and lowered to perform routine ground maintenance. The principal purpose of that equipment is to provide emergency access.

4.3.1 Modifications to Excavation and Ground Control Activities

The Air Intake Shaft Station was not modified during this reporting period. Ground control activities were limited to routine maintenance.

4.3.2 Instrumentation

Radial convergence point and extensometer instrumentation data near the Air Intake Shaft Station are presented in Section 5.0 as part of the discussion on the performance of the access drifts. Twenty rock bolt load cells are installed in the Air Intake Shaft Station.

5.0 PERFORMANCE OF ACCESS DRIFTS

This section describes the geomechanical performance of the underground access drifts. The Waste Disposal Area is discussed in Section 6.0 and the Salt Disposal Investigation areas are discussed in Section 7.0. Four major north-south drifts in the WIPP underground are intersected by shorter east-west cross-drifts. Drift dimensions range from 13 ft (4 m) to 21 ft (6.4 m) high and from 14 ft (4.3 m) to 33 ft (9.2 m) wide.

5.1 Modifications to Excavation and Ground Control Activities

Floor trimming and rock bolting were performed during this reporting period, Table 5-1 summarizes these activities.

5.2 Instrumentation

This section discusses instrumentation details in the access drifts.

5.2.1 Extensometers

Seventeen extensometers continue to be monitored at various locations in the access drifts. Where displacement data were available, annual displacement rates were calculated (see Section 1.4.3) for each active installation and compared to the annual displacement rates from the previous reporting period.

Table 5-1 Summary of Modifications and Ground Control Activities in the Access Drifts July 1, 2015 to June 30, 2016

Location	Work Activity
SDI Lube Bay at S90	4-ft Mechanical Bolts and Chainlink Mesh on Ribs
E0 from N150 to N300	4-ft Mechanical Bolts and Chainlink Mesh on Ribs
E140-N1400 Miters	4-ft Mechanical Bolts and Chainlink Mesh on Ribs
W30 from S90 to S550	4-ft Mechanical Bolts and Chainlink Mesh on Ribs
E140 from N780 to N1100	4-ft Mechanical Bolts and Chainlink Mesh on Ribs
E140-S550	4-ft Mechanical Bolts and Chainlink Mesh on Ribs
N300 Drift from E0 to AIS	4-ft Mechanical Bolts and Chainlink Mesh on Ribs
E300 from S3310 to S3650	4-ft Mechanical Bolts Pinning Existing Mesh
E140-S550	4-ft Mechanical Bolts Pinning Existing Mesh
Panel 7, Room 1	14-ft Dywidag Roof Bolt Pattern
Panel 7, Room 2	14-ft Dywidag Roof Bolt Pattern
Panel 7, Room 3	14-ft Dywidag Roof Bolt Pattern
Panel 7, Room 5	14-ft Dywidag Roof Bolt Pattern
Panel 7, S2180 Drift	14-ft Dywidag Roof Bolt Pattern
Panel 7, S2520 Drift	14-ft Dywidag Roof Bolt Pattern
E300 from S2180 to S3650	14-ft Dywidag Roof Bolt Pattern
Mine Wide (Non CA)	14-ft Dywidag Roof Bolts Replacement
E0, E140, W30, W170	14-ft Dywidag Roof Bolts Replacement
All cross cuts included.	14-ft Dywidag Roof Bolts Replacement

Extensometer data are obtained by measuring the displacement from the reference head anchor (collar) to each fixed anchor of the extensometer. These measurements are scheduled to be made at least monthly throughout the WIPP underground.

Many of the E-140 extensometers indicate movement in the roof beam that may be attributed to shallow fracturing and the effects of anhydrite stringer separations in the roof. Lateral deformation in the roof beam may influence the extensometer readings, causing an increase in the measured displacement. Although the extensometer data indicate continued deformation and breakup of the lower beam, the roof bolt anchorage zone remains competent.

5.2.2 Convergence Points

Convergence point data are obtained by measuring the change in distance between fixed points anchored into the rock across an opening, either from rib to rib or from roof to floor. The measurement end-points constitute a "chord." Figure 5-1 shows typical convergence point array configurations along with typical chord designations.

Normally within this section a listing of the newly installed or reinstalled convergence points is available in Table 5-2. New and Replacement Convergence Points Installed in the Access Drifts July 1, 2015 through June 30, 2016. Under this reporting period there were no installation or reinstallation of convergence points due in part to no substantial floor trimming or new mining activities in the access drifts. Therefore, Table 5-2 is not being included this year.

Where possible, annual closure rates were calculated from convergence point array data gathered in the access drifts. Approximately 360 convergence points are located in the access drifts. A complete tabulation of these convergence point data and calculated closure rates is presented in the supporting data document for this report.

Locations with increases in annual vertical closure rates of greater than twenty percent are shown in Table 5-3.

Table 5-3 Vertical Closure Rate Changes in Excess of Twenty Percent in the Access Drifts

[WA-R4] Location	Chord[1]	Last Reading Date	Closure Rate 2015 to 2016 in/yr (cm/yr)	Closure Rate 2014 to 2015 in/yr (cm/yr)	Rate Percent Change
E300-S2916	A-C	05/24/16	13.0 (33.0)	2.3 (5.8)	465%
S90-W120	A-C	05/05/16	0.7 (1.8)	0.3 (0.8)	133%
E300-S1687	A-C	05/24/16	1.8 (4.6)	0.8 (2.0)	125%
S90-W620	A-C	05/10/16	0.9 (2.3)	0.4 (1.0)	125%
E140-S460	B-D	05/03/16	1.3 (3.3)	0.6 (1.5)	103%
N780-E70	A-C	11/17/15	1.7(4.3)	0.9(2.3)	89%
E300-N1100	A-C	04/06/16	2.8 (7.1)	1.6 (4.1)	75%
E300-S250	A-C	04/06/16	1.0 (2.5)	0.6 (1.5)	67%
N215-W620	A-C	04/06/16	1.0 (2.5)	0.6 (1.5)	67%
S90-W590	B-D	05/10/16	0.5 (1.3)	0.3 (0.8)	67%
E140-N1100	A-C	04/06/16	2.3 (5.8)	1.4 (3.6)	64%
S1000-E160	A-C	05/03/16	0.8 (2.0)	0.5 (1.3)	60%
W170-S850	B-D	02/04/16	0.8 (2.0)	0.5 (1.3)	60%
E0-N75	A-C	11/17/15	2.3(5.8)	1.5(3.8)	53%
E140-N1420	A-C	04/06/16	2.2 (5.6)	1.5 (3.8)	52%
CORE-W10	A-C	05/05/16	1.2 (3.0)	0.8 (2.0)	51%
CORE-W62	A-C	02/04/16	1.5 (3.8)	1.0 (2.5)	51%
W30-S1150	A-C	11/17/15	1.8(4.6)	1.2(3.0)	50%
S90-W120	A-C	05/05/16	0.6 (1.5)	0.4 (1.0)	50%
S90-W400	A-C	05/10/16	0.6 (1.5)	0.4 (1.0)	50%

Table 5-3 Vertical Closure Rate Changes in Excess of Twenty Percent in the Access Drifts (Continued)

[WA-R5] Location	Chord[1]	Last Reading Date	Closure Rate 2015 to 2016 in/yr (cm/yr)	Closure Rate 2014 to 2015 in/yr (cm/yr)	Rate Percent Change
S90-W590	A-C	5/10/16	0.6 (1.5)	0.4 (1.0)	50%
W170-S1150	C-G	05/05/16	1.2 (3.0)	0.8 (2.0)	50%
W170-S400	A-C	05/05/16	0.9 (2.3)	0.6 (1.5)	50%
E140-S1225	H-F	05/03/16	3.1 (7.9)	2.1 (5.3)	49%
CORE-W20	A-C	05/05/16	1.1 (2.8)	0.8 (2.0)	46%
E140-S1450	L-H	05/03/16	3.3 (8.4)	3.0 (7.6)	10%
W170-S1150	B-D	02/04/16	1.0 (2.5)	0.7 (1.8)	43%
E140-N1266	A-C	04/06/16	3.3 (8.4)	2.3 (5.8)	42%
CORE-W30	A-C	05/05/16	1.2 (3.0)	0.9 (2.3)	41%
N250-E220	B-D	01/08/16	2.1 (5.3)	1.5 (3.8)	40%

S90-W770	B-D	05/10/16	0.7 (1.8)	0.5 (1.3)	40%
W170-N150	A-C	05/05/16	0.7 (1.8)	0.5 (1.3)	40%
W170-S850	H-F	02/04/16	0.7 (1.8)	0.5 (1.3)	40%
W30-S2275	A-C	12/08/15	5.3 (13.5)	3.8 (9.7)	39%
E300-N1341	A-C	04/06/16	3.4 (8.6)	2.5 (6.4)	36%
N250-E220	H-F	04/06/16	1.9 (4.8)	1.4 (3.6)	36%
E300-S1450	A-C	05/24/16	2.3 (5.8)	1.7 (4.3)	35%
E140-N460	A-C	04/06/16	2.7 (6.9)	2.0 (5.1)	34%
E140-N150	A-C	04/06/16	2.1 (5.3)	1.6 (4.1)	33%
E140-N940	A-C	04/06/16	4.6 (11.7)	3.4 (8.6)	33%
E300-S850	A-E	05/24/16	0.8 (2.0)	0.6 (1.5)	33%
N215-W500	A-C	04/06/16	1.2 (3.0)	0.9 (2.3)	33%
N300-W170	A-C	04/06/16	1.6 (4.1)	1.2 (3.0)	33%
W170-S850	A-E	05/05/16	0.8 (2.0)	0.6 (1.5)	33%
E300-N170	H-F	04/06/16	2.1 (5.3)	1.6 (4.1)	31%
W170-S1000	A-C	05/05/16	1.3 (3.3)	1.0 (2.5)	30%
W30-S2750	A-C	06/02/16	4.8 (12.2)	3.7 (9.4)	30%
W170-S1150	H-F	11/03/15	0.9(2.3)	0.7(1.8)	29%
E0-N460	A-C	04/06/16	2.2 (5.6)	1.7 (4.3)	29%
E0-N780	A-C	04/06/16	2.1 (5.3)	1.6 (4.1)	29%
W170-S90	A-C	05/05/16	0.9 (2.3)	0.7 (1.8)	29%
E140-S1450/1456	A-G	05/03/16	5.0(12.7)	3.9 (9.9)	28%
E140-N355	A-C	04/06/16	2.9 (7.4)	2.3 (5.8)	27%
E300-N1262	A-C	04/06/16	3.4 (8.6)	2.7 (6.9)	26%

Table 5-3 Vertical Closure Rate Changes in Excess of Twenty Percent in the Access Drifts (Continued)

S3650-E55	A-C	06/02/16	4.4 (11.2)	3.5 (8.9)	26%
E300-N170	A-E	04/06/16	2.5 (6.4)	2.0 (5.1)	25%
E300-S45	H-F	04/06/16	1.5 (3.8)	1.2 (3.0)	25%
E300-S90	A-C	04/06/16	1.5 (3.8)	1.2 (3.0)	25%
E300-S1000	A-C	05/24/16	1.0 (2.5)	0.8 (2.0)	25%
E300-S3480	A-C	04/05/16	3.5 (8.9)	2.8 (7.1)	25%
S3650-W100	A-C	06/02/16	3.5 (8.9)	2.8 (7.1)	25%
W170-S1150	A-E	05/05/16	1.0 (2.5)	0.8 (2.0)	25%
W170-S3565	A-C	06/02/16	3.0 (7.6)	2.4 (6.1)	25%
W30-S1950	A-C	05/03/16	3.5 (8.9)	2.8 (7.1)	25%
CORE-W51	A-C	05/05/16	1.4 (3.6)	1.1 (2.8)	23%
N250-E220	A-E	04/06/16	3.2 (8.1)	2.6 (6.6)	23%
E300-N45	A-E	04/06/16	2.2 (5.6)	1.8 (4.6)	22%

S1600-E110	A-C	05/03/16	1.1 (2.8)	0.9 (2.3)	22%
W170-S700	A-C	05/05/16	1.1 (2.8)	0.9 (2.3)	22%
W30-S250	A-C	05/03/16	1.1 (2.8)	0.9 (2.3)	22%
W30-S500	A-C	05/03/16	1.1 (2.8)	0.9 (2.3)	22%
W30-S850	B-D	05/03/16	1.1 (2.8)	0.9 (2.3)	22%
E140-S262	A-C	05/03/16	1.8 (4.6)	1.5 (3.8)	21%
E140-S700	E-F	05/03/16	1.5 (3.8)	1.2 (3.0)	21%
E300-S45	A-E	04/06/16	1.7 (4.3)	1.4 (3.6)	21%

[1] Chord is defined in Section 5.2.2.

5.3 Analysis of Convergence Point and Extensometer Data

Vertical loading on mine pillars results in lateral stresses on the roof and floor beams. The composition of those beams, in part, determines how these structures will react to the horizontal stresses. In particular, horizontally continuous anhydrite stringers (see Section 2.2.2) divide the beam itself into a series of smaller independent beams.

Lateral strain on the beam imposed by vertical loading on the pillars is accommodated by vertical displacement over the mined opening. This requires that the horizontally oriented beam separate along the most favorable, or weakest, planes.

Where anhydrite stringers interpose the beam, they constitute a plane of weakness, and delamination occurs. The material is confined in the plane above, so that the roof accommodates the lateral strain by bending convex into the mined opening.

Two distinct results come of this action. First, voids form within the beam as the portions closer to the opening move away from those deeper within the beam. Second, the convex portion of the bended plane is subjected to tensile loading perpendicular to the axis of the drift and superficial tears known as "tensile fractures" develop generally parallel to the axis of the drift.

Where anhydrite stringers are small and discontinuous or not present at all within the beam, horizontal loading is accommodated along shear planes. These develop at angles of approximately 35 degrees with respect to the horizontal. In some cases, a plane develops preferentially on one side of the drift, and the bulk of material is pushed into the mined opening on that side. This may be thought of as a cantilevered beam.

Whatever the mechanism; vertical displacement into the mined opening is measured by convergence monitoring. Convergence points consider the displacement between two opposing surfaces: either the roof and floor or the two ribs. Extensometers consider the displacement between one surface (usually the back) and one or more points within the beam. Where a convergence point and an extensometer are adjacent to one another, it is possible to determine the individual displacements of both floor and roof beams.

This data is used to analyze the stability and mechanics of the beam, and in determining what actions may be taken to ensure the safety of personnel and equipment consistent with the safe operation of the facility.

5.4 Excavation Performance

Approximately 330 readings are collected and assessed regularly from convergence point arrays throughout the WIPP underground. Due to the affect rock temperature has on salt creep, convergence rates vary seasonally, typically increasing during the warmer summer months and decreasing during the cooler and drier winter months. These temperature affects are more pronounced nearer the fresh air intake.

The performance of the access drift excavations during this reporting period was within acceptable criteria. "Acceptable criteria" means that a drift remains accessible, and the ground can be controlled by routine maintenance. Standard remedial ground control in some areas was required to maintain the performance of the excavations. The accessible drifts remain stable and controlled. Most of the annualized rates remain steady, indicating stability. Of the 250 convergence locations measured in the access drifts only 71 locations (28%) had annual closure rates in excess of 20% from the previous year's value. Of those 71 locations the average closure rate was 1.9 inches/year and the average change in rate between consecutive years was 0.5 inch/year.

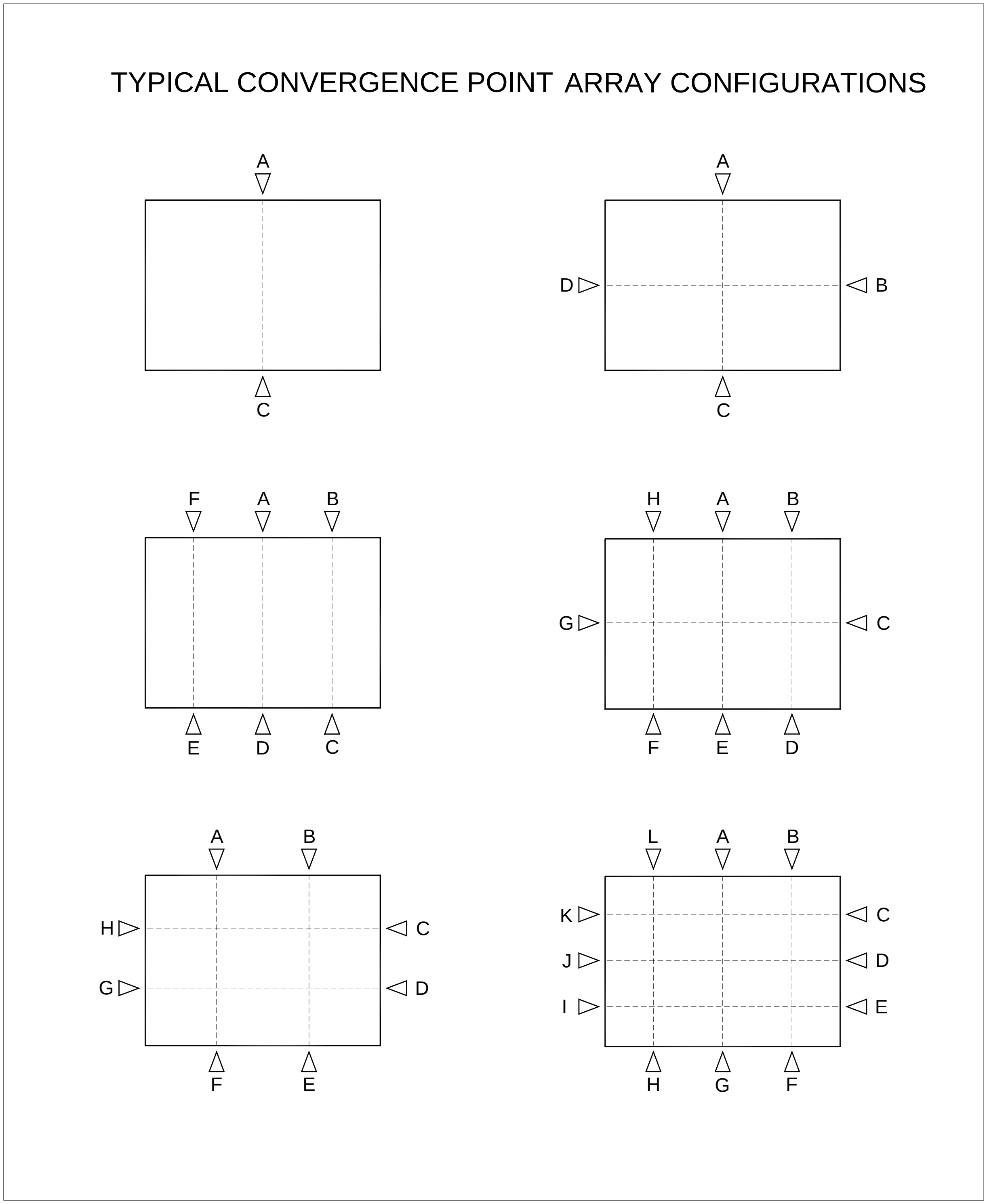

Figure 5-1 Typical Convergence Point Array Configurations Showing Anchor Designations

6.0 PERFORMANCE OF THE WASTE DISPOSAL AREA

The Waste Disposal Area as of June 30, 2016, consisted of Panels 1, 2, 3, 4, 5, 6, 7 and a partially mined Panel 8. Panels 1, 2, 3, 4, 5 and 6 were closed during previous reporting periods.

6.1 History

Excavation of Panel 1 began in May 1986 with the mining of the access entries. Initially, the disposal rooms and drifts were developed as pilot drifts that were later excavated to nominal operational dimensions of 13 ft (4 m) high, 33 ft (10 m) wide, and 300 ft (91 m) long. Room 1 was completed to these dimensions in August 1986, and pilot drifts for Rooms 2 and 3 were excavated in January and February 1987. Rooms 2 and 3 were completed in February and March 1988, and Rooms 4 through 7 were completed in May 1988. Four short access drifts designed to lead to smaller test alcoves were excavated north off the S-1600 drift and Rooms 4-7 in June 1989. Only the access drifts to the alcoves were completed; the alcoves themselves were not excavated. Panel 1 waste emplacement (in Rooms 1, 2, 3, 7, adjacent areas of S 1600, and all of S-1950) was completed during a prior reporting period, and the panel is closed to all access. The Panel 1 access entries, S-1600 and S-1950, which extend from the E-300 drift to the isolation walls, remain open, and the instrumentation in this area continues to be maintained and monitored.

Excavation of the Panel 2 Waste Disposal Area began in September 1999 with the mining of access entries. Initially, the disposal rooms and drifts were developed as pilot drifts that were trimmed to finished dimensions. Room 1 was completed in January 2000, and pilot drifts for Rooms 2 and 3 were excavated in February 2000. Pilot drifts were completed for Rooms 4 through 6 in April 2000. The pilot drift for Room 7 was excavated in May 2000. All the rooms were excavated to final dimensions by August 2000. Waste emplacement in Panel 2 was completed during a prior reporting period, and the panel is closed to all access. The Panel 2 access entries, S-2150 and S-2520, which extend from the E-300 drift to the isolation walls, remain open, and the instrumentation in this area continues to be maintained and monitored.

Excavation of Panel 3 waste disposal rooms began in May 2002 with the mining of access entries to Panel 3. As with Panel 2, initially, the disposal rooms and drifts were developed as pilot drifts that were trimmed to finished dimensions. All the rooms were excavated to final dimensions by the end of March 2004. Waste emplacement in Panel 3 was completed in February 2007. Substantial barriers and bulkheads were installed in the exhaust and intake drifts of Panel 3 to prevent access into the panel and to isolate it from the ventilation circuit.

Panel 4 access drift mining began in January 2005. The disposal rooms were initially developed as pilot drifts and were later trimmed to final dimensions. Mining was completed by June 2006. Waste emplacement in Panel 4 was completed in March

2009. Substantial barriers and bulkheads were installed in the exhaust and intake drifts of Panel 4 to prevent access into the panel and to isolate it from the ventilation circuit.

Panel 5 excavation activities began in June 2006. The panel was initially mined to less-than-final dimensions and later trimmed to specification. Mining was complete by February 2008. Waste emplacement was conducted from March 2009 through July 2011. Isolation walls were completed in November 2011. Instrumentation and regular observations will continue in the accessible area up to the isolation walls.

Panel 6 mining began in April 2008. The panel was initially mined to less- than-final dimensions and later trimmed to specification. Mining was complete by April 2010. Waste emplacement began in March of 2011 and was completed in January of 2014.

Panel 7 mining began in April of 2010 and was completed in August of 2011. Initial mining placed the floor within two feet of a polyhalitic halite bed (designated PH-4) which sits atop a thick anhydrite bed designated MB-139. Horizontal stresses caused significant uplift and the floor was then mined down through MB-139 and backfilled with run of mine salt. The remediation of the floor was completed in January of 2013. Subsequent geomechanical monitoring indicates stable vertical convergence. RH waste emplacement began in Panel 7 in September 2013 and CH waste emplacement began in January 2014.

6.2 Modifications to Excavations and Ground Control Activities

Ground control activities were severely restricted during this reporting period primarily due to the consequences of the radioactive release. One limitation was the additional personal protective equipment (PPE) that is required to be worn in a contaminated area. Another limitation is the reduced ventilation due to the requirement to filter the exhaust air leaving the mine. The reduced ventilation limited the number of diesel-powered equipment that could be ran simultaneously. Broken rock bolt replacement was being performed on a priority basis; E140, southern E300, the south main drifts (Panel 9) and Panel 7. The south mains proved to be too large of an effort to properly maintain and the decision was made to close the mains at S2750. This allowed pattern bolting to be concentrated on Panel 7 and broken bolt replacement to occur at other essential areas. Areas of Panel 7 have been placed under restricted access until pattern rock bolting can occur.

In January 2015 a rock fall a small rock fall was discovered in the access drift into Panel 3 (S2750 east of E300). A large rock had fallen through a gap in the chainlink mesh. The mesh was in the process of being supported by rock bolts at the time of the fire and the release. Subsequent small rock falls have also occurred in this area.

A rock fall occurred in the access drift into Panel 4. The fall was discovered on September 27, 2016. The area had been restricted due to numerous rock bolt plate failures.

During this reporting period the Mine Safety and Health Administration (MSHA) issued approximately 30 citations for ground control issues. Almost all were related to a lack of ground control maintenance. Ground control maintenance and many other WIPP operations functions were significantly impacted by the release. However, none of the areas under the MSHA citations actually had instability as indicated by either the geomechanical data or physical observations conducted by the geotechnical group.

6.3 Instrumentation

Panel 7 instrumentation consists of the following:

- Forty-nine vertical convergence points, distributed as fourteen each in the intake and exhaust drifts and three in each of the rooms; and
- Eleven wire extensometers, distributed as two in each of the intake and exhaust drifts and one in each of the rooms.

A schematic of the geomechanical instrumentation layout found in Panel 7 is shown in Figure 6-1.

Due to the fire and the radiological release, convergence measurements were not taken in Panel 7 between January 29, 2014 and February 1, 2015. However, the remote monitoring of the extensometers in Panel 7 continued on a weekly basis.

6.4 Excavation Performance

Waste handling activities in Panels 1-6 have been completed, and geomechanical monitoring inside these panels has been discontinued.

Horizontal and vertical convergence rates, calculated at the center of each of the rooms, in Panel 7 were compared between this and the previous reporting period. All seven rooms in the panel experienced increases in their rates of closure from the previous reporting period.

6.5 Analysis of Extensometer and Convergence Point Data

Geomechanical instrumentation is installed in each disposal room and at select locations in the panel access drifts. As anticipated, these installations show a general increase in room closure rate and roof beam deformation with time. Overall, the panel is experiencing age-appropriate roof beam deformation for a panel that is without a full complement of rock bolts. A reduction in the rates of roof beam deformation will occur once the rooms are pattern bolted.

Although Panels 1 through 6 are closed, convergence monitoring continues in the panel entries between E-300 and the explosion isolation walls (Panels 1 and 2), and the substantial and isolation barriers (Panels 3 and 4) as well as, between W170 and the explosion isolation wall (Panel 5). As of the end of the reporting period the isolation of

Panel 6 had not been completed. Monitoring has been discontinued in the Panel 4 intake drift (S3650) which is closed to access due to elevated volatile organic compound (VOC) levels and at S2750 (Panel 3 exhaust drift) due to ground conditions. Monitoring data indicate generally steady long term trends. Incidences of short term acceleration are largely attributed to creep deformation of the pillars, which results in increasing lateral loading of the roof beam and the growth of separations along anhydrite stringers.

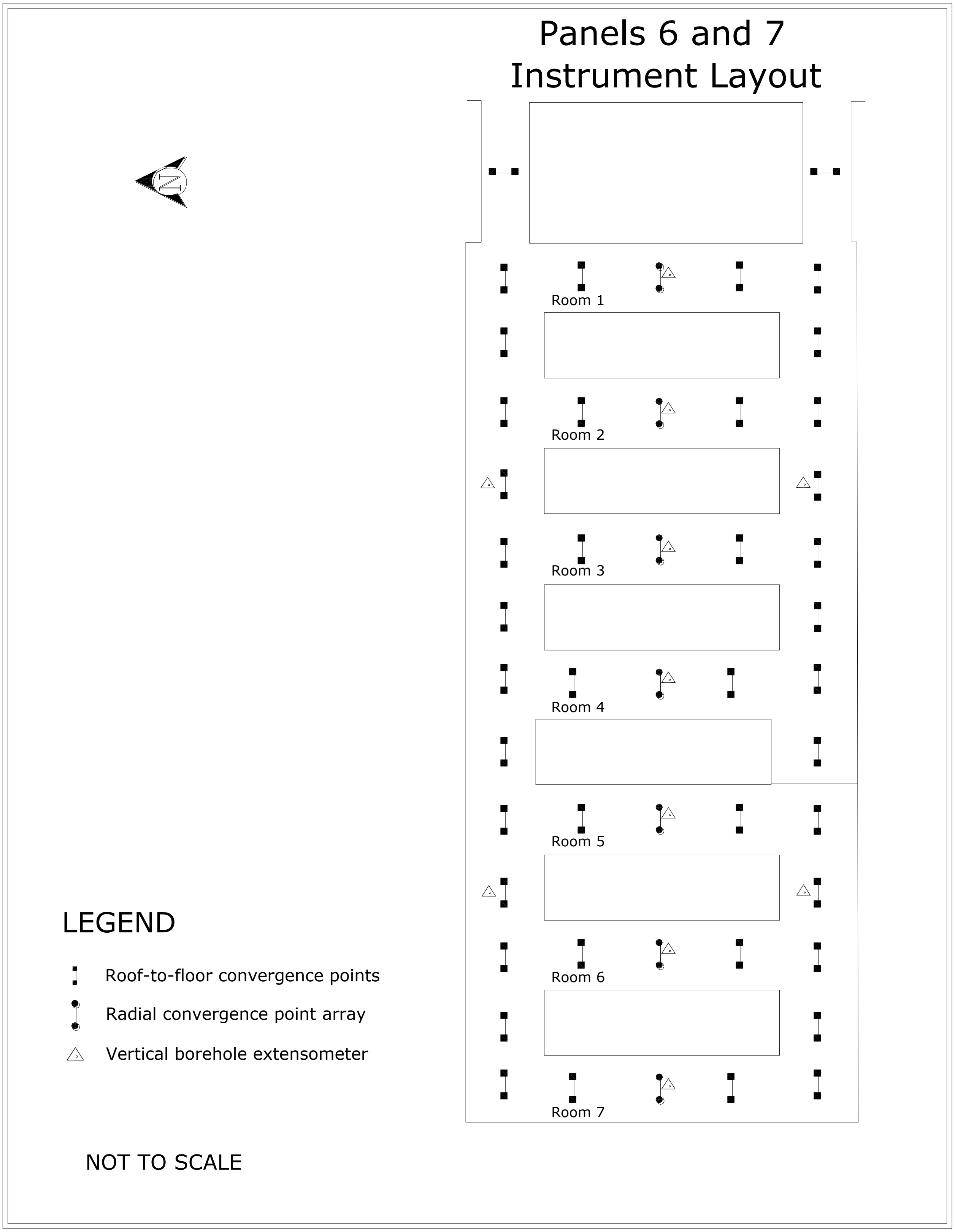

Figure 6-1 Location of Geomechanical Instruments in Panels 6 and 7

7.0 PERFORMANCE OF THE SALT DISPOSAL INVESTIGATIONS AND SALT DEFENSE DISPOSAL INVESTIGATIONS

This chapter describes the geomechanical performance of the Salt Disposal Investigation (SDI) and SDDI areas (hereafter referred to as SDI). Development of the area began in January 2012. When completed, most of the area will have nominal dimensions of 13 feet high and 16 feet wide.

7.1 Ground Control Program

Due to the relatively narrow drifts (nominally 16 feet across) and favorable mining horizon, ground control plans in the SDI area are confined to routine maintenance such as spot-bolting where localized drummy surface features develop. More substantial engineered ground control systems may be applied in the event that ongoing geomechanical monitoring and analysis of the area identify a need.

7.2 Instrumentation

Forty-nine convergence arrays have been installed in the SDI area. The arrays are read on a periodic basis.

7.3 Analysis of Convergence Point Data

As a rule, the area behaves as expected, with relatively high initial rates rapidly decreasing as the stresses redistribute to load the surrounding salt pillars.

7.4 Excavation Performance

One object of the SDI project is to observe the behavior of the salt in response to high heat sources emplaced within the mined openings. It is expected that the performance of these areas, in particular those nearest the experimental heat sources, will exhibit rapid creep movement. However, a comparison between the rates of closure between this reporting period and the previous reporting period show that every measured location in SDI shows a reduction in the rate of roof to floor closure. This is to be expected as the reduction in the higher initial strain following excavation has been realized and the excavations are settling into the steady state phase of salt creep.

8.0 GEOSCIENCE PROGRAM

The activities of the geoscience program were not performed during the July 1, 2015 – June 30, 2016 reporting period primarily due to logistical problems associated with the radiological release, e.g., reduced ventilation minimized diesel equipment operation and the unavailability of non-diesel equipment in Panel 7. A description of the various aspects of the geoscience program is presented in the remainder of Section 8.0.

The Geoscience Program confirms the suitability of the site through the collection of various geologic data and excavation characteristics from the underground. These include the inspection of open observation holes for fractures (separations) and offsets (lateral displacements) in roof beams and the mapping of fracture development on roof surfaces. Data collected through these activities support the design and evaluation of ground support systems.

Normally, the following activities are performed:

- Observation hole inspections
- Fracture mapping
- Stratigraphic Mapping
- Drilling and Geologic Core Descriptions

Fracture development in the roof is primarily caused by the concentration of compressive stresses in the roof beam and is influenced by the size and shape of the excavation and the stratigraphy in the immediate vicinity of the opening. In a thick roof beam, pillar deformations induce lateral compressive stresses into the immediate roof and floor. With time, the buildup of stress causes differential movement along stratigraphic boundaries. This differential movement is identified as offsets in observation holes and by the bends in failed rock bolts. Large strains associated with lateral movements can induce fracturing in the roof, which is frequently seen near the ribs; however, this process may take a long time (years) to develop.

At the upper repository horizon, clay or anhydrite stringers exert significant influence over the effective thickness of the roof beam. The presence of these stringers causes the roof beam to behave as a series of thin independent beams. Little or no tensile support is provided across the stringer interface. As horizontal end-loading continues, each beam can deflect downward causing a tensile fracture to develop along the bottom of the beam. These tensile fractures can develop in relatively new excavations soon after separation occurs along the stringer interface.

8.1 Observation Hole Inspections

Geotechnical observation holes are drilled at various locations throughout the underground facility. A location may contain one or more holes arranged in an array. These holes are drilled to depths that allow the monitoring of fracture development and offsetting and are inspected for the development of those features. Roof observation holes usually extend up past clays G and H (Figure 8-1 and Figure 8-2).

The clay seams nearest the excavation surfaces define the immediate roof beam. The roof beam is bounded by Clay G in most of the access drifts and Panels 1, 2, 7 and 8. Some areas, such as the Salt Shaft Station, portions of the E-0 and E-140 drifts, the south mains south of S-2620, and Panels 3, 4, 5, and 6 are excavated to Clay G and so have roof beams bounded by Clay H.

The offset in an observation hole is determined by visually estimating the degree of occlusion. The direction of offset along clay seams is observed as the movement of the strata nearer to the observer relative to the strata farther away. Typically, the nearer strata move toward the center of the excavation (Figure 8-3 and Figure 8-4). Based on previous observations in the underground, the magnitude of offset is usually greater in holes located near ribs than in those located along excavation centerlines. Offsetting along the clay layers is observable until total offset is reached or visibility is obstructed by intervening offsets at other clay seams or fractures.

Observation holes are inspected for fractures, using an aluminum rod with a flattened steel wire probe attached to one end perpendicular to the rod (referred to as a "scratch rod"). Fractures and clay seams are located by moving the probe along the inside of the hole until it is snagged in one of these features. Depth to each feature is recorded, as is the magnitude of separations encountered. A fiber scope camera is available for use in addition to the scratch rod to visually document features of interest in a hole.

A list of new holes drilled between July, 1 2015 and June 30, 2016 are presented in Table 8-1. In addition, a record of the boreholes scratched during the reporting period is presented in Table 8-2.

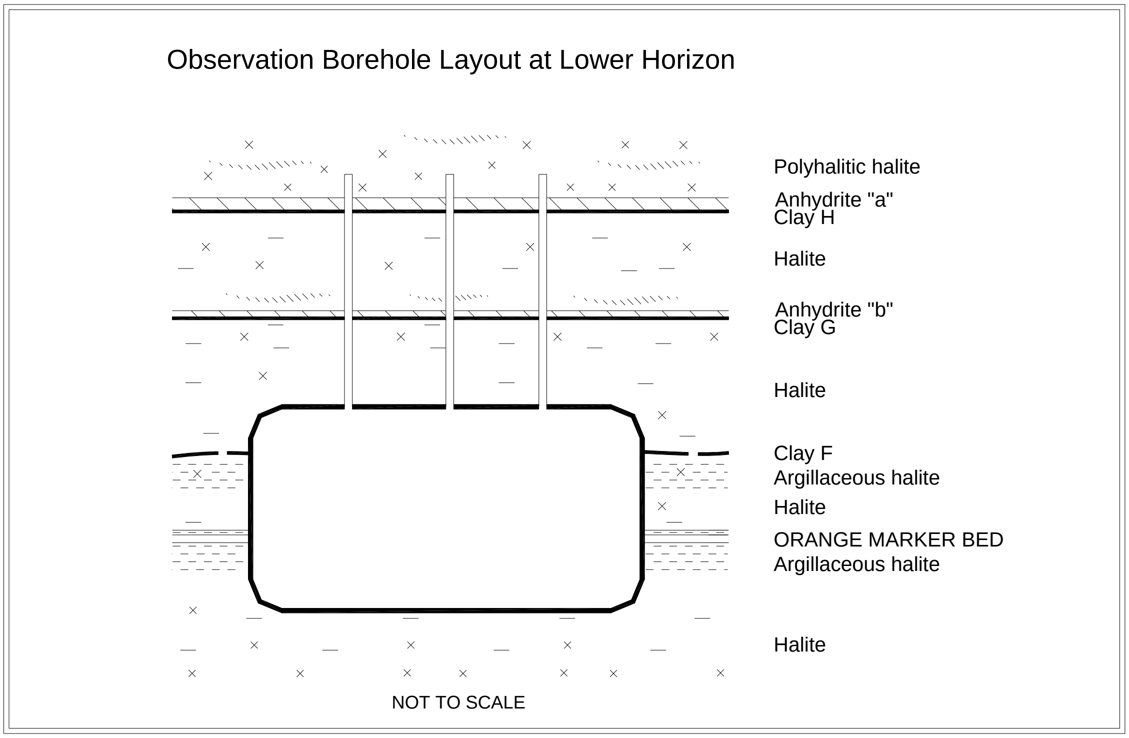

Figure 8-1 Example of Observation Hole Layout at Lower Horizon

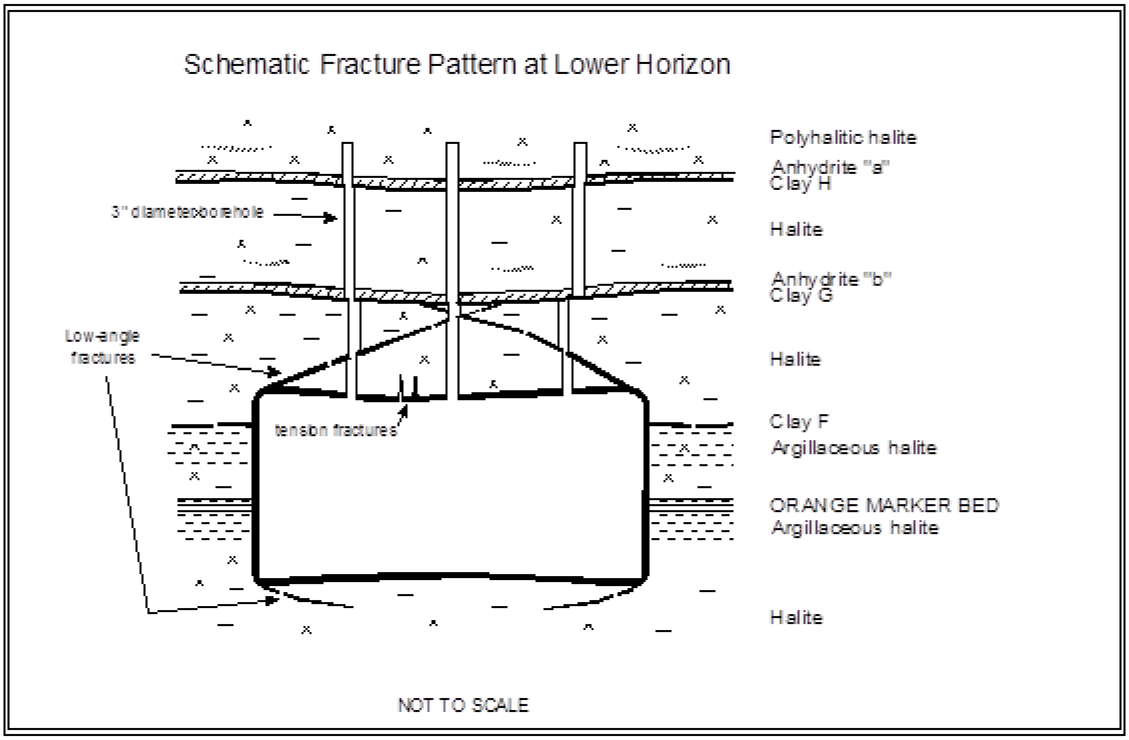

Figure 8-2 Typical Fracture Pattern at Lower Horizon

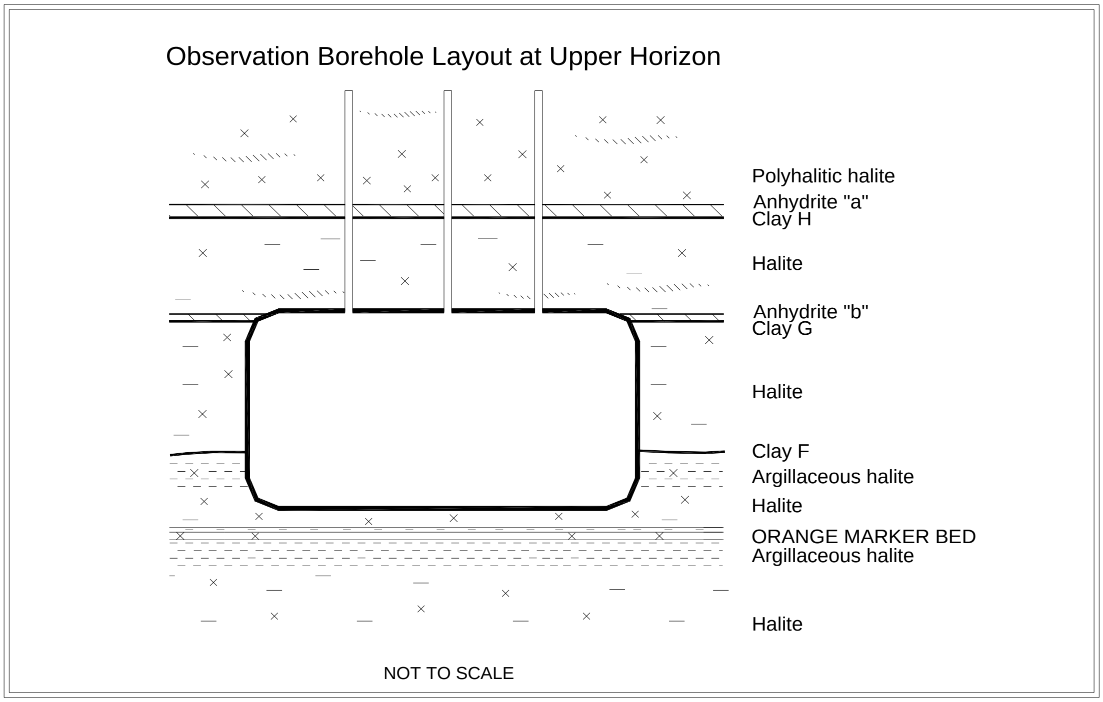

Figure 8-3 Example Observation Hole Layout at Upper Horizon

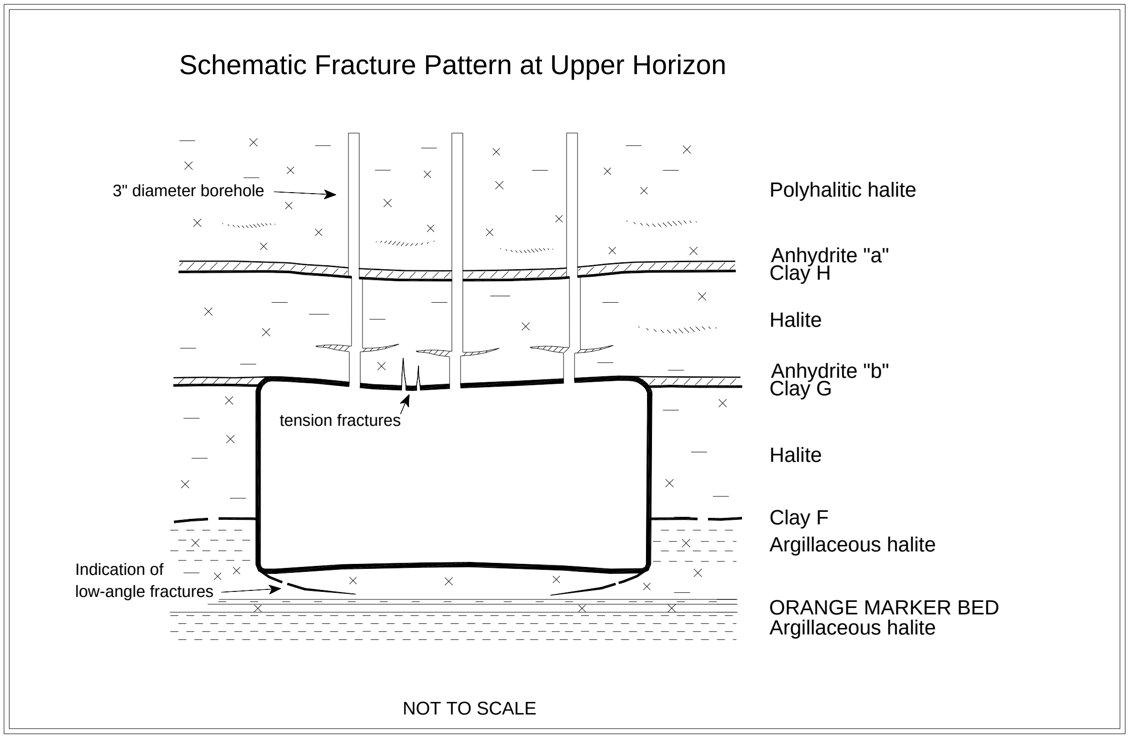

Figure 8-4 Typical Fracture Patterns at Upper Horizon

8.2 Fracture Mapping

Routine mapping documents the progression of fractures in the roof exposed on the excavation surfaces of the drifts and rooms in the underground repository. The fracture surveys are generally performed on an annual basis, and the fracture maps are updated. The fracture maps facilitate the analysis of strain in the immediate roof-beam, because they document the development and propagation of fractures through time.

8.3 Stratigraphic Mapping

Stratigraphic mapping is the identification and partitioning of the sequence of rock strata based on their form, distribution, and lithologic composition. It is used to verify that there are no nonconformities in the geology within the waste disposal horizon at WIPP.

8.4 Drilling and Geologic Core Descriptions

As new panels and new experimental areas are excavated, holes are typically drilled and cored vertically into the back and into the floor to depths of 50 feet to identify and describe the stratigraphic units present.

9.0 SUMMARY

At the inception of WIPP, criteria were developed that address the design requirements (DOE, 1984). They pertained to all aspects of the mined facility and its operation as a pilot plant for the demonstration of technical and operational methods for permanent disposal of contact-handled and remote-handled TRU waste. In 1994, as the WIPP focus moved toward the permanent disposal of TRU waste, these design requirements were reassessed and replaced by a new set of requirements called system design descriptions. Table 9-1 shows the comparison of these design requirements with conditions actually observed in the underground from July 2015 through June 2016.

Replacement of failed rock bolts was performed at various locations during this reporting period. The pre-release pace of bolt replacement could not be met due to the additional PPE and the reduction in ventilation. This resulted in some areas being placed under restricted access or prohibited access until ground maintenance could be performed. Some areas, while awaiting rock bolting, experienced rock falls.

The *in situ* performance of the accessible, bolted, excavations generally continues to satisfy the appropriate design criteria. The return to routine maintenance of ground control systems was not achieved during this reporting period. Future changes to the planned life of some of the openings may require a change to the geometry of the access drifts (removing unstable roof beam or rib spalls, or milling the floor for added clearance), or the addition of ground control (roof removal, installing bolts, mesh, or straps).

In addition to underground instrumentation, qualitative assessments of fracture development are documented through mapping the underground repository and inspecting the observation holes. Although, as indicated in Section 8.0, no significant geoscience activities occurred during the current reporting period the accumulation of many years of collected information acquired from these programs contributes to the understanding of the dynamic geomechanical processes in the WIPP underground. This aids in the design of effective ground control and support systems.

Table 9-1 Comparison of Excavation Performance to System Design Requirements

Requirement	Comments
"The lining shall be designed for a hydrostatic pressure. . . ."	Water pressure observed on piezometers located behind the shaft liners remains below design levels.
"The key shall be designed to resist the lateral pressure generated by salt creep."	Visual inspections of all shaft keys do not indicate any deterioration due to creep loading.
"The key shall be designed to retain the rock formation and will be provided with chemical seal rings and a water collection ring with drains to prevent water from flowing down the unlined shaft from the lining above."	Shaft inspection observations show no indication of instability due to salt dissolution. No water has been observed flowing along the rock-liner interface.
"The underground waste disposal facilities shall be designed to provide space and adequate access for the underground equipment and temporary storage space to support underground operations."	Geomechanical instrument data and visual observations indicate that the current design provides adequate access and storage and disposal space. Ground control maintenance is performed as necessary to maintain access. If ground control activities cannot be performed in a timely manner and the geomechanical data suggest potential instability, access to the drift is to be restricted or even prohibited until ground remediation can occur.
"Entries and subentries to the underground disposal area and the experimental areas shall be provided and sized for personnel safety, adequate air flow, and space for equipment."	Deformation of excavation remains within the required limits. Normal periodic maintenance consisting of rock bolting, wire meshing, trimming, and scaling continue throughout accessible areas of the repository. Areas such as the waste transport route undergo periodic floor trims in order to maintain adequate operating height.
"Geomechanical instrumentation shall be provided to measure the cumulative deformation of the rock mass surrounding mined drifts. . . ."	Geomechanical instrumentation is operated and maintained to meet this requirement. This annual report provides a summary and analysis of the geomechanical data.

10.0 REFERENCES

ASTM, 2006, D6026-06, *Standard Practice for Using Significant Digits in Geotechnical Data*.

Public Law 96-164, *Department of Energy National Security and Military Applications of Nuclear Energy Authorization Act of 1980*.

Title 40 CFR Part 191, "Environmental Radiation Protection Standards for Management and Disposal of Spent Nuclear Fuel, High-Level and Transuranic Radioactive Wastes."

Title 40 CFR Part 194, "Criteria for the Certification and Re-certification of the Waste Isolation Pilot Plant's Compliance with the 40 CFR Part 191 Disposal Regulations."

U.S. Environmental Protection Agency, 1998, "Criteria for the Certification and Recertification of the Waste Isolation Pilot Plant's Compliance with the Disposal Regulations: Certification Decision," Federal Register, Vol. 63, No. 95, pp. 27354, May 18, 1998, Washington, DC

Holt, R. M., and D. W. Powers, 1990, *Geologic Mapping of the Air Intake Shaft at the Waste Isolation Pilot Plant*, DOE/WIPP 90-051, Waste Isolation Pilot Plant, Carlsbad, New Mexico.

Holt, R. M., and D. W. Powers, 1984, *Geotechnical Activities in the Waste Handling Shaft, Waste Isolation Pilot Plant (WIPP) Project, Southeastern New Mexico*, WTSD TME 038, Waste Isolation Pilot Plant, Carlsbad, New Mexico.

New Mexico Environment Department (NMED), 2016, Waste Isolation Pilot Plant Hazardous Waste Facility Permit, NM4890139088-TSDF, Santa Fe, New Mexico.

Powers, D. W., and R. M. Holt, 1993, *The Upper Cenozoic Gatuña Formation of Southeastern New Mexico, New Mexico Geological Society Guidebook*, 44th Field Conference, Carlsbad Region, New Mexico and West Texas, D. W. Love et al., Eds., pp 271-282.

Powers, D. W., and R. M. Holt, 1995, *Gatuña Formation (Miocene to Pleistocene) Geology and Paleohydrology*, prepared for Westinghouse Waste Isolation Division by International Technology Corporation, Albuquerque, New Mexico.

Powers, D. W., S. J. Lambert, S. E. Shaffer, L. R. Hill, and W. D. Weart, Eds.,1978, *Geological Characterization Report, Waste Isolation Pilot Plant (WIPP) Site, Southeastern New Mexico, Vols. I and II*, SAND 78 1596; Sandia National Laboratories, Albuquerque, New Mexico.

U.S. Department of Energy (DOE), 2000, *Brine Generation Study, DOE/WIPP 00-2000, Waste Isolation Pilot Plant*, Carlsbad, New Mexico.

U.S. Department of Energy (DOE), 1986a, *Interim Geotechnical Field Data Report, DOE/WIPP 86-012*, Waste Isolation Pilot Plant, Carlsbad, New Mexico.

U.S. Department of Energy (DOE), 1986b, *Waste Isolation Pilot Plant Design Validation Final Report*, DOE/WIPP 86-010; Prepared by Bechtel National, Inc., for the U.S. Department of Energy, San Francisco, California.

U.S. Department of Energy (DOE), 1986c, *Geotechnical Activities in the Exhaust Shaft*, DOE/WIPP 86-008, Waste Isolation Pilot Plant, Carlsbad, New Mexico.

U.S. Department of Energy (DOE), 1985, *Quarterly Geotechnical Field Data Report*, DOE/WIPP-221, Waste Isolation Pilot Plant, Carlsbad, New Mexico.

U.S. Department of Energy (DOE), 1984, *Design Criteria, Waste Isolation Pilot Plant (WIPP) Revised Mission Concept-IIA*, DOE/WIPP-071; Waste Isolation Pilot Plant, Carlsbad, New Mexico.

U.S. Department of Energy (DOE), 1983, *Summary of the Results of the Evaluation of the WIPP Site and Preliminary Design Validation Program*, DOE/WIPP-161; Waste Isolation Pilot Plant, Carlsbad, New Mexico.

ISSUED

DOE/WIPP-17-3560
Volume 2

Waste Isolation Pilot Plant

Geotechnical Analysis Report For July 2015 – June 2016

Supporting Data

U.S. Department of Energy

October 2017

This page was intentionally left blank.

This document has been submitted as required to:

U.S. Department of Energy
Office of Scientific and Technical Information
PO Box 62
Oak Ridge, TN 37831
(865) 576-8401

Additional information about this document may be obtained by calling 1-800-336-9477

Unlimited, publicly available full-text scientific and technical reports produced since 1991 are available online at Information Bridge (www.osti.gov/bridge).

U.S Department of Energy and its contractors may obtain full-text reports produced prior to 1991 in paper form for a processing fee from:

U.S. Department of Energy
Office of Scientific and Technical Information
P.O. Box 62
Oak Ridge, TN 37831-0062
Telephone: (865) 576-8401
Facsimile: (865) 576-5728
E-mail: reports@osti.gov

Available for sale to the public from:

U.S. Department of Commerce
National Technical Information Service
5301 Shawnee Rd
Alexandra, VA 22312
Phone: (800) 553-6847 or (703) 605-6000
Fax: (703) 605-6900
Email: info@ntis.gov

This page was intentionally left blank.

FOREWORD AND ACKNOWLEDGMENTS

This report contains an assessment of the geotechnical status of the Waste Isolation Pilot Plant (WIPP). During the excavation of the principal underground access and experimental areas, the status was reported quarterly. Since 1987, when the initial construction phase was completed, reports have been published annually. This report presents and analyzes data collected from July 1, 2015, to June 30, 2016.

This Geotechnical Analysis Report (GAR) was written to meet the needs of several audiences. It satisfies requirements contained in the WIPP Hazardous Waste Facility Permit[1] (HWFP) and the Certification of Compliance[2] with Subparts B and C, Title 40 *Code of Federal Regulations* (CFR) Part 191, "Environmental Radiation Protection Standards for Management and Disposal of Spent Nuclear Fuel, High-Level and Transuranic Radioactive Wastes." It focuses on the geotechnical performance of the various components of the underground facility, including the shafts, shaft stations, access drifts, and waste disposal areas. The results of investigations of excavation effects and other geotechnical studies are also included.

The report compares the geotechnical performance of the repository to the design criteria. It describes the techniques that were used to acquire the data. The depth and breadth of the evaluation of the different components of the underground facility vary according to the types and quantities of data available and the complexity of the recorded geotechnical responses. Graphic documentation of data and tabular documentation of instrument history can be provided upon request.

This GAR was prepared by Nuclear Waste Partnership LLC (NWP) for the U.S. Department of Energy (DOE), Carlsbad Field Office (CBFO), in Carlsbad, New Mexico. Work was supported by the DOE under Contract No. DE-EM0001971.

[1] New Mexico Environment Department (NMED), 2016, Waste Isolation Pilot Plant Hazardous Waste Facility Permit, NM4890139088-TSDF, Santa Fe, NM

[2] U.S. Environmental Protection Agency, 1998, "Criteria for the Certification and Recertification of the Waste Isolation Pilot Plant's Compliance with the Disposal Regulations: Certification Decision," Federal Register, Vol. 63, No. 95, pp. 27354, May 18, 1998, Washington, DC

This page was intentionally left blank.

Table of Contents

List of Tables

List of Figures

Salt Handling Shaft and Key

Salt Handling Shaft Station

Waste Shaft Station

Air Intake Shaft Station

Access Drifts

Waste Disposal Areas

Waste Disposal Area Panel 1

Waste Disposal Area Panel 2

Waste Disposal Area Panel 5

Waste Disposal Area Panel 6

Waste Disposal Area Panel 7

Waste Disposal Area Panel 8

Salt Disposal Investigations

1.0 Introduction

This report is a compilation of geotechnical data presented as plots for each active instrument installed in the underground at the Waste Isolation Pilot Plant (WIPP) through June 30, 2016. A summary of the geotechnical analyses that were performed using the enclosed data is provided in Volume 1 of the Geotechnical Analysis Report (GAR).

1.1 Instrumentation

Geomechanical instrument data included in this report reflect the measurements of the geomechanical response of the underground. The instruments consist of convergence points, borehole extensometers, rockbolt load cells, pressure cells, strain gages, piezometers, and joint meters.

Closure measurements are taken at convergence points. Rock displacement is calculated by measuring the distance between two opposing points. Displacement is monitored over time and is plotted as closure versus time. Annual rates of closure are calculated for the convergence data and are compared with annual closure rates from previous reporting periods.

Borehole extensometers are used to determine the absolute movements of the ground around the openings. With these instruments, rods or wires are placed into a hole and anchored at various depths. The displacement at the extensometer head (located near the excavation face) is measured relative to each of the fixed anchors. These data are used in the extensometer *displacement* plots presented here. Annual rates of displacement are calculated for each extensometer and are compared with the annual displacement rate reported during the previous reporting period.

Rockbolt load cells are used to determine the ground loading and the effectiveness of rockbolts. Plots consist of load versus time for each instrumented bolt.

Earth pressure cells and strain gages are used in and around the shaft liners to determine their loads. These are also depicted in time-based plots. Monitoring of these instruments indicates whether there is any stress buildup in the shaft lining systems.

Piezometers are used to measure the gauge pressure of groundwater. They have been installed in the shafts at varying elevations to monitor the hydraulic head acting on the shaft liners. Plots from piezometers are presented as pressure versus time.

Joint meters are installed perpendicular to a crack and monitor any changes in separation of the crack which may occur over time.

1.2 Data Plot Explanation

Data are presented in graphical form for ease in interpretation. Time-based plots are used in this report. Each plot generally consists of a legend in the upper right-hand corner that gives the array name and specific location of the instrument or point evaluated. The legend ties the graphical cross-sectional representation of the drift or shaft typically presented in the lower right-hand corner to the symbols on the curve in the graph. For extensometers, each anchor is designated with an alpha character "A" closest to the collar and "B," "C," "D," or "E" for the furthest point from the collar (the deepest anchor). For convergence points, the horizontal and vertical sections of the drift are referred to as chords. Breaks in the graph for convergence data and a numeric designator added to the legend typically indicate that the convergence point was lost due to normal mine maintenance activities and later reinstalled.

1.3 Report Organization

Chapter 1.0 provides an introduction to this Supporting Data volume of the GAR. Chapter 2.0 provides instrument data analysis for the Salt Handling shaft, followed by data plots for the piezometers, earth pressure cells, spot welded strain gages, and embedment strain gages installed in the Salt Handling shaft. Chapter 3.0 provides instrument data analysis for the Salt Handling Shaft Station and Waste Shaft Station and an instrument data summary only for the area immediately surrounding the Air Intake Shaft, and data plots for extensometers, convergence points, and rockbolt load cells for all three locations. Chapter 4.0 provides instrument data analysis for the access drifts followed by data plots for the extensometers, convergence points, joint meters and rock bolt load cells. Chapter 5.0 provides instrument data analysis for the Waste Disposal Area followed by data plots for the extensometers and convergence points. Chapter 6.0 provides convergence point instrument data analysis for the Salt Disposal Investigations (SDI) area. Chapter 7.0 provides geologic data collected through the mapping of fractures, stratigraphic mapping and the observed displacements in vertical boreholes.

2.0 Instrumentation Summary for Shafts

Originally, the Salt, Waste and Exhaust Shafts were instrumented with geomechanical instrumentation. The instrument readings from the Waste and Exhaust Shafts are no longer available due to failed instruments, broken cabling and/or inoperative, obsolete data acquisition equipment. Table 2-1 presents data and analysis of the Salt Shaft instrumentation. Plots of the instrument data are presented as Figures 2-1 through 2-30.

Table 2-1
Salt Handling Shaft Data Analysis

Piezometers

Field Tag	Level feet	Figure Number	Date of 2015-2016 Max. Reading	2015-2016 Maximum Pressure Readings (psi)	Date of 2014-2015 Max. Reading	2014-2015 Maximum Pressure Readings (psi)	Change in Maximum Pressure From Previous Year (psi)	Comments
37X-PE-00201	580	2-1	06/14/16	91.9	7/29/2014	73.4	18.5	
37X-PE-00202	580	2-1	06/14/16	105.6	6/14/2014	105.6	0	
37X-PE-00203	620	2-2	06/14/16	187.5	7/29/2014	144.4	43.1	
37X-PE-00204	620	2-3	06/14/16	82.7	7/29/2014	144.8	-62.1	
37X-PE-00206	691	2-4	06/14/16	174.4	7/29/2014	156.3	18.1	
37X-PE-00210	802	2-5	06/14/16	-0.8	7/29/2014	58.3	-59.1	
37X-PE-00211	850	2-6	06/14/16	54.8	7/29/2014	42.1	12.7	
37X-PE-00212	850	2-7	06/14/16	88	07/29/14	90.8	-2.8	

Earth Pressure Cells

Field Tag	Level feet	Figure Number	Date of 2015-2016 Max. Reading	2015-2016 Maximum Pressure Readings (psi)	Date of 2013-2014 Max. Reading	2014-2015 Maximum Pressure Readings (psi)	Change in Maximum Pressure From Previous Year (psi)	Comments
37X-WE-00203	862.4	2-8	06/14/16	6.3	7/29/2014	5.1	1.2	

Table 2-1
Salt Handling Shaft Data Analysis, continued

Embedment Strain Gages								
Field Tag	Level feet	Figure Number	Date of 2015-2016 Max. Reading	2015-2016 Maximum Strain Readings (με)	Date of 2014-2015 Max. Reading	2014-2015 Maximum Strain Readings (με)	Change in Maximum Strain From Previous Year (με)	Comments
37X-ZE-00210	856.3	2-9	06/14/16	1006	7/29/2014	1005	1	
37X-ZE-00211	856.3	2-10	06/14/16	326	7/29/2014	338	-12	
37X-ZE-00212	856.3	2-11	06/14/16	-590	7/29/2014	-595	5	
37X-ZE-00213	856.3	2-12	06/14/16	407	7/29/2014	400	7	
37X-ZE-00214	856.3	2-13	06/14/16	126	7/29/2014	122	4	
37X-ZE-00215	856.3	2-14	06/14/16	134	7/29/2014	137	-3	
37X-ZE-00216	856.3	2-15	06/14/16	669	7/29/2014	663	6	
37X-ZE-00235	856.3	2-16	06/14/16	-355	7/29/2014	-349	-6	
37X-ZE-00236	856.3	2-17	06/14/16	55	7/29/2014	116	-61	
37X-ZE-00237	856.3	2-18	06/14/16	123	7/29/2014	117	6	
37X-ZE-00238	856.3	2-19	06/14/16	555	7/29/2014	550	5	

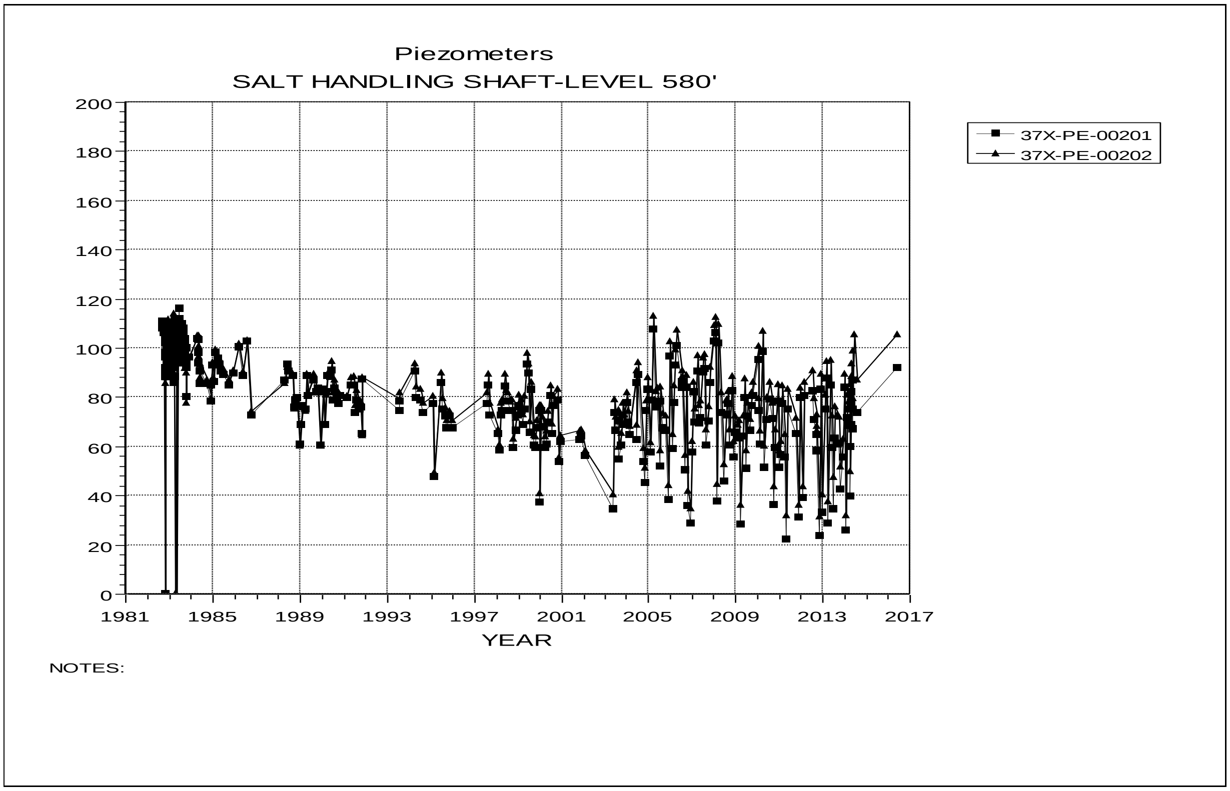

Figure 2-1 Piezometer Salt Handling Shaft – Level 580 at the Forty-niner Member

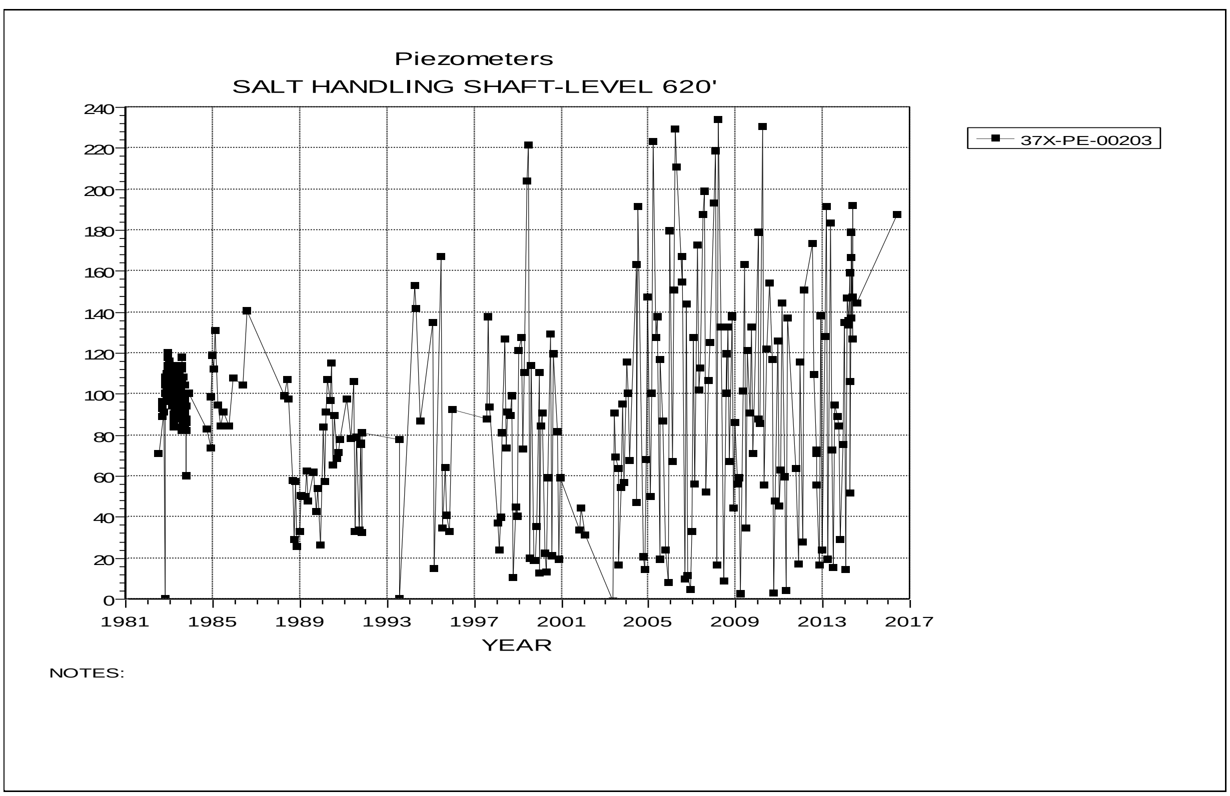

Figure 2-2 Piezometers Salt Handling Shaft – Level 620 at the Magenta Dolomite Member

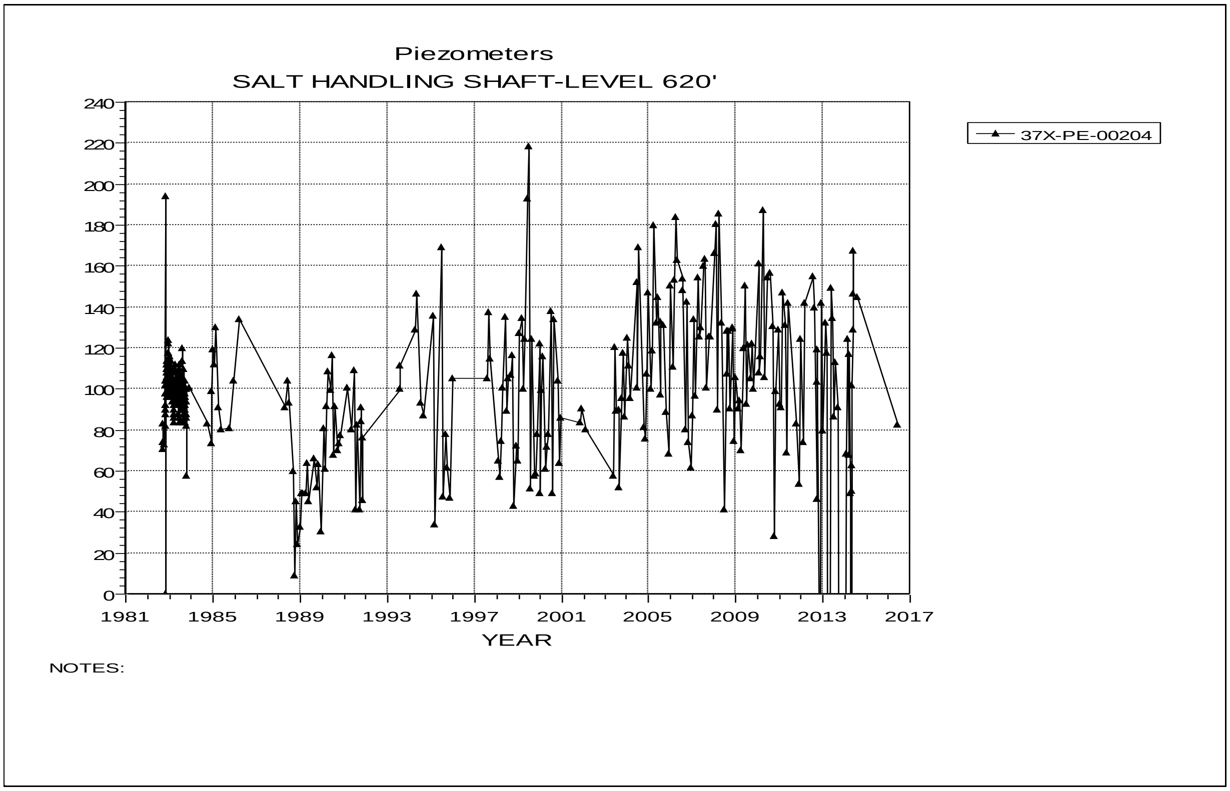

Figure 2-3 Piezometers Salt Handling Shaft – Level 620
at the Magenta Dolomite Member

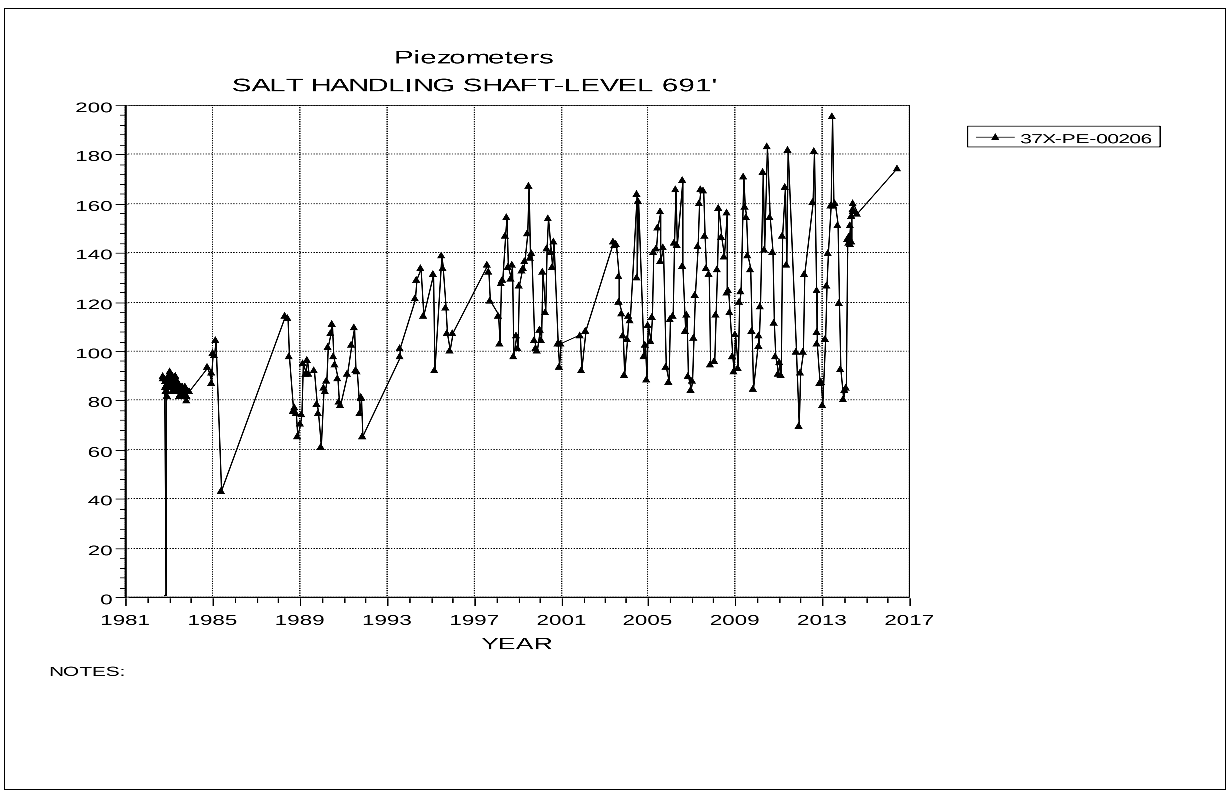

Figure 2-4 Piezometers Salt Handling Shaft – Level 691
at the Tamarisk Member

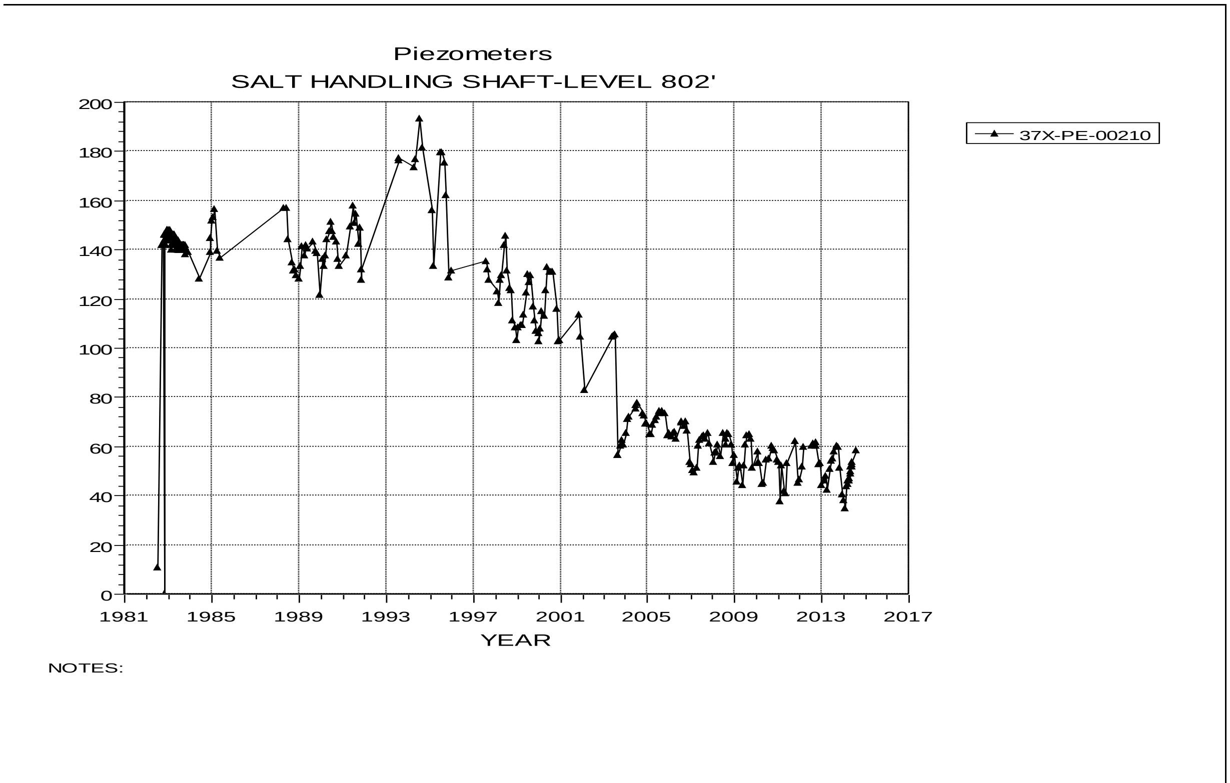

Figure 2-5 Piezometers Salt Handling Shaft – Level 802 at the Los Medaños Member

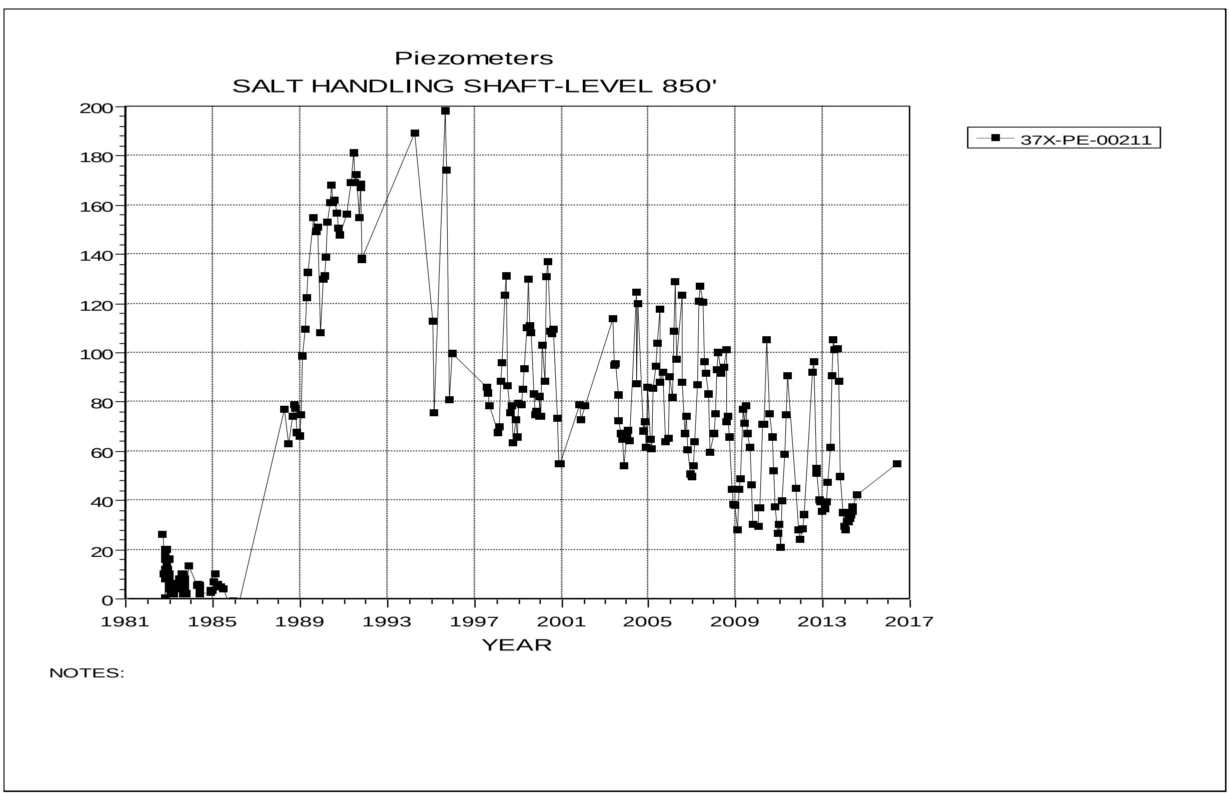

Figure 2-6 Piezometers Salt Handling Shaft – Level 850 at the Rustler-Salado Contact

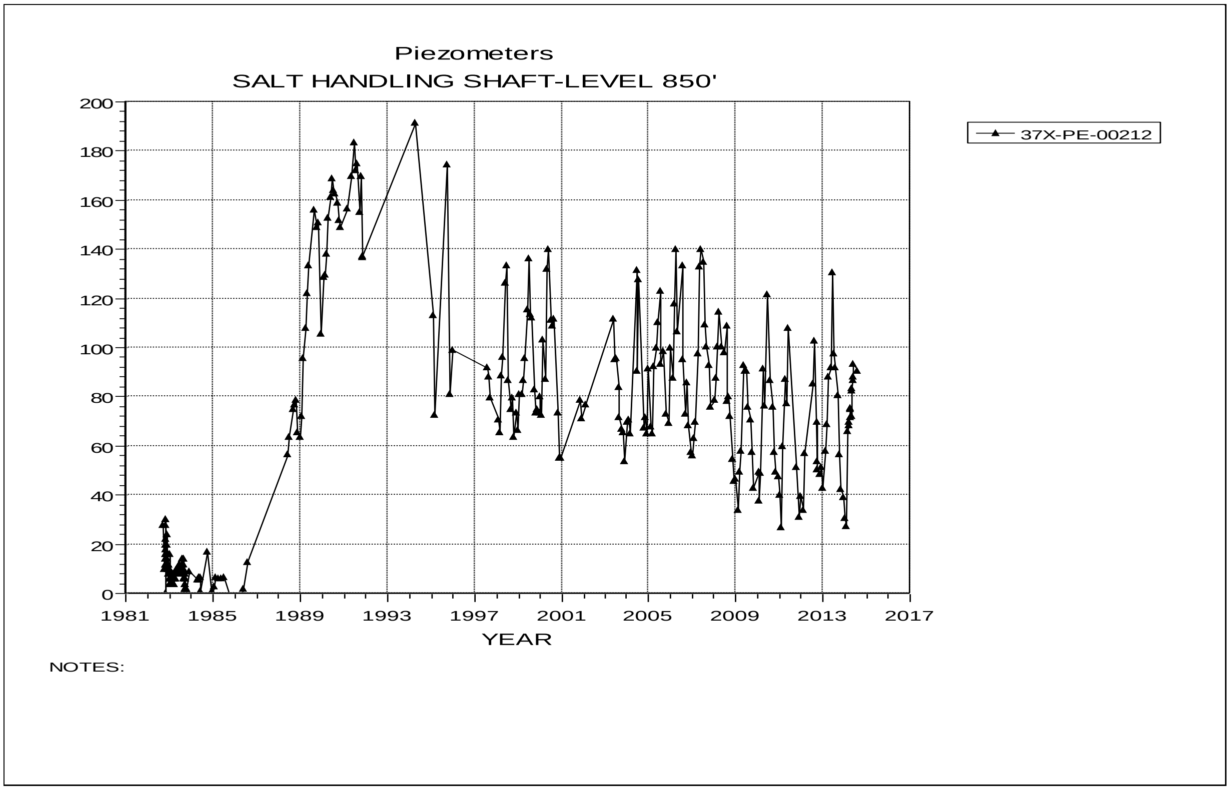

Figure 2-7 Piezometers Salt Handling Shaft –
Level 850 at the Rustler-Salado Contact

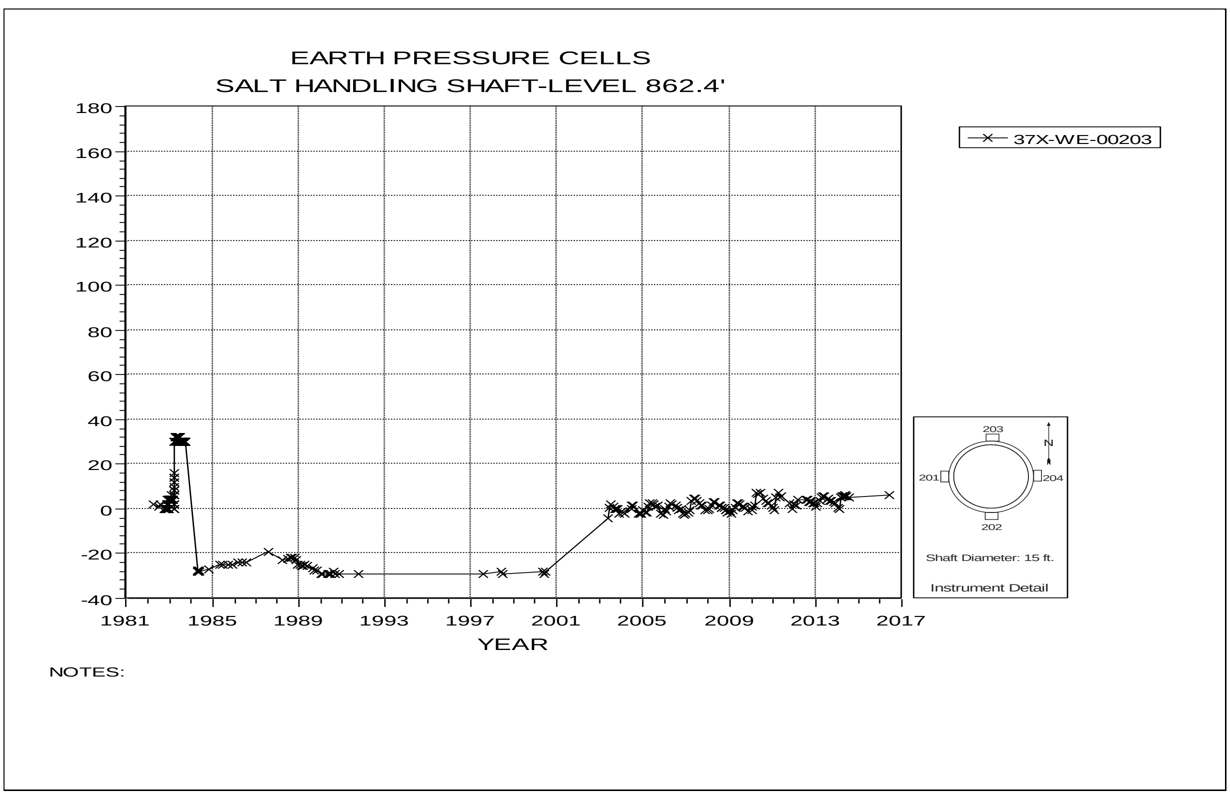

Figure 2-8 Earth Pressure Cell –
Salt Handling Shaft Key – Level 862.4

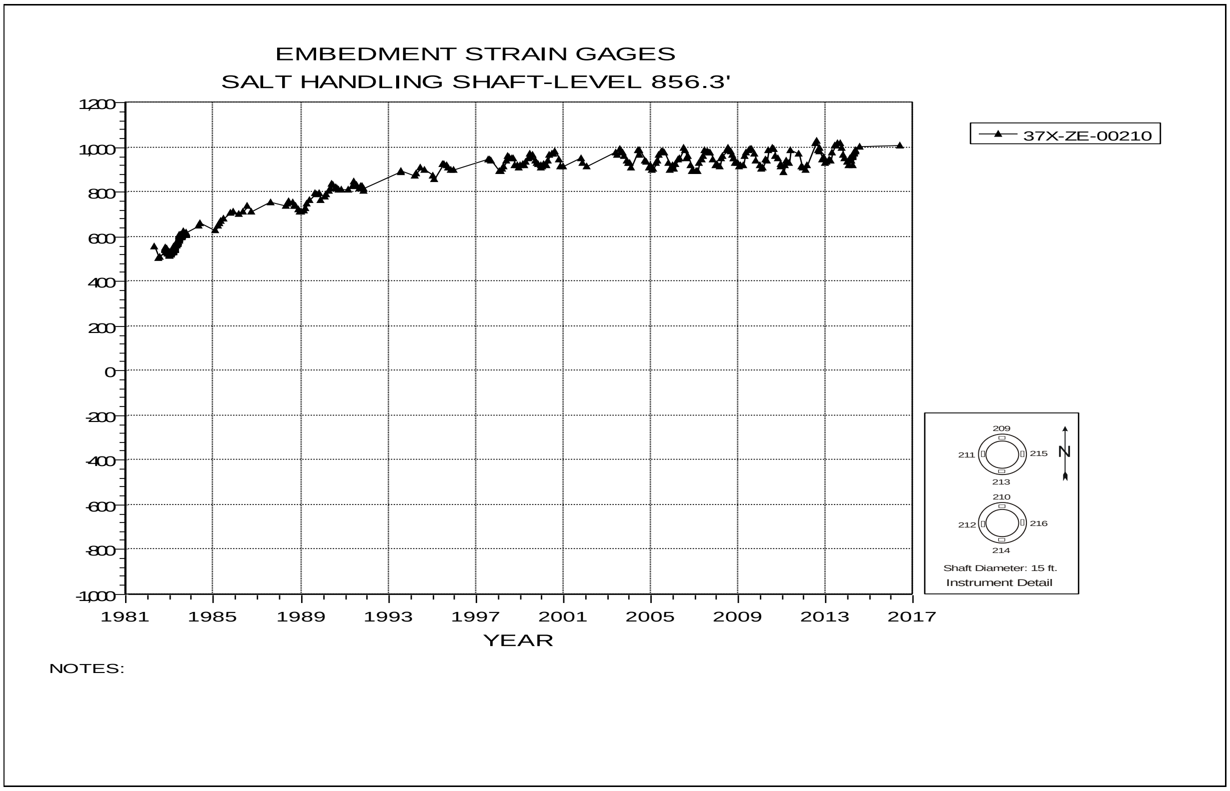

Figure 2-9 Embedment Strain Gage –
Salt Handling Shaft Key – Level 856.3

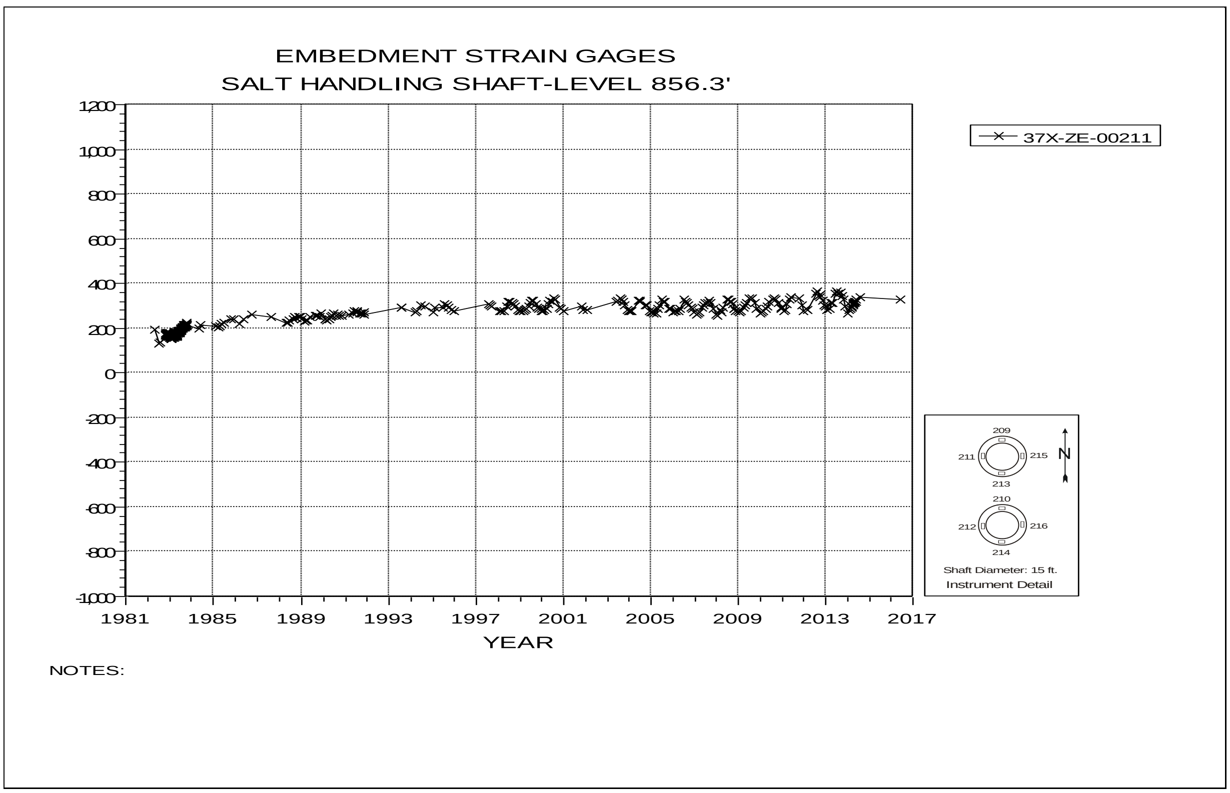

Figure 2-10 Embedment Strain Gage –
Salt Handling Shaft Key – Level 856.3

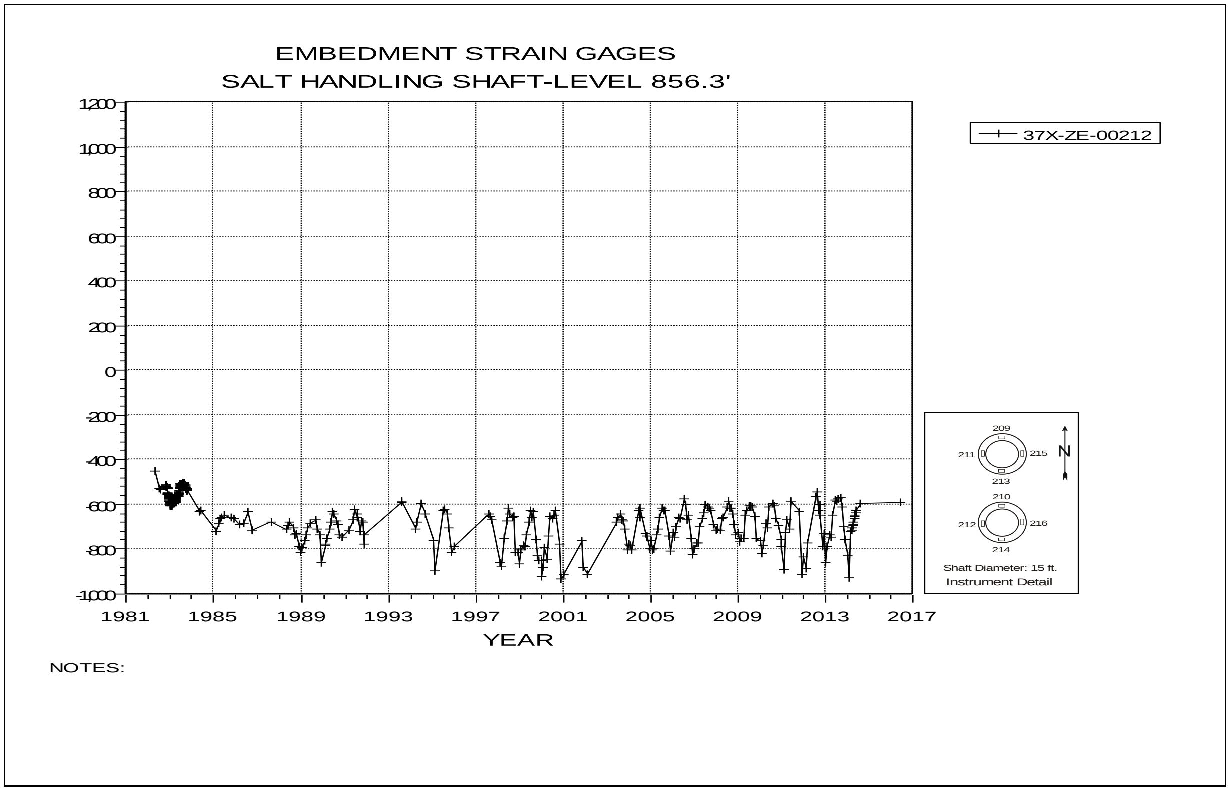

Figure 2-11 Embedment Strain Gage –
Salt Handling Shaft Key – Level 856.3

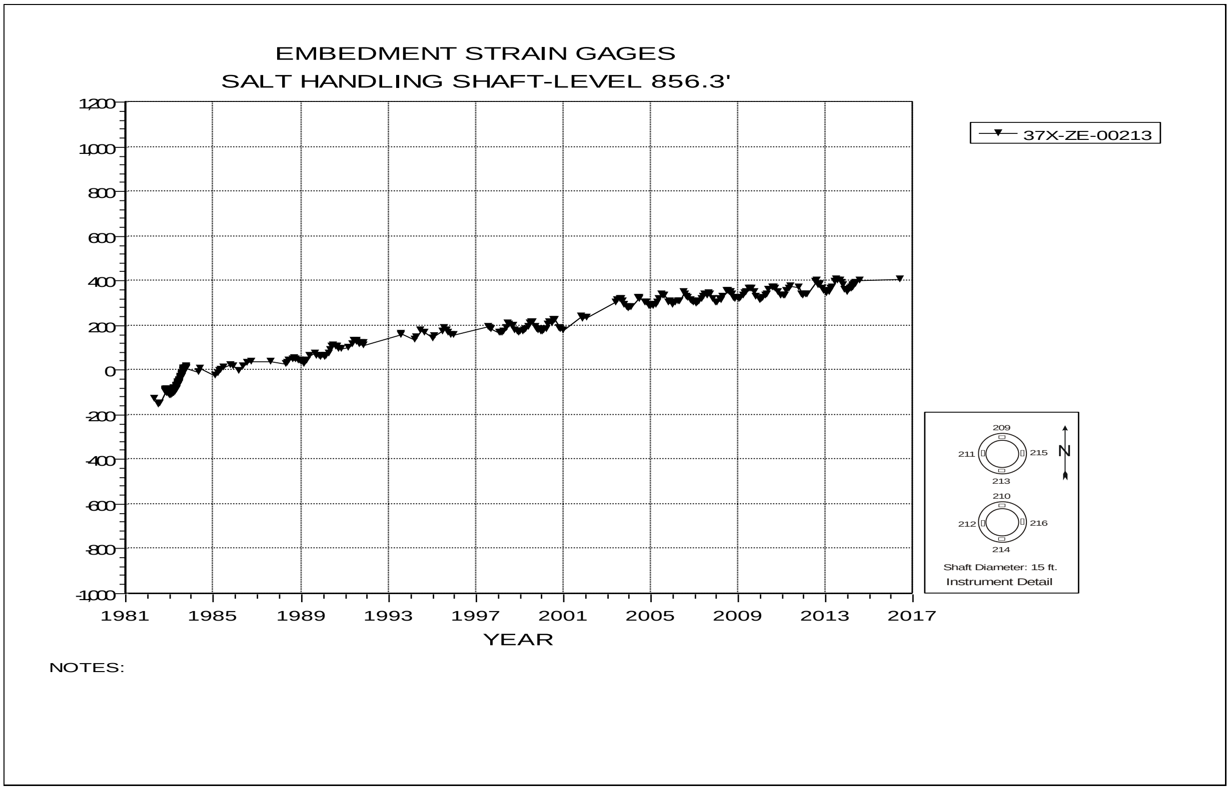

Figure 2-12 Embedment Strain Gage –
Salt Handling Shaft Key – Level 856.3

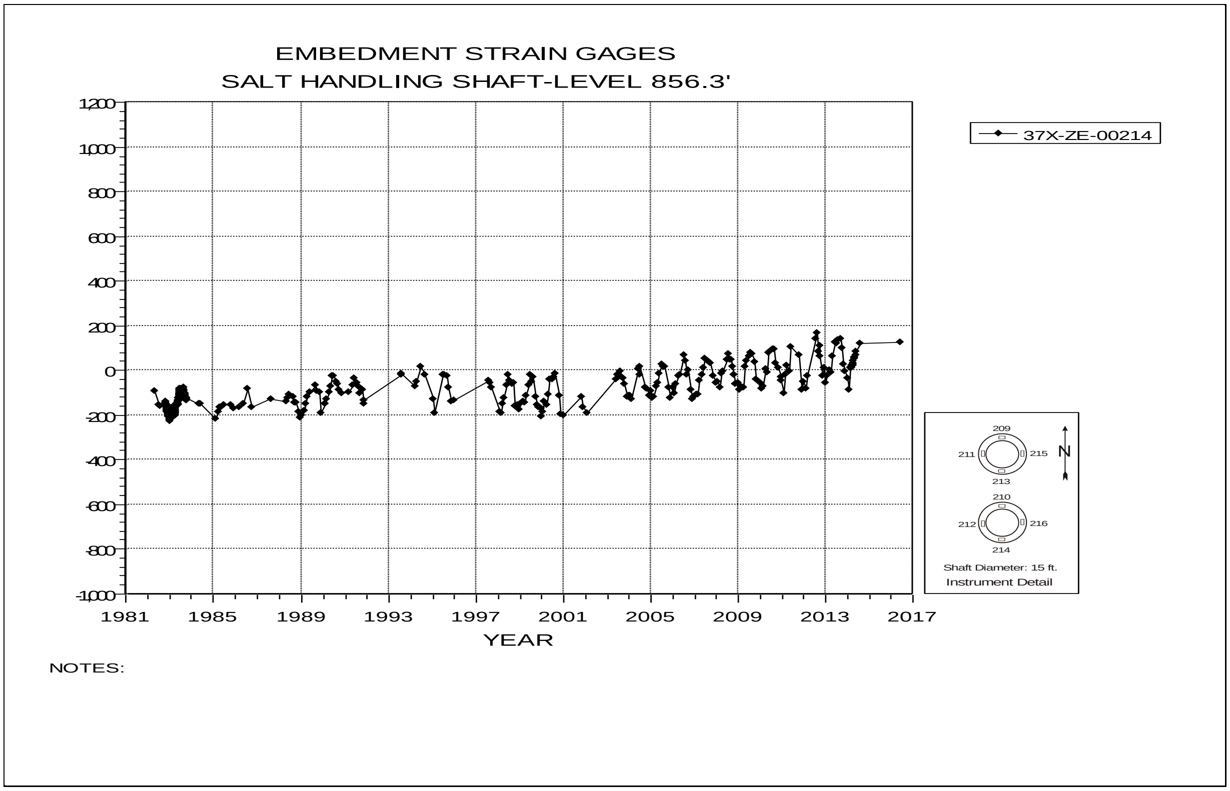

Figure 2-13 Embedment Strain Gage –
Salt Handling Shaft Key – Level 856.3

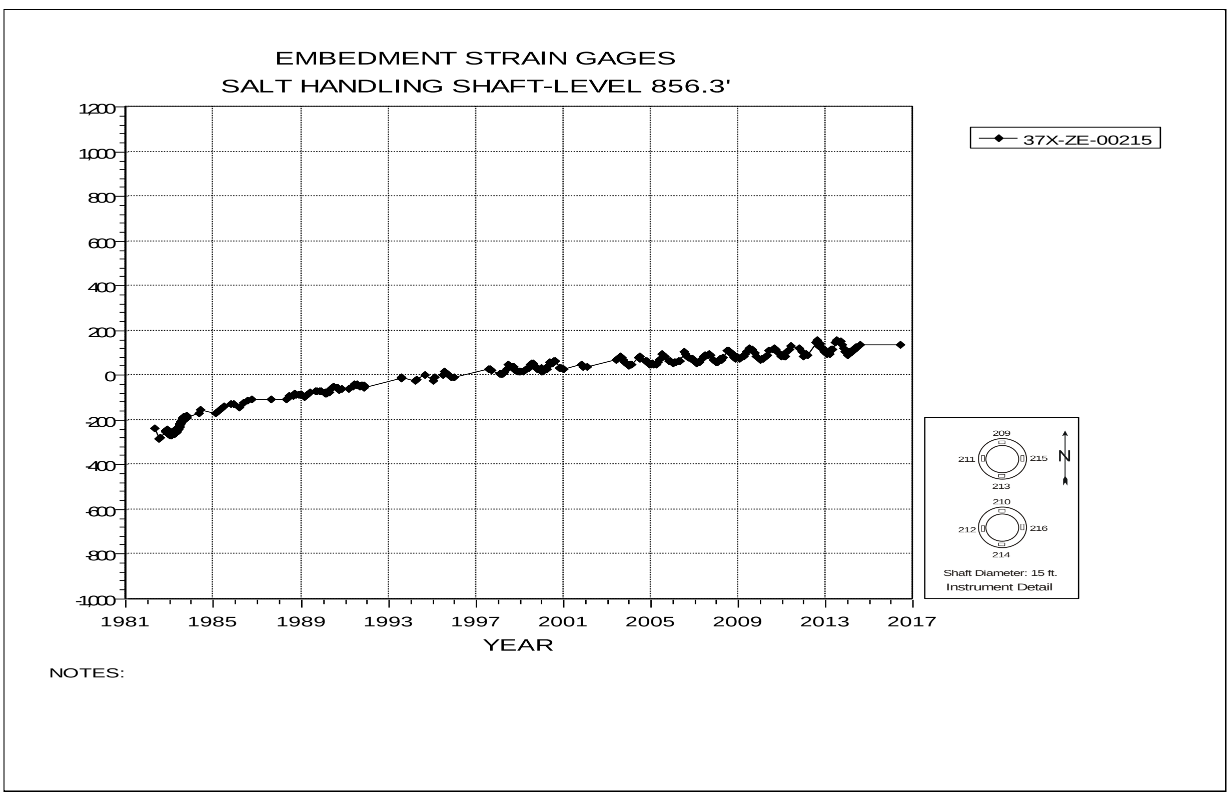

Figure 2-14 Embedment Strain Gage –
Salt Handling Shaft Key – Level 856.3

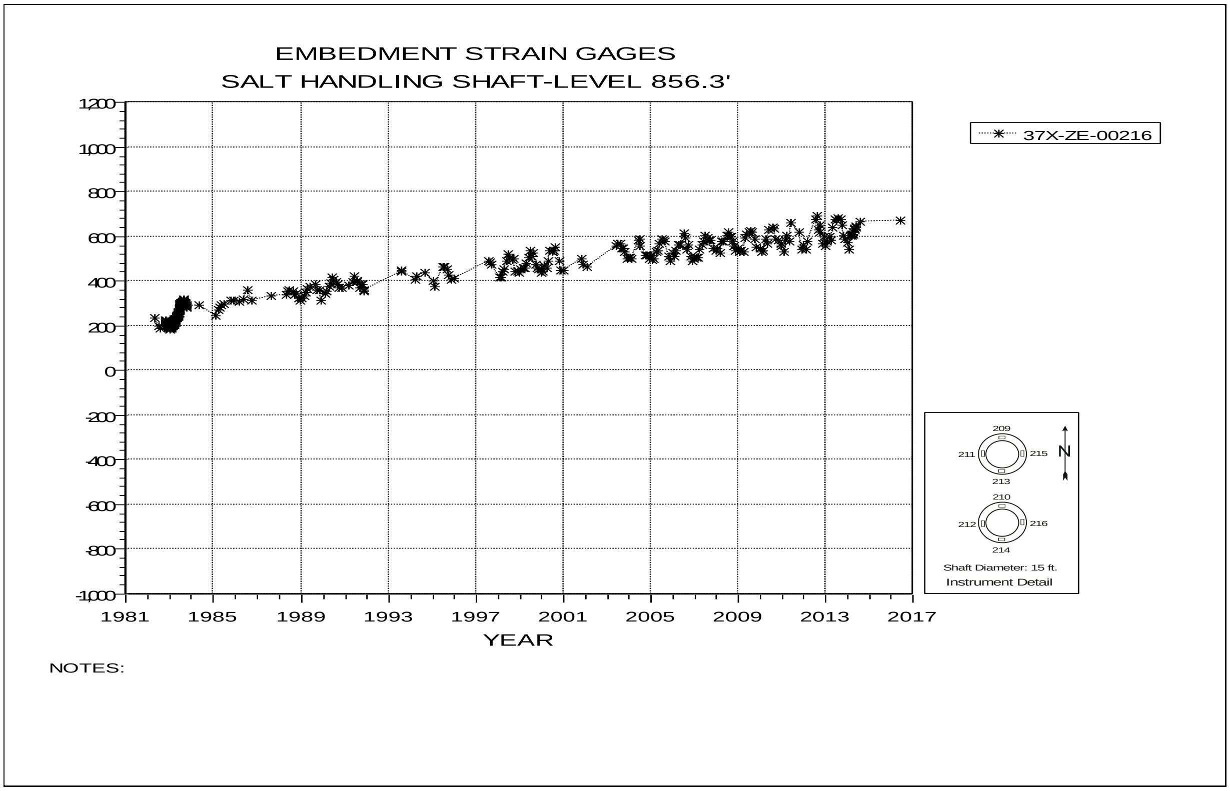

Figure 2-15 Embedment Strain Gage –
Salt Handling Shaft Key – Level 856.3

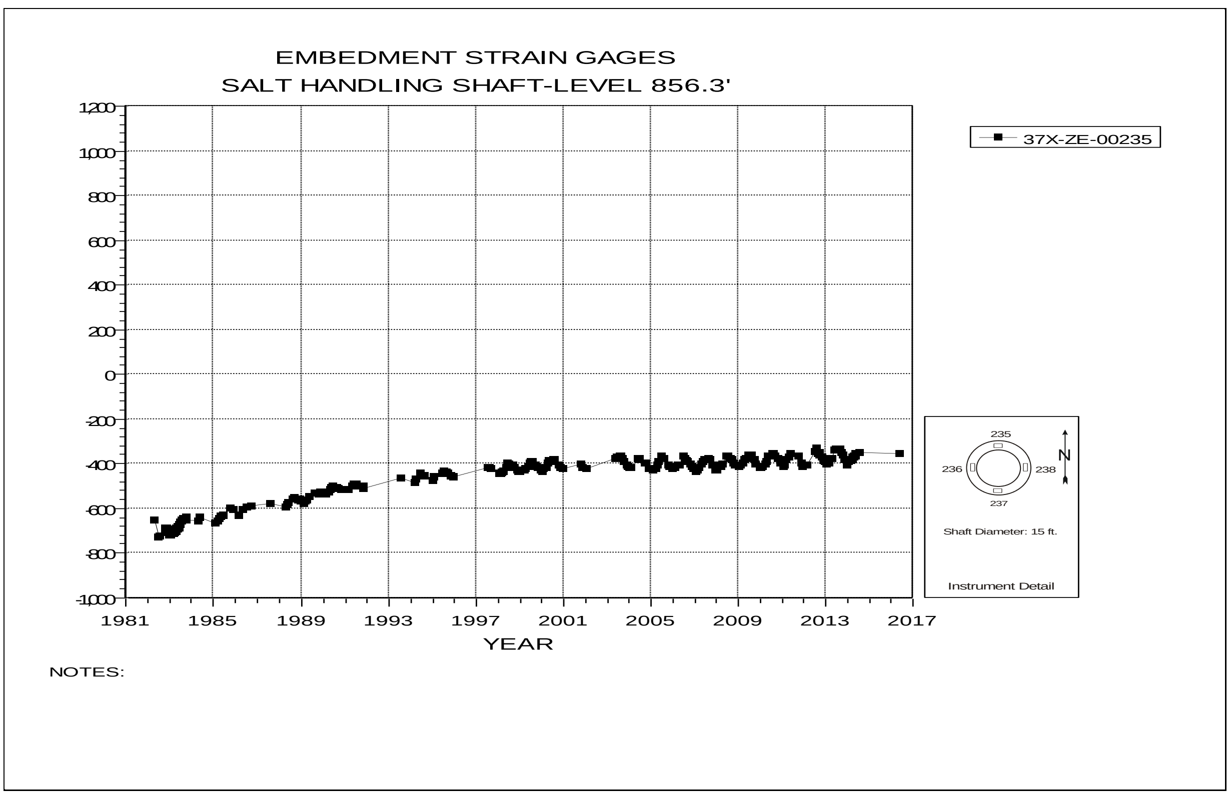

Figure 2-16 Embedment Strain Gage –
Salt Handling Shaft Key – Level 856.3

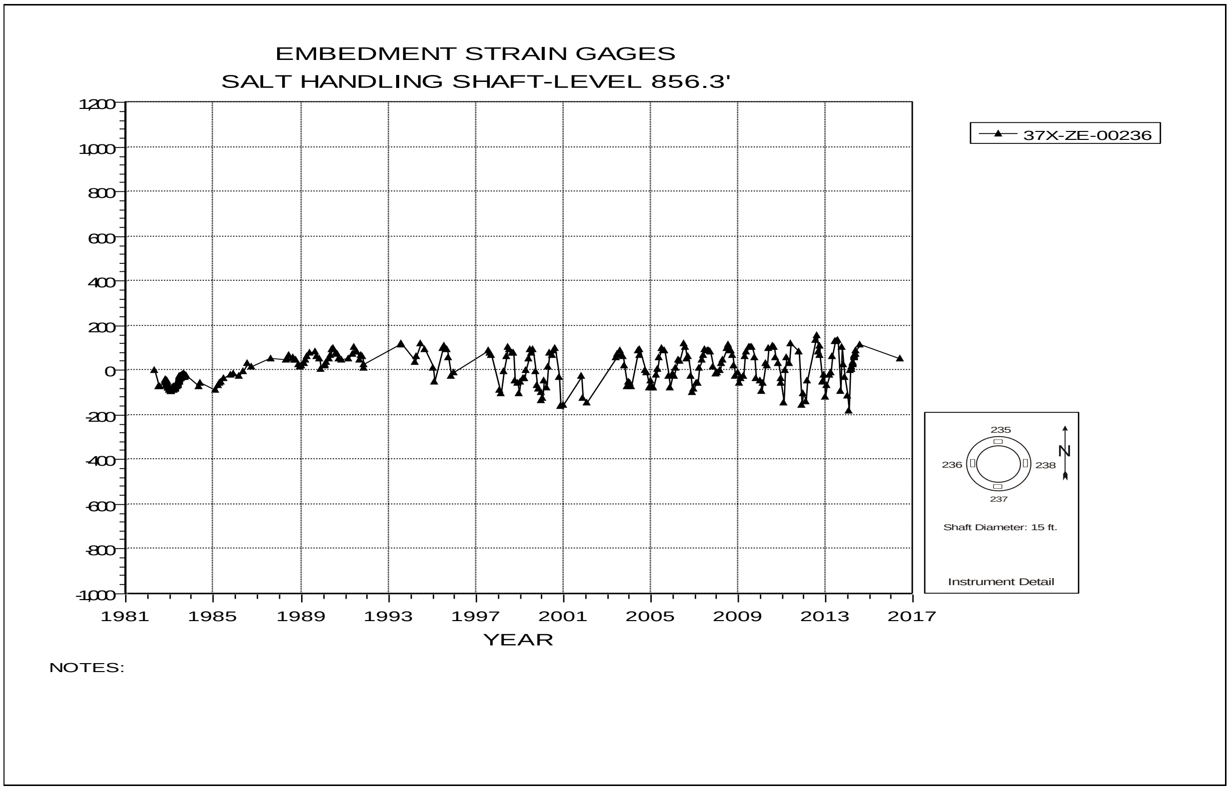

Figure 2-17 Embedment Strain Gage –
Salt Handling Shaft Key – Level 856.3

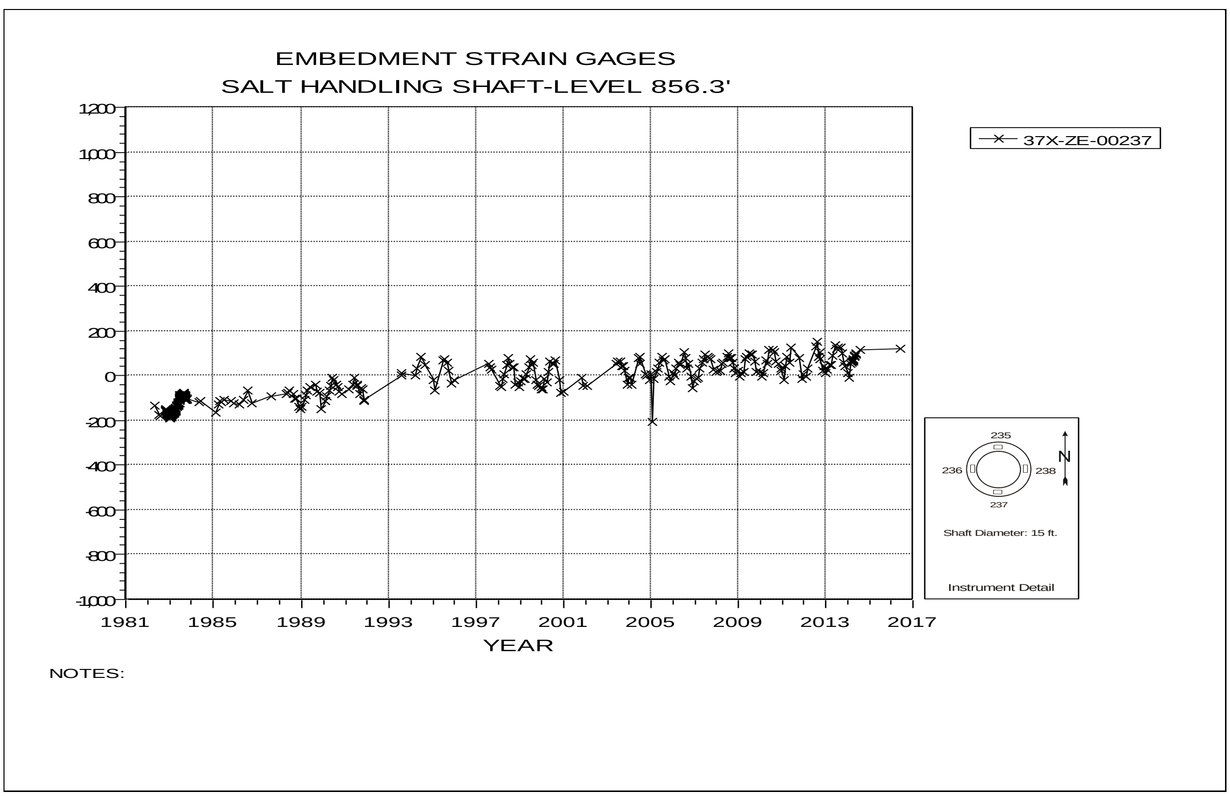

Figure 2-18 Embedment Strain Gage –
Salt Handling Shaft Key – Level 856.3

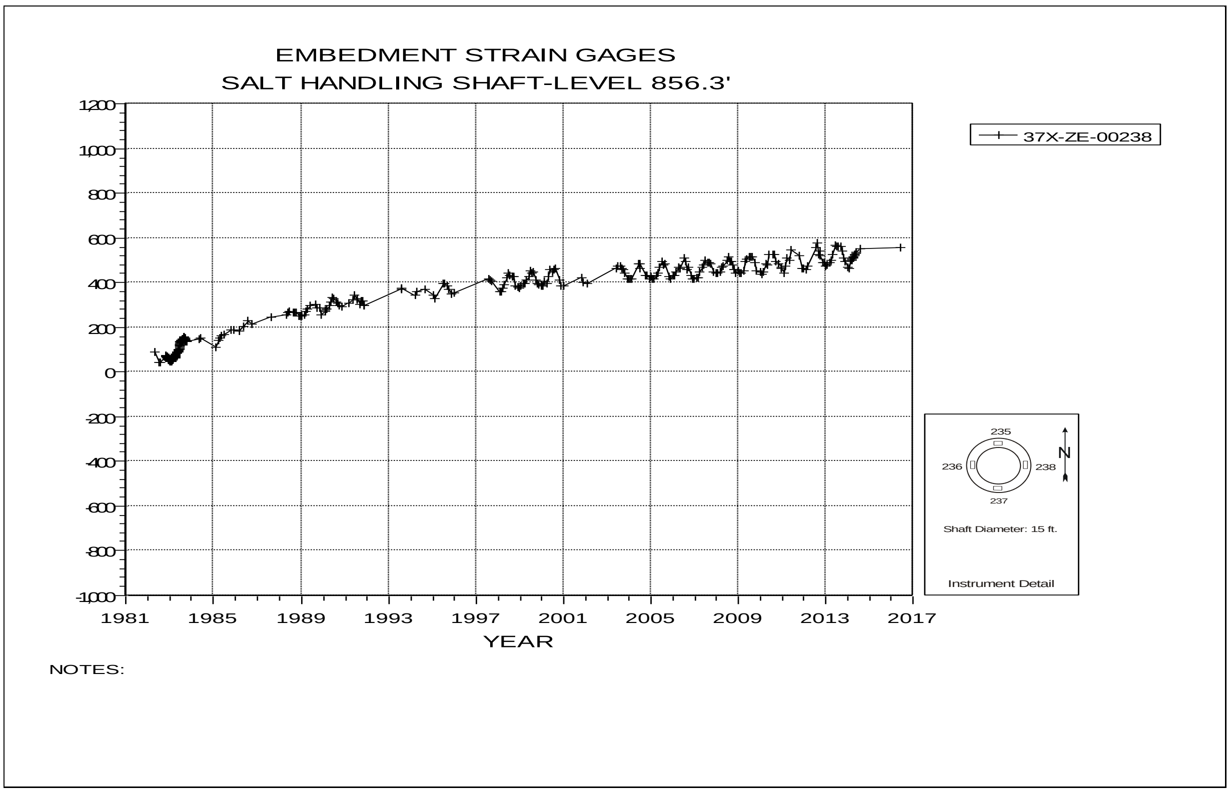

Figure 2-19 Embedment Strain Gage –
Salt Handling Shaft Key – Level 856.3

3.0 Instrumentation Summary for Shaft Stations

Instrumentation data analysis for the Salt Handling Shaft Station, Waste Shaft Station, and the area around the Air Intake Shaft follow. Table 3-1 presents data analyses for each of the Salt Handling Shaft Station instruments. Figures 3-1 through 3-7 present plots of the instrumentation data for the Salt Handling Shaft Station.

Table 3-2 presents data and analysis for the Waste Shaft Station. Plots from the instrumentation in the Waste Shaft Station are presented as Figures 3-8 and 3-9.

Table 3-3 and Figures 3-9 through 3-14 present the data from rock bolt load cells and borehole extensometers located in the immediate area around the Air Intake Shaft.

Table 3-1
Salt Handling Shaft Station Data Analysis

Convergence Points

Field Tag	Location	Figure Number	Last Reading 2015-2016		Cumulative Displacement (inches)	Closure Rate 2015 to 2016 (in/year)	Closure Rate 2014 to 2015 (in/year)	Rate Change Percent	Comments
			Date	Inches					
E0-S18-8 A-E	E0-S18	3-1	04/06/16	7.749	28.90	2.6	1.2	117%	
E0-S18-6 B-D	E0-S18	3-2	04/06/16	8.626	31.73	2.7	1.3	108%	
E0-S18-5 H-F	E0-S18	3-2	04/06/16	5.139	19.60	2.1	0.7	200%	
E0-S30-6 A-C	E0-S30	3-3	04/06/16	7.769	29.80	2.6	1.2	117%	
E0-S65-5 A-C	E0-S65	3-4	04/06/16	5.641	21.00	2.3	0.8	188%	

Extensometers

Field Tag	Location	Figure Number	Date of Last Reading	Collar Displacement Relative to Deepest Anchor (inches)	Displacement Rate 2015 to 2016 (in/year)	Displacement Rate 2014 to 2015 (in/year)	Rate Change Percent	Comments
51X-GE-01026-2	E0-S30	3-5	04/06/16	-13.18	-52.0	0.0	N/A	
51X-GE-01027-2	E0-S60	3-6	04/06/16	-13.83	-53.0	0.0	N/A	

ISSUED

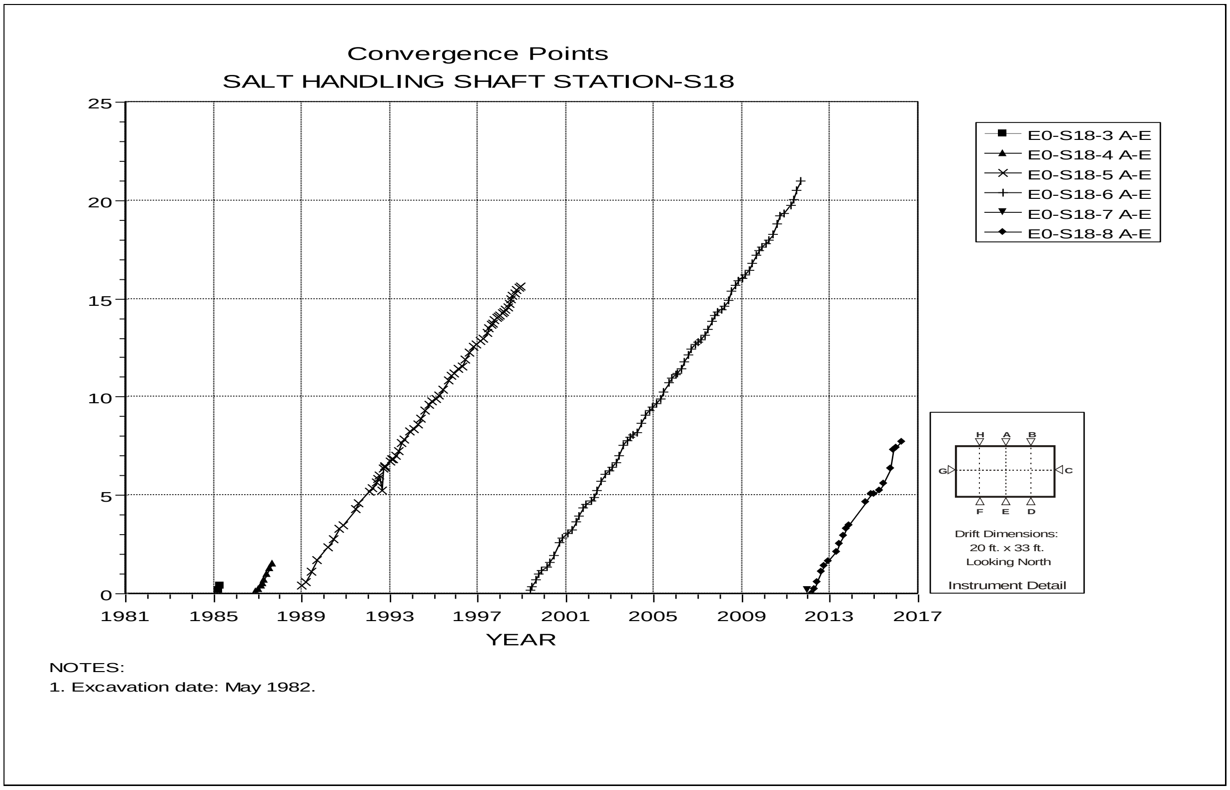

Figure 3-1 Convergence Point Array –
Salt Handling Shaft Station at S18 – Centerline – Roof to Floor

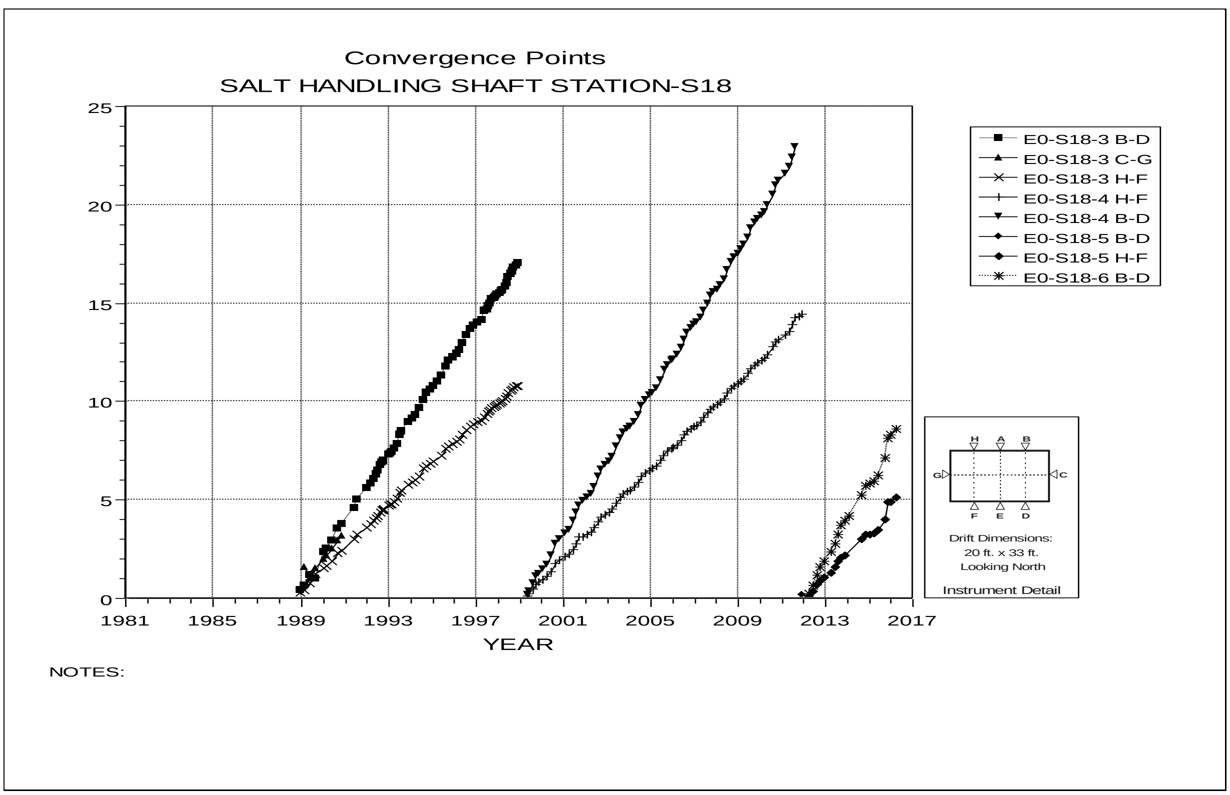

Figure 3-2 Convergence Point Array –
Salt Handling Shaft Station at S18 – East Quarter Point – Roof to Floor

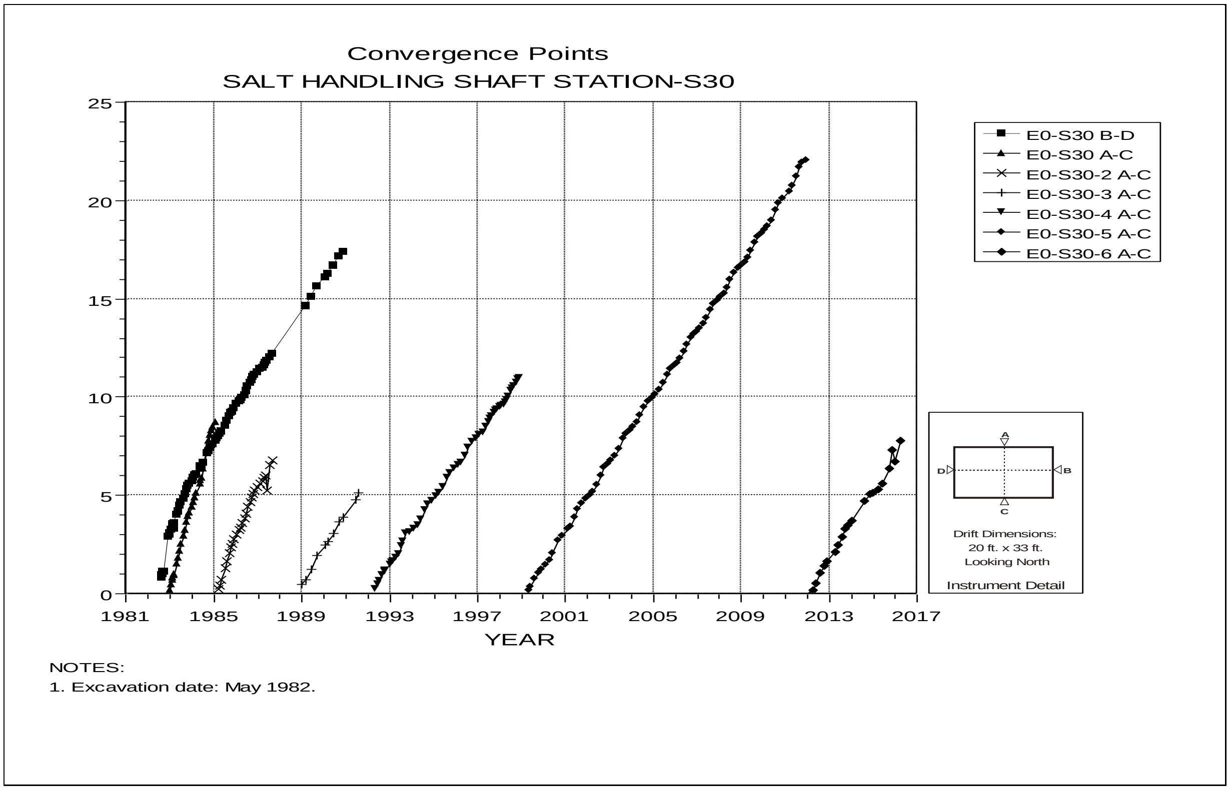

Figure 3-3 Convergence Point Array –
Salt Handling Shaft Station at S30 – Roof to Floor

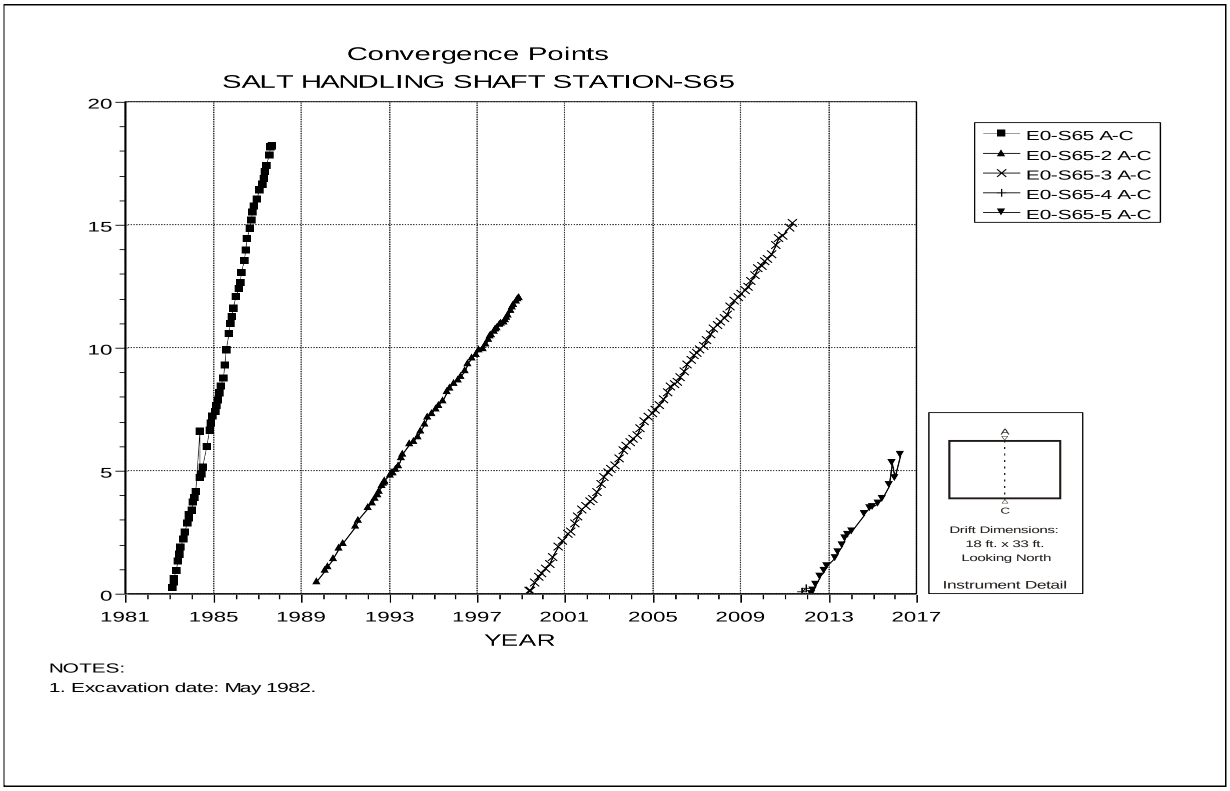

Figure 3-4 Convergence Point Array –
Salt Handling Shaft Station at S65 – Roof to Floor

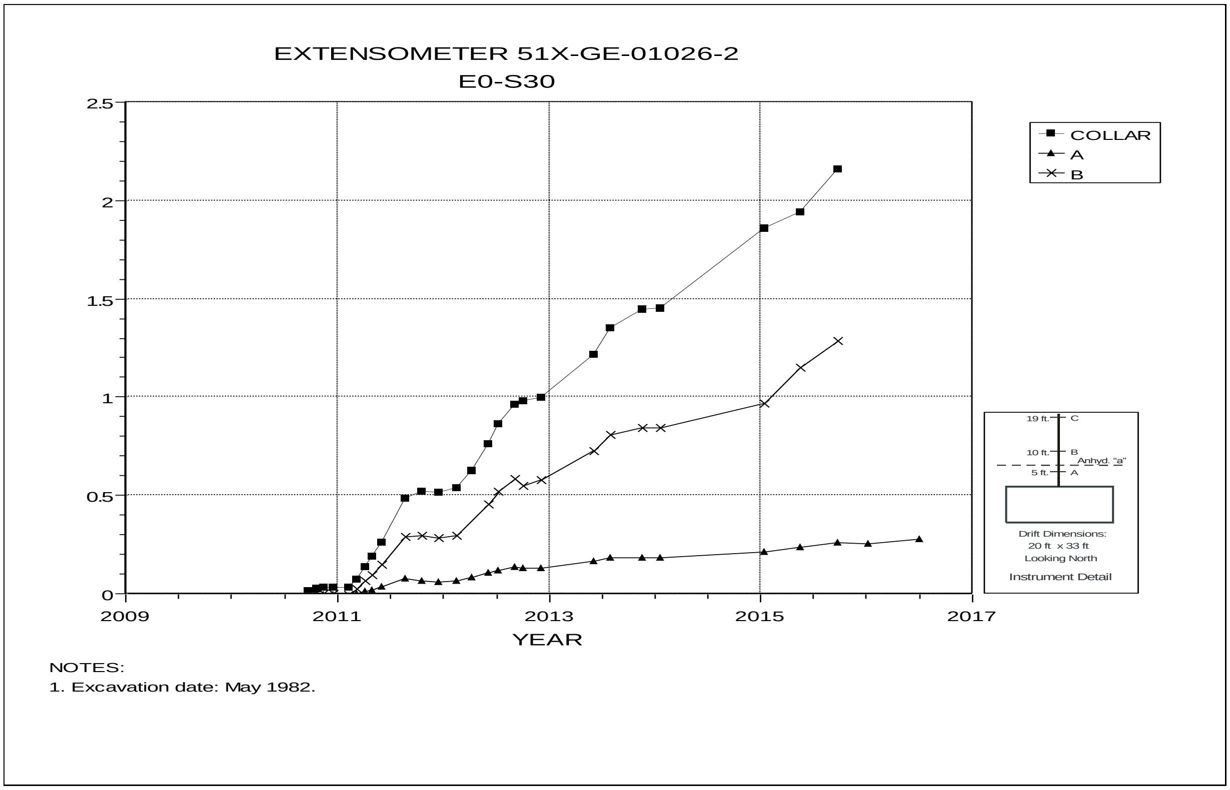

Figure 3-5 Extensometer 51X-GE-01026-2 –
Salt Handling Shaft Station at E0 S30 – Roof

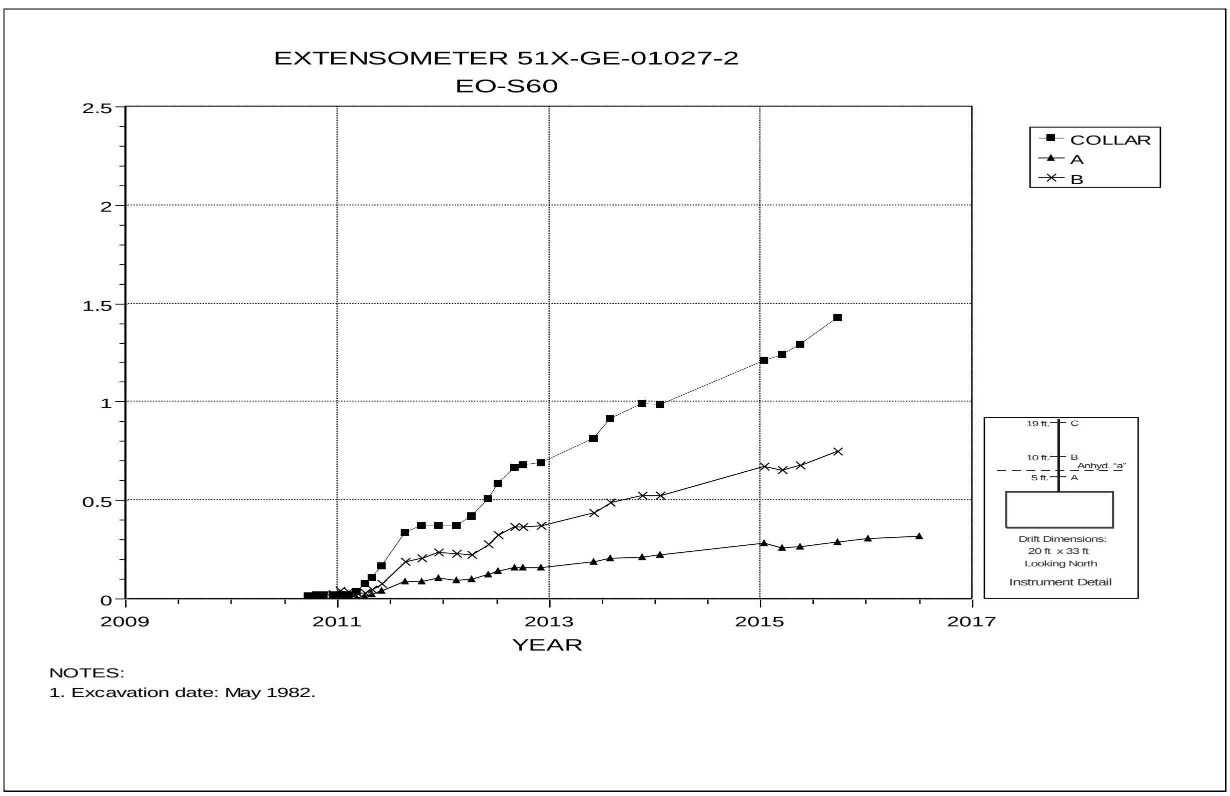

Figure 3-6 Extensometer 51X-GE-01027-2 –
Salt Handling Shaft Station at E0 S60 – Roof

Table 3-2
Waste Shaft Station Data Analysis

Extensometers

Fieldtag	Location	Figure Number	Date of Last Reading	Collar Displacement Relative to Deepest Anchor (inches)	Displacement Rate 2015 to 2016 (in/year)	Displacement Rate 2014 to 2015 (in/year)	Rate Change Percent	Comments
51X-GE-00268	Waste Shaft Station at W30	3-7	02/04/16	7.333	0.0	0.1	-100%	Calculations based on data from anchor D.
51X-GE-00404-2	Waste Shaft Station at E35	3-8	10/05/15	1.579	0.3	0.3	0%	

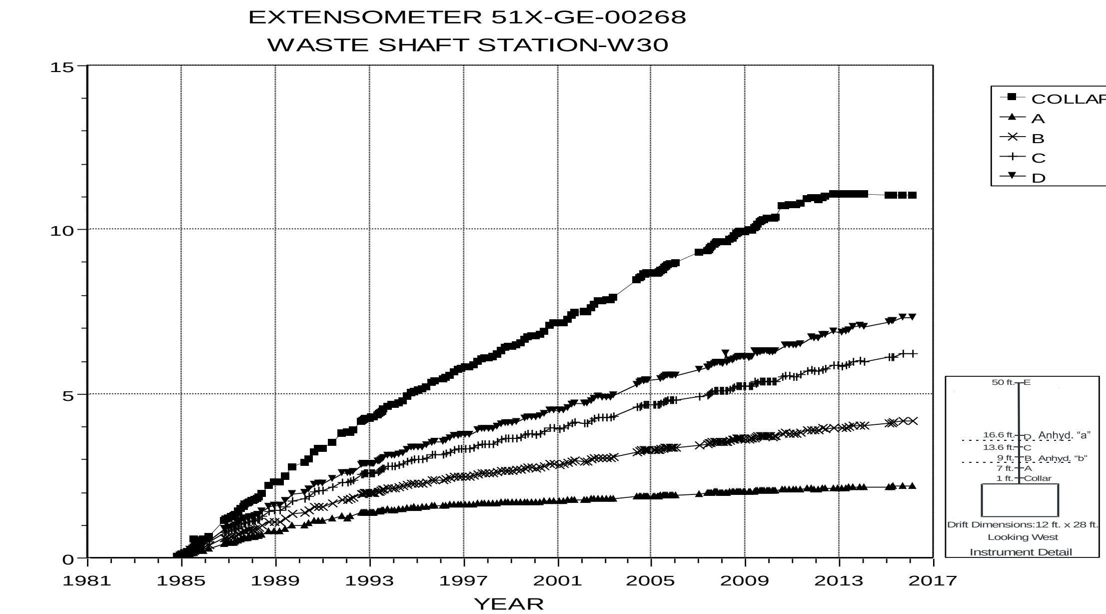

NOTES:
1. Excavation date: November 1982.
2. The Collar anchor (anchor E) is out of range. Select CFI to view the plot.

Figure 3-7 Extensometers 51X-GE-00268
Waste Shaft Station at W30 – Roof

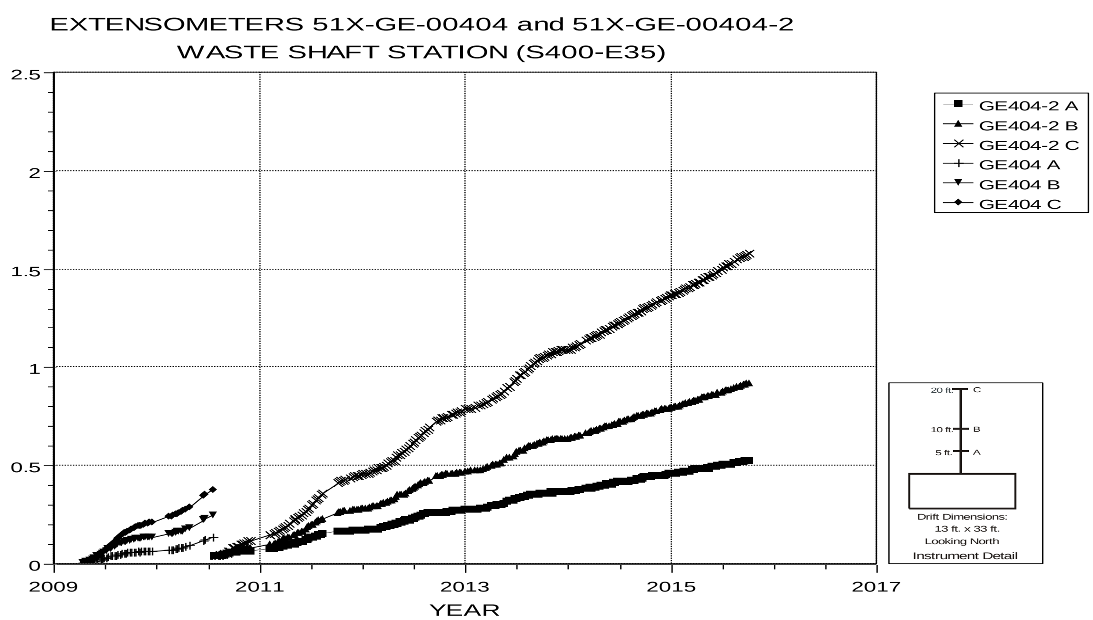

NOTES:
1. Excavation date: November 1982.
2. Extensometer 51X-GE-00404 was replaced by 51X-GE-00404-2 in July 2010.

Figure 3-8 Extensometers 51X-GE-00404 and 51-GE-00404-2
Waste Shaft Station at E35 – Roof

Table 3-3
Air Intake Shaft Station Data Analysis

Extensometers

Field Tag	Location	Figure Number	Date of Last Reading	Collar Displacement Relative to Deepest Anchor (Inches)	Displacement Rate 2014 to 2015 in/year	Displacement Rate 2013 to 2014 in/year	Rate Change Percent	Comments
41X-GE-00122	W620- S65	3-9	06/27/16	4.105	0.2	0.2	0%	Calculations performed from anchor B data
41X-GE-00123	W620- N93	3-10	06/27/16	4.31	0.2	0.2	0%	Calculations performed from anchor A data.

Rockbolt Load Cells

Field Tag	Location	Figure Number	Date of Initial Reading	Date of Last Reading[3]	Load[3] (kips)	Comments
51X-WG-00236	AIS Station Brow - South	3-11	01/19/93	06/27/16	1.69	
51X-WG-00237	AIS Station Brow - South	3-11	01/19/93	06/27/16	1.025	
51X-WG-00238	AIS Station Brow - South	3-11	01/19/93	06/27/16	45.495	
51X-WG-00239	AIS Station Brow - South	3-11	01/19/93	06/27/16	1.053	
51X-WG-00240	AIS Station Brow - South	3-11	01/19/93	06/27/16	1.64	
51X-WG-00241	AIS Station Brow - South	3-12	01/19/93	06/27/16	51.45	
51X-WG-00242	AIS Station Brow - South	3-12	01/19/93	06/27/16	25.647	
51X-WG-00243	AIS Station Brow - South	3-12	01/19/93	06/27/16	27.767	
51X-WG-00244	AIS Station Brow - South	3-12	12/24/94	06/27/16	0.733	
51X-WG-00245	AIS Station Brow - South	3-12	01/19/93	06/27/16	25.098	
51X-WG-00246	AIS Station Brow - North	3-13	01/19/93	06/27/16	1.493	
51X-WG-00247	AIS Station Brow - North	3-13	01/19/93	06/27/16	18.324	
51X-WG-00248	AIS Station Brow - North	3-13	01/19/93	06/27/16	0.342	
51X-WG-00249	AIS Station Brow - North	3-13	01/19/93	06/27/16	10.882	
51X-WG-00250	AIS Station Brow - North	3-13	12/24/94	06/27/16	25.754	
51X-WG-00251	AIS Station Brow - North	3-14	01/19/93	06/27/16	25.754	
51X-WG-00253	AIS Station Brow - North	3-14	01/19/93	06/27/16	66.954	
51X-WG-00254	AIS Station Brow - North	3-14	01/19/93	06/27/16	4.97	
51X-WG-00255	AIS Station Brow - North	3-14	01/19/93	06/27/16	18.119	

[3] N/A—Rock bolt has broken or the load cell has been damaged. These will not be displayed in the future unless they are replaced.

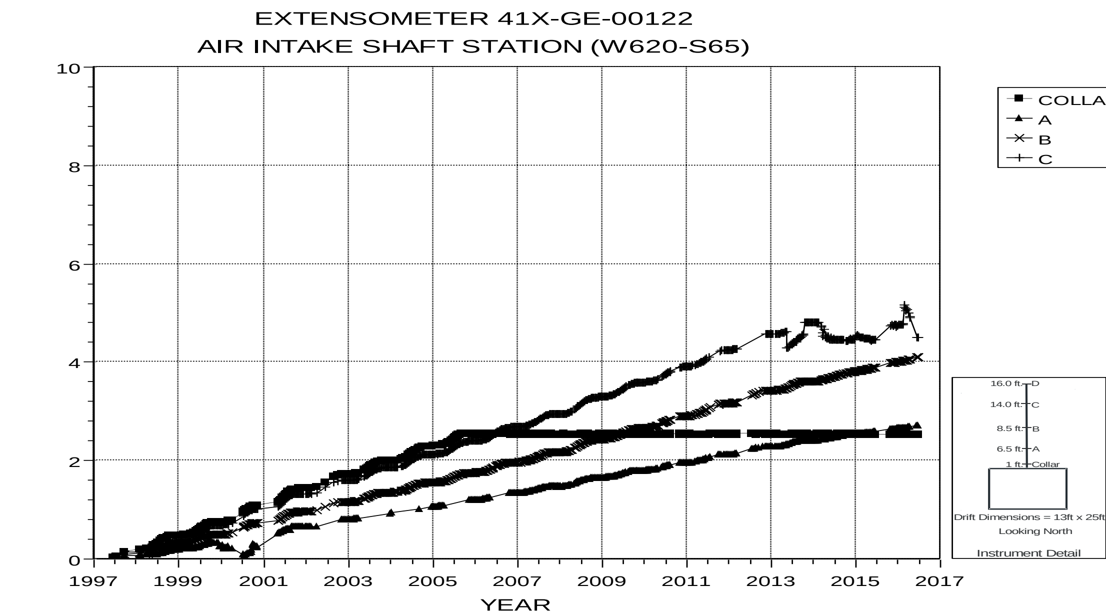

NOTES:
1. Excavation date: January 1988.
2. The Collar (Anchor 'D') and Anchor 'C' have exceeded their maximum ranges, select CFI to view the plot..

Figure 3-9 Extensometer 41X-GE-00122 –
Air Intake Shaft Station at W620 S65 – Roof

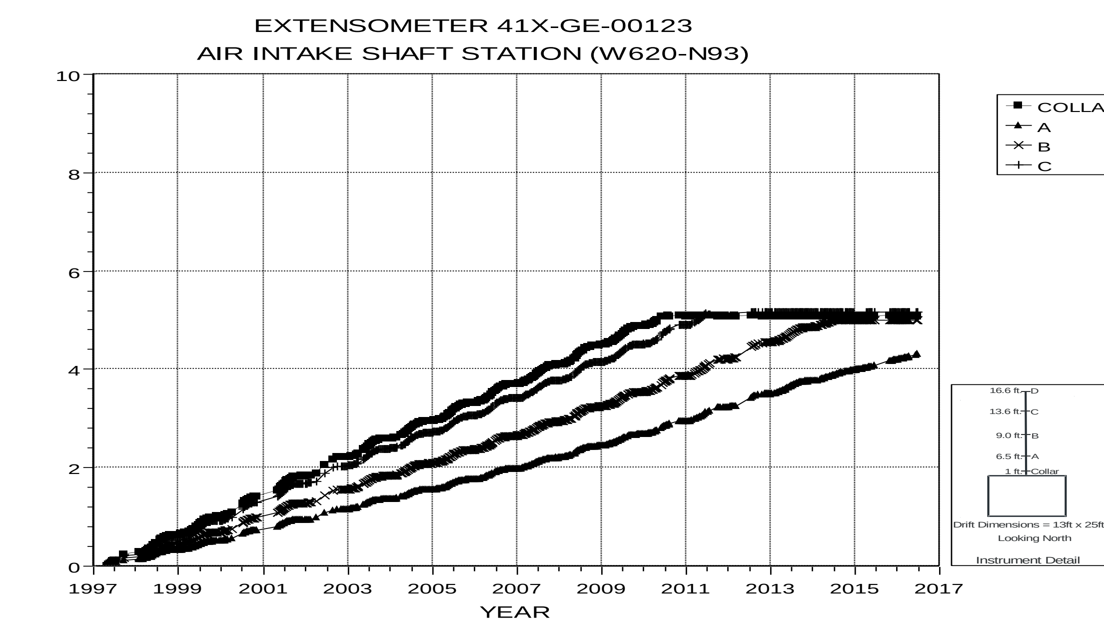

NOTES:
1. Excavation date: January 1988.
2. Anchors 'B', 'C' and the Collar anchor (Anchor 'D') have reached their maximum ranges.
3. Select 'CFI' to view the plot.

Figure 3-10 Extensometer 41X-GE-00123 –

Air Intake Shaft Station at W620 N93 – Roof

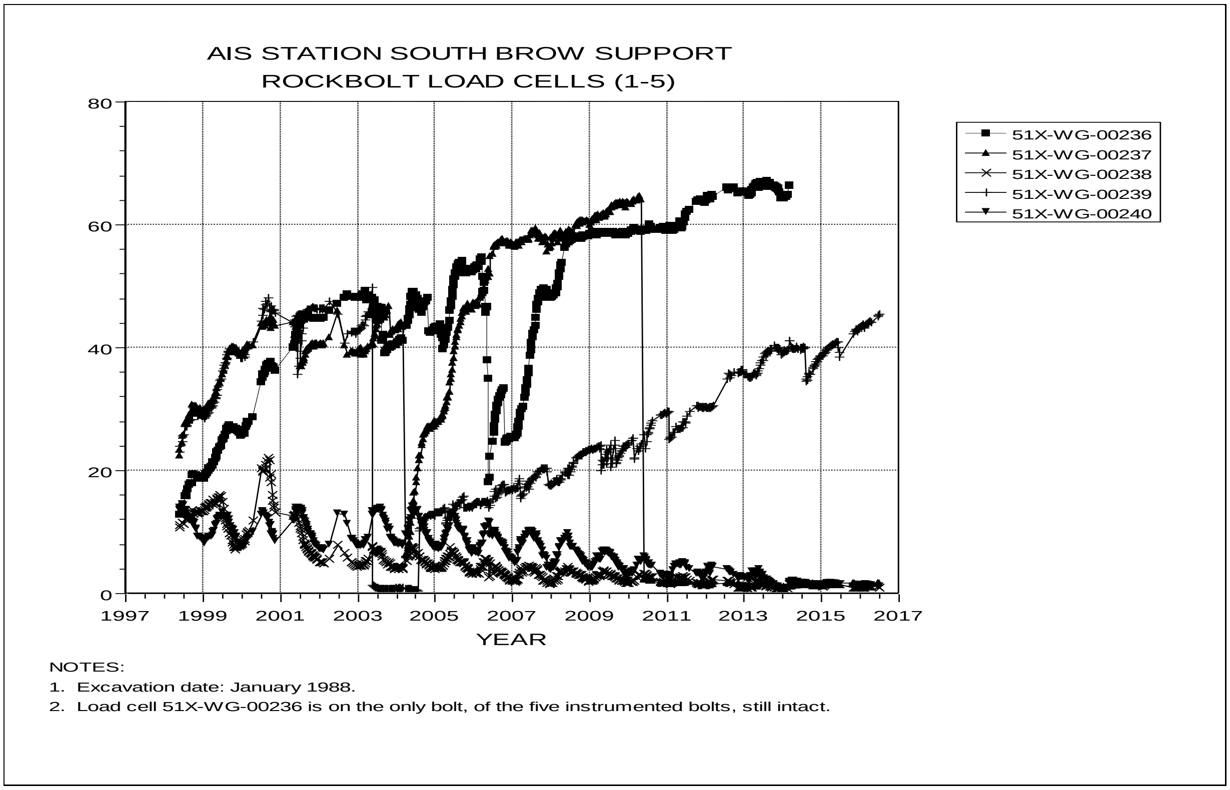

Figure 3-11 Rockbolt Load Cells –
Air Intake Shaft Station – South Brow Support – Bolts (1-5)

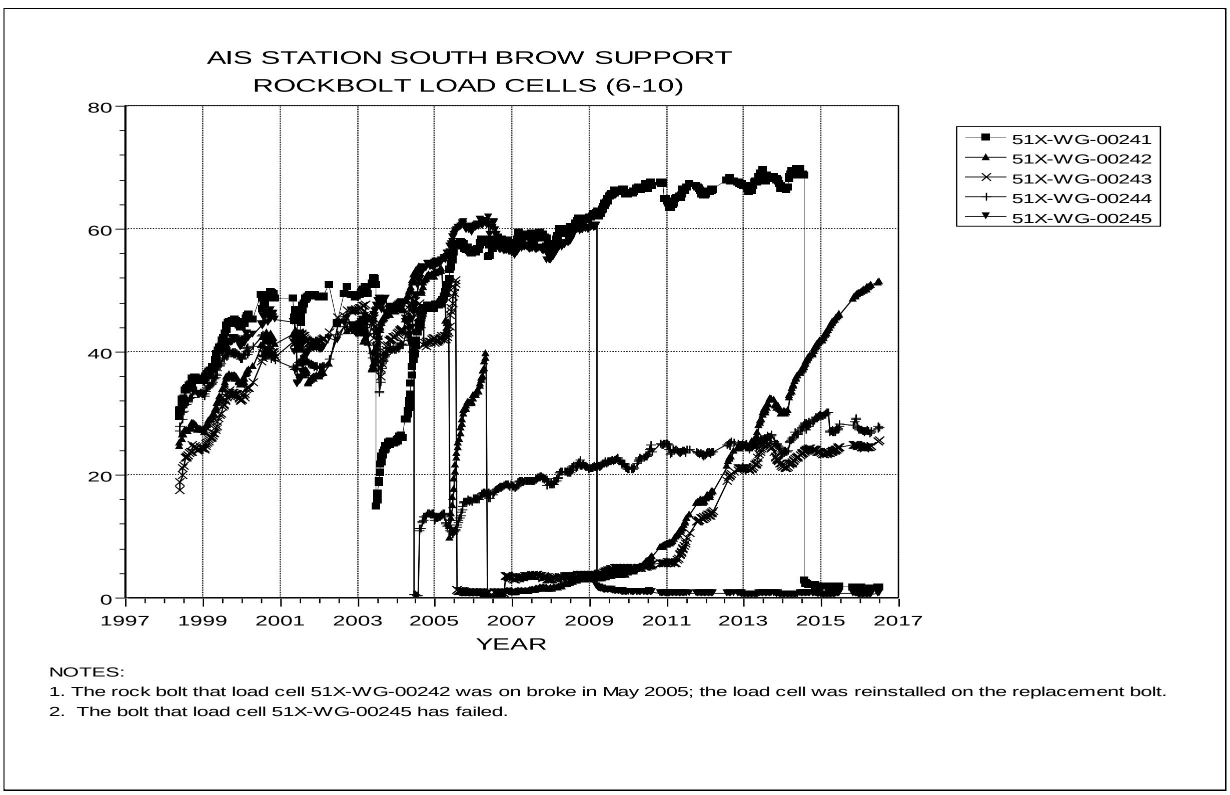

Figure 3-12 Rockbolt Load Cells –
Air Intake Shaft Station – South Brow Support – Bolts (6-10)

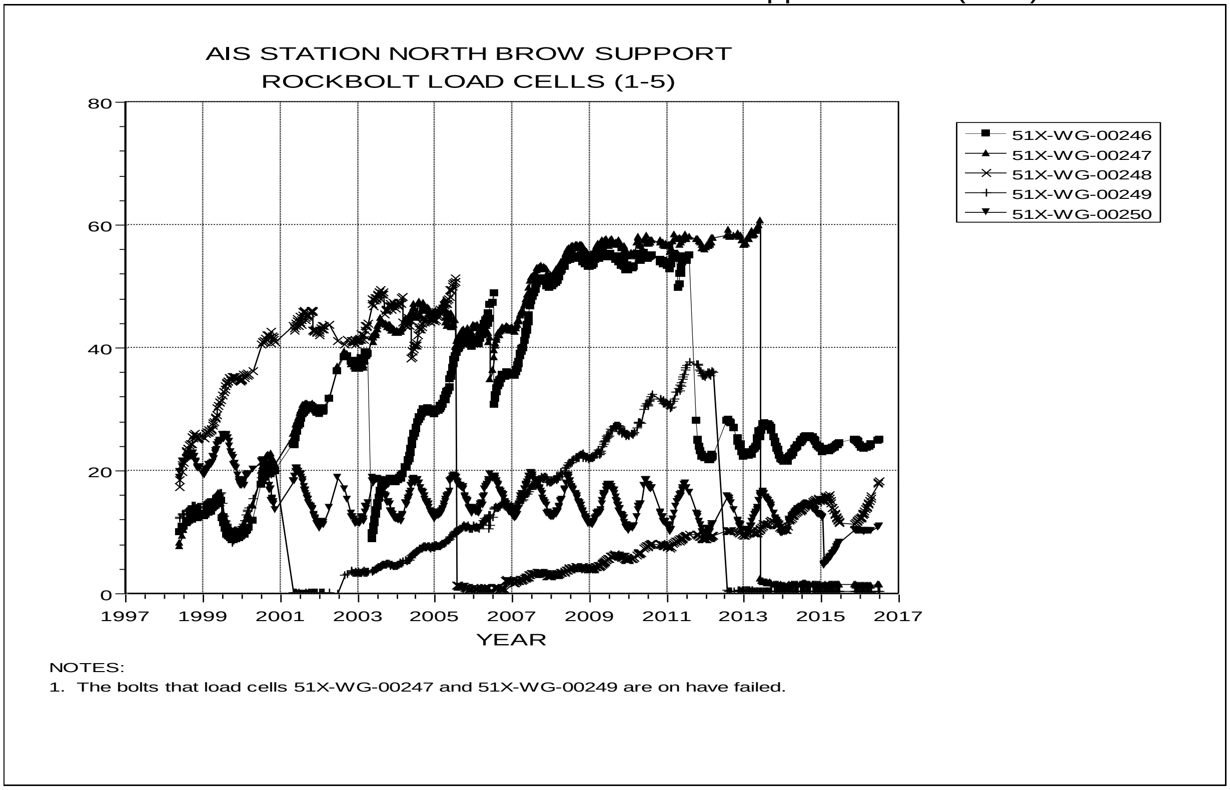

Figure 3-13 Rockbolt Load Cells –
Air Intake Shaft Station – North Brow Support – Bolts (1-5)

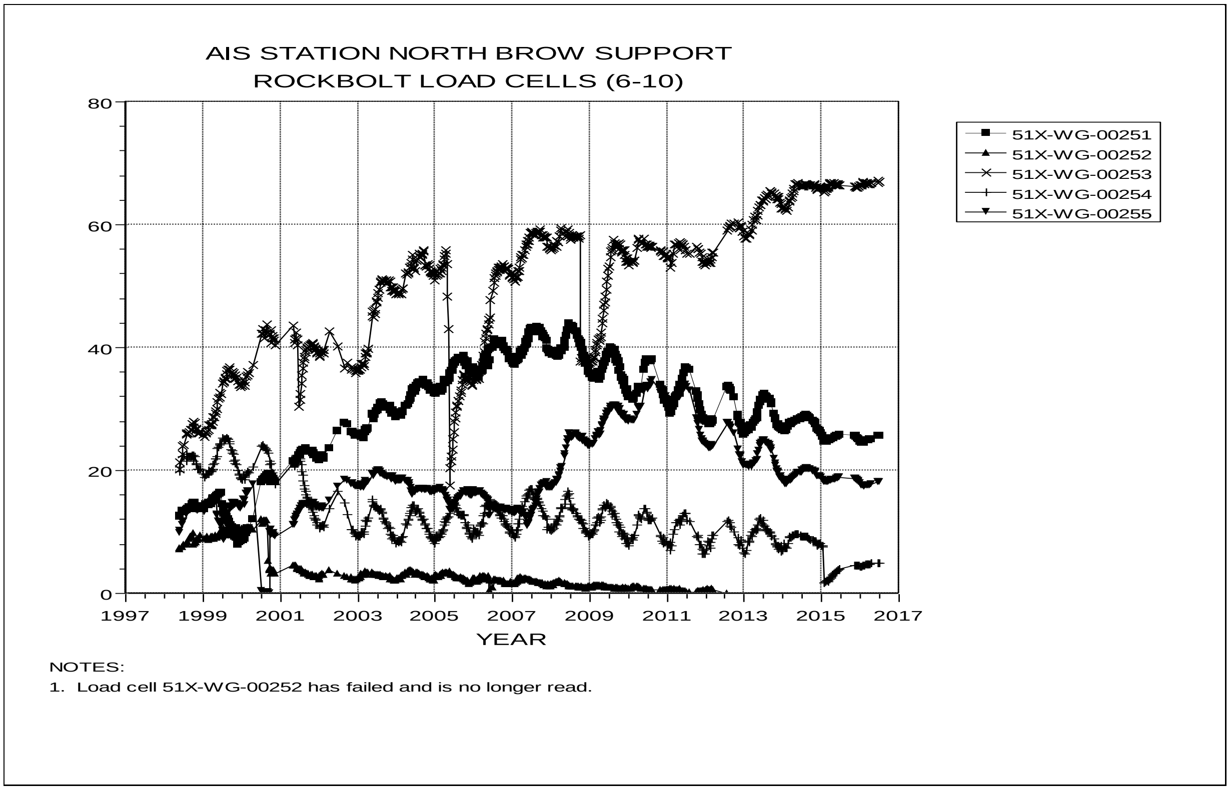

Figure 3-14 Rockbolt Load Cells –
Air Intake Shaft Station – North Brow Support – Bolts (6-10)

This page was intentionally left blank.

4.0 Instrumentation Summary for the Access Drifts

This chapter presents the instrumentation data and data analyses for the access drifts throughout the WIPP underground. Table 4-1 provides the results of analyses performed on the instrument data including displacement, convergence rates, and rock bolt loading.

Figures 4-1 through 4-20 present data from borehole extensometers installed in the access drifts while Figures 4-21 through 4-244 present the convergence point data. Figure 4-245 through 4-249 presents data from joint meters installed at the S1950/E300 overcast and the access drifts.

Table 4-1
Access Drifts Data Analysis

Extensometers

Field Tag	Location	Figure Number	Date of Last Reading	Collar Displacement Relative to Deepest Anchor (inches)	Displacement Rate[4] 2015 to 2016 (in/year)	Displacement Rate 2014 to 2015 (in/year)	Rate Change Percent[4]	Comments
51X-GE-00355	E0-N300	4-1	06/27/16	7.267	0.5	0.4	25%	
51X-GE-00353	E0-N626	4-2	06/27/16	10.024	0.9	0.7	29%	
51X-GE-00352	E0-N940	4-3	06/27/16	9.644	1.0	0.7	43%	
51X-GE-00105-3	E140-N150	4-4	01/08/16	1.689	-7.1	N/A	N/A	
51X-GE-00364	E140-N1266	4-5	06/27/16	8.919	1.4	0.9	56%	
51X-GE-00372	E140-S146	4-6	10/05/15	5.834	0.8	0.7	14%	
51X-GE-00472	E140-S1000	4-7	05/05/16	6.957	0.2	0.3	-33%	
51X-GE-00464	E140-S1025	4-8	05/05/16	5.277	0.0	-0.1	-100%	
51X-GE-00428-2	E140-S1150	4-9	05/05/16	9.311	2.1	3.0	-30%	
51X-GE-00429	E140-S1450	4-10	05/05/16	9.398	3.0	2.7	11%	
51X-GE-00430	E140-S1669	4-11	03/22/16	10.297	2.7	3.7	-27%	
51X-GE-00431	E140-S1775	4-12	05/05/16	9.708	2.7	2.3	17%	
51X-GE-00432	E140-S1850	4-13	05/05/16	8.618	2.3	2.4	-4%	
51X-GE-00374	E300-N1186	4-14	06/27/16	8.65	1.2	0.6	100%	
51X-GE-00388	E300-N1266	4-15	06/27/16	6.752	1.1	0.6	83%	
51X-GE-00373	E300-N1341	4-16	06/27/16	7.036	1.0	0.6	67%	
51X-GE-00474	S1000-E120	4-17	05/05/16	1.638	0.1	0.1	0%	
51X-GE-00473	S1000-E160	4-18	07/09/15	1.342	N/A	0.1	N/A	
51X-GE-00442	S1600-E120	4-19	12/15/15	-0.684	-13.3	-18.9	-30%	
51X-GE-00415	W170-S2998	4-20	08/11/15	10.734	1.0	-12.3	-108%	

Table 4-1
Access Drifts Data Analysis

Convergence Points									
Field Tag	Location	Figure Number	Last Reading 2015-2016 Date	Last Reading 2015-2016 Inches	Cumulative Displacement (inches)	Closure Rate 2015 to 2016 (in/year)	Closure Rate 2014 to 2015 (in/year)	Rate Change Percent	Comments
CORE-W10 A-C	Core Storage W10	4-21	05/05/16	26.69	26.69	1.2	0.8	50%	
CORE-W117 A-C	Core Storage W117	4-21	11/03/15	27.782	27.782	N/A	0.9	0%	
CORE-W133 A-C	Core Storage W133	4-21	02/04/16	28.291	28.291	N/A	N/A	0%	
CORE-W20 A-C	Core Storage W20	4-21	05/05/16	25.491	25.491	1.1	0.8	38%	
CORE-W30 A-C	Core Storage W30	4-21	05/05/16	26.918	26.918	1.2	0.9	33%	
CORE-W51 A-C	Core Storage W51	4-21	05/05/16	31.221	31.221	1.4	1.1	27%	
E0-N75 A-C	E0-N75	4-22	04/06/16	27.865	27.865	2.9	1.5	93%	
E0-N225-2 A-C	E0-N225	4-23	04/06/16	26.531	26.531	2.5	1.2	108%	
E0-N460-3 A-C	E0-N460	4-24	04/06/16	31.906	51.995	2.2	1.7	29%	
E0-N562 A-C	E0-N562	4-25	04/06/16	25.886	25.886	3.2	N/A	0	
E0-N626-4 A-C	E0-N626	4-26	01/08/16	30.437	71.396	2.2	N/A	0	
E0-N780-2 A-C	E0-N780	4-27	04/06/16	26.971	47.393	2.1	1.6	31%	
E0-N940-5 A-C	E0-N940	4-28	04/06/16	28.682	76.734	1.6	2.1	-24%	
E0-N1110-5 A-C	E0-N1110	4-29	4/6/2016	18.851	53.275	0.6	1.2	-47%	
E0-N1266-4 A-C	E0-N1266	4-30	4/6/2016	29.512	29.512	1.3	1.7	-26%	
E140-N5-7 A-C	E140-N5	4-31	04/06/16	8.609	55.502	3.0	2.5	20%	
E140-N150-6 A-C	E140-N150	4-32	04/06/16	5.579	36.325	2.1	1.6	31%	
E140-N220-4 A-C	E140-N220	4-33	04/06/16	8.781	50.938	3.1	2.6	19%	
E140-N355-2 A-C	E140-N355	4-34	04/06/16	21.866	30.41	2.9	2.3	26%	
E140-N460-3 A-C	E140-N460	4-35	04/06/16	30.263	51.094	2.7	2.0	35%	
E140-N562-2 A-C	E140-N562	4-36	04/06/16	31.572	43.389	2.3	2.5	-8%	
E140-N626-3 A-C	E140-N626	4-37	04/06/16	42.153	74.723	2.8	3.3	-15%	
E140-N686-2 A-C	E140-N686	4-38	04/06/16	32.862	46.001	1.8	2.3	-22%	
E140-N780-2 A-C	E140-N780	4-39	09/23/15	37.664	69.421	8.3	2.7	207%	
E140-N940-2 A-C	E140-N940	4-40	04/06/16	39.987	39.987	4.6	3.4	35%	

Table 4-1
Access Drifts Data Analysis (continued)

Convergence Points (continued)

Field Tag	Location	Figure Number	Last Reading 2015-2016 Date	Last Reading 2015-2016 Inches	Cumulative Displacement (inches)	Closure Rate[4] 2015 to 2016 (in/year)	Closure Rate 2014 to 2015 (in/year)	Rate Change Percent[4]	Comments
E140-N1100-2 A-C	E140-N1100	4-41	04/06/16	19.061	38.784	2.3	1.4	64%	
E140-N1266-3 A-C	E140-N1266	4-42	04/06/16	29.865	67.62	3.3	2.3	43%	
E140-N1420-2 A-C	E140-N1420	4-43	04/06/16	20.685	37.155	2.2	1.5	47%	
E140-S90-4 A-C	E140-S90	4-44	04/06/16	18.095	35.808	2.5	N/A	N/A	
E140-S262-5 A-C	E140-S262	4-45	05/03/16	7.043	44.064	1.8	1.5	20%	
E140-S460-6 A-C	E140-S460	4-46	12/10/15	9.394	60.13	-0.8	1.9	-142%	
E140-S460-2 B-D	E140-S460	4-46	05/03/16	31.904	37.848	1.3	0.6	117%	
E140-S550-6 A-C	E140-S550	4-47	05/03/16	10.28	52.247	2.0	1.8	11%	
E140-S700-8 A-D	E140-S700	4-48	05/03/16	12.19	42.23	2.3	2.1	10%	
E140-S700-6 B-C	E140-S700	4-49	05/03/16	12.624	42.656	-2.7	2.4	-213%	
E140-S700-6 E-F	E140-S700	4-50	05/03/16	8.699	28.696	1.5	1.2	25%	
E140-S850-10 A-C	E140-S850	4-51	05/03/16	7.95	65.686	2.6	2.3	13%	
E140-S1000-4 A-C	E140-S1000	4-52	05/03/16	5.319	45.666	1.7	1.5	13%	
E140-S1025-5 A-C	E140-S1025	4-53	05/03/16	5.979	33.386	1.9	1.7	12%	
E140-S1075-5 A-E	E140-S1075	4-54	05/03/16	9.159	37.961	3.1	3.0	3%	
E140-S1075-5 B-D	E140-S1075	4-55	05/03/16	4.108	26.199	1.4	1.2	17%	
E140-S1075-5 H-F	E140-S1075	4-56	05/03/16	6.25	27.57	2.2	1.9	16%	
E140-S1150-5 A-G	E140-S1150	4-57	05/03/16	12.929	83.103	4.6	4.6	0%	
E140-S1150-7 B-F	E140-S1150	4-58	05/03/16	-12.707	19.75	N/A	3.5	N/A	
E140-S1150-6 L-H	E140-S1150	4-59	05/03/16	5.77	31.568	1.7	1.8	-6%	
E140-S1225-5 A-E	E140-S1225	4-60	05/03/16	12.121	48.616	2.4	4.6	-48%	
E140-S1225-5 B-D	E140-S1225	4-61	05/03/16	9.263	45.187	2.8	3.2	-13%	
E140-S1225-4 H-F	E140-S1225	4-62	05/03/16	7.938	33.321	3.1	2.1	48%	
E140-S1300-5 A-C	E140-S1300	4-63	05/03/16	4.522	42.465	-0.4	2.3	-117%	
E140-S1378-4 A-E	E140-S1375/1378	4-64	05/03/16	11.736	54.277	3.7	3.5	6%	
E140-S1378-4 B-D	E140-S1378	4-65	05/03/16	6.995	6.995	1.9	2.7	-30%	

Table 4-1
Access Drifts Data Analysis (continued)

Convergence Points (continued)

Field Tag	Location	Figure Number	Last Reading 2015-2016		Cumulative Displacement (inches)	Closure Rate 2015 to 2016 (in/year)	Closure Rate 2014 to 2015 (in/year)	Rate Change Percent	Comments
			Date	Inches					
E140-S1378-4 H-F	E140-S1375/1378	4-66	05/03/16	14.151	60.013	3.3	5.3	-38%	
E140-S1450-6 A-G	E140-S1450/1456	4-67	05/03/16	13.178	93.985	5.0	3.9	28%	
E140-S1450-4 B-F	E140-S1450/1456	4-68	5/3/2016	6.633	54.121	1.3	2.2	-40%	
E140-S1450-3 I-E	E140-S1450/1456	4-69	05/03/16	8.633	26.725	1.5	1.0	50%	
E140-S1450-4 L-H	E140-S1450/1456	4-70	05/03/16	10.507	51.022	4.3	3.0	43%	
E140-S1534-4 A-E	E140-S1534	4-71	05/03/16	7.869	61.352	1.0	2.7	-63%	
E140-S1534-5 B-D	E140-S1534	4-72	05/03/16	8.263	42.81	3.9	2.2	77%	
E140-S1534-4 H-F	E140-S1534	4-73	03/18/16	8.328	46.266	2.4	2.6	-8%	
E140-S1600-7 A-C	E140-S1600	4-74	05/03/16	8.533	50.479	3.8	2.4	58%	
E140-S1687-4 A-E	E140-S1687	4-75	05/03/16	11.361	60.5	3.5	3.6	-3%	
E140-S1687-4 B-D	E140-S1687	4-76	05/03/16	8.091	44.833	2.8	2.5	12%	
E140-S1687-4 H-F	E140-S1687	4-77	05/03/16	10.094	46.862	3.1	3.3	-6%	
E140-S1775-4 A-G	E140-S1775	4-78	05/03/16	13.042	81.228	4.0	4.1	-2%	
E140-S1775-5 B-F	E140-S1775	4-79	05/03/16	12.937	70.35	4.1	4.1	0%	
E140-S1775-3 I-E	E140-S1775	4-80	05/03/16	17.113	31.334	2.1	1.3	62%	
E140-S1775-4 L-H	E140-S1775	4-81	05/03/16	6.902	39.487	2.4	2.4	0%	
E140-S1862-4 A-E	E140-S1862	4-82	05/03/16	12.04	65.038	3.6	3.7	-3%	
E140-S1862-4 B-D	E140-S1862	4-83	05/03/16	13.016	61.677	4.0	4.1	-2%	
E140-S1862-4 H-F	E140-S1862	4-84	05/03/16	6.6	32.953	2.0	1.9	5%	
E140-S1950-7 A-C	E140-S1950	4-85	05/03/16	13.114	69.504	4.1	4.4	-7%	
E140-S2007-8 A-C	E140-S2007	4-86	06/02/16	16.283	60.81	4.7	5.0	-6%	
E140-S2634-2 A-C	E140-S2634	4-87	06/02/16	15.539	72.514	4.5	4.5	0%	
E140-S2750-4 A-C	E140-S2750	4-88	06/02/16	11.196	37.531	3.9	3.3	18%	
E140-S2833-3 A-C	E140-S2833	4-89	06/02/16	33.837	54.636	3.9	4.5	-13%	
E140-S2915-3 A-C	E140-S2915	4-90	06/02/16	22.913	49.129	2.9	2.6	12%	
E140-S2998-3 A-C	E140-S2998	4-91	06/02/16	25.762	52.917	3.4	3.1	10%	
E140-S3080-2 A-C	E140-S3080	4-92	06/02/16	28.402	44.541	4.3	5.0	-14%	
E140-S3195-2 A-C	E140-S3195	4-93	06/02/16	31.01	57.265	4.4	5.1	-14%	

Table 4-1
Access Drifts Data Analysis (continued)

Convergence Points (continued)

Field Tag	Location	Figure Number	Last Reading 2015-2016 Date	Last Reading 2015-2016 Inches	Cumulative Displacement (inches)	Closure Rate[4] 2015 to 2016 (in/year)	Closure Rate 2014 to 2015 (in/year)	Rate Change Percent[4]	Comments
E140-S3295-2 A-C	E140-S3295	4-94	06/02/16	19.226	26.931	3.0	2.9	3%	
E140-S3325 A-C	E140-S3325	4-95	06/02/16	26.187	26.187	2.9	2.8	4%	
E140-S3395-2 A-C	E140-S3395	4-96	06/02/16	26.02	41.178	3.3	3.5	-6%	
E140-S3480-2 A-C	E140-S3480	4-97	06/02/16	32.995	47.295	4.8	5.5	-13%	
E140-S3565-2 A-C	E140-S3565	4-98	06/02/16	26.837	38.165	4.3	5.9	-27%	
E140-S3650-2 A-C	E140-S3650	4-99	06/02/16	16.231	22.851	3.0	2.6	15%	
E300-N45-2 A-E	E300-N45	4-100	04/06/16	5.464	38.345	2.2	1.8	22%	
E300-N45-2 H-F	E300-N45	4-101	04/06/16	4.826	34.365	2.0	N/A	N/A	
E300-N170-3 A-E	E300-N170	4-102	04/06/16	6.072	39.546	2.5	2.0	25%	
E300-N170-3 H-F	E300-N170	4-102	04/06/16	5.035	35.33	2.1	1.6	31%	
E300-N1100-2 A-C	E300-N1100	4-103	4/6/2016	6.016	8.241	2.8	1.6	73%	
E300-N1262-4 A-C	E300-N1262	4-104	04/06/16	11.35	33.413	3.4	2.7	26%	
E300-N1341-3 A-C	E300-N1341	4-105	04/06/16	10.154	30.752	3.4	2.5	36%	
E300-S45-3 A-E	E300-S45	4-106	04/06/16	4.456	31.66	1.7	1.4	21%	
E300-S45-3 B-D	E300-S45	4-107	04/06/16	4.988	30.179	1.9	1.6	19%	
E300-S45-3 H-F	E300-S45	4-108	04/06/16	3.817	27.066	1.5	1.2	25%	
E300-S90-3 A-C	E300-S90	4-109	04/06/16	3.496	23.773	1.5	1.2	25%	
E300-S250-2 A-C	E300-S250	4-110	04/06/16	12.3	16.685	1.0	0.6	67%	
E300-S250-2 B-D	E300-S250	4-110	01/08/16	13.02	17.066	1.3	N/A	N/A	
E300-S700-2 A-C	E300-S700	4-111	05/24/16	7.796	27.526	1.6	1.5	7%	
E300-S850-2 A-E	E300-S850	4-112	05/24/16	3.997	19.079	0.8	0.6	33%	
E300-S850-2 B-D	E300-S850	4-113	01/18/16	3.737	15.038	2.2	0.6	267%	
E300-S850-2 H-F	E300-S850	4-114	01/18/16	2.978	13.441	0.7	0.7	0%	
E300-S1000-2 A-C	E300-S1000	4-115	05/24/16	5.45	24.995	1.0	0.8	25%	
E300-S1150-4 A-E	E300-S1150	4-116	05/24/16	11.681	28.76	2.0	1.8	11%	
E300-S1150-4 B-D	E300-S1150	4-117	01/18/16	3.777	15.882	0.9	0.8	13%	
E300-S1150-4 H-F	E300-S1150	4-118	01/18/16	4.143	15.899	0.9	0.9	0%	

Table 4-1
Access Drifts Data Analysis (continued)

Convergence Points (continued)

Field Tag	Location	Figure Number	Last Reading 2015-2016		Cumulative Displacement (inches)	Closure Rate[4] 2015 to 2016 (in/year)	Closure Rate 2014 to 2015 (in/year)	Rate Change Percent[4]	Comments
			Date	Inches					
E300-S1300-2 A-C	E300-S1300	4-119	05/24/16	9.768	23.302	1.8	1.7	6%	
E300-S1450-2 A-C	E300-S1450	4-120	05/24/16	10.17	19.152	2.3	1.7	35%	
E300-S1687-2 A-C	E300-S1687	4-121	05/24/16	7.932	17.789	1.8	0.8	125%	
E300-S1775-2 A-C	E300-S1775	4-122	05/24/16	9.487	18.282	2.2	1.9	16%	
E300-S1862-2 A-C	E300-S1862	4-123	05/24/16	10.727	20.18	2.0	1.9	5%	
E300-S2065-2 A-C	E300-S2065	4-124	05/24/16	11.702	22.813	2.3	2.7	-15%	
E300-S2275-2 A-C	E300-S2275	4-125	05/24/16	16.044	29.47	3.0	2.8	7%	
E300-S2350-2 A-C	E300-S2350	4-126	05/24/16	23.959	39.523	4.9	4.7	4%	
E300-S2425-2 A-C	E300-S2425	4-127	05/24/16	20.956	37.178	4.4	4.3	2%	
E300-S2634-2 A-C	E300-S2634	4-128	05/24/16	11.954	25.339	2.5	2.2	14%	
E300-S2833-2 A-C	E300-S2833	4-129	05/24/16	16.571	32.863	3.1	5.3	-42%	
E300-S2916-4 A-C	E300-S2916	4-130	04/05/16	13.127	38.197	2.1	2.3	-10%	
E300-S2998-4 A-C	E300-S2998	4-131	05/24/16	22.662	57.412	4.2	6.0	-30%	
E300-S3195 A-C	E300-S3195	4-132	05/24/16	40.369	40.369	4.8	6.6	-27%	
E300-S3480 A-C	E300-S3480	4-133	04/05/16	22.704	22.704	3.5	2.8	25%	
N140-E90-3 A-C	N140-E90	4-134	4/6/2016	1.742	20.377	1.0	0.6	63%	
N215-W500-2 A-C	N215-W500	4-135	04/06/16	16.778	35.107	1.2	0.9	33%	
N215-W500-2 B-D	N215-W500	4-136	04/06/16	16.118	22.936	1.1	N/A	N/A	
N215-W620-2 A-C	N215-W620	4-137	04/06/16	12.924	29.142	1.0	0.6	67%	
N250-E220-3 A-E	N250-E220	4-138	04/06/16	7.825	47.783	3.2	2.6	23%	
N250-E220-3 B-D	N250-E220	4-139	01/08/16	4.314	40.454	2.1	1.5	40%	
N250-E220-3 H-F	N250-E220	4-140	04/06/16	4.591	32.879	1.9	1.4	36%	
N300-W170-2 A-C	N300-W170	4-141	04/06/16	20.507	42.767	1.6	1.2	33%	
N300-W170-2 B-D	N300-W170	4-141	04/06/16	21.429	29.624	1.3	N/A	N/A	
N460-E70-3 A-C	N460-E70	4-142	04/06/16	22.04	38.486	2.8	1.1	155%	
N780-E70 A-C	N780-E70	4-143	01/08/16	18.488	18.488	3.8	0.9	322%	
S90-W120 A-C	S90-W120	4-144	05/05/16	10.442	10.442	0.6	0.4	50%	
S90-W120 B-D	S90-W120	4-144	05/05/16	11.228	11.228	0.7	0.3	133%	

Table 4-1
Access Drifts Data Analysis (continued)

Convergence Points (continued)									
Field Tag	Location	Figure Number	Last Reading 2015-2016 Date	Last Reading 2015-2016 Inches	Cumulative Displacement (inches)	Closure Rate[4] 2015 to 2016 (in/year)	Closure Rate 2014 to 2015 (in/year)	Rate Change Percent[4]	Comments
S90-W400-3 A-C	S90-W400	4-145	05/10/16	1.393	20.245	0.6	0.4	50%	
S90-W400-3 B-D	S90-W400	4-145	05/10/16	1.407	19.744	0.6	0.2	200%	
S90-W590-2 A-C	S90-W590	4-146	05/10/16	6.666	15.995	0.6	0.4	50%	
S90-W590-2 B-D	S90-W590	4-146	05/10/16	11.273	15.08	0.5	0.3	67%	
S90-W620 A-C	S90-W620	4-147	05/10/16	30.011	30.011	0.9	0.4	125%	
S90-W770 A-C	S90-W770	4-148	05/10/16	21.376	21.376	0.8	0.7	14%	
S90-W770-3 B-D	S90-W770	4-148	05/10/16	6.378	19.699	0.7	0.5	40%	
S90-W905 A-C	S90-W905	4-149	05/10/16	19.479	19.479	1.2	1.1	9%	
S105-W920 A-C	S105-W920	4-150	05/10/16	7.769	7.769	0.9	0.8	13%	
S700-E55-2 A-C	S700-E55	4-151	2/4/2016	10.274	14.416	1.7	2.1	-19%	
S1000-E58-4 A-C	S1000-E58	4-152	05/03/16	14.546	30.012	1.2	N/A	N/A	
S1000-E120-3 A-C	S1000-E120	4-153	05/03/16	12.814	21.254	1.0	0.9	11%	
S1000-E160 -3 A-C	S1000-E160	4-154	05/03/16	7.552	15.762	0.8	0.5	60%	
S1000-W98-2 A-C	S1000-W98	4-155	05/03/16	23.693	42.441	2.0	N/A	N/A	
S1300-E120 A-C	S1300-E120	4-156	05/03/16	18.943	18.943	0.9	0.8	13%	
S1300-E160 A-C	S1300-E160	4-157	05/03/16	31.861	31.861	2.0	1.8	11%	
S1300-W100-3 A-C	S1300-W100	4-158	05/03/16	22.85	46.853	0.7	N/A	N/A	

Table 4-1
Access Drifts Data Analysis (continued)

Convergence Points (continued)

Field Tag	Location	Figure Number	Last Reading 2014-2015 Date	Last Reading 2014-2015 Inches	Cumulative Displacement (inches)	Closure Rate[4] 2015 to 2016 (in/year)	Closure Rate 2014 to 2015 (in/year)	Rate Change Percent[4]	Comments
S1600-E110-2 A-C	S1600-E110	4-159	05/03/16	3.357	20.079	1.1	0.9	22%	
S1600-E170-2 A-C	S1600-E170	4-160	05/03/16	3.687	21.998	1.2	1.0	20%	
S1950-E113-4 A-C	S1950-E113	4-161	05/03/16	14.558	18.434	1.2	1.2	0%	
S1950-E281-3 A-C	S1950-E281	4-162	05/24/16	20.691	27.233	1.4	1.4	0%	
S1950-E284-3 A-C	S1950-E284	4-163	05/24/16	21.285	27.897	1.5	1.5	0%	
S2180-E220 A-C	S2180-E220	4-164	05/24/16	22.583	22.583	1.8	1.8	0%	
S2180-W100-3 A-C	S2180-W100	4-165	06/09/16	19.383	37.566	3.6	N/A	N/A	
S2520-E220 A-C	S2520-E220	4-166	05/24/16	27.536	27.536	1.6	1.6	0%	
S2520-W100-2 A-C	S2520-W100	4-167	08/20/15	11.396	31.076	N/A	3.0	N/A	
S2750-E55-2 A-C	S2750-E55	4-168	06/02/16	21.764	38.445	2.7	2.8	-4%	
S2750-E220-2 A-C	S2750-E220	4-169	05/24/16	14.369	35.766	2.5	4.2	-40%	
S2750-W93-3 A-C	S2750-W93	4-170	06/02/16	7.811	40.219	2.4	2.9	-17%	
S3080-E220-2 A-C	S3080-E220	4-171	05/24/16	32.235	34.94	3.3	4.8	-31%	
S3080-W100 A-C	S3080-W100	4-172	06/02/16	45.078	45.078	4.0	5.0	-20%	
S3310-E55 A-C	S3310-E55	4-173	06/02/16	35.397	35.397	2.8	4.0	-30%	
S3310-E220 A-C	S3310-E220	4-174	05/24/16	42.145	42.145	2.7	5.2	-48%	
S3310-W100-3 A-C	S3310-W100	4-175	06/02/16	36.063	42.341	4.3	4.9	-12%	
S3650-E55-2 A-C	S3650-E55	4-176	06/02/16	19.577	22.91	4.4	3.5	26%	
S3650-E220-2 A-C	S3650-E220	4-177	06/02/16	22.203	25.56	4.7	4.2	12%	
S3650-W100-2 A-C	S3650-W100	4-178	6/2/2016	20.261	26.278	3.5	2.8	24%	
W30-S120-3 A-C	W30-S120	4-179	05/03/16	2.122	29.768	0.8	0.8	0%	
W30-S250-5 A-C	W30-S250	4-180	05/03/16	11.685	37.918	1.1	0.9	22%	
W30-S400-2 A-C	W30-S400	4-181	05/03/16	9.003	26.831	0.7	0.7	0%	
W30-S500-3 A-C	W30-S500	4-182	05/03/16	2.481	32.888	1.1	0.9	22%	
W30-S700-5 A-C	W30-S700	4-183	05/03/16	12.136	46.413	1.6	1.5	7%	
W30-S850-6 A-E	W30-S850	4-184	05/03/16	4.467	34.484	1.8	1.5	20%	
W30-S850-5 B-D	W30-S850	4-185	05/03/16	2.95	23.359	1.1	0.9	22%	

Table 4-1
Access Drifts Data Analysis (continued)

Convergence Points (continued)

Field Tag	Location	Figure Number	Last Reading 2014-2015		Cumulative Displacement (inches)	Closure Rate 2015 to 2016 (in/year)	Closure Rate 2014 to 2015 (in/year)	Rate Change Percent	Comments
			Date	Inches					
W30-S850-4 H-F	W30-S850	4-186	05/03/16	4.652	26.849	1.8	1.6	13%	
W30-S1000-5 A-C	W30-S1000	4-187	05/03/16	10.937	49.116	1.5	1.7	-12%	
W30-S1150-2 A-C	W30-S1150	4-188	05/03/16	25.273	26.774	7.2	4.0	80%	
W30-S1300-2 A-C	W30-S1300	4-189	05/03/16	11.674	32.912	1.9	1.7	12%	
W30-S1453-2 A-C	W30-S1453	4-190	11/03/15	15.161	29.228	2.8	3.1	-10%	
W30-S1600-3 A-C	W30-S1600	4-191	05/03/16	14.875	34.005	2.5	2.4	4%	
W30-S1775-4 A-C	W30-S1775	4-192	09/15/15	6.673	28.014	N/A	3.0	N/A	
W30-S1950-3 A-C	W30-S1950	4-193	05/03/16	8.066	37.74	3.5	2.8	25%	
W30-S2067-4 A-C	W30-S2067	4-194	02/04/16	8.223	35.163	3.2	2.8	14%	
W30-S2275-4 A-C	W30-S2275	4-195	12/08/15	18.613	39.293	5.3	3.8	39%	
W30-S2350-4 A-C	W30-S2350	4-196	12/08/15	23.879	43.188	5.5	5.3	4%	
W30-S2425-4 A-C	W30-S2425	4-197	12/08/15	16.136	34.424	4.1	3.7	11%	
W30-S2520-4 A-C	W30-S2520	4-198	08/20/15	5.619	34.608	N/A	3.3	N/A	
W30-S2685-3 A-C	W30-S2685	4-199	06/02/16	14.882	33.772	2.7	2.5	8%	
W30-S2750-3 A-C	W30-S2750	4-200	06/02/16	12.341	31.055	4.8	3.7	30%	
W30-S2833-4 A-C	W30-S2833	4-201	06/02/16	11.631	34.73	2.6	3.1	-16%	
W30-S2916-2 A-C	W30-S2916	4-202	06/02/16	11.754	52.803	2.9	3.5	-17%	
W30-S2998-2 A-C	W30-S2998	4-203	06/02/16	14.986	39.43	4.5	5.3	-15%	
W30-S3080 A-C	W30-S3080	4-204	06/02/16	33.336	33.336	2.7	2.4	13%	
W30-S3195 A-C	W30-S3195	4-205	06/02/16	32.595	32.595	3.5	3.8	-8%	
W30-S3310 A-C	W30-S3310	4-206	06/02/16	24.497	24.497	2.0	1.8	11%	
W30-S3650-2 A-C	W30-S3650	4-207	06/02/16	15.133	20.785	2.2	2.3	-4%	
W170-N150-3 A-C	W170-N150	4-208	05/05/16	5.122	13.474	0.7	0.5	40%	
W170-S5-2 A-C	W170-S5	4-209	05/05/16	1.419	17.615	0.6	0.5	20%	
W170-S5-2 B-D	W170-S5	4-209	05/05/16	12.831	20.597	0.8	0.5	60%	

Table 4-1
Access Drifts Data Analysis (continued)

Convergence Points (continued)

Field Tag	Location	Figure Number	Last Reading 2014-2015		Cumulative Displacement (inches)	Closure Rate[4] 2015 to 2016 (in/year)	Closure Rate 2014 to 2015 (in/year)	Rate Change Percent[4]	Comments
			Date	Inches					
W170-S90-3 A-C	W170-S90	4-210	05/05/16	12.686	19.888	0.9	0.7	29%	
W170-S232-2 A-C	W170-S232	4-211	05/05/16	9.315	14.904	0.6	0.5	20%	
W170-S232-2 B-D	W170-S232	4-211	05/05/16	12.766	15.408	0.7	0.4	75%	
W170-S400 A-C	W170-S400	4-212	05/05/16	18.325	18.325	0.9	0.6	50%	
W170-S560-4 A-C	W170-S560	4-213	05/05/16	5.932	16.751	0.8	0.7	14%	
W170-S560-3 B-D	W170-S560	4-213	11/03/15	4.959	17.787	N/A	0.6	N/A	
W170-S700-3 A-C	W170-S700	4-214	05/05/16	2.404	27.682	1.1	0.9	22%	
W170-S850-8 A-E	W170-S850	4-215	05/05/16	1.776	22.73	0.8	0.6	33%	
W170-S850-8 B-D	W170-S850	4-216	02/04/16	1.465	17.656	0.8	0.5	60%	
W170-S850-3 C-G	W170-S850	4-217	05/05/16	15.898	26.711	1.0	0.5	100%	
W170-S850-8 H-F	W170-S850	4-218	02/04/16	1.285	15.744	0.7	0.5	40%	
W170-S1000-3 A-C	W170-S1000	4-219	05/05/16	8.794	31.707	1.3	1.0	30%	
W170-S1150-5 A-E	W170-S1150	4-220	05/05/16	2.16	27.201	1.0	0.8	25%	
W170-S1150-5 B-D	W170-S1150	4-221	02/04/16	1.854	19.853	1.0	0.7	43%	
W170-S1150-2 C-G	W170-S1150	4-222	05/05/16	18.393	29.97	1.2	0.8	50%	
W170-S1150-3 H-F	W170-S1150	4-223	02/04/16	2.109	19.266	1.9	0.7	171%	
W170-S1300-4 A-C	W170-S1300	4-224	05/05/16	16.135	37.093	2.4	2.0	20%	
W170-S1445-4 A-C	W170-S1445	4-225	05/05/16	13.912	25.204	2.1	1.9	11%	
W170-S1600-4 A-C	W170-S1600	4-226	05/05/16	16.86	31.625	3.1	2.9	7%	
W170-S1779-3 A-C	W170-S1779	4-227	05/05/16	14.688	29.659	2.4	2.2	9%	
W170-S1950-3 A-C	W170-S1950	4-228	05/03/16	12.527	25.708	1.9	1.8	6%	
W170-S2180-3 A-C	W170-S2180	4-229	06/09/16	9.418	32.982	2.3	N/A	N/A	
W170-S2275 A-C	W170-S2275	4-230	06/09/16	22.733	22.733	1.9	1.9	0%	
W170-S2350 A-C	W170-S2350	4-231	06/09/16	29.847	29.847	2.6	2.4	8%	
W170-S2425 A-C	W170-S2425	4-232	06/09/16	25.262	25.262	1.8	1.8	0%	
W170-S2520-2 A-C	W170-S2520	4-233	08/12/15	13.443	34.038	N/A	3.6	N/A	

Table 4-1
Access Drifts Data Analysis (continued)

Convergence Points (continued)									
Field Tag	Location	Figure Number	Last Reading 2014-2015		Cumulative Displacement (inches)	Closure Rate[4] 2015 to 2016 (in/year)	Closure Rate[4] 2014 to 2015 (in/year)	Rate Change Percent[4]	Comments
			Date	Inches					
W170-S2685-2 A-C	W170-S2685	4-234	06/02/16	29.957	31.803	2.0	N/A	N/A	
W170-S2833-3 A-C	W170-S2833	4-235	6/2/2016	13.333	51.246	6.2	5.6	11%	
W170-S2916 A-C	W170-S2916	4-236	06/02/16	39.246	39.246	3.0	3.0	0%	
W170-S2998-2 A-C	W170-S2998	4-237	06/02/16	9.233	51.248	3.3	3.1	6%	
W170-S3080 A-C	W170-S3080	4-238	06/02/16	36.921	36.921	3.4	3.2	6%	
W170-S3195 A-C	W170-S3195	4-239	06/02/16	38.198	38.198	4.1	4.4	-7%	
W170-S3310 A-C	W170-S3310	4-240	06/02/16	28.379	28.379	2.3	2.1	10%	
W170-S3395 A-C	W170-S3395	4-241	06/02/16	36.365	36.365	3.0	3.3	-9%	
W170-S3480 A-C	W170-S3480	4-242	06/02/16	46.053	46.053	6.0	6.1	-2%	
W170-S3565 A-C	W170-S3565	4-243	06/02/16	23.197	23.197	3.0	2.4	25%	
W170-S3650-2 A-C	W170-S3650	4-244	06/02/16	14.684	22.329	2.3	2.1	10%	

Table 4-1
Access Drifts Data Analysis (continued)

Joint Meters

Field Tag	Location	Figure Number	Date	Cumulative Displacement (inches)	Closure Rate 2015 to 2016 (in/year) [4]	Closure Rate 2014 to 2015 (in/year)	Rate Change Percent[4]	Comments
51X-CG-02706	S1950-E300	4-245	05/05/16	2.9	0.3	N/A	N/A	
51X-CG-02707	S1950-E300	4-245	05/05/16	2.4	0.1	N/A	N/A	
51X-CG-02876-2	E140-S1505	4-246	05/05/16	-0.3	0.0	-0.008	-150%	
51X-CG-02883-3	E140-S1529	4-247	05/05/16	-0.3	-0.2	-0.048	258%	
51X-CG-02885-2	E140-S1545	4-248	05/05/16	0.9	0.1	0.09	-20%	
51X-CG-02875-2	E140-S1795	4-249	05/05/16	0.6	0.0	0.051	-90%	

[4] N/A – Insufficient data available to perform the calculation. This is usually due to the inability to read the instruments because of activities such as the removal of an instrument due to floor, rib or back trimming; locations blocked by equipment or waste disposal; installation timing, access issues, etc.

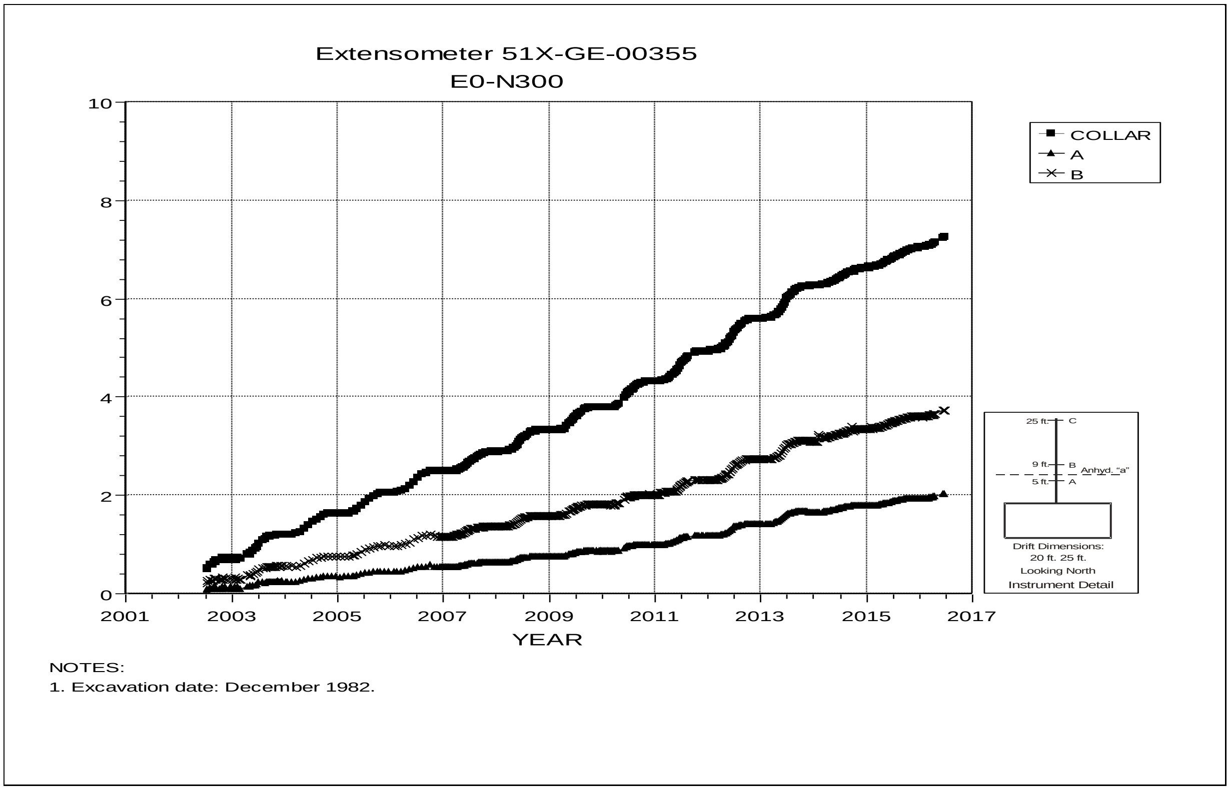

Figure 4-1 Extensometer 51X-GE-00355 –
E0 N300 – Roof

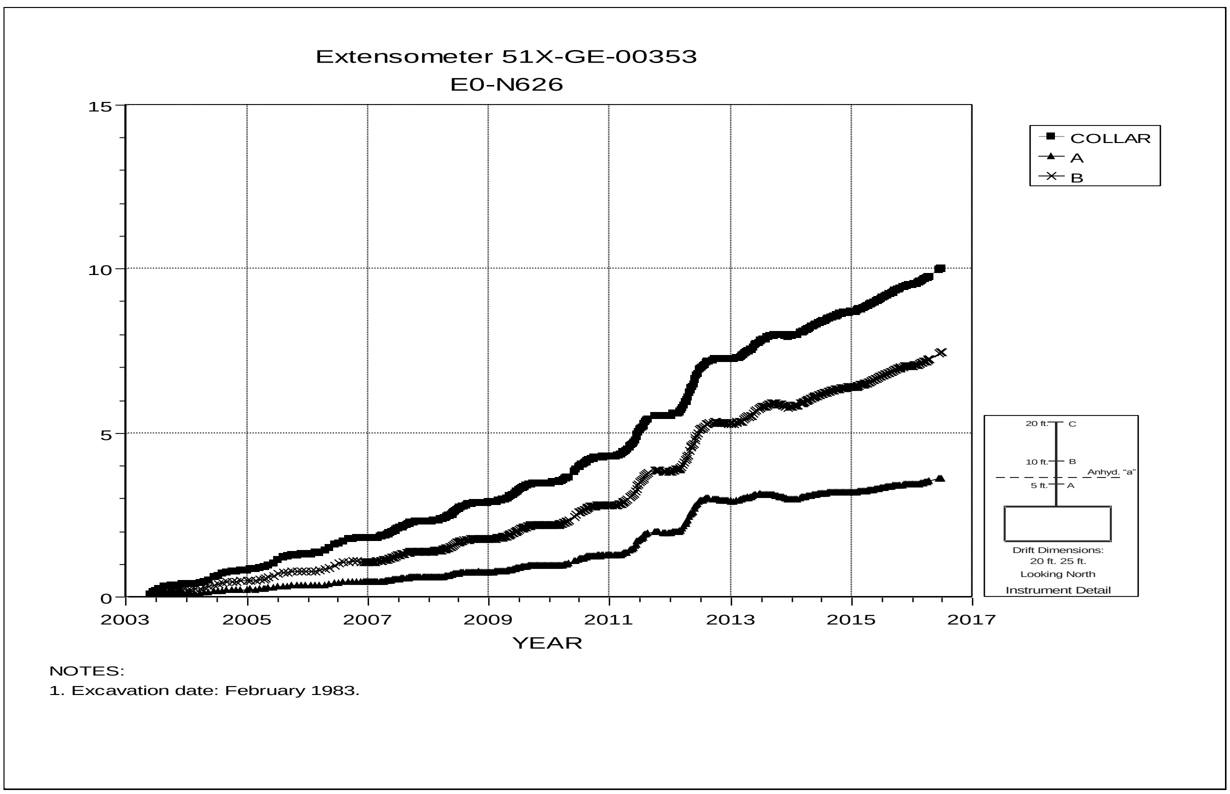

Figure 4-2 Extensometer 51X-GE-00353 –
E0 N626 – Roof

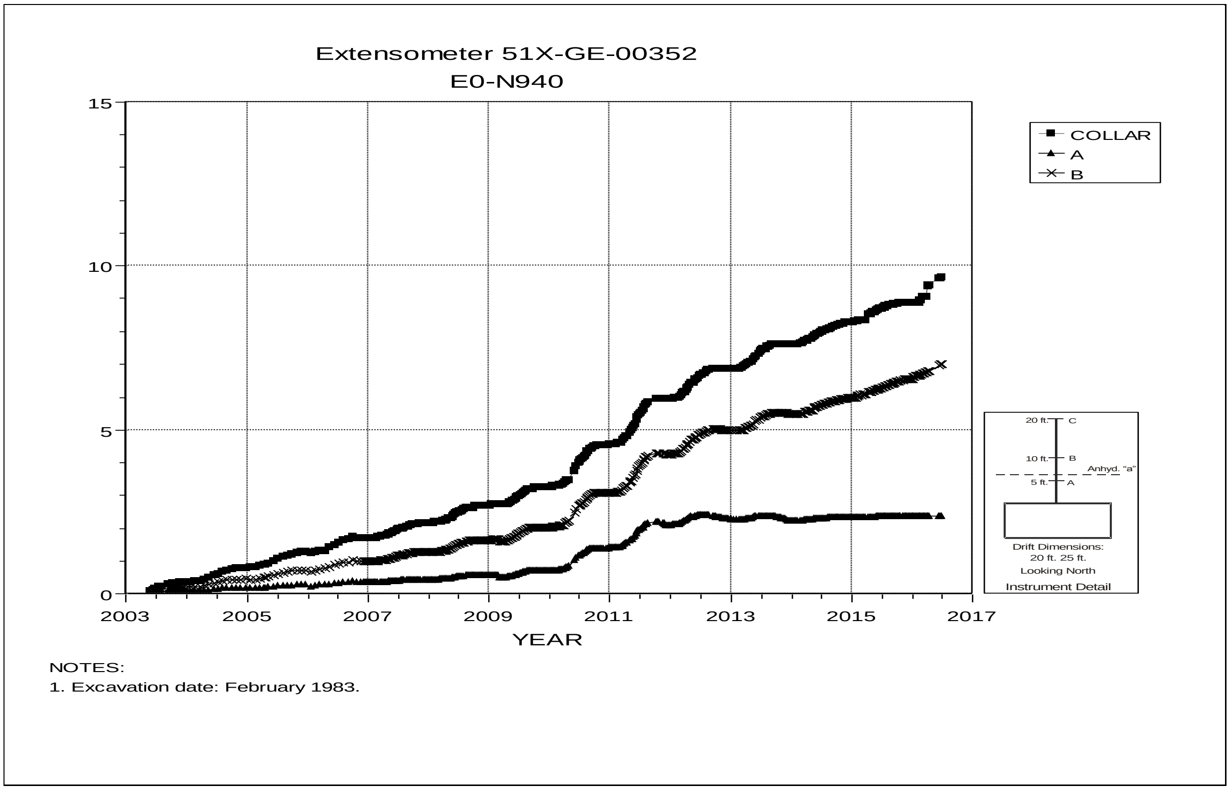

Figure 4-3 Extensometer 51X-GE-00352 –
E0 N940 – Roof

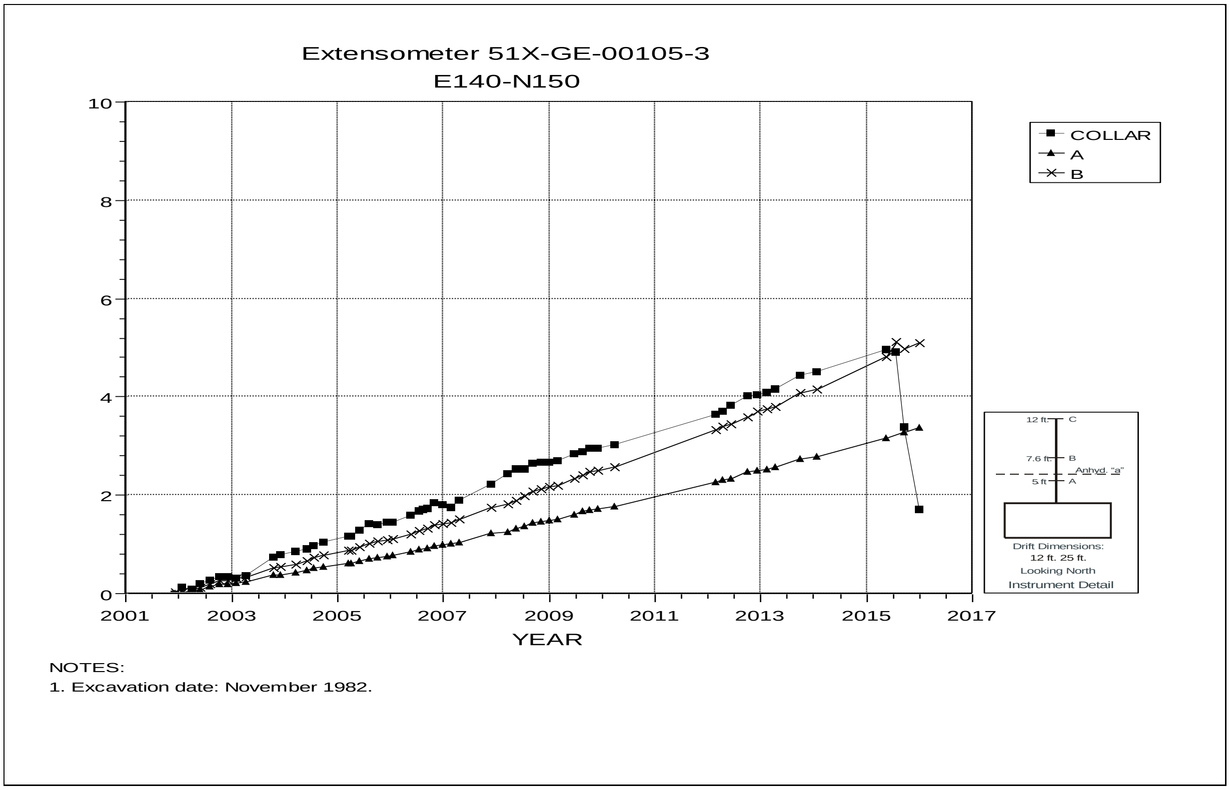

Figure 4-4 Extensometer 51X-GE-00105-3 –
E140 N150 – Roof

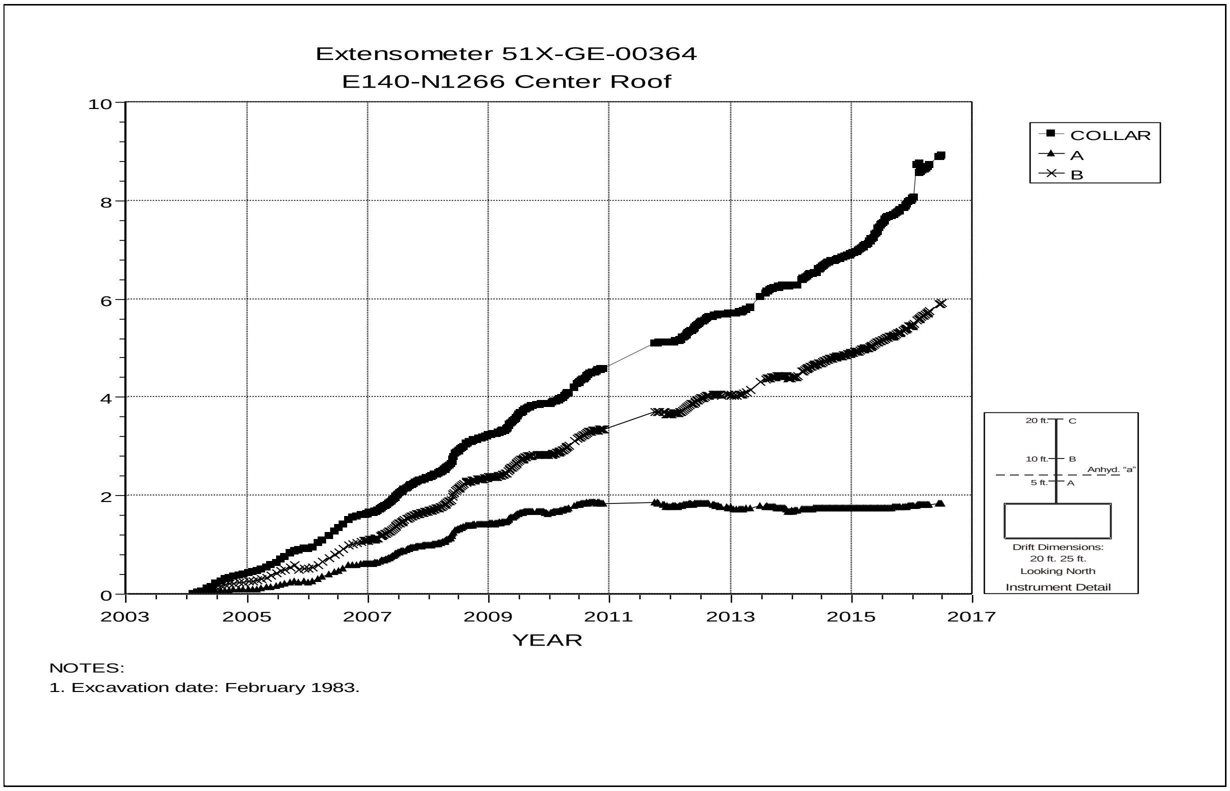

Figure 4-5 Extensometer 51X-GE-00364 –
E140 N1266 – Roof

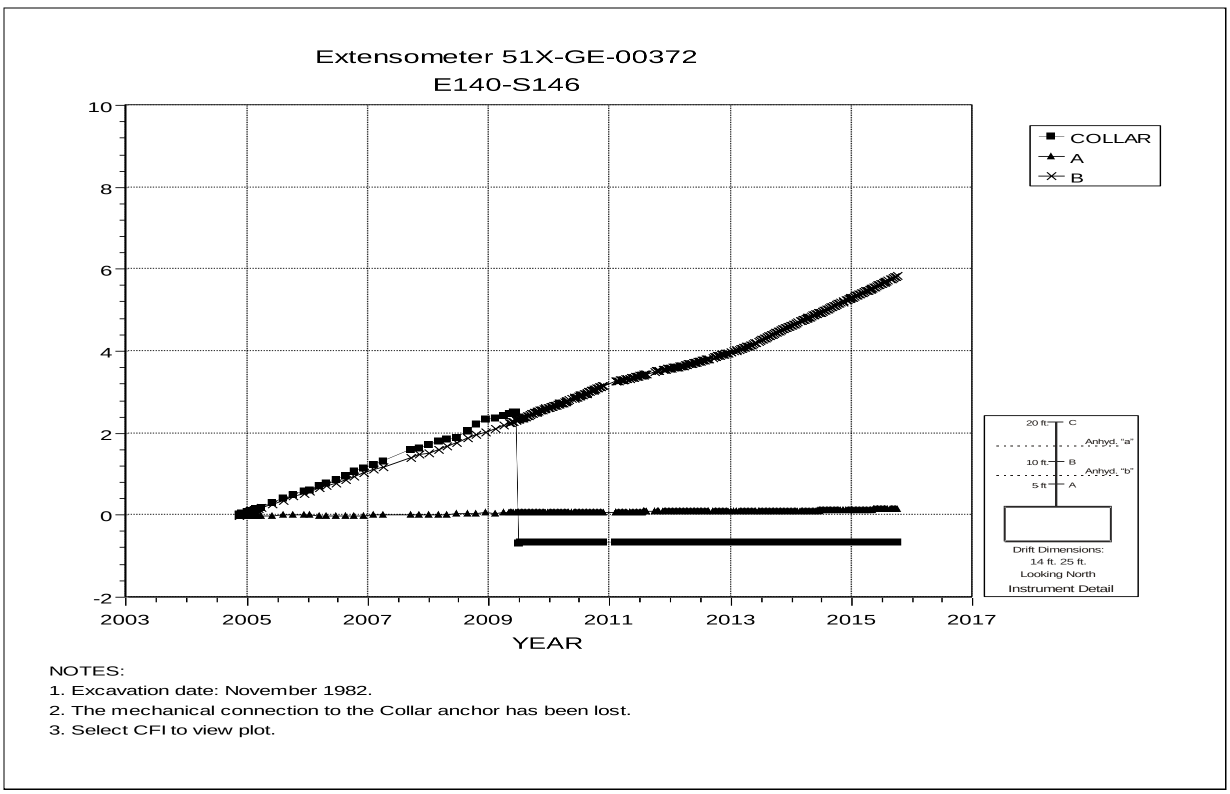

Figure 4-6 Extensometer 51X-GE-00372 –
E140 S146 – Roof

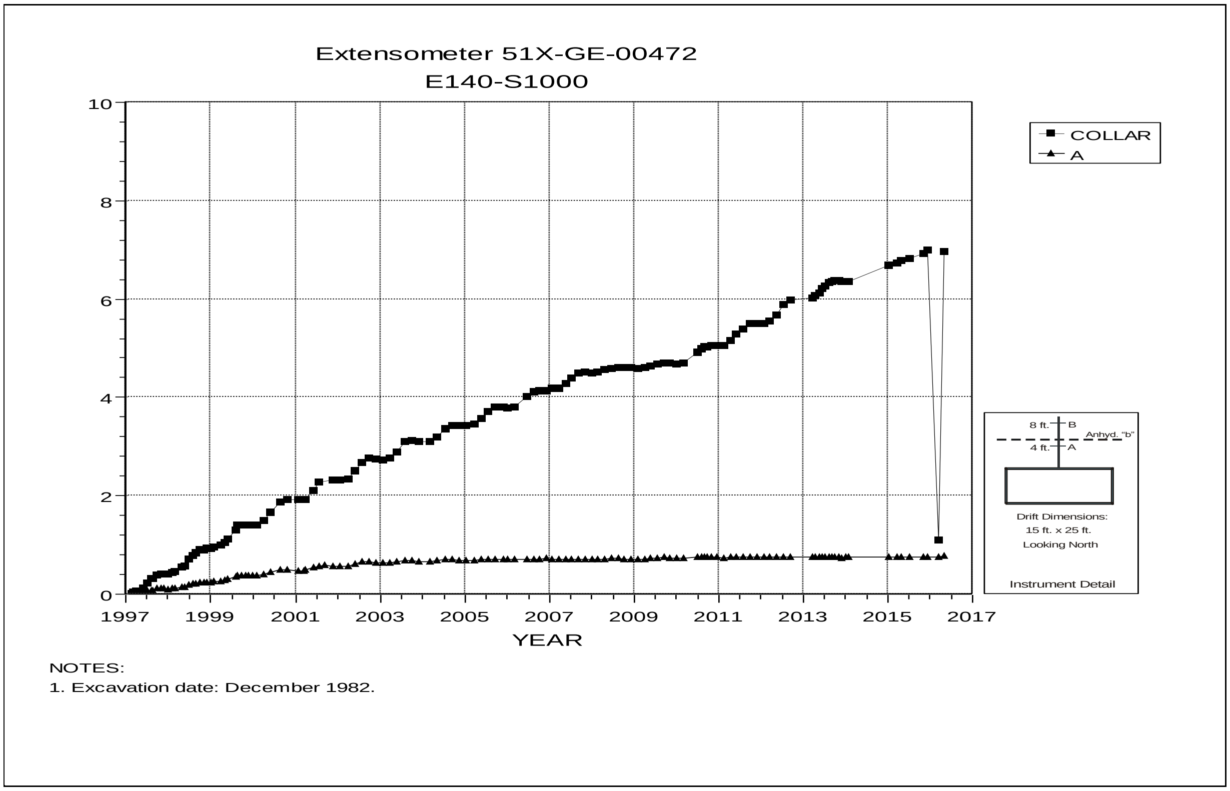

Figure 4-7 Extensometer 51X-GE-00472–
E140 S1000 – Roof

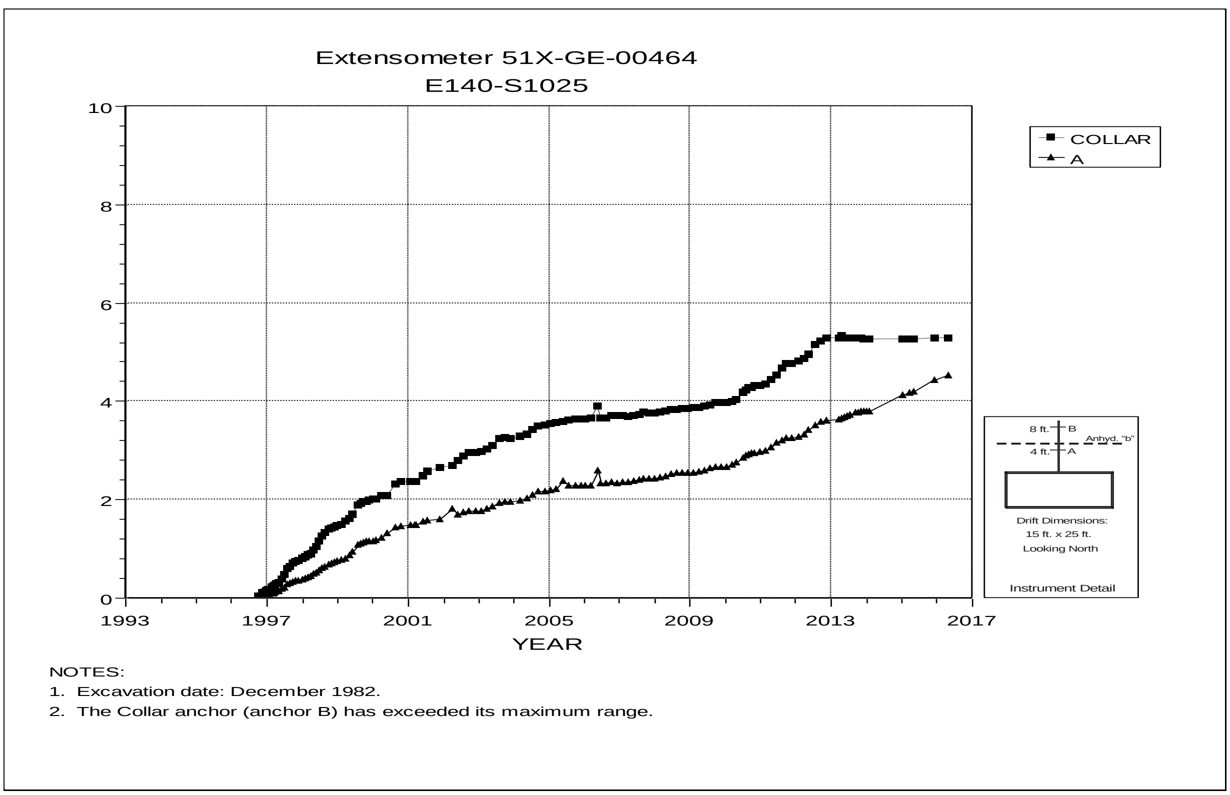

Figure 4-8 Extensometer 51X-GE-00464 –
E140 S1025 – Roof

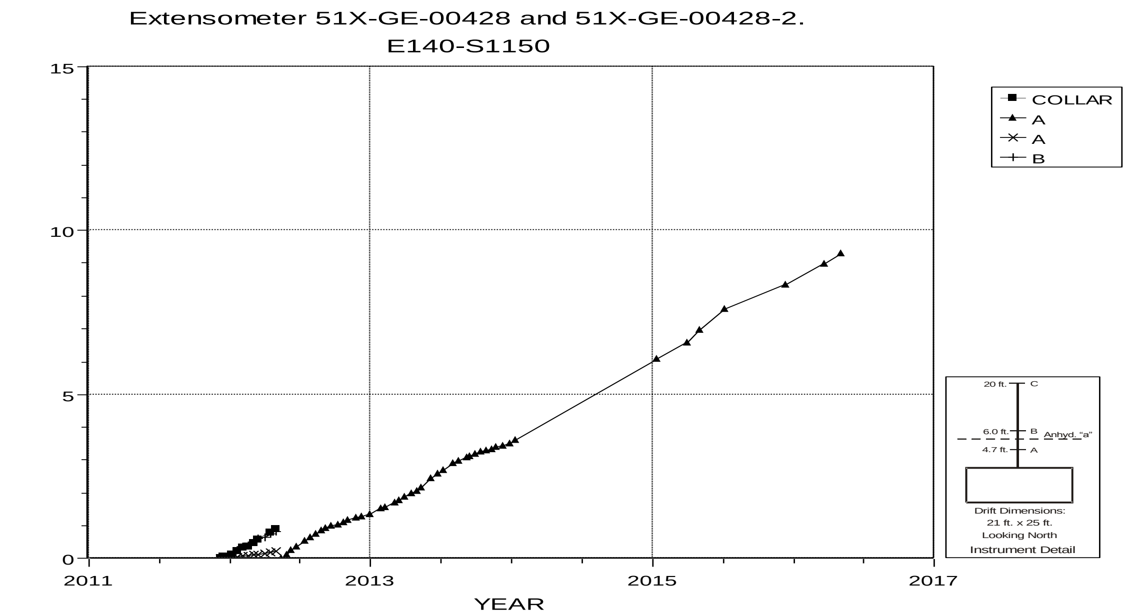

NOTES:
1. Excavation date: December 1982.
2. Single anchor 51X-GE-00428-2 replaced 51X-GE-00428.

Figure 4-9 Extensometers 51X-GE-00428-2 –
E140 S1150 – Roof

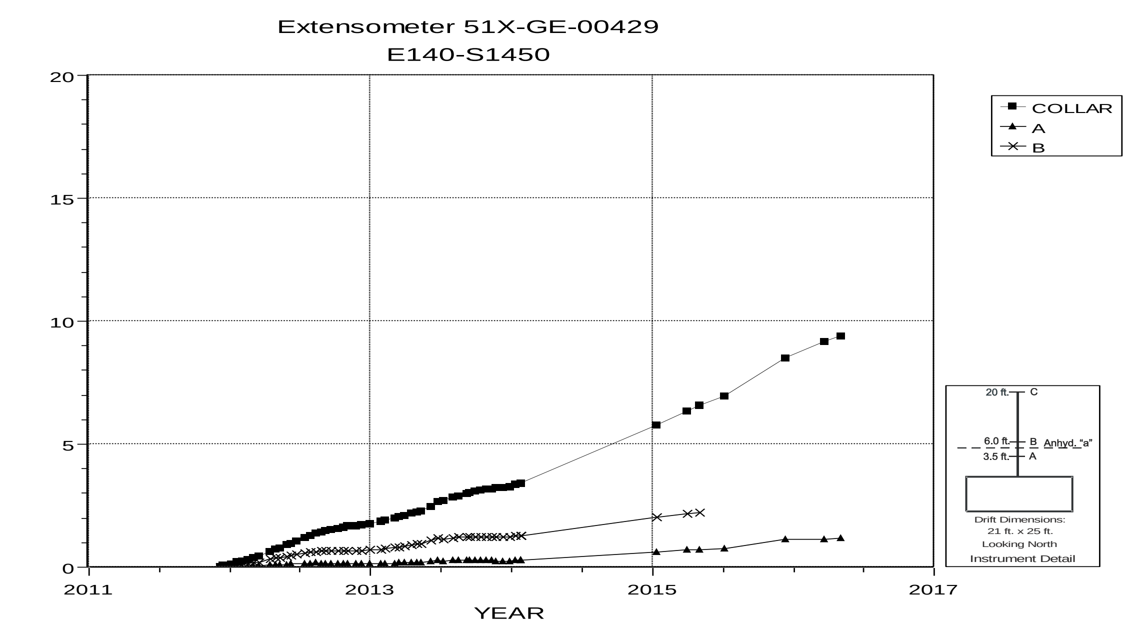

NOTES:
1. Excavation date: December 1982.
2. The mechanical connection to anchor 'B' has broken.

Figure 4-10 Extensometers 51X-GE-00429 –
E140 S1450 – Roof

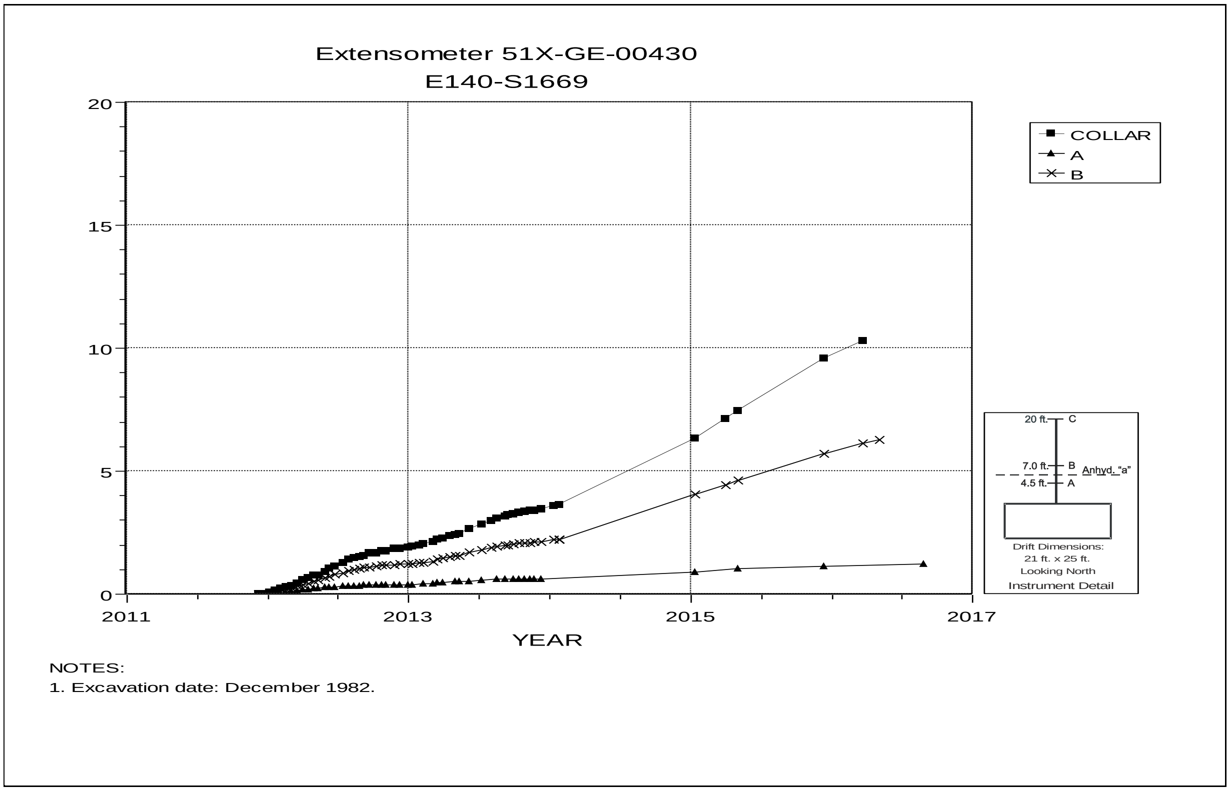

Figure 4-11 Extensometer 51X-GE-00430 –
E140 S1669 – Roof

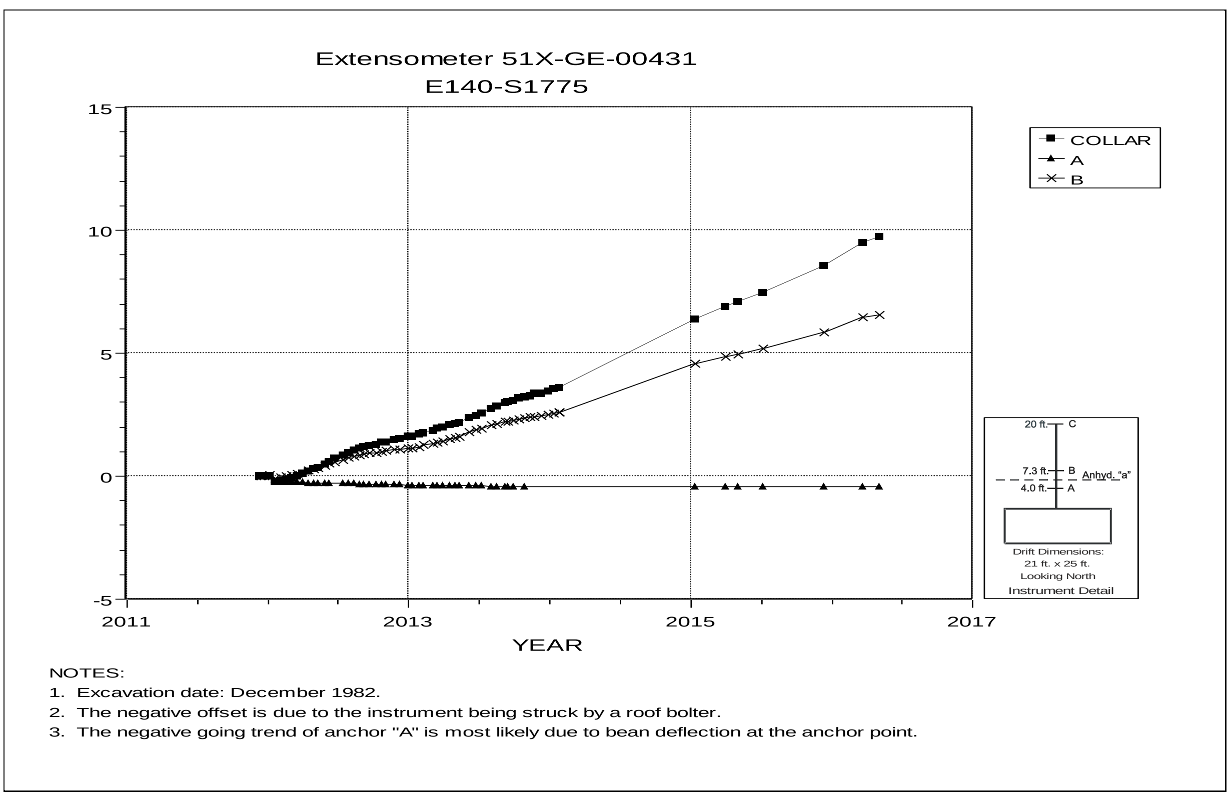

Figure 4-12 Extensometer 51X-GE-00431–
E140 S1775 – Roof

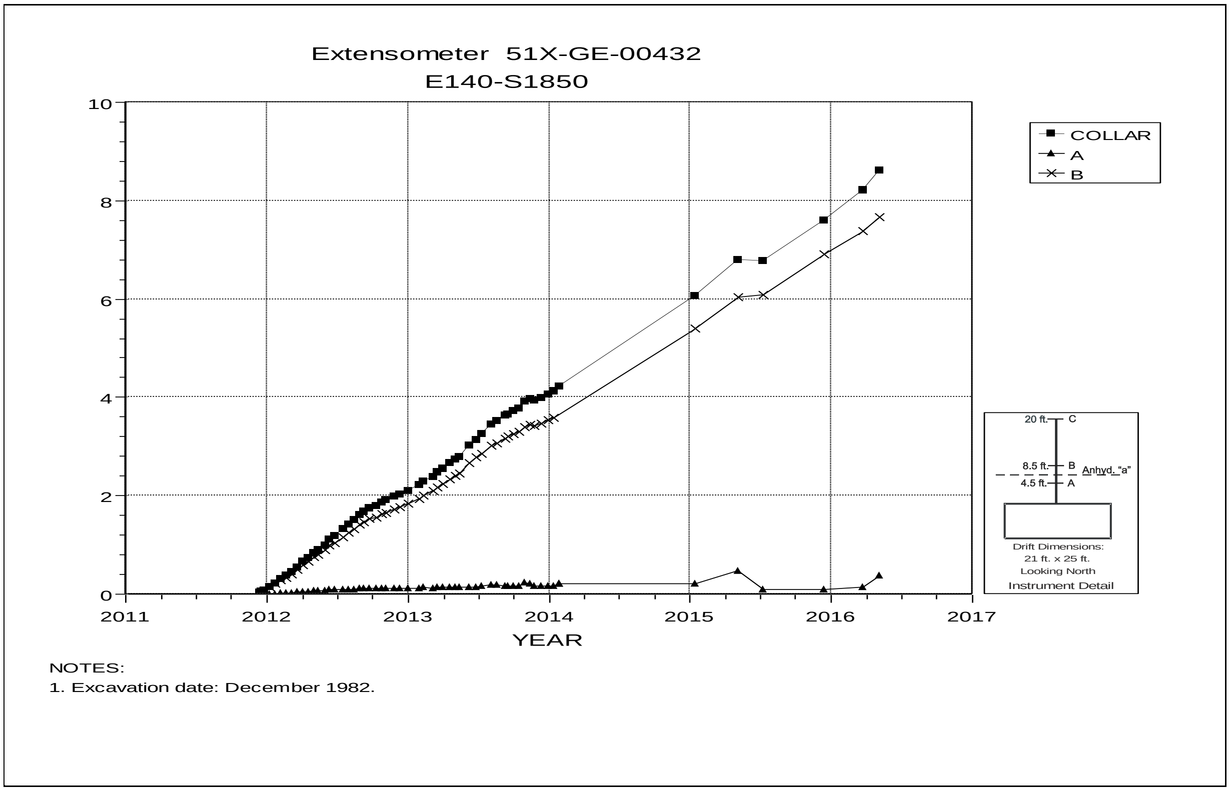

Figure 4-13 Extensometer 51X-GE-00432 –
E140 S1850 – Roof

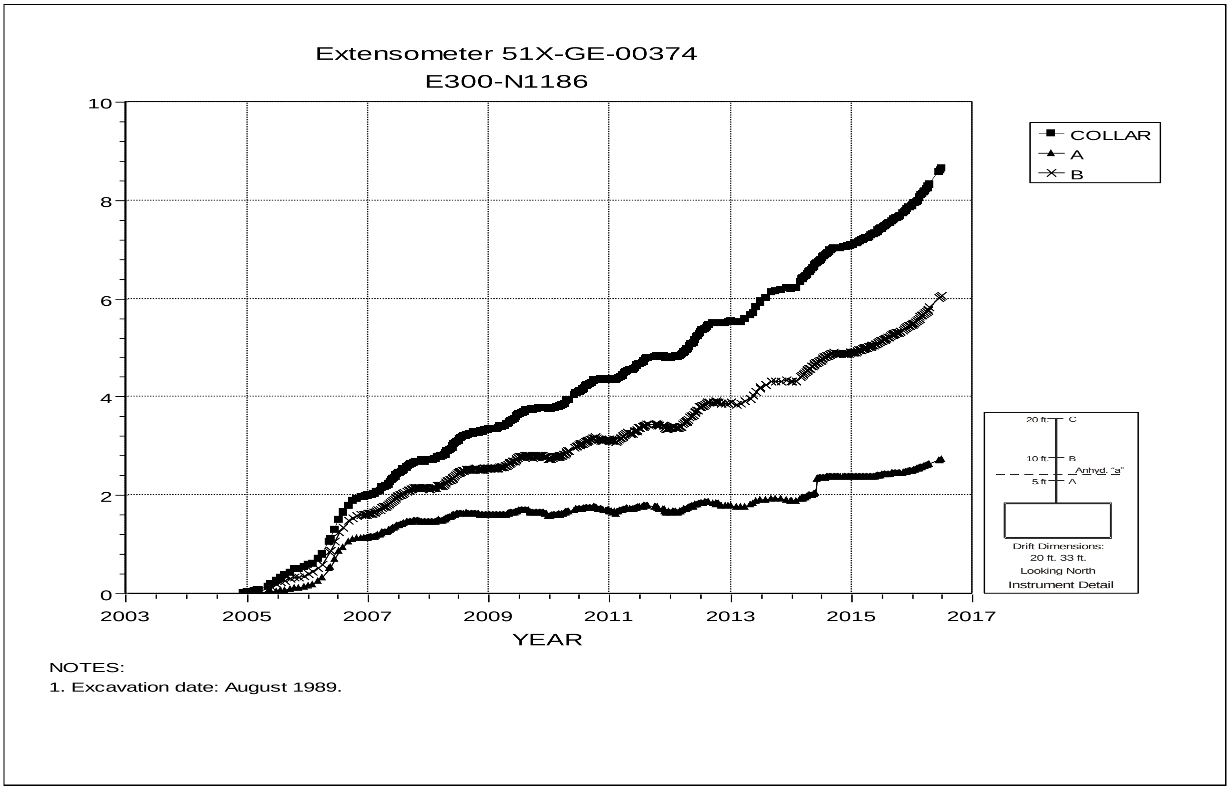

Figure 4-14 Extensometer 51X-GE-00374 –
E300 N1186 – Roof

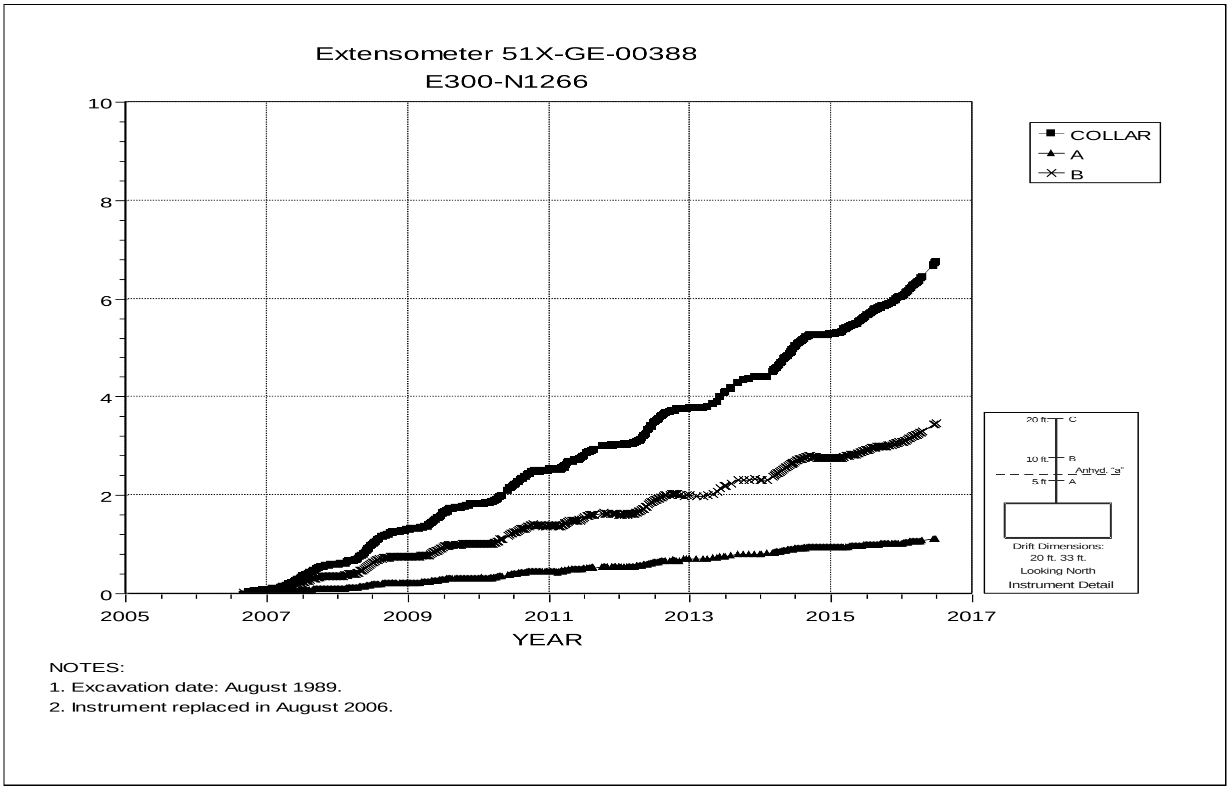

Figure 4-15 Extensometer 51X-GE-00388-
E300 N1266 – Roof

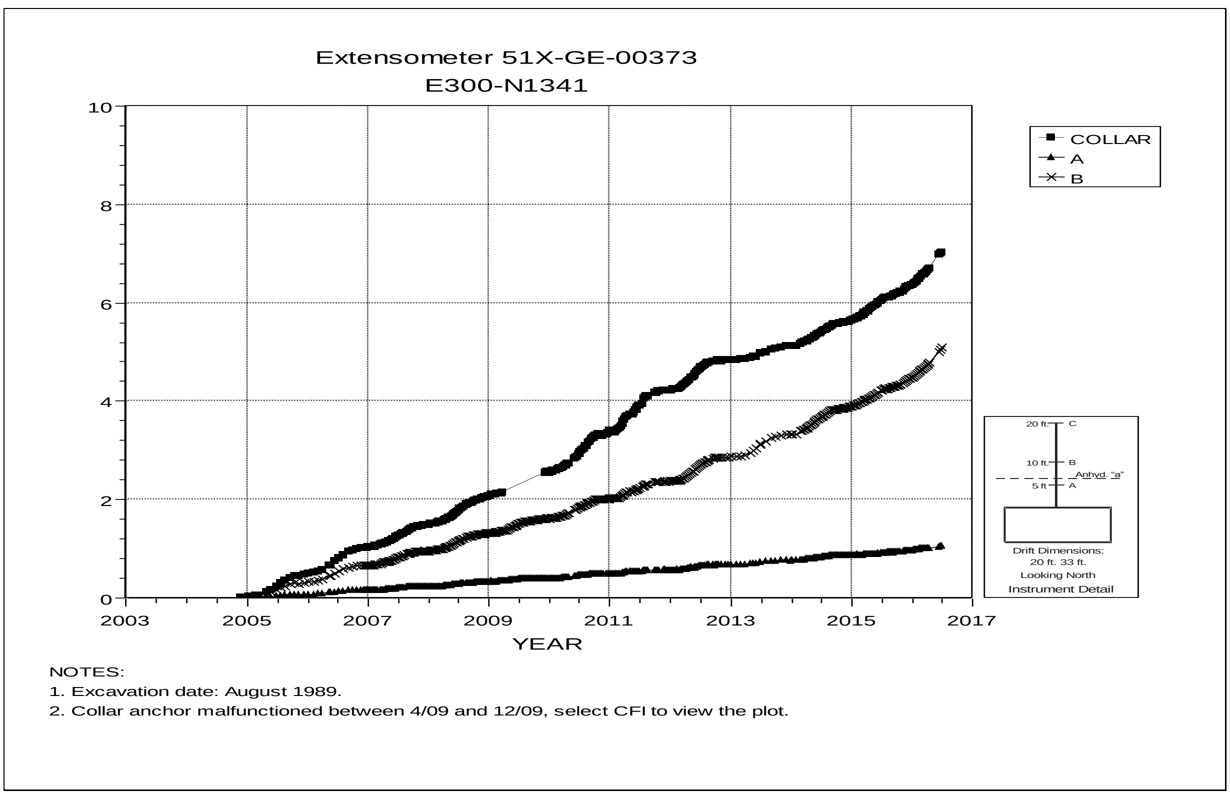

Figure 4-16 Extensometer 51X-GE-00373 –
E300 N1341 – Roof

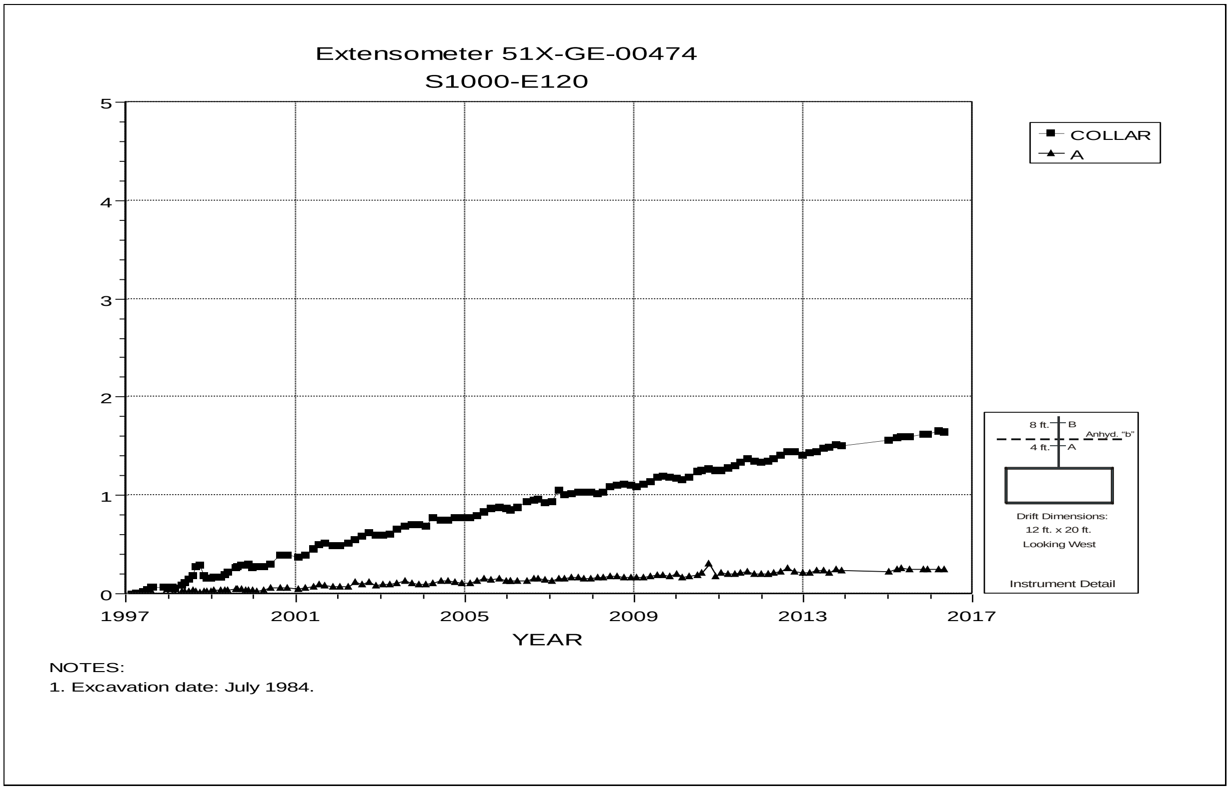

Figure 4-17 Extensometer 51X-GE-00474 –
S1000 E120–Roof

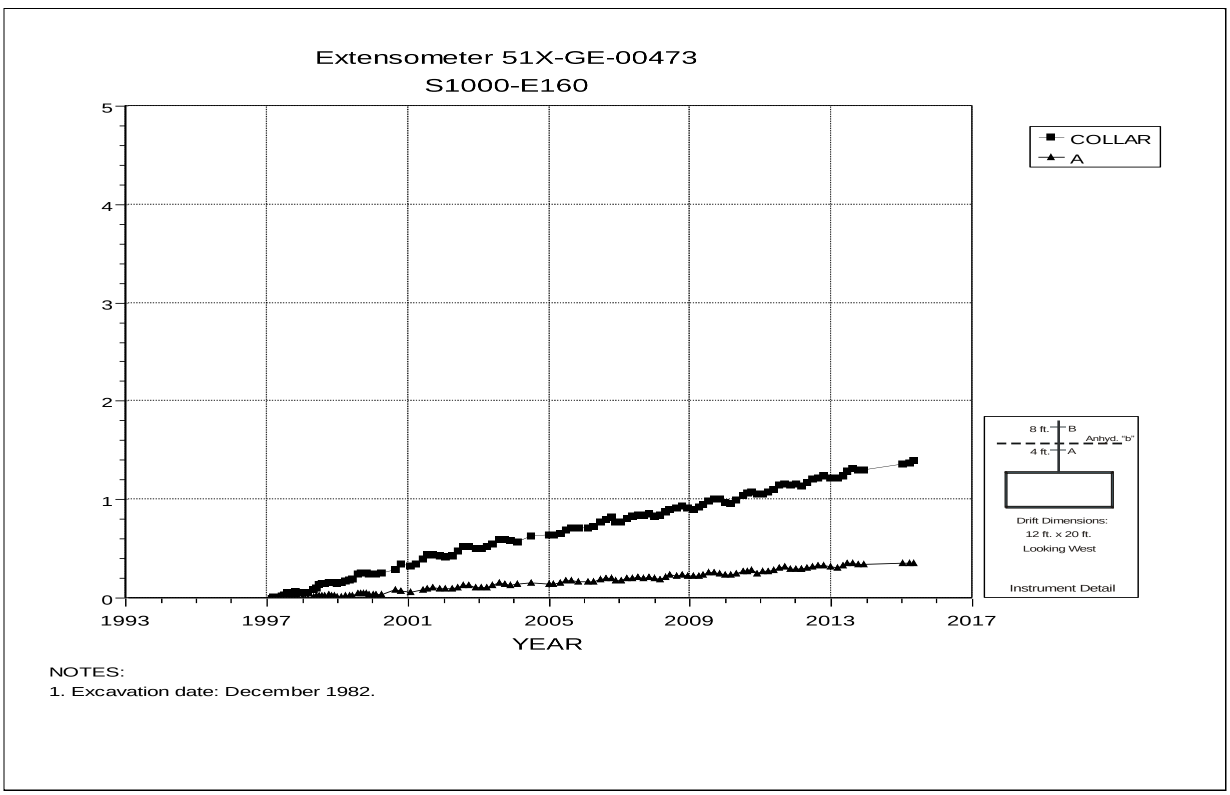

Figure 4-18 Extensometer 51X-GE-00473 –
S1000 E160–Roof

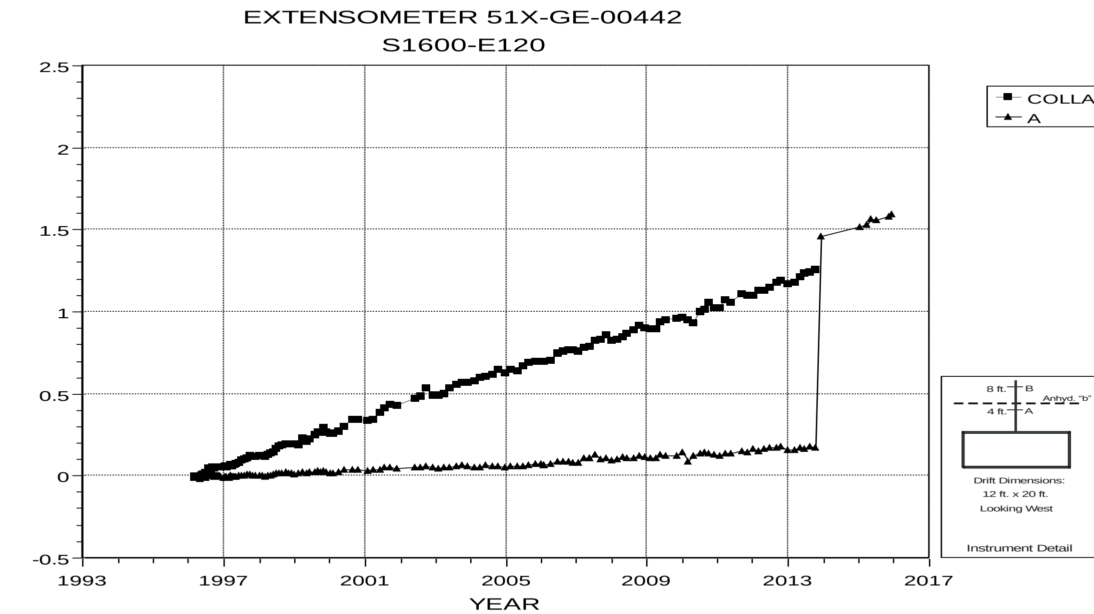

NOTES:
1. Excavation date: June 1984.

Figure 4-19 Extensometer 51X-GE-00442 –
S1600 E120–Roof

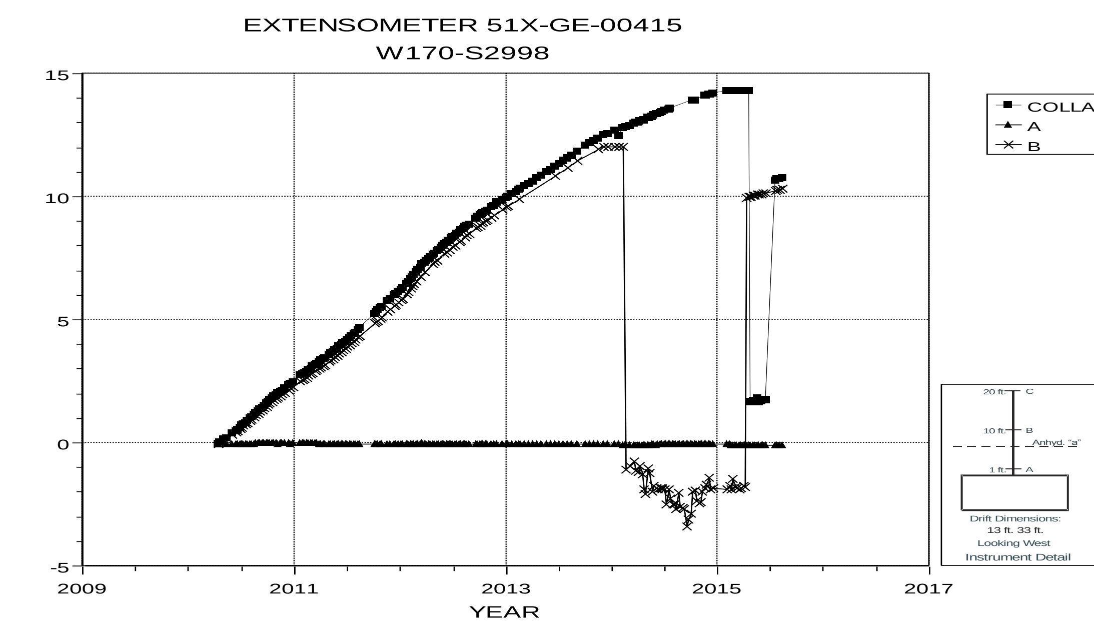

NOTES:
1. Excavation date: August 2001.
2. Anchor B has reached its maximum range and has failed.

Figure 4-20 Extensometer 51X-GE-00415 –
W170 S2998–Roof

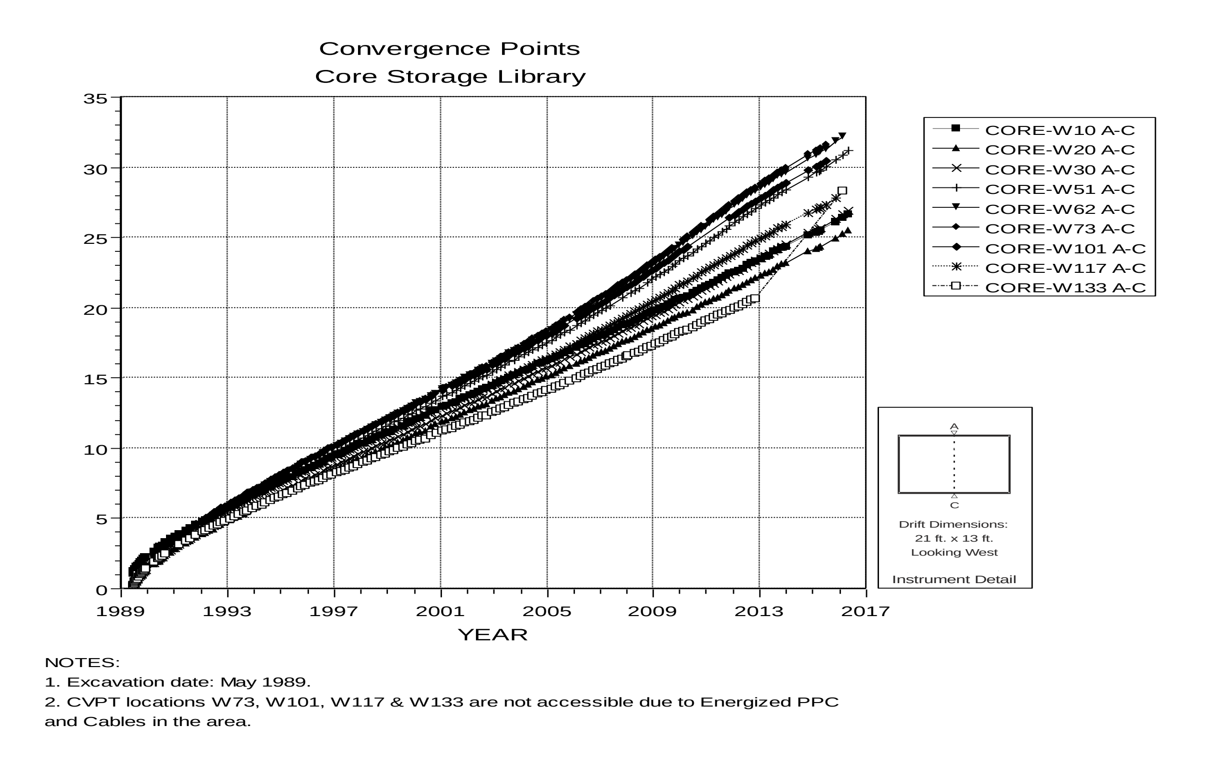

Figure 4-21 Core Storage Library – Roof to Floor

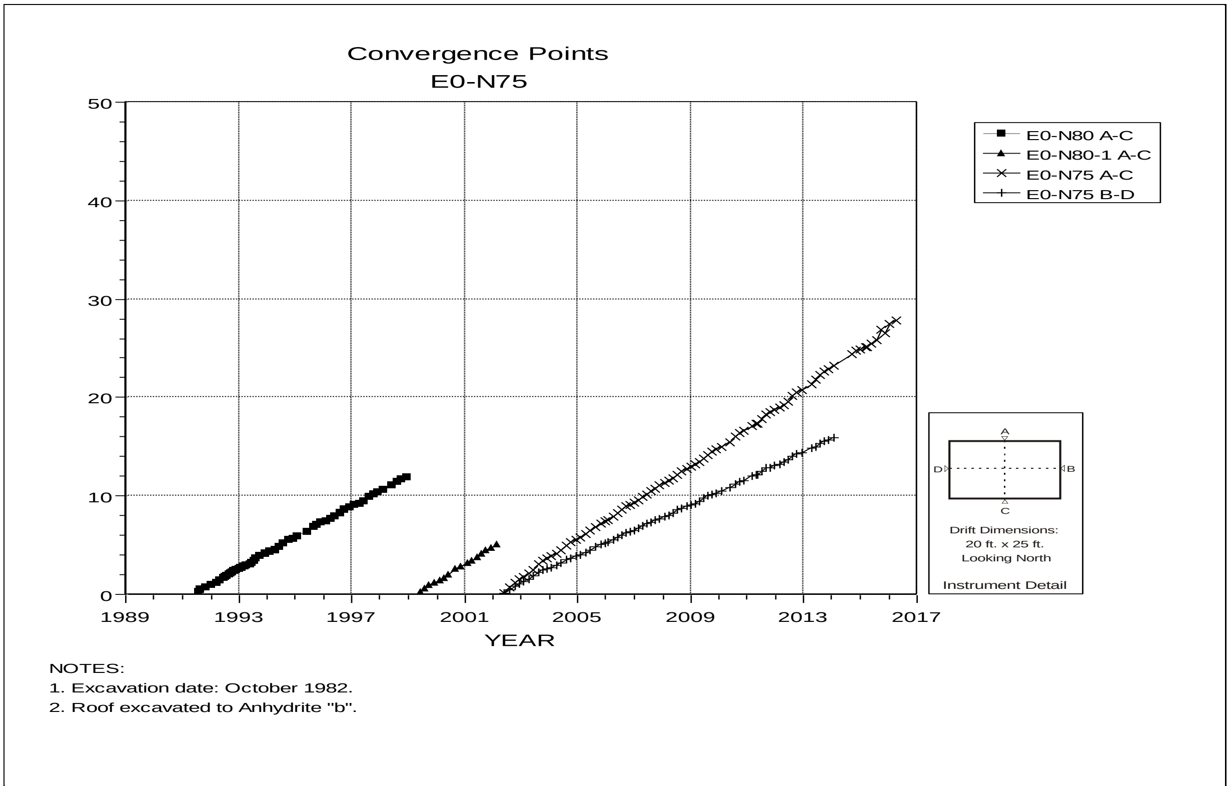

Figure 4-22 Convergence Point Array –
E0 N75 – All Chords

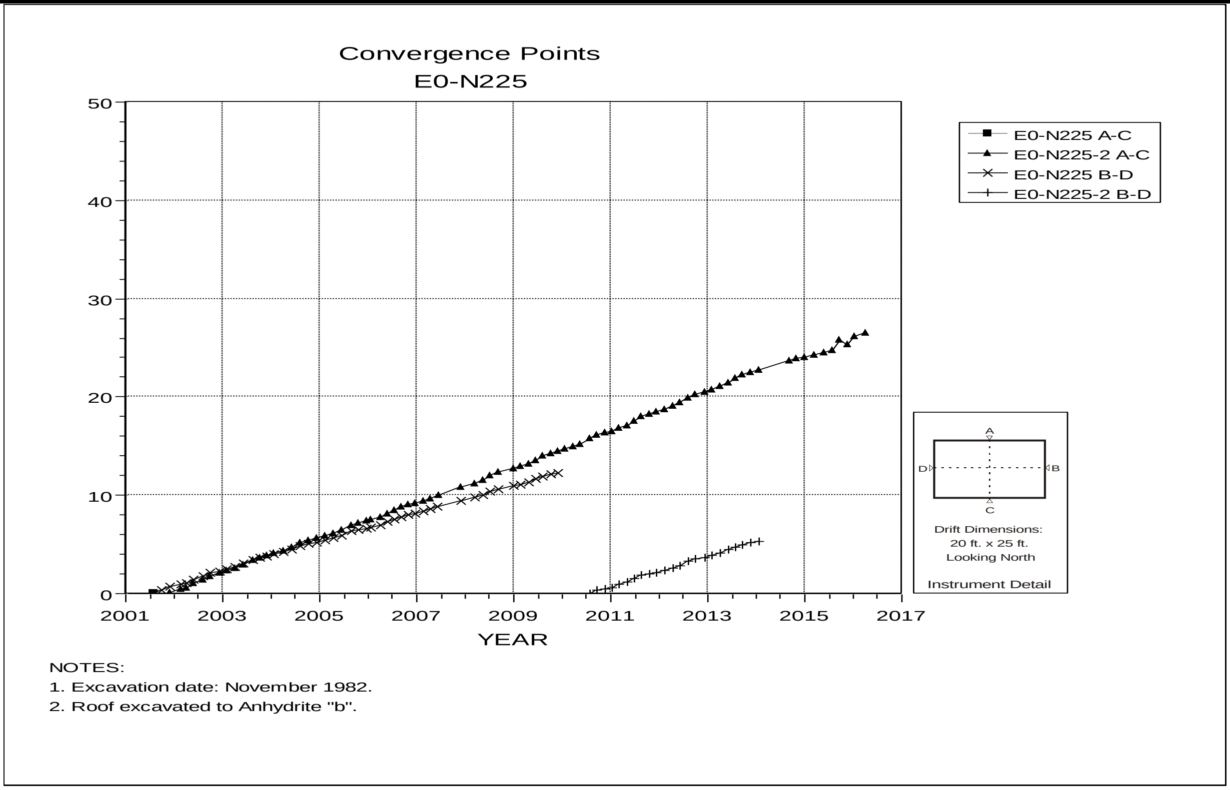

Figure 4-23 Convergence Point Array –
E0 N225 – All Chords

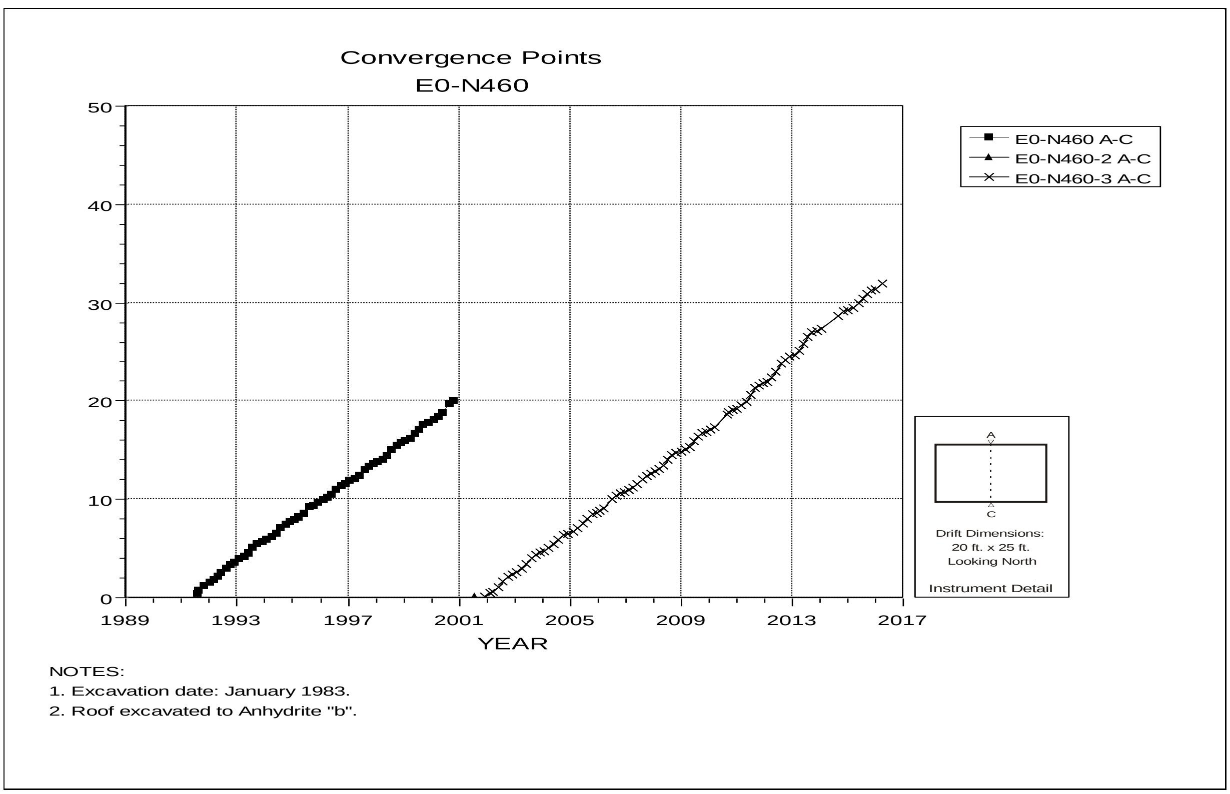

Figure 4-24 Convergence Point Array –
E0 N460 – Roof to Floor

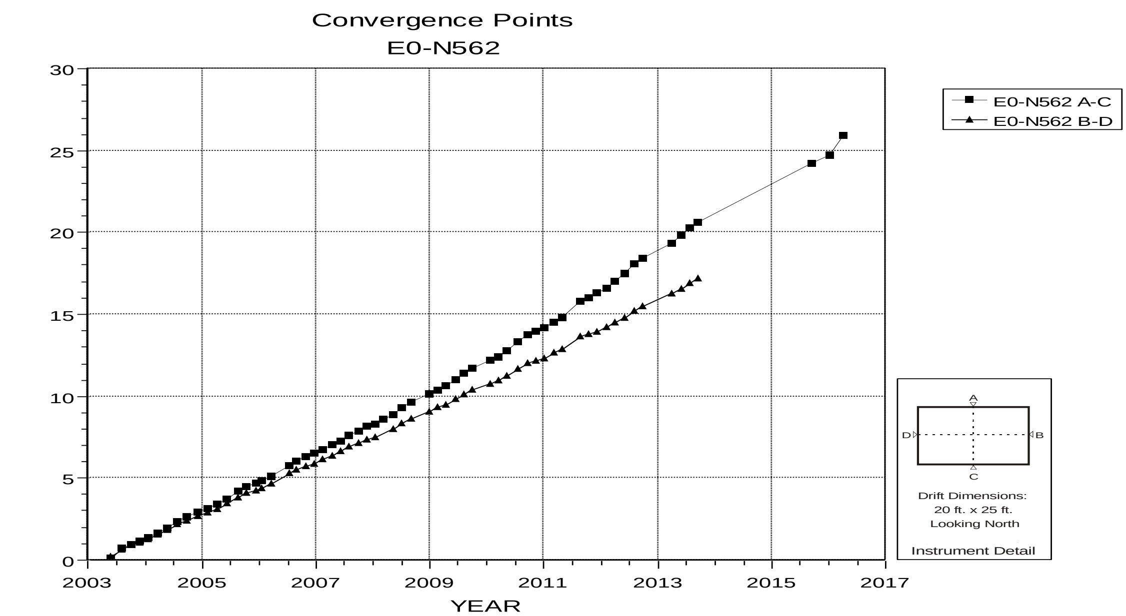

NOTES:
1. Excavation date: February 1983.
2. The RC floor point is covered by a muck pile.

Figure 4-25 Convergence Point Array –
E0 N562 – Roof to Floor

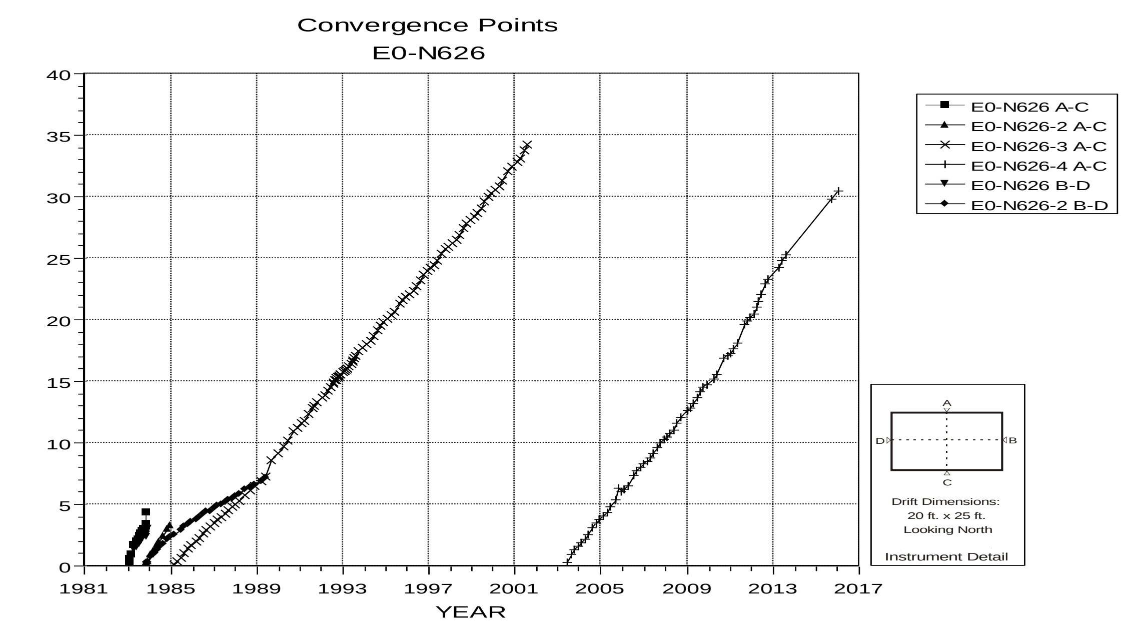

NOTES:
1. Excavation date: February 1983.
2. Roof excavated to Anhydrite "b".
3. The RC floor point is covered by a muck pile.

Figure 4-26 Convergence Point Array –
E0 N626 – Roof to Floor

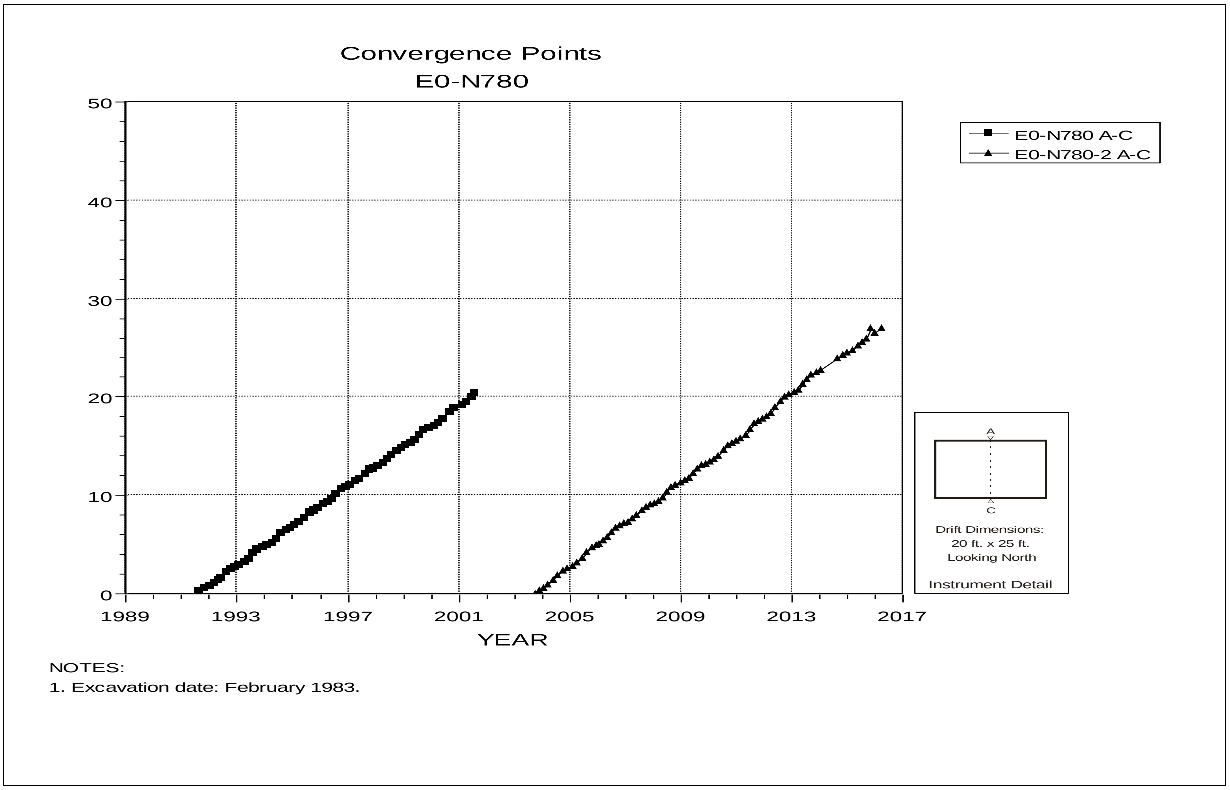

Figure 4-27 Convergence Point Array –
E0 N780 – Roof to Floor

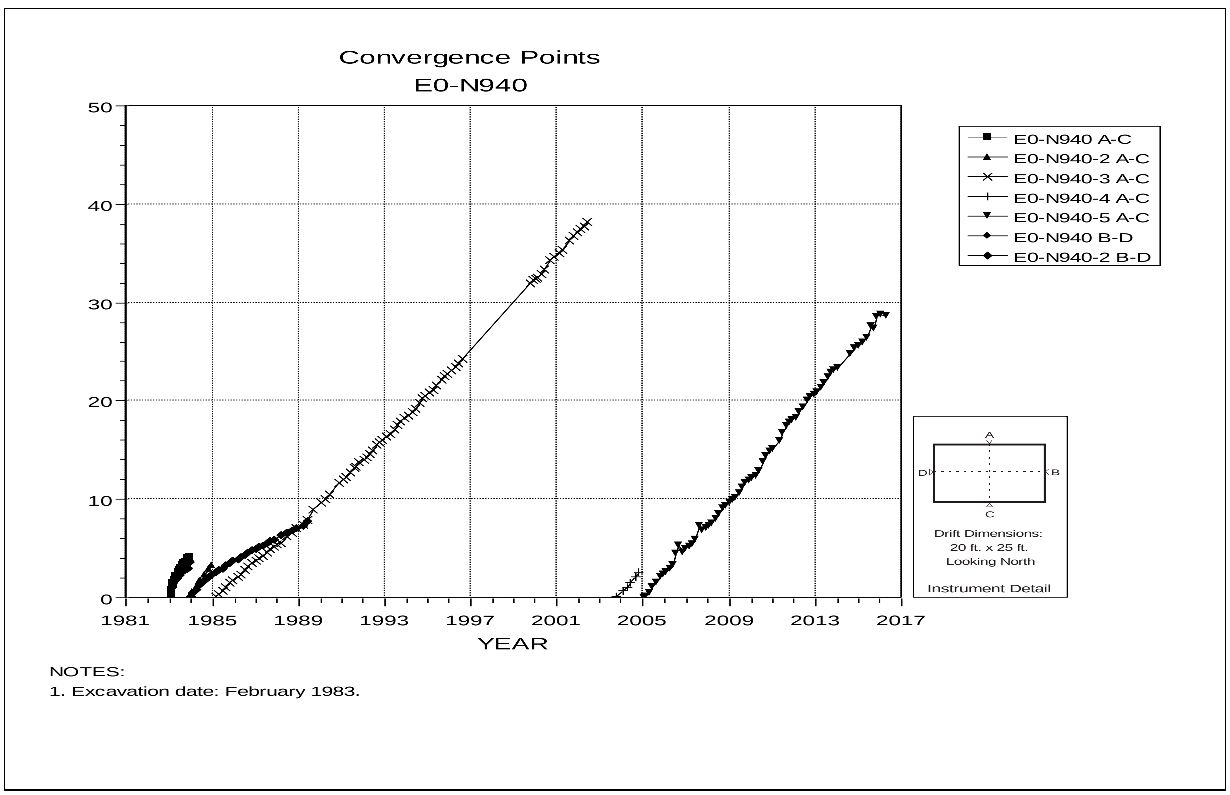

Figure 4-28 Convergence Point Array –
E0 N940 – All Chords

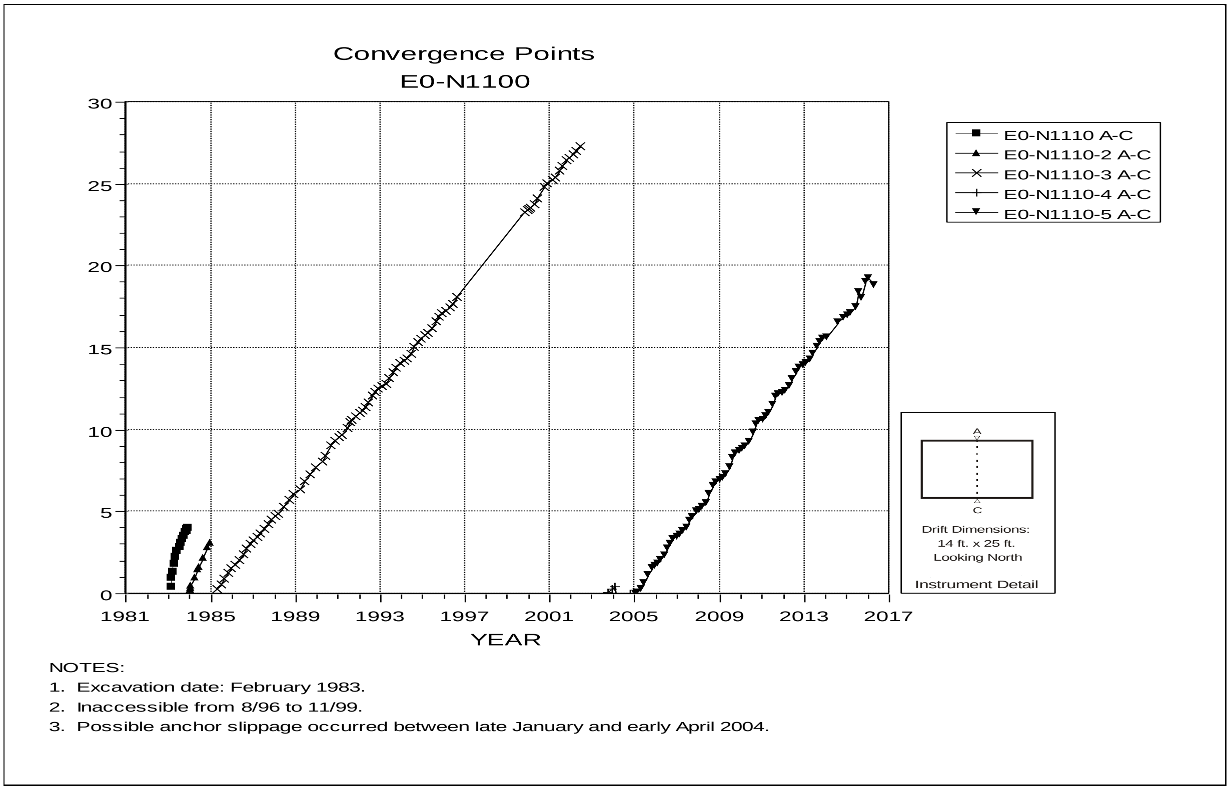

Figure 4-29 Convergence Point Array –
E0 N1100 – Roof to Floor

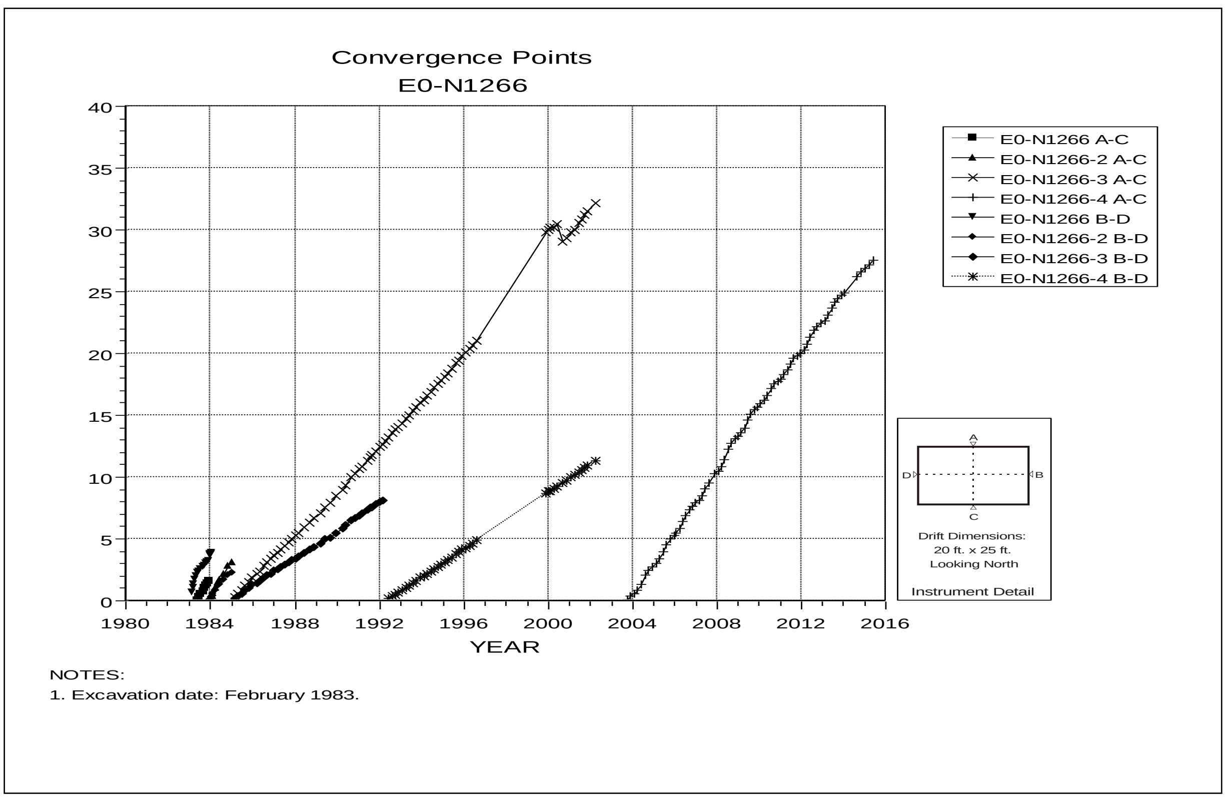

Figure 4-30 Convergence Point Array –
E0 N1266 – All Chords

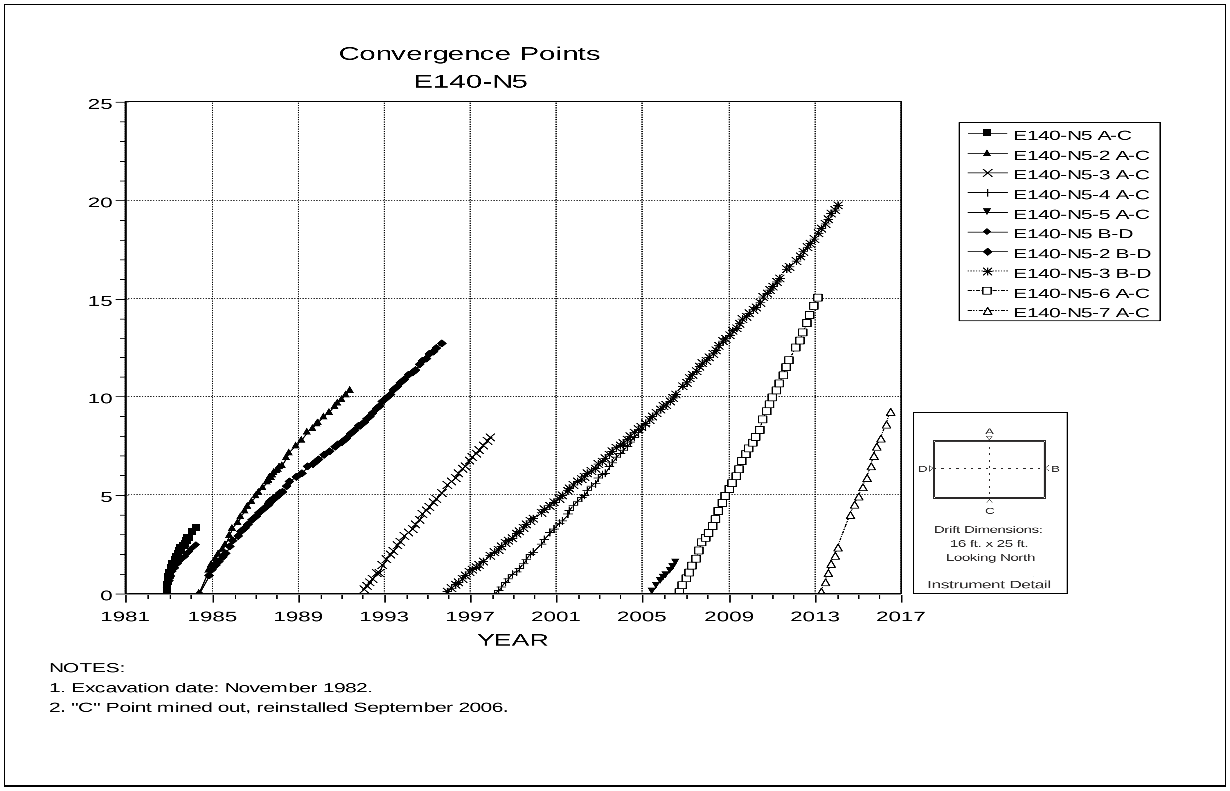

Figure 4-31 Convergence Point Array –
E140 N5 – All Chords

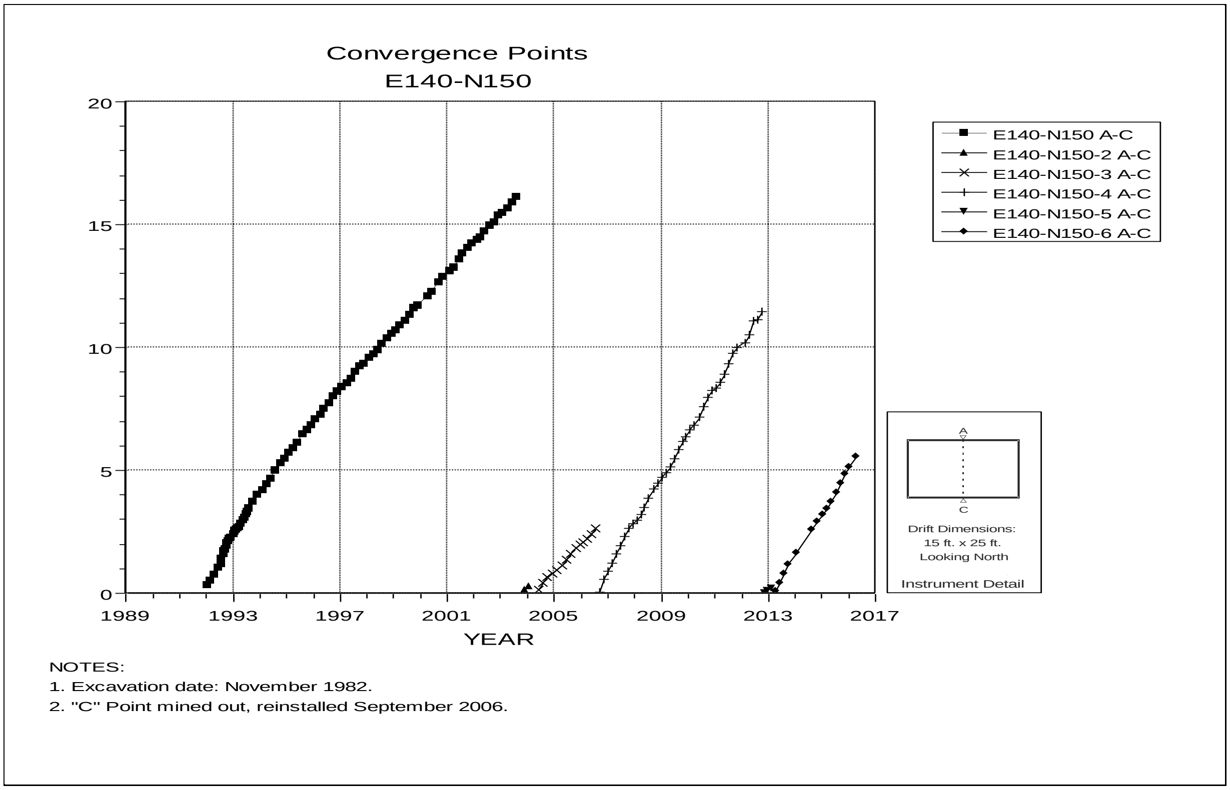

Figure 4-32 Convergence Point Array –
E140 N150 – Roof to Floor

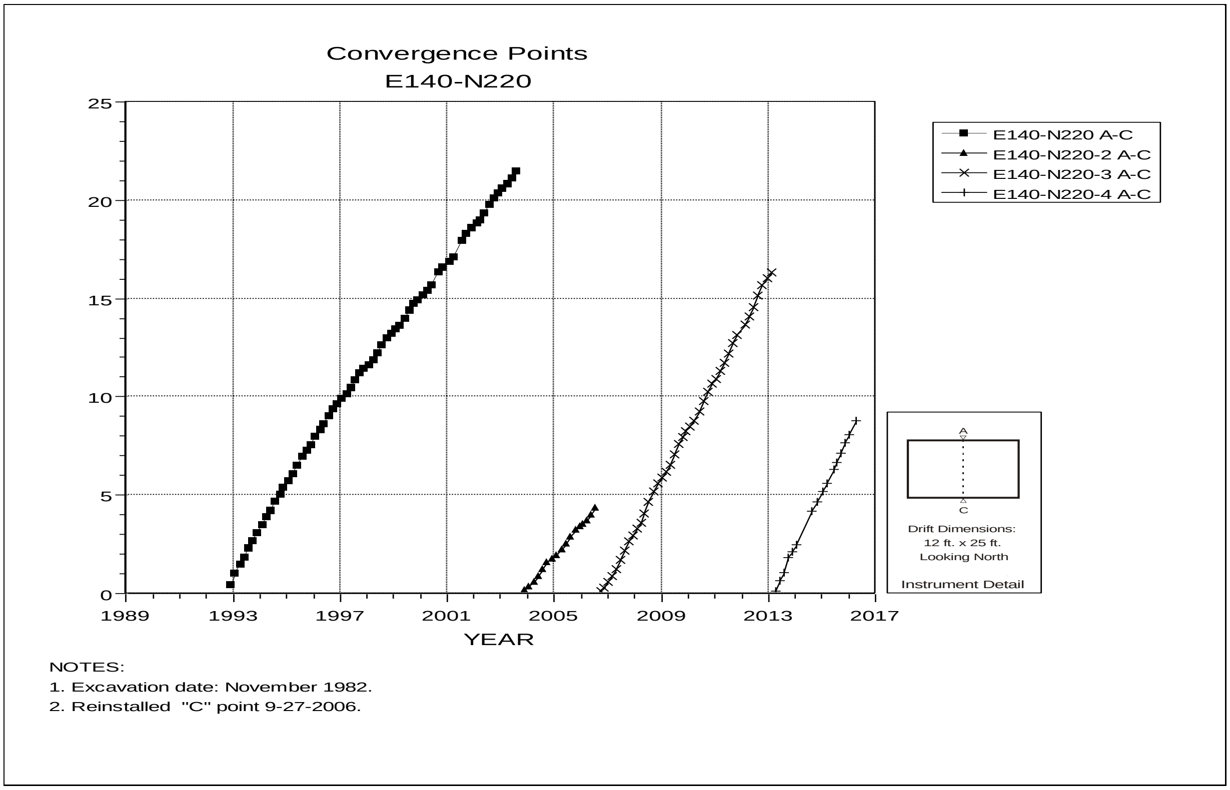

Figure 4-33 Convergence Point Array –
E140 N220 – Roof to Floor

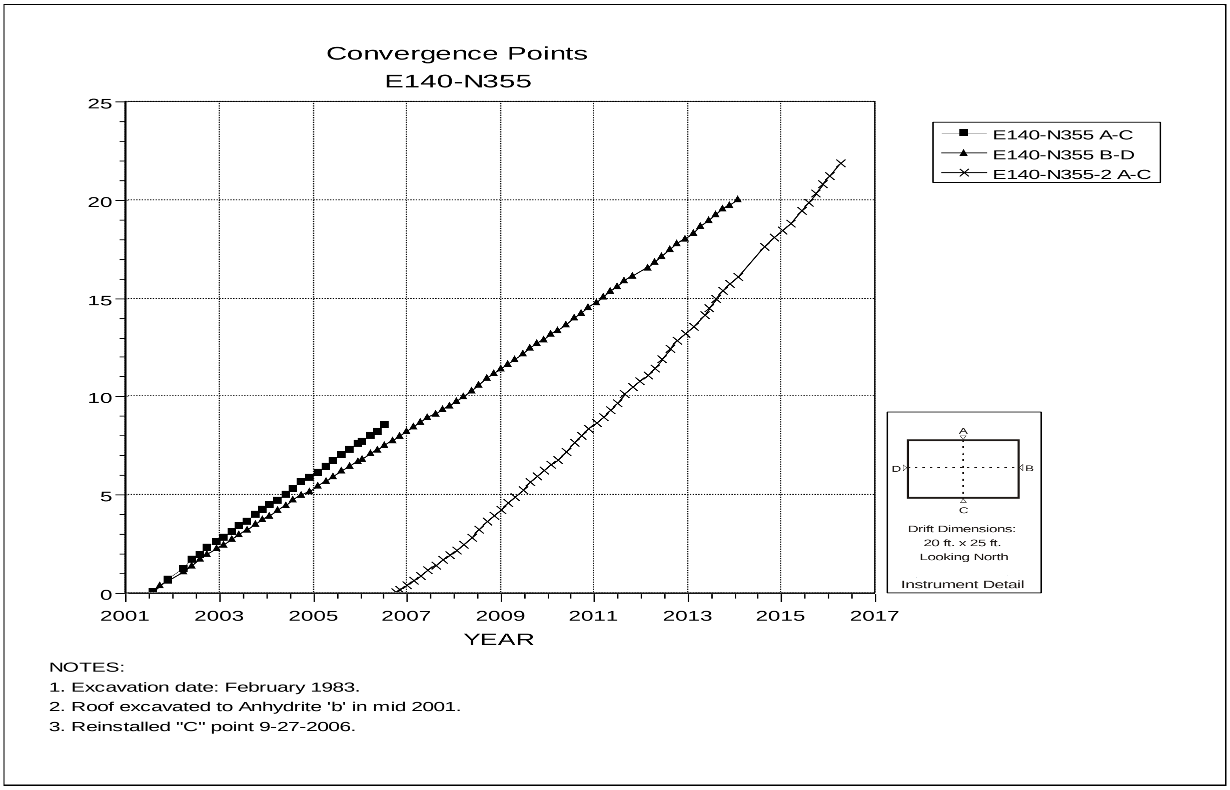

Figure 4-34 Convergence Point Array –
E140 N355 – All Chords

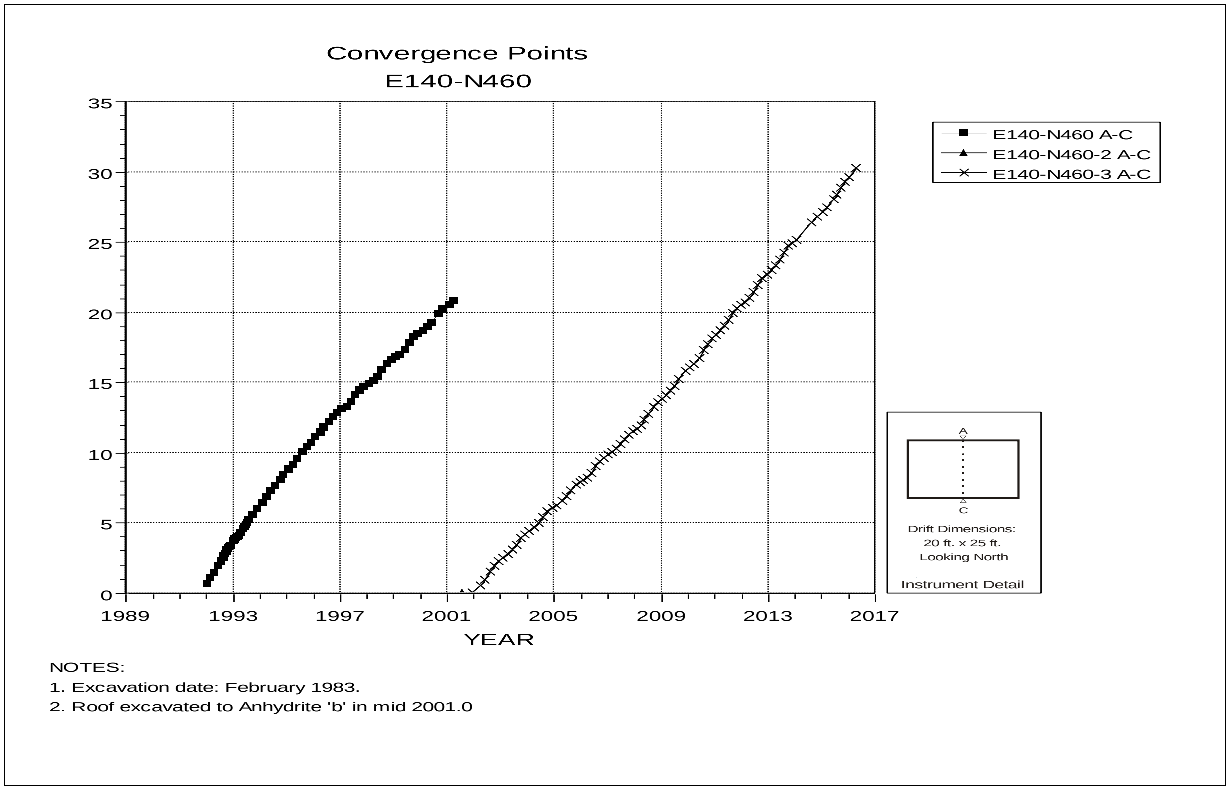

Figure 4-35 Convergence Point Array –
E140 N460 – Roof to Floor

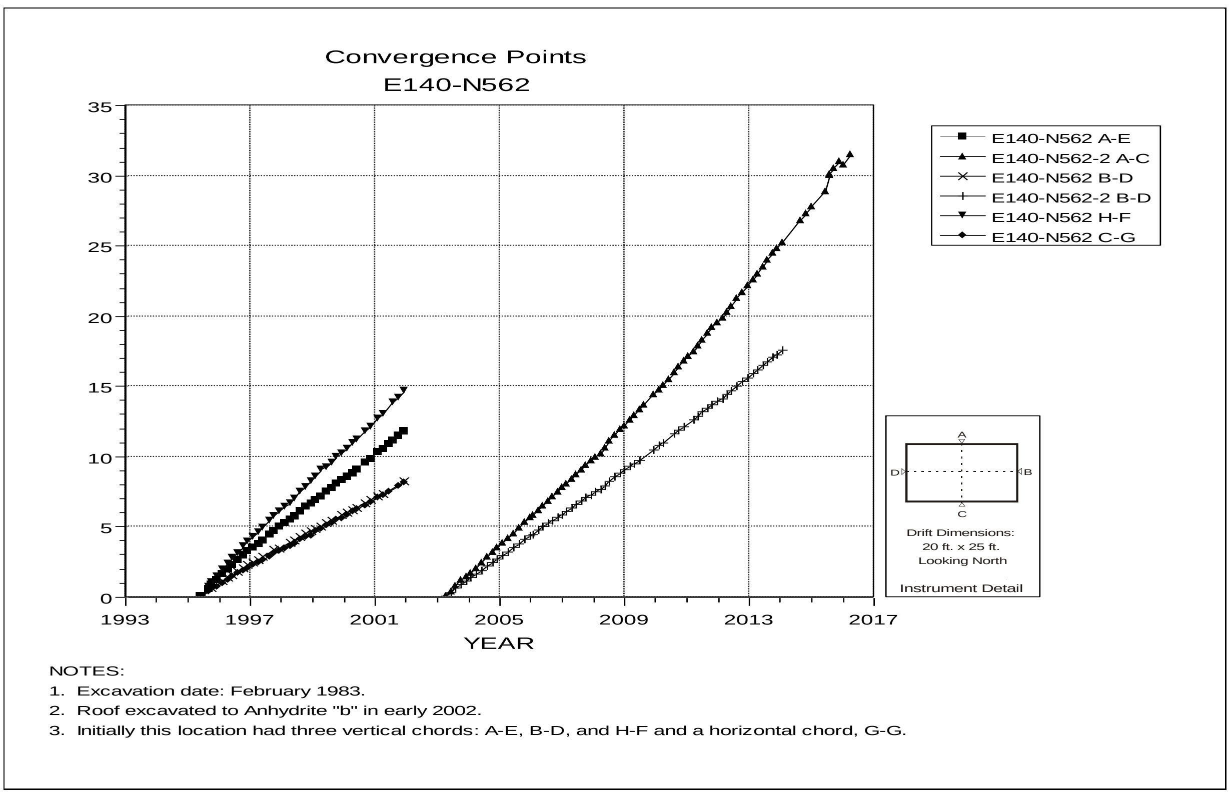

Figure 4-36 Convergence Point Array –
E140 N562 – All Chords

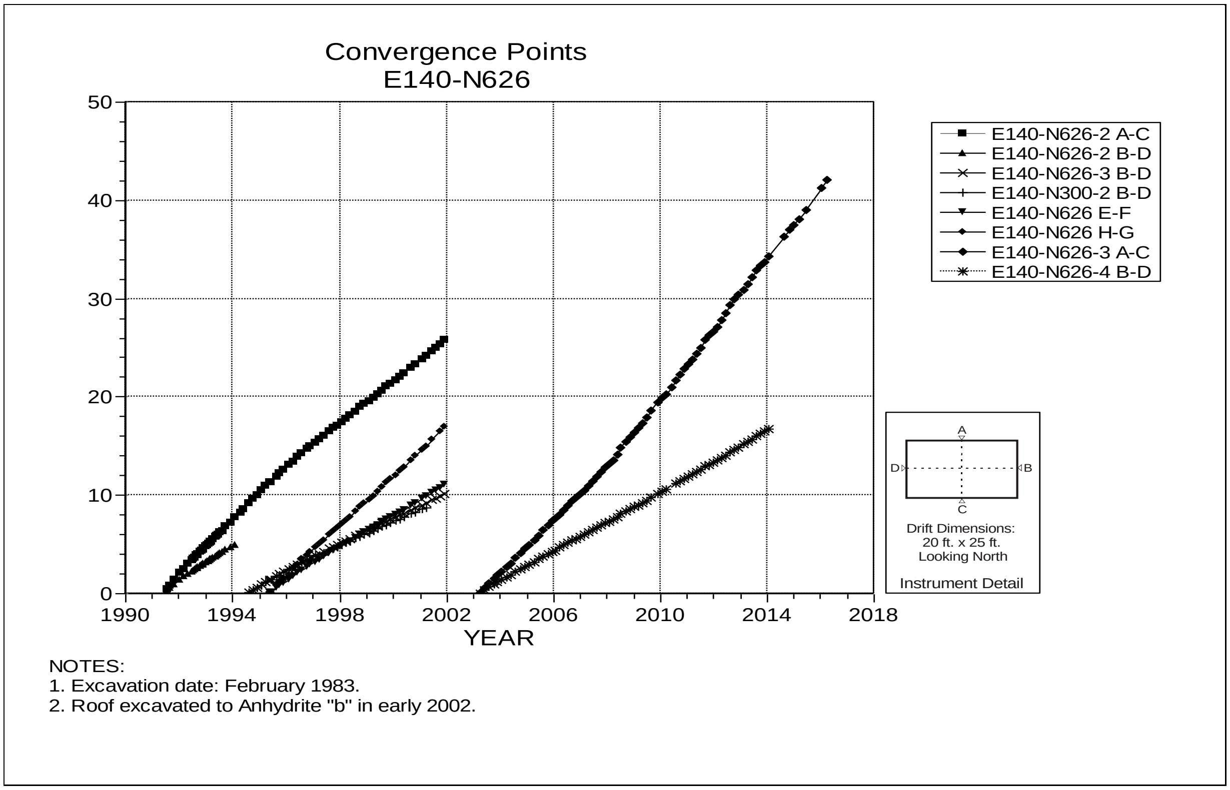

Figure 4-37 Convergence Point Array –
E140 N626 – All Chords

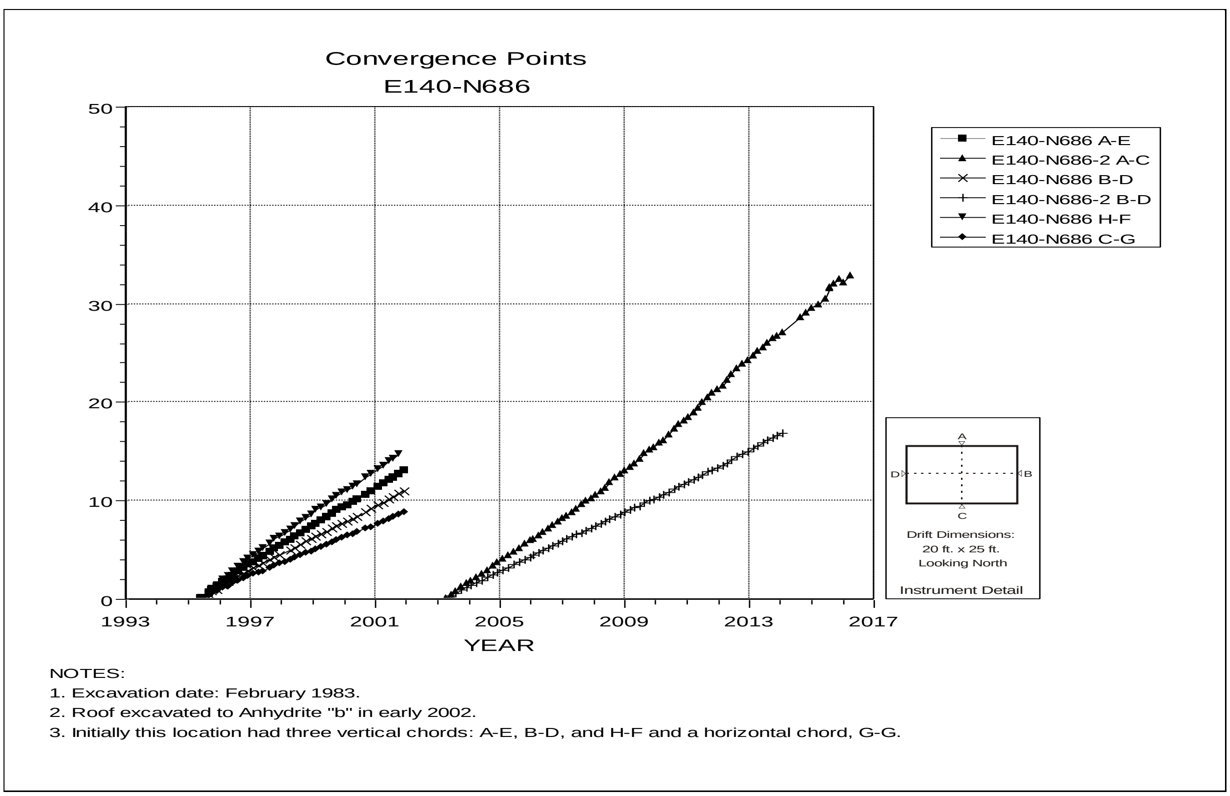

Figure 4-38 Convergence Point Array –

ISSUED

E140 N686 – All Chords

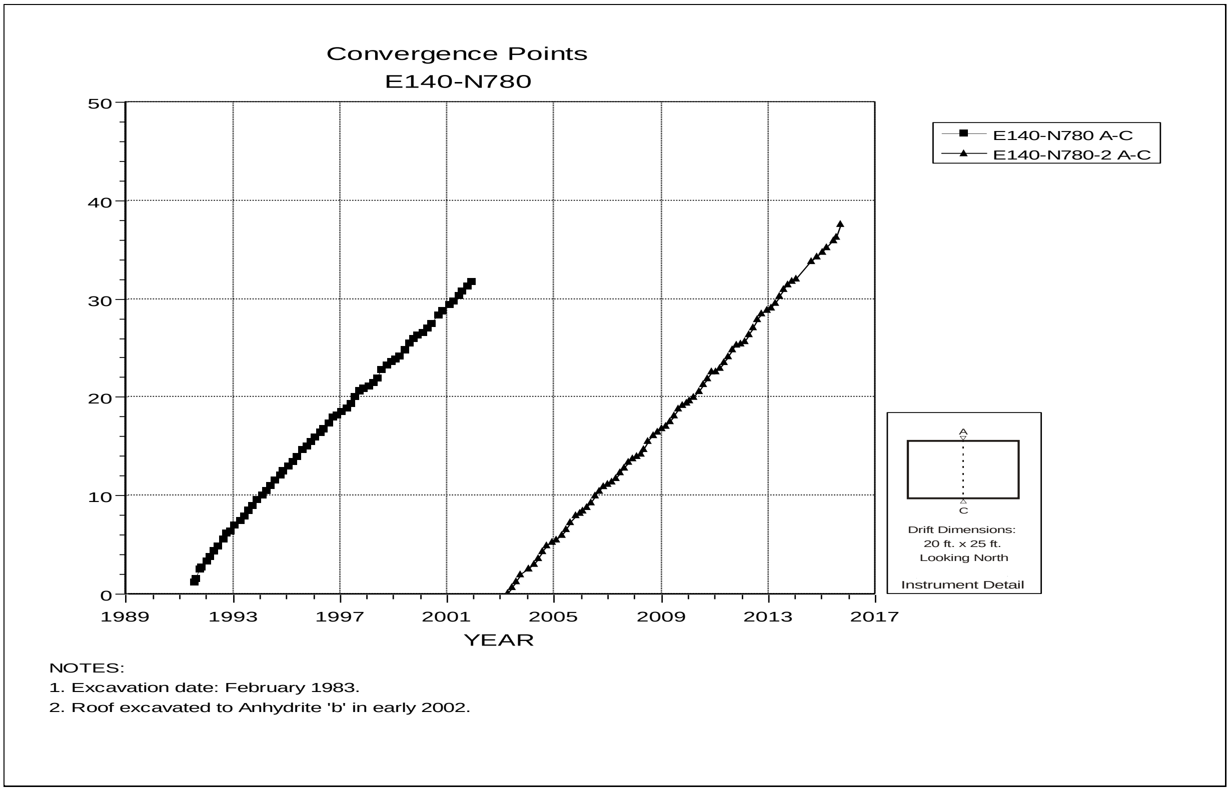

Figure 4-39 Convergence Point Array –
E140 N780 – Roof to Floor

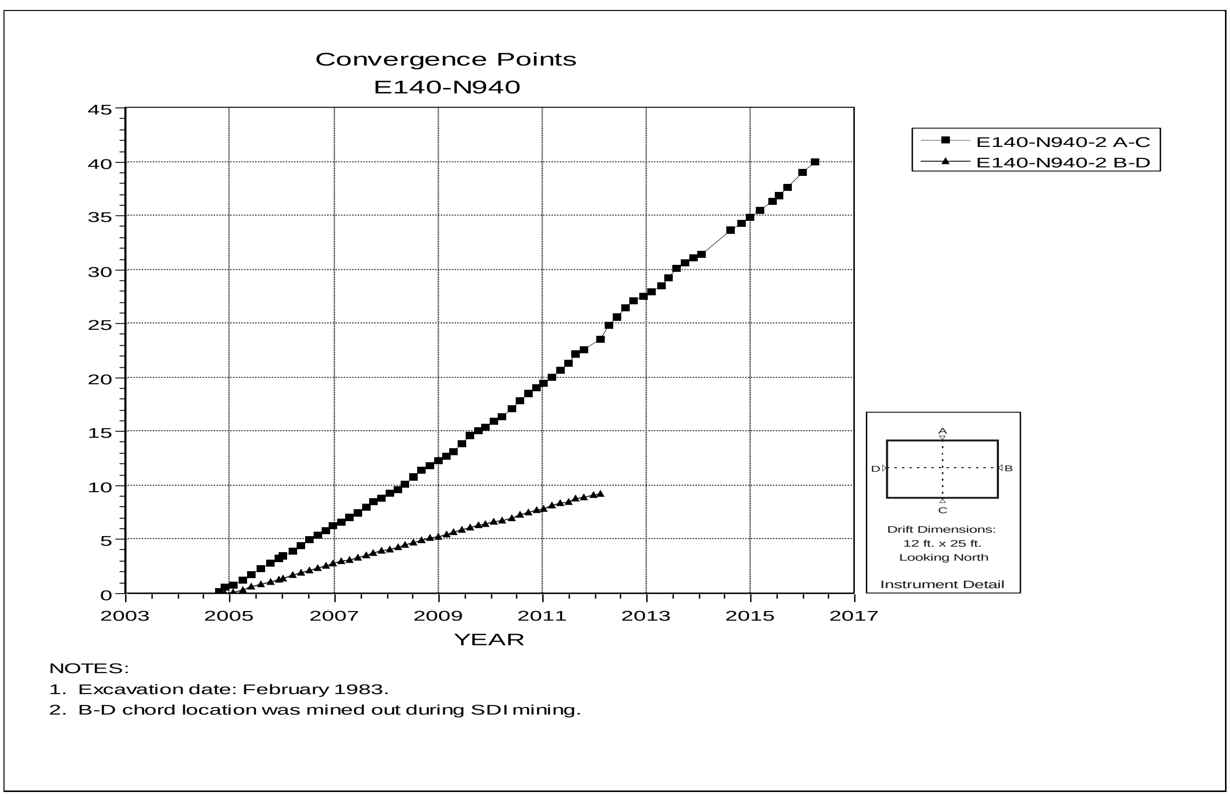

Figure 4-40 Convergence Point Array –
E140 N940 – All Chords

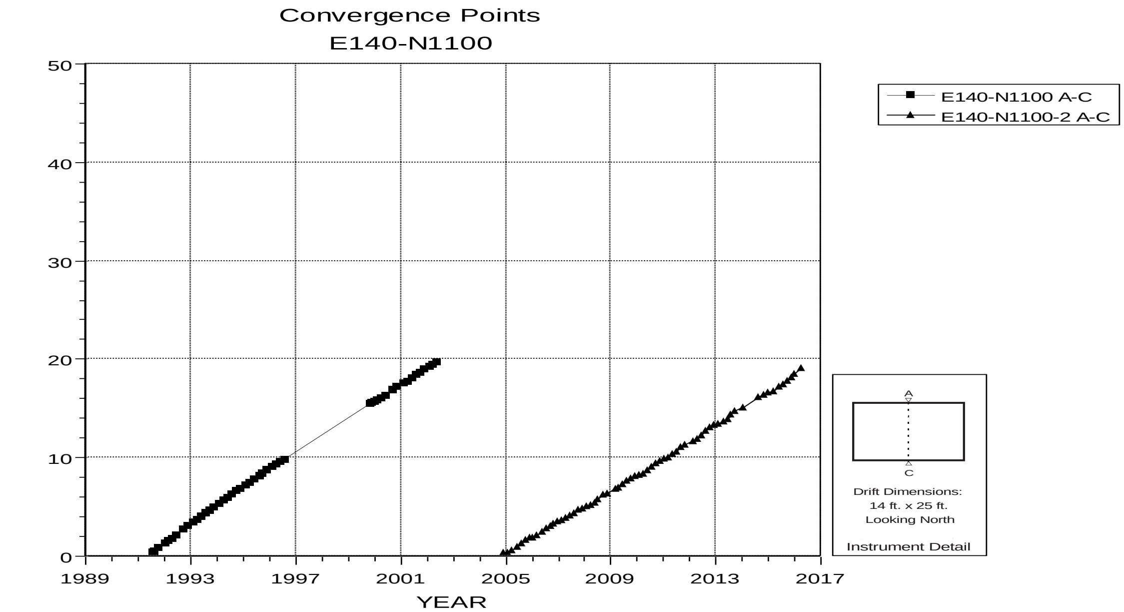

NOTES:
1. Excavation date: February 1983.
2. Inaccessible from 08/96 to 11/99.

Figure 4-41 Convergence Point Array –
E140 N1100 – Roof to Floor

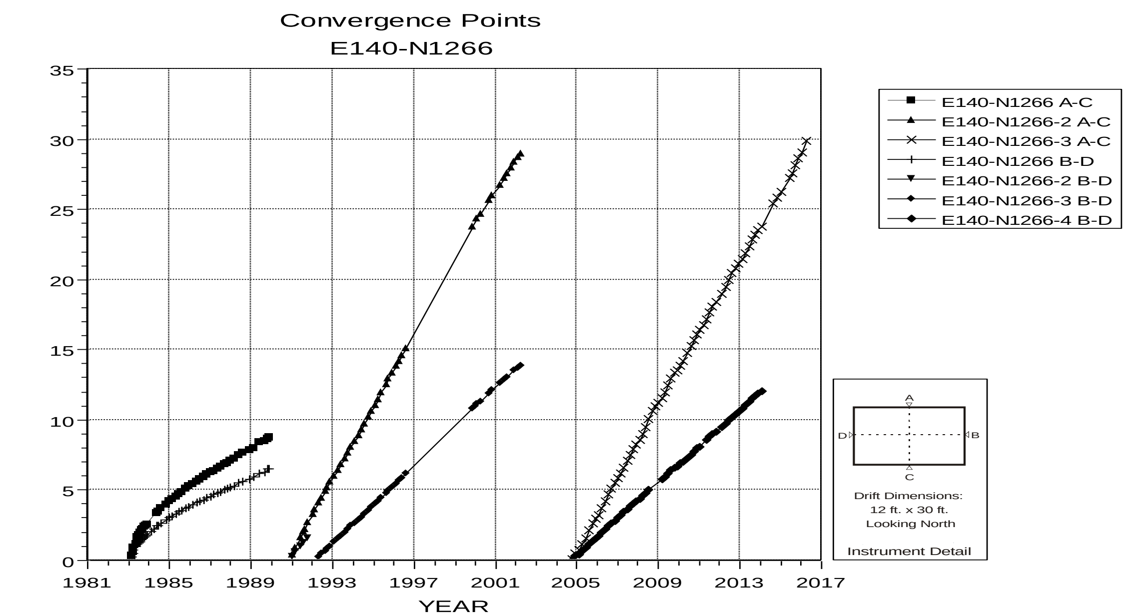

NOTES:
1. Excavation date: February 1983.
2. Enlarged from 8ft x 14ft in January 1990.
3. Inaccessible from 8/ 96 to 11/99.

Figure 4-42 Convergence Point Array –
E140 N1266 – Roof to Floor

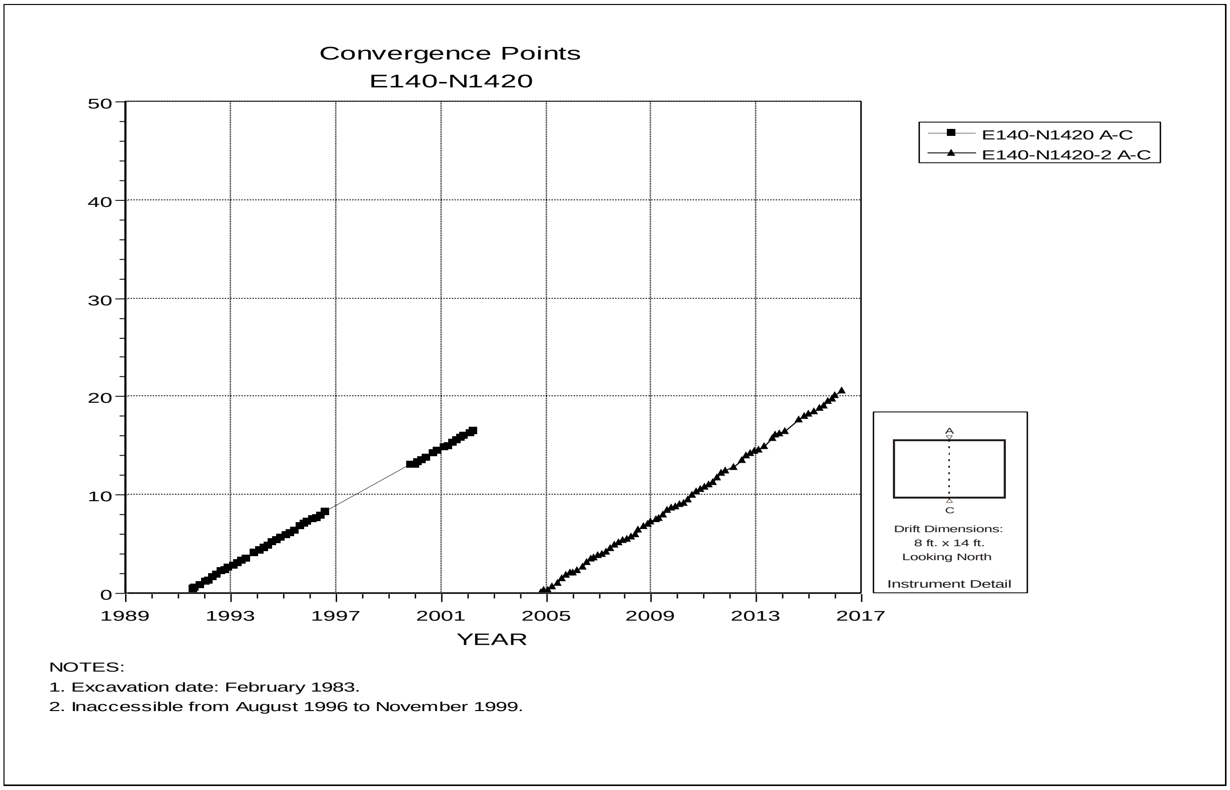

Figure 4-43 Convergence Point Array –
E140 N1420 – Roof to Floor

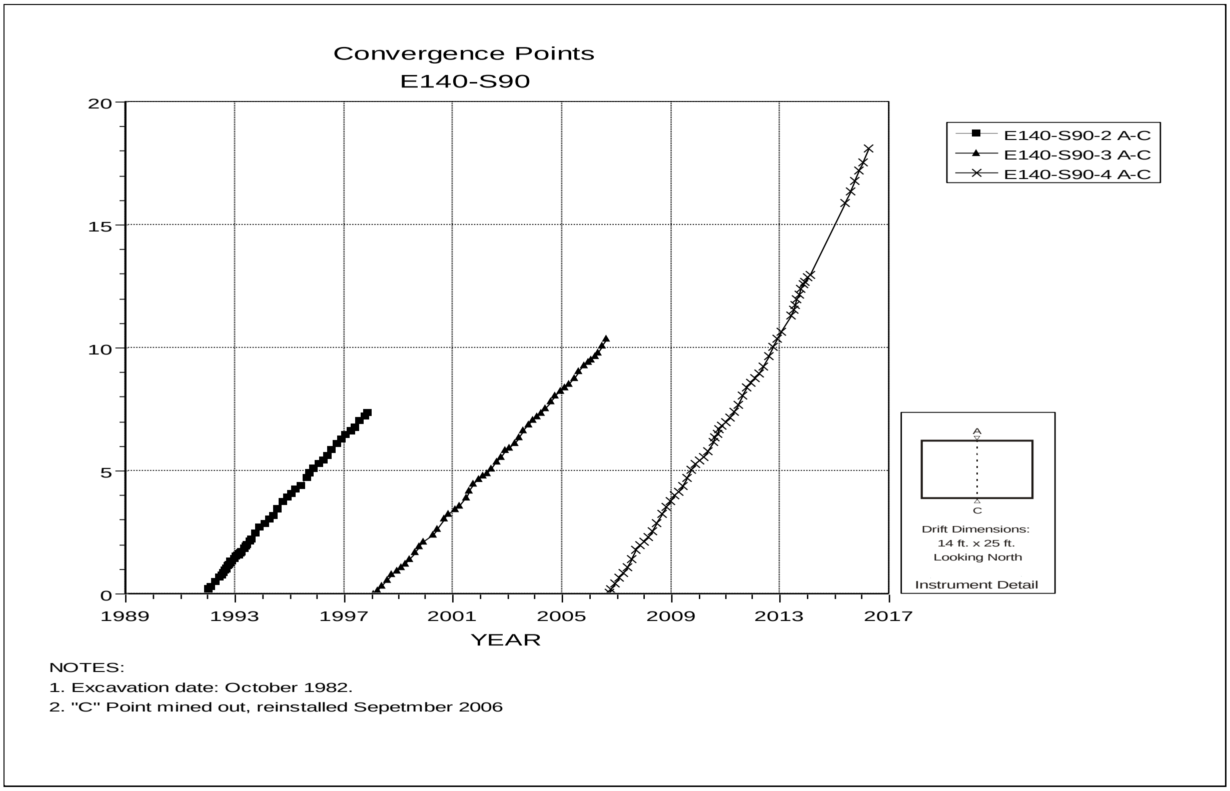

Figure 4-44 Convergence Point Array –
E140 S90 – Roof to Floor

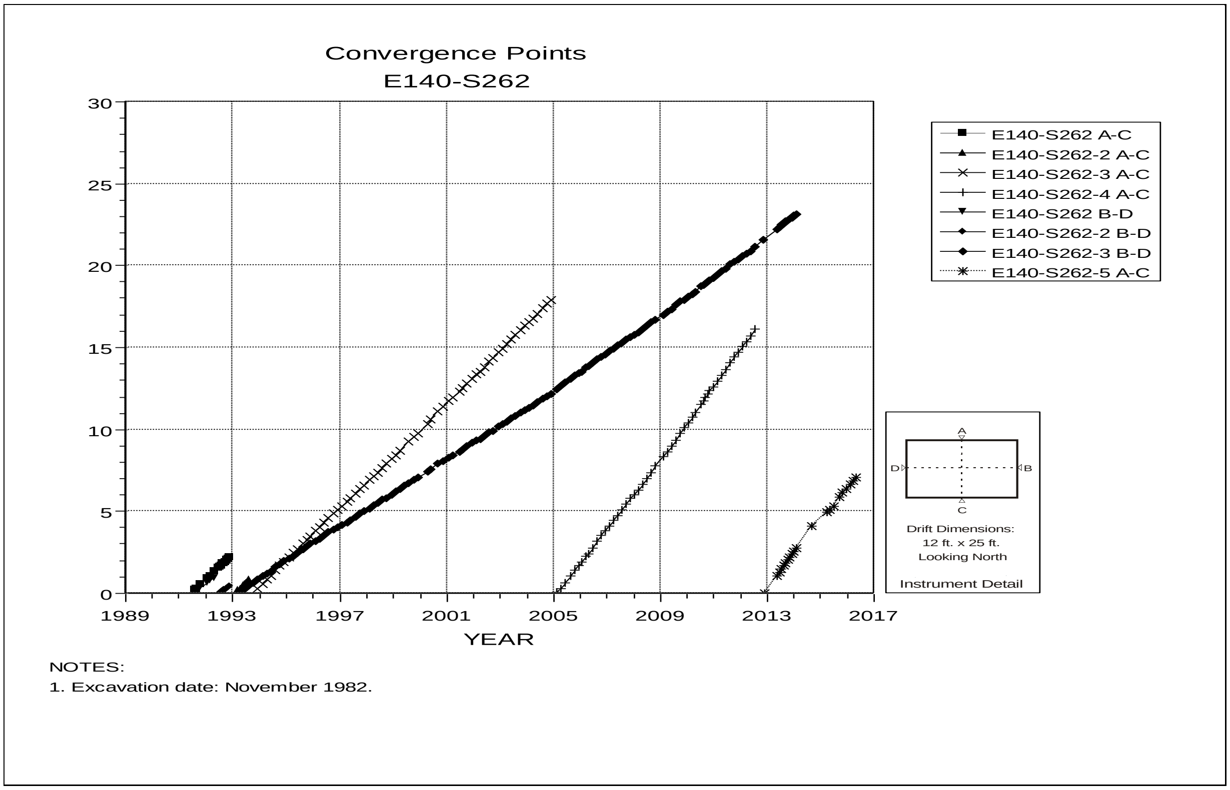

Figure 4-45 Convergence Point Array –
E140 S262 – All Chords

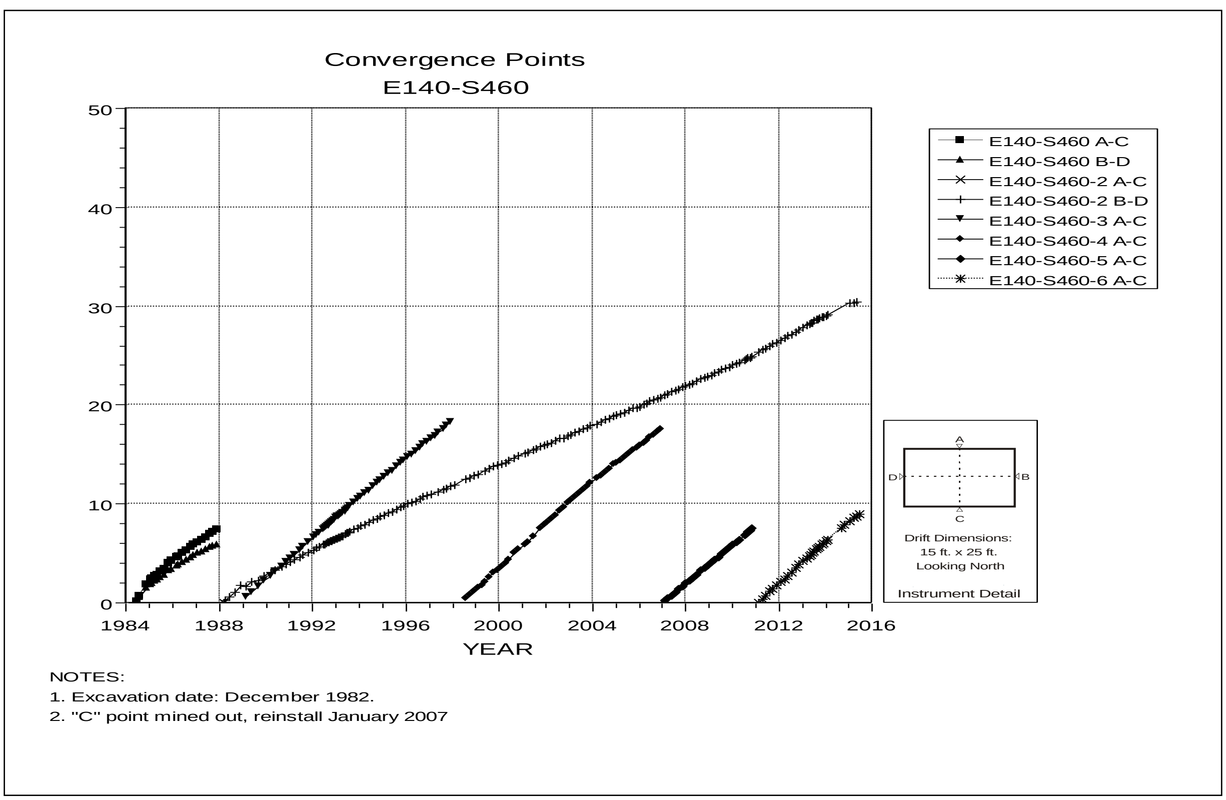

Figure 4-46 Convergence Point Array –
E140 S460 – All Chords

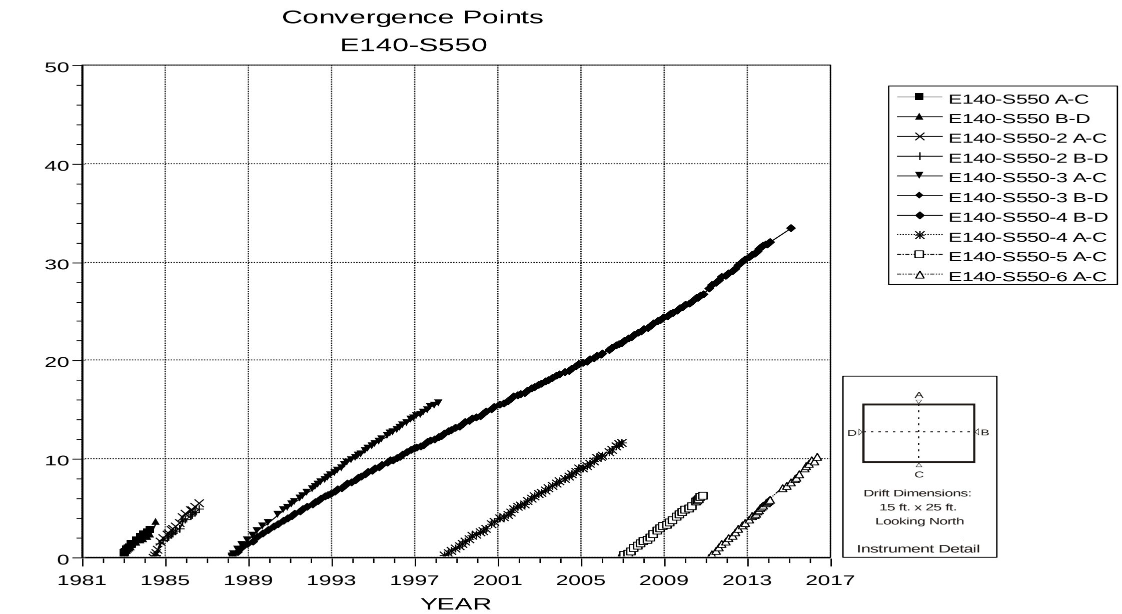

NOTES:
1. Excavation date: December 1982.

Figure 4-47 Convergence Point Array –
E140 S550 – All Chords

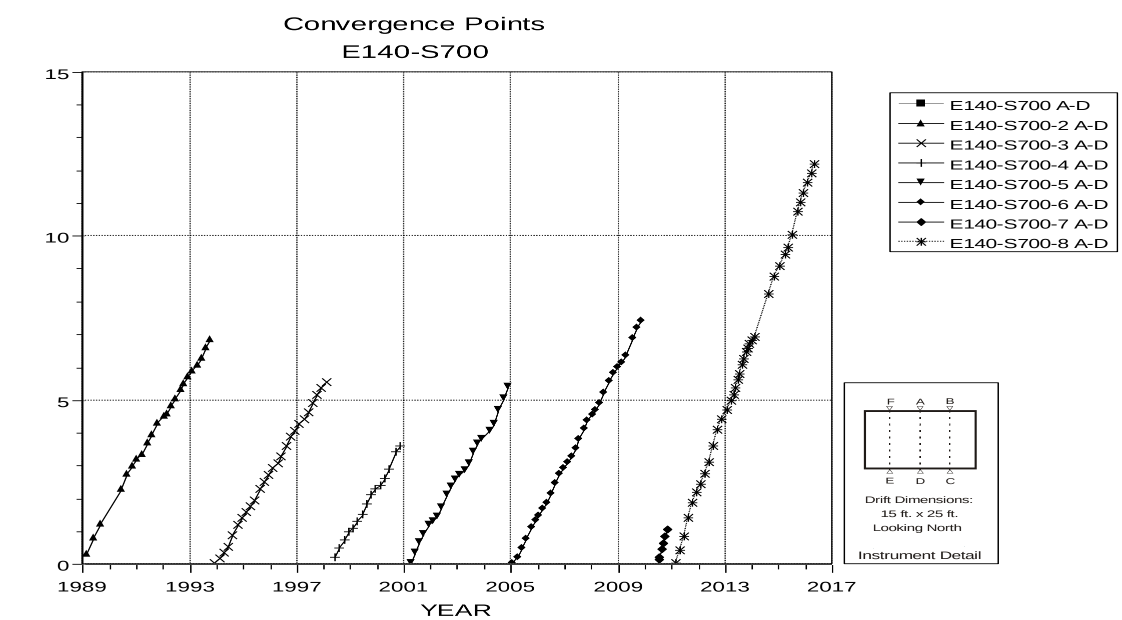

NOTES:
1. Excavation date: December 1982.

ISSUED

Figure 4-48 Convergence Point Array –
E140 S700 – Roof to Floor – Centerline

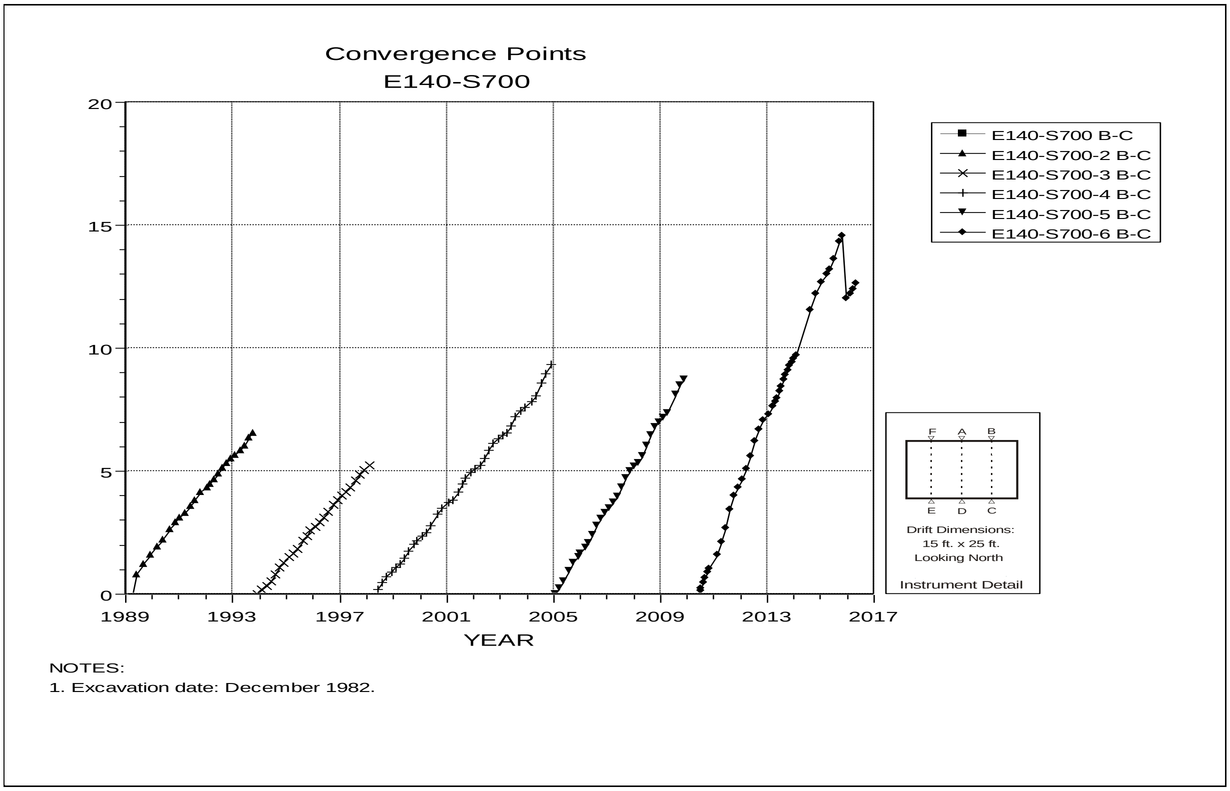

Figure 4-49 Convergence Point Array –
E140 S700 – Roof to Floor – East Quarter Point

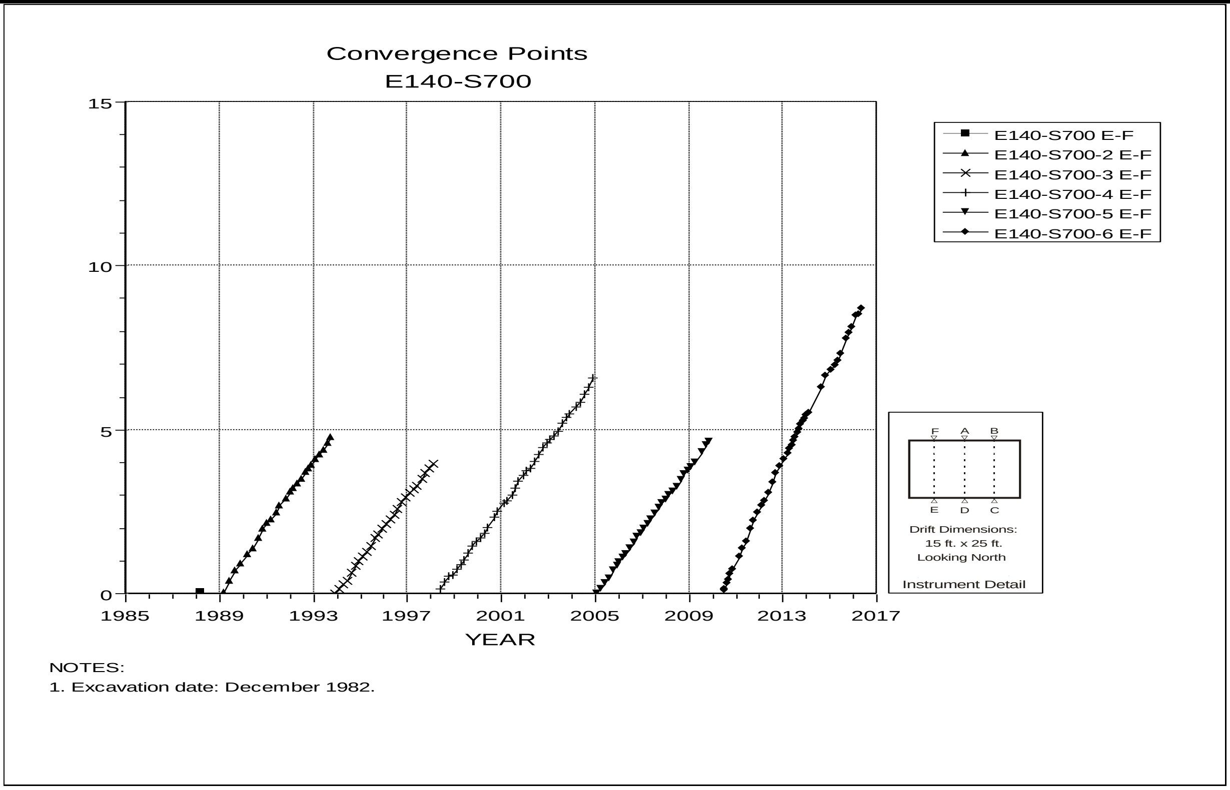

Figure 4-50 Convergence Point Array –
E140 S700 – Roof to Floor – West Quarter Point

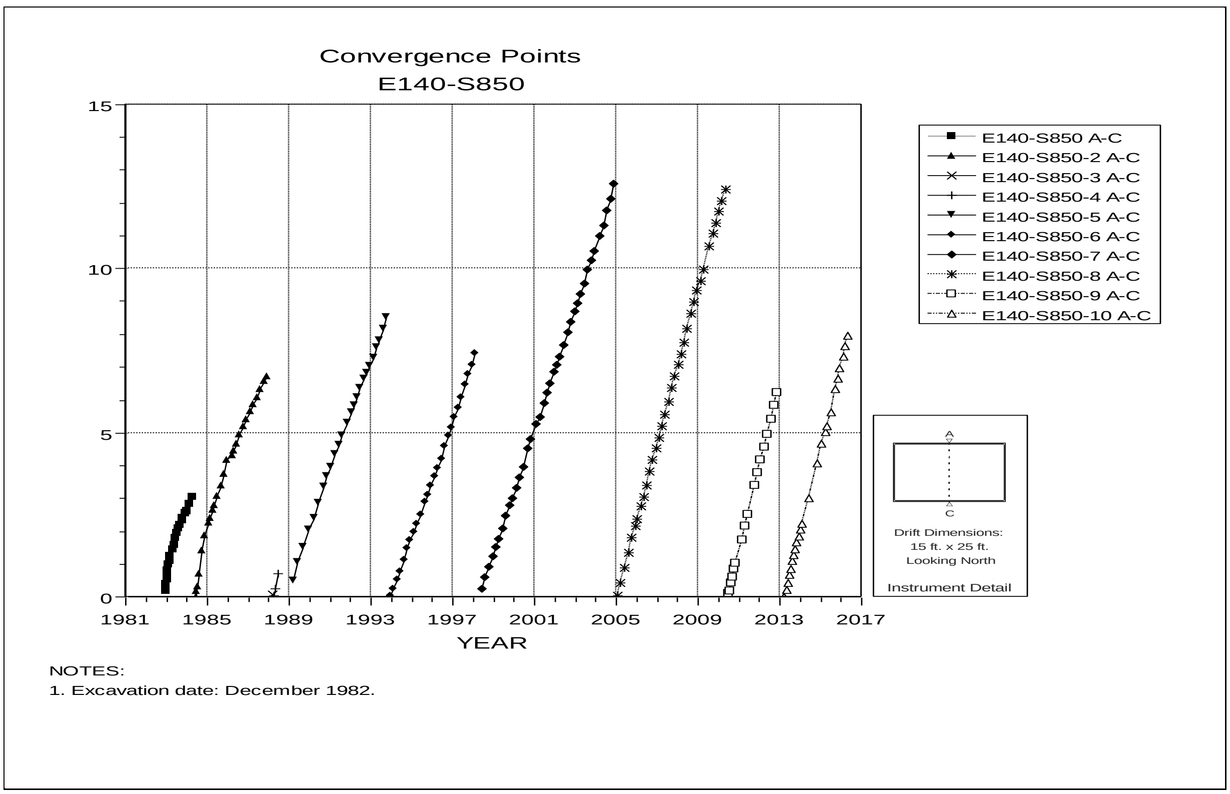

Figure 4-51 Convergence Point Array –
E140 S850 – Roof to Floor

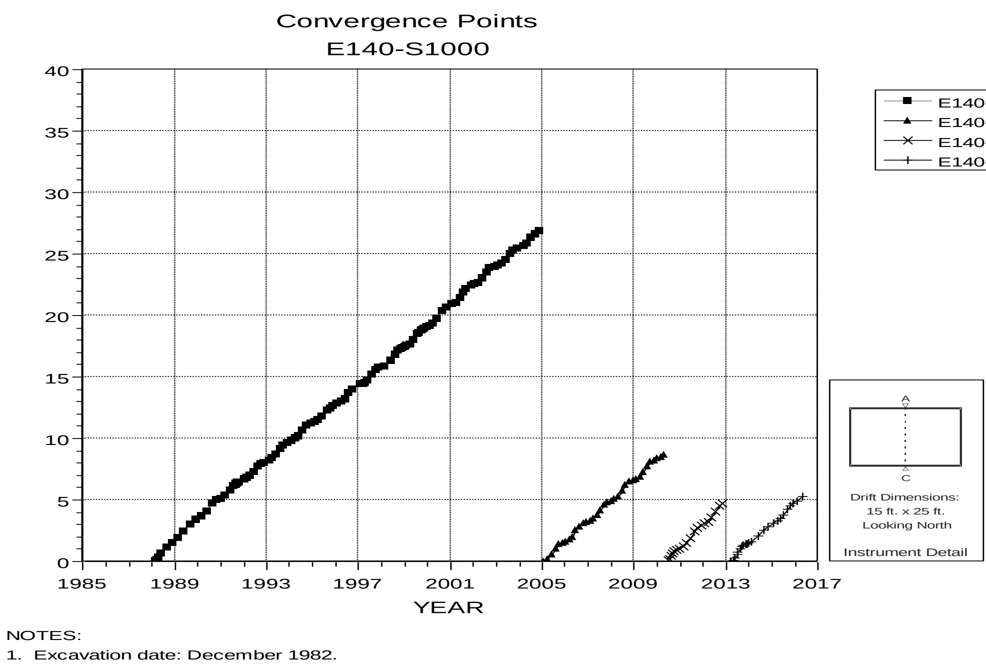

Figure 4-52 Convergence Point Array –
E140 S1000 – Roof to Floor

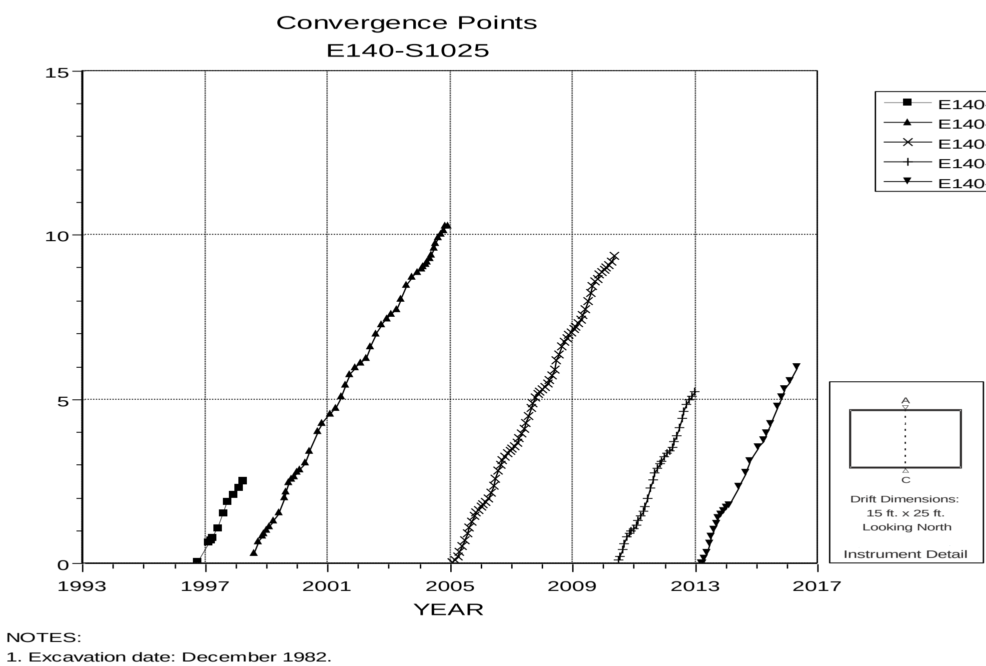

Figure 4-53 Convergence Point Array –
E140 S1025 – Roof to Floor

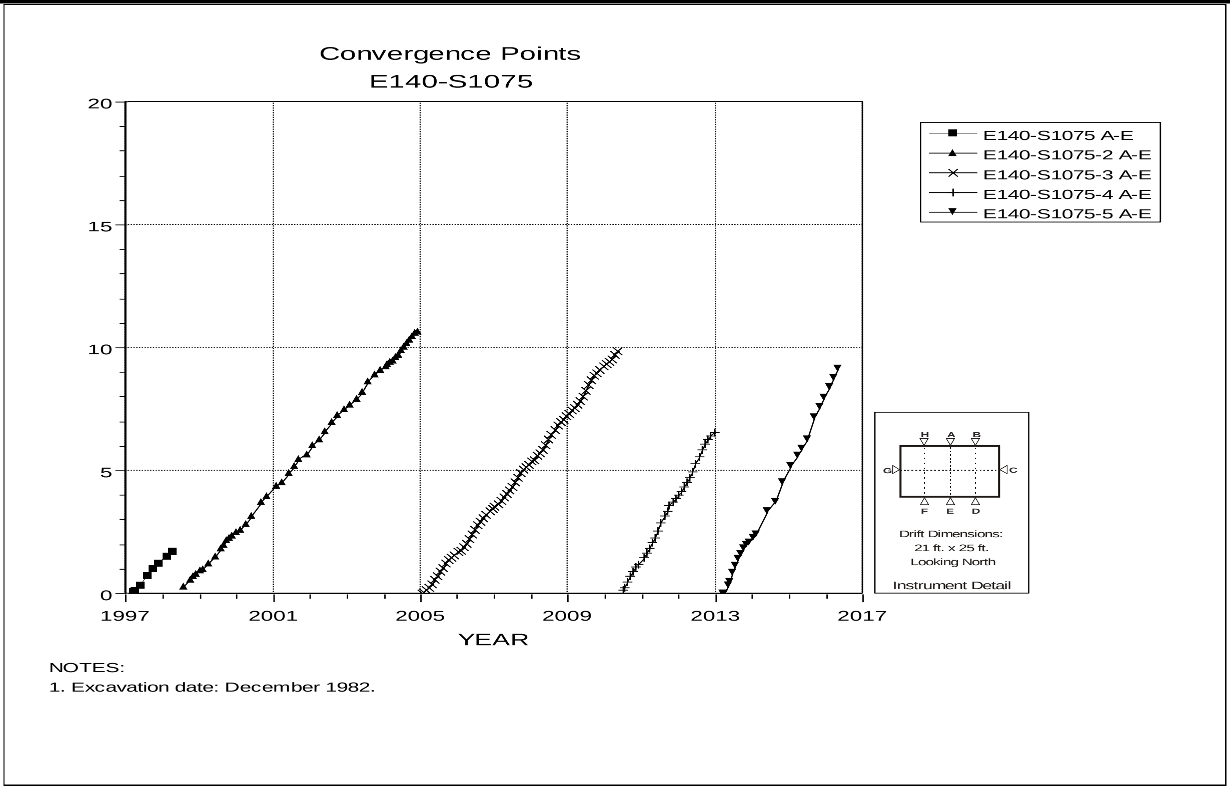

Figure 4-54 Convergence Point Array –
E140 S1075 – Roof to Floor – Centerline

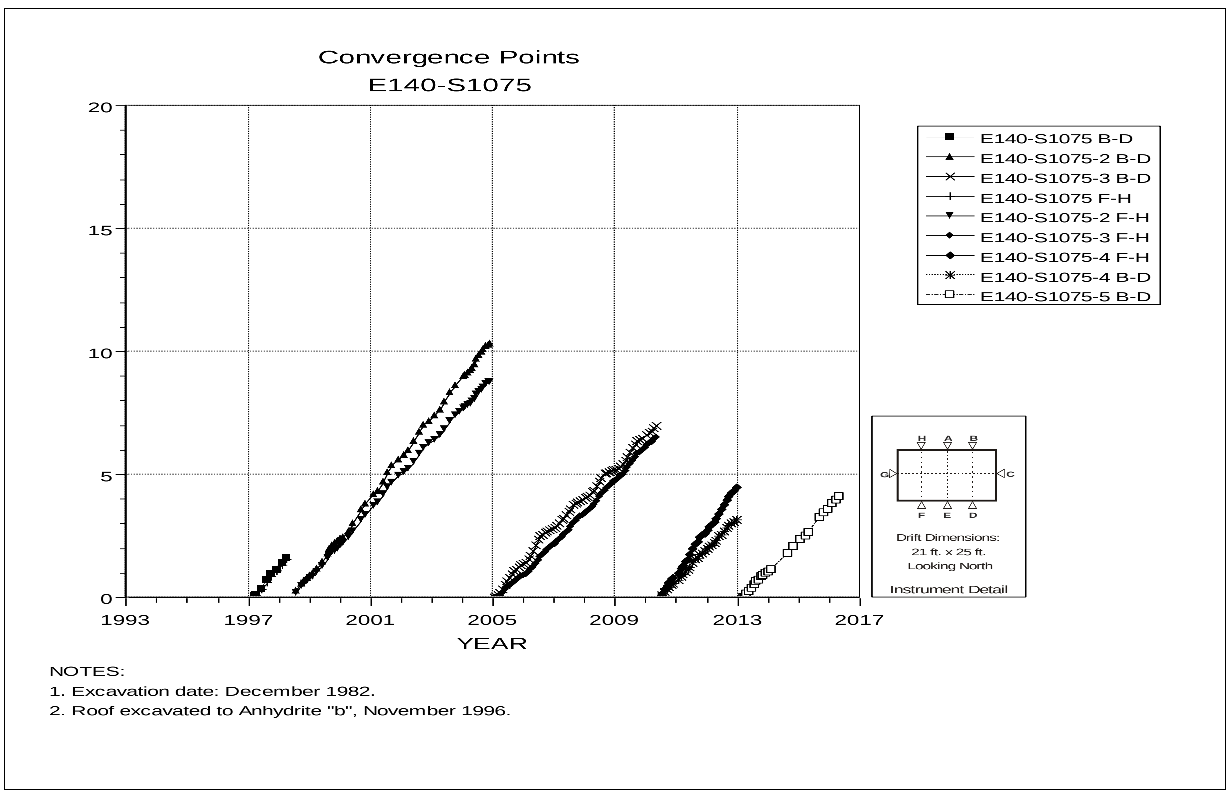

Figure 4-55 Convergence Point Array –
E140 S1075 – Roof to Floor – East Quarter Point

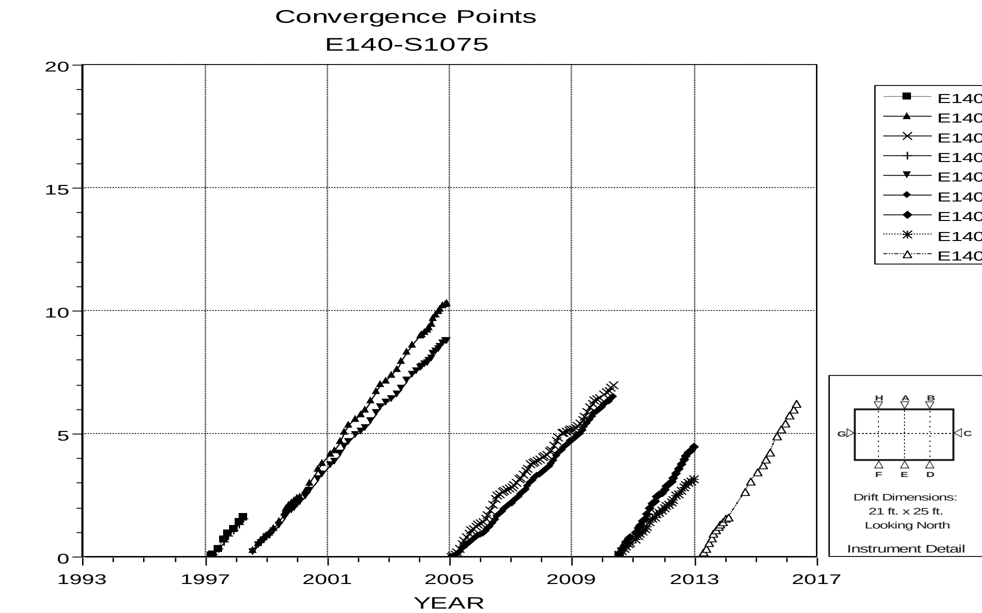

NOTES:
1. Excavation date: December 1982.
2. Roof excavated to Anhydrite "b", November 1996.

Figure 4-56 Convergence Point Array –
E140 S1075 – Roof to Floor – West Quarter Point

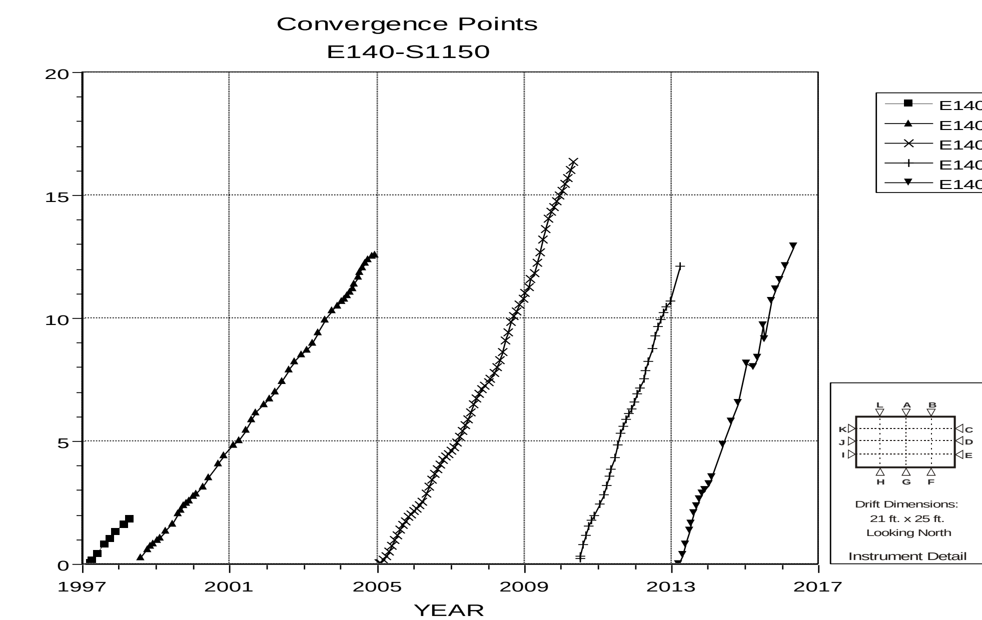

NOTES:
1. Excavation date: December 1982.
2. Roof excavated to Anhydrite "b", November 1996.

Figure 4-57 Convergence Point Array –
E140 S1150 – Roof to Floor – Centerline

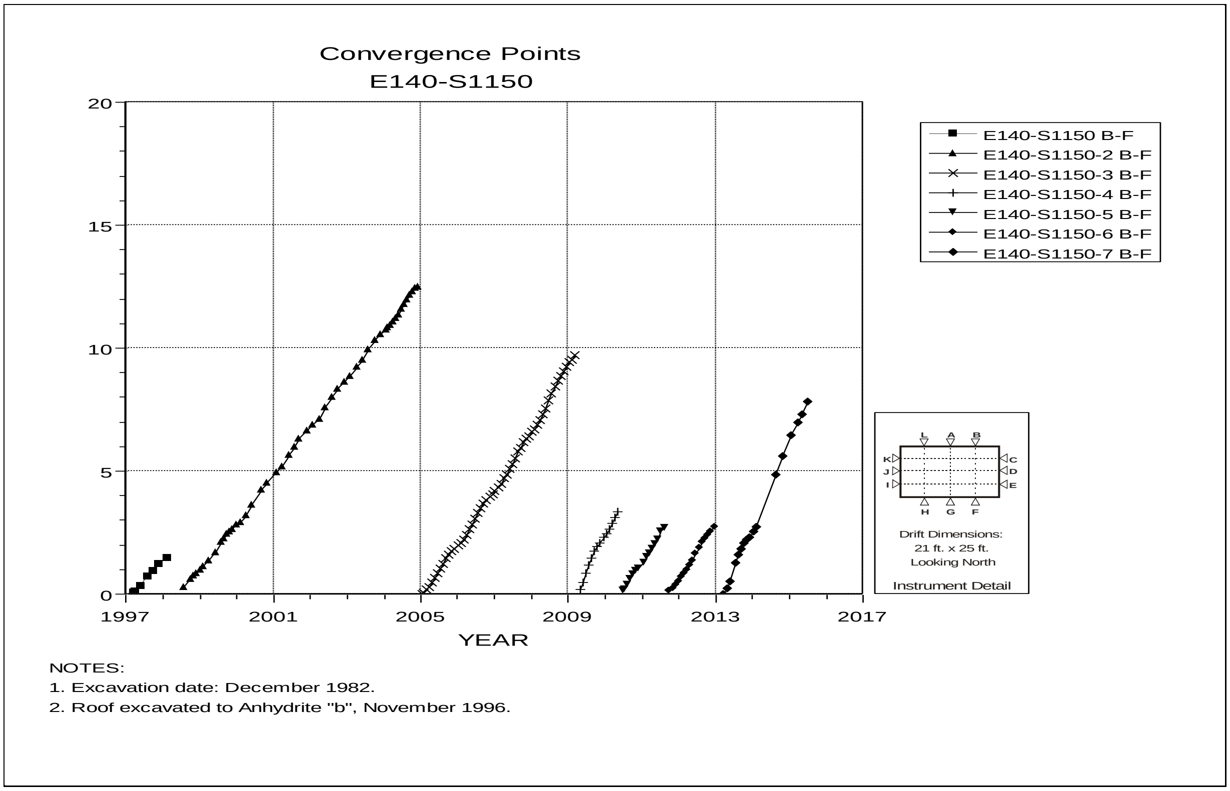

Figure 4-58 Convergence Point Array –
E140 S1150 – Roof to Floor – East Quarter Point

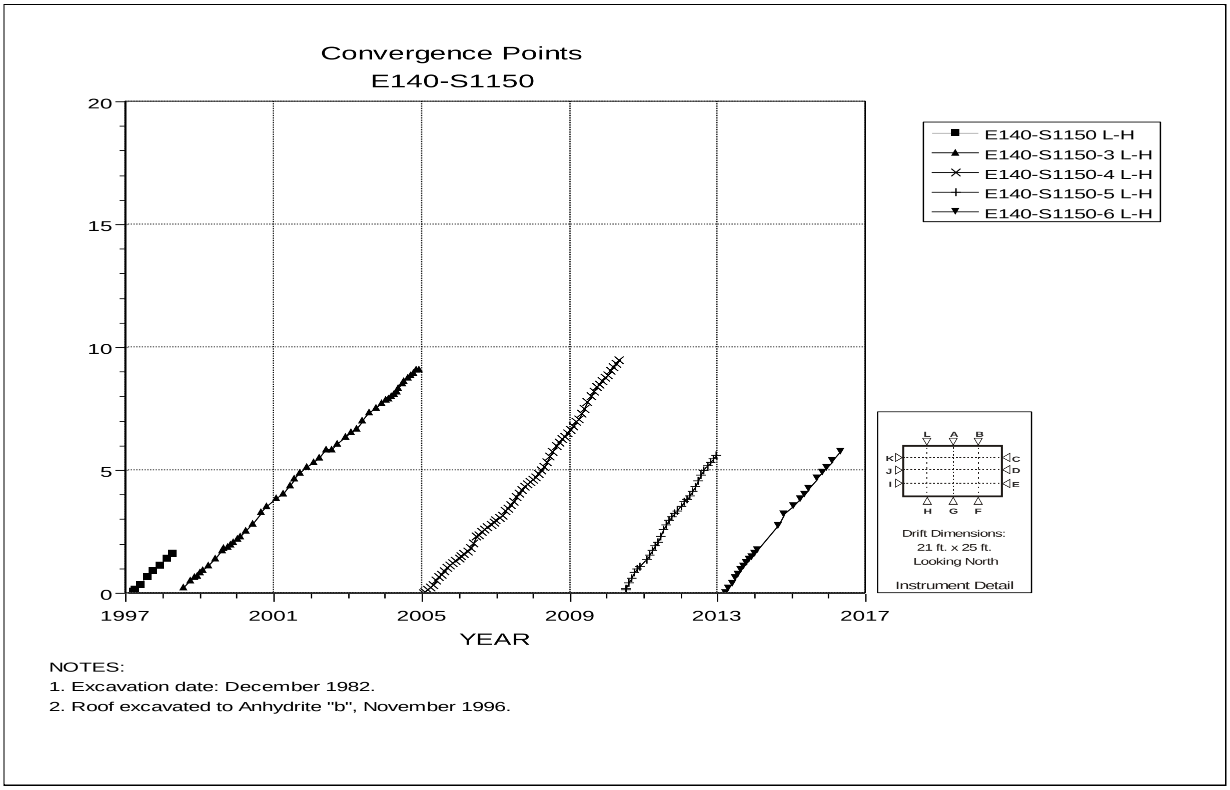

Figure 4-59 Convergence Point Array –
E140 S1150 – Roof to Floor – West Quarter Point

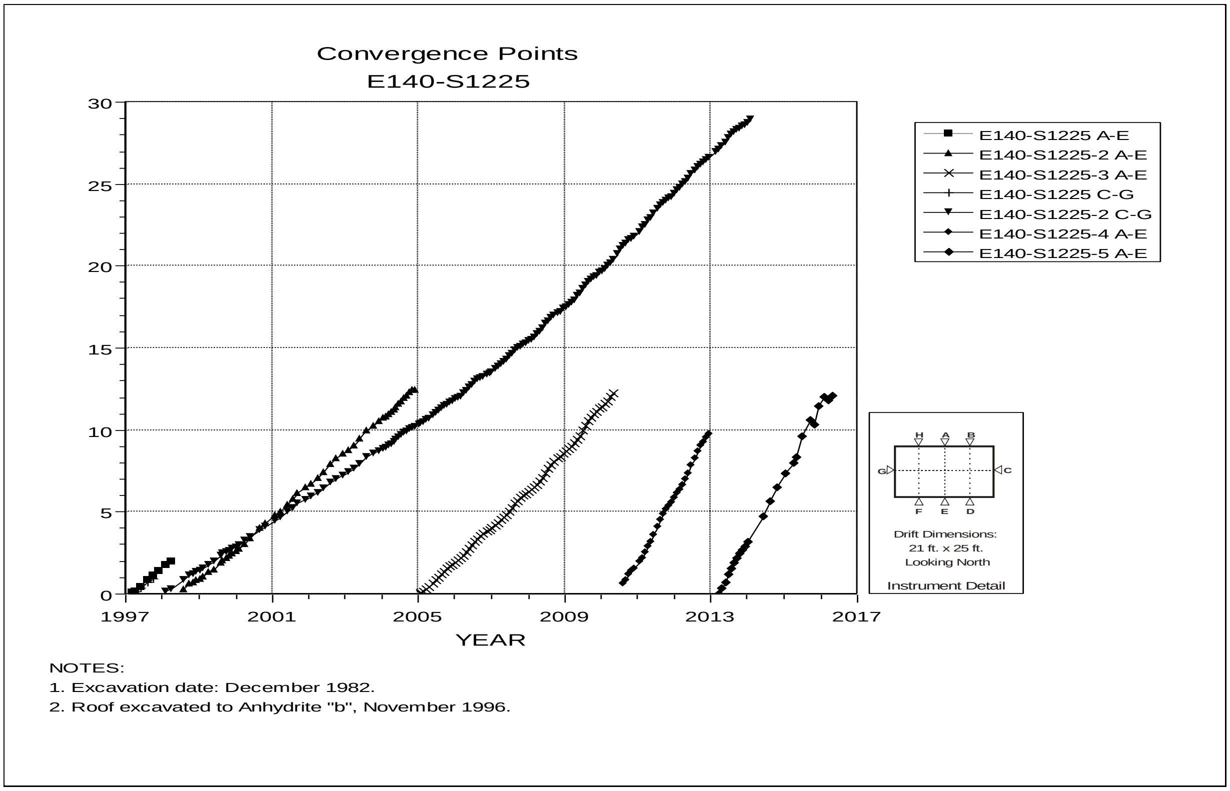

Figure 4-60 Convergence Point Array –
E140 S1225 – Roof to Floor – Centerline

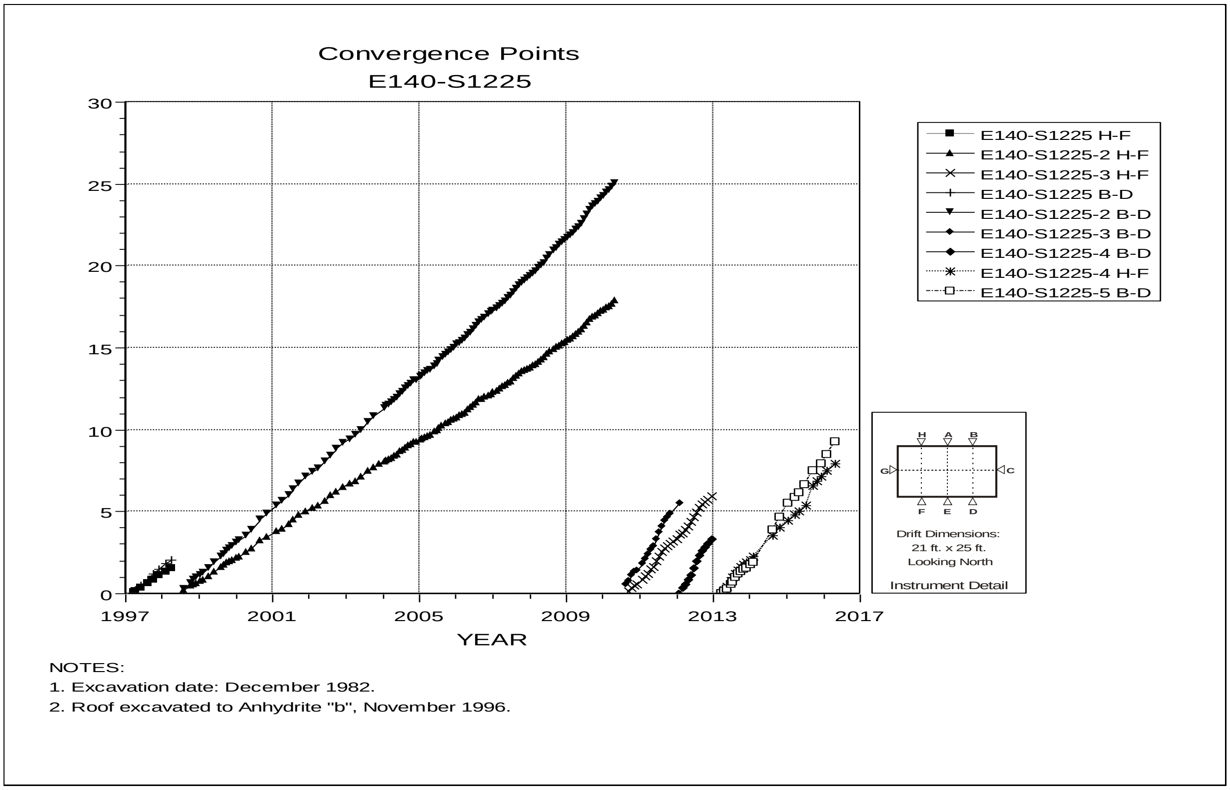

Figure 4-61 Convergence Point Array –
E140 S1225 – Roof to Floor – East Quarter Point

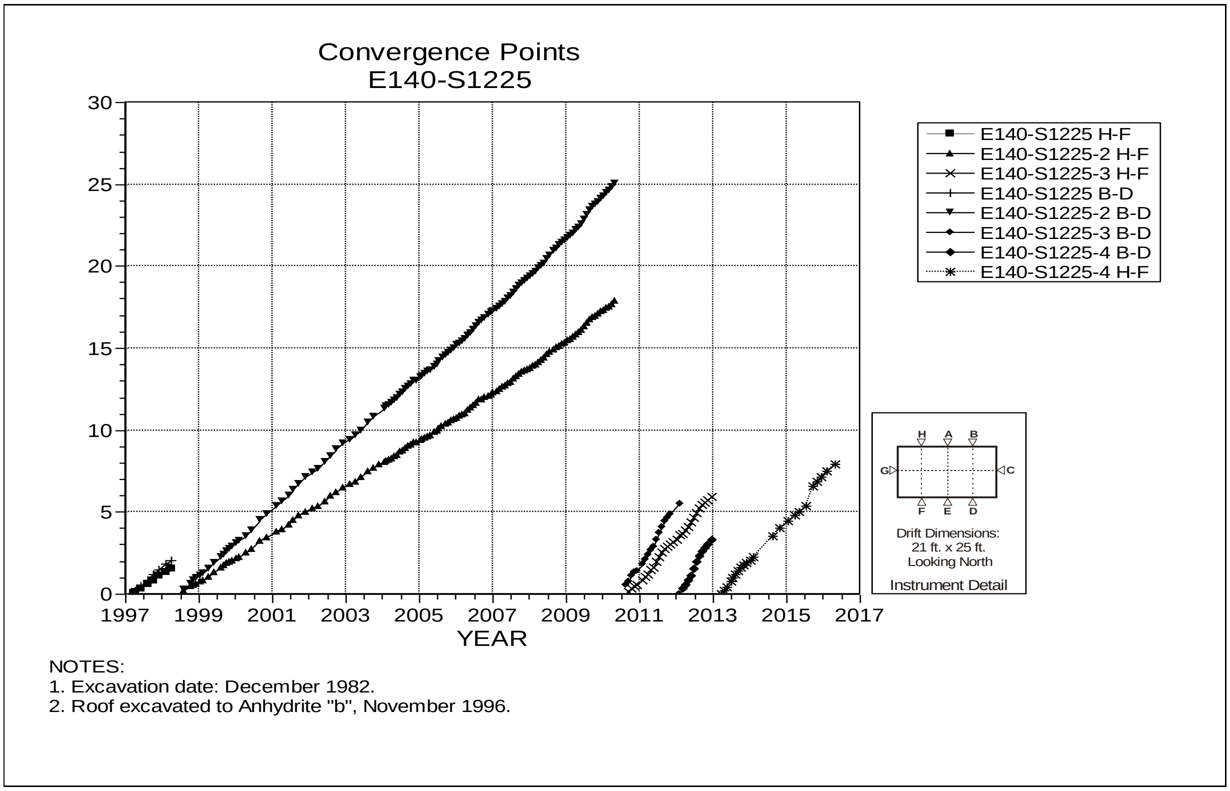

Figure 4-62 Convergence Point Array–
E140 S1225 – Roof to Floor – West Quarter Point

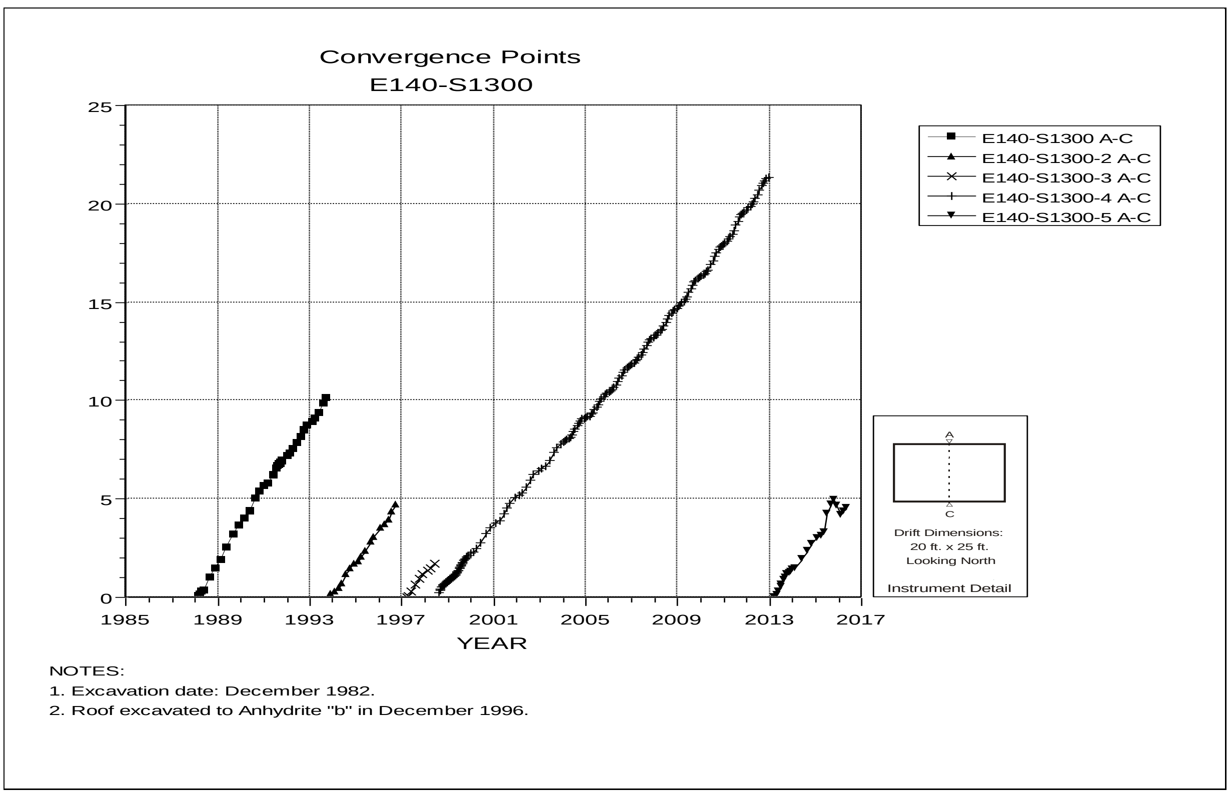

Figure 4-63 Convergence Point Array –
E140 S1300 – Roof to Floor

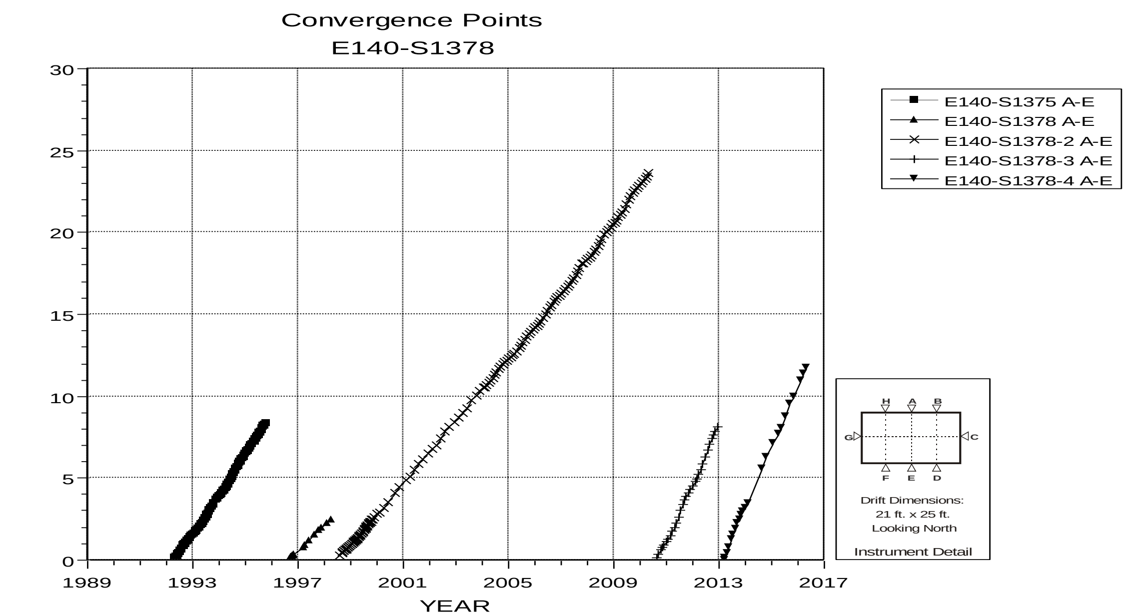

NOTES:
1. Excavation date: December 1982.
2. Roof excavated to Anhydrite "b" in December 1995.

Figure 4-64 Convergence Point Array –
E140 S1378 – Roof to Floor – Centerline

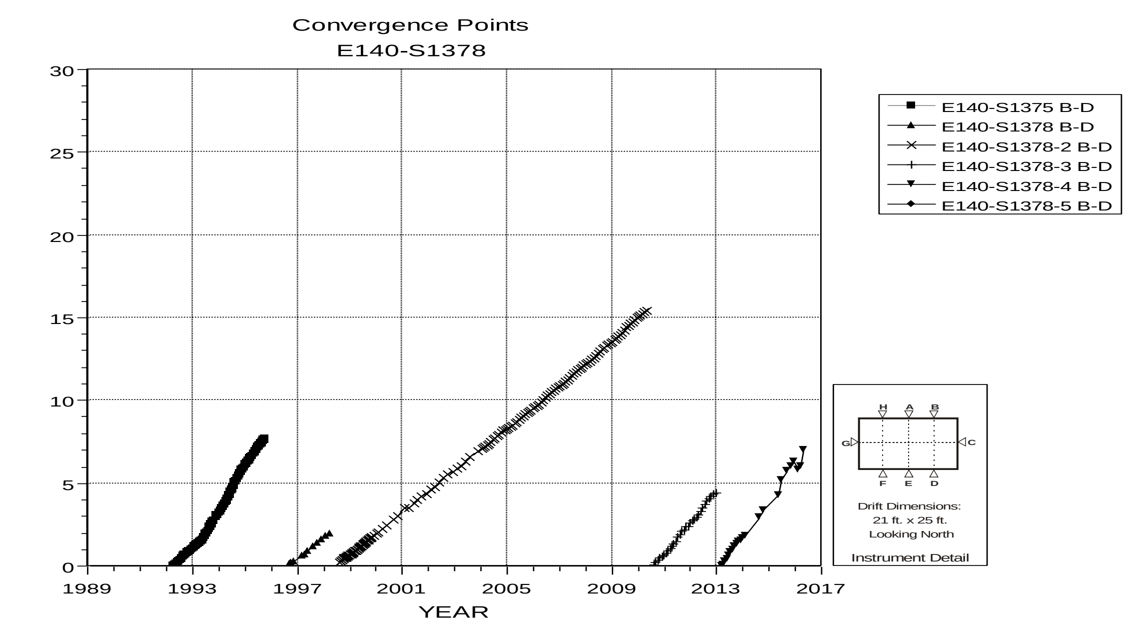

NOTES:
1. Excavation date: December 1982.
2. Roof excavated to Anhydrite "b" in December 1995.

Figure 4-65 Convergence Point Array –
E140 S1378 – Roof to Floor – West Quarter Point

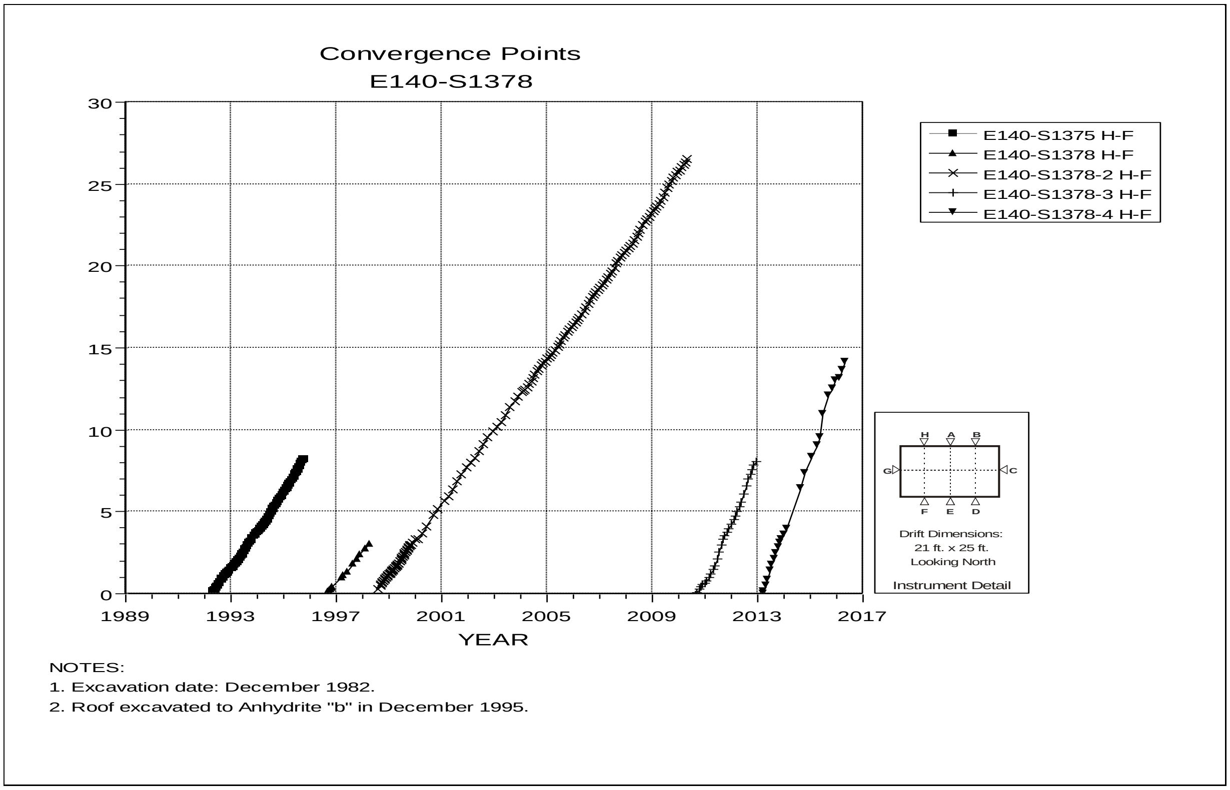

Figure 4-66 Convergence Point Array –
E140 S1378 – Roof to Floor – East Quarter Point

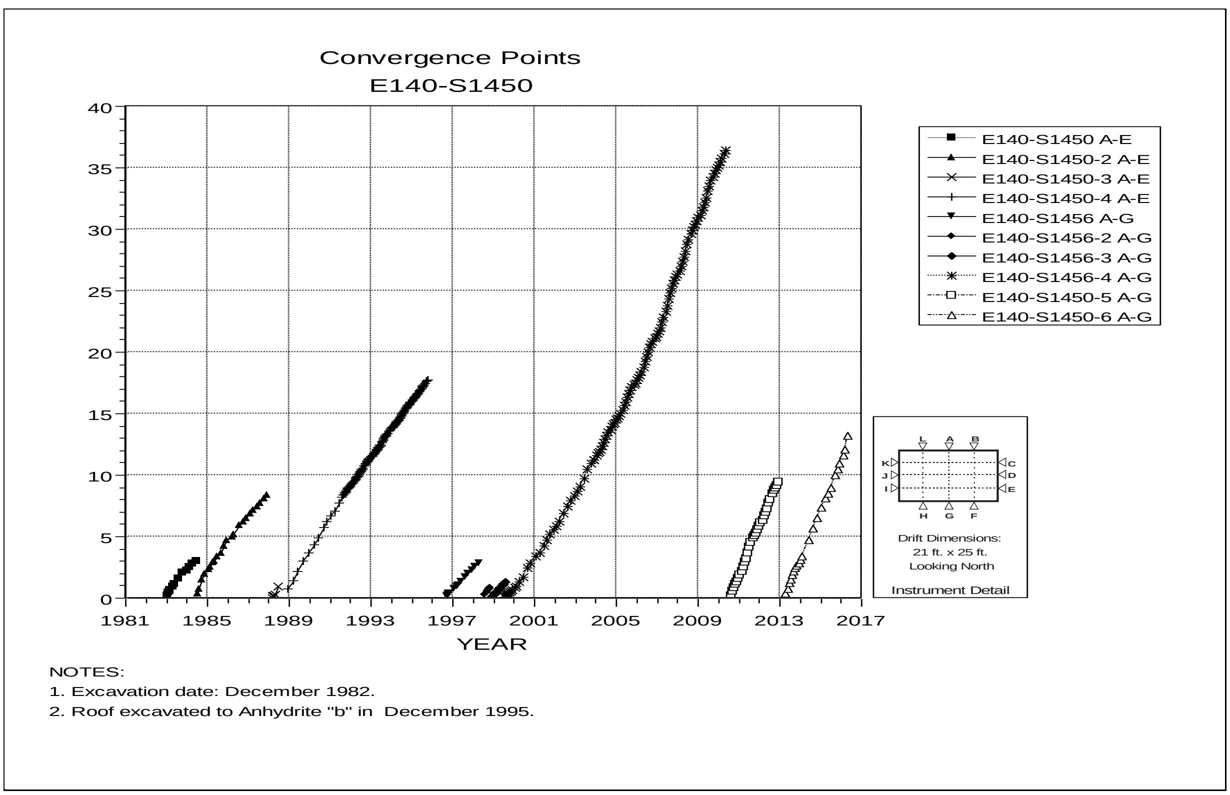

Figure 4-67 Convergence Point Array –
E140 S1450 – Roof to Floor – Centerline

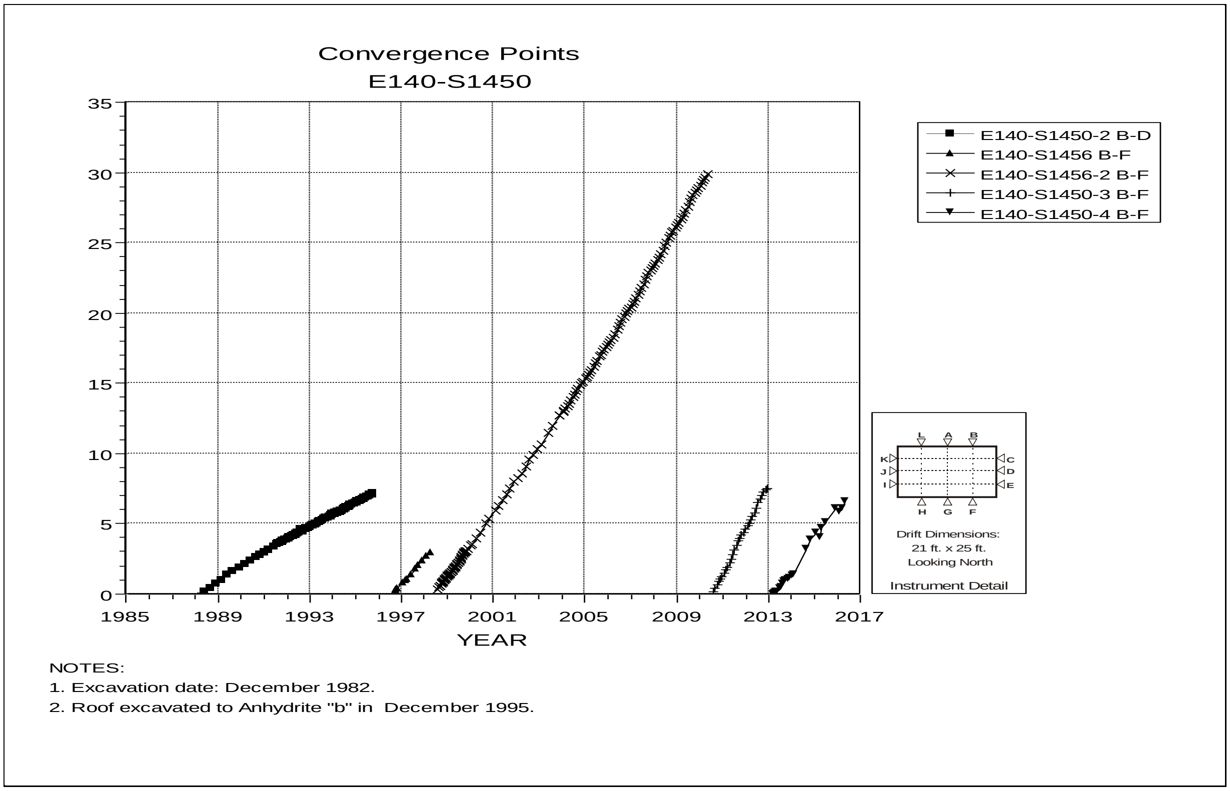

Figure 4-68 Convergence Point Array –
E140 S1450 – Roof to Floor – East Quarter Point

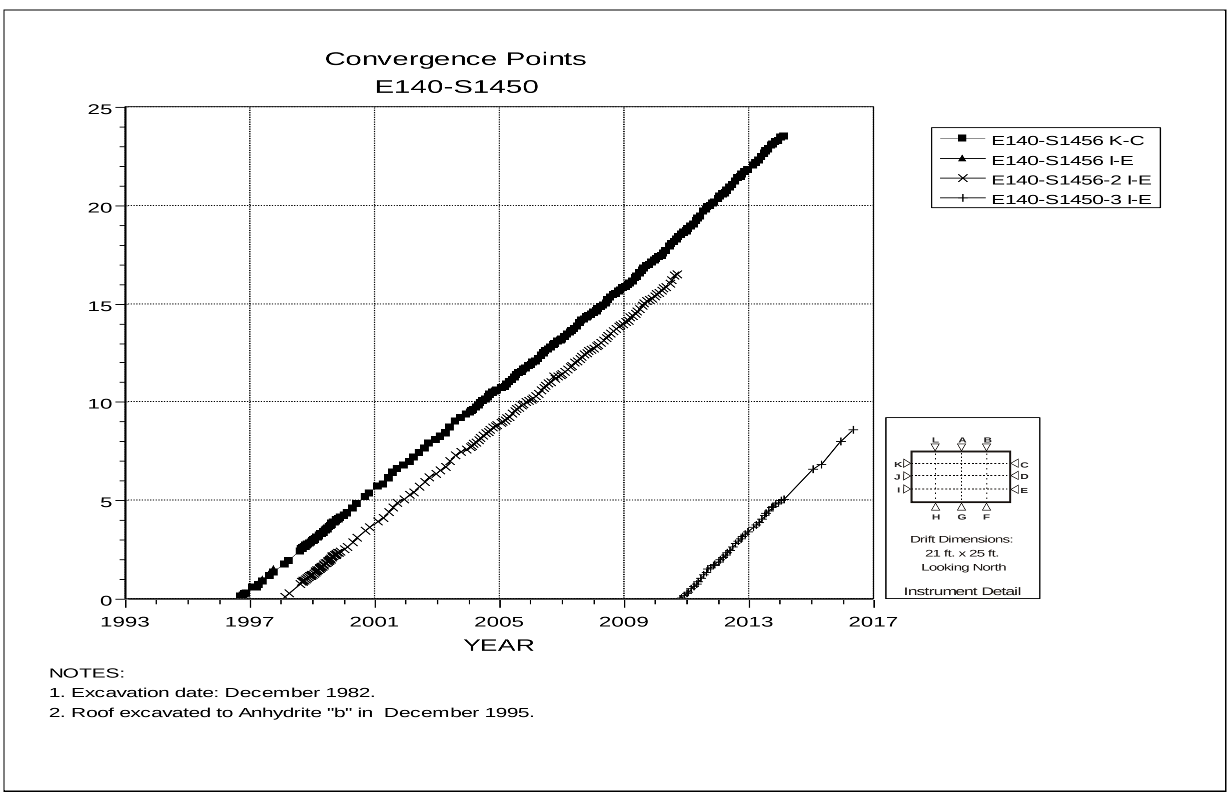

Figure 4-69 Convergence Point Array –
E140 S1450 – Rib to Rib

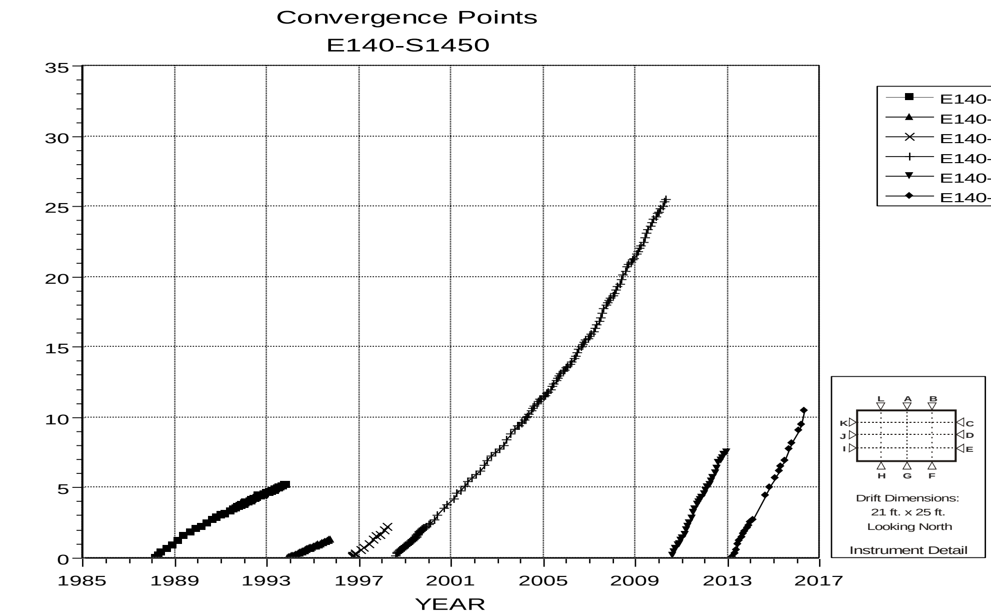

NOTES:
1. Excavation date: December 1982.
2. Roof excavated to Anhydrite "b" in December 1995.

Figure 4-70 Convergence Point Array –
E140 S1450 – Roof to Floor – West Quarter Point

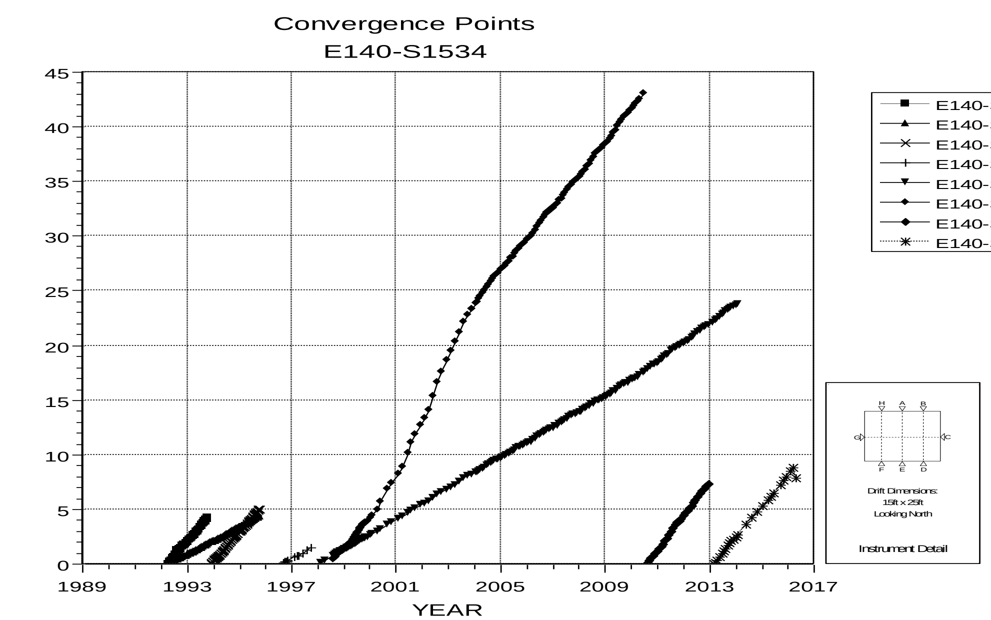

NOTES:
1. Excavation date: December 1982.
2. Roof excavated to Anhydrite "b" in December 1995.
3. Replaced by E140-S1534.

Figure 4-71 Convergence Point Array –
E140 S1534 – Roof to Floor – Centerline and Rib to Rib

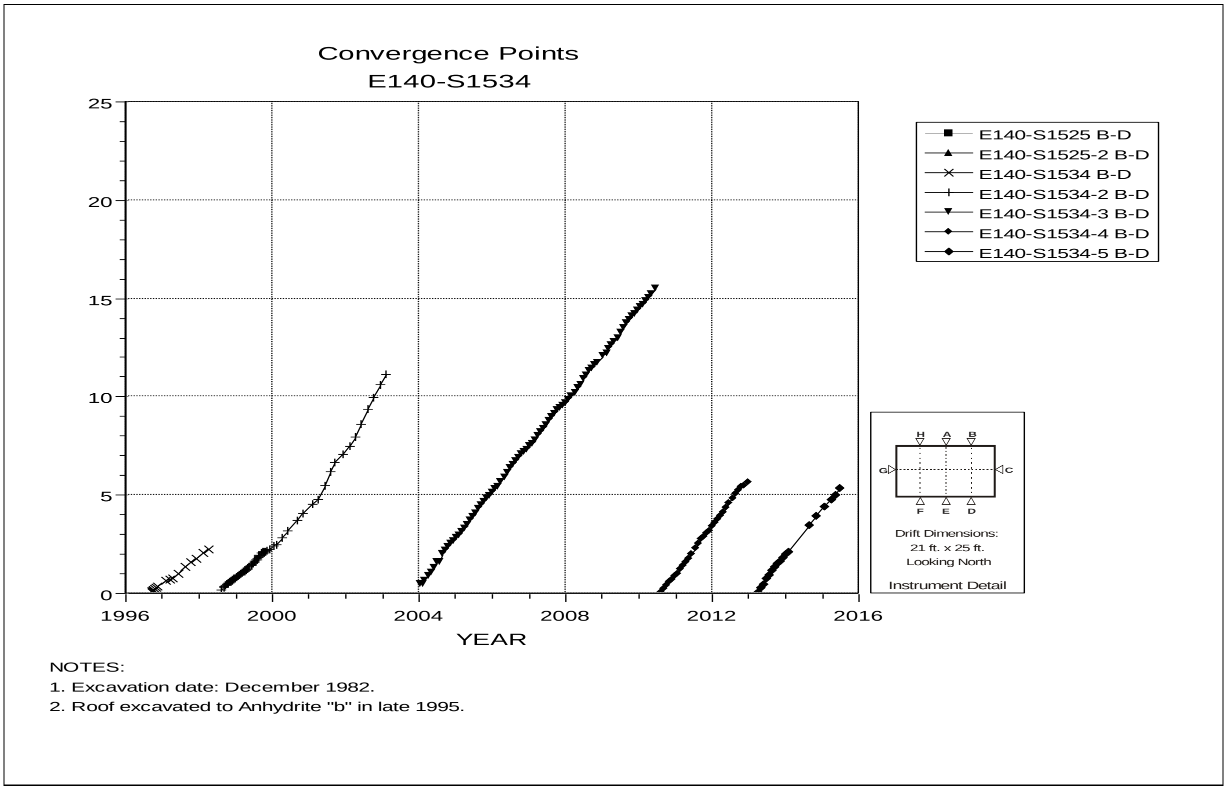

Figure 4-72 Convergence Point Array –
E140 S1534 – Roof to Floor – East Quarter Point

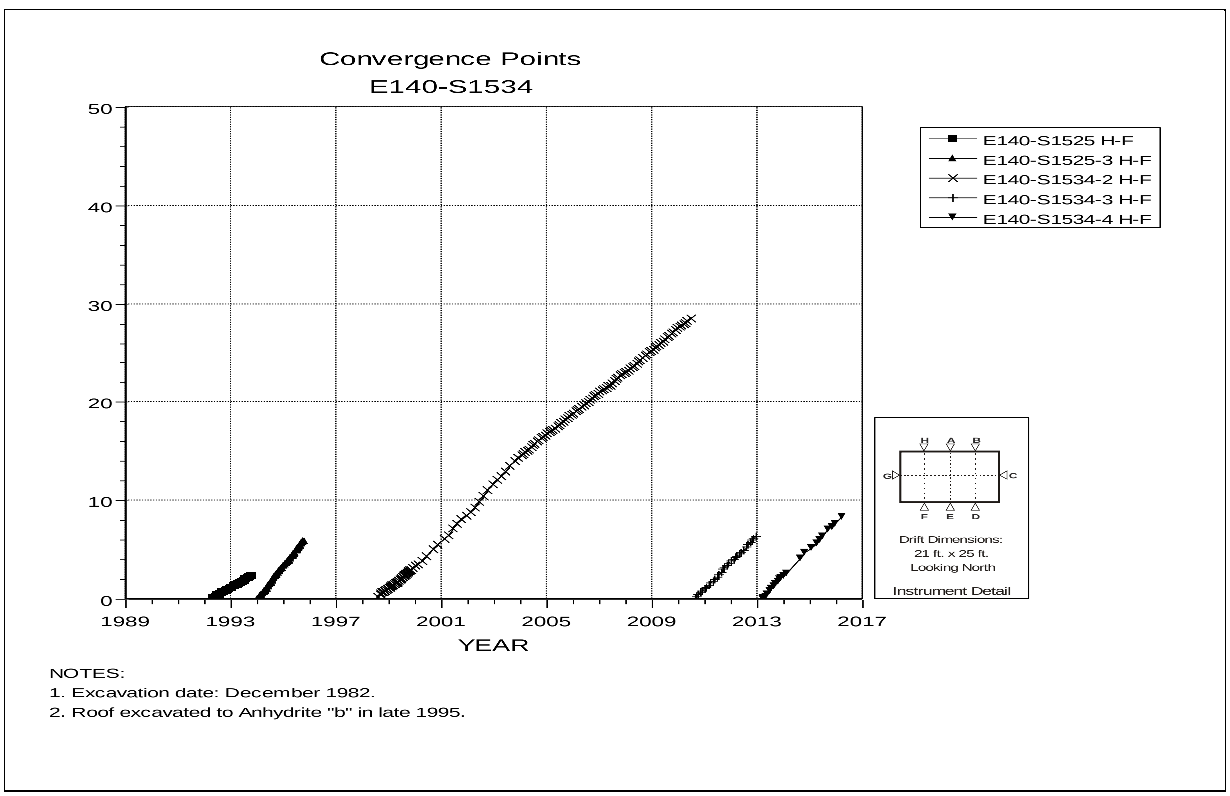

Figure 4-73 Convergence Point Array –

E140 S1534 – Roof to Floor – West Quarter Point

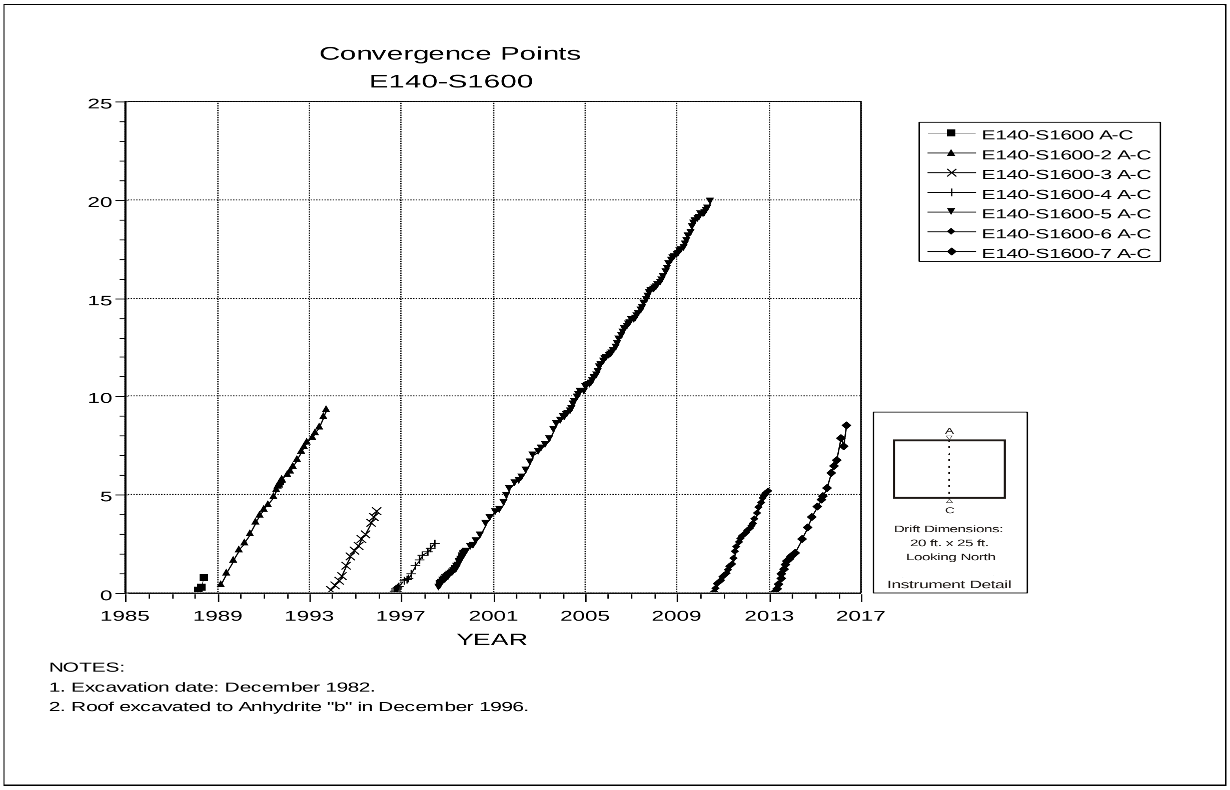

Figure 4-74 Convergence Point Array –
E140 S1600 – Roof to Floor

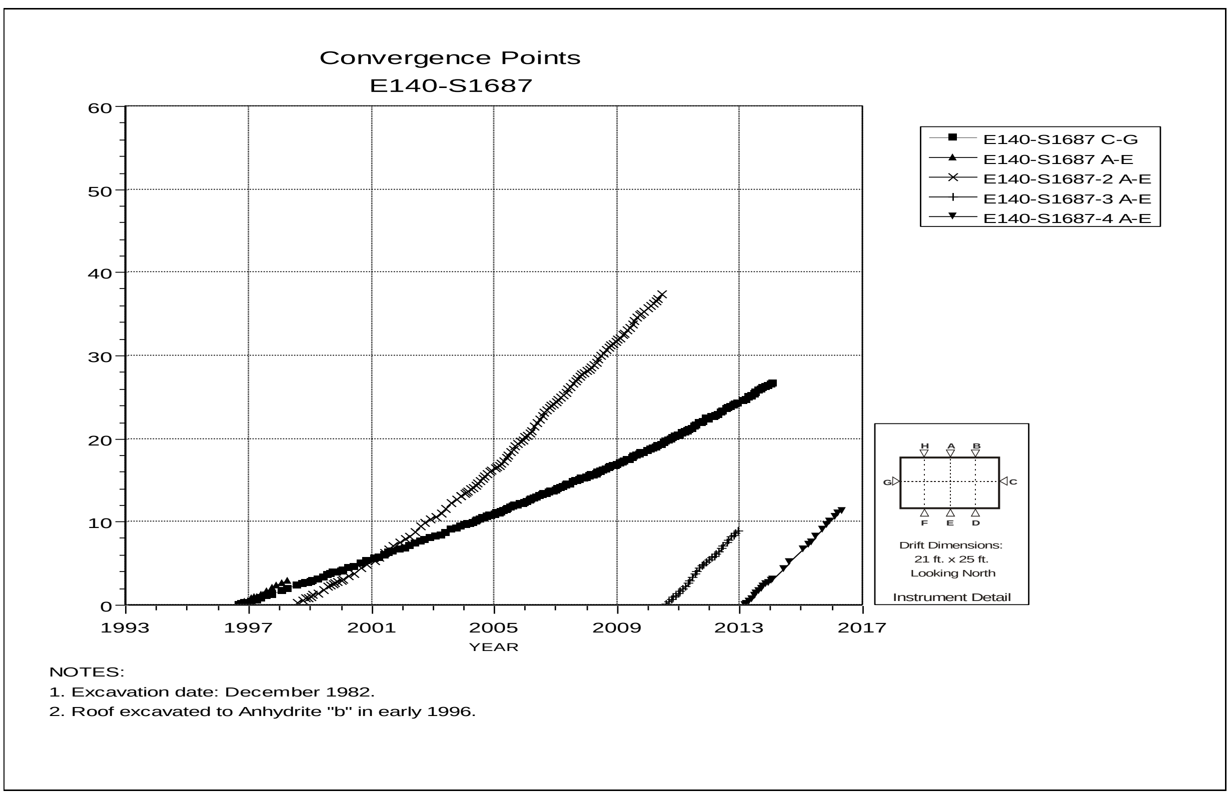

Figure 4-75 Convergence Point Array –
E140 S1687 – Roof to Floor – Centerline and Rib to Rib

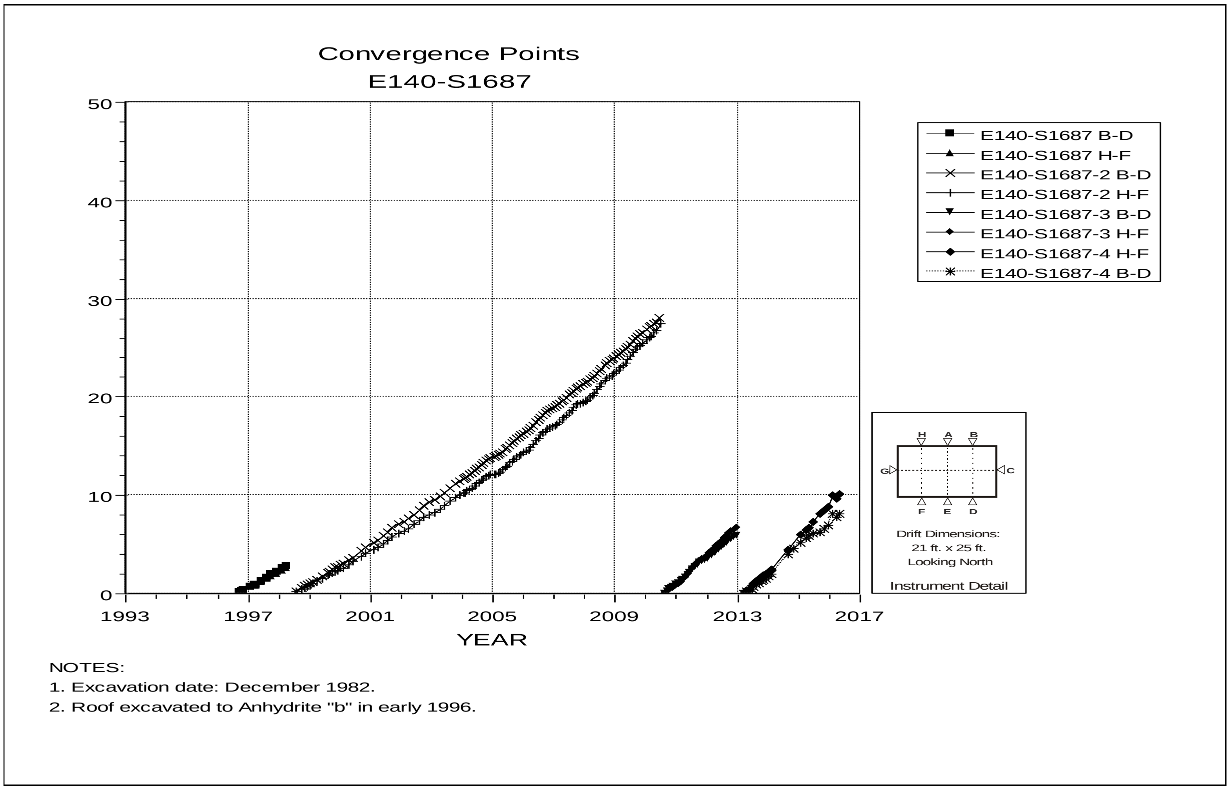

Figure 4-76 Convergence Point Array –
E140 S1687 – Roof to Floor – East Quarter Point

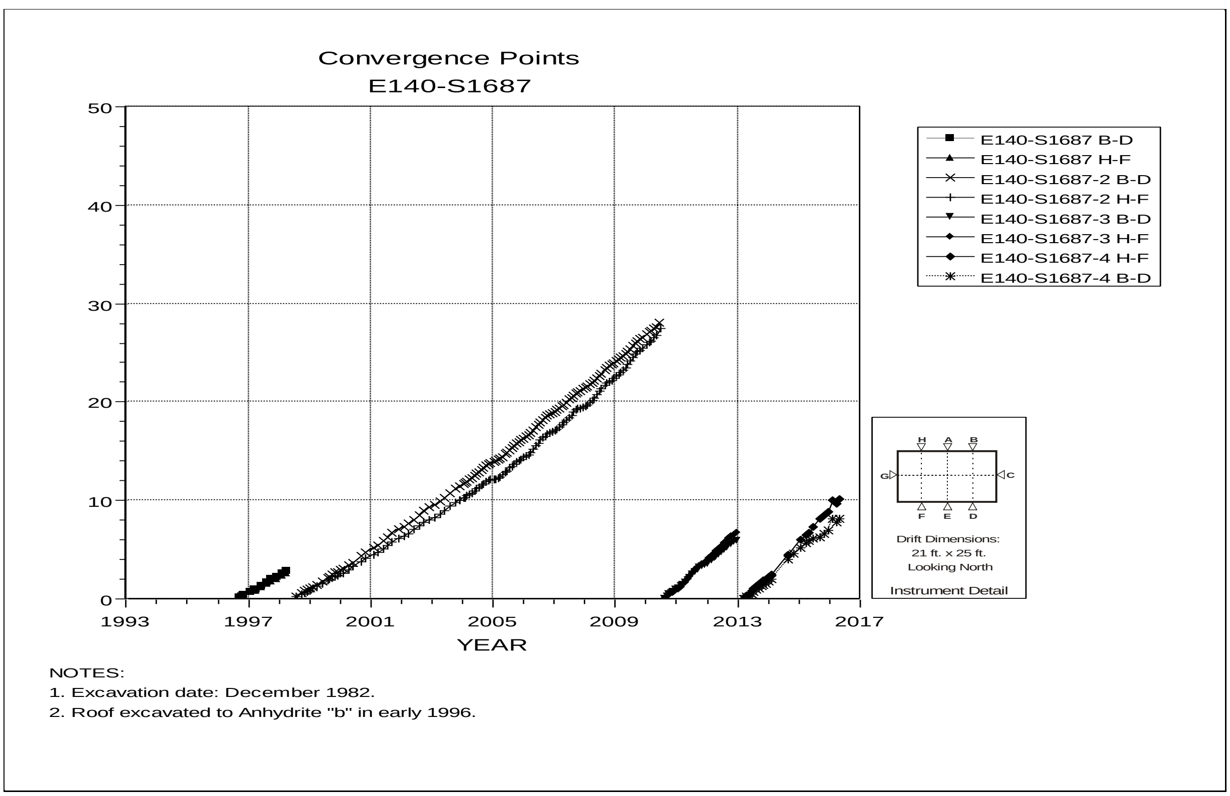

Figure 4-77 Convergence Point Array –
E140 S1687 – Roof to Floor – West Quarter Point

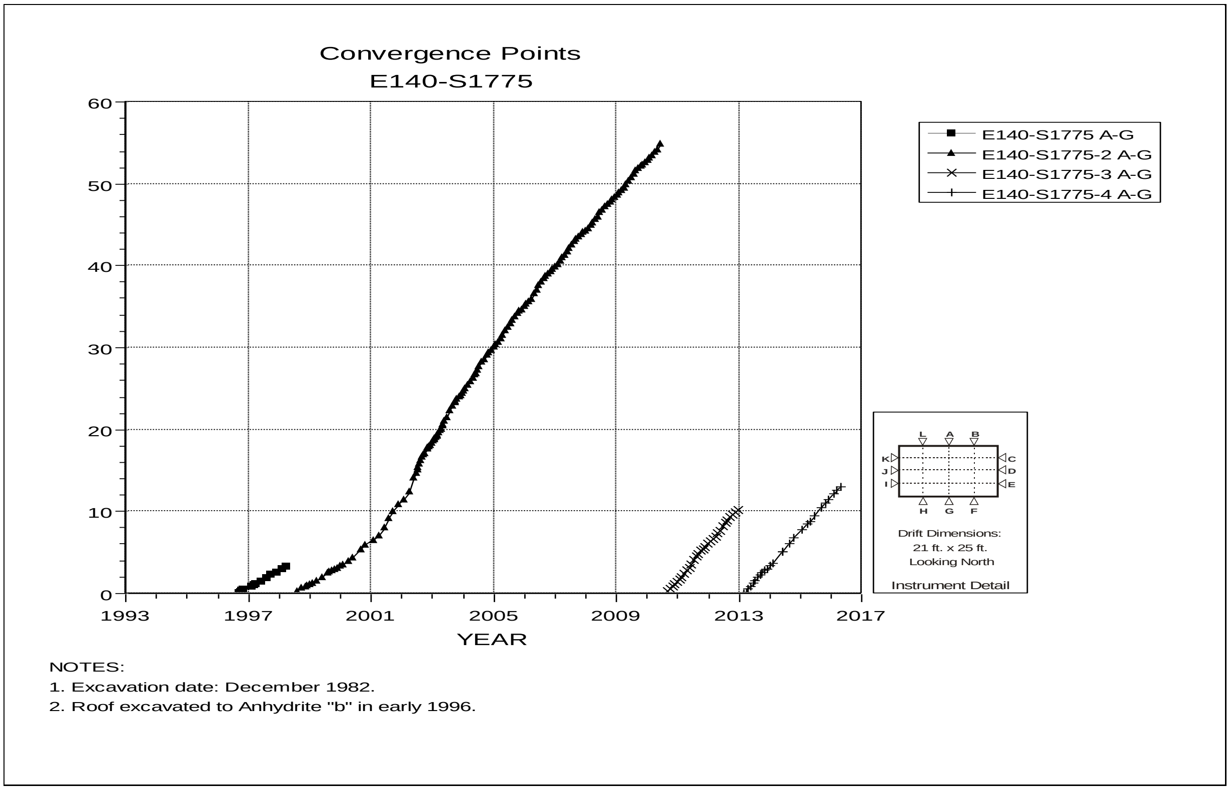

Figure 4-78 Convergence Point Array –
E140 S1775 – Roof to Floor – Centerline

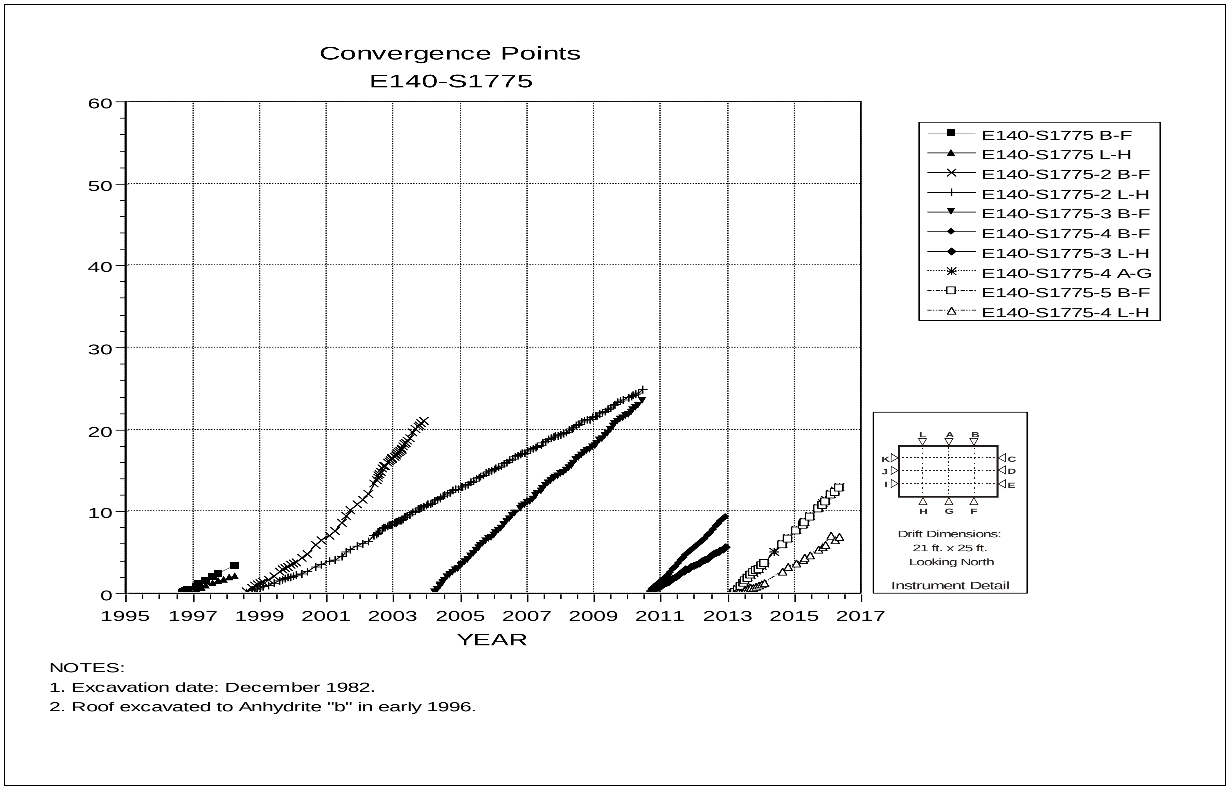

Figure 4-79 Convergence Point Array –

E140 S1775 – Roof to Floor – East Quarter Point

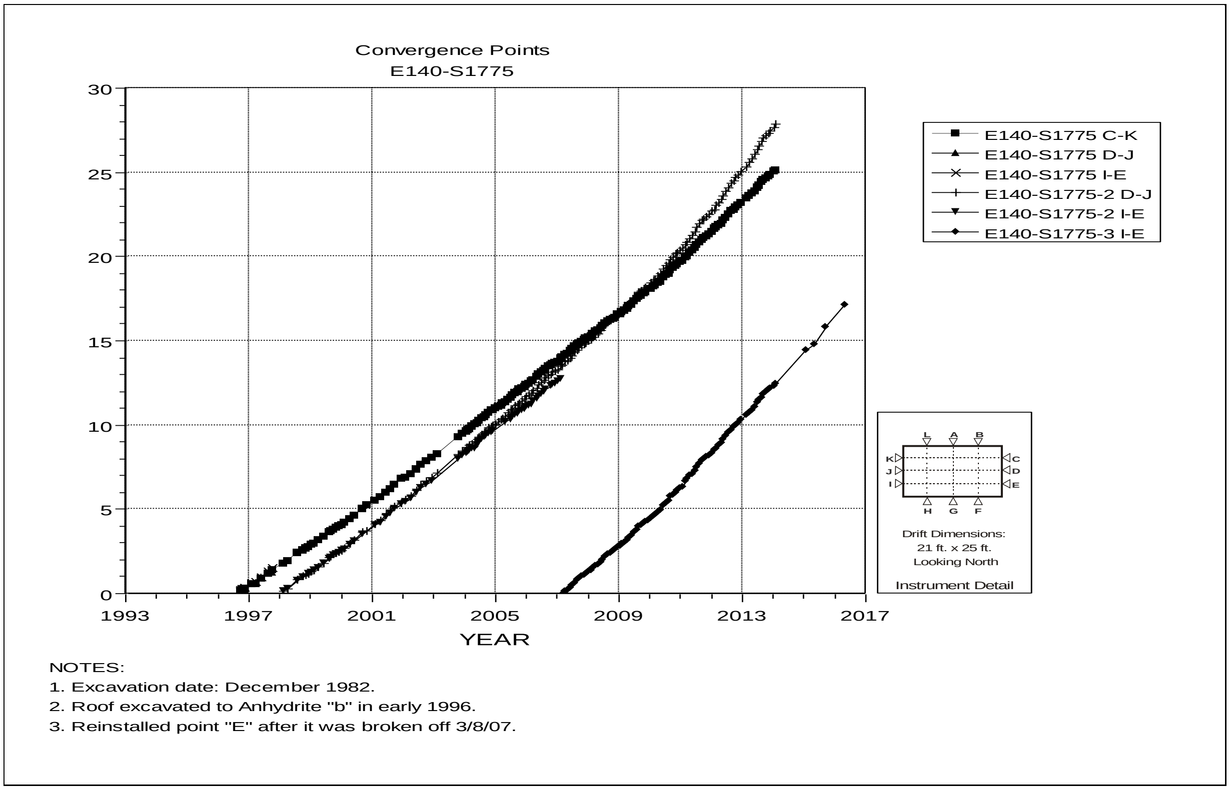

Figure 4-80 Convergence Point Array –
E140 S1775 – Rib to Rib

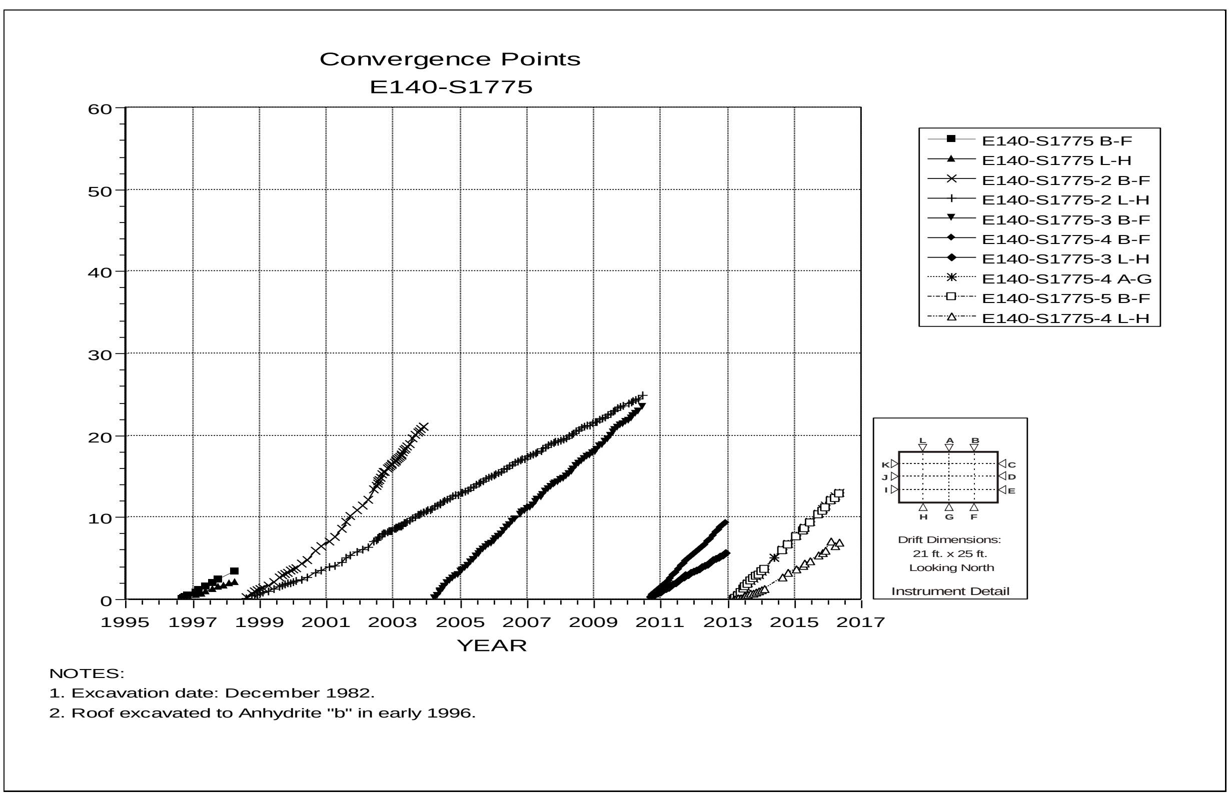

Figure 4-81 Convergence Point Array –

E140 S1775 – Roof to Floor – West Quarter Point

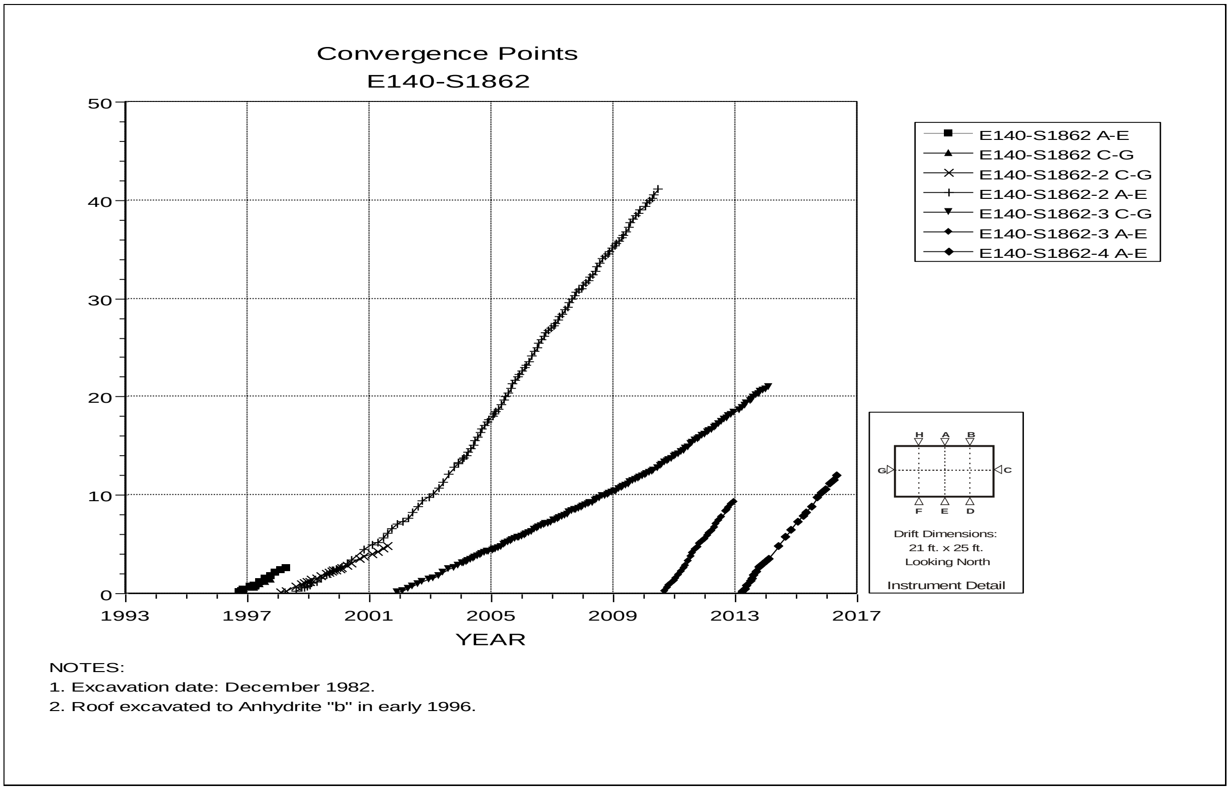

Figure 4-82 Convergence Point Array –
E140 S1862 – Roof to Floor – Centerline

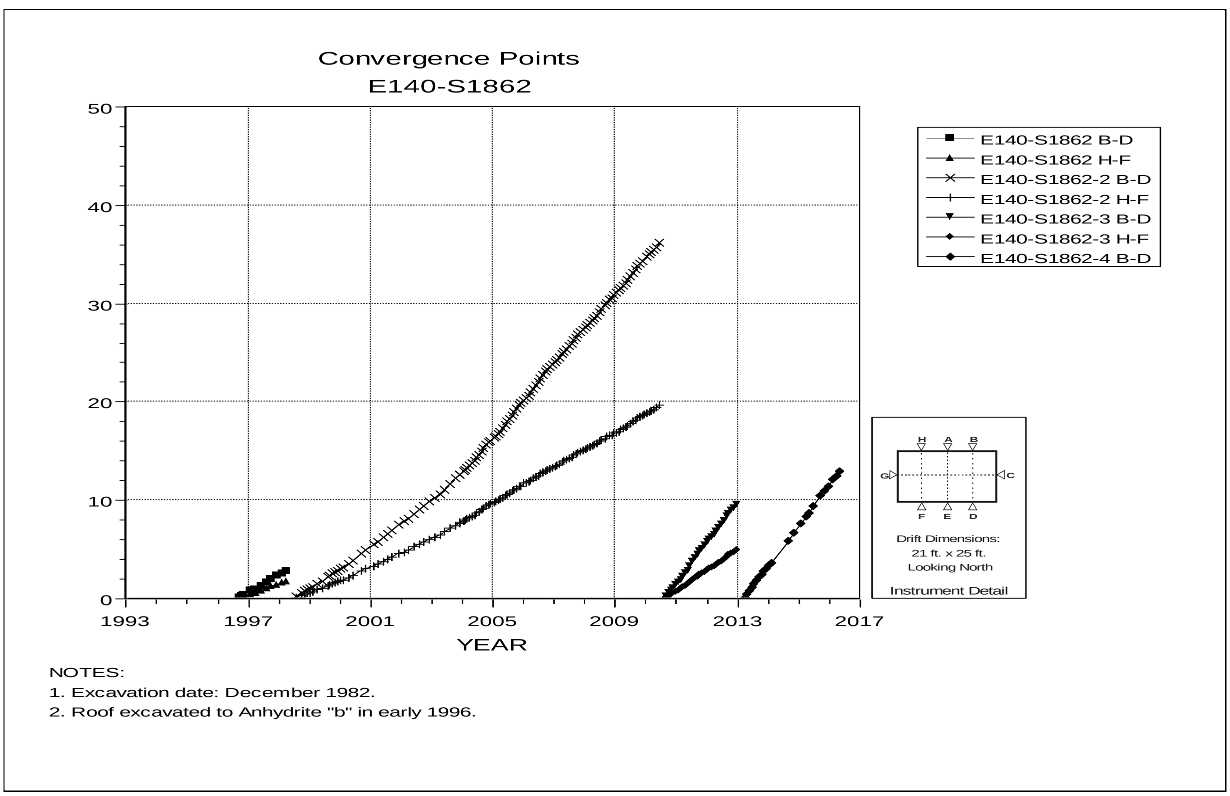

Figure 4-83 Convergence Point Array –

E140 S1862 – Roof to Floor – East Quarter Point

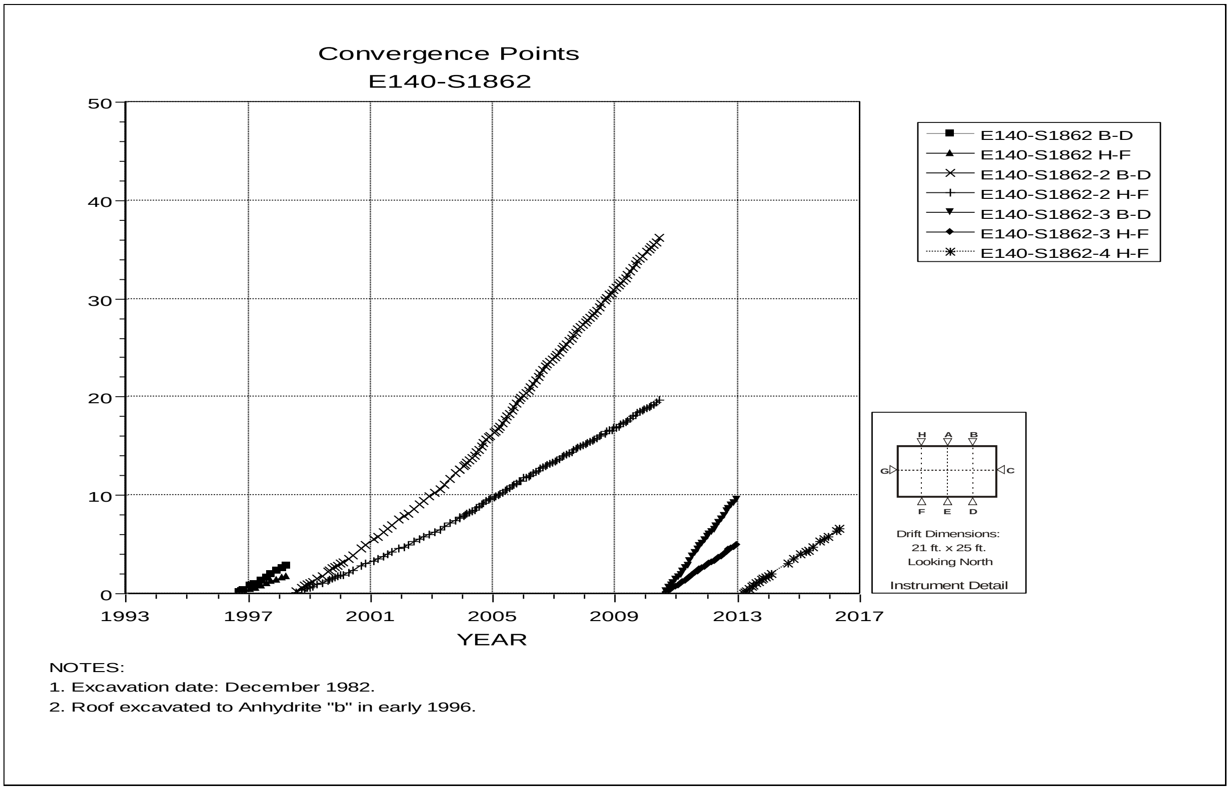

Figure 4-84 Convergence Point Array –
E140 S1862 – Roof to Floor – West Quarter Point

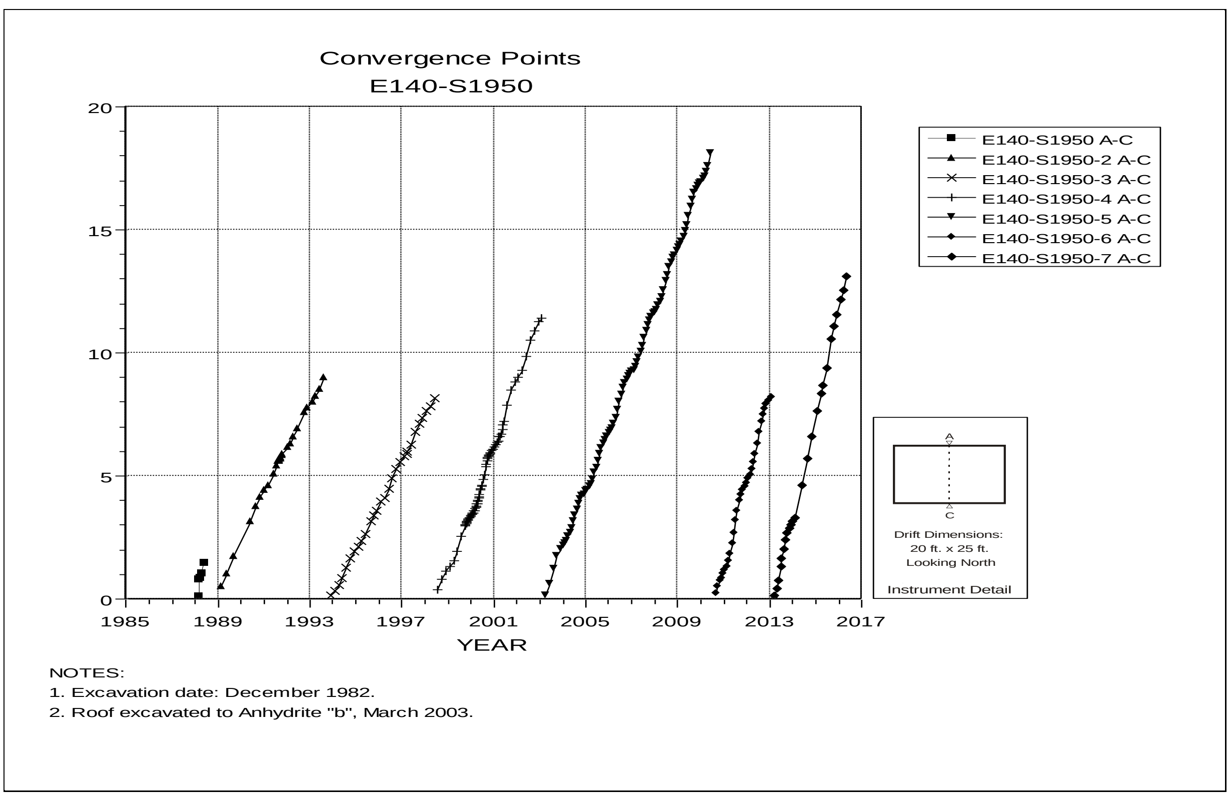

Figure 4-85 Convergence Point Array –

E140 S1950 – Roof to Floor

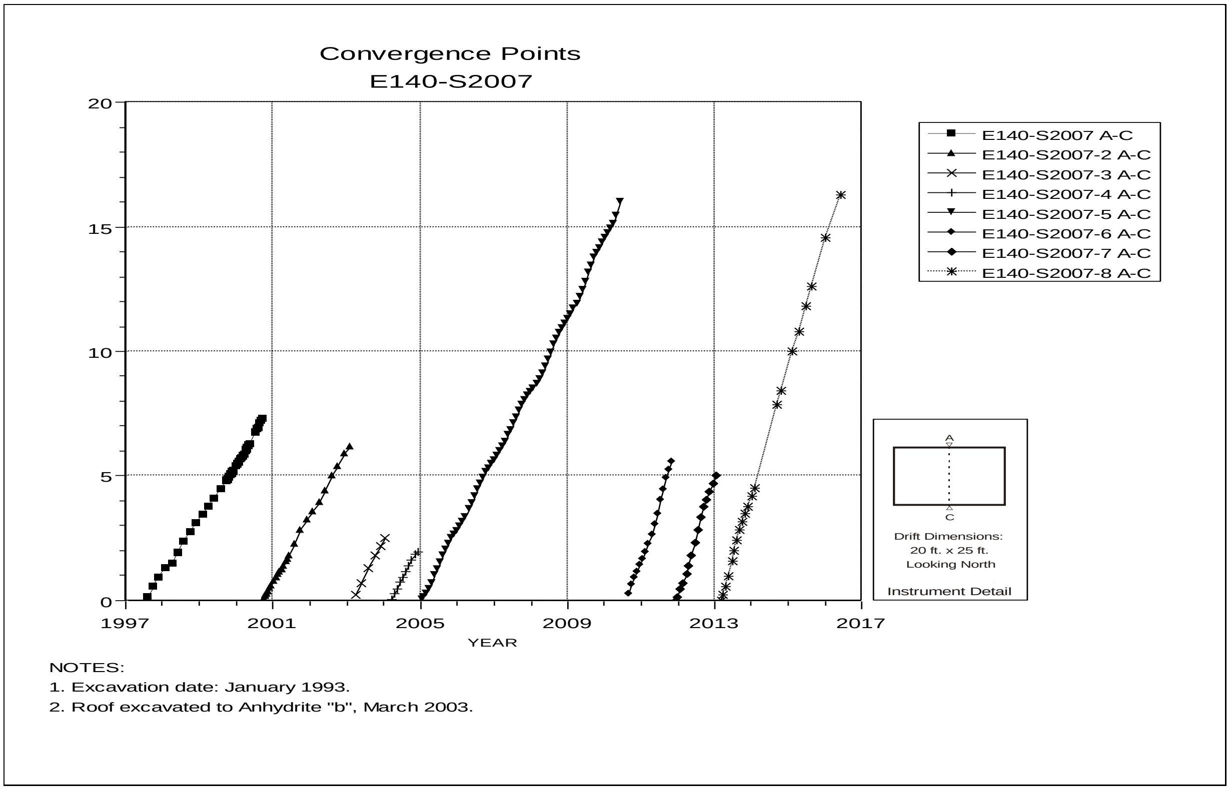

Figure 4-86 Convergence Point Array –
E140 S2007 – Roof to Floor

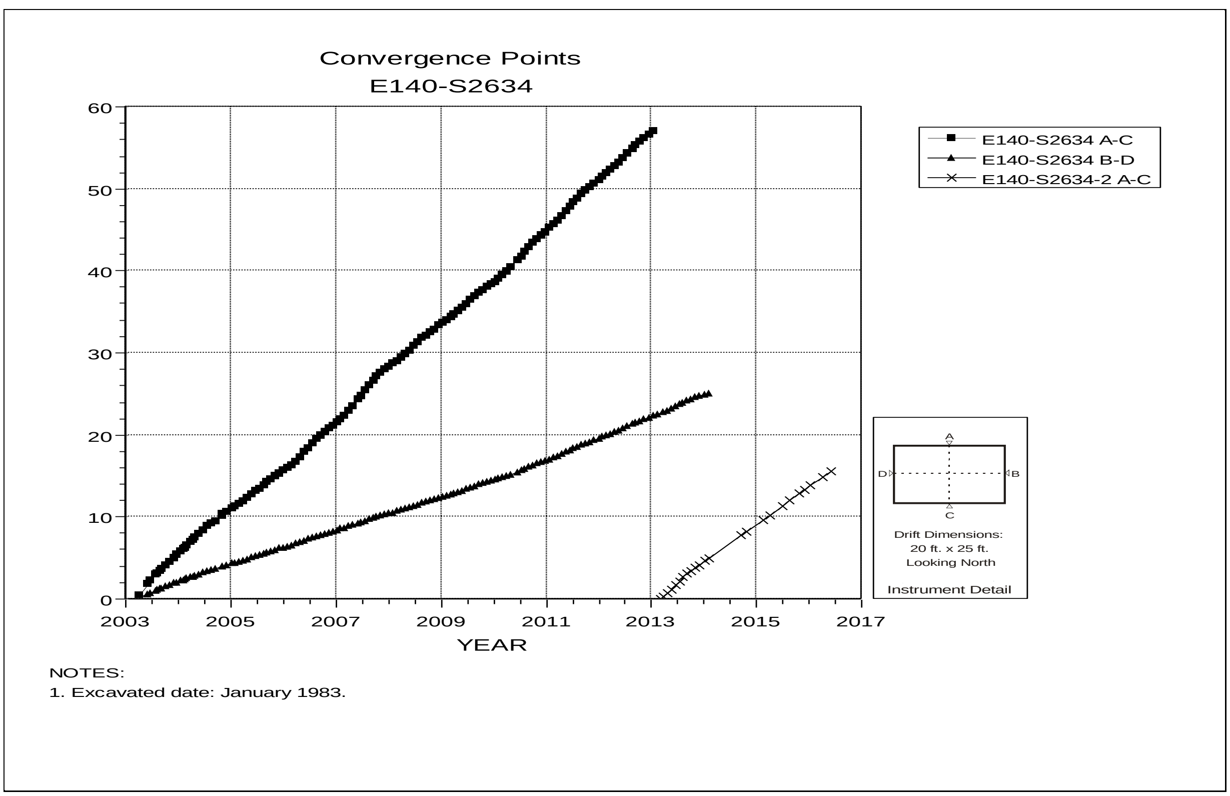

Figure 4-87 Convergence Point Array –

E140 S2634 – All Chords

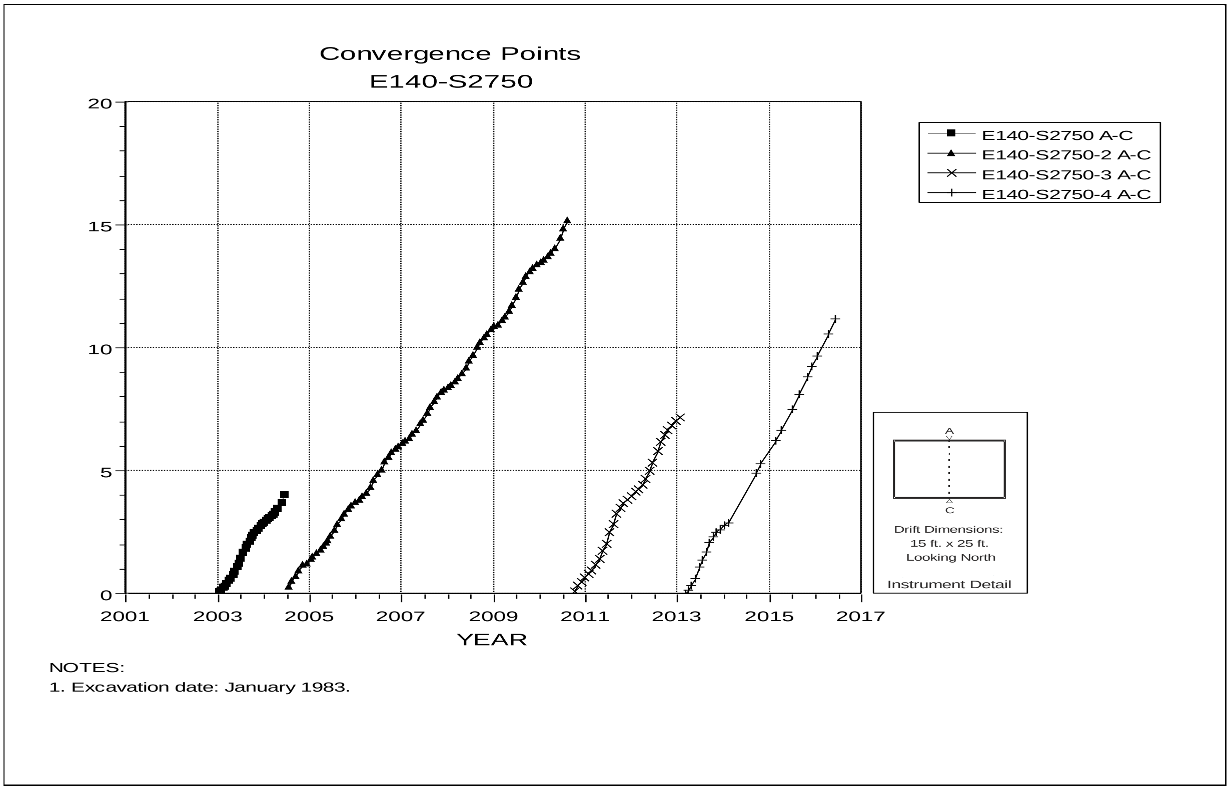

Figure 4-88 Convergence Point Array –
E140 S2750 – Roof to Floor

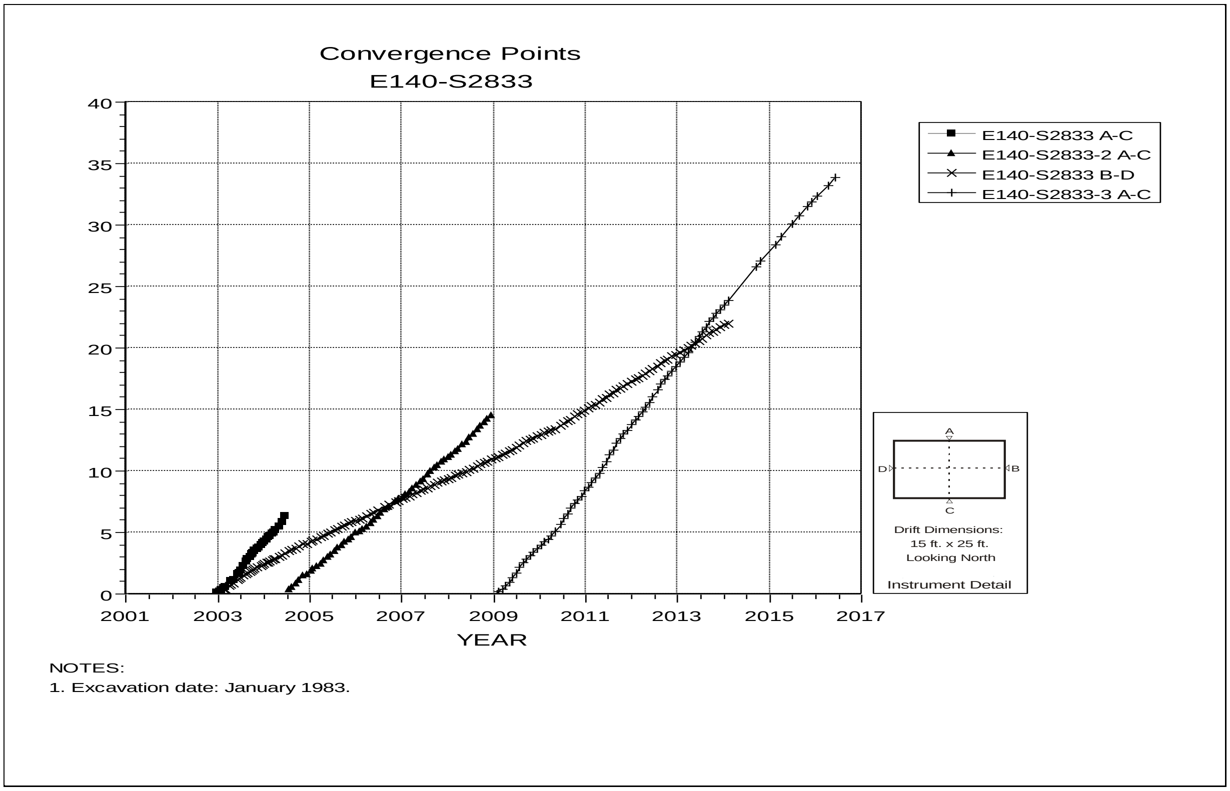

Figure 4-89 Convergence Point Array –

E140 S2833 – Roof to Floor

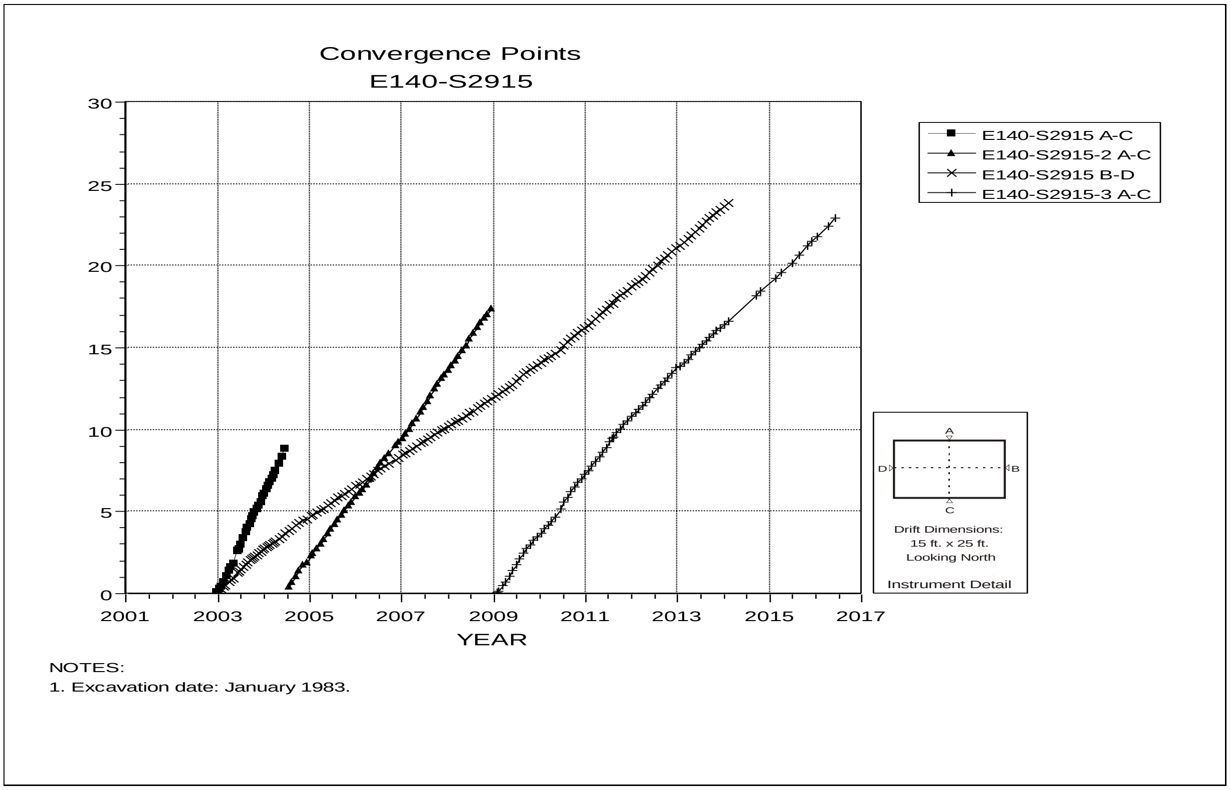

Figure 4-90 Convergence Point Array –
E140 S2915 – All Chords

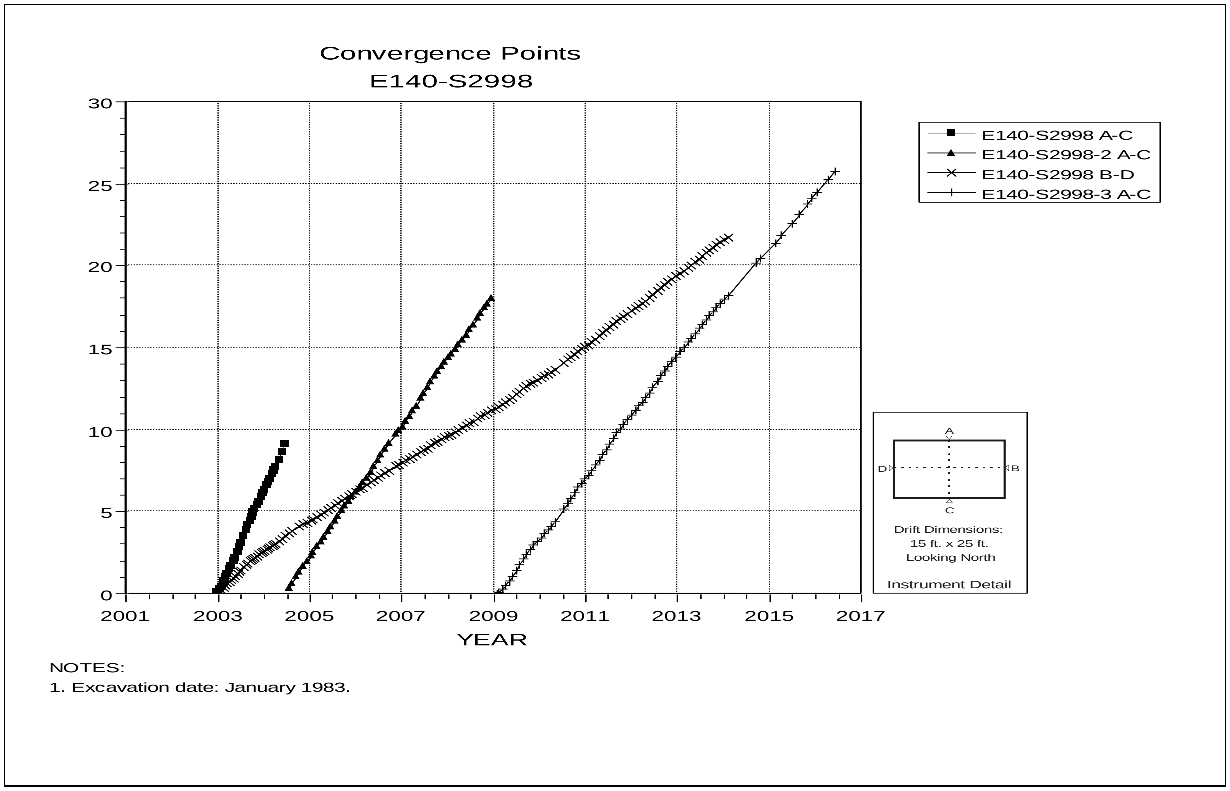

Figure 4-91 Convergence Point Array –

E140 S2998 – Roof to Floor

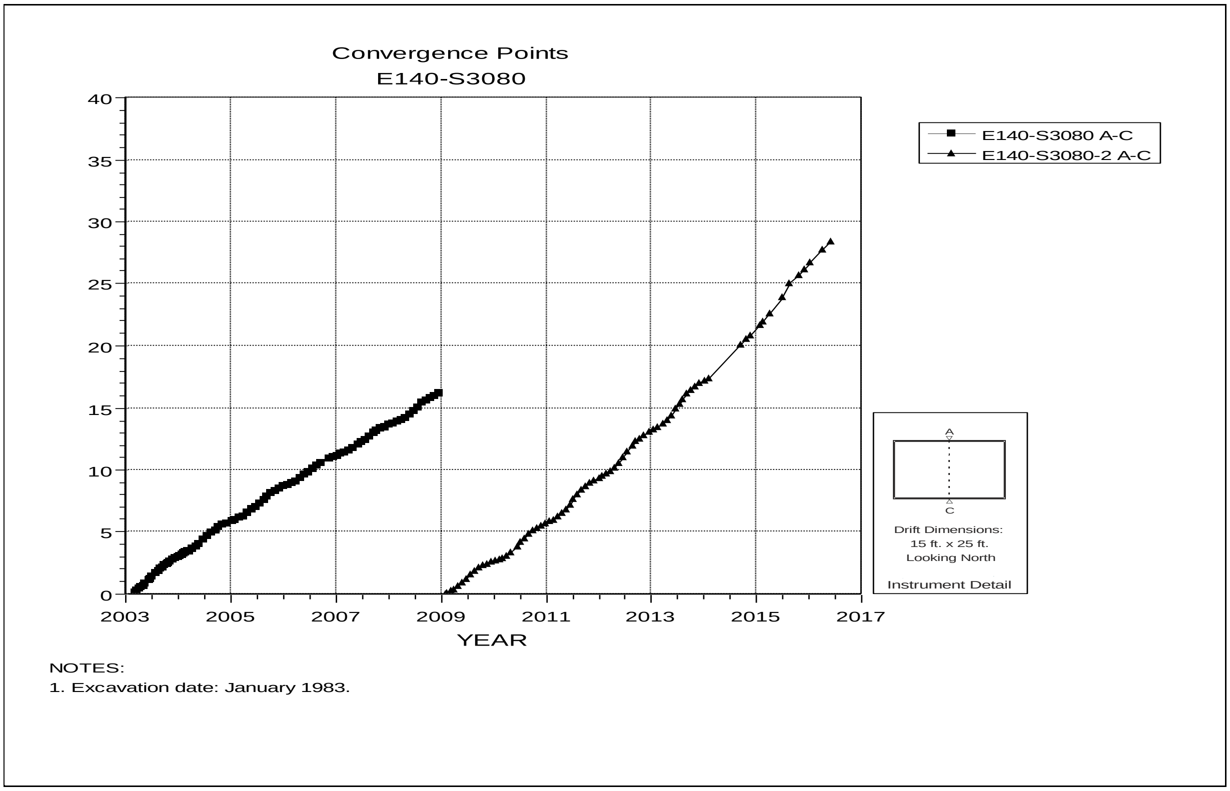

Figure 4-92 Convergence Point Array –
E140 S3080 – Roof to Floor

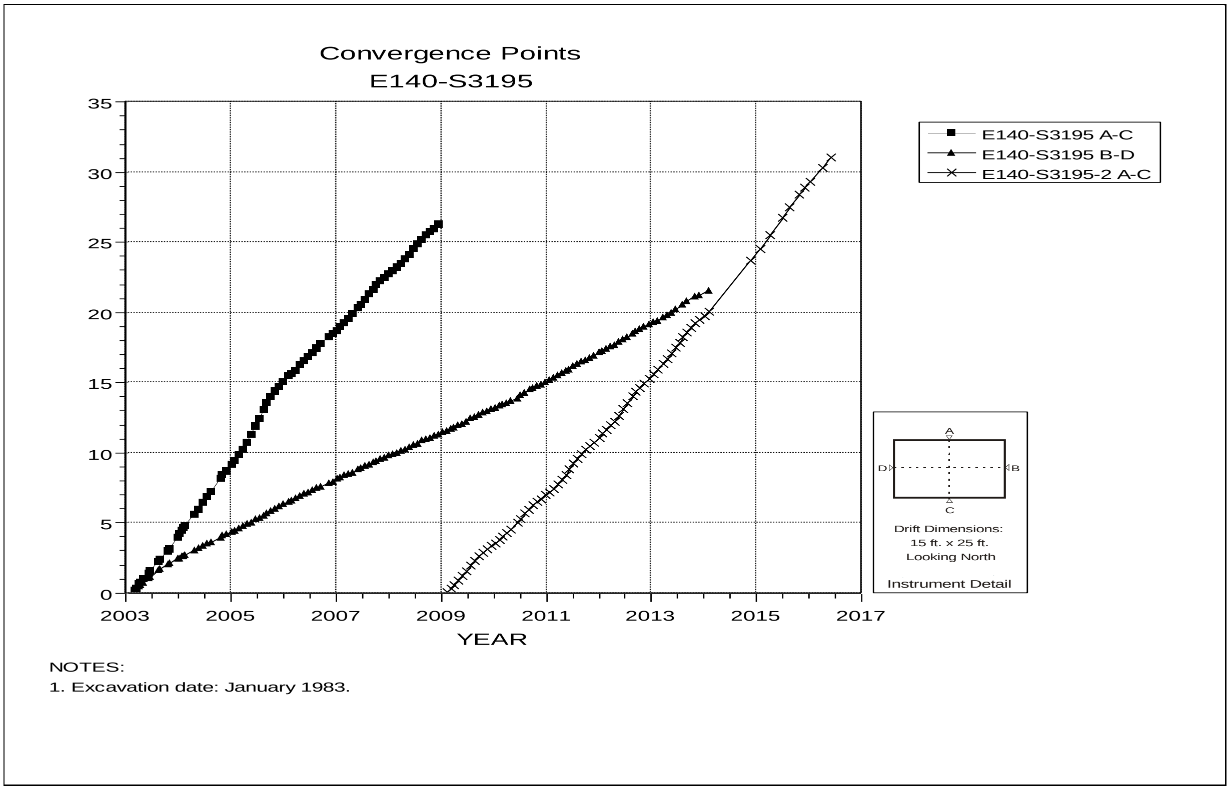

Figure 4-93 Convergence Point Array –
E140 S3195 – Roof to Floor

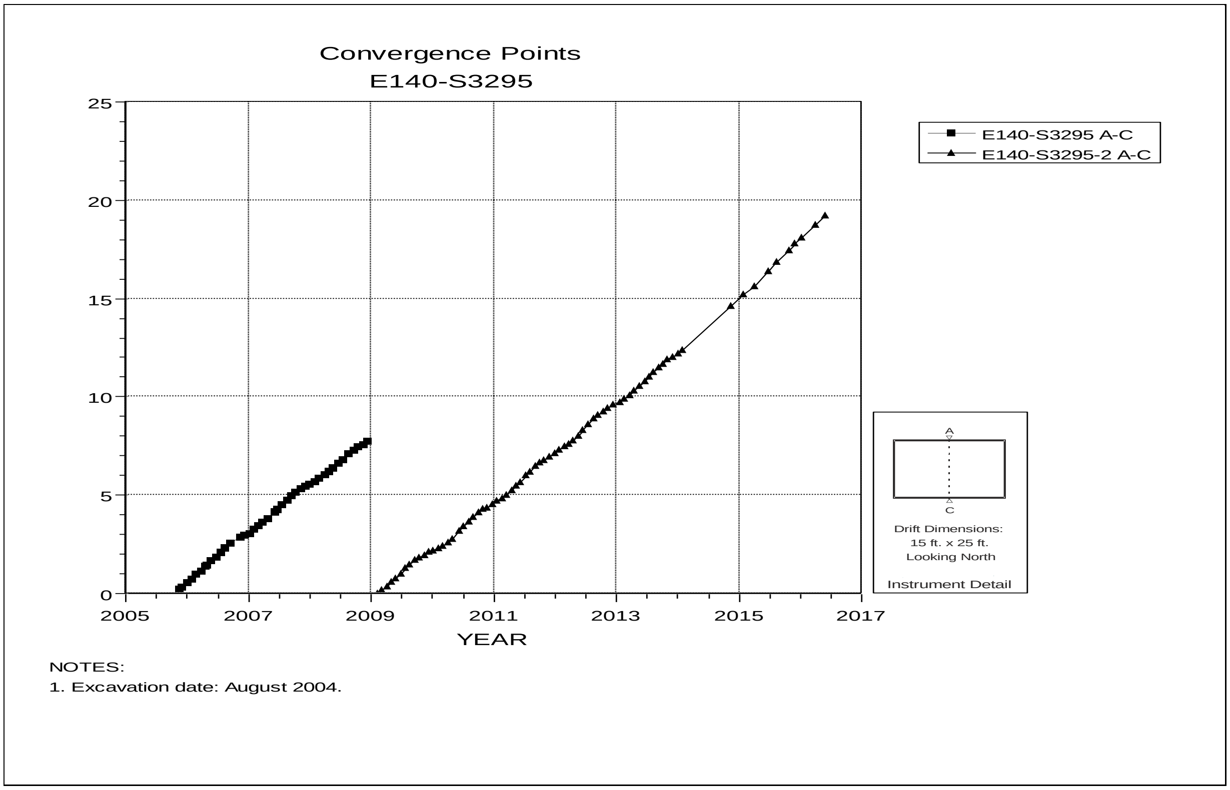

Figure 4-94 Convergence Point Array –
E140 S3295 – Roof to Floor

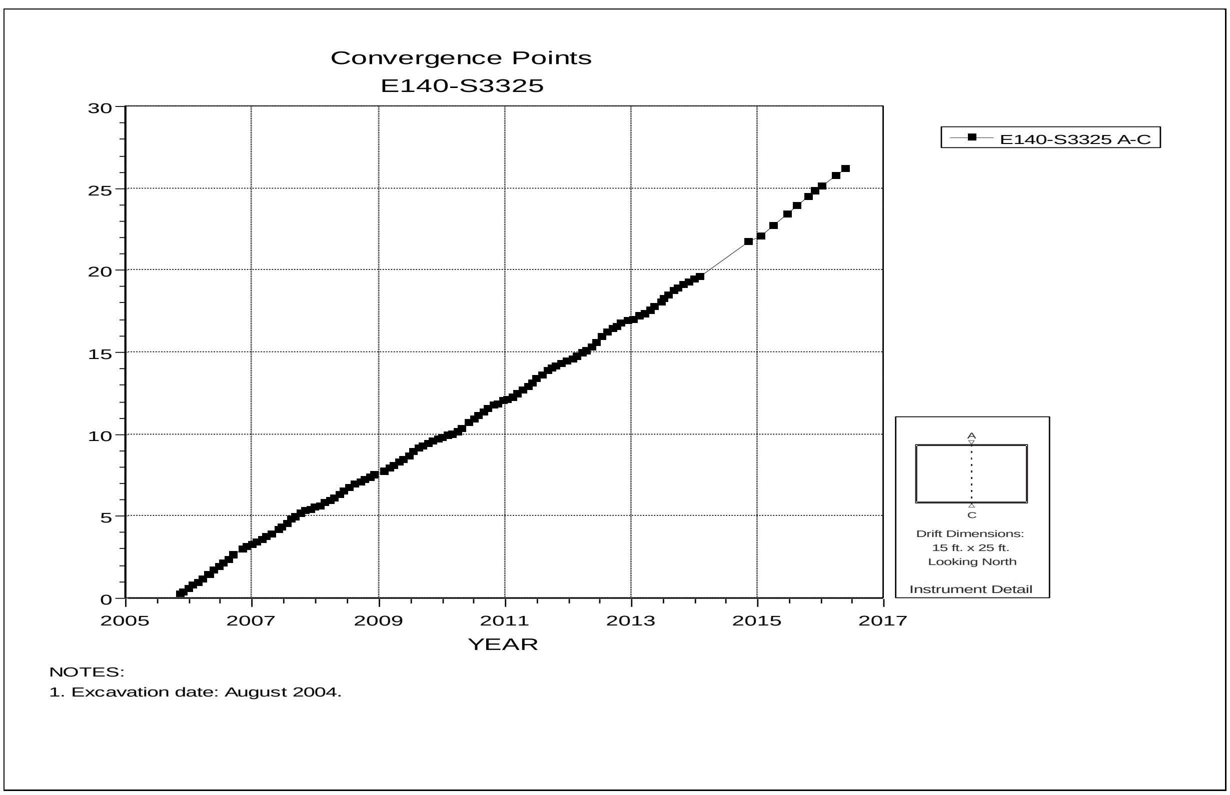

ISSUED

Figure 4-95 Convergence Point Array –
E140 S3325 – Roof to Floor

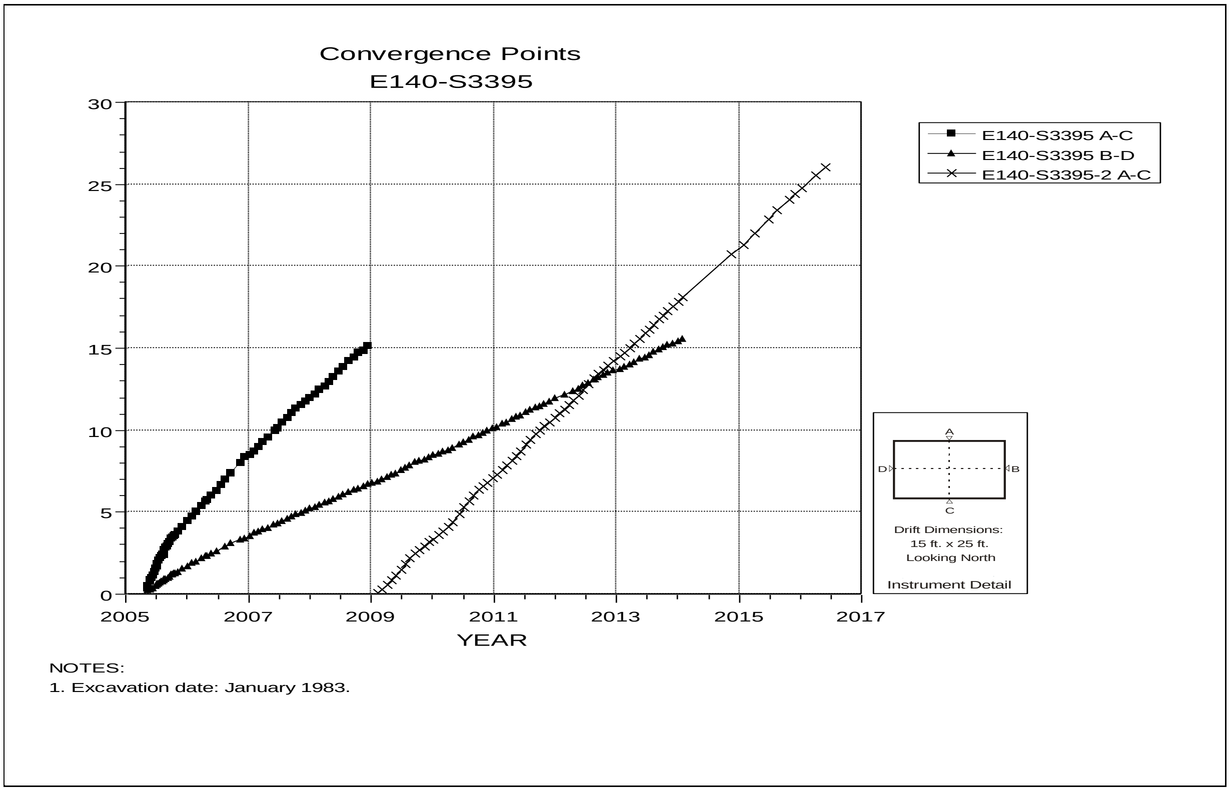

Figure 4-96 Convergence Point Array –
E140 S3395 – Roof to Floor

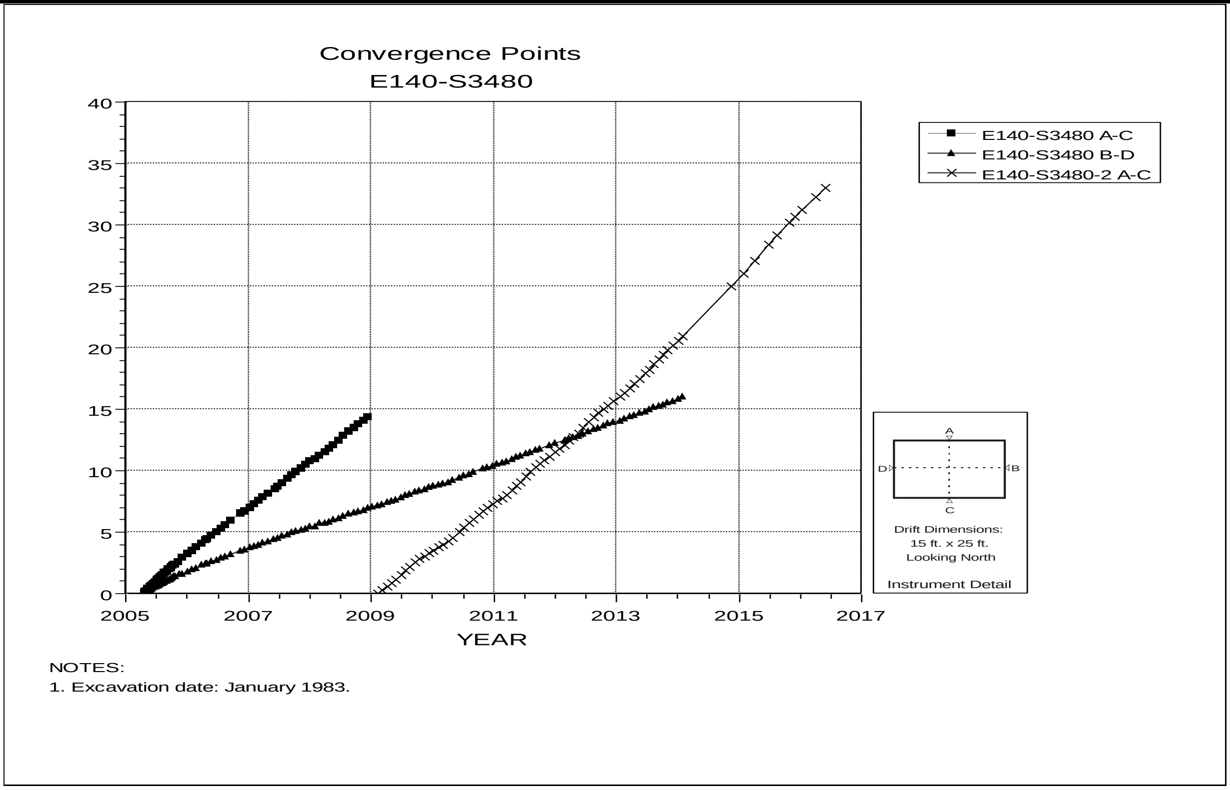

Figure 4-97 Convergence Point Array –
E140 S3480 – Roof to Floor

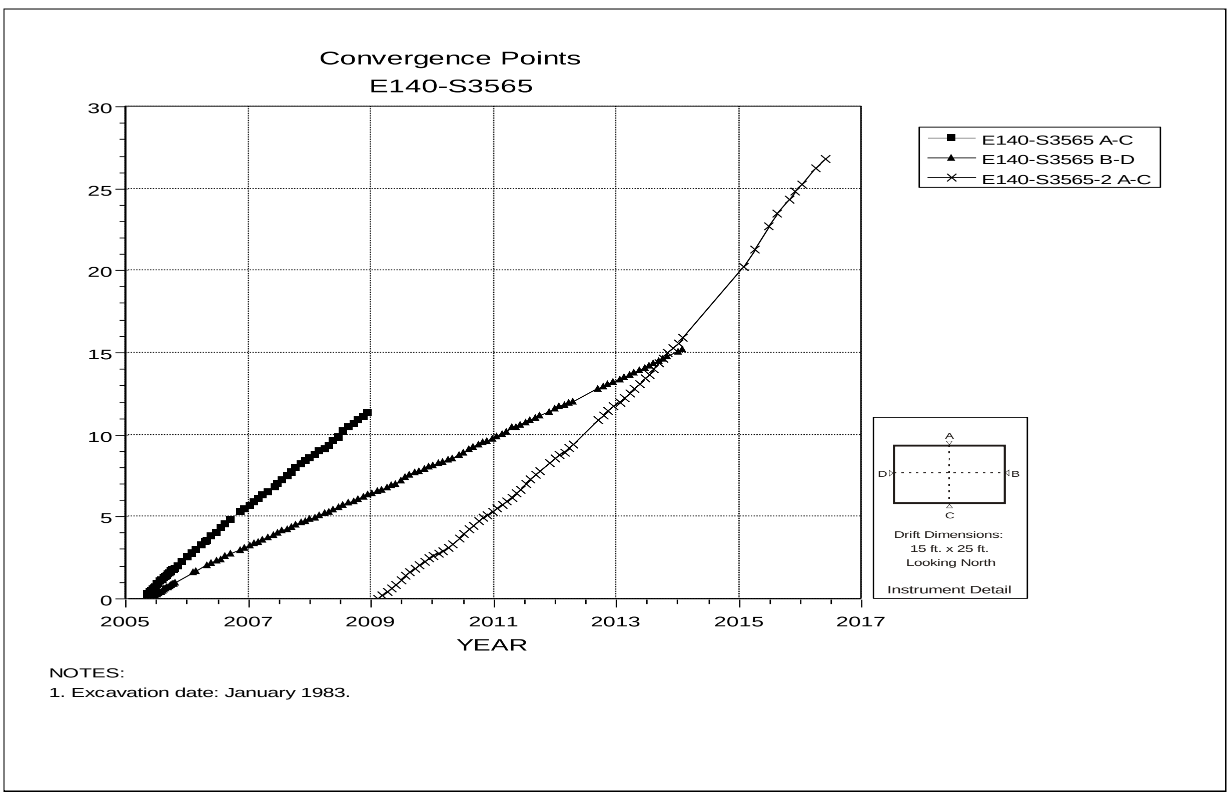

Figure 4-98 Convergence Point Array –
E140 S3565 – Roof to Floor

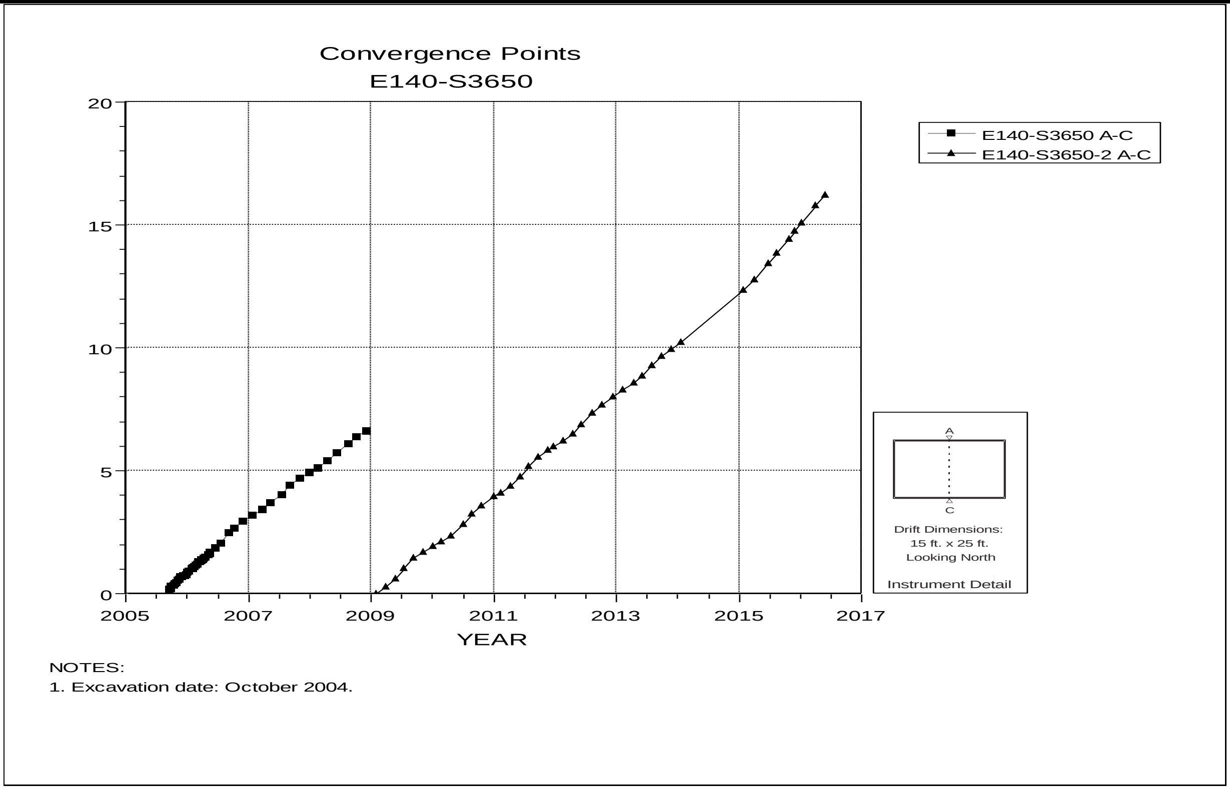

Figure 4-99 Convergence Point Array –
E140 S3650 – Roof to Floor

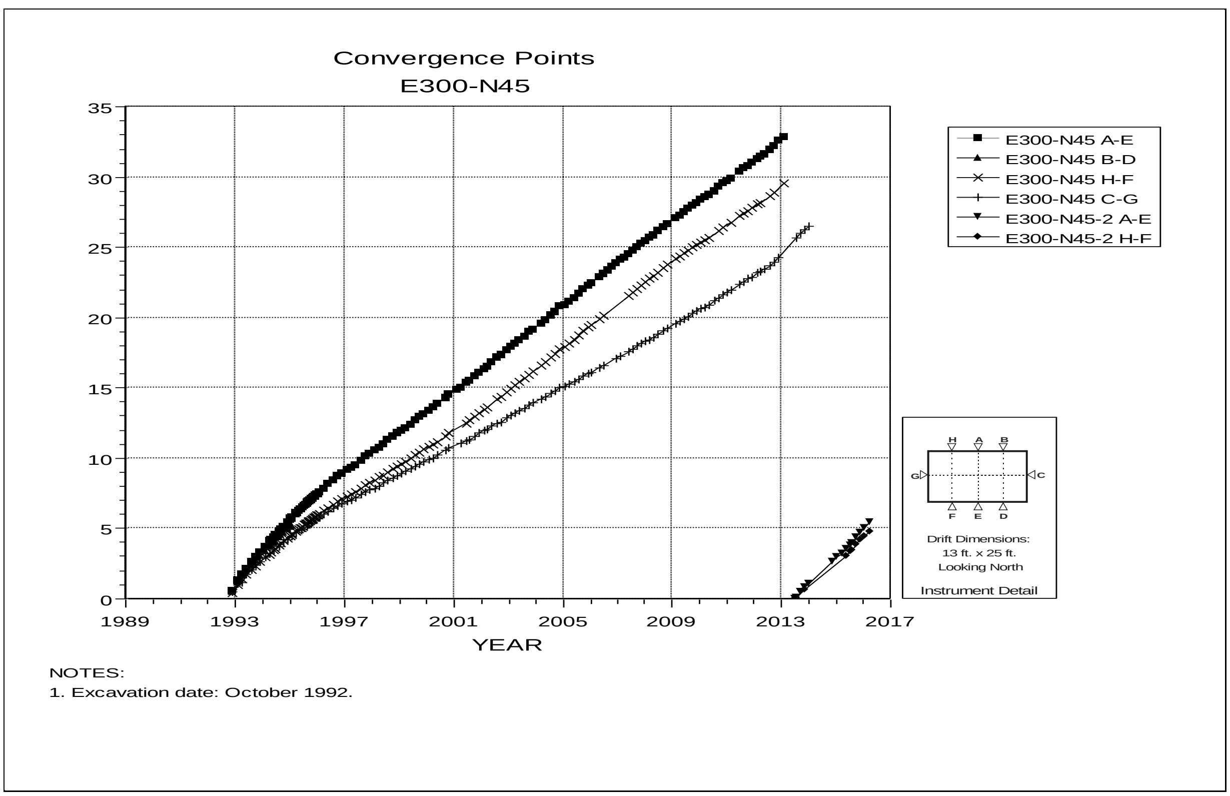

Figure 4-100 Convergence Point Array –
E300 N45 – All Chords

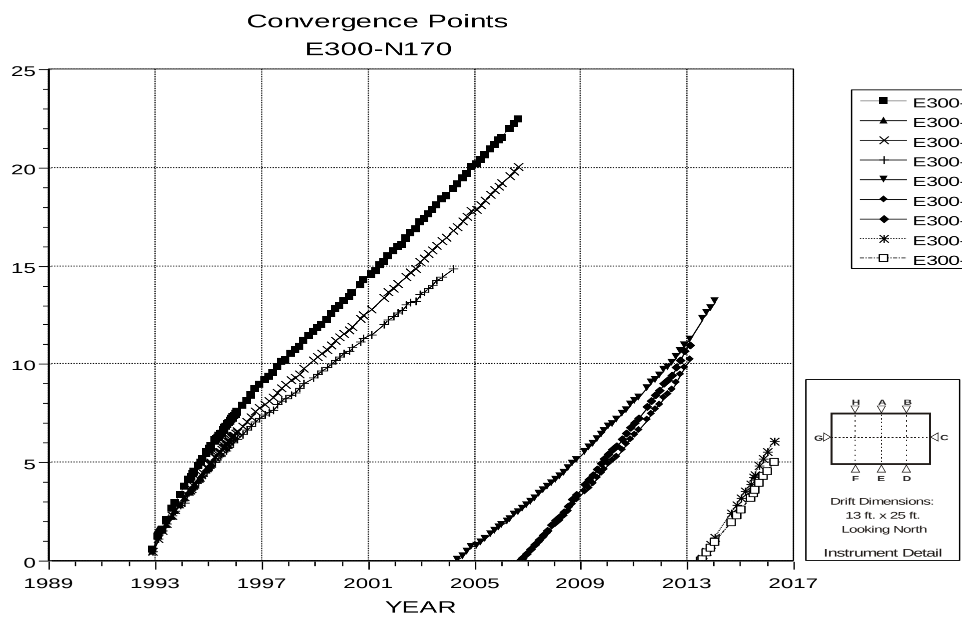

NOTES:
1. Excavation date: October 1992.
2. Reinstalled "E" and "F" points 9-27-2006.

Figure 4-101 Convergence Point Array –
E300 N170 – Roof to Floor – Centerline

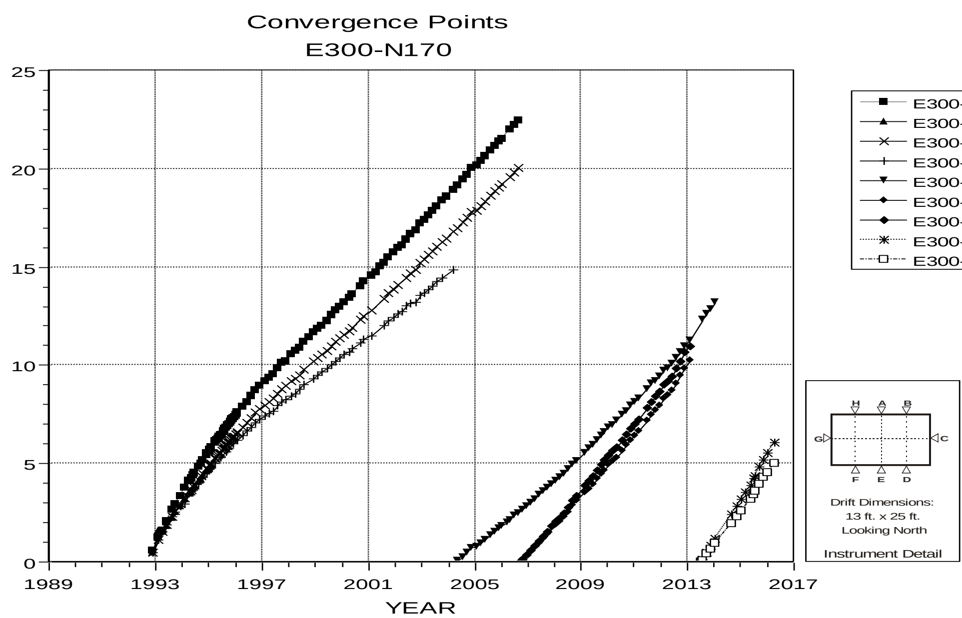

NOTES:
1. Excavation date: October 1992.
2. Reinstalled "E" and "F" points 9-27-2006.

Figure 4-102 Convergence Point Array –
E300 N170 – Roof to Floor – West Quarter Point

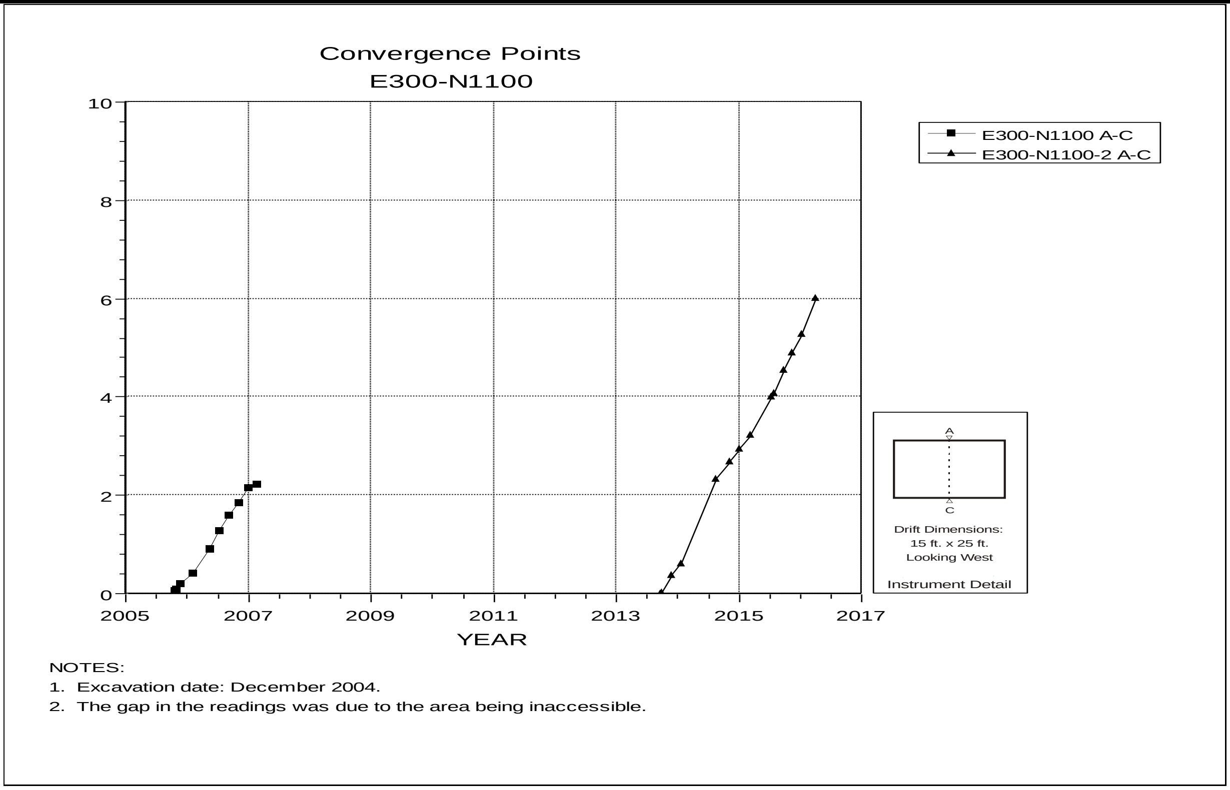

Figure 4-103 Convergence Point Array –
E300 N1100– Roof to Floor

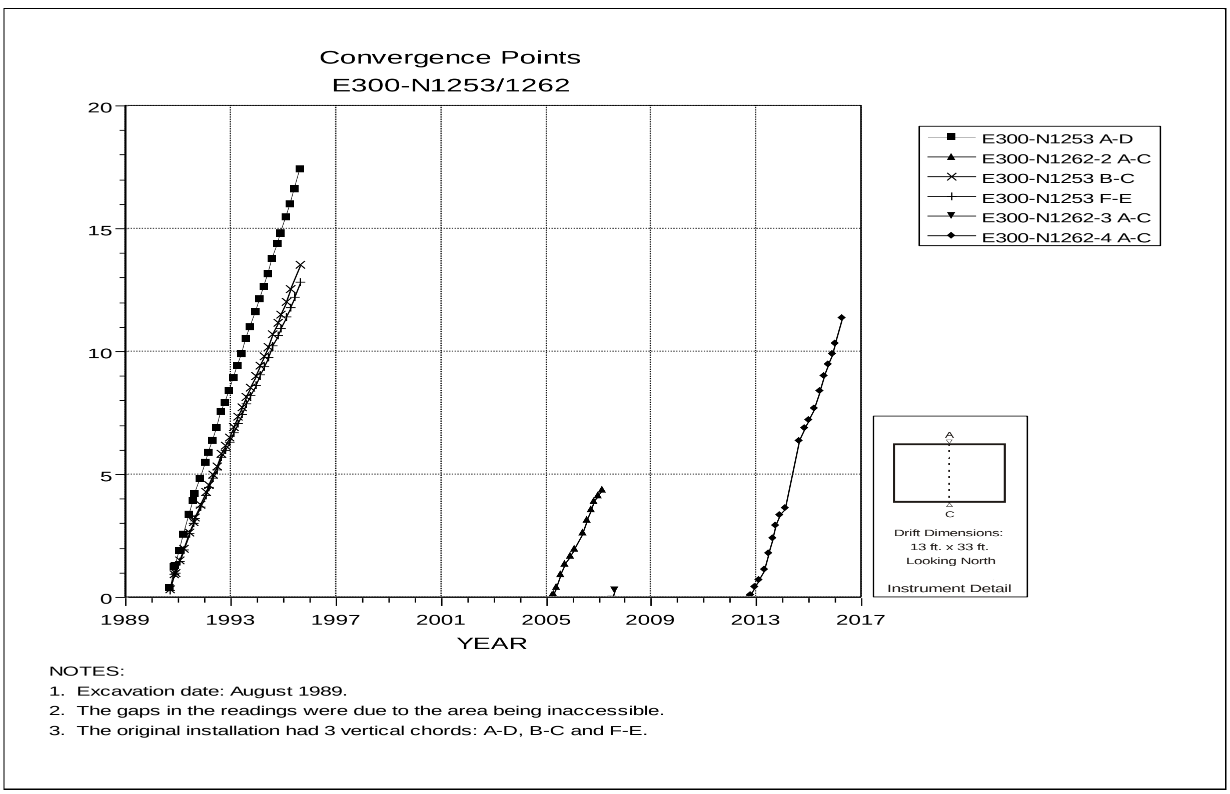

Figure 4-104 Convergence Point Array –
E300 N1262 – Roof to Floor

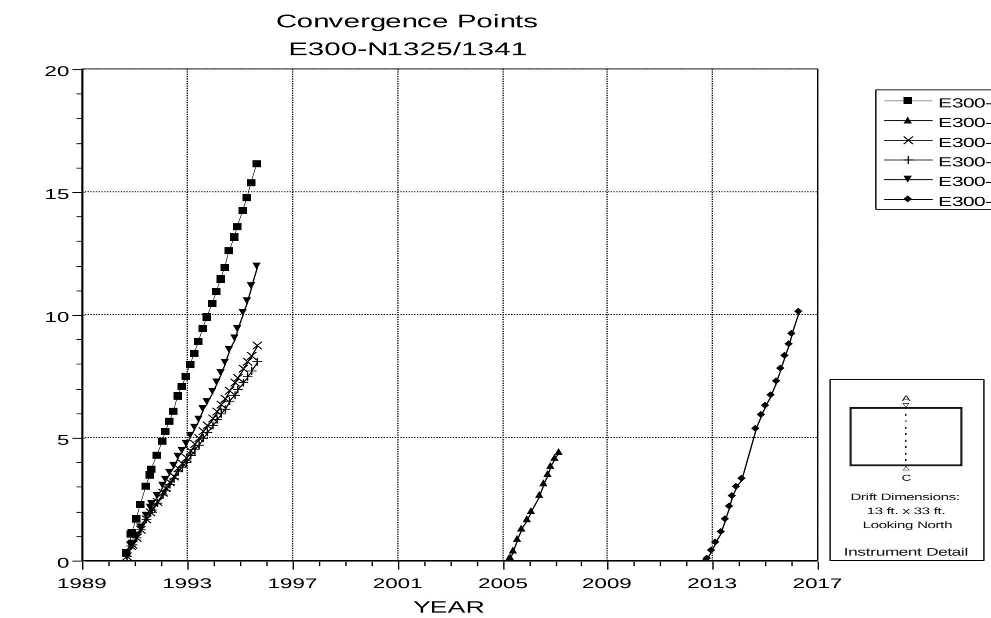

NOTES:
1. Excavation date: August 1989.
2. The gaps in the readings were due to the area being inaccessible.
3. The original installation had 3 vertical chords: A-D, B-C and F-E and horizontal chord C-G.

Figure 4-105 Convergence Point Array –
E300 N1341 – All Chords

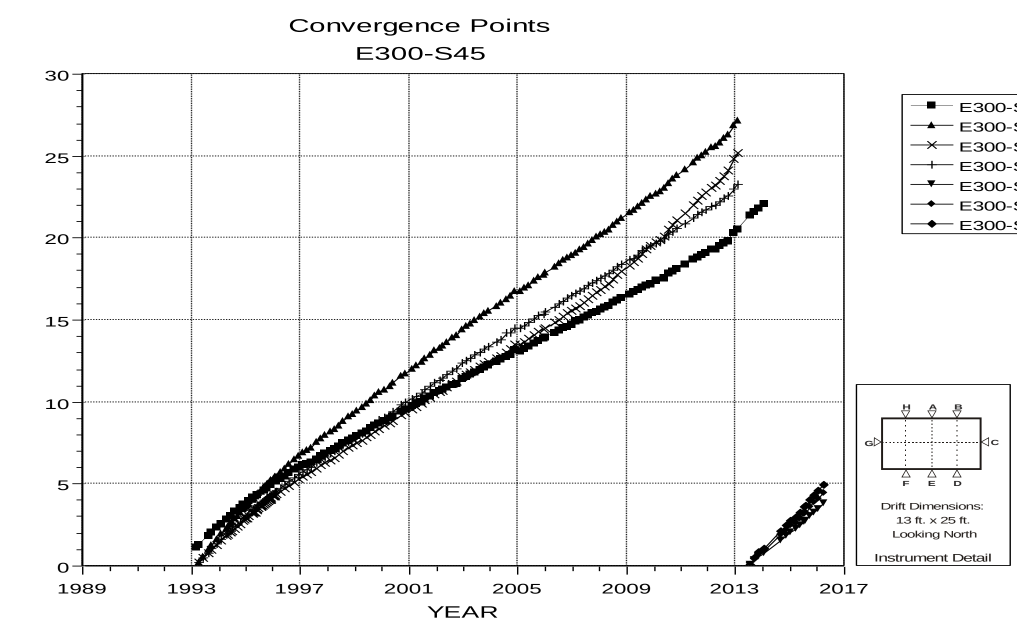

NOTES:
1. Excavation date: October 1992
2. The initial A-F, B-D and H-F chords were only read at installation.

Figure 4-106 Convergence Point Array –
E300 S45 – Roof to Floor – Centerline

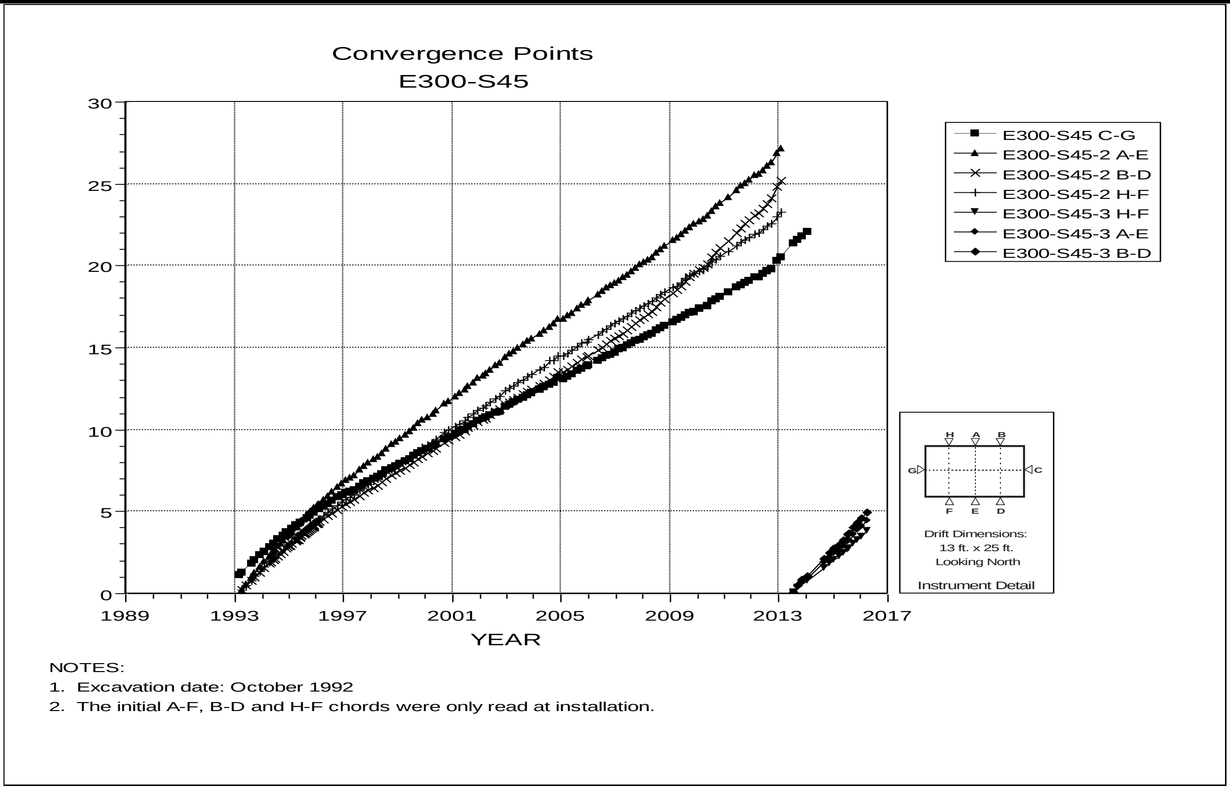

Figure 4-107 Convergence Point Array –
E300 S45 – Roof to Floor – East Quarter Point

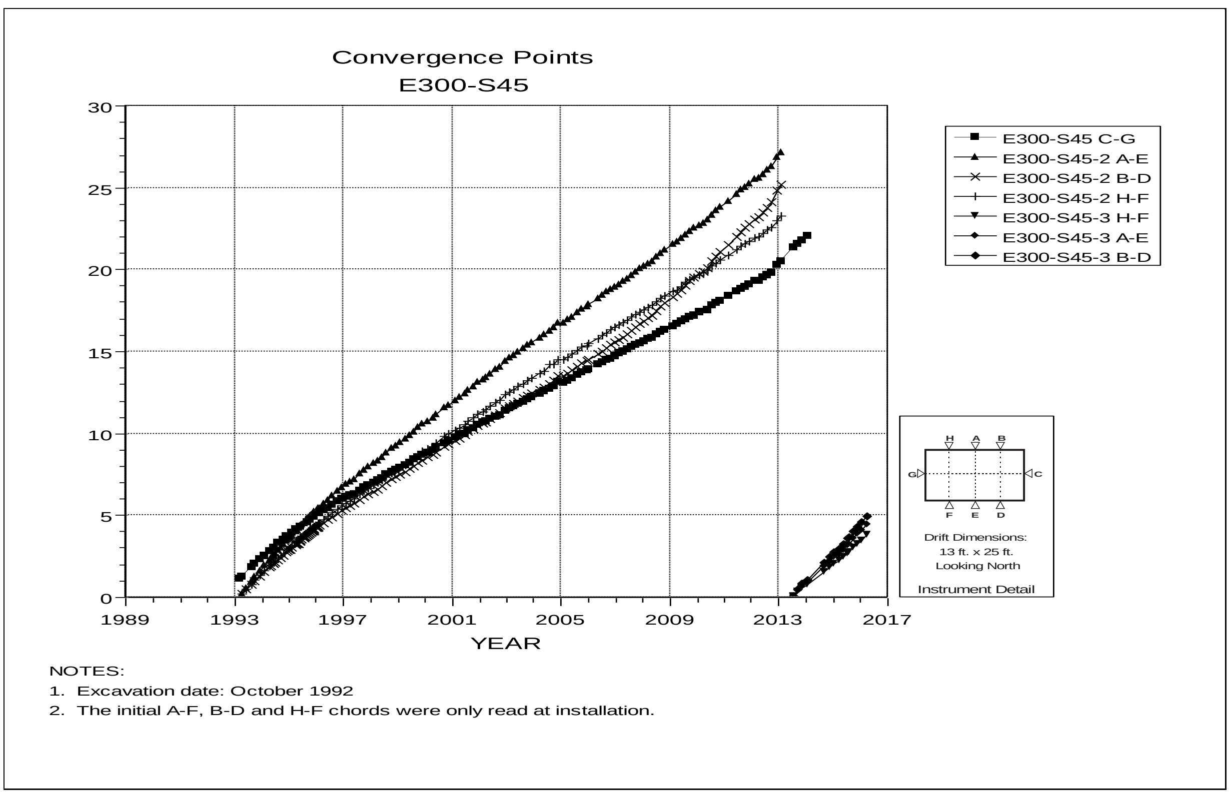

Figure 4-108 Convergence Point Array –
E300 S45 – Roof to Floor – West Quarter Point

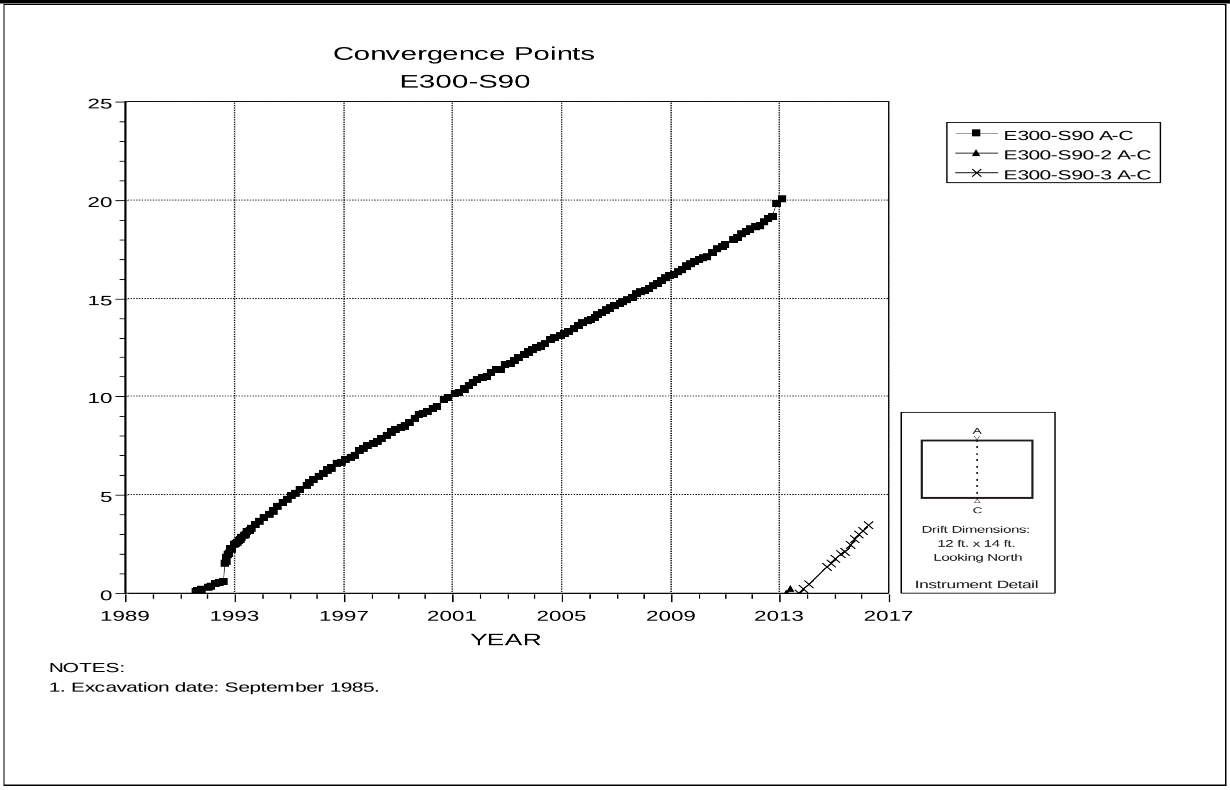

Figure 4-109 Convergence Point Array –
E300 S90 – Roof to Floor

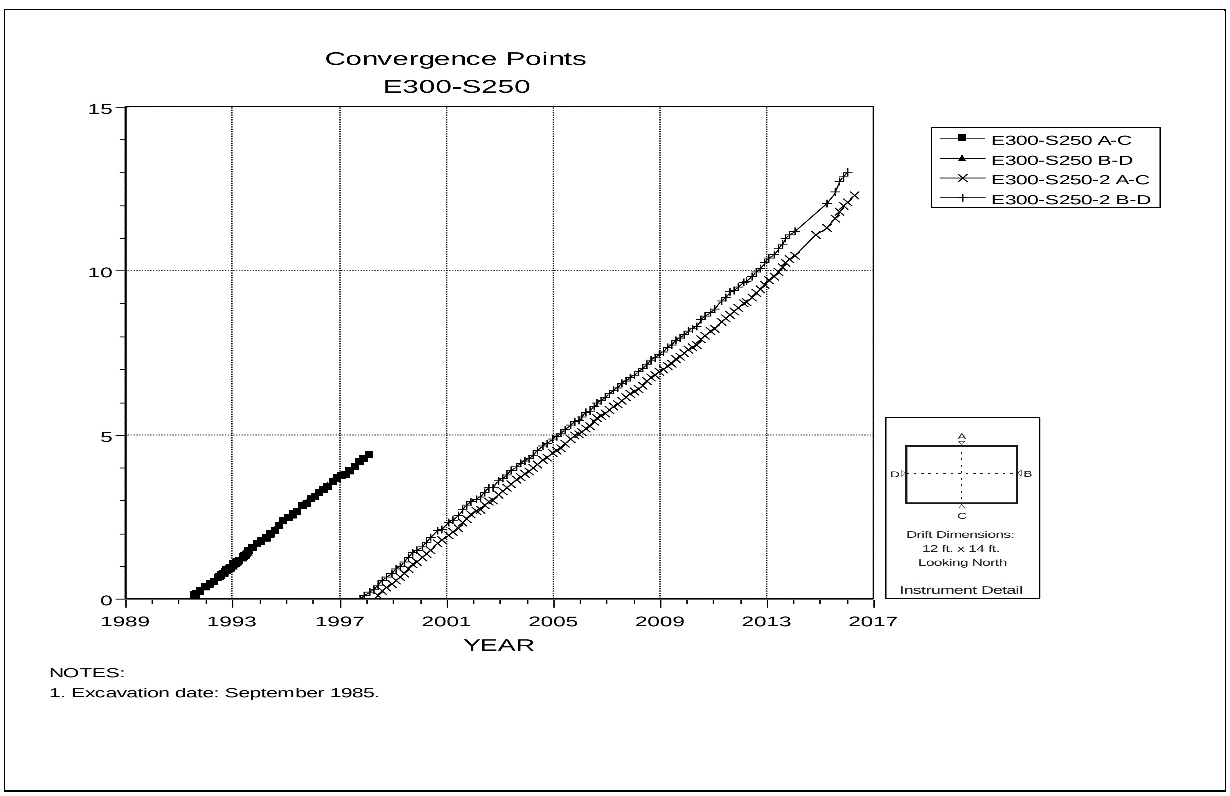

Figure 4-110 Convergence Point Array –
E300 S250 – Roof to Floor

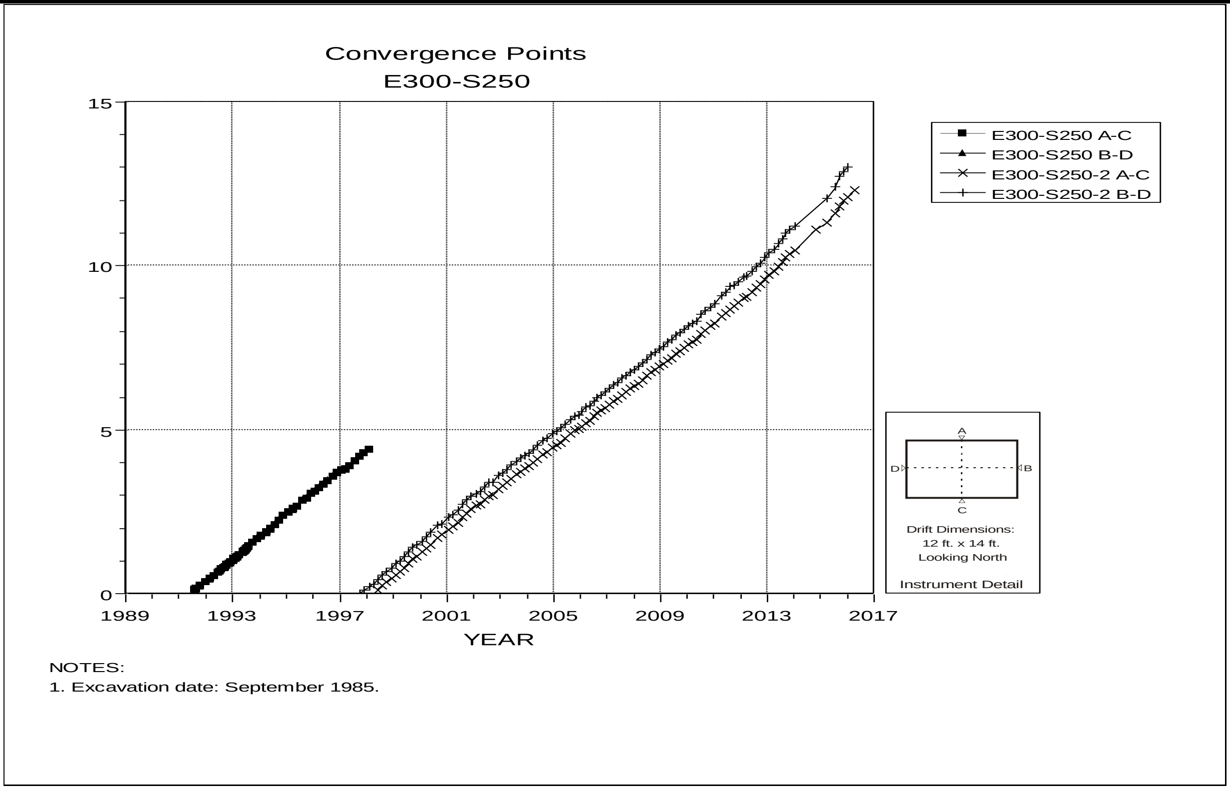

Figure 4-111 Convergence Point Array –
E300 S250 – Rib to Rib

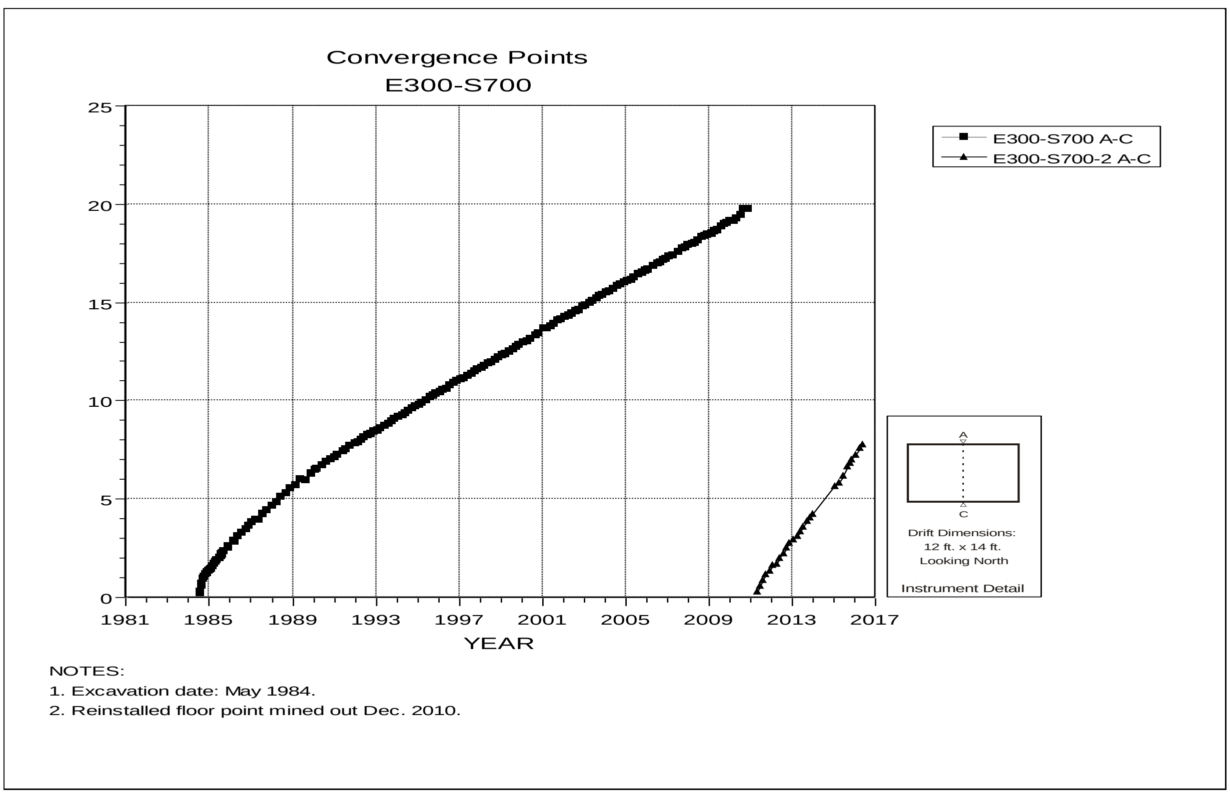

Figure 4-112 Convergence Point Array –
E300 S700 – Roof to Floor

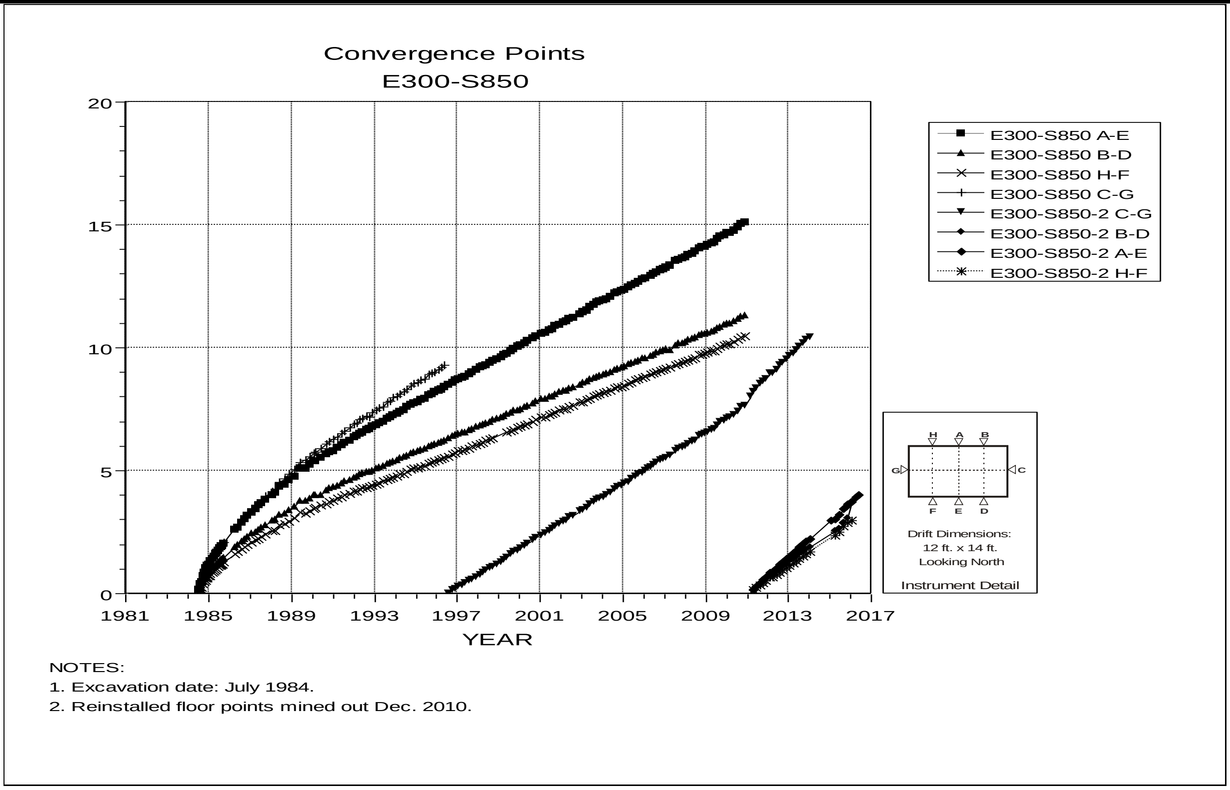

Figure 4-113 Convergence Point Array –
E300 S850 – Roof to Floor – Centerline

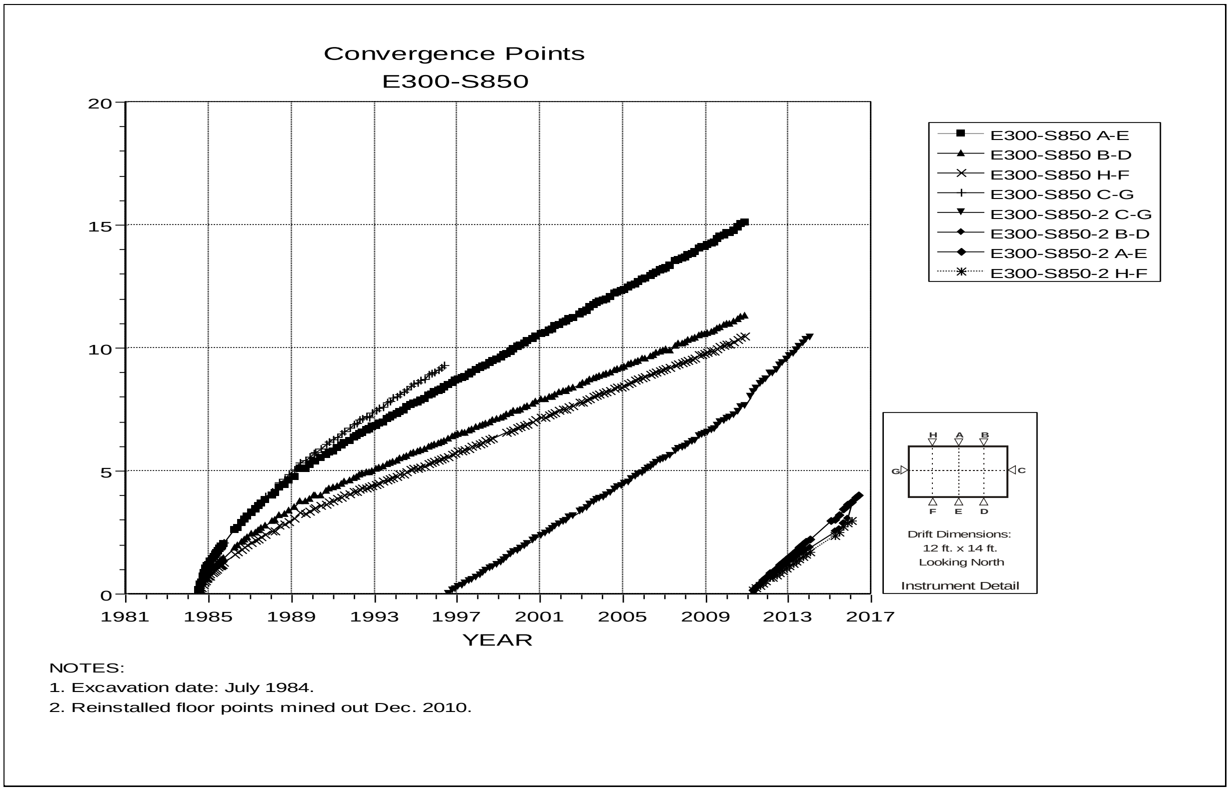

Figure 4-114 Convergence Point Array –
E300 S850 – Roof to Floor – East Quarter Point

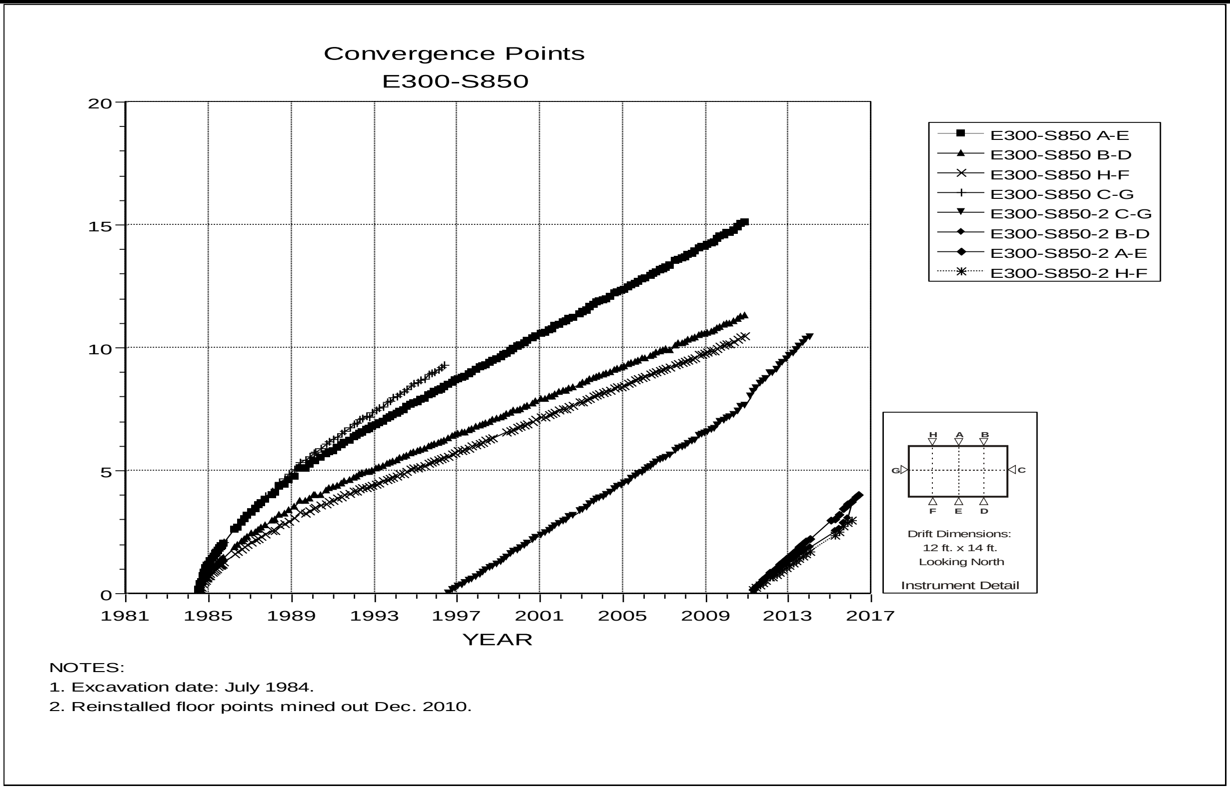

Figure 4-115 Convergence Point Array –
E300 S850 – Roof to Floor – West Quarter Point

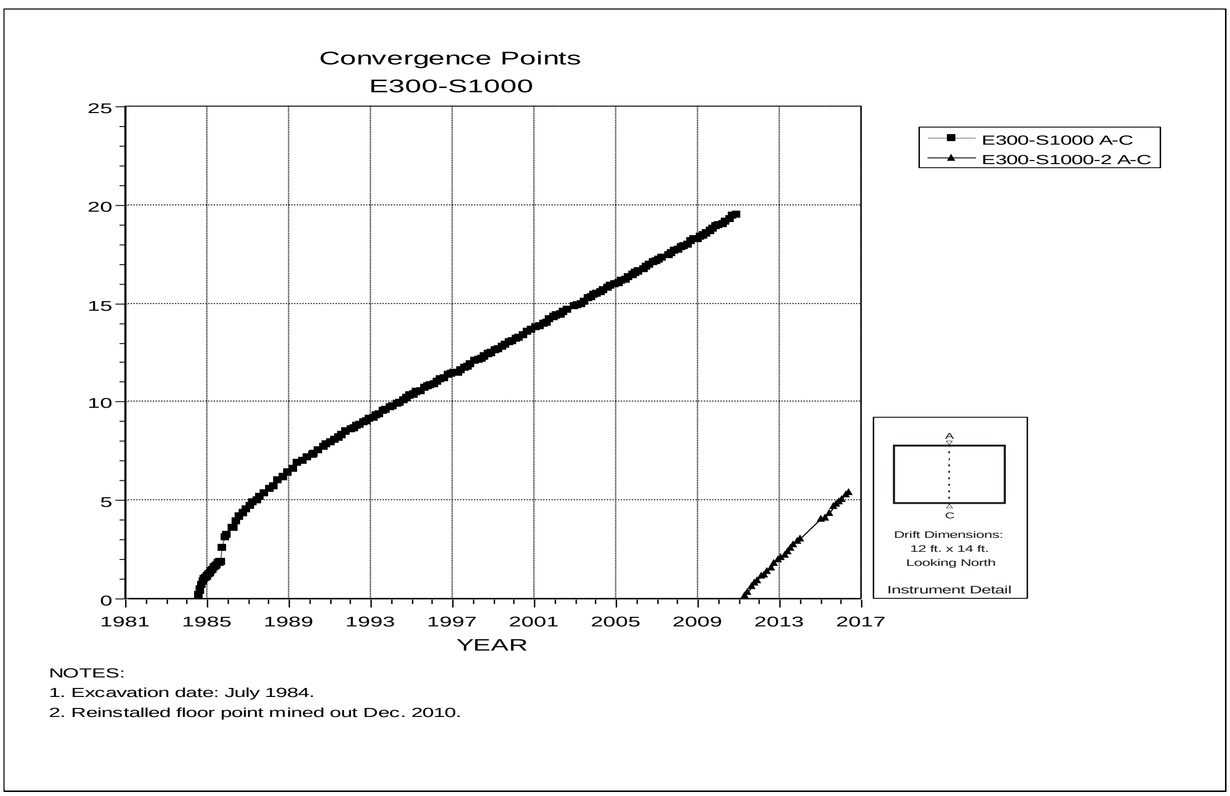

Figure 4-116 Convergence Point Array –
E300 S1000 – Roof to Floor

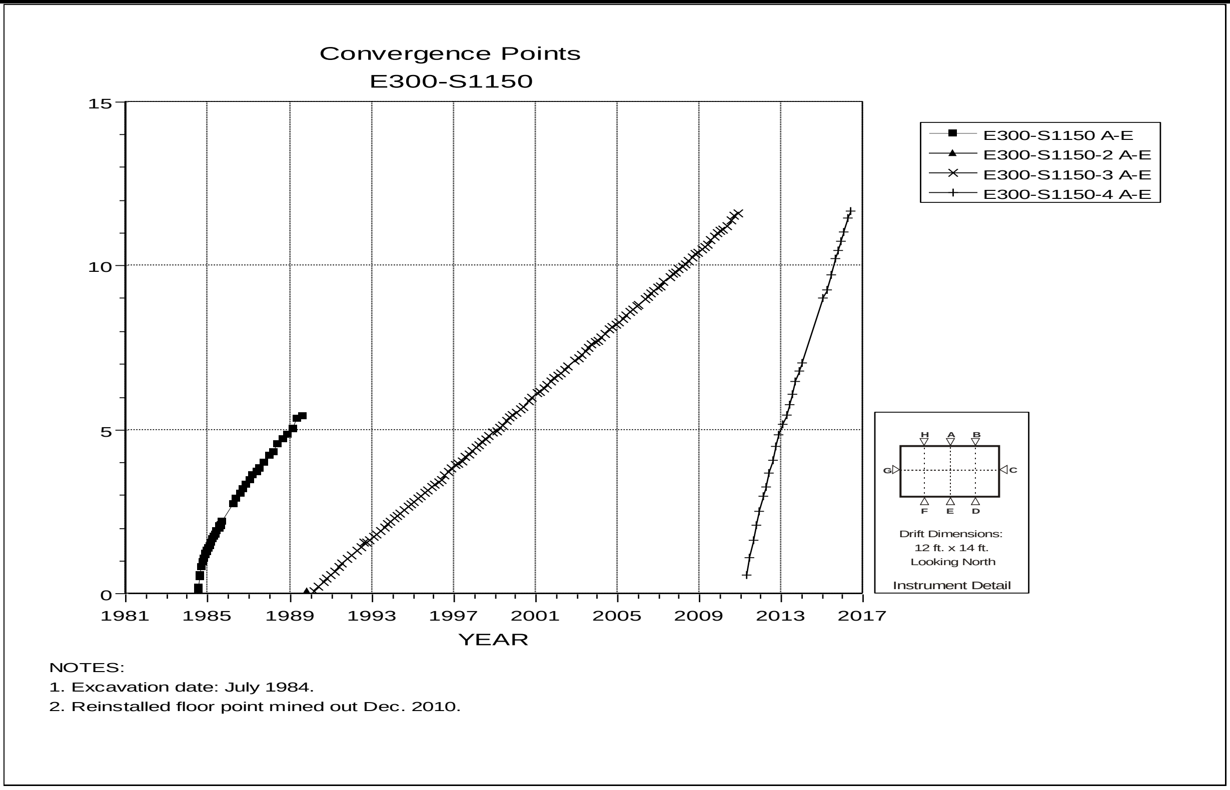

Figure 4-117 Convergence Point Array –
E300 S1150 – Roof to Floor – Centerline

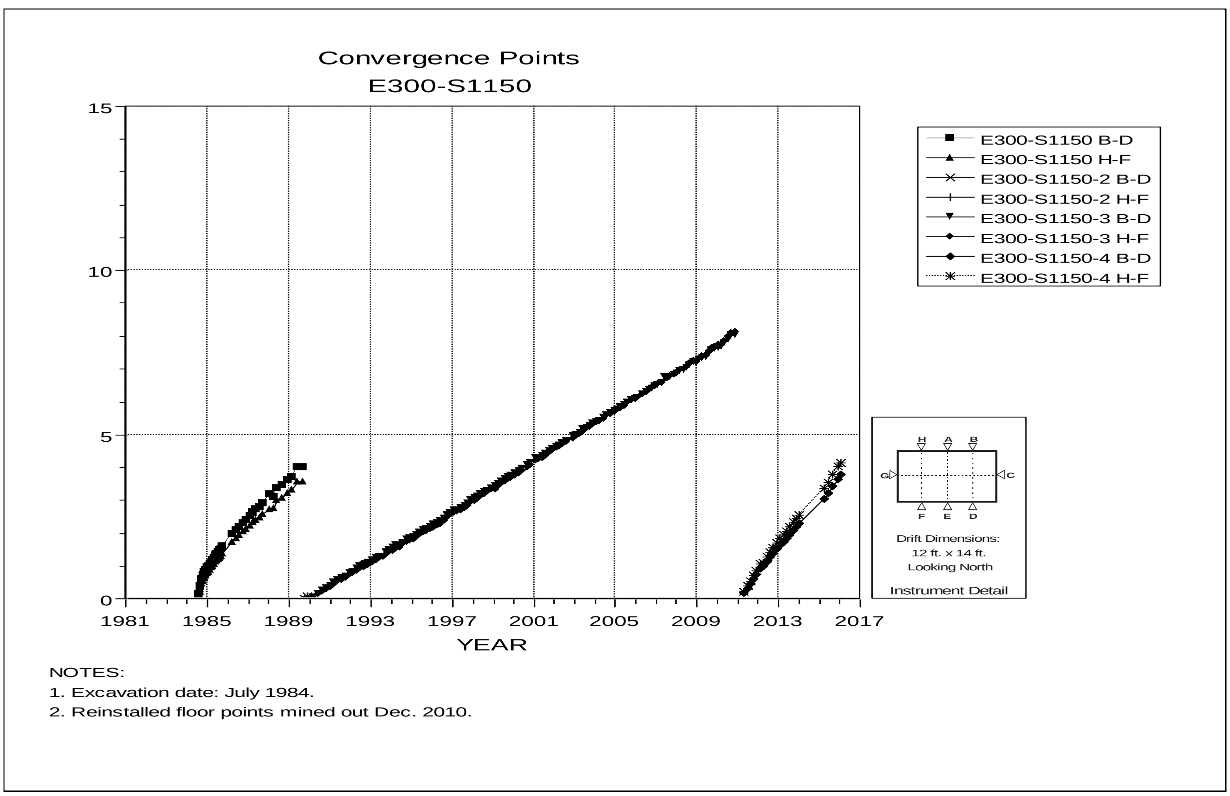

Figure 4-118 Convergence Point Array –
E300 S1150 – Roof to Floor – East Quarter Point

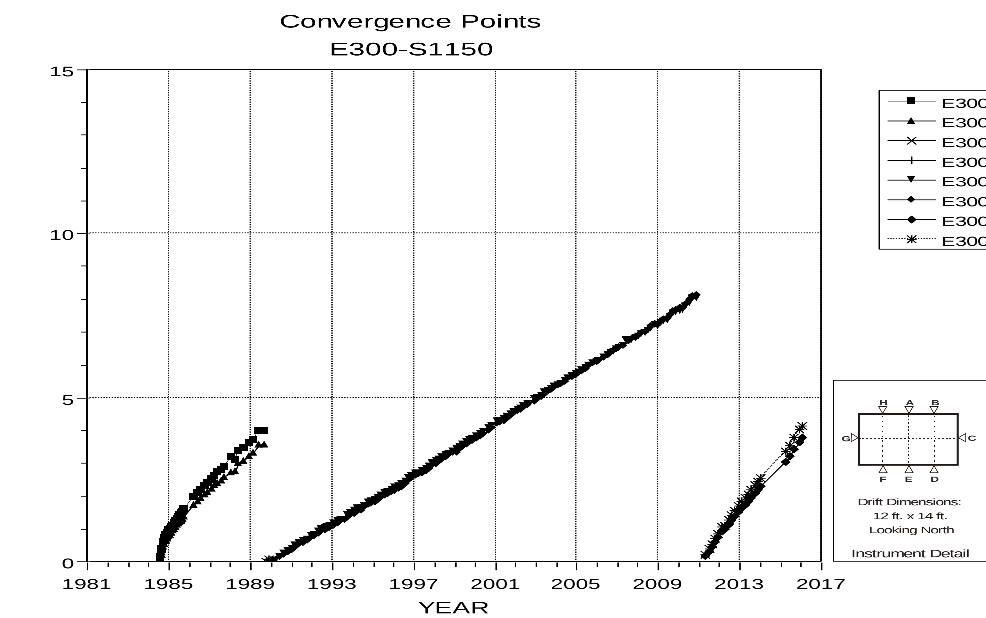

NOTES:
1. Excavation date: July 1984.
2. Reinstalled floor points mined out Dec. 2010.

Figure 4-119 Convergence Point Array –
E300 S1150 – Roof to Floor – West Quarter Point

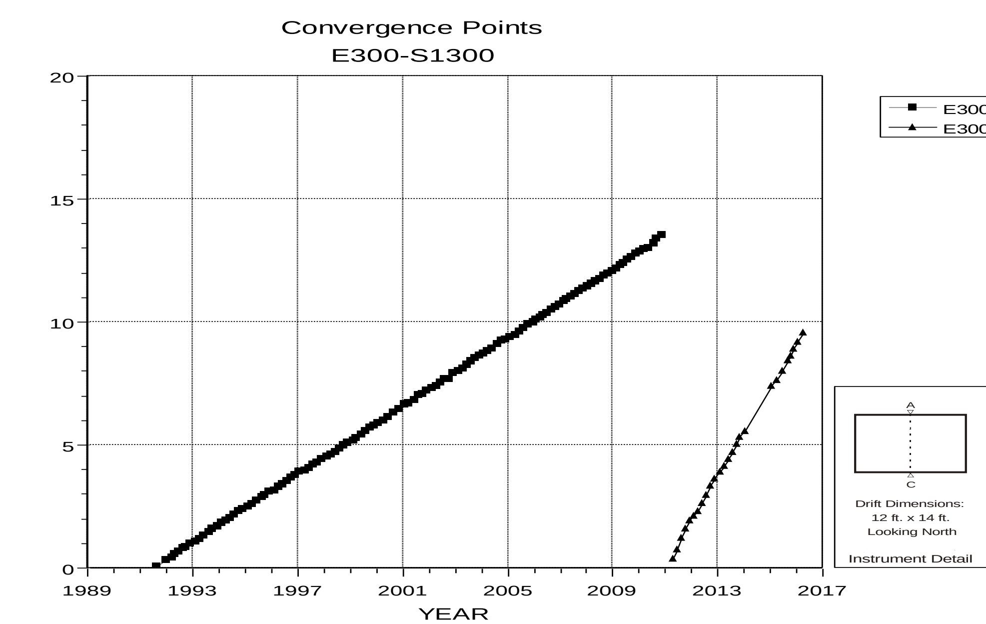

NOTES:
1. Excavation date: July 1984.
2. Reinstalled floor point mined out Dec. 2010.

Figure 4-120 Convergence Point Array –
E300 S1300 – Roof to Floor

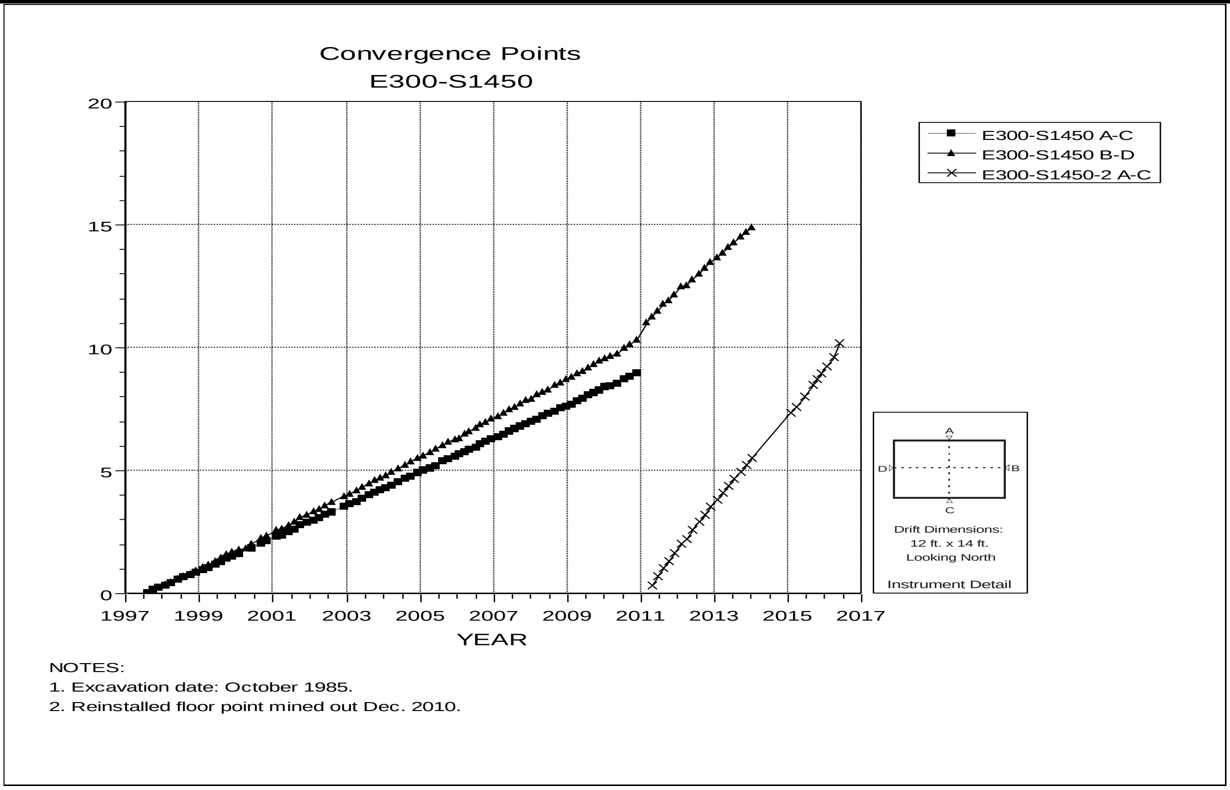

Figure 4-121 Convergence Point Array –
E300 S1450 – Roof to Floor

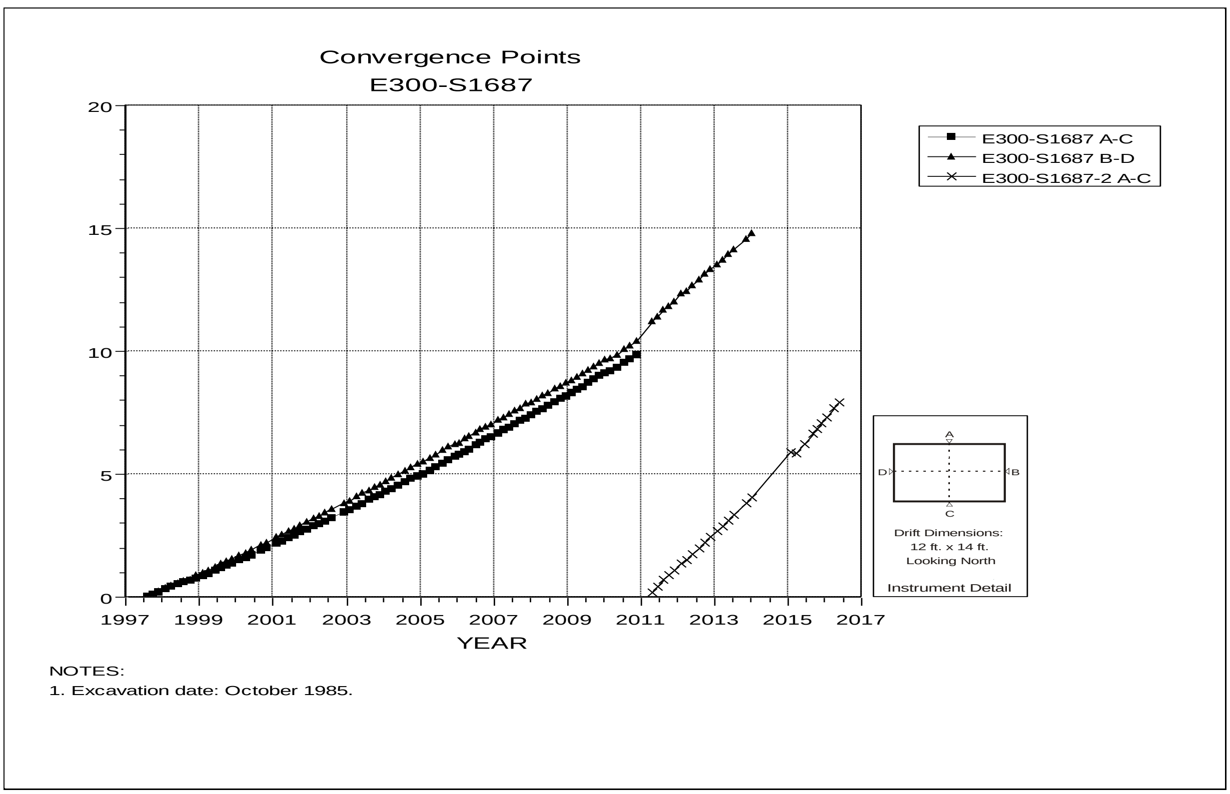

Figure 4-122 Convergence Point Array –
E300 S1687 – Roof to Floor

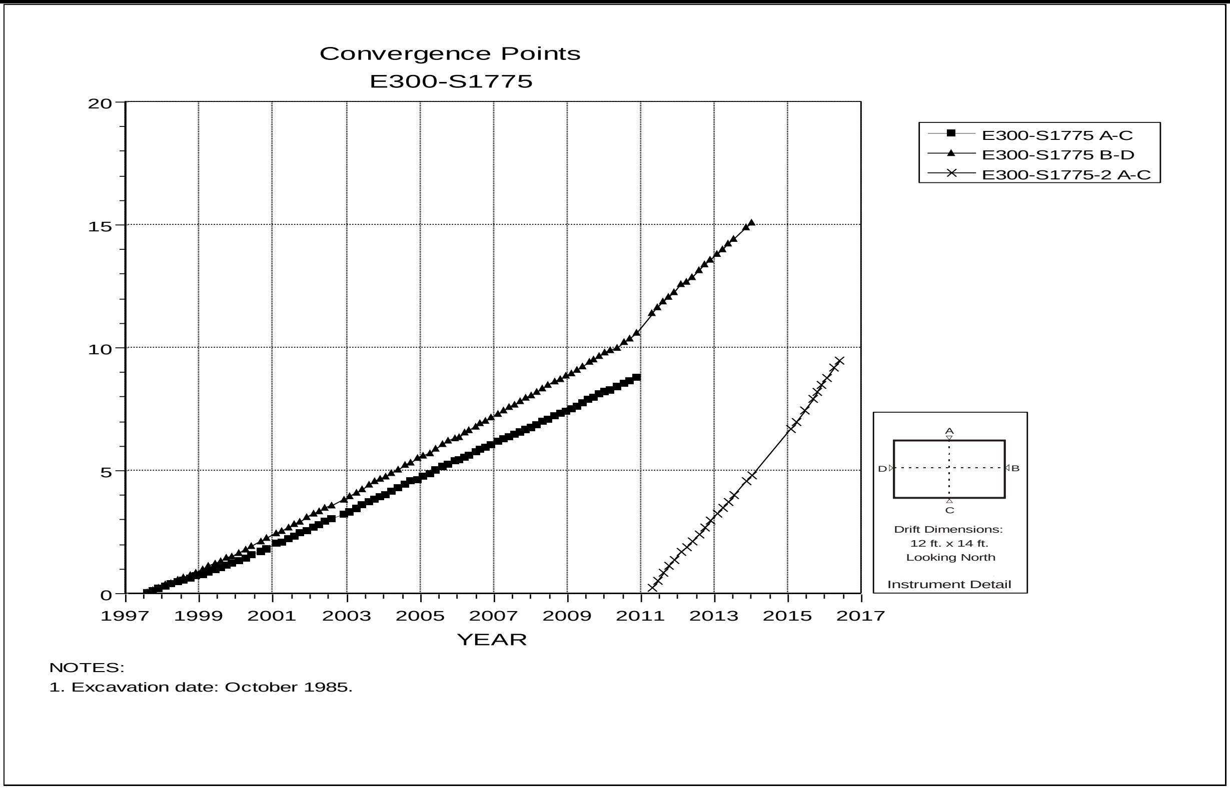

Figure 4-123 Convergence Point Array –
E300 S1775 – All Chords

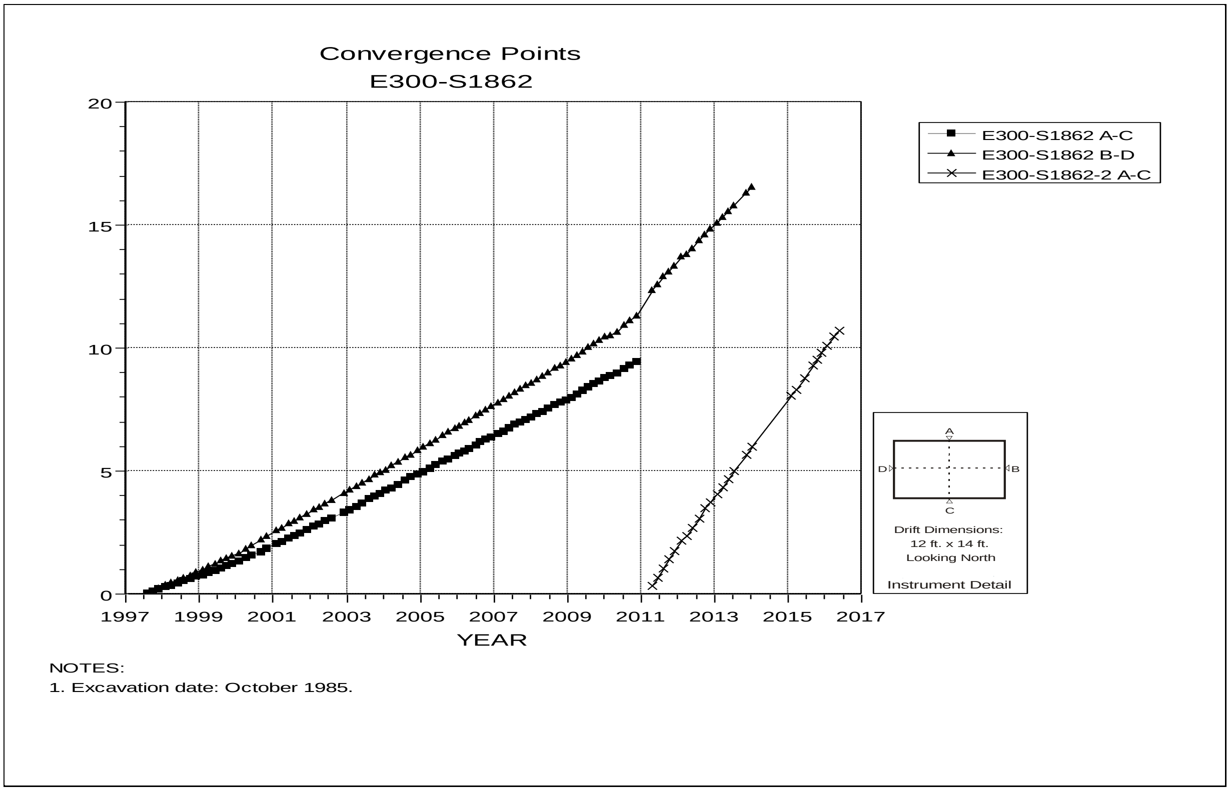

Figure 4-124 Convergence Point Array –
E300 S1862 – All Chords

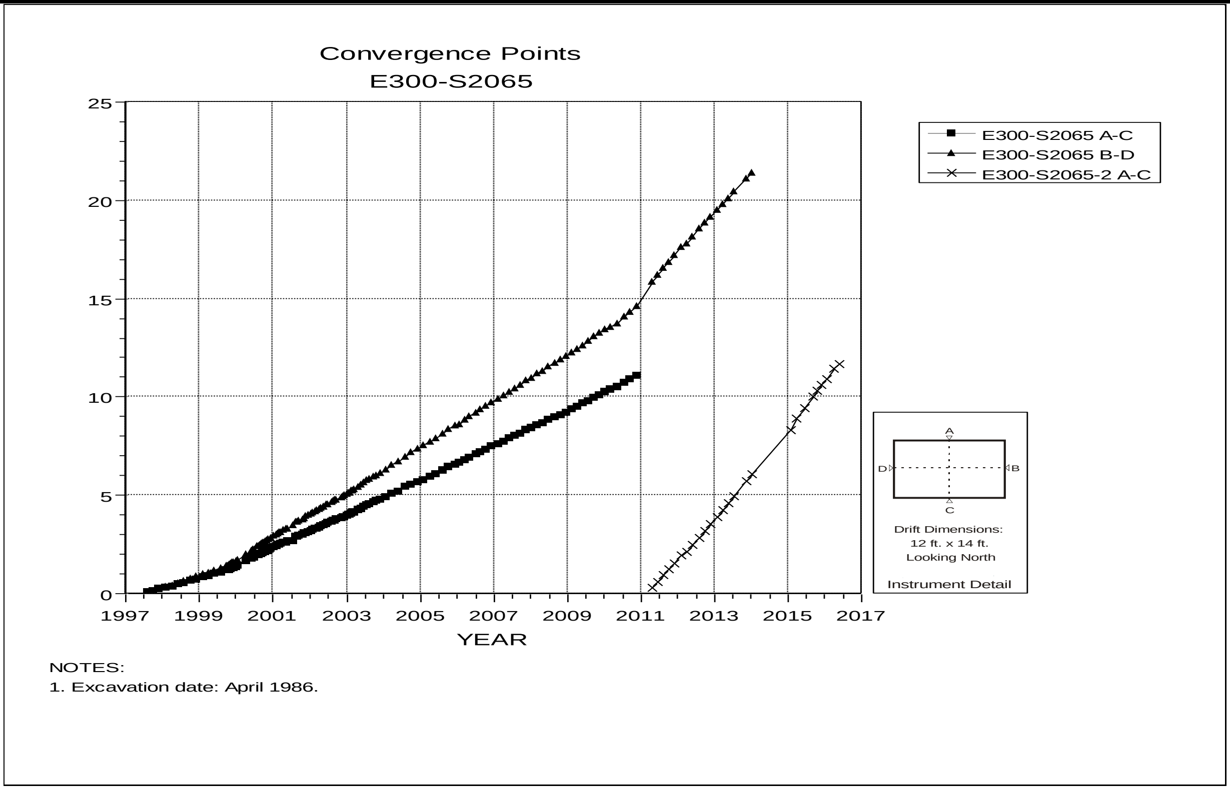

Figure 4-125 Convergence Point Array –
E300 S2065 – Roof to Floor

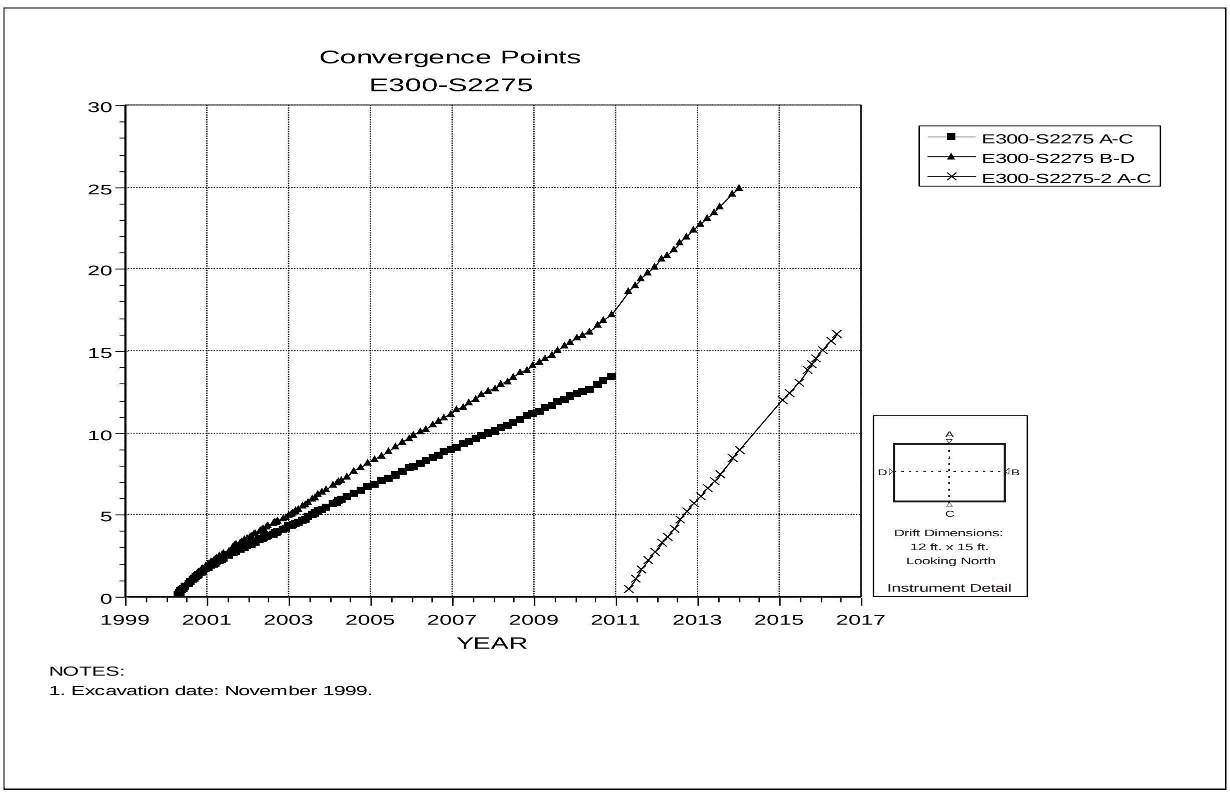

Figure 4-126 Convergence Point Array –
E300 S2275 – All Chords

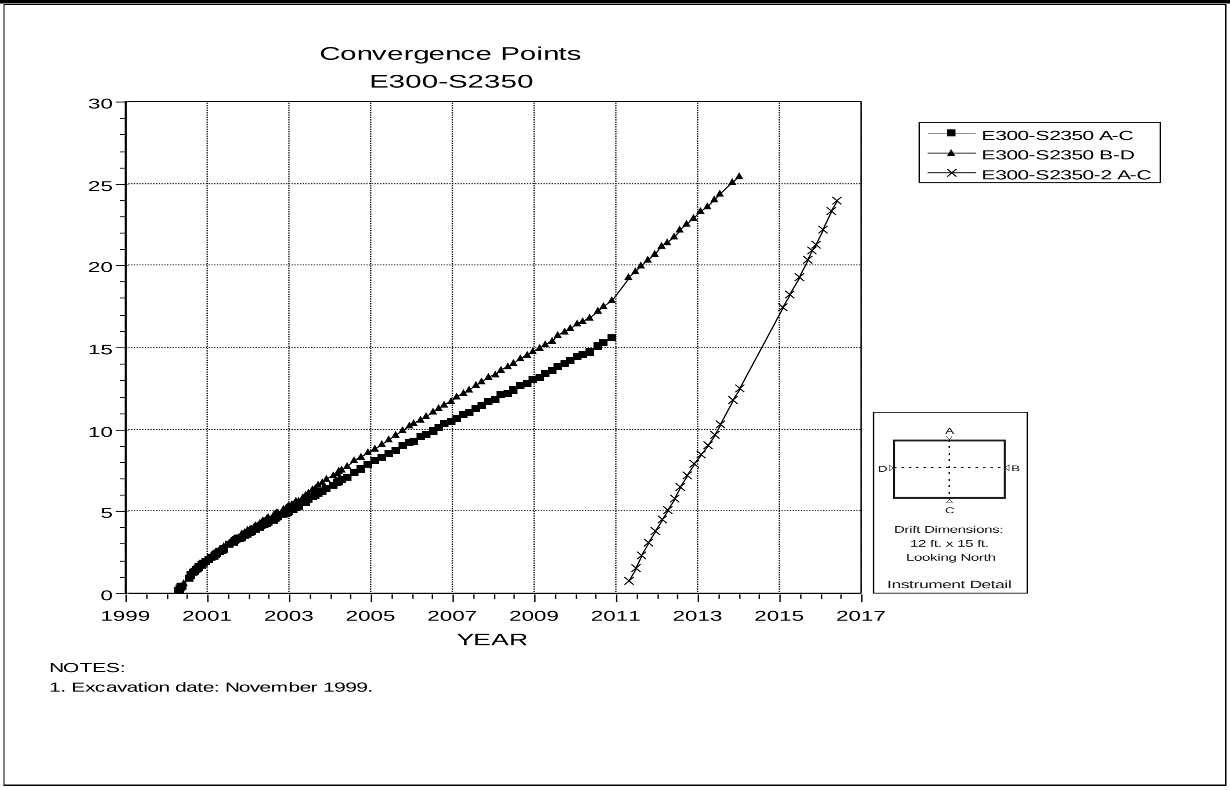

Figure 4-127 Convergence Point Array –
E300 S2350 – All Chords

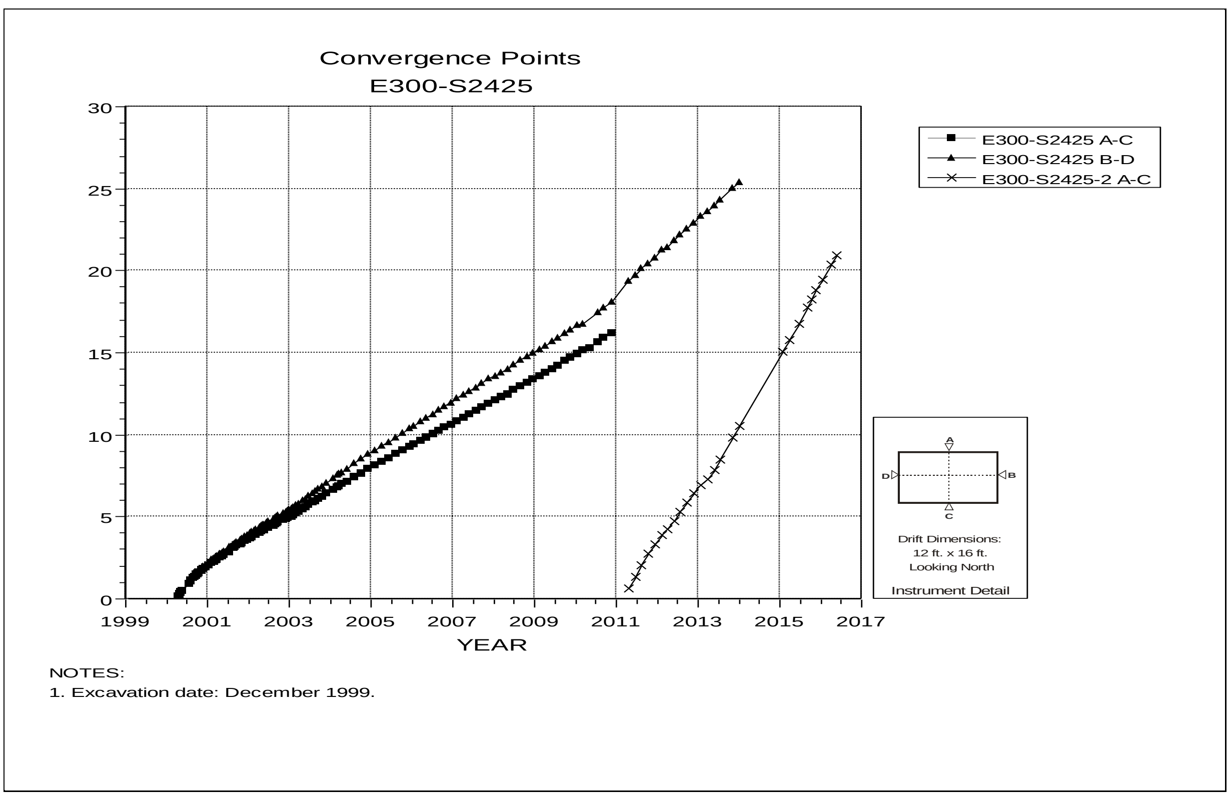

Figure 4-128 Convergence Point Array –
E300 S2425 – All Chords

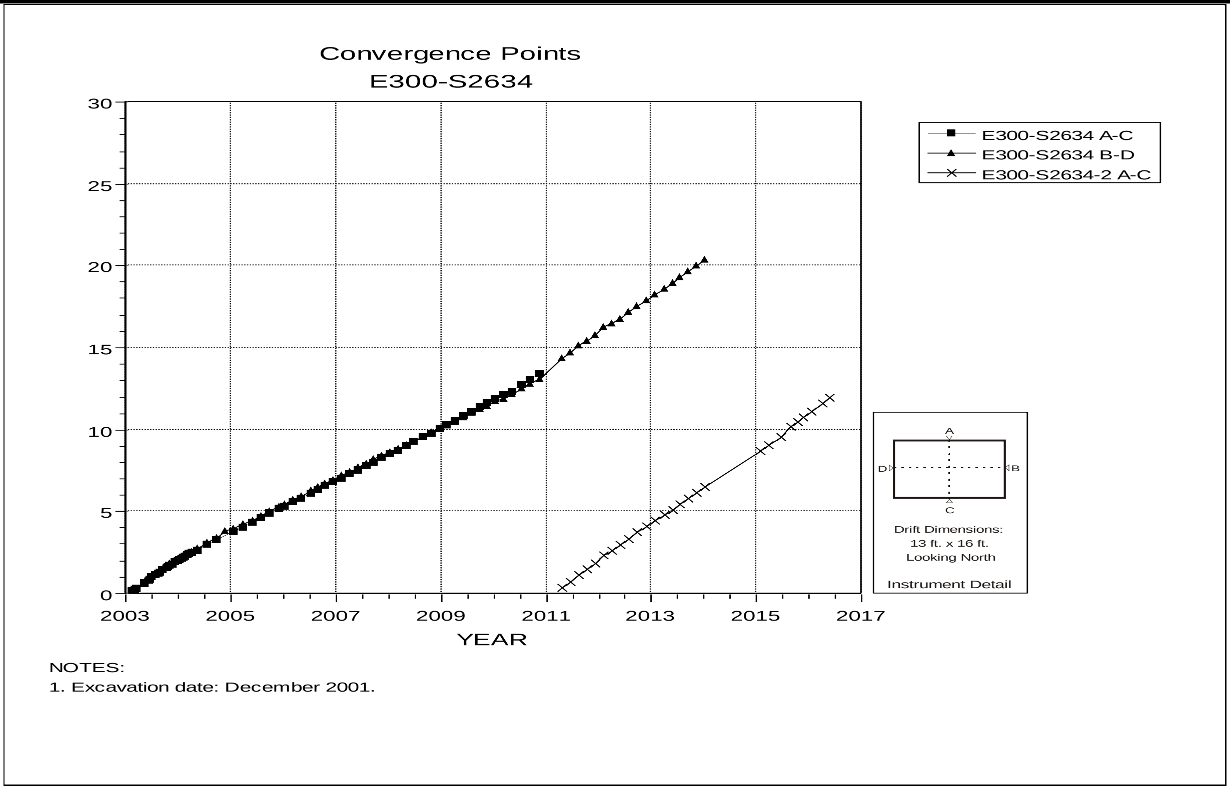

Figure 4-129 Convergence Point Array –
E300 S2634 – All Chords

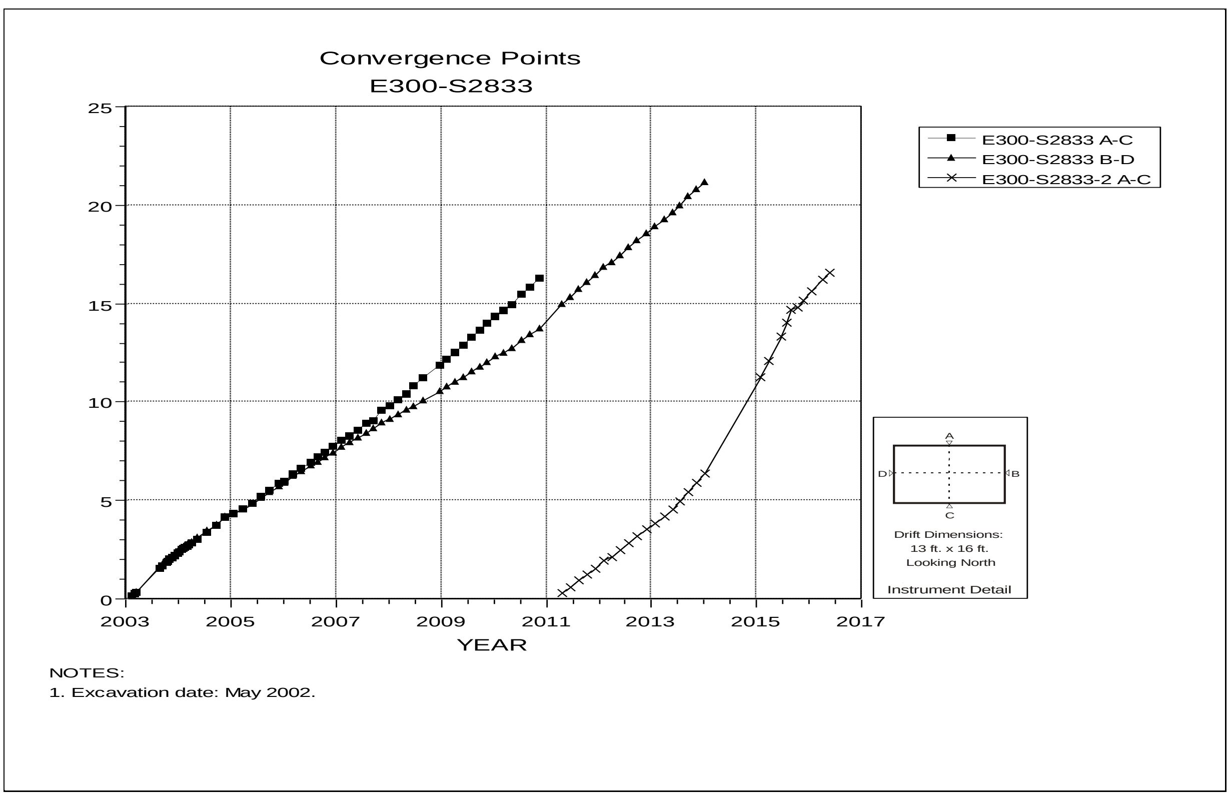

Figure 4-130 Convergence Point Array –
E300 S2833 – All Chords

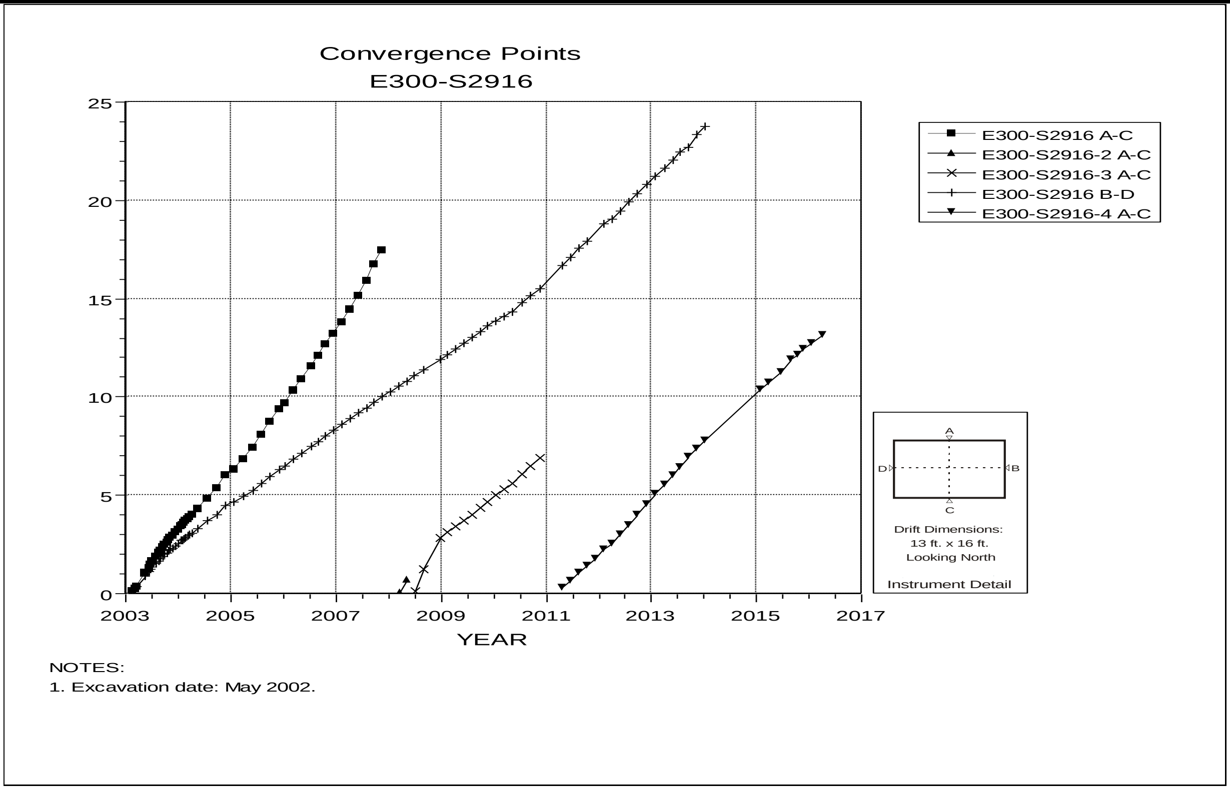

Figure 4-131 Convergence Point Array –
E300 S2916 – All Chords

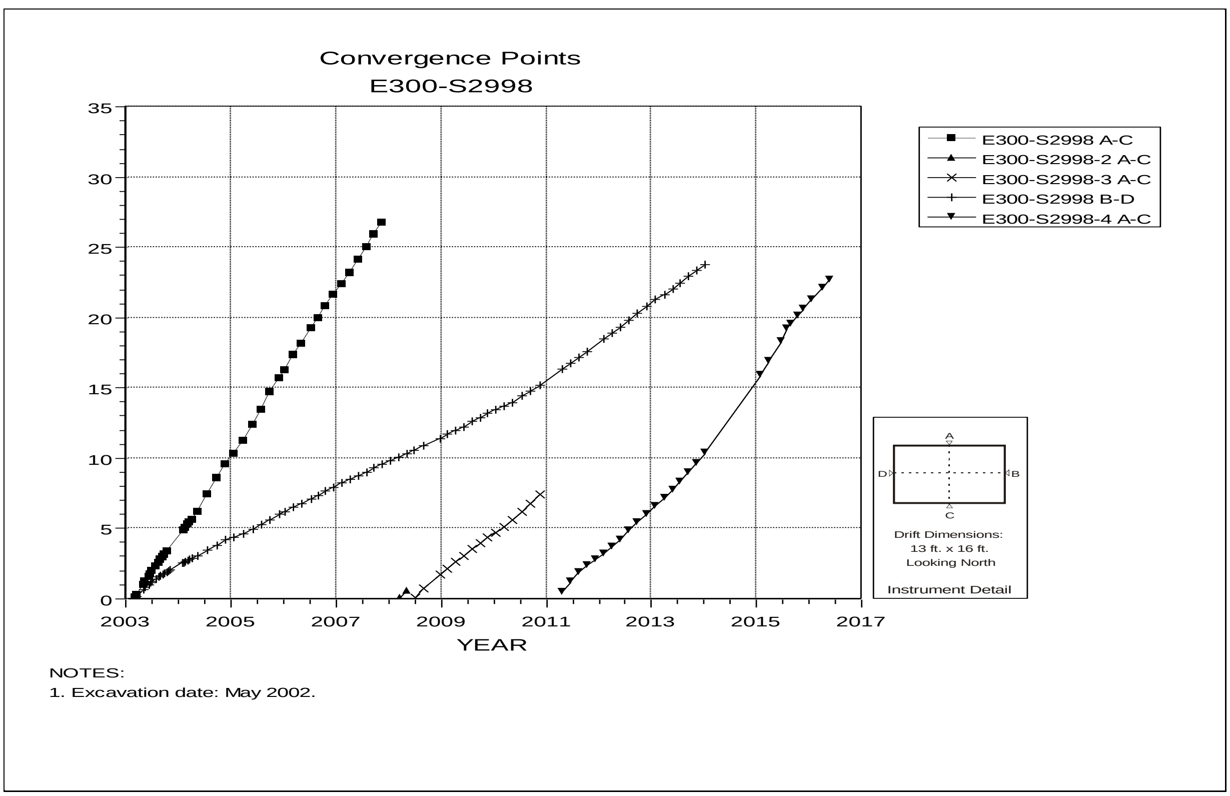

Figure 4-132 Convergence Point Array –
E300 S2998 – All Chords

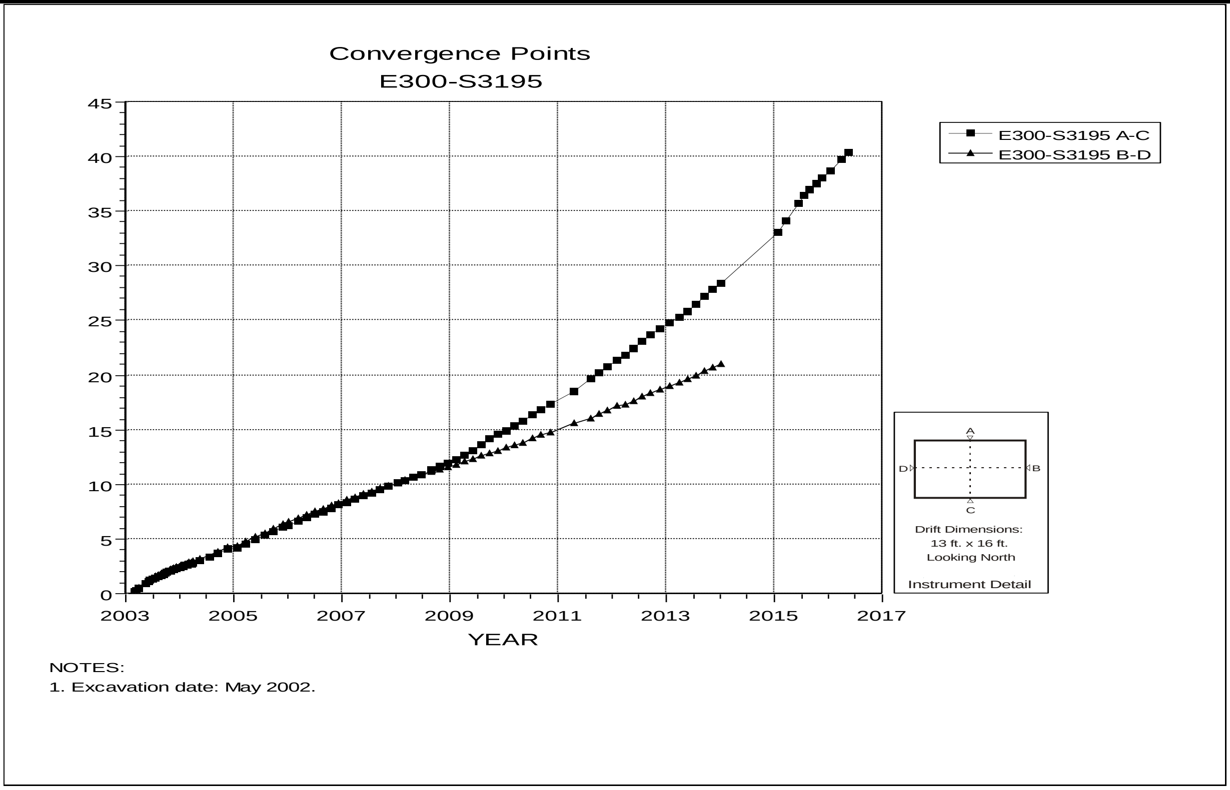

Figure 4-133 Convergence Point Array –
E300 S3195 – All Chords

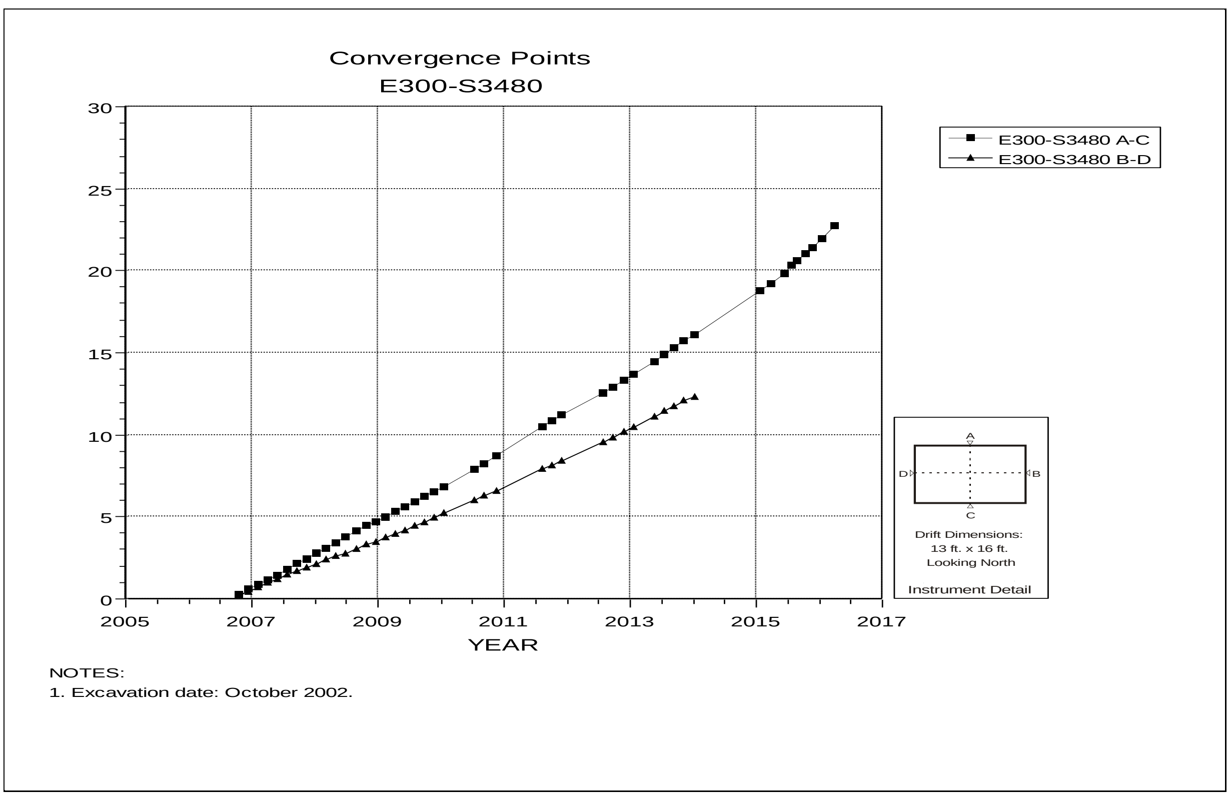

Figure 4-134 Convergence Point Array –
E300 S3480 – All Chords

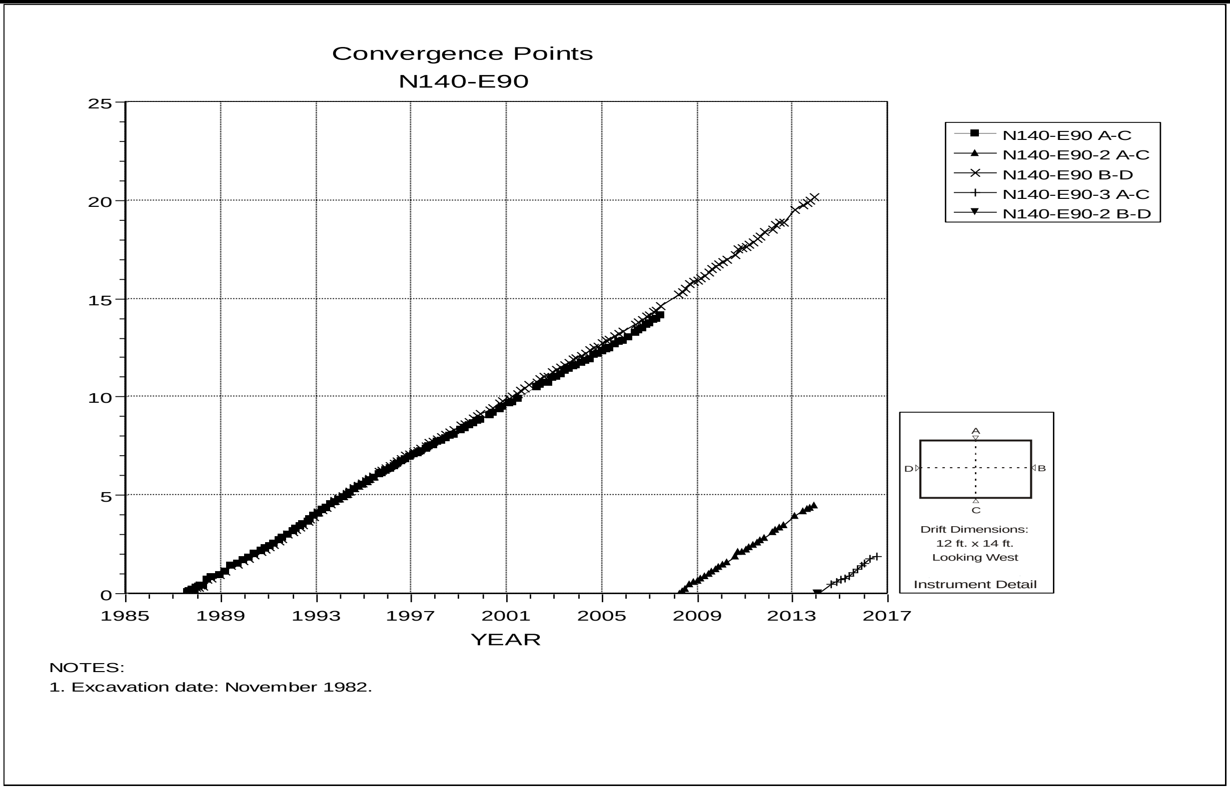

Figure 4-135 Convergence Point Array –
N140 E90 – All Chords

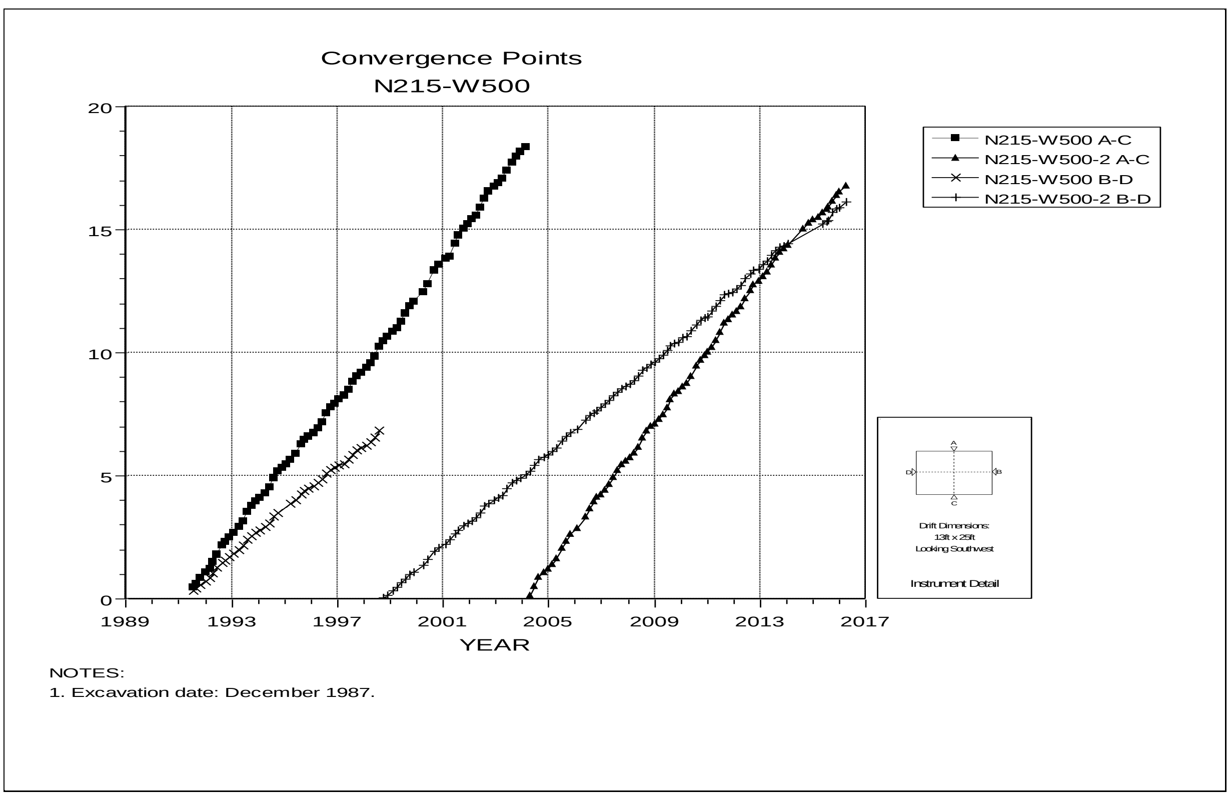

Figure 4-136 Convergence Point Array –
N215 W500 – All Chords

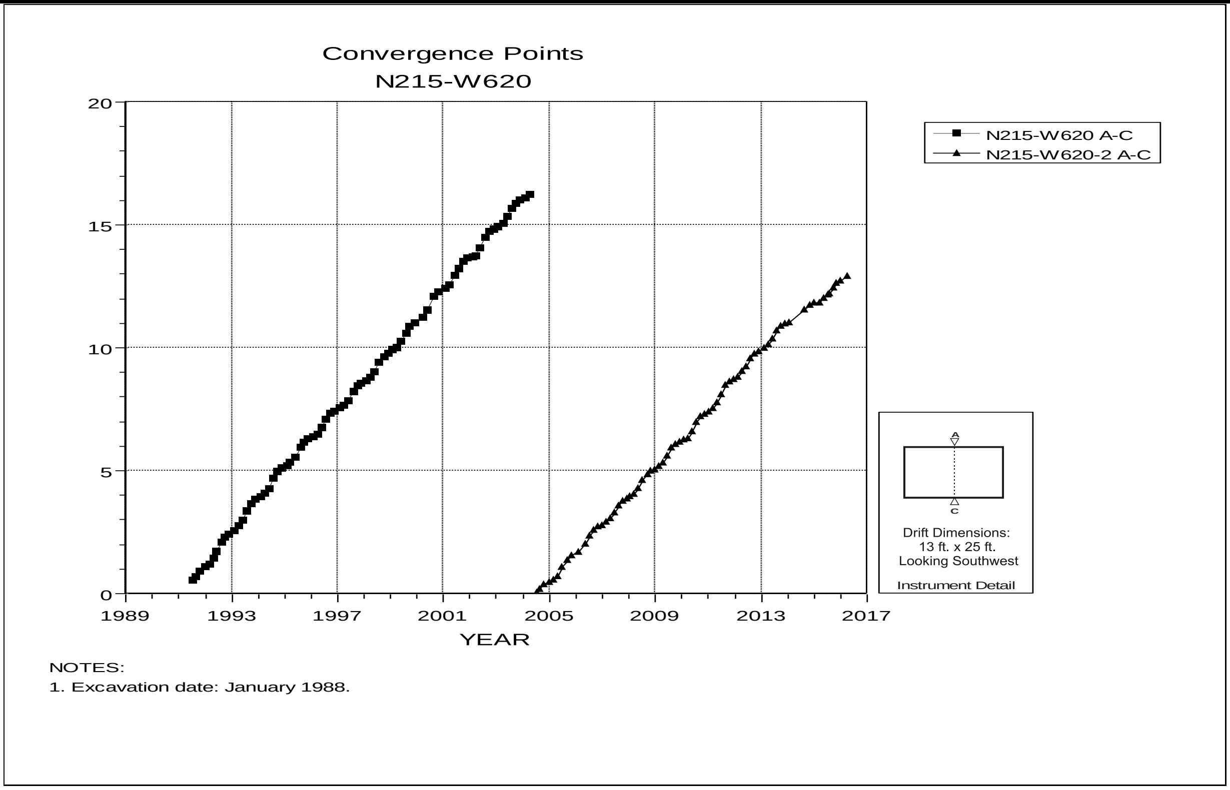

Figure 4-137 Convergence Point Array –
N215 W620 – Roof to Floor

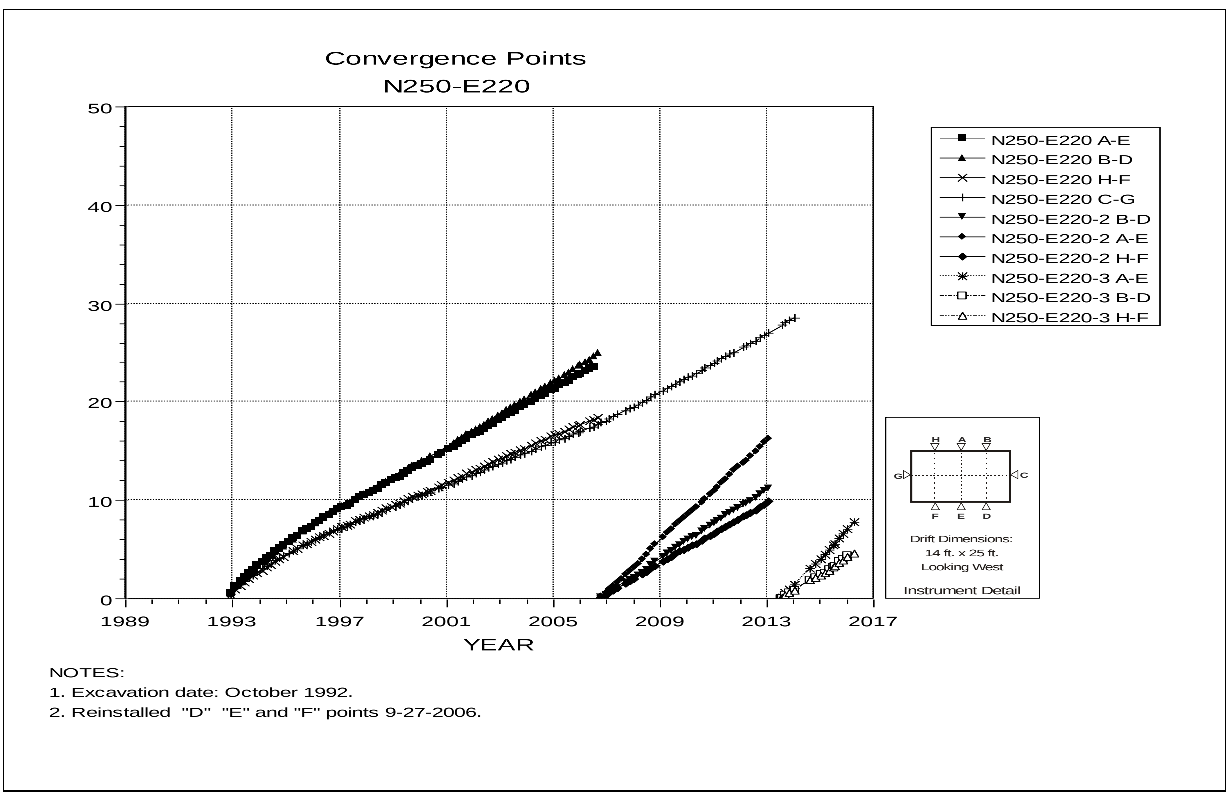

Figure 4-138 Convergence Point Array –
N250 E220 – Roof to Floor – Centerline

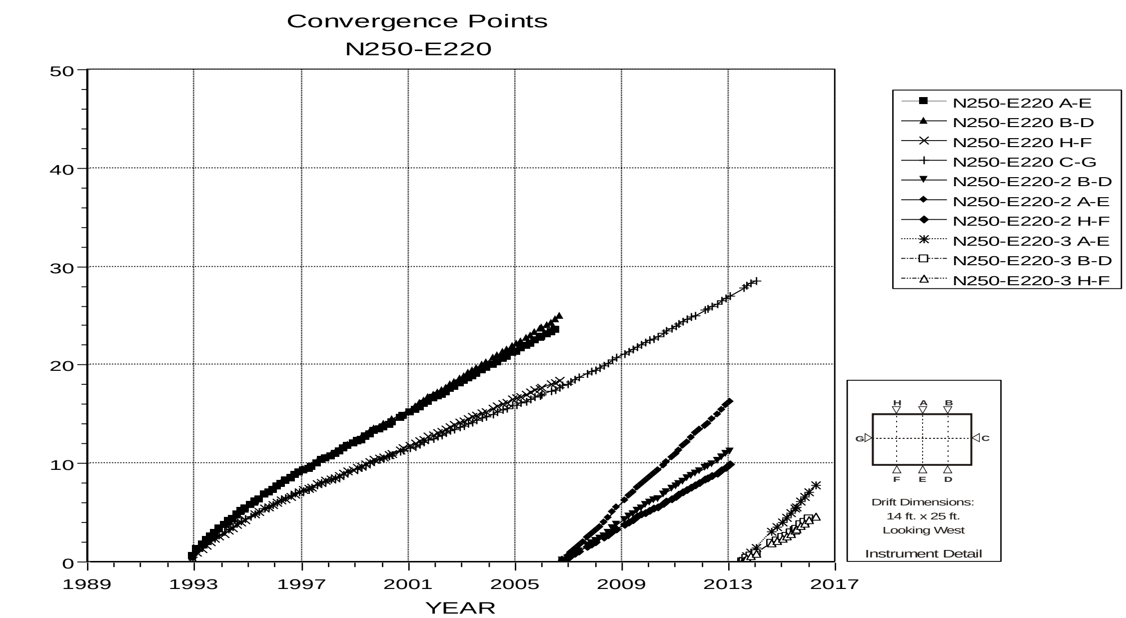

NOTES:
1. Excavation date: October 1992.
2. Reinstalled "D" "E" and "F" points 9-27-2006.

Figure 4-139 Convergence Point Array –
N250 E220 – Roof to Floor – East Quarter Point

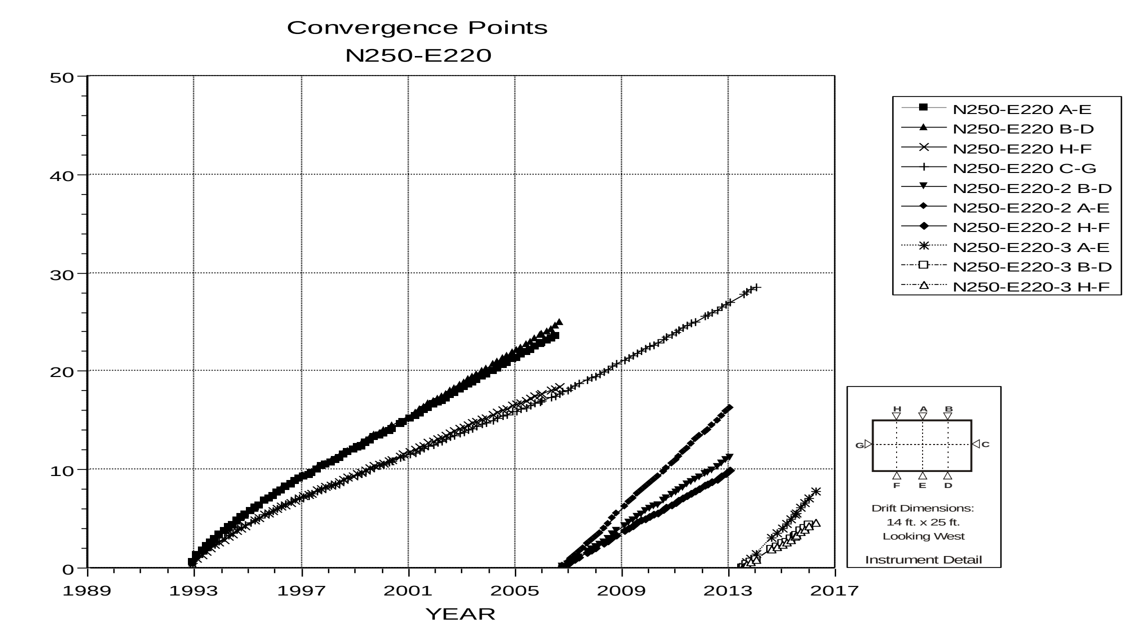

NOTES:
1. Excavation date: October 1992.
2. Reinstalled "D" "E" and "F" points 9-27-2006.

Figure 4-140 Convergence Point Array –
N250 E220 – Roof to Floor – West Quarter Point

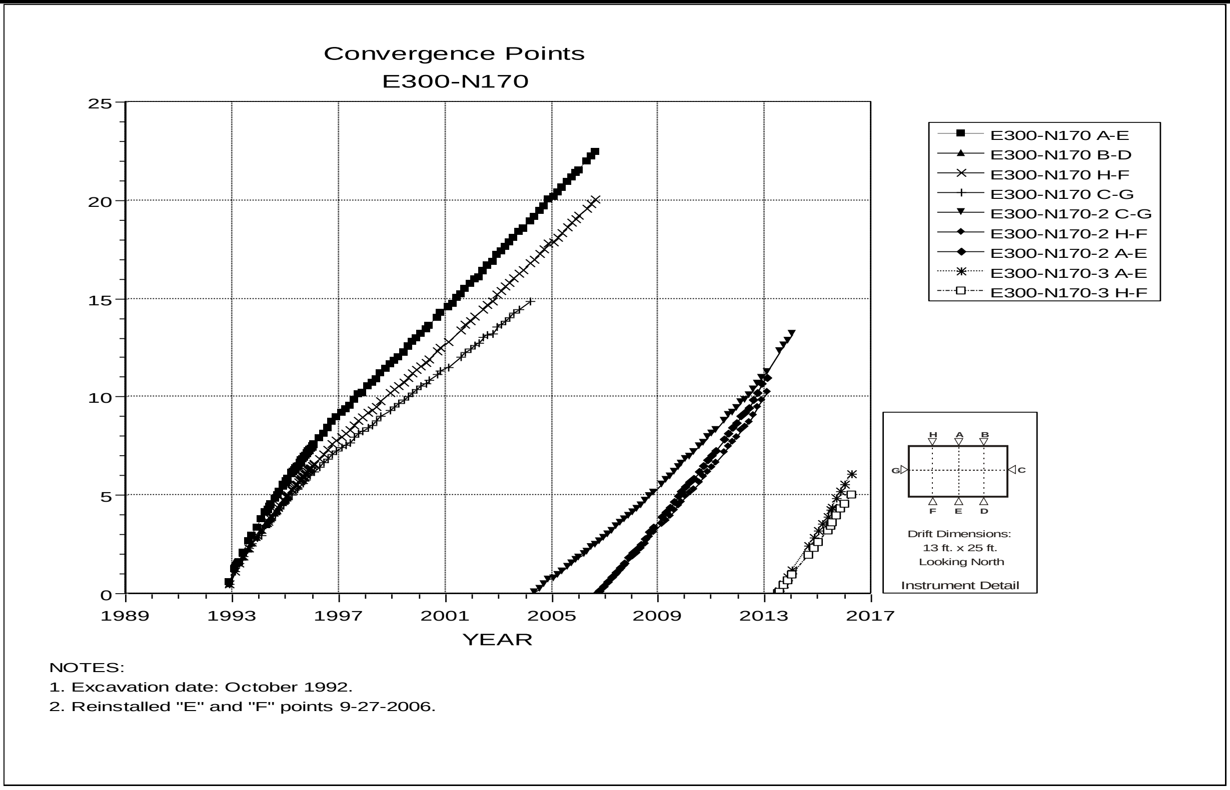

Figure 4-141 Convergence Point Array –
E300 N170 – All Chords

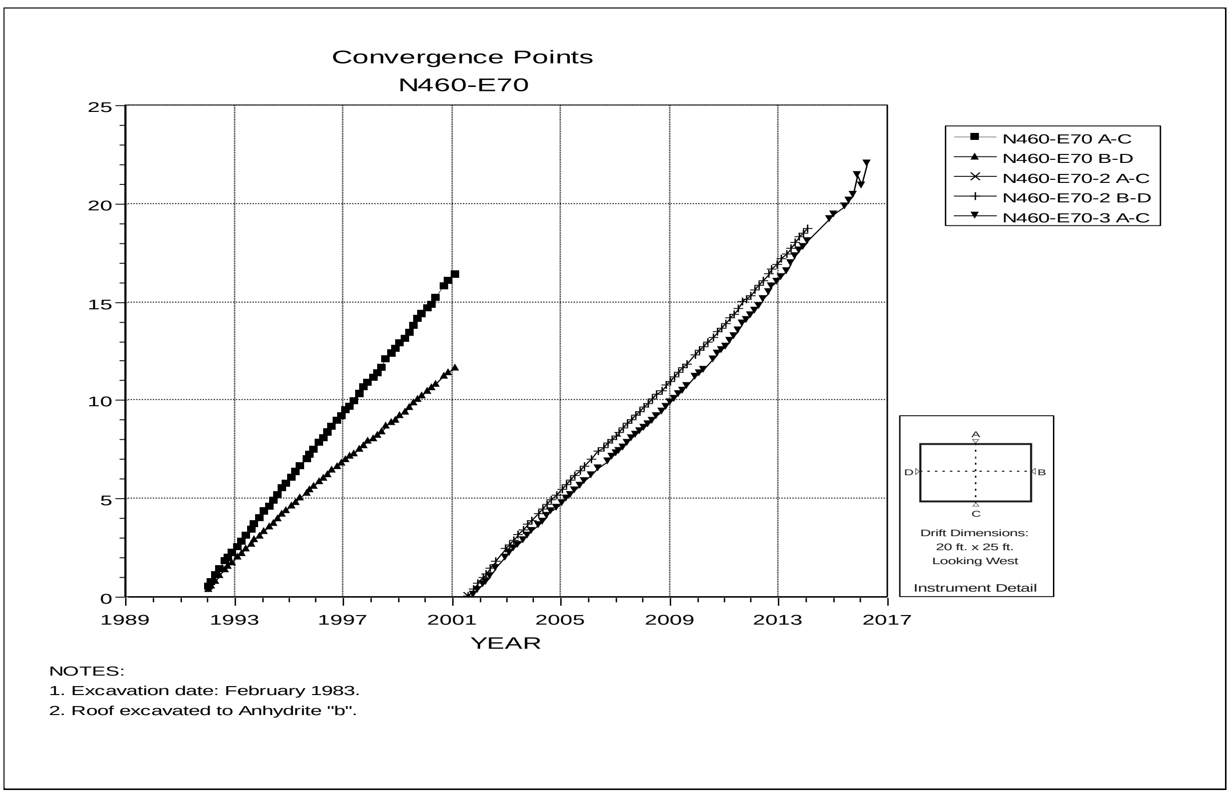

Figure 4-142 Convergence Point Array –
N460 E70 – All Chords

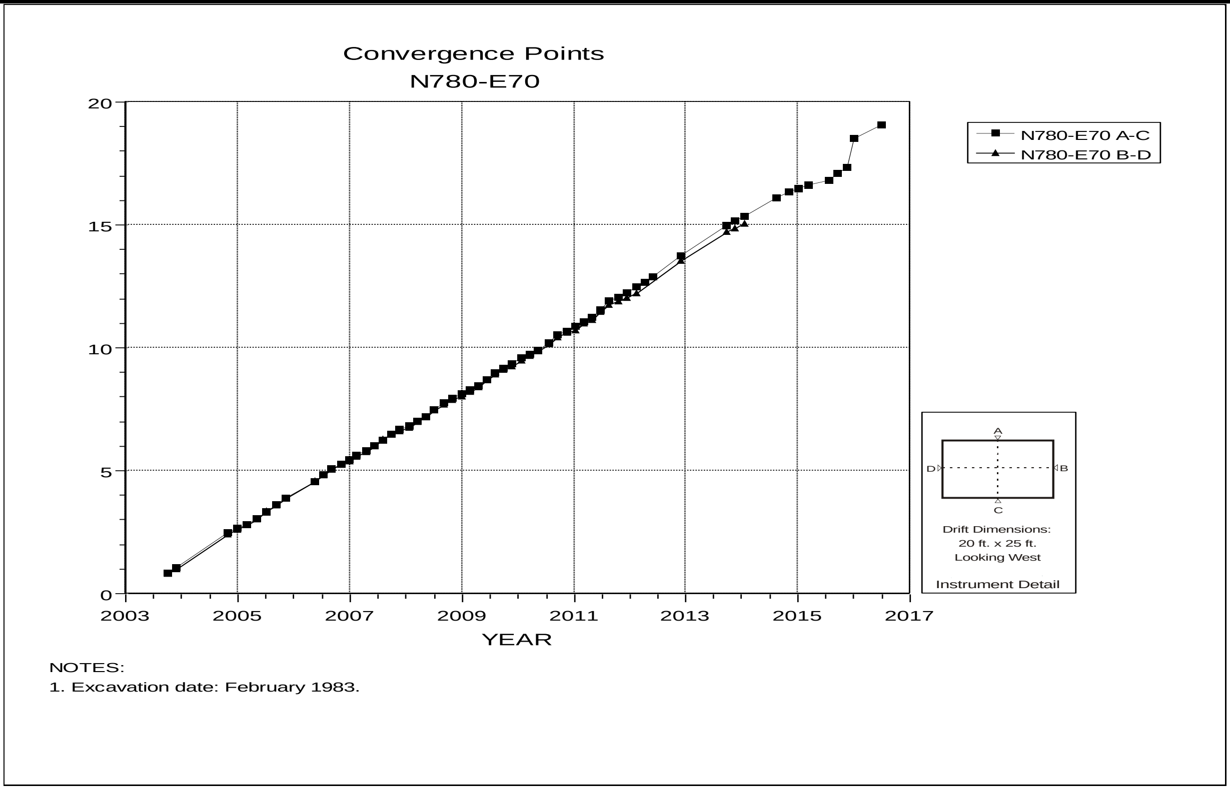

Figure 4-143 Convergence Point Array –
N780 E70 – All Chords

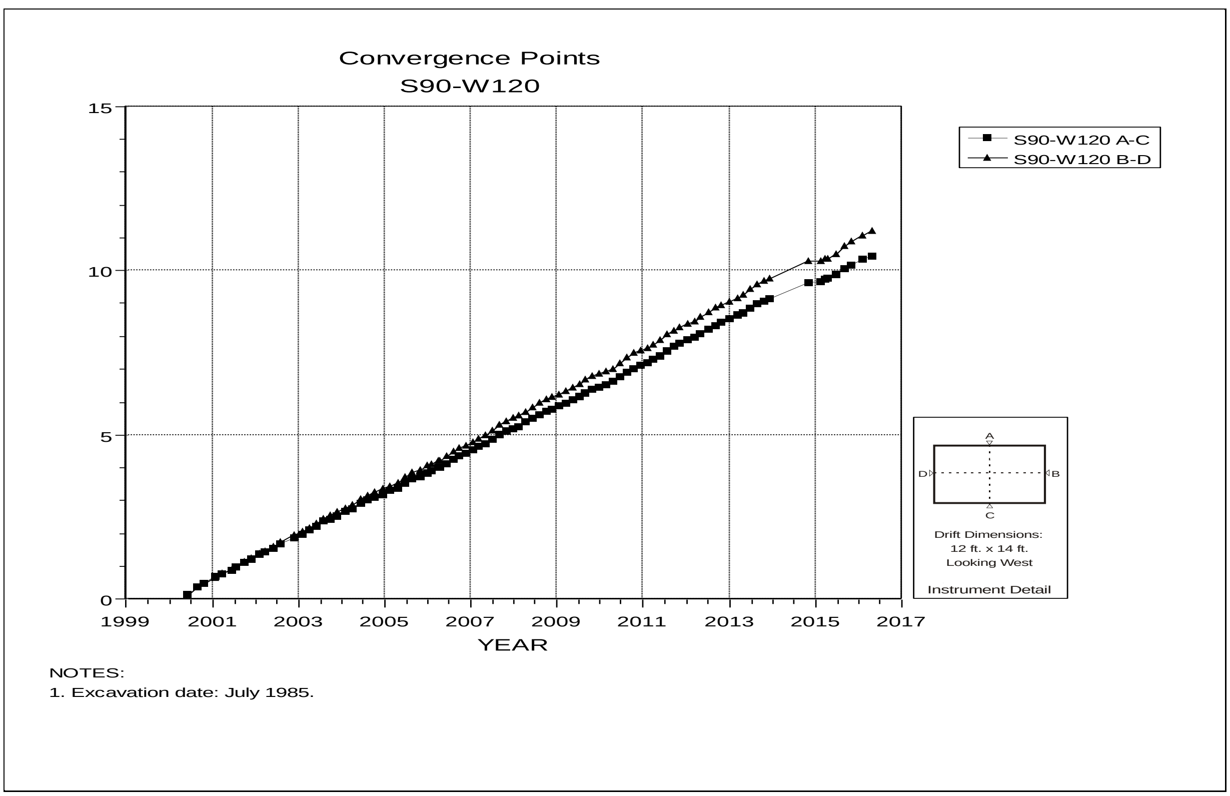

Figure 4-144 Convergence Point Array –
S90 W120 – All Chords

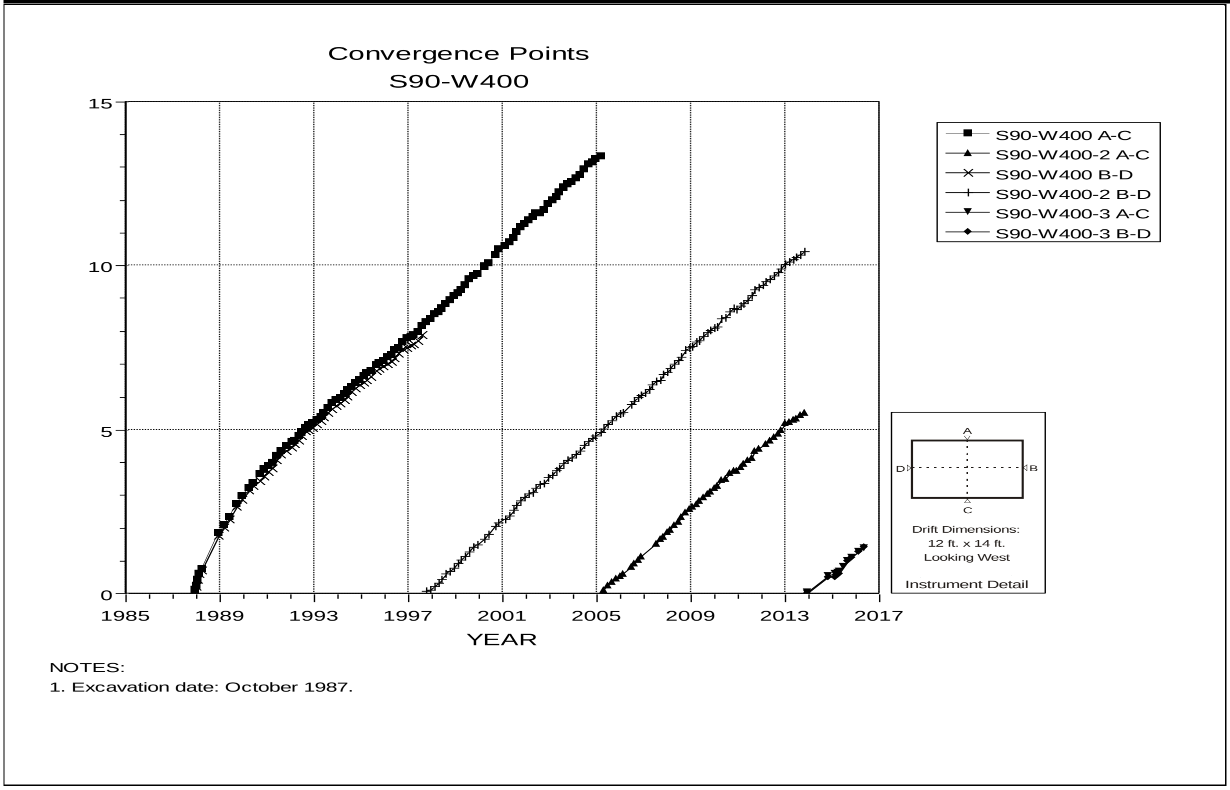

Figure 4-145 Convergence Point Array –
S90 W400 – All Chords

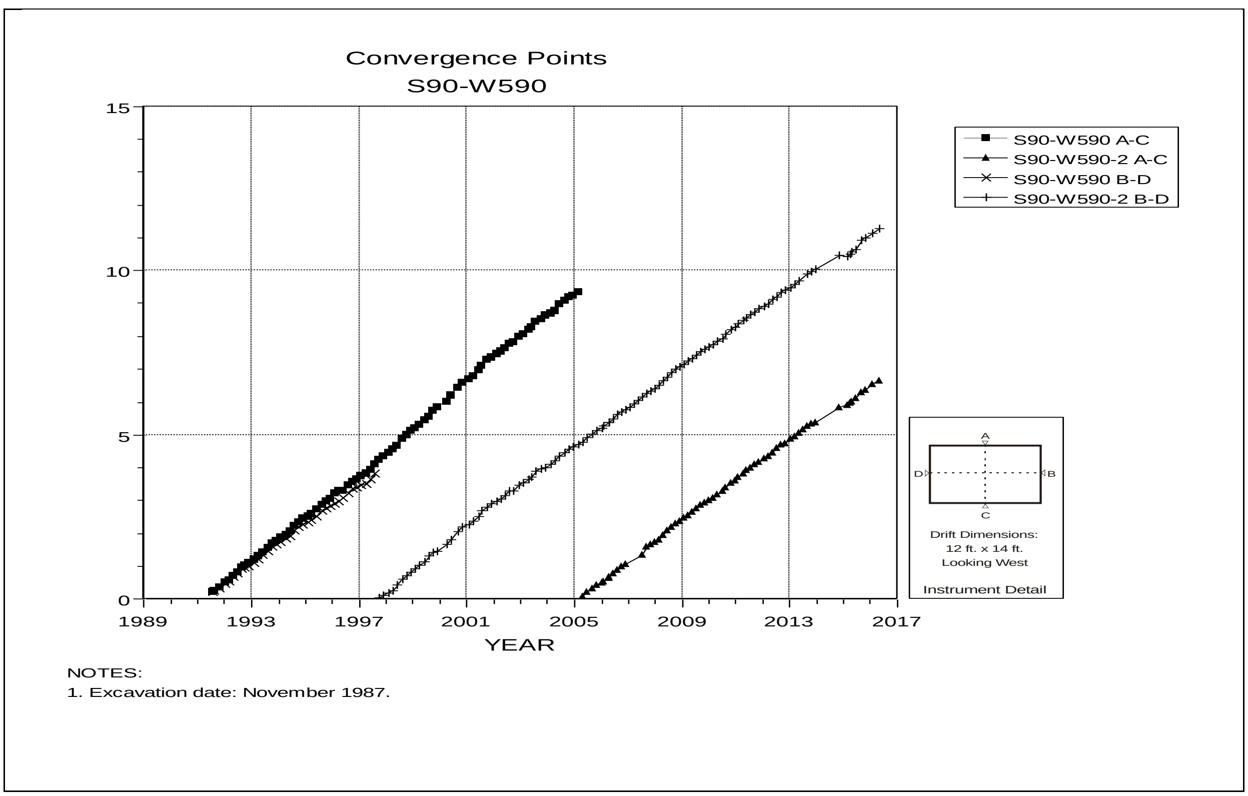

Figure 4-146 Convergence Point Array –
S90 W590 – All Chords

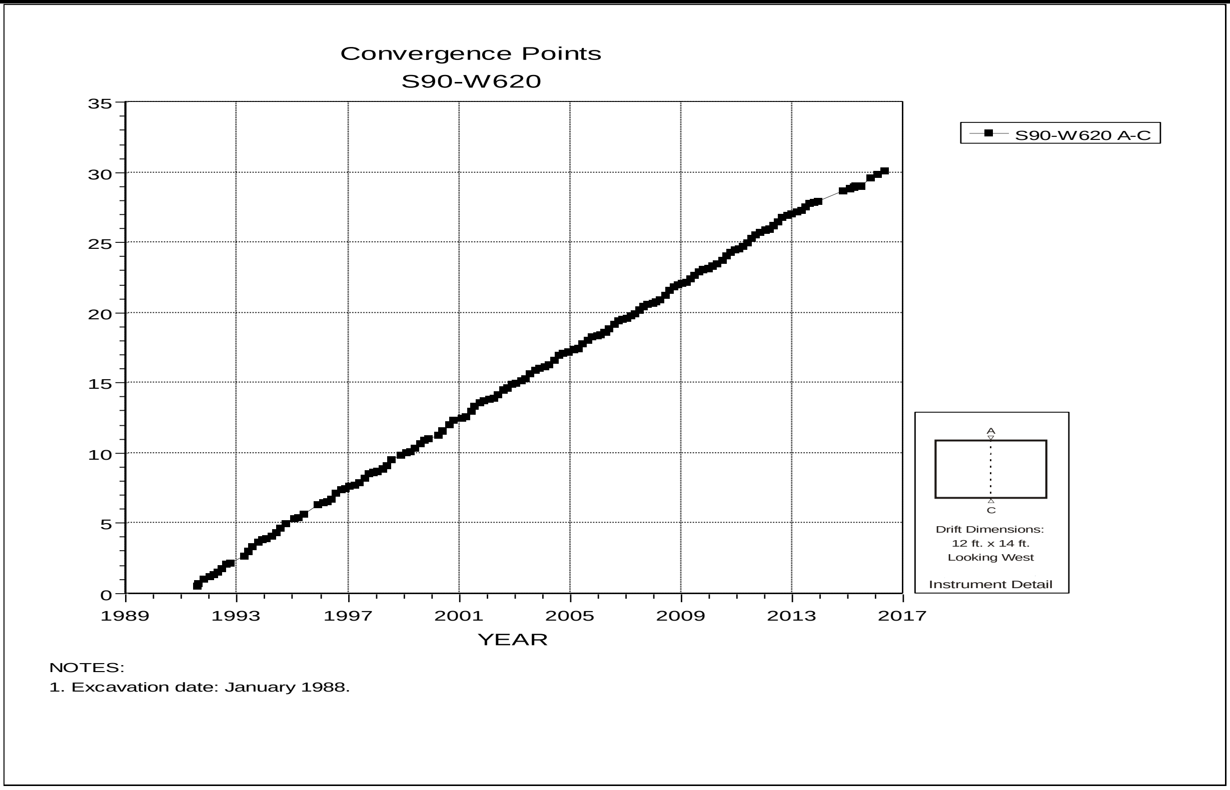

Figure 4-147 Convergence Point Array –
S90 W620 – Roof to Floor

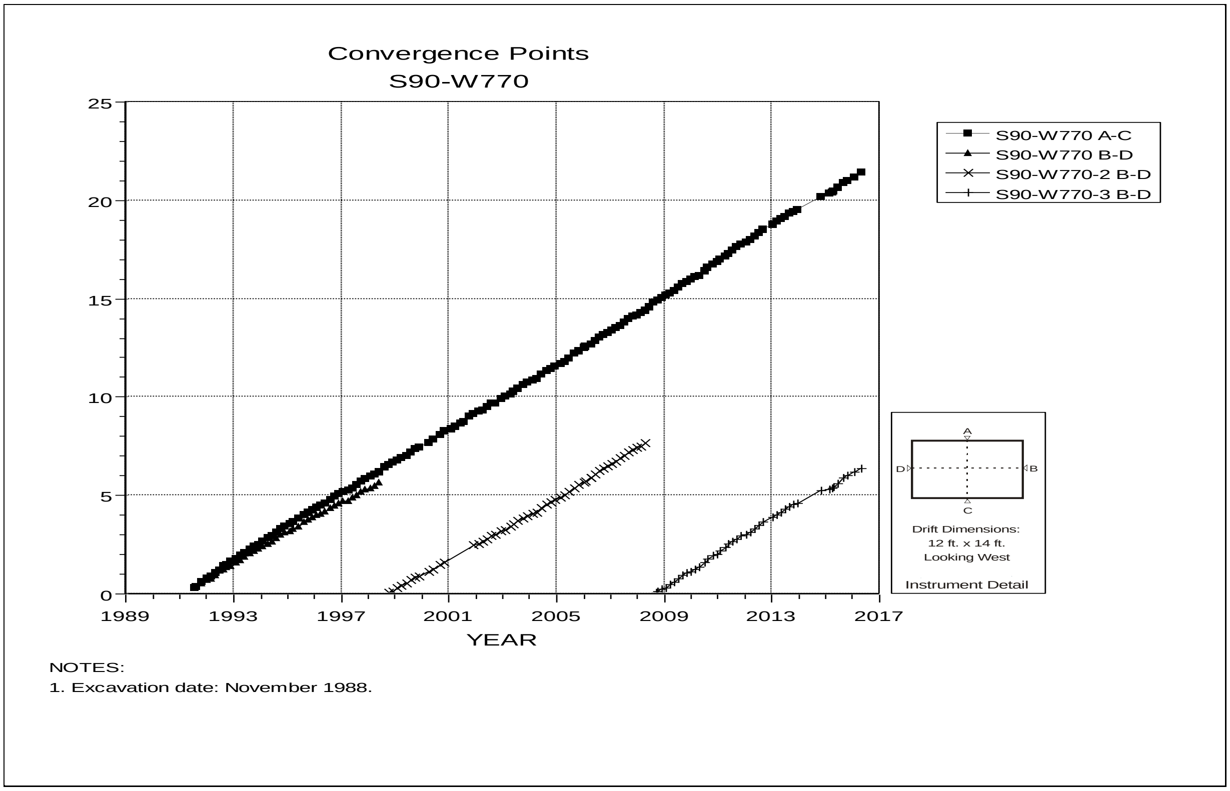

Figure 4-148 Convergence Point Array –
S90 W770 – All Chords

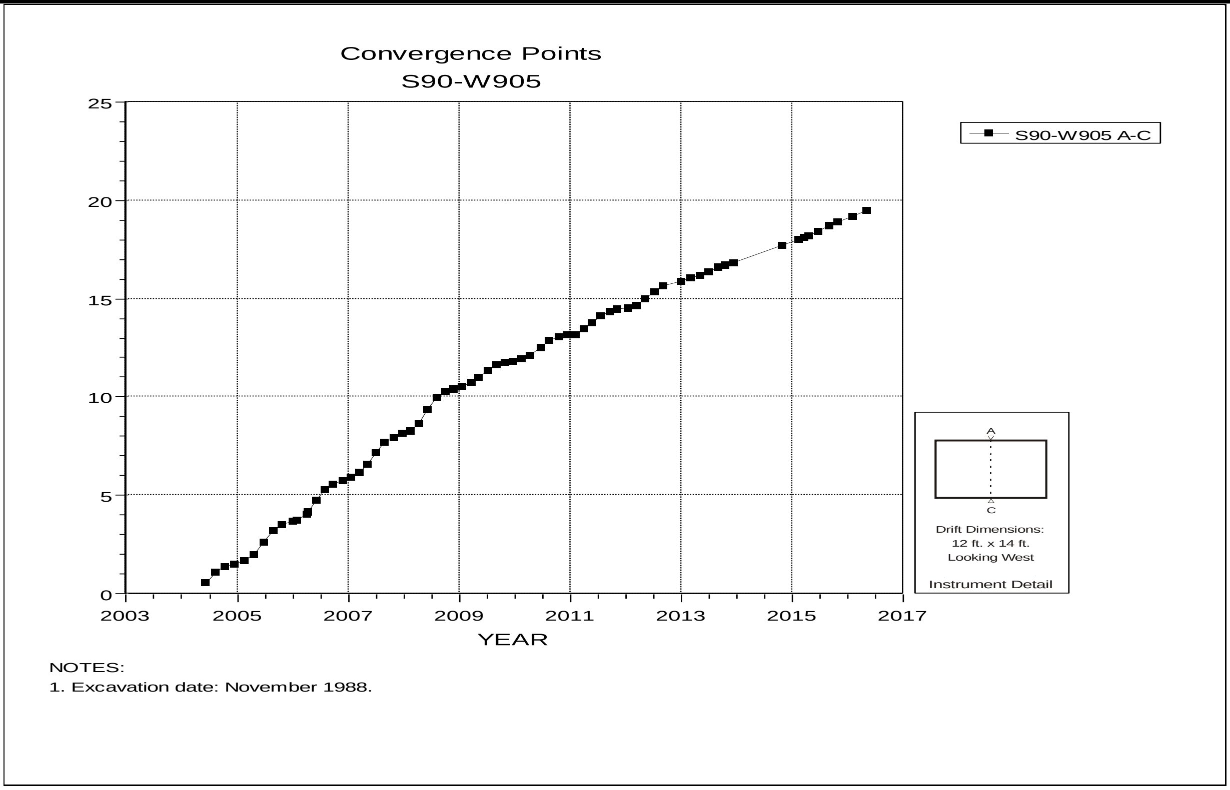

Figure 4-149 Convergence Point Array –
S90 W905 – Roof to Floor

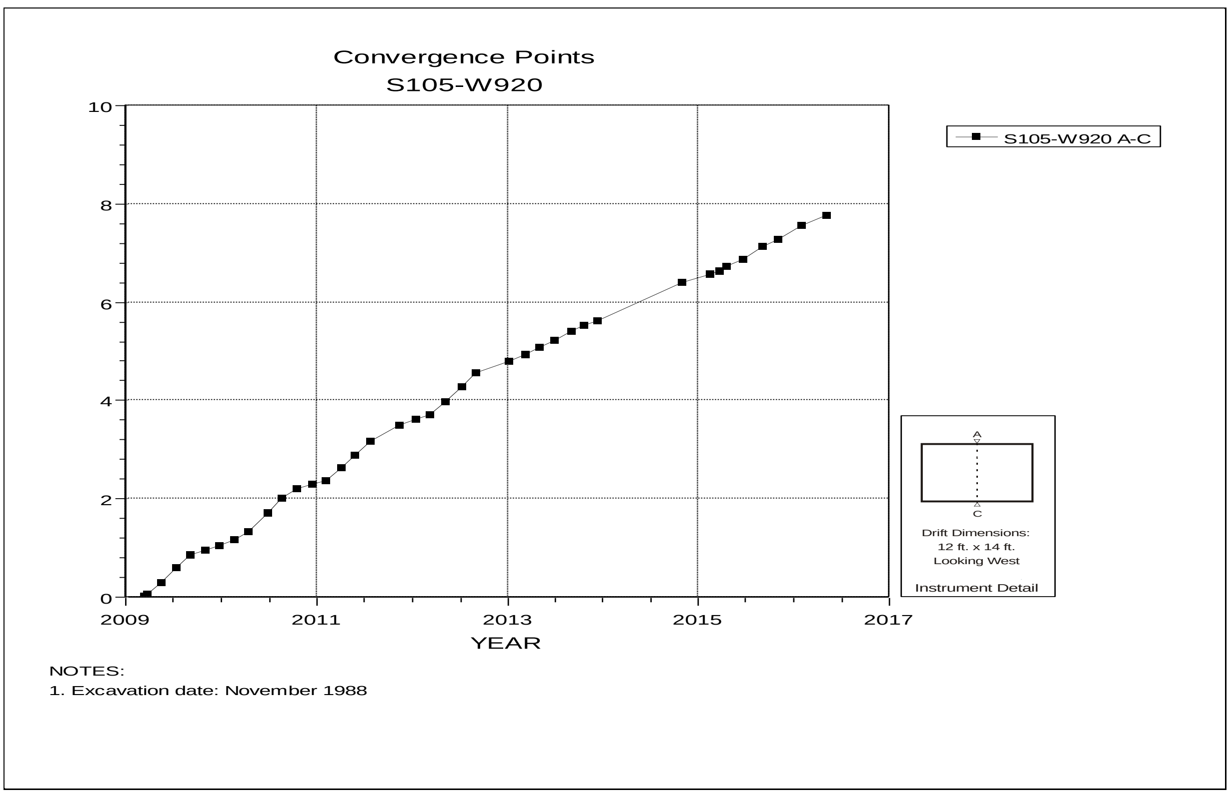

Figure 4-150 Convergence Point Array –
S105 W920 – Roof to Floor

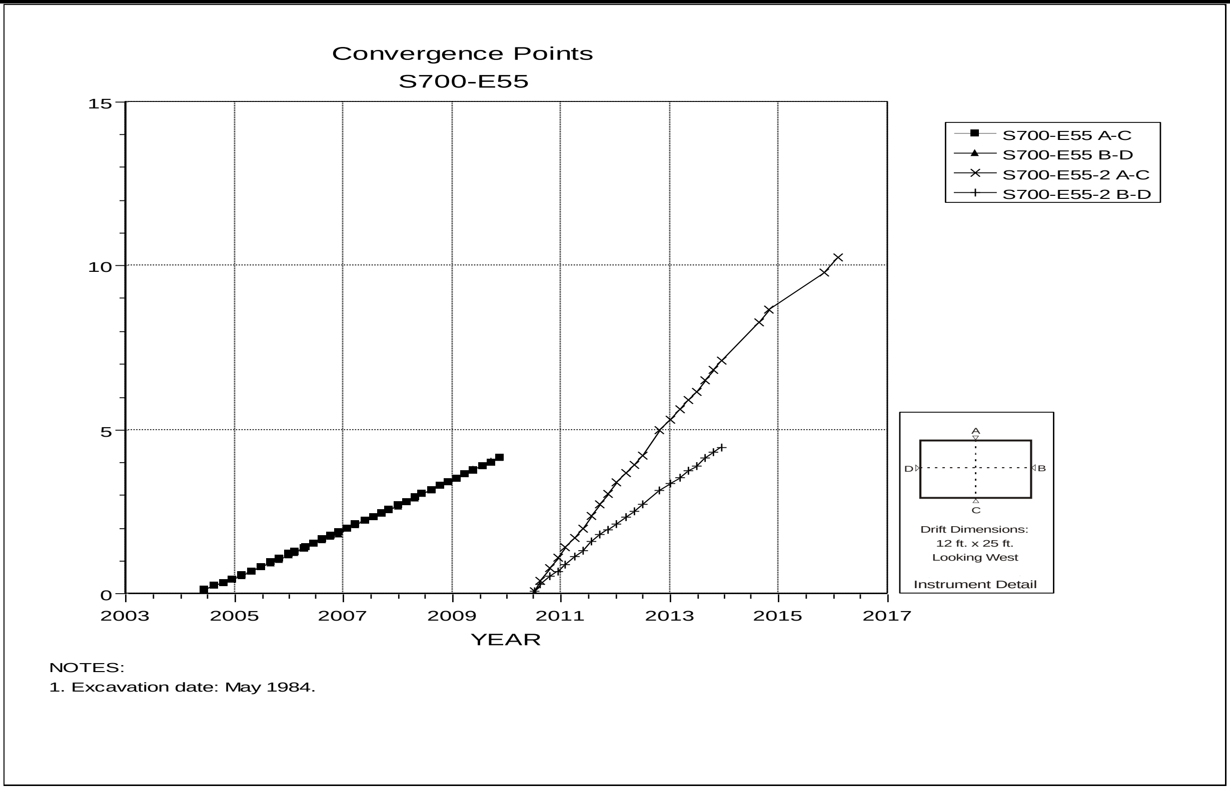

Figure 4-151. Convergence Point Array –
S700 E55 – All Chords

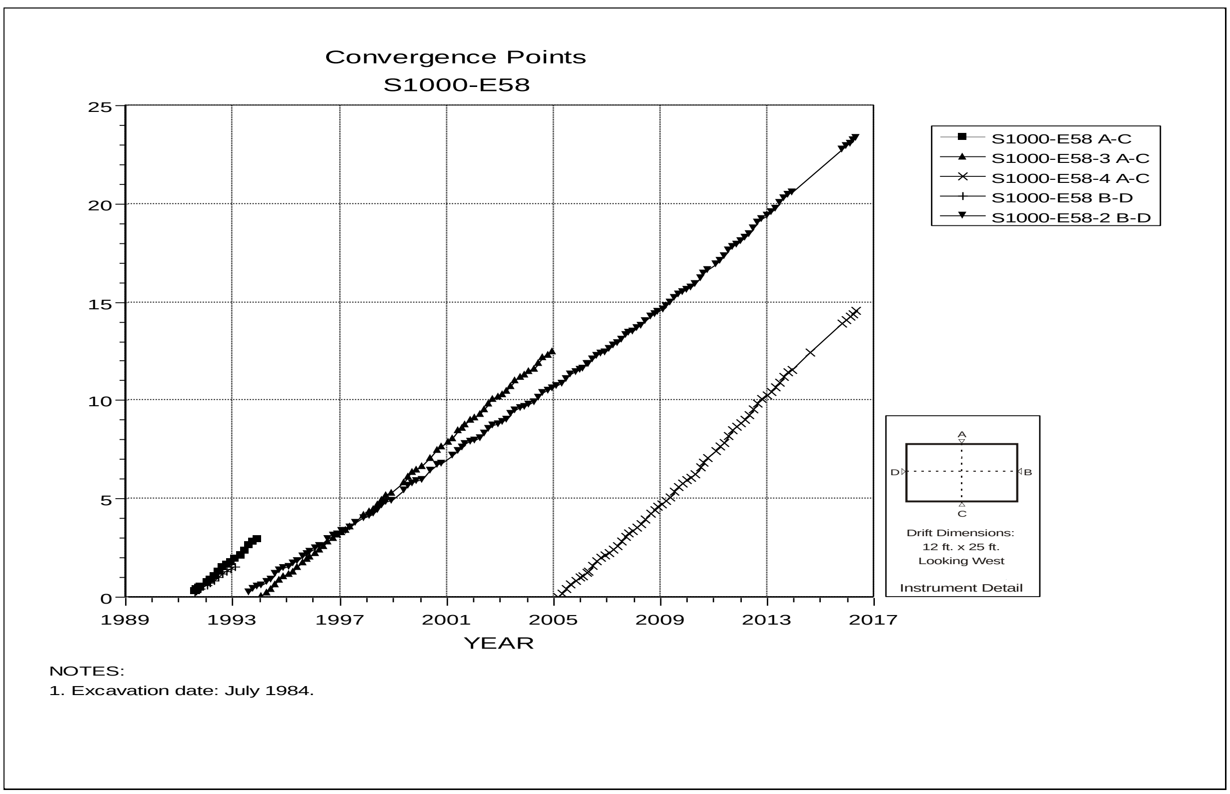

Figure 4-152 Convergence Point Array –
S1000 E58 – All Chords

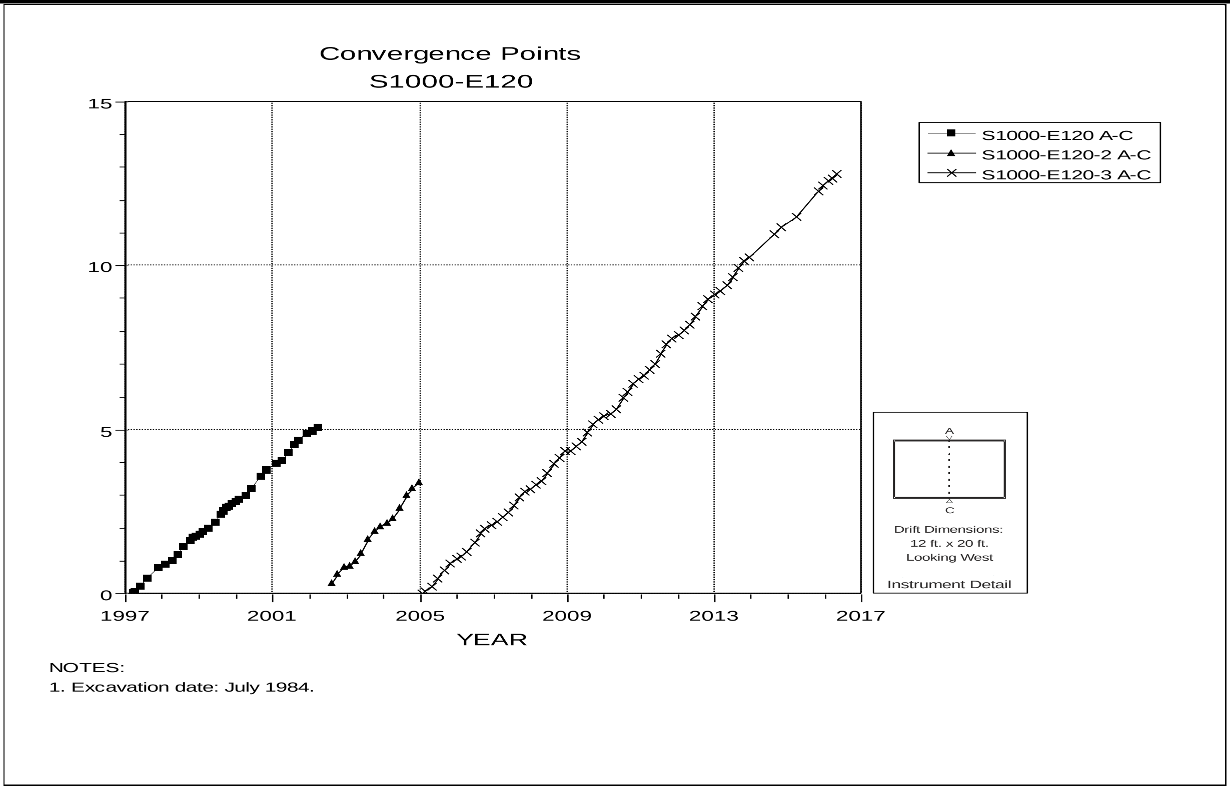

Figure 4-153 Convergence Point Array –
S1000 E120 – Roof to Floor

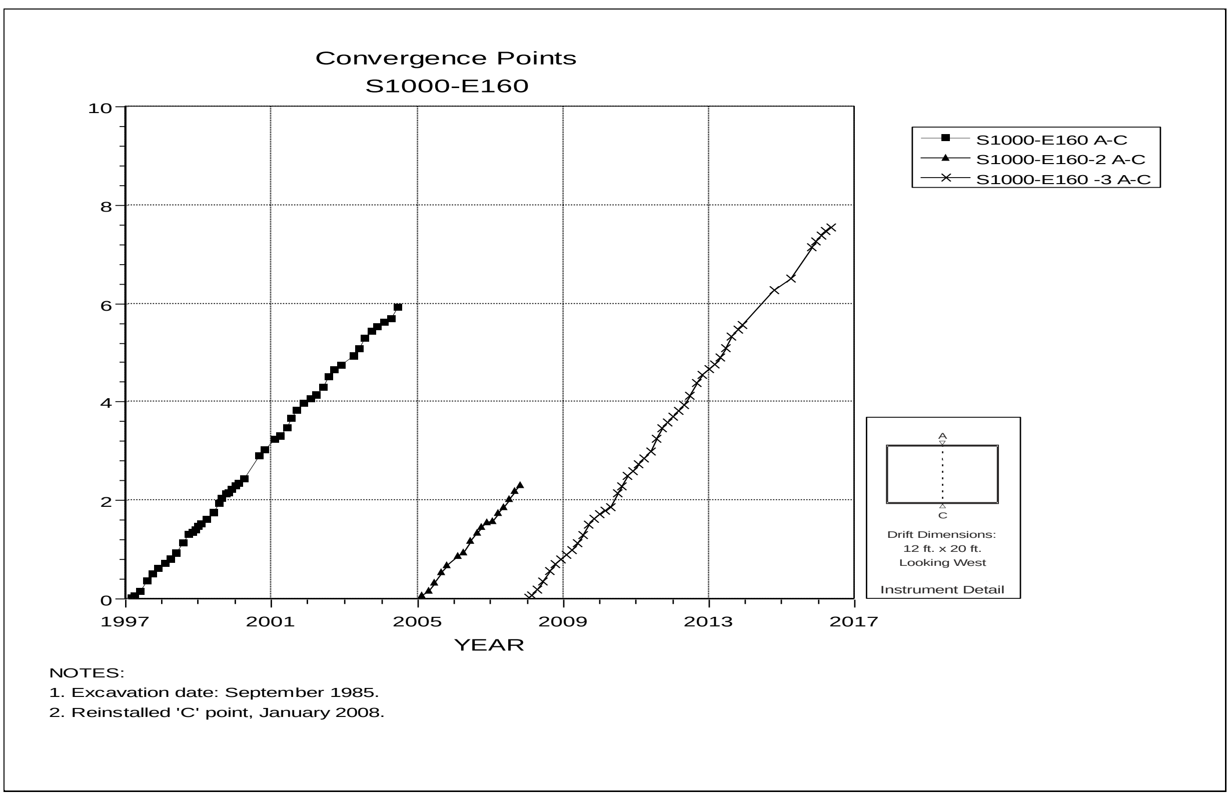

Figure 4-154 Convergence Point Array –
S1000 E160 – Roof to Floor

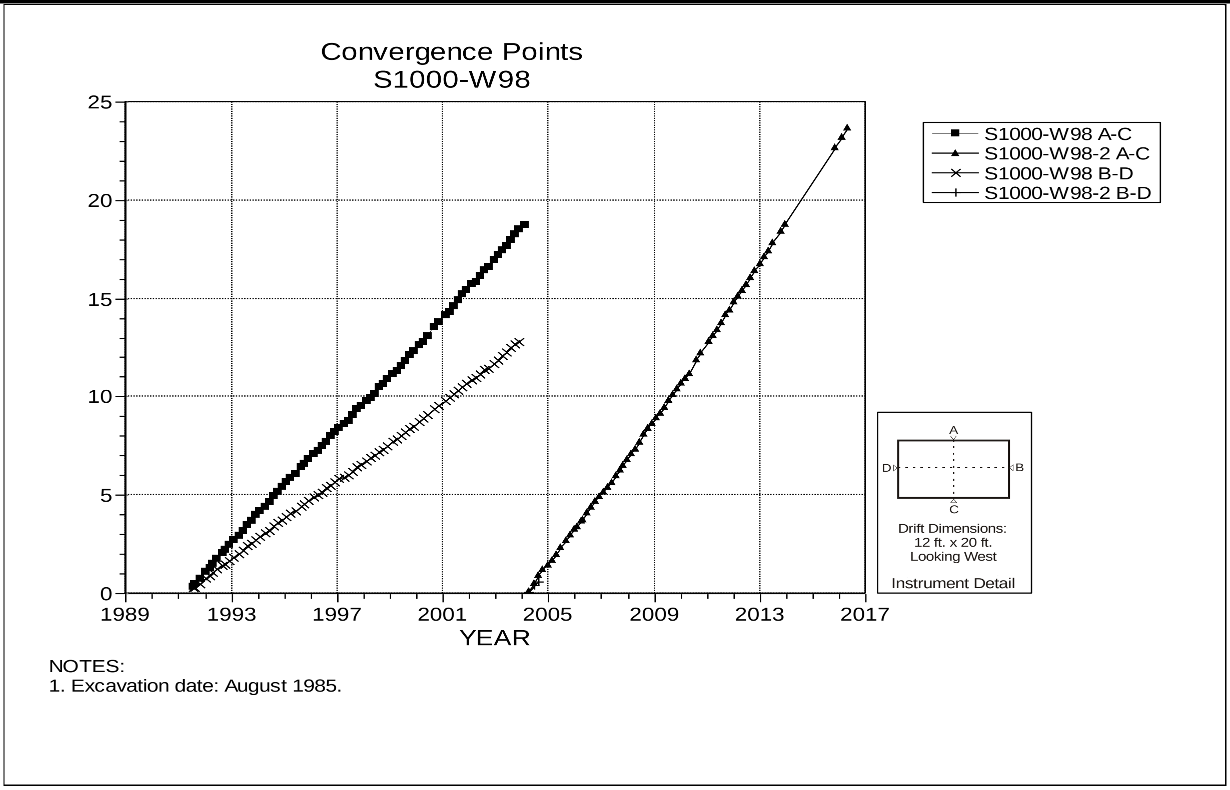

Figure 4-155 Convergence Point Array –
S1000 W98 – Roof to Floor

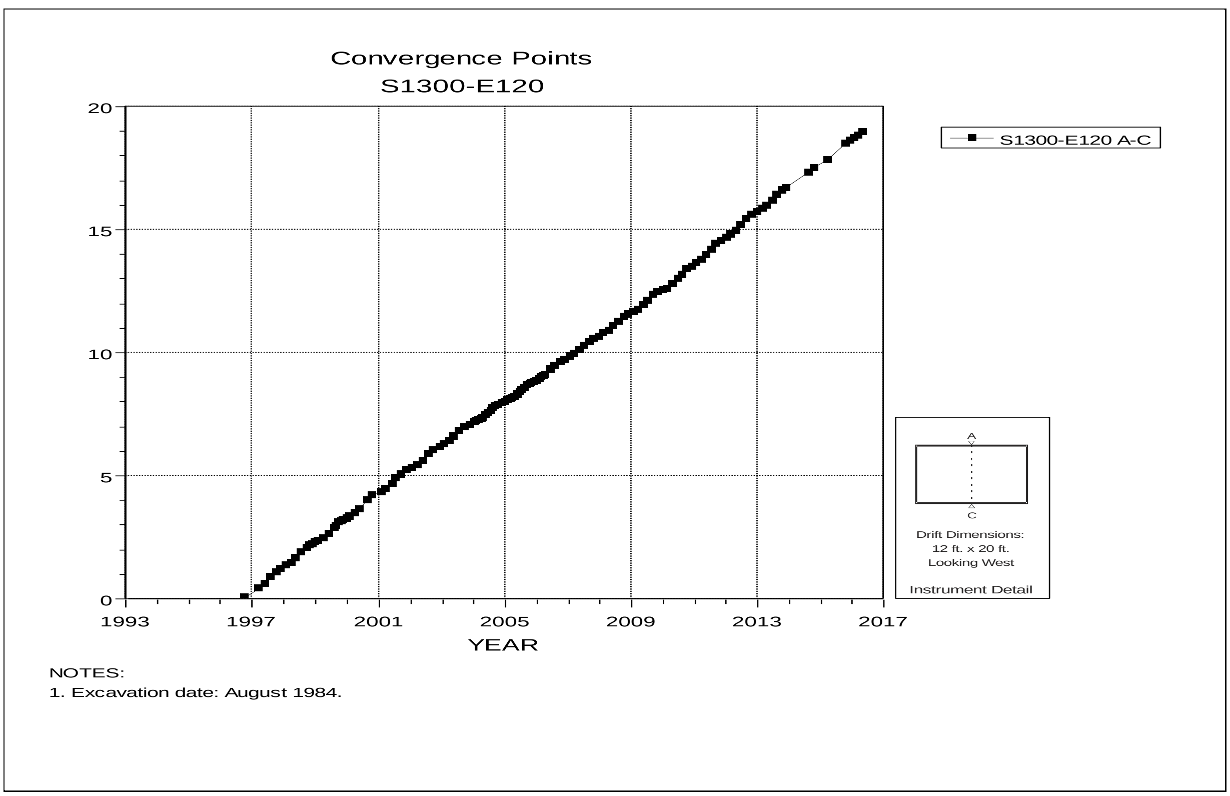

Figure 4-156 Convergence Point Array –
S1300 E120 – Roof to Floor

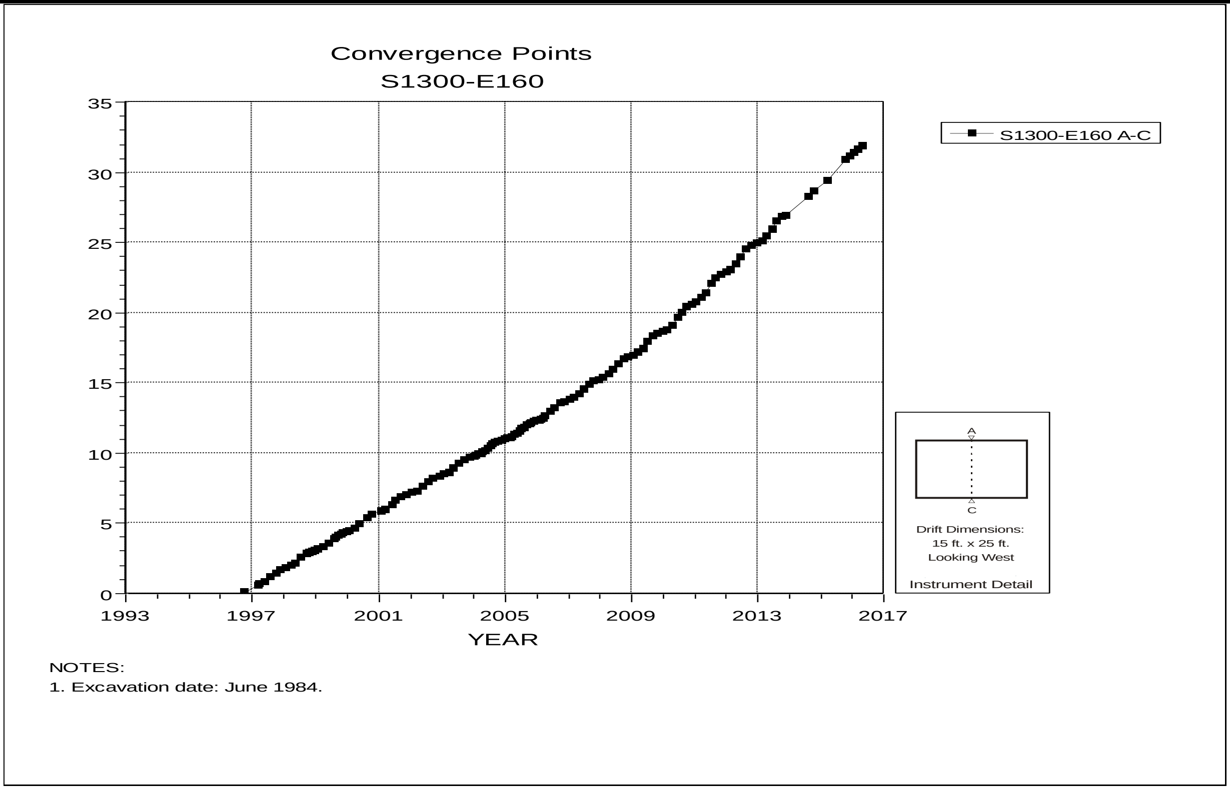

Figure 4-157 Convergence Point Array –
S1300 E160 – Roof to Floor

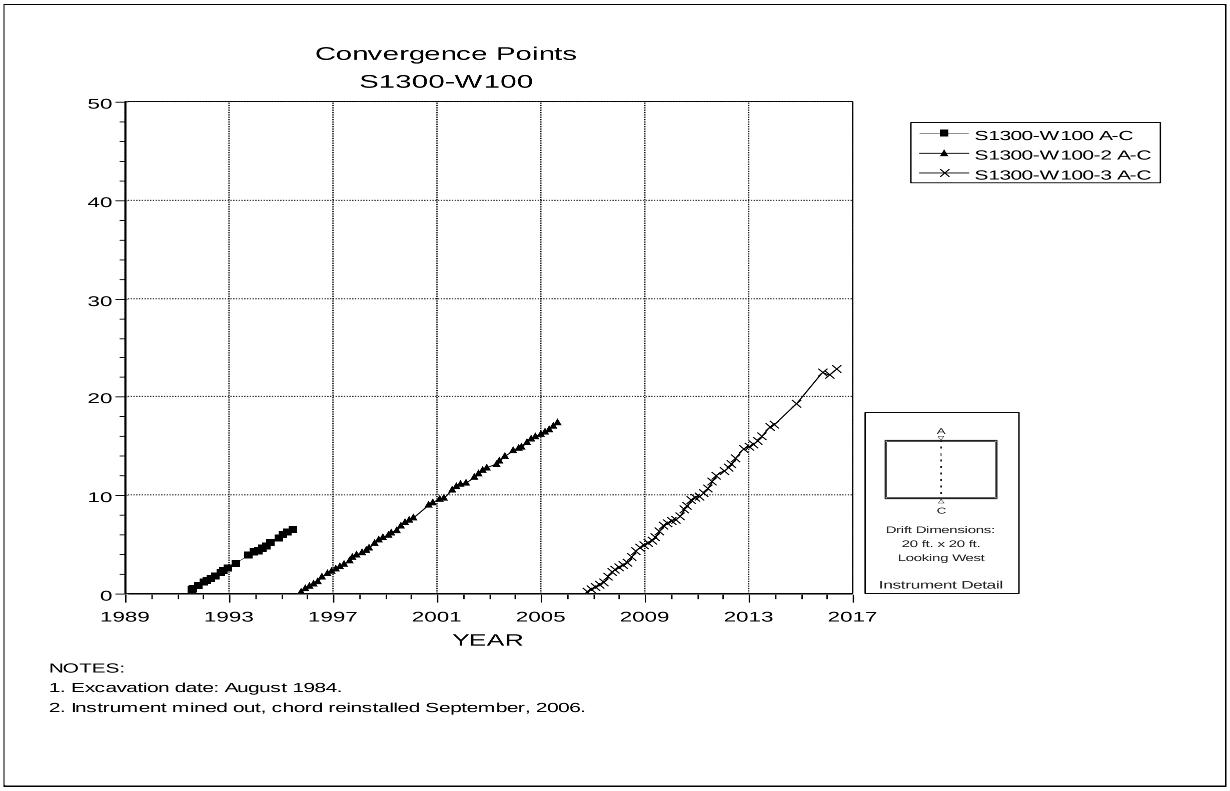

Figure 4-158 Convergence Point Array –
S1300 W100 – Roof to Floor

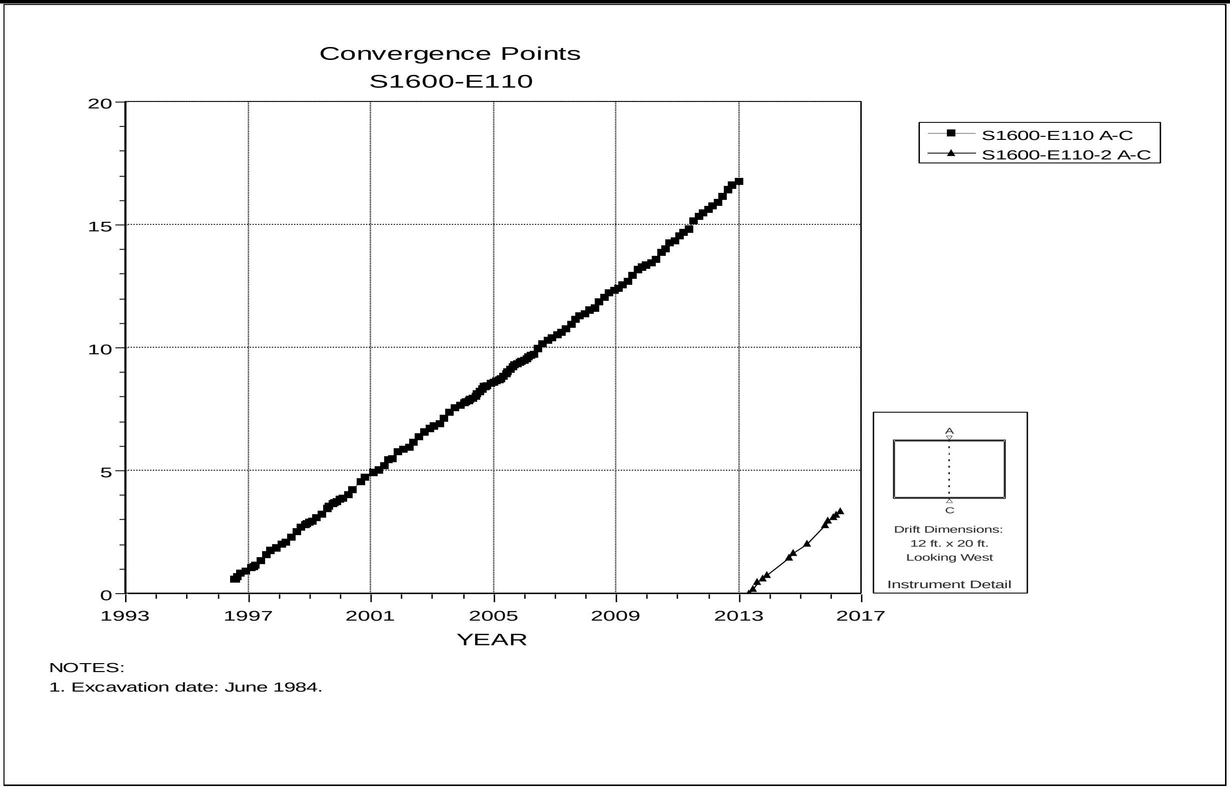

Figure 4-159 Convergence Point Array –
S1600 E110 – Roof to Floor

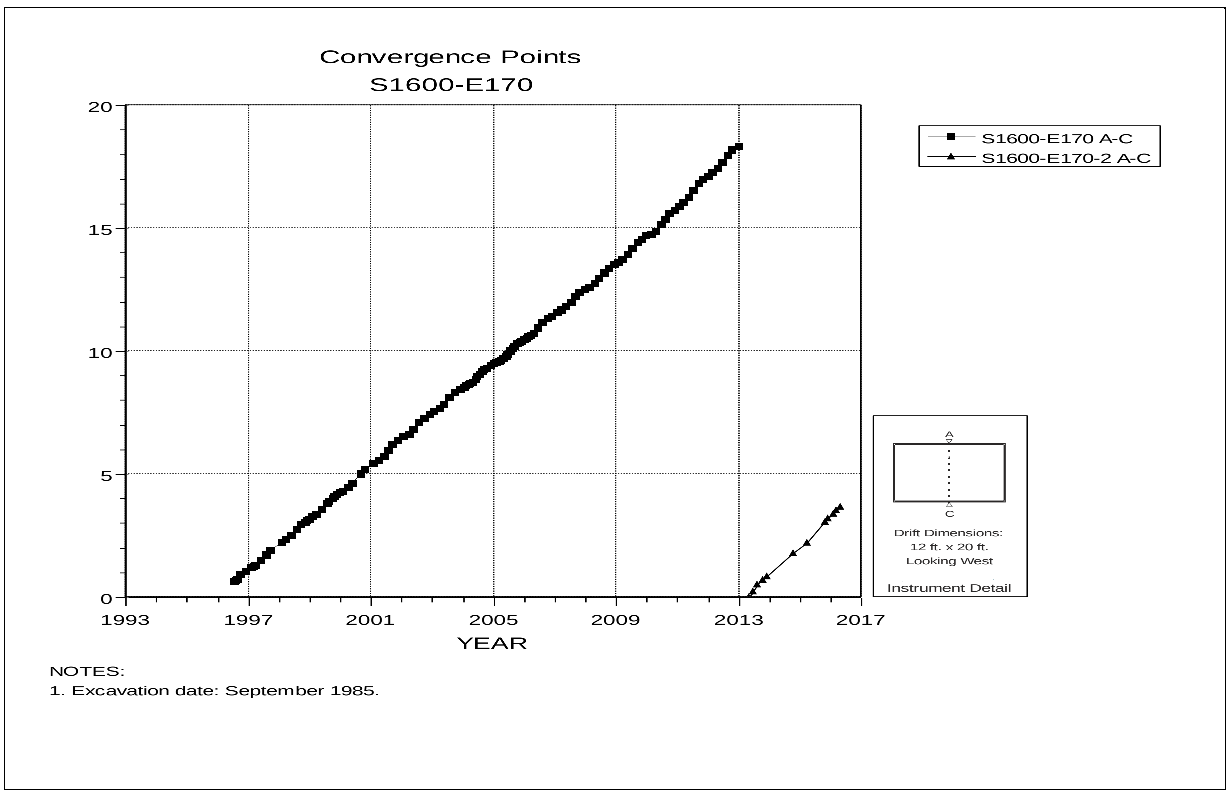

Figure 4-160 Convergence Point Array –
S1600 E170 – Roof to Floor

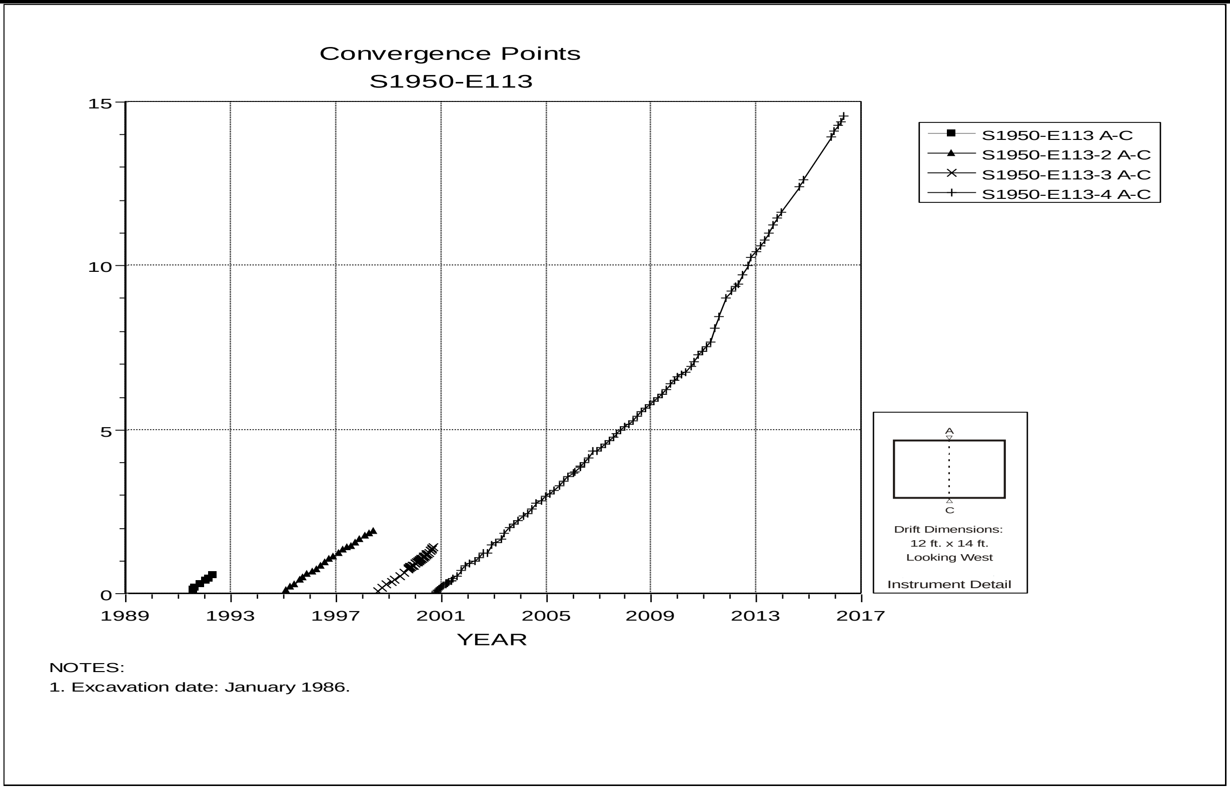

Figure 4-161 Convergence Point Array –
S1950 E113 – Roof to Floor

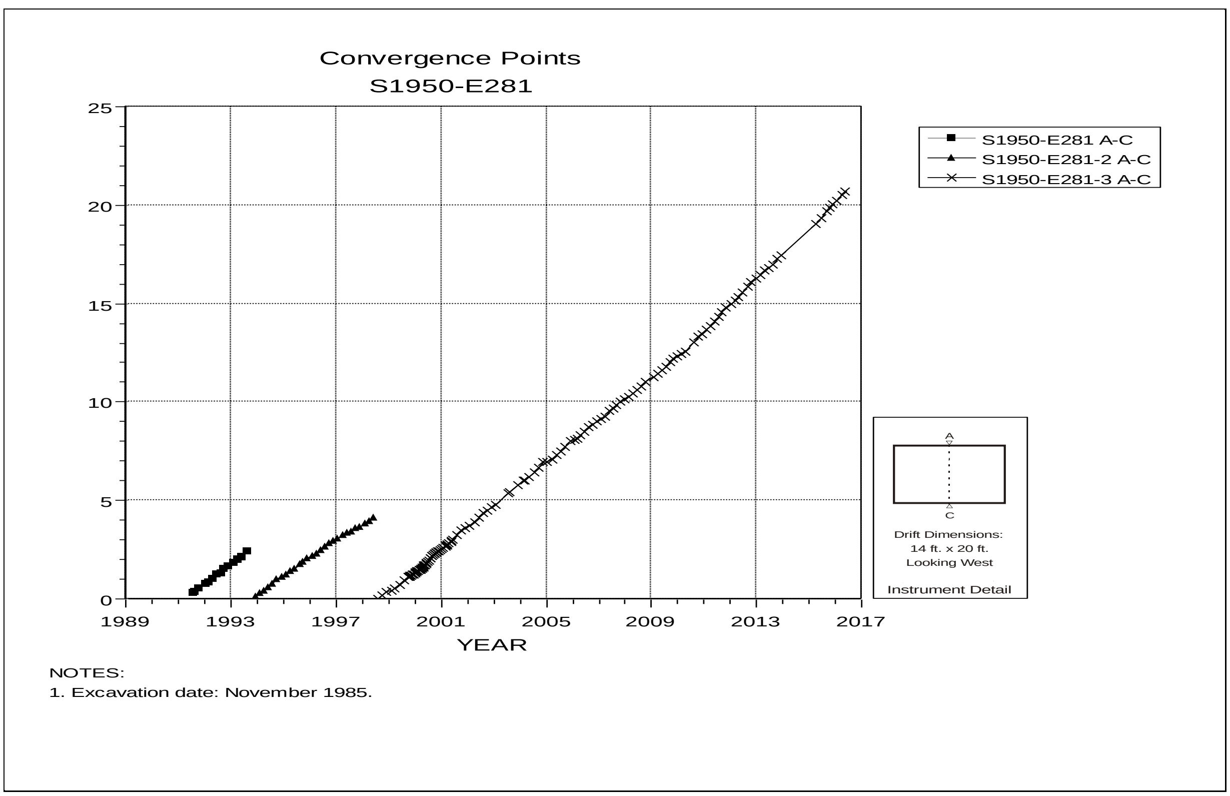

Figure 4-162 Convergence Point Array –
S1950 E281 – Roof to Floor Floor

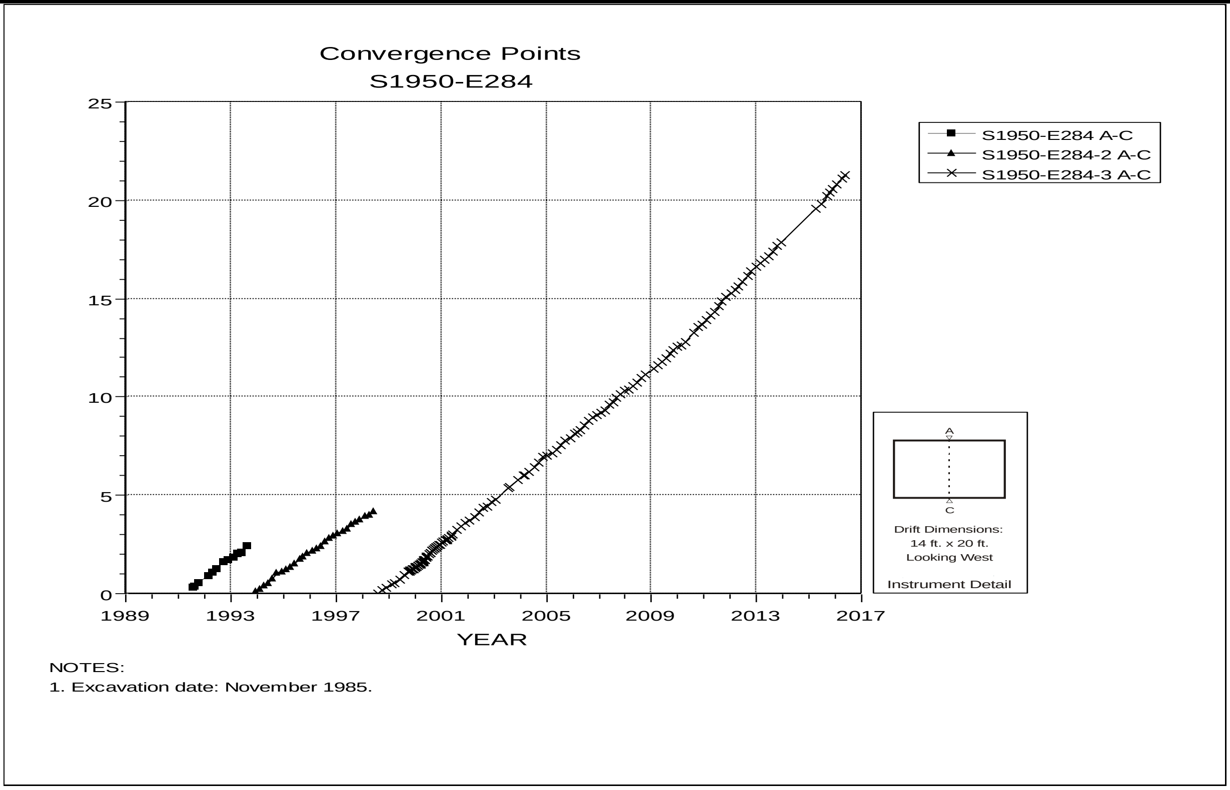

Figure 4-163 Convergence Point Array –
S1950 E284 – Roof to Floor

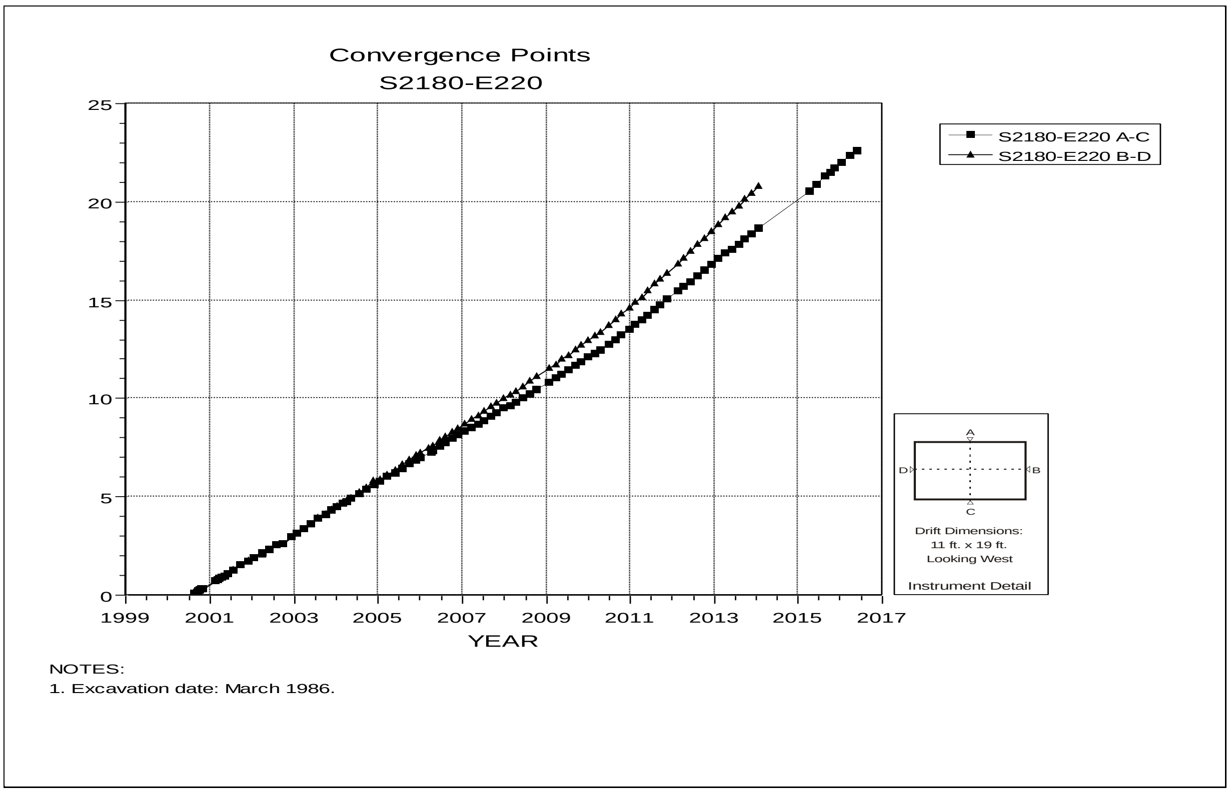

Figure 4-164 Convergence Point Array –
S2180 E220 – All Chords

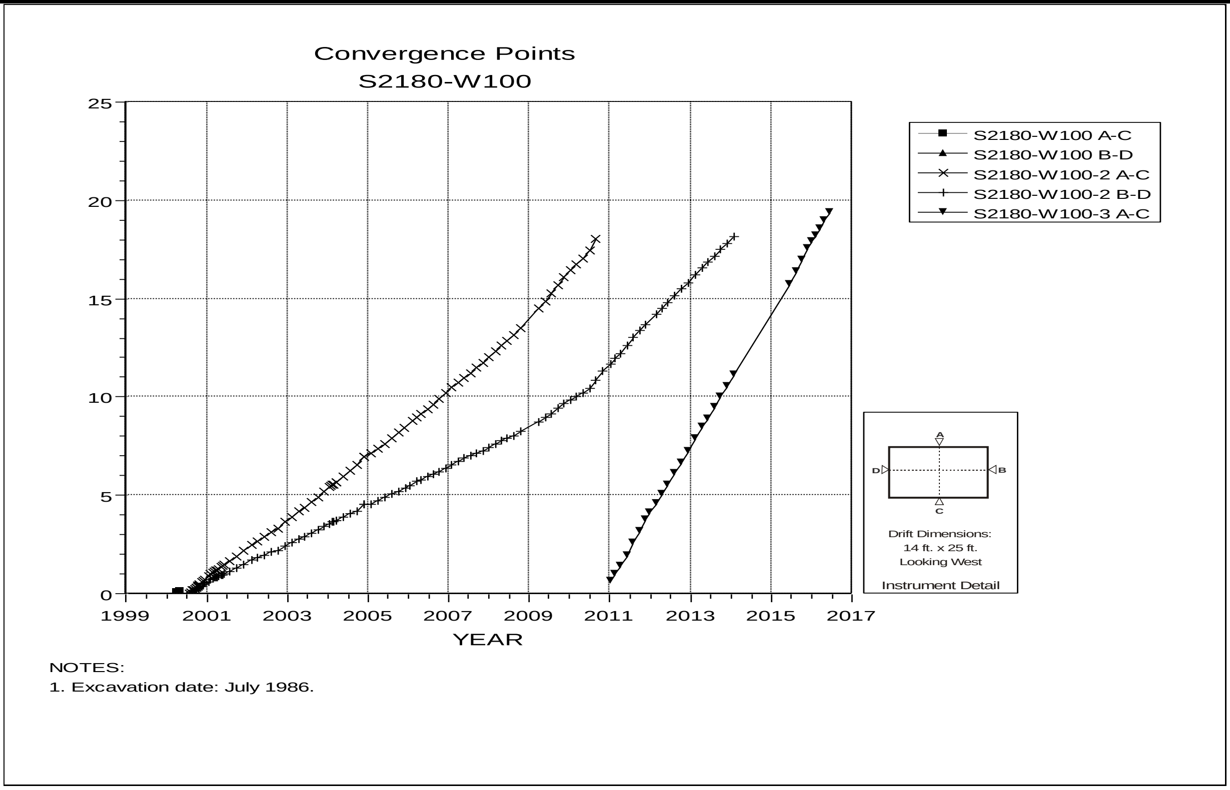

Figure 4-165 Convergence Point Array –
S2180 W100 – All Chords

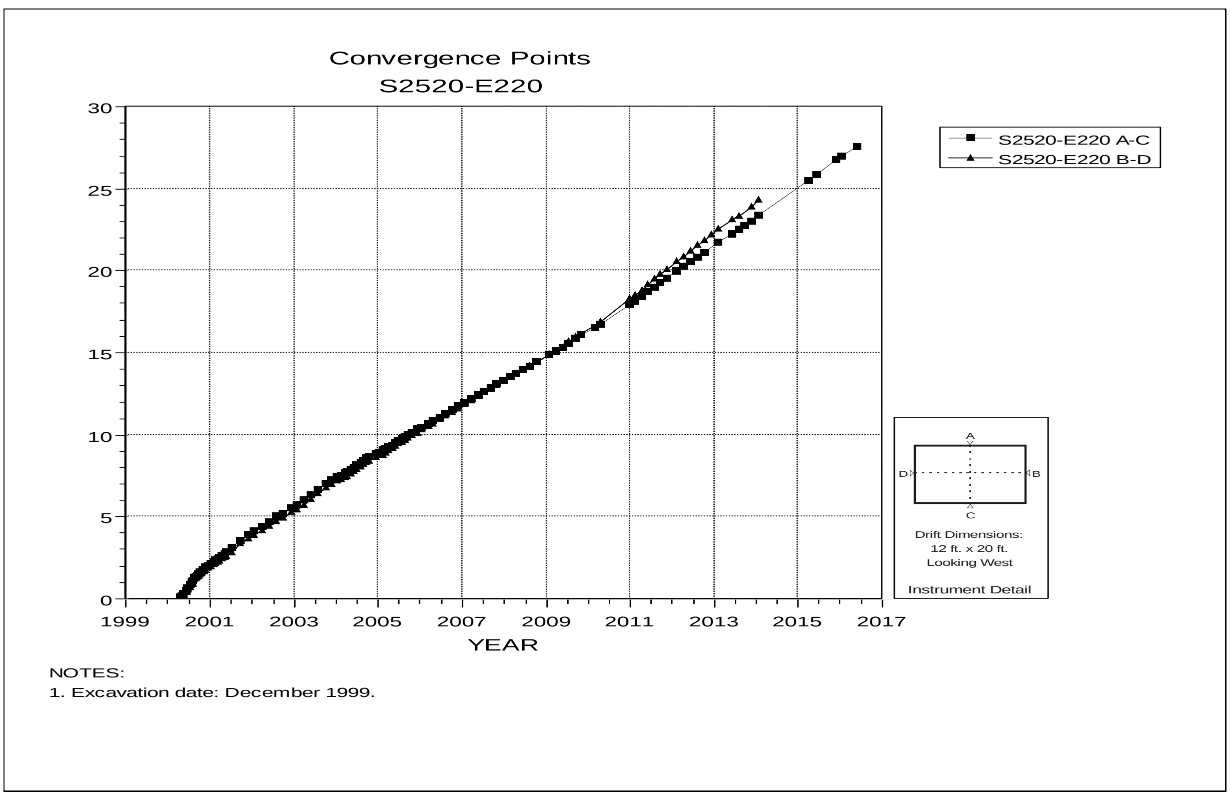

Figure 4-166 Convergence Point Array –
S2520 E220 – All Chords

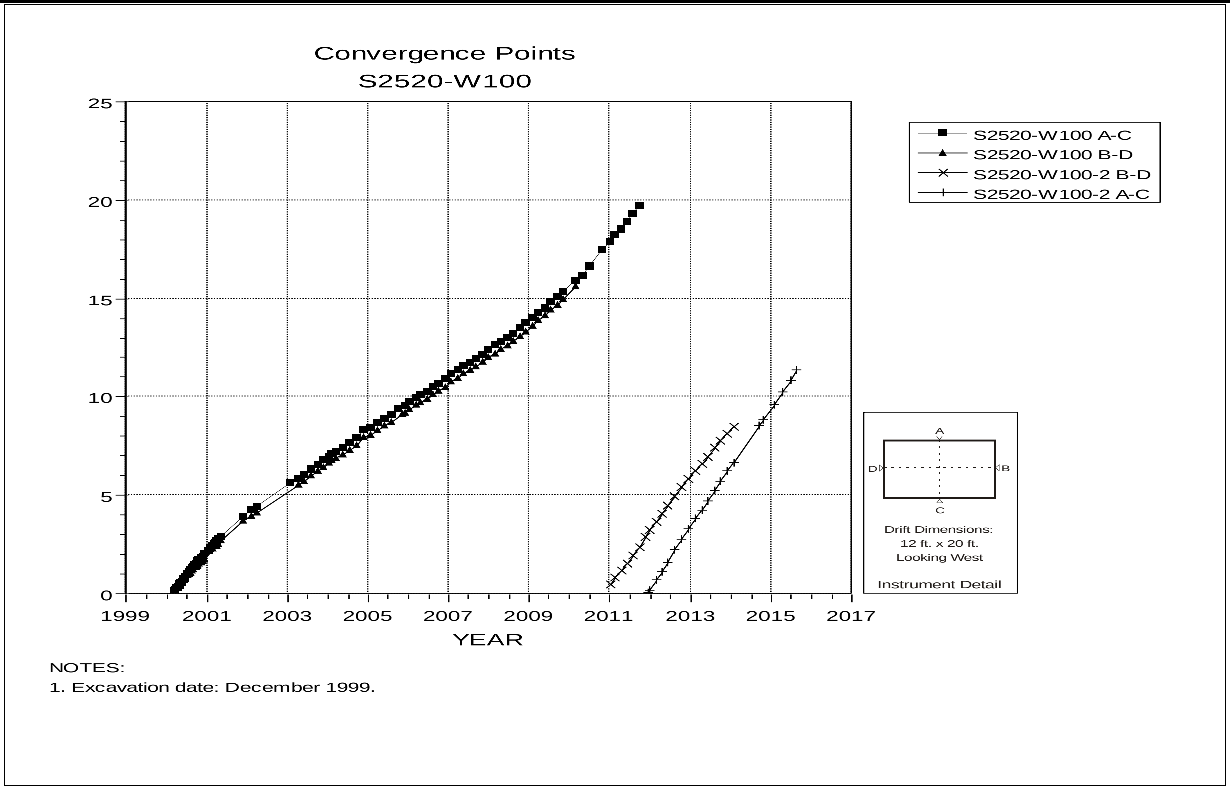

Figure 4-167 Convergence Point Array –
S2520 W100 – All Chords

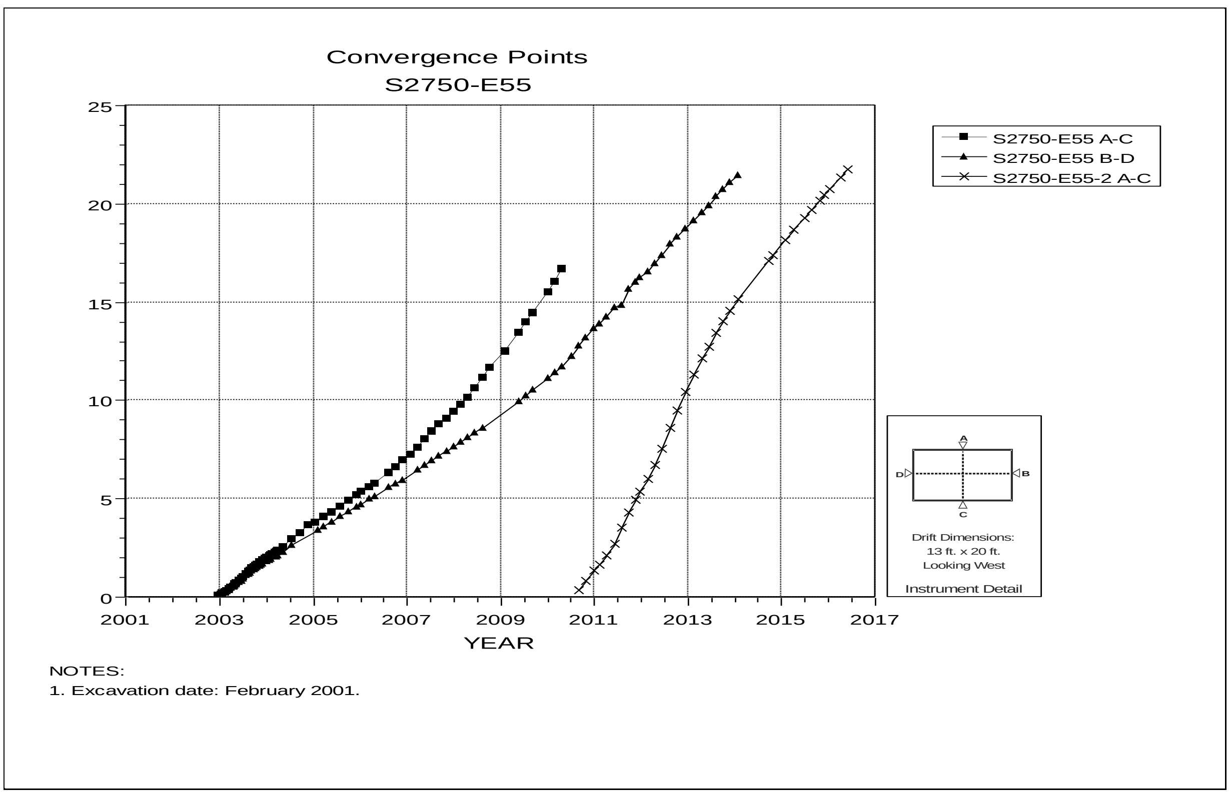

Figure 4-168 Convergence Point Array-
S2750 E55 – All Chords

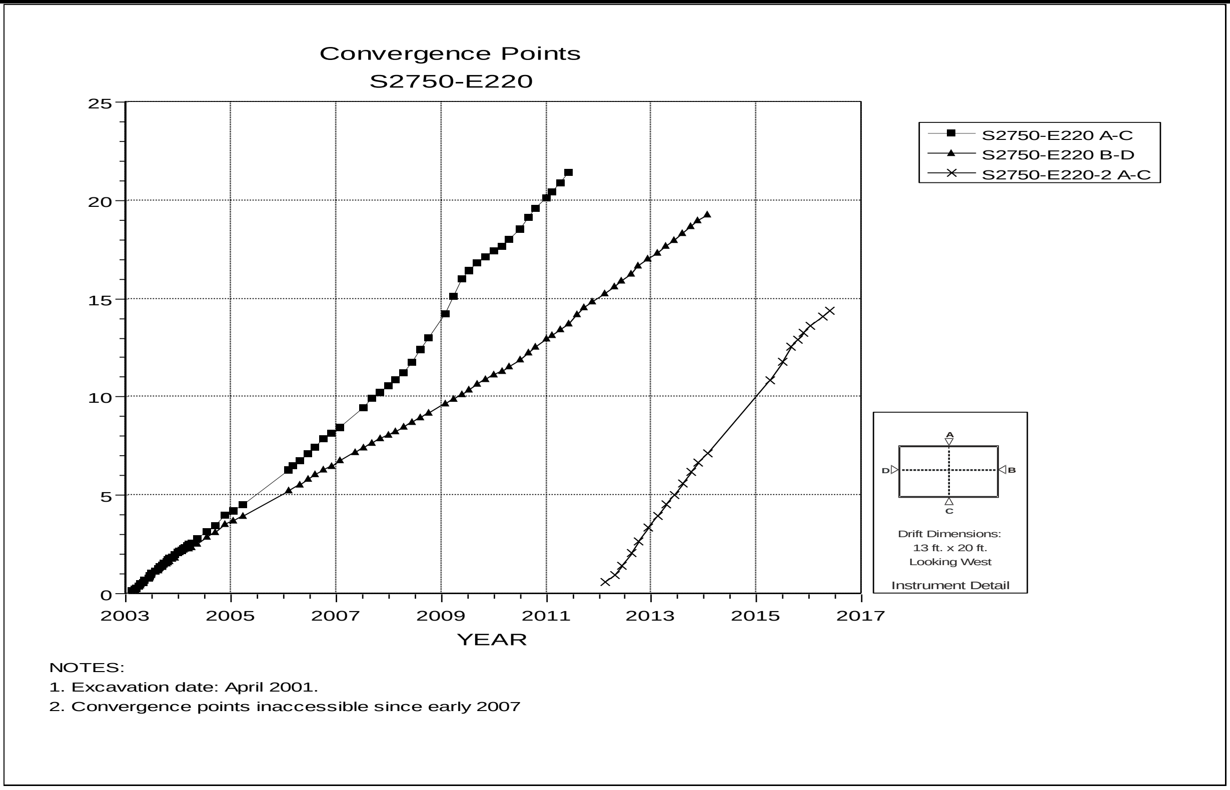

Figure 4-169 Convergence Point Array –
S2750 E220 – All Chords

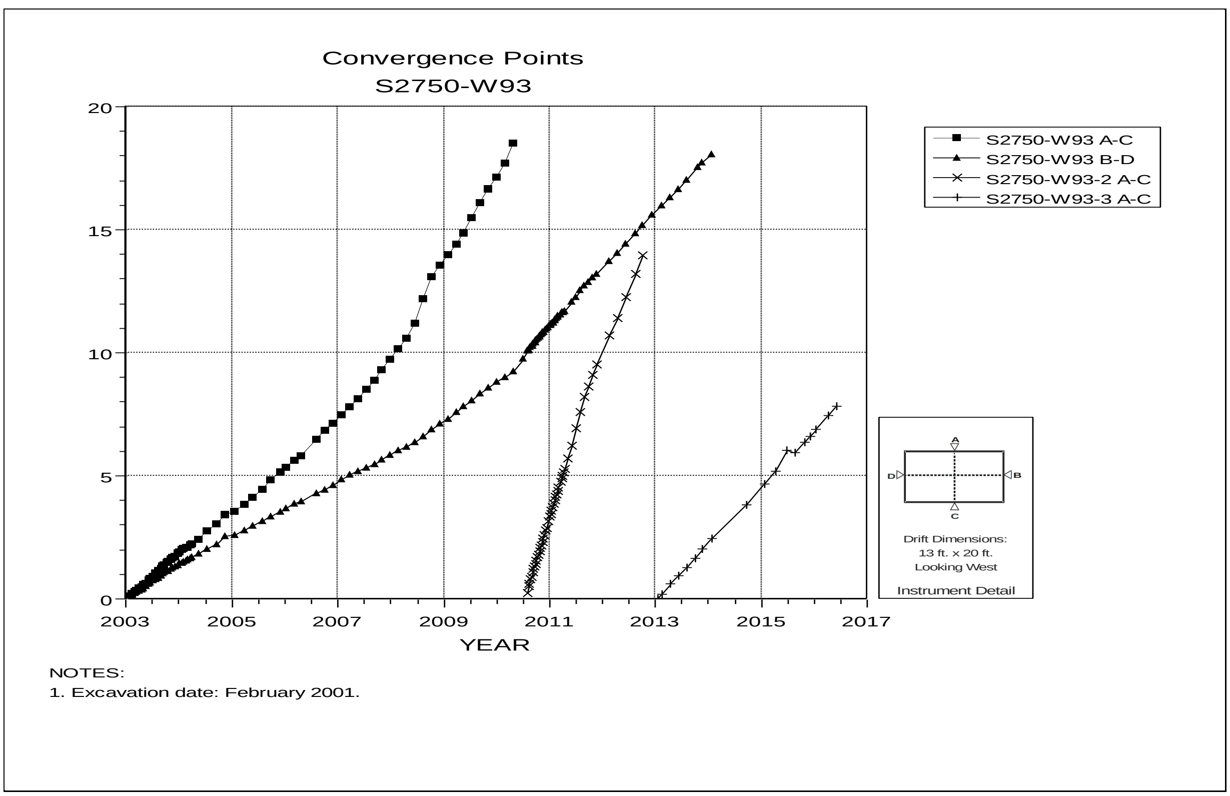

Figure 4-170 Convergence Point Array –
S2750 W93 – All Chords

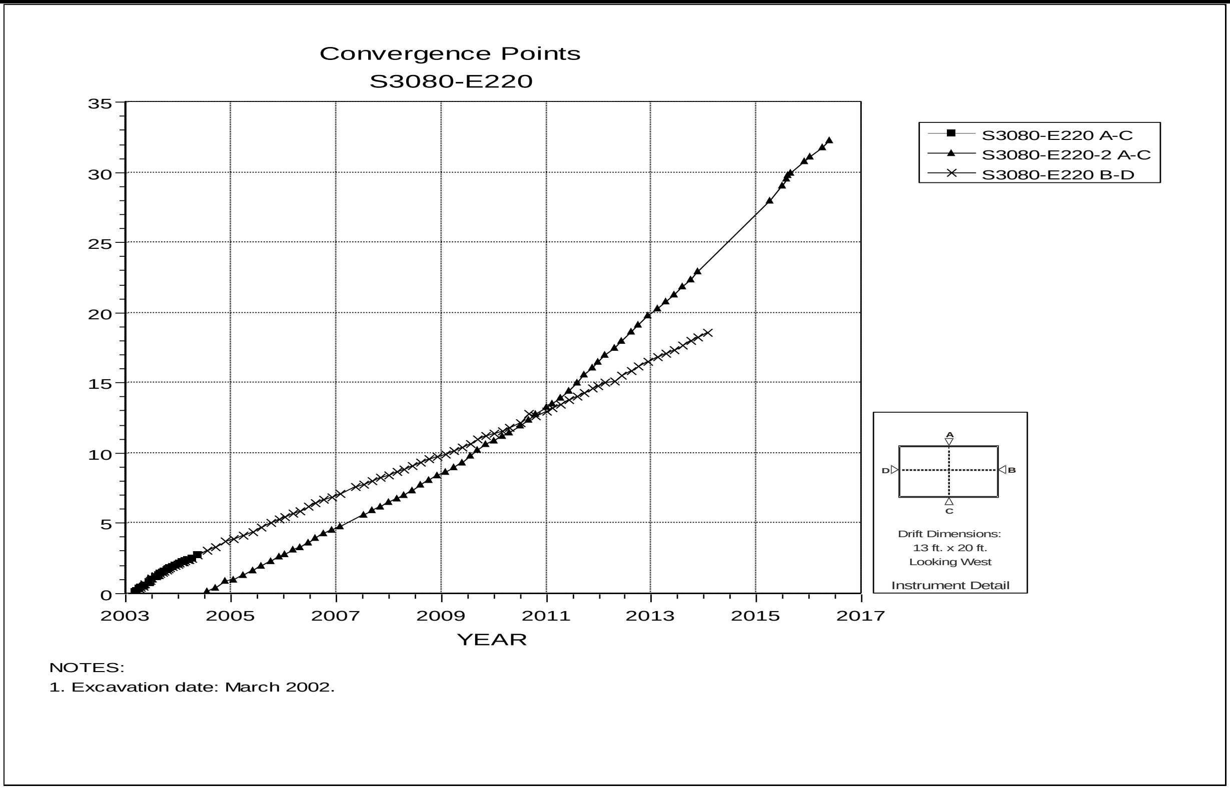

Figure 4-171 Convergence Point Array –
S3080 E220 – All Chords

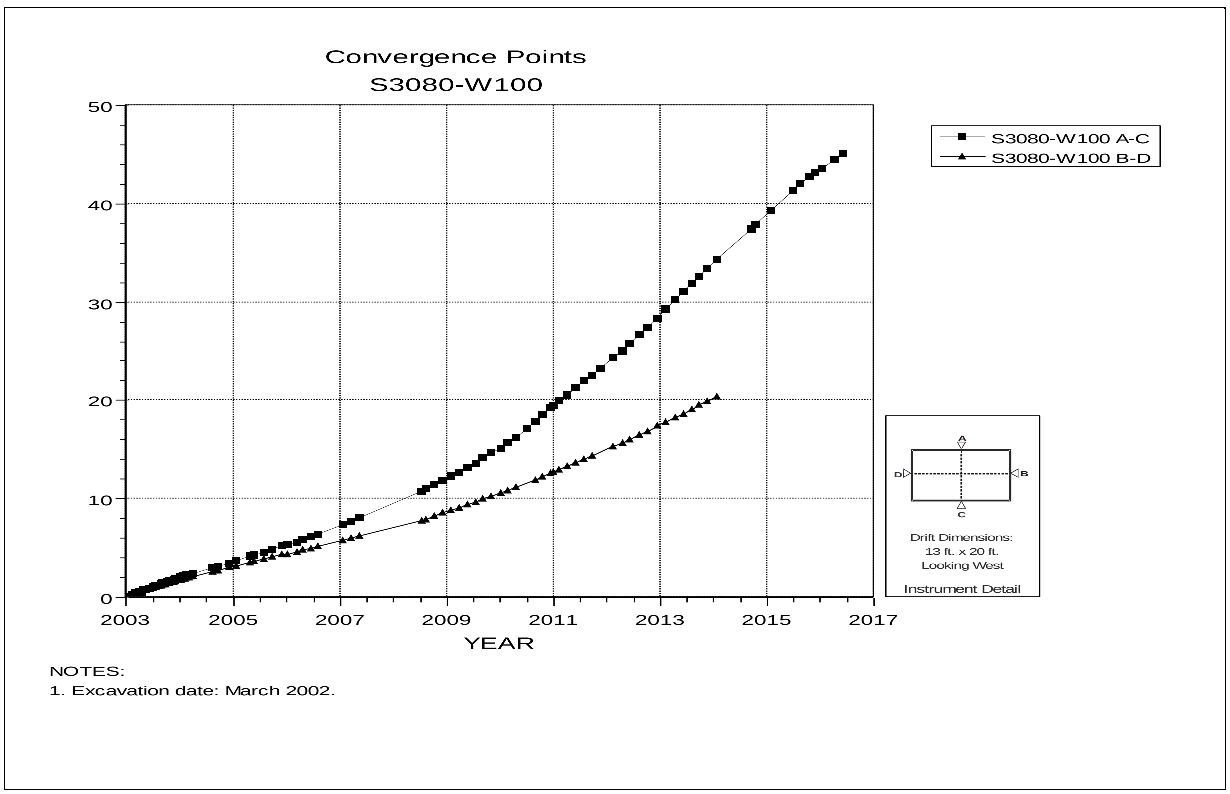

Figure 4-172 Convergence Point Array –
S3080 W100 – All Chords

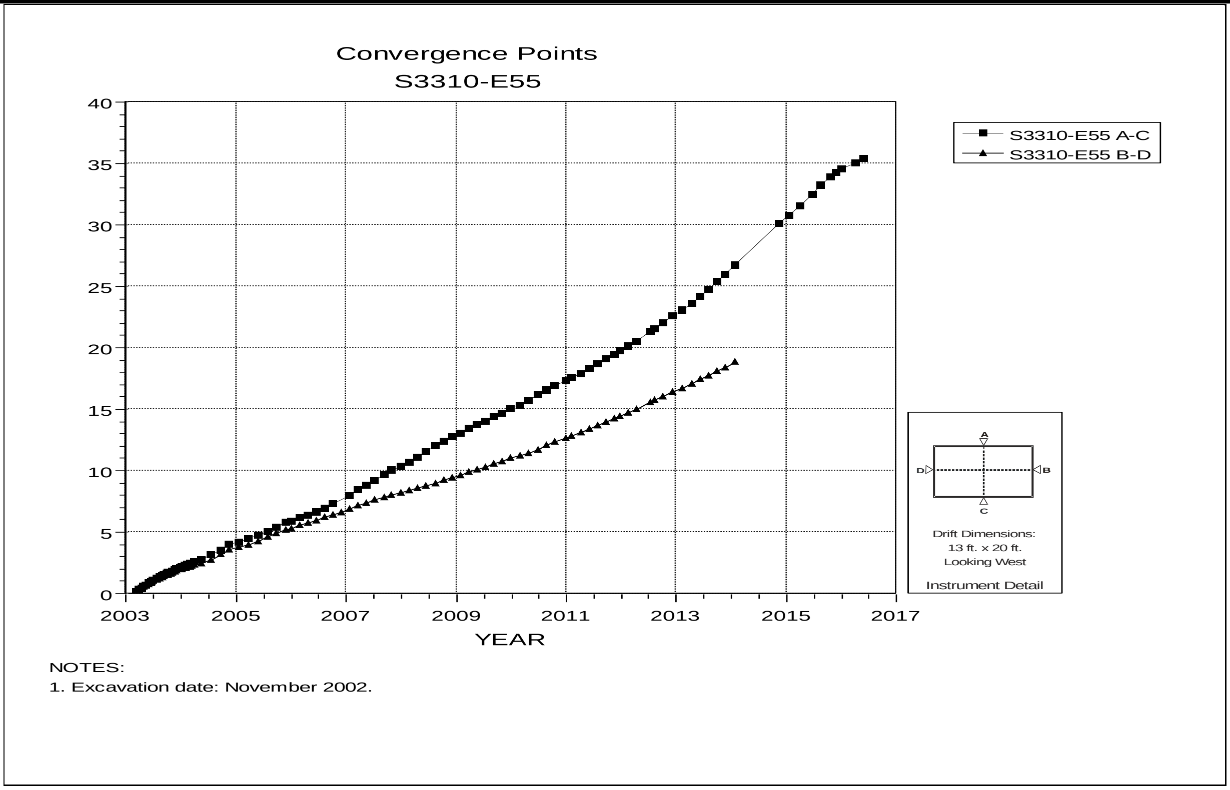

Figure 4-173 Convergence Point Array –
S3310 E55 – All Chords

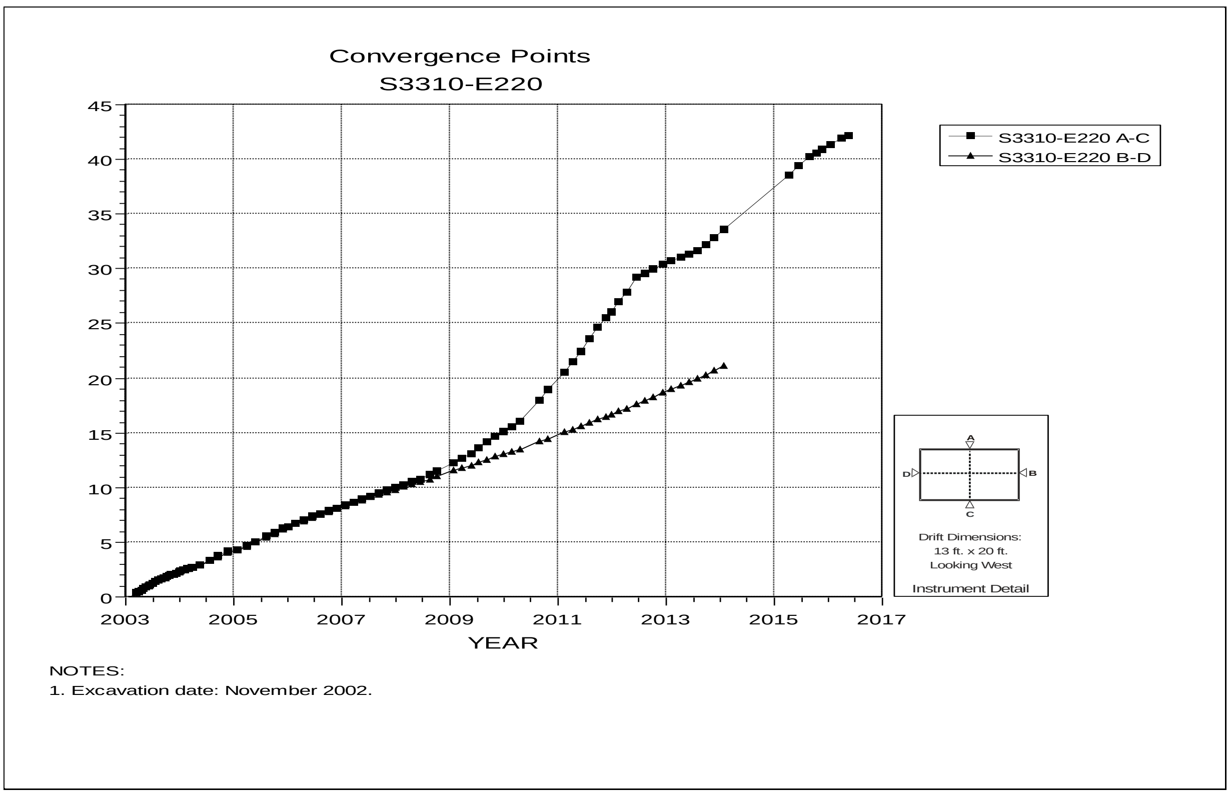

Figure 4-174 Convergence Point Array –
S3310 E220 – All Chords

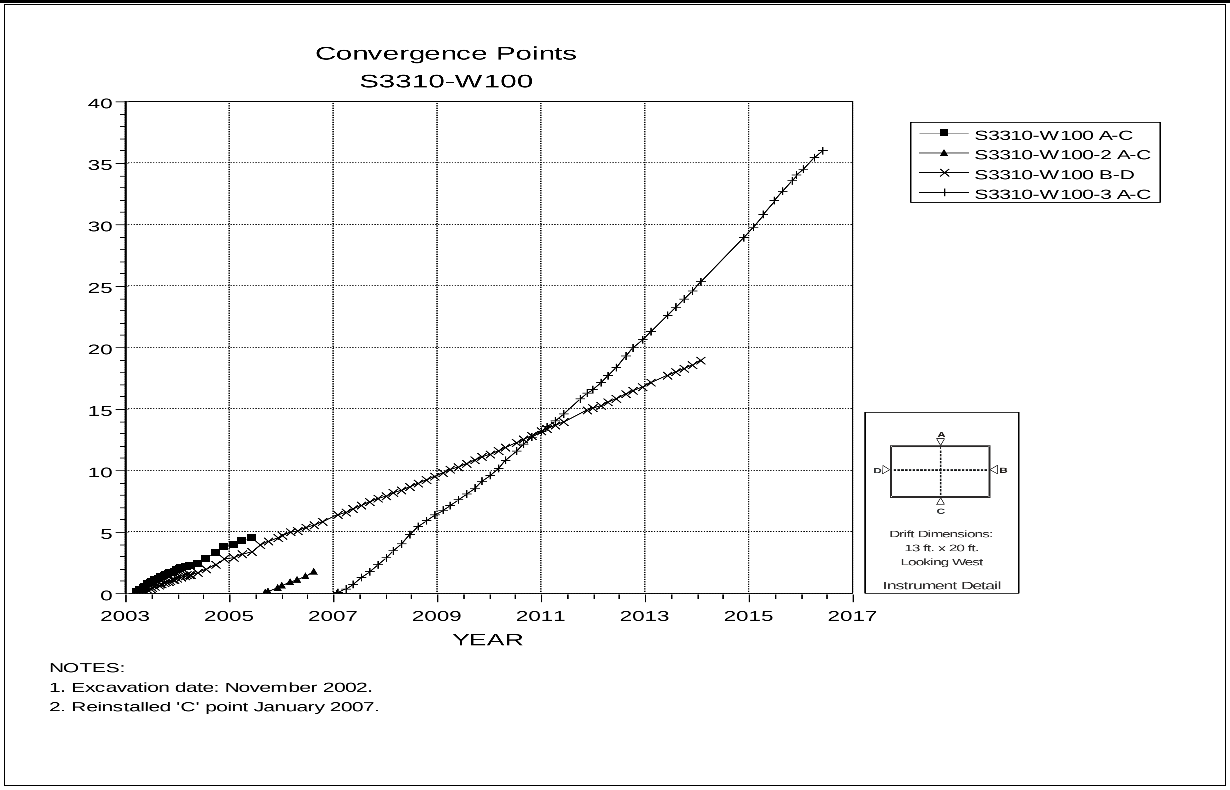

Figure 4-175 Convergence Point Array –
S3310 W100 – All Chords

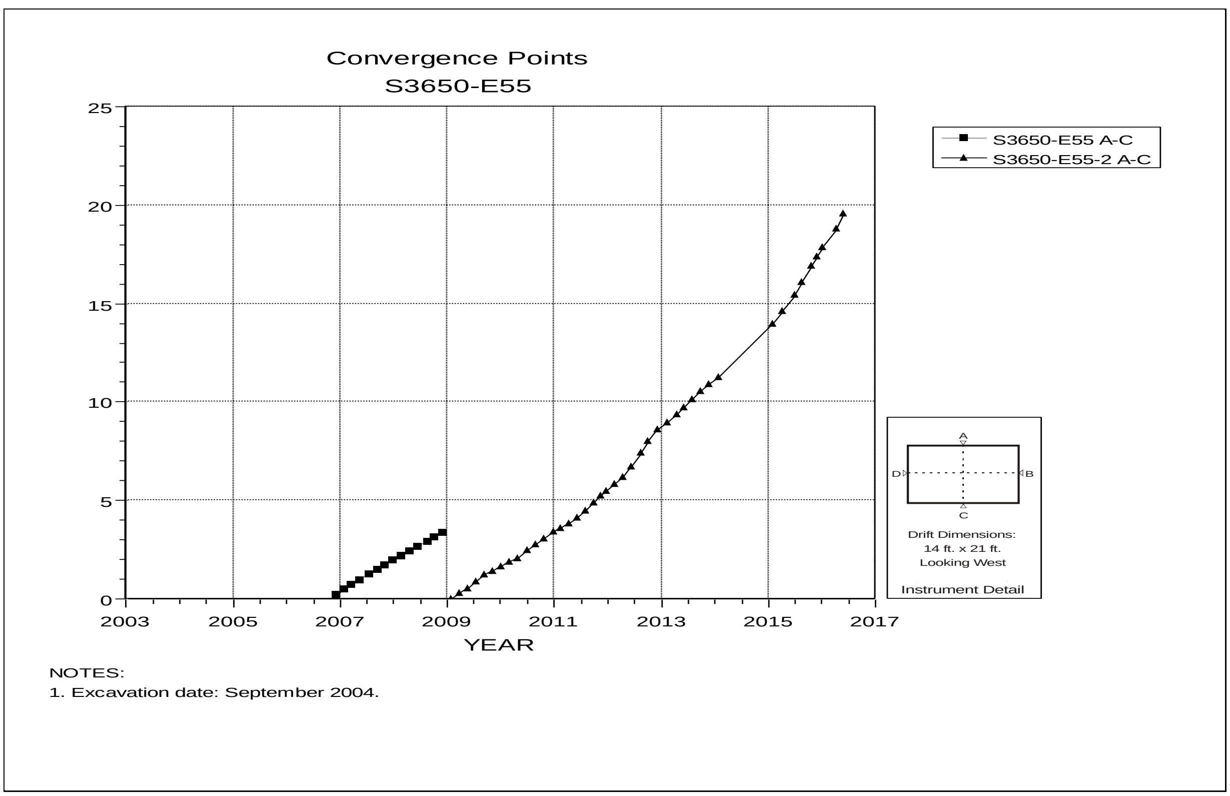

Figure 4-176 Convergence Point Array –
S3650 E55 – Roof to Floor

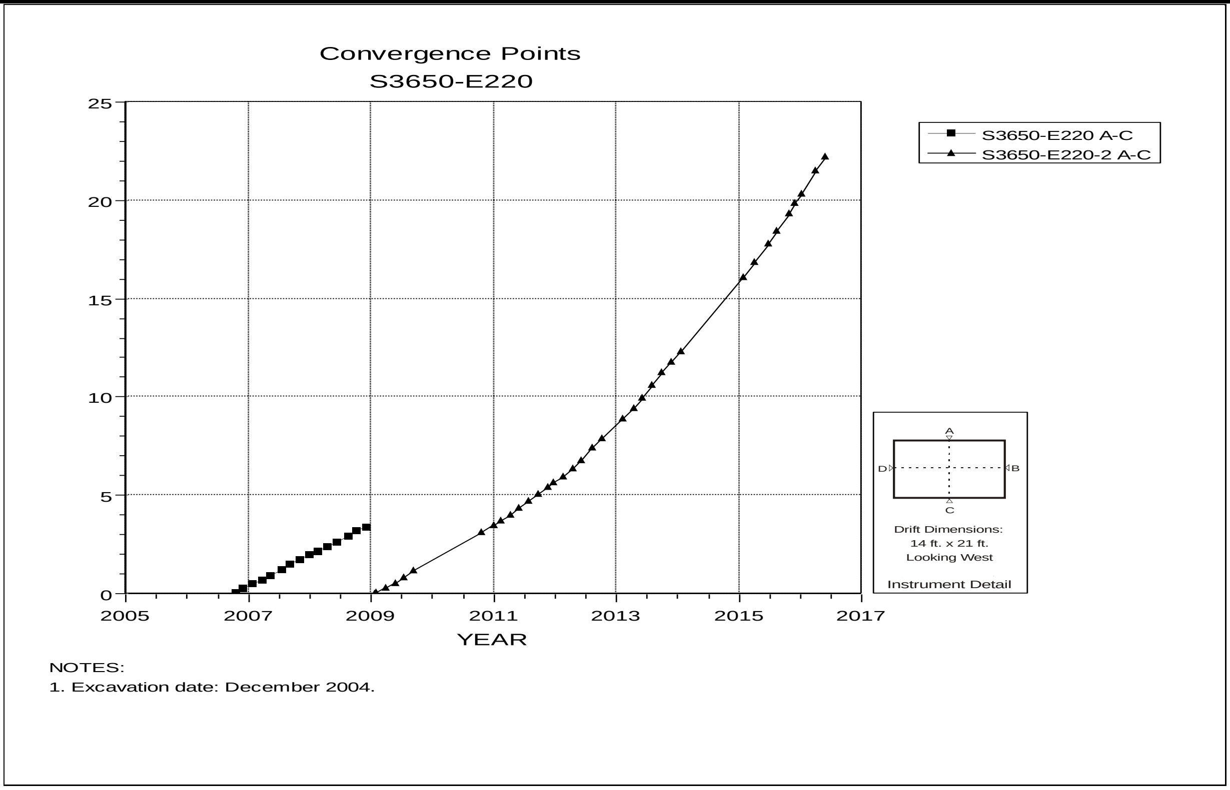

Figure 4-177 Convergence Point Array –
S3650 E220 – Roof to Floor

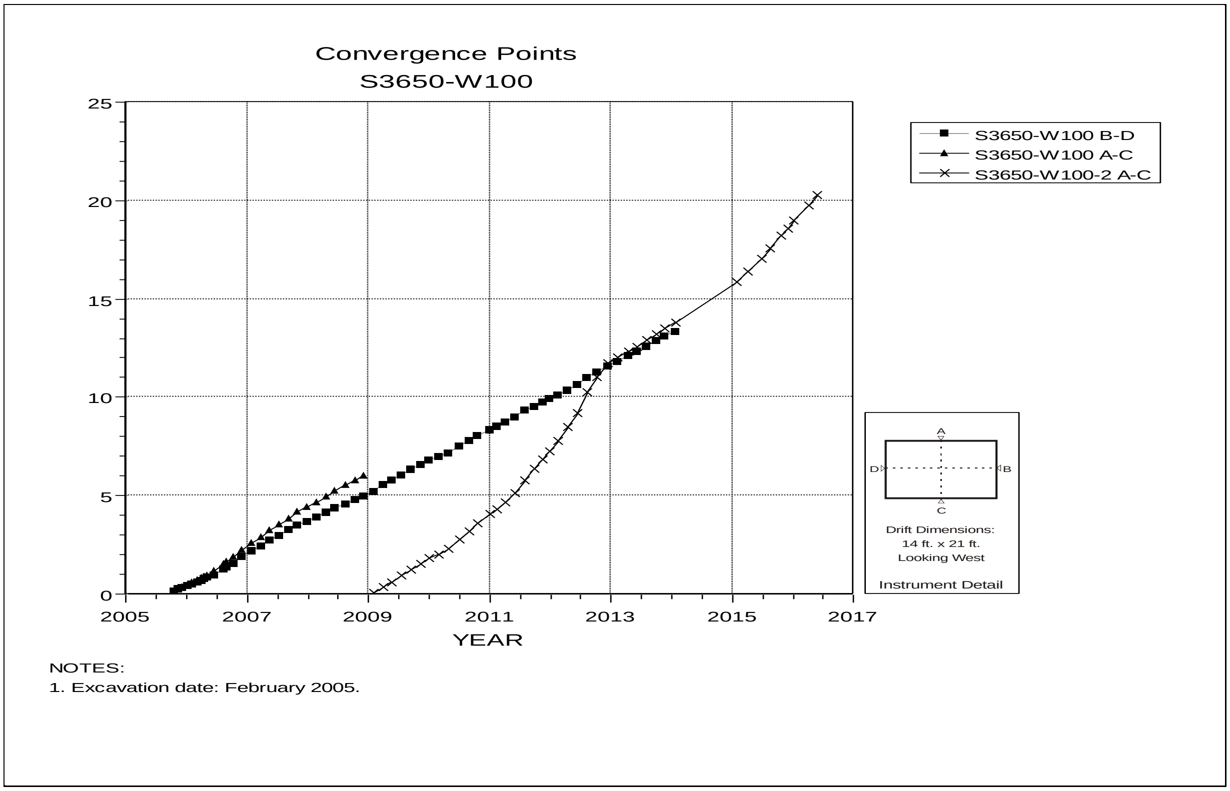

Figure 4-178 Convergence Point Array –
S3650 W100 – All Chords

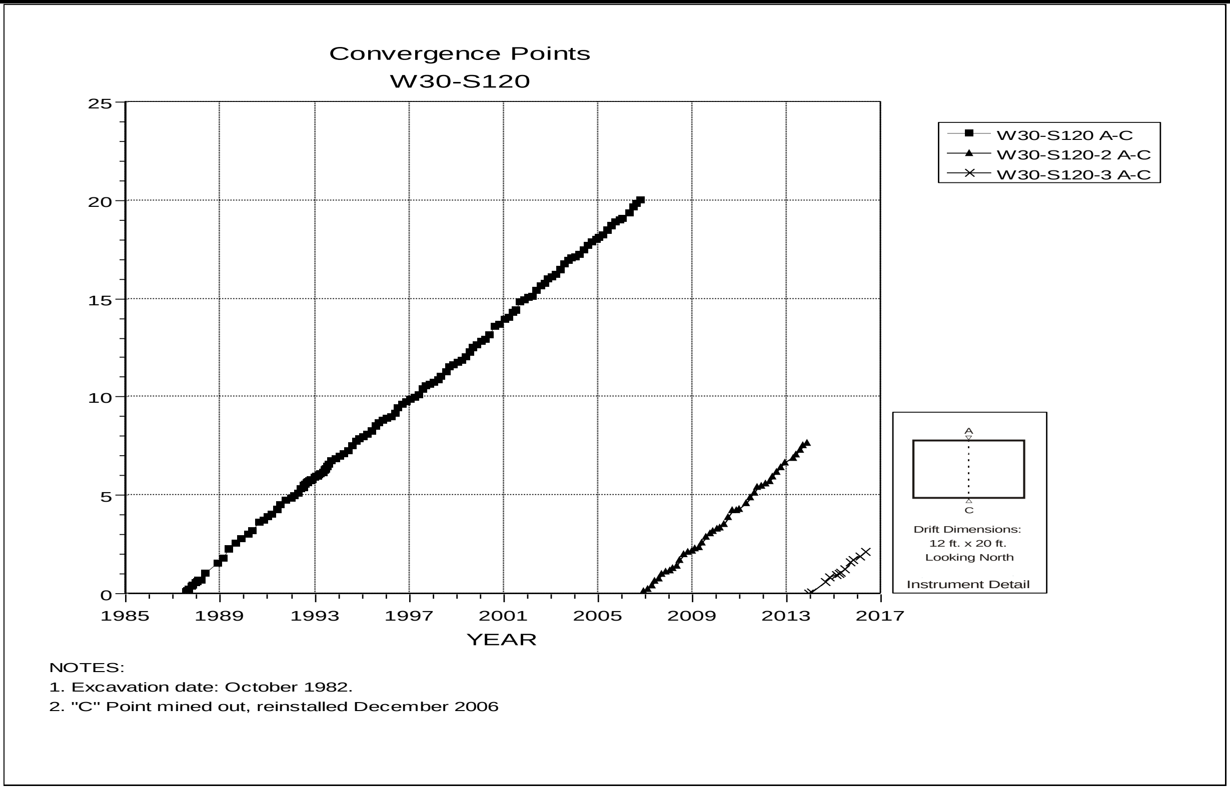

Figure 4-179 Convergence Point Array –
W30 S120 – Roof to Floor

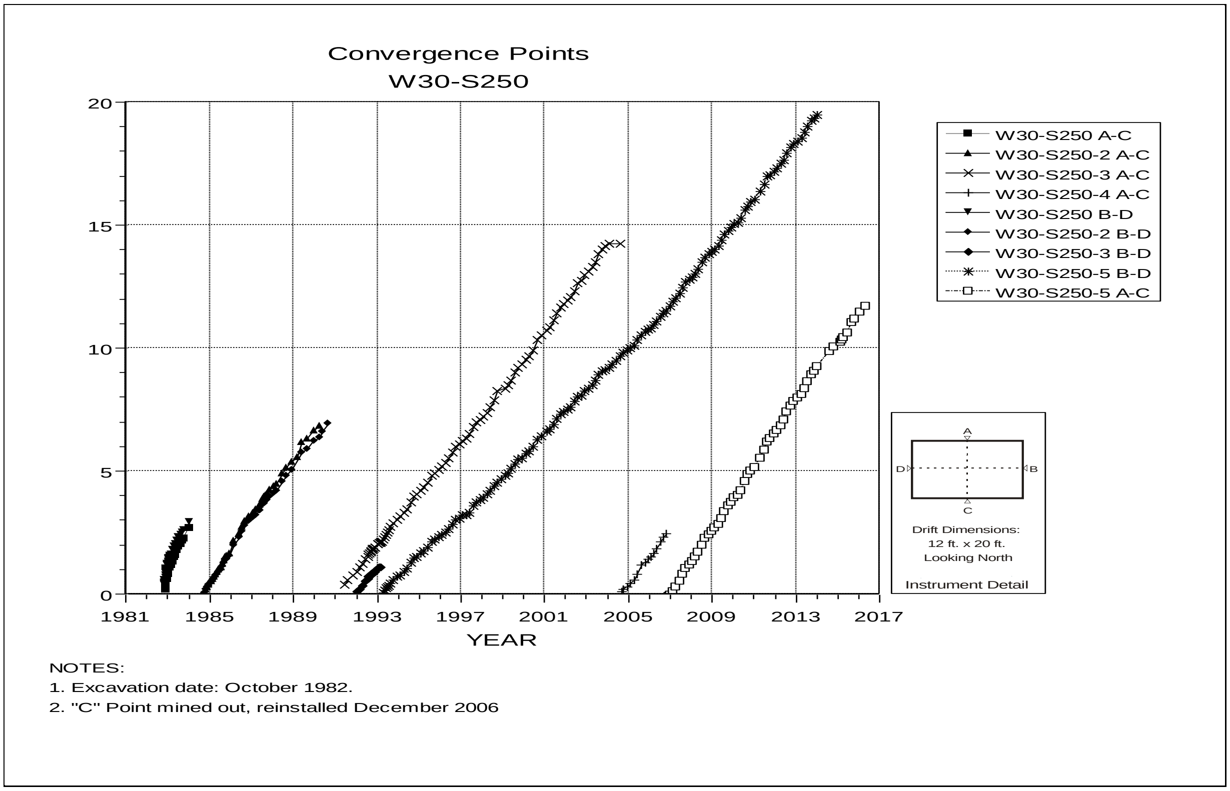

Figure 4-180 Convergence Point Array –
W30 S250 – Roof to Floor

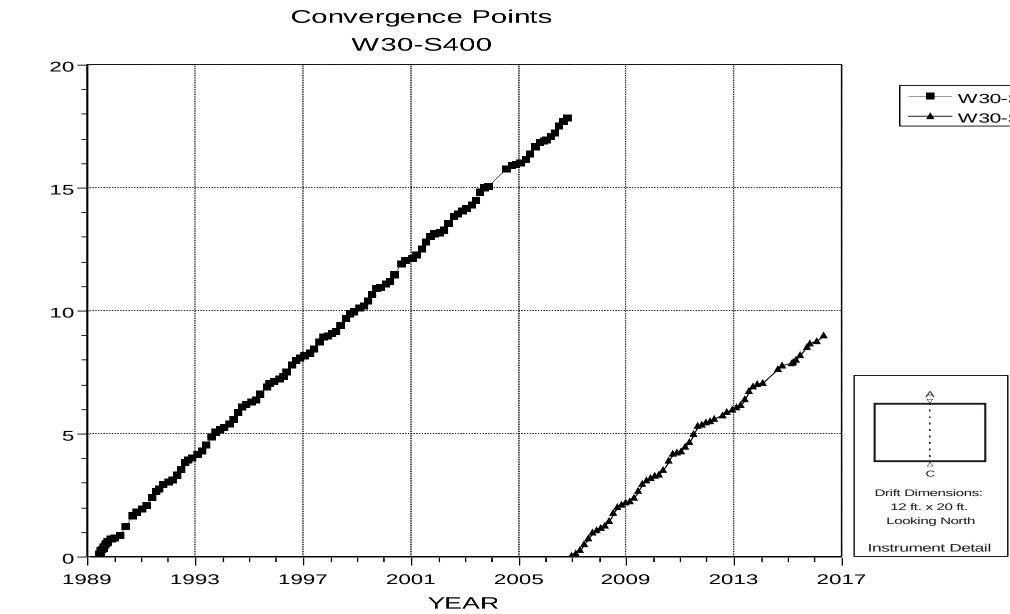

NOTES:
1. Excavation date: October 1982.
2. "C" Point mined out, reinstalled December 2006.

Figure 4-181 Convergence Point Array –
W30 S400 – Roof to Floor

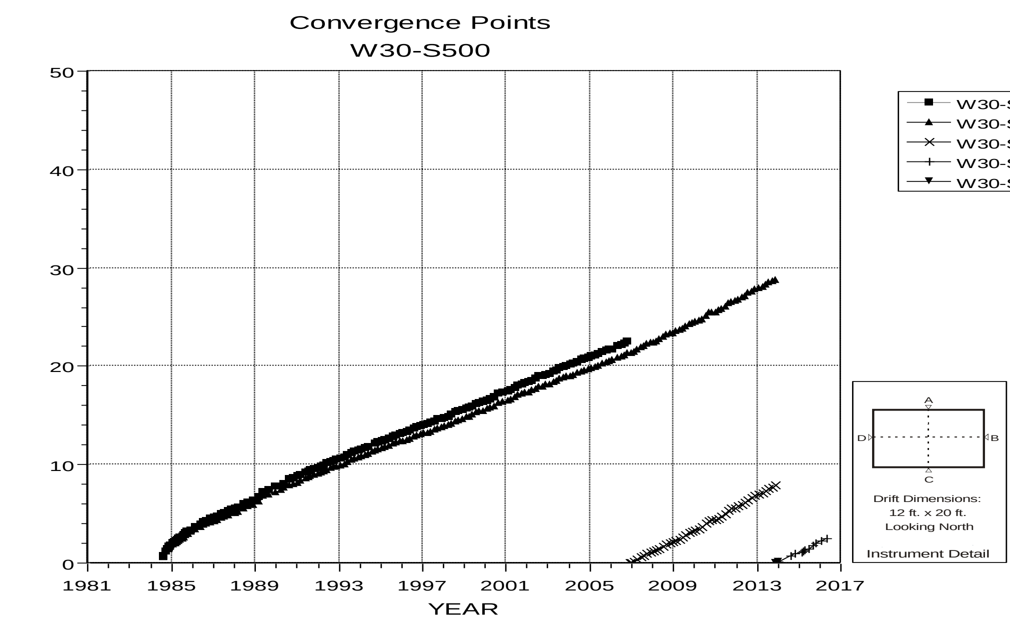

NOTES:
1. Excavation date: August 1984.
2. "C" Point mined out, reinstalled December 2006

Figure 4-182 Convergence Point Array –
W30 S500 – Roof to Floor

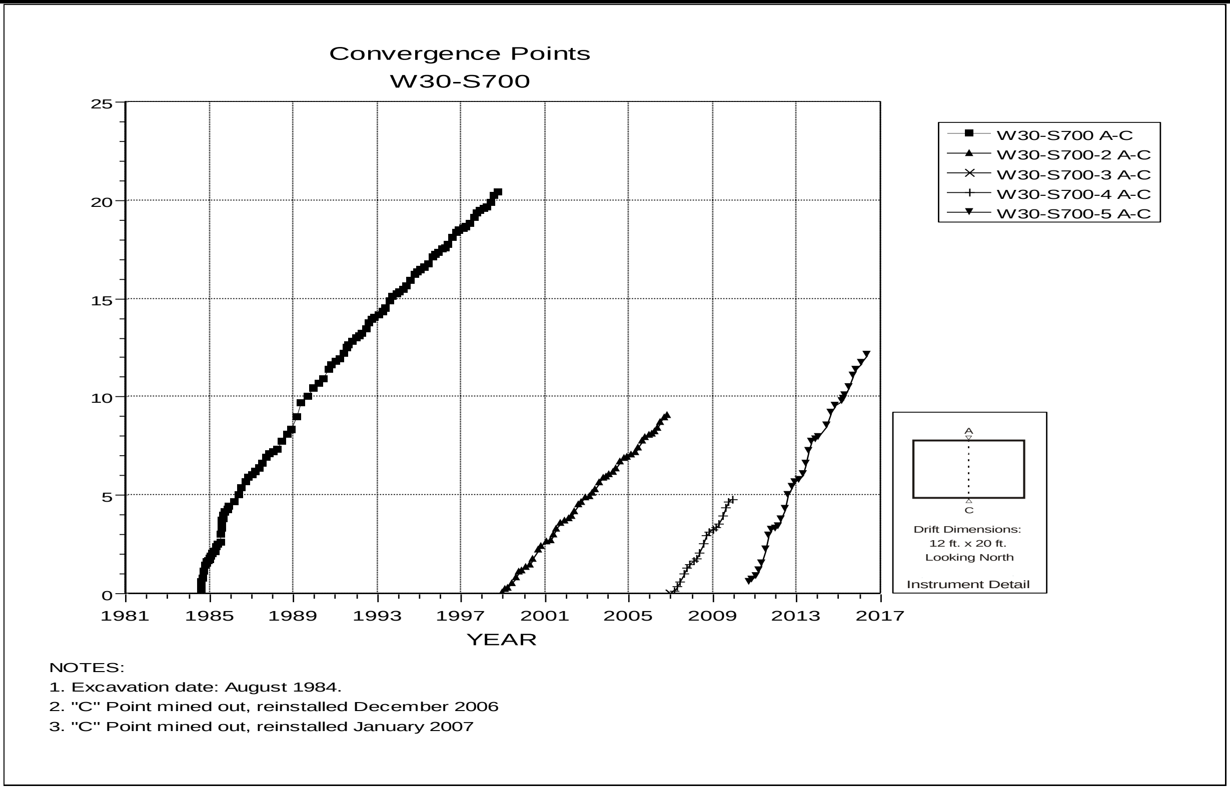

Figure 4-183 Convergence Point Array –
W30 S700 – Roof to Floor

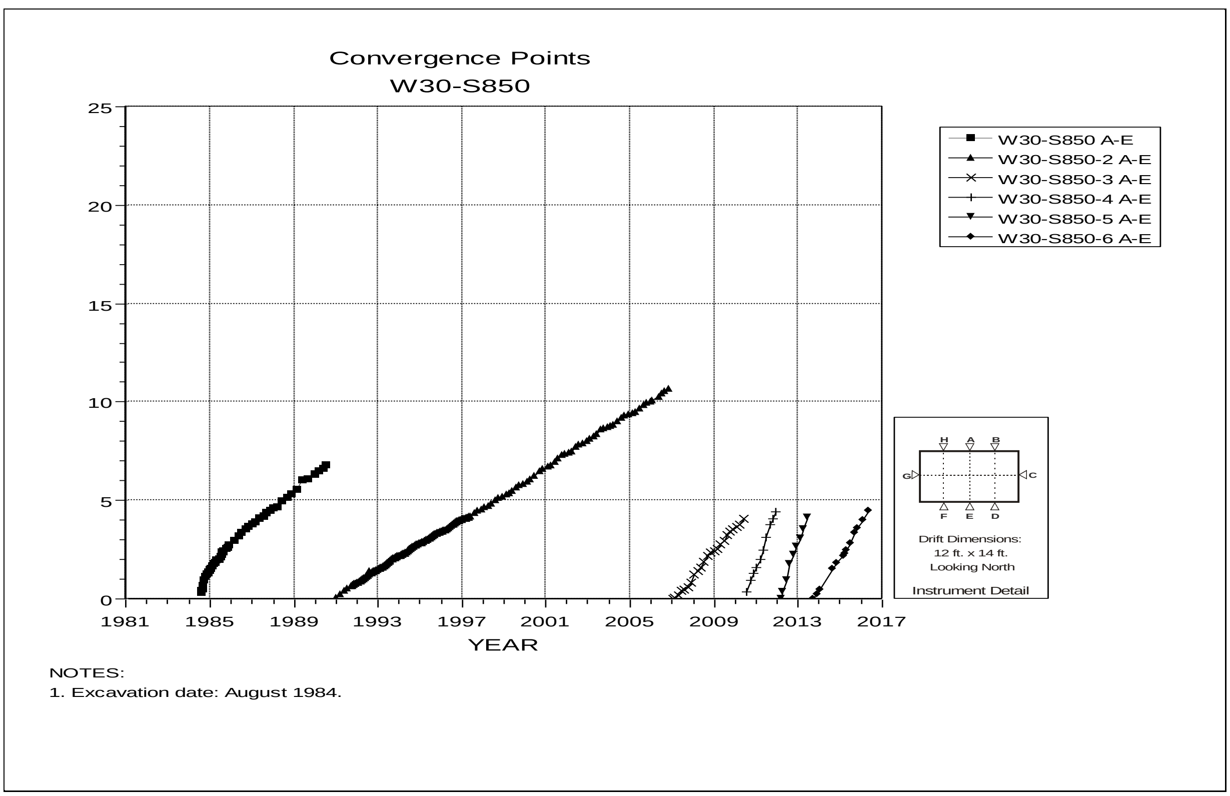

Figure 4-184 Convergence Point Array –
W30 S850 – Centerline – Roof to Floor

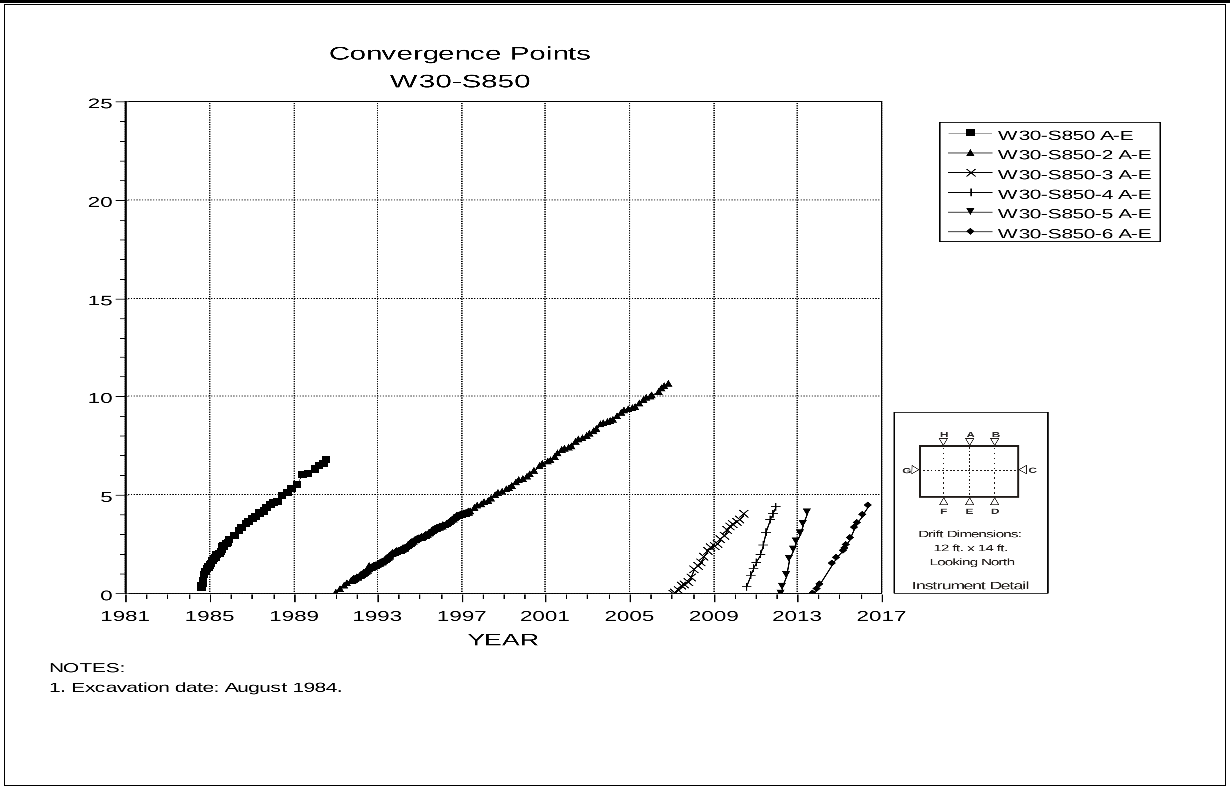

Figure 4-185 Convergence Point Array –
W30 S850 – Roof to Floor – East Quarter Point

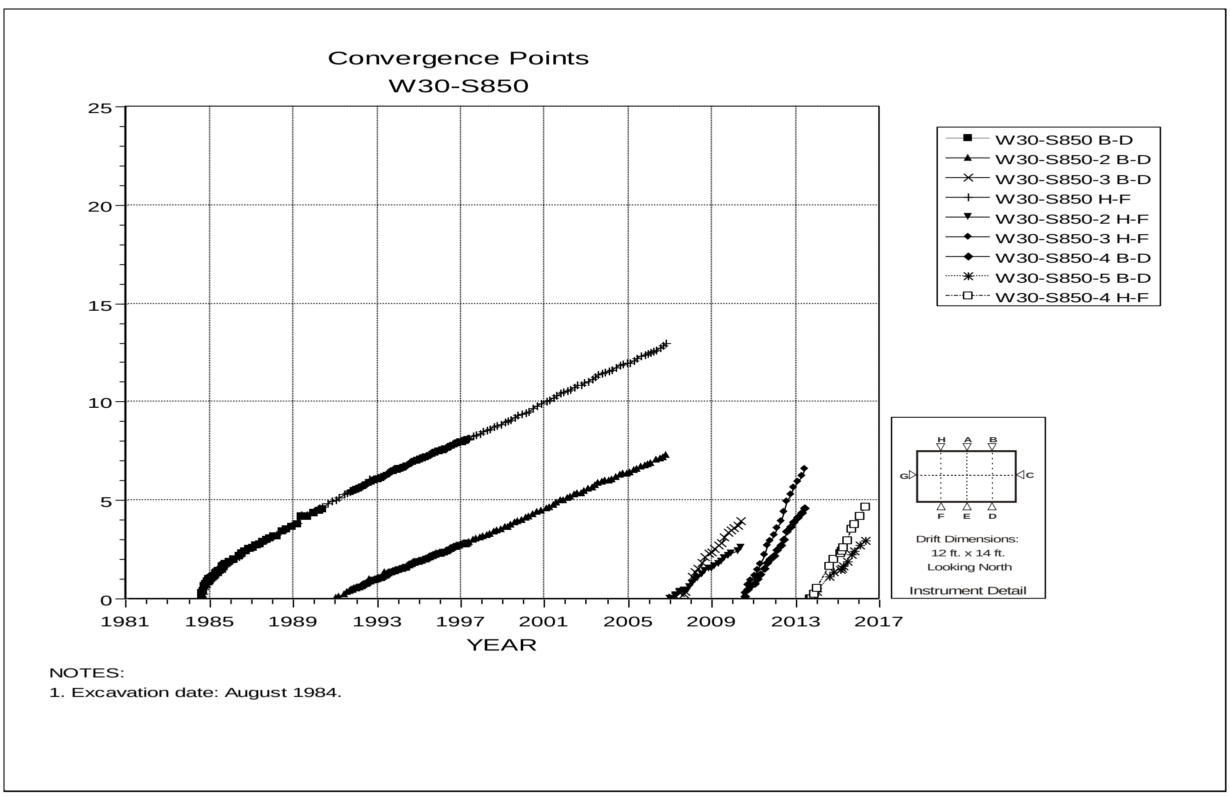

Figure 4-186 Convergence Point Array –
W30 S850 – Roof to Floor – West Quarter Point

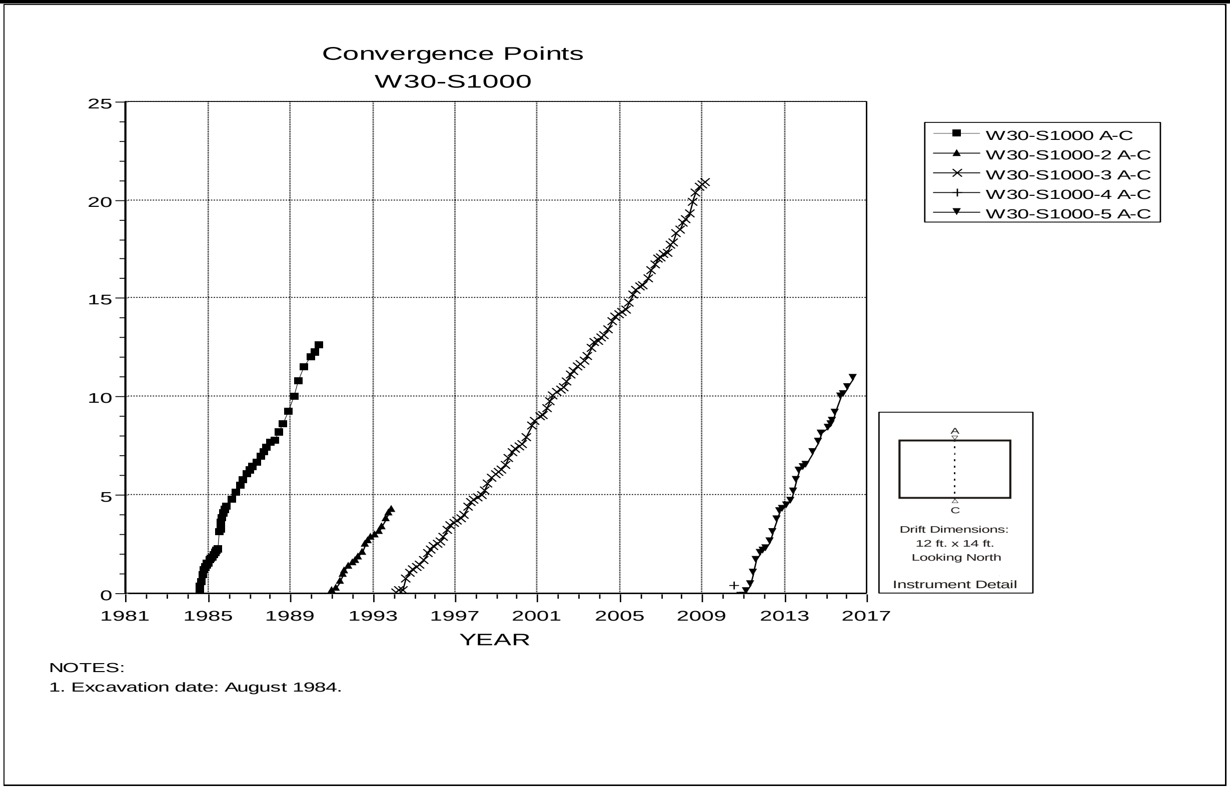

Figure 4-187 Convergence Point Array –
W30 S1000 – Roof to Floor

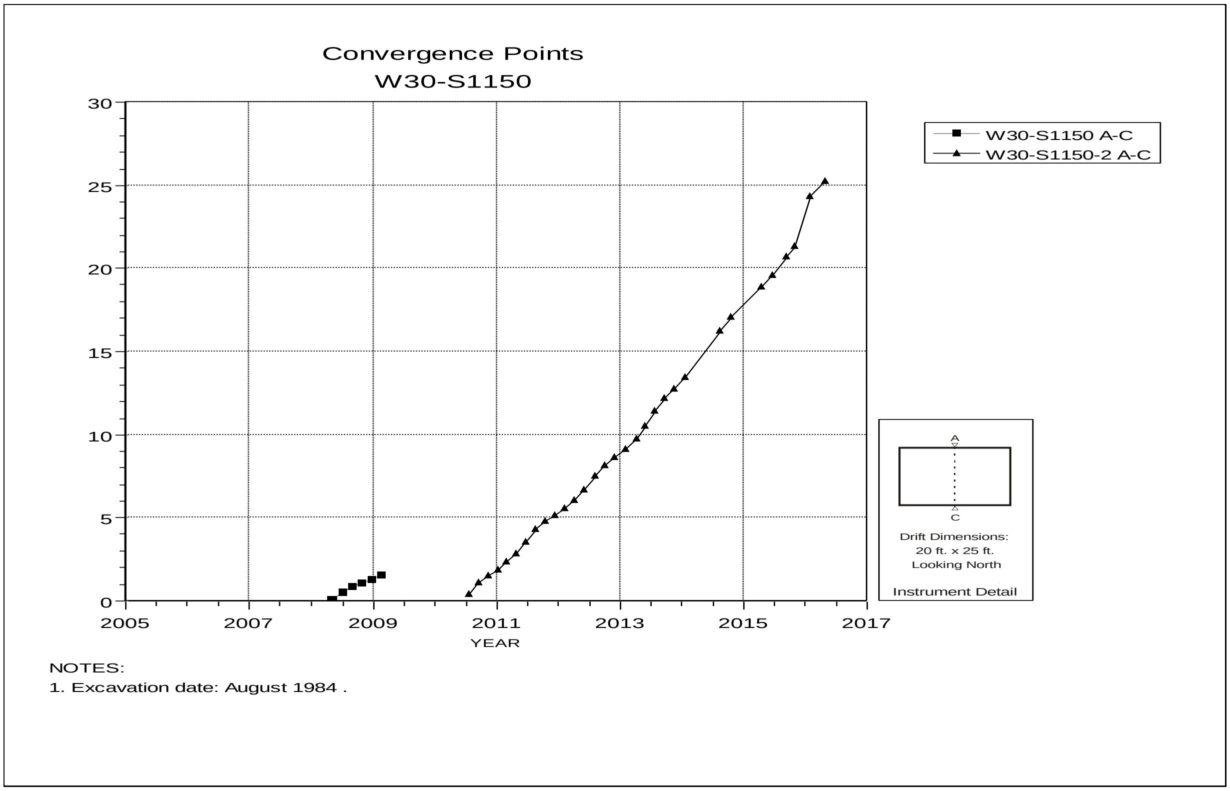

Figure 4-188 Convergence Point Array –
W30 S1150 – Roof to Floor Floor

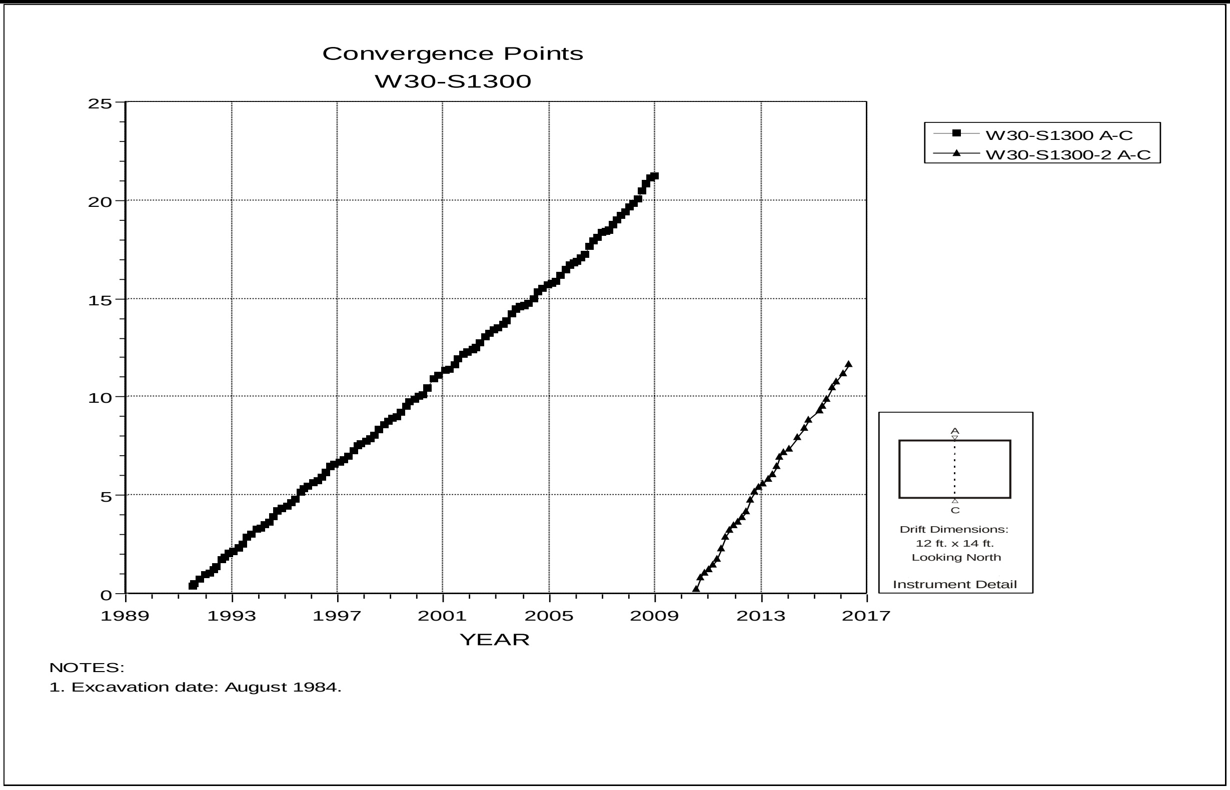

Figure 4-189 Convergence Point Array –
W30 S1300 – Roof to Floor

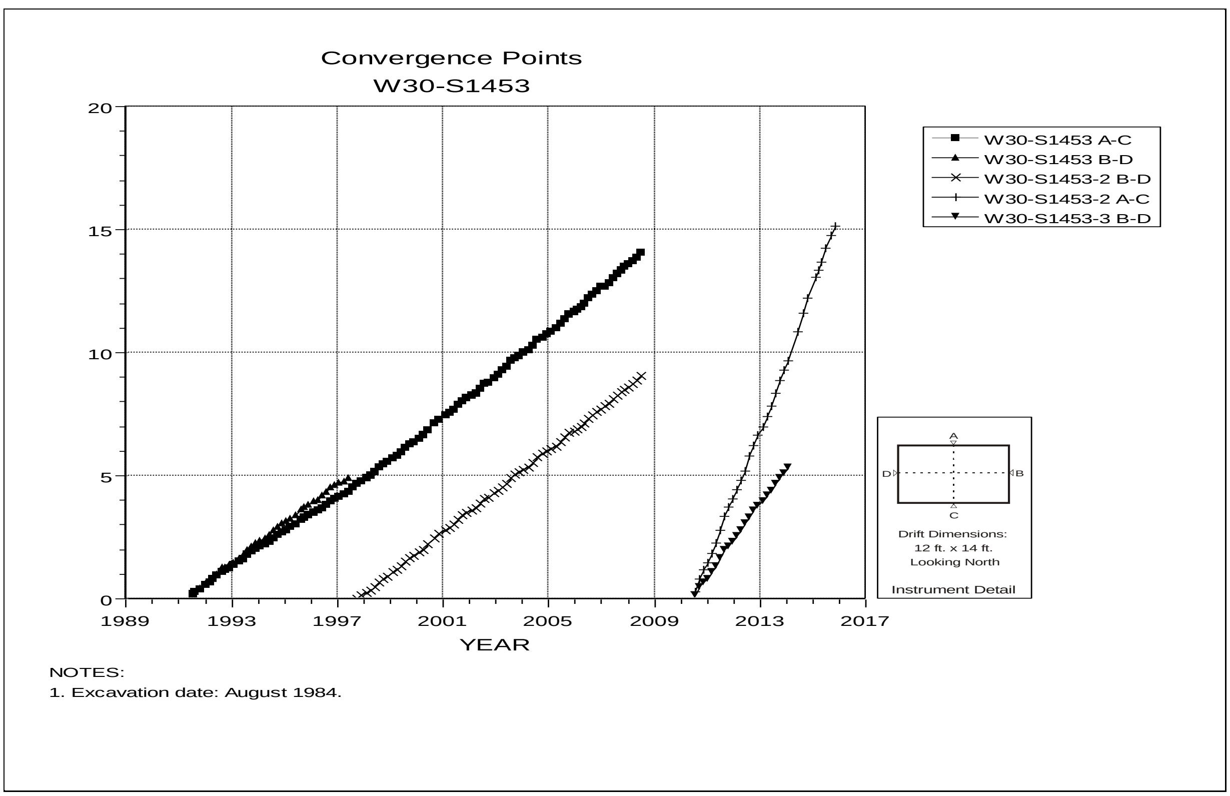

Figure 4-190 Convergence Point Array –
W30 S1453 – All Chords

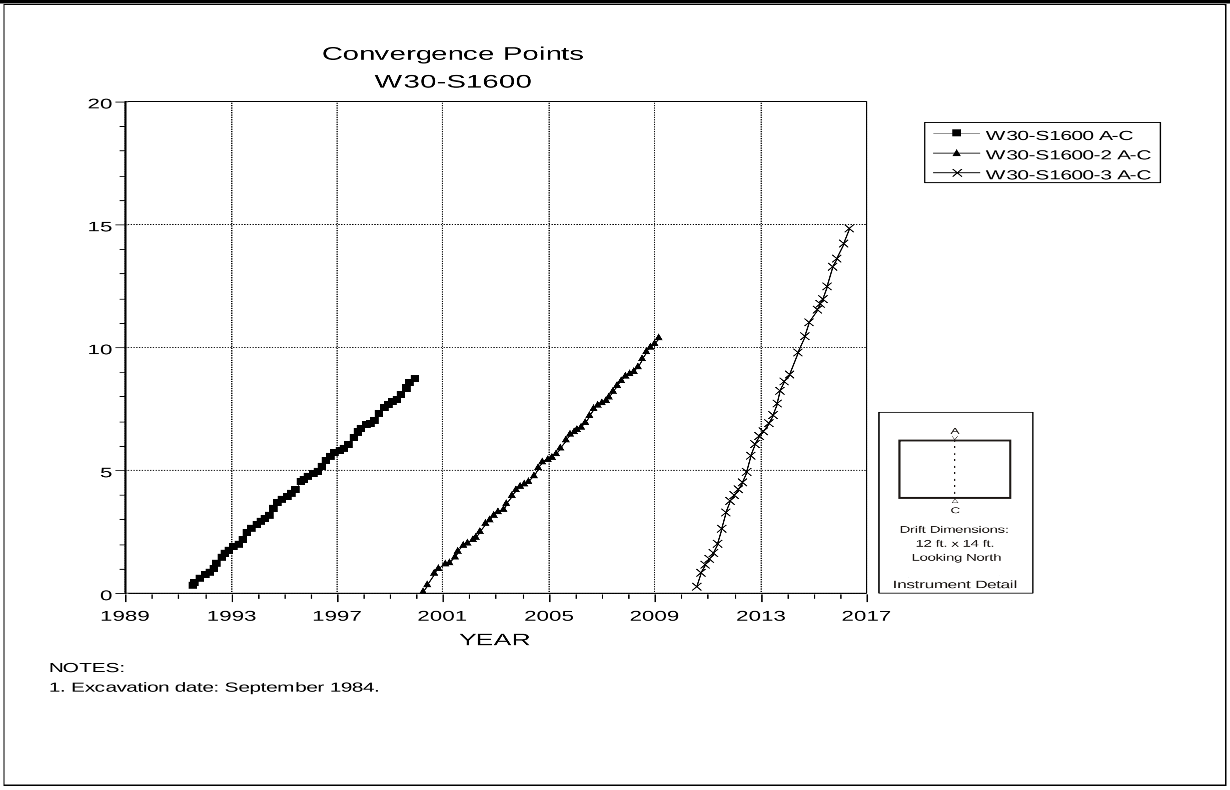

Figure 4-191 Convergence Point Array –
W30 S1600 – Roof to Floor

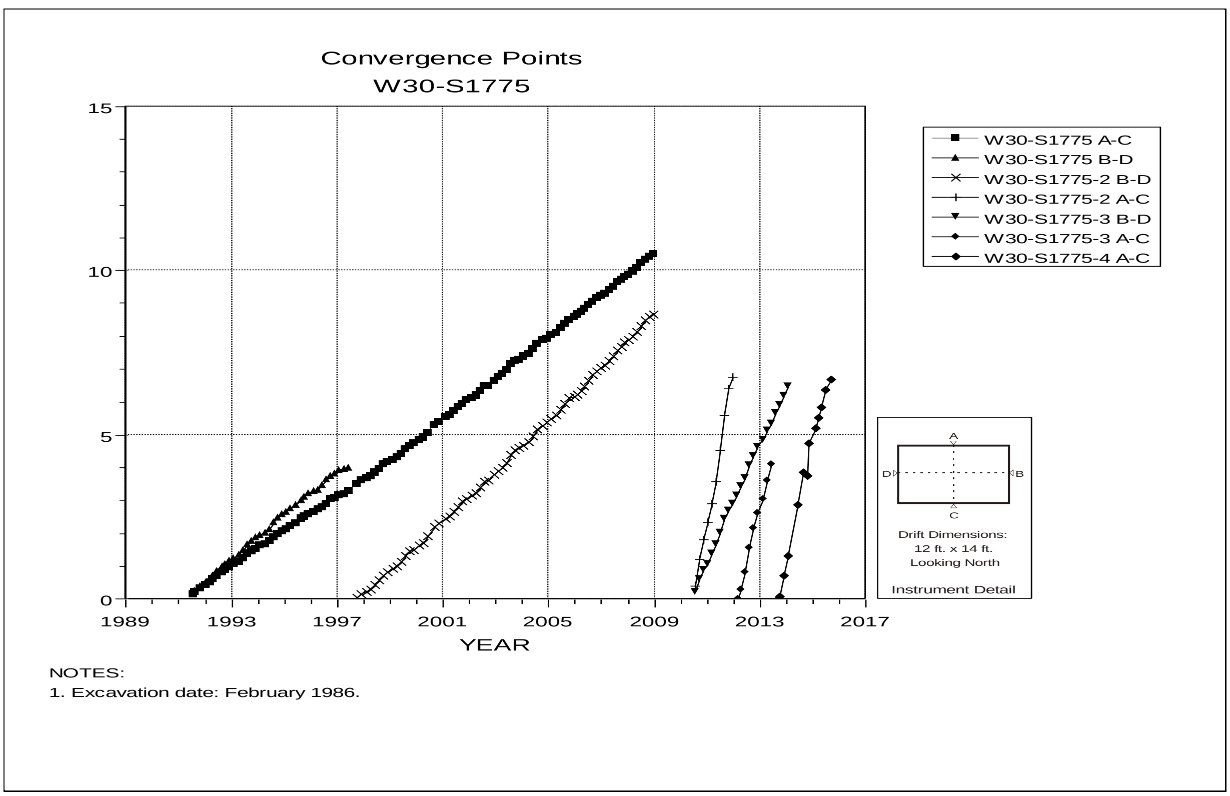

Figure 4-192 Convergence Point Array –
W30 S1775 – Roof to Floor

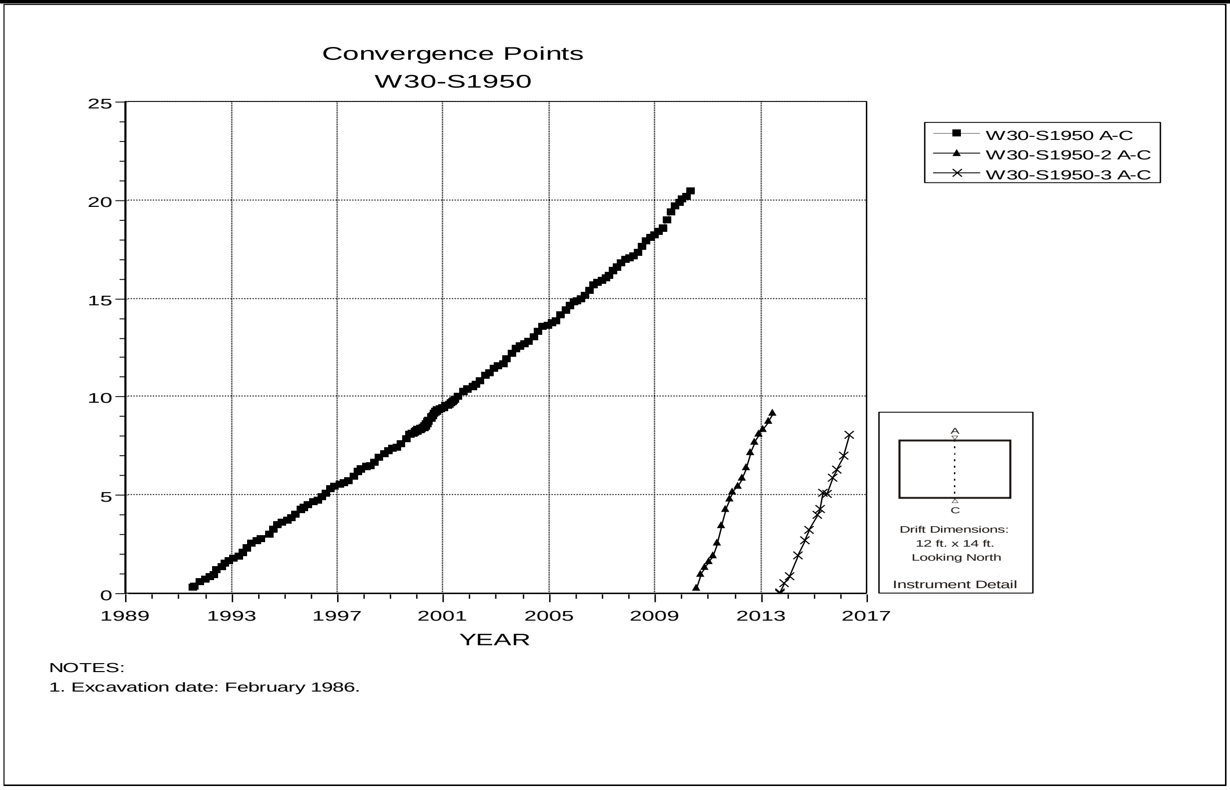

Figure 4-193 Convergence Point Array –
W30 S1950 – Roof to Floor

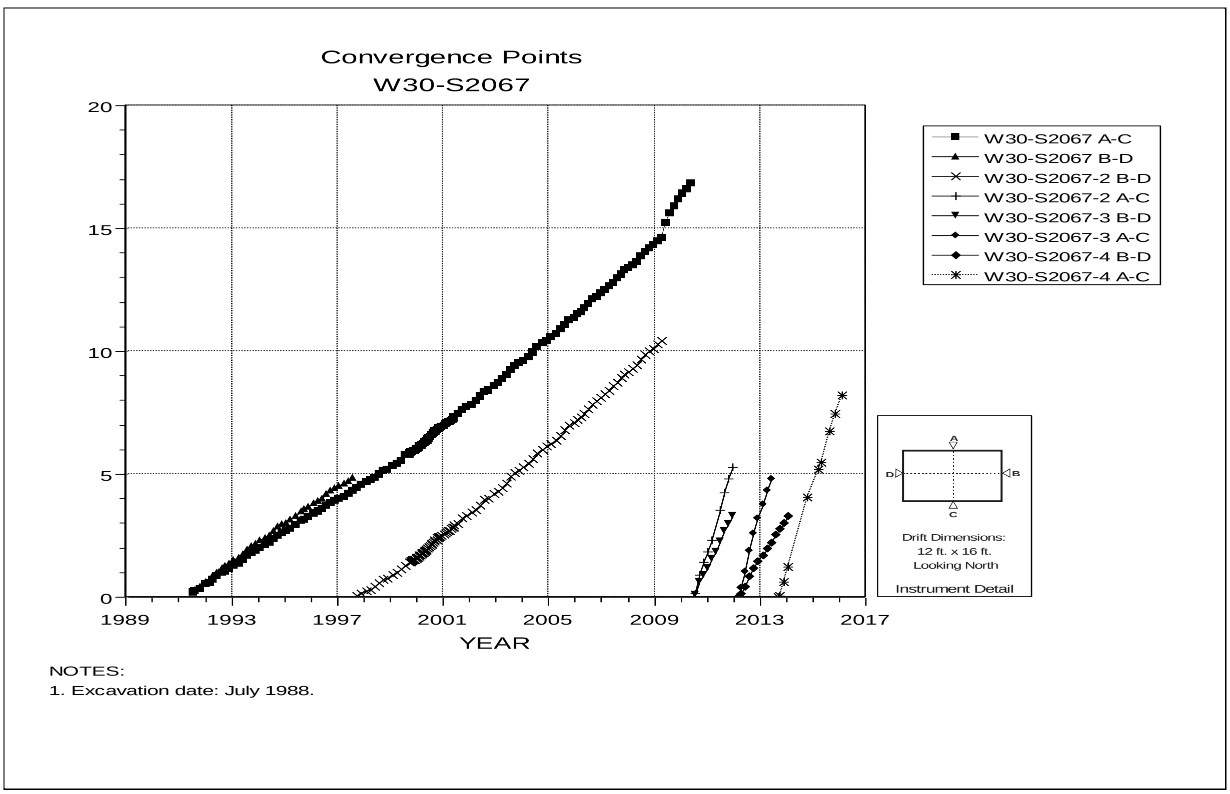

Figure 4-194 Convergence Point Array –
W30 S2067 – All Chords

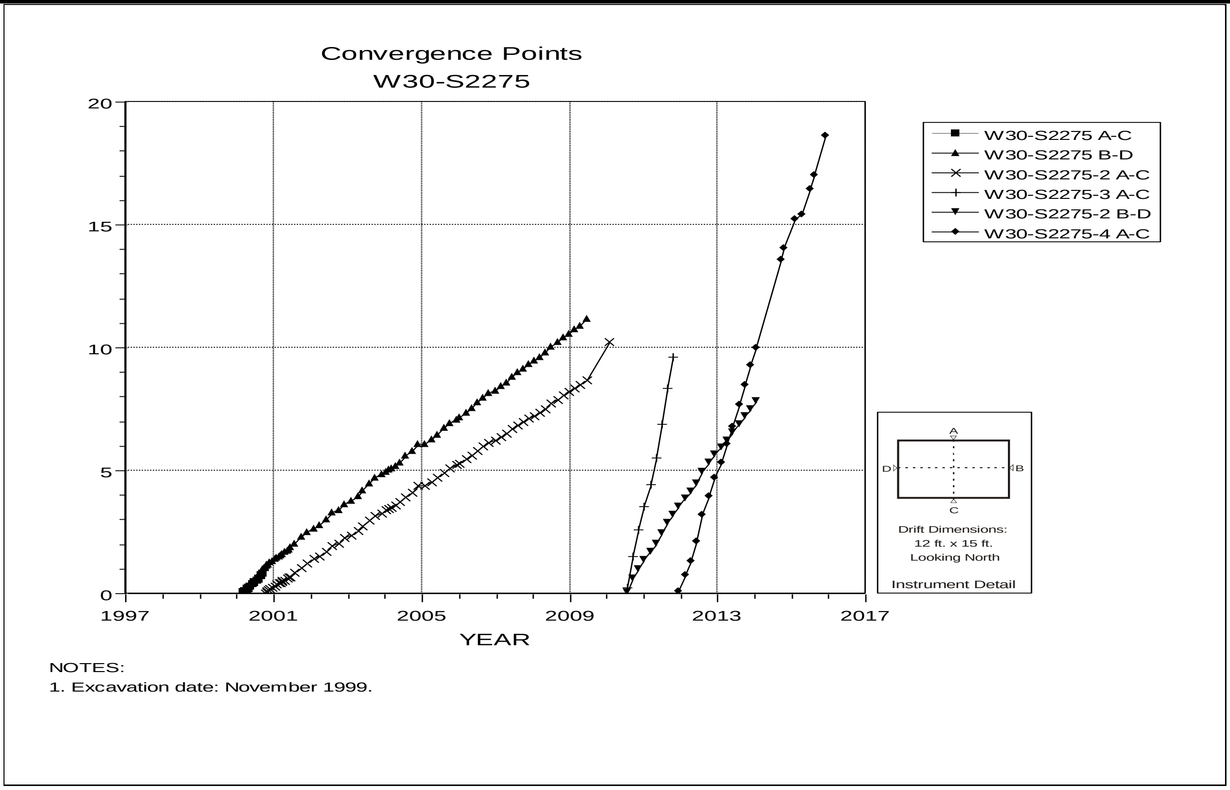

Figure 4-195 Convergence Point Array –
W30 S2275 – All Chords

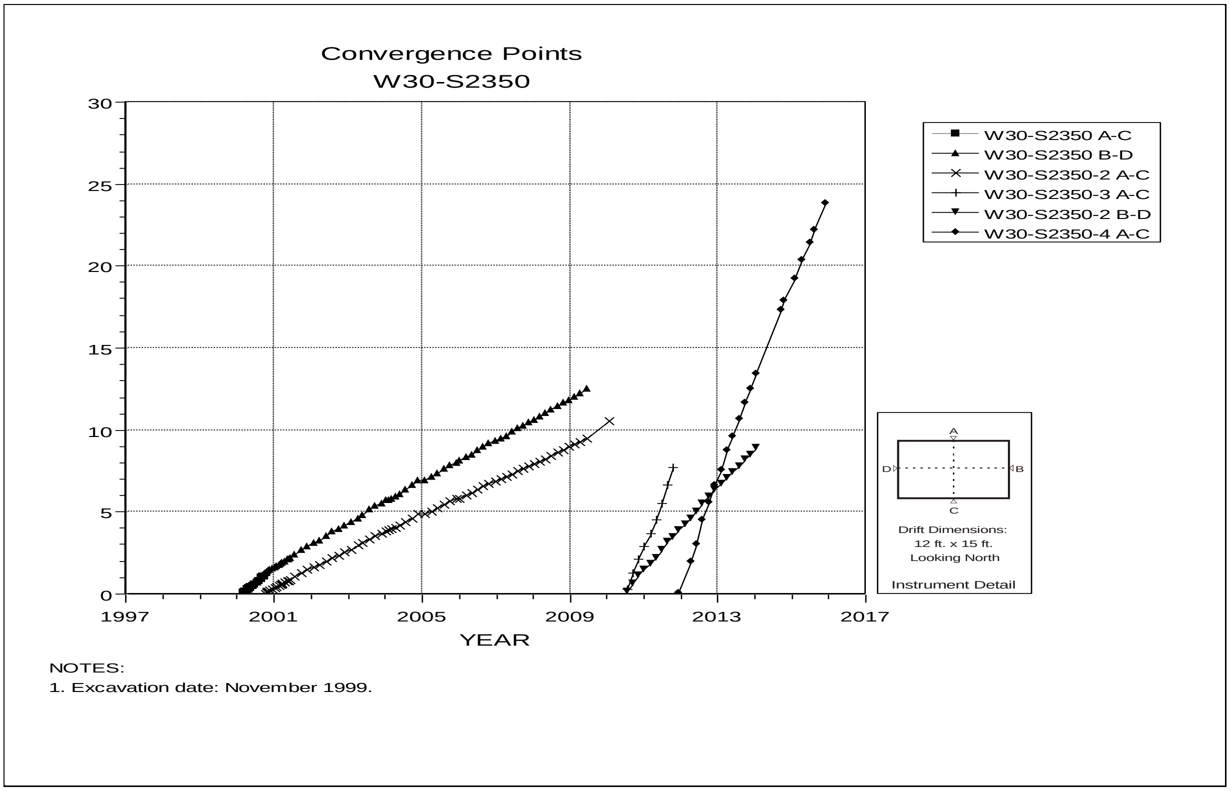

Figure 4-196 Convergence Point Array –
W30 S2350 – All Chords

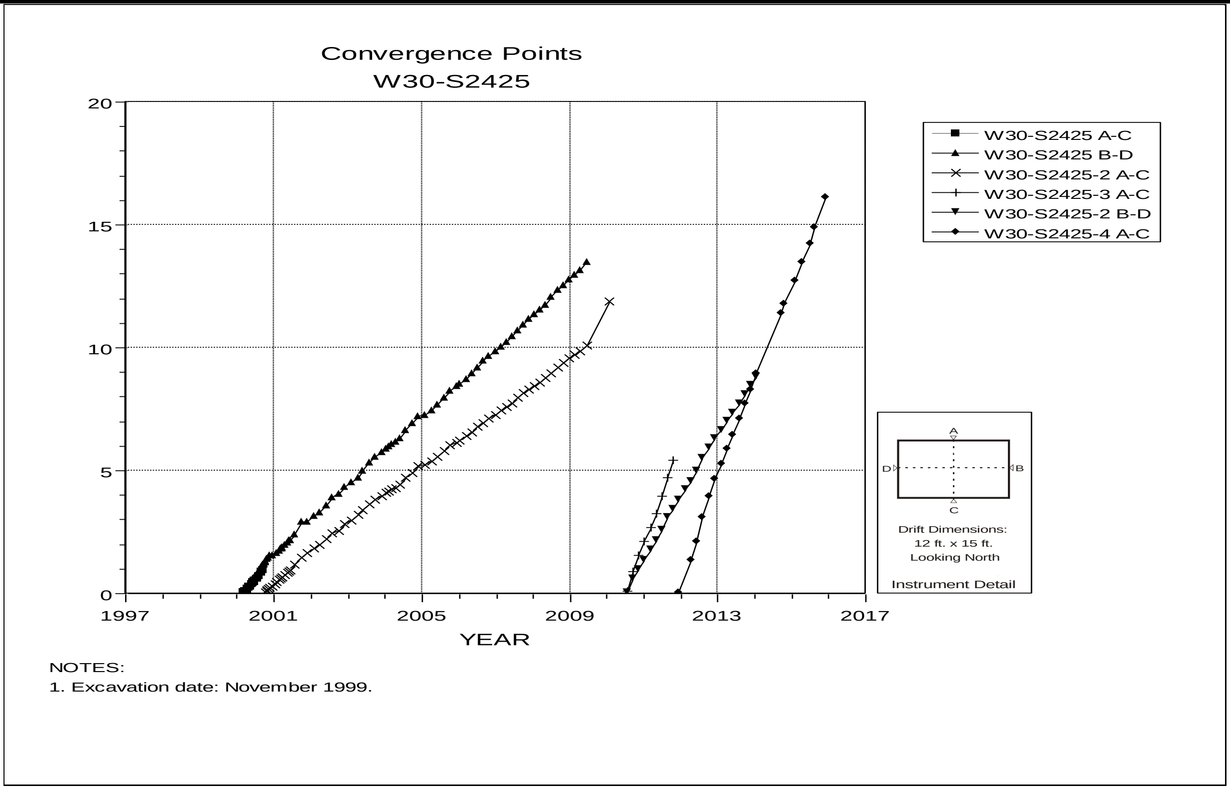

Figure 4-197 Convergence Point Array –
W30 S2425 – All Chords

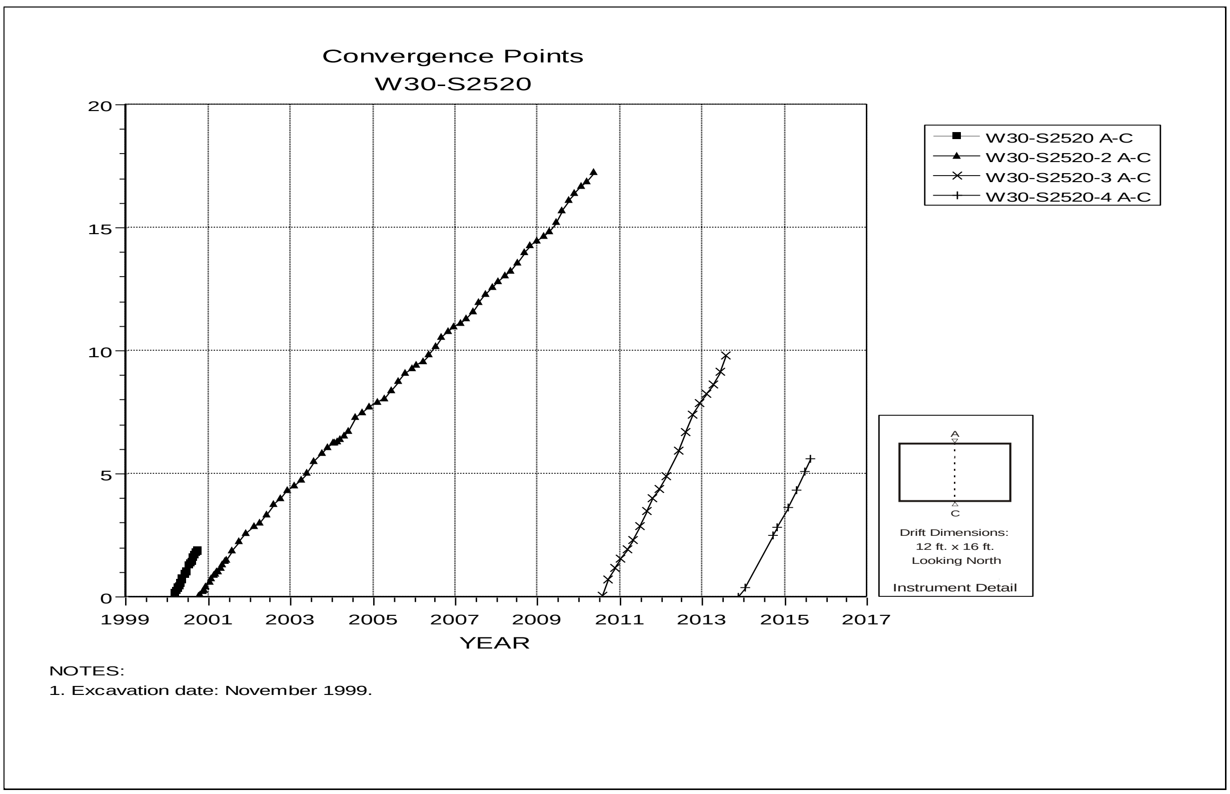

Figure 4-198 Convergence Point Array –
W30 S2520– Roof to Floor

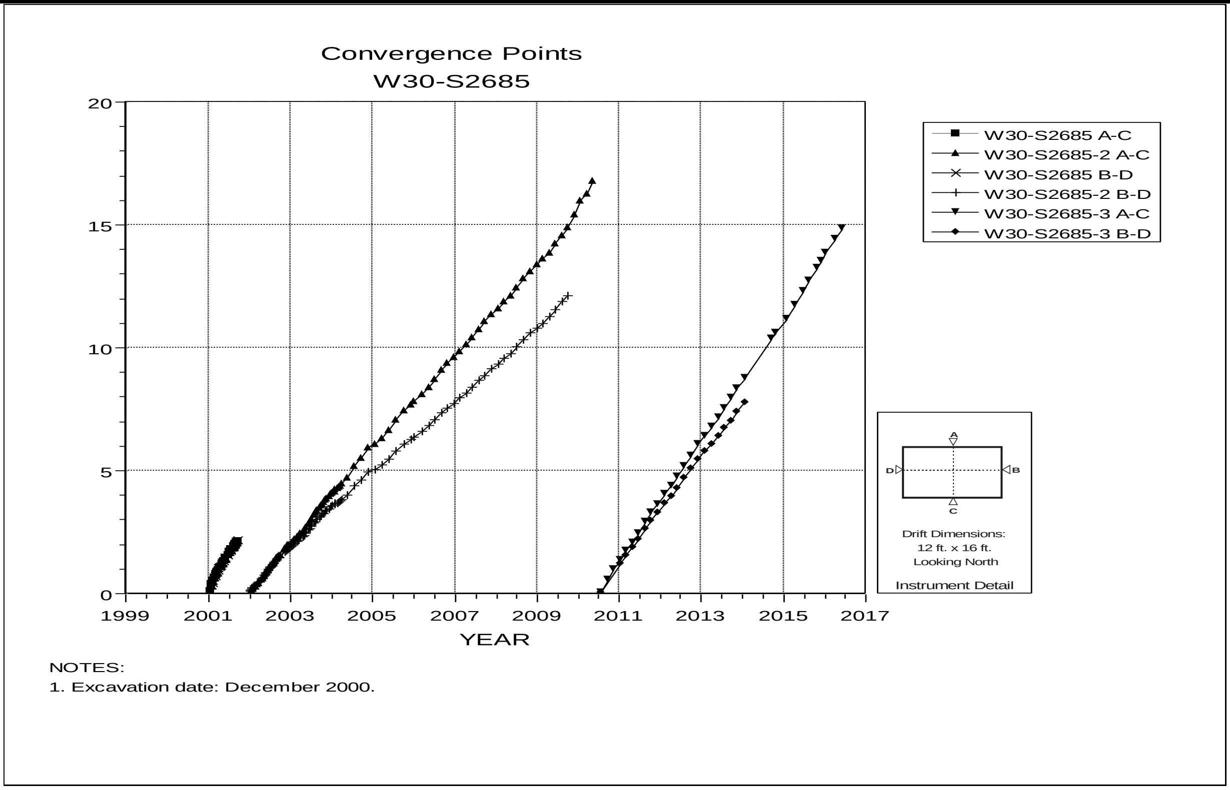

Figure 4-199 Convergence Point Array –
W30 S2685 – All Chords

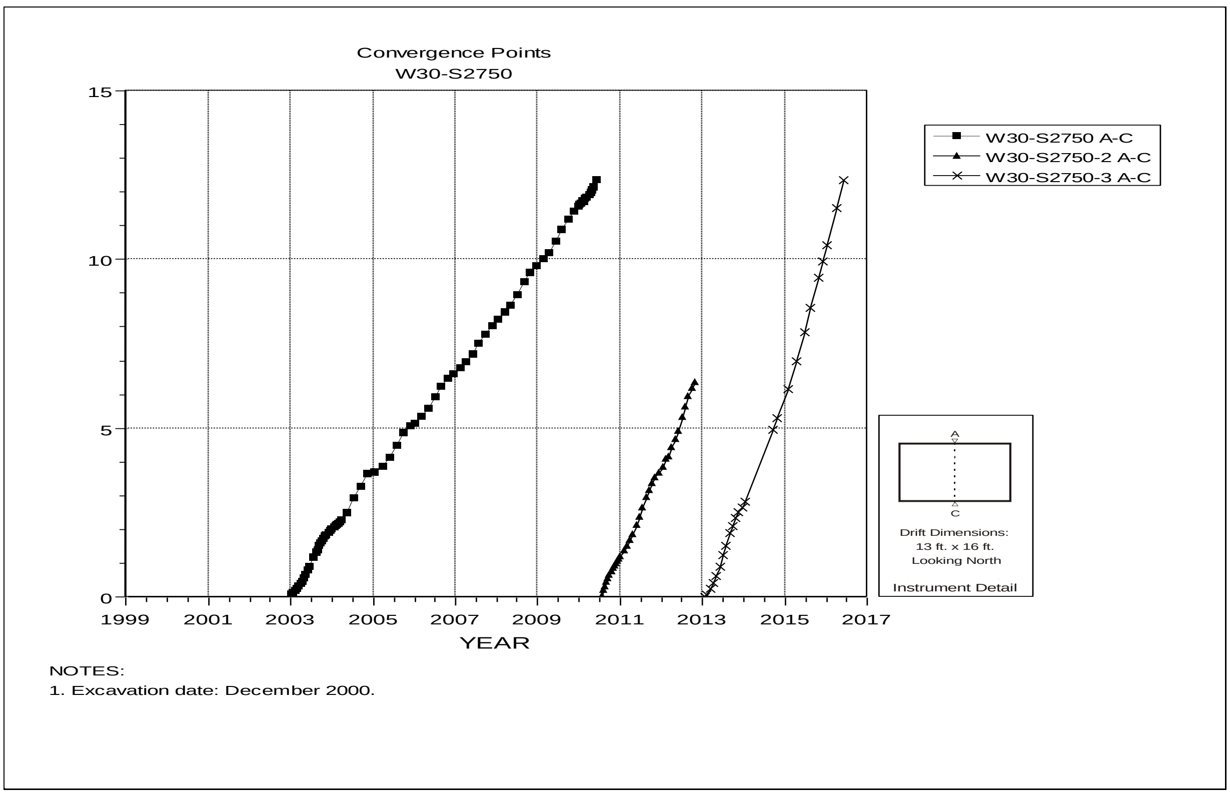

Figure 4-200 Convergence Point Array –
W30 S2750 – Roof to Floor

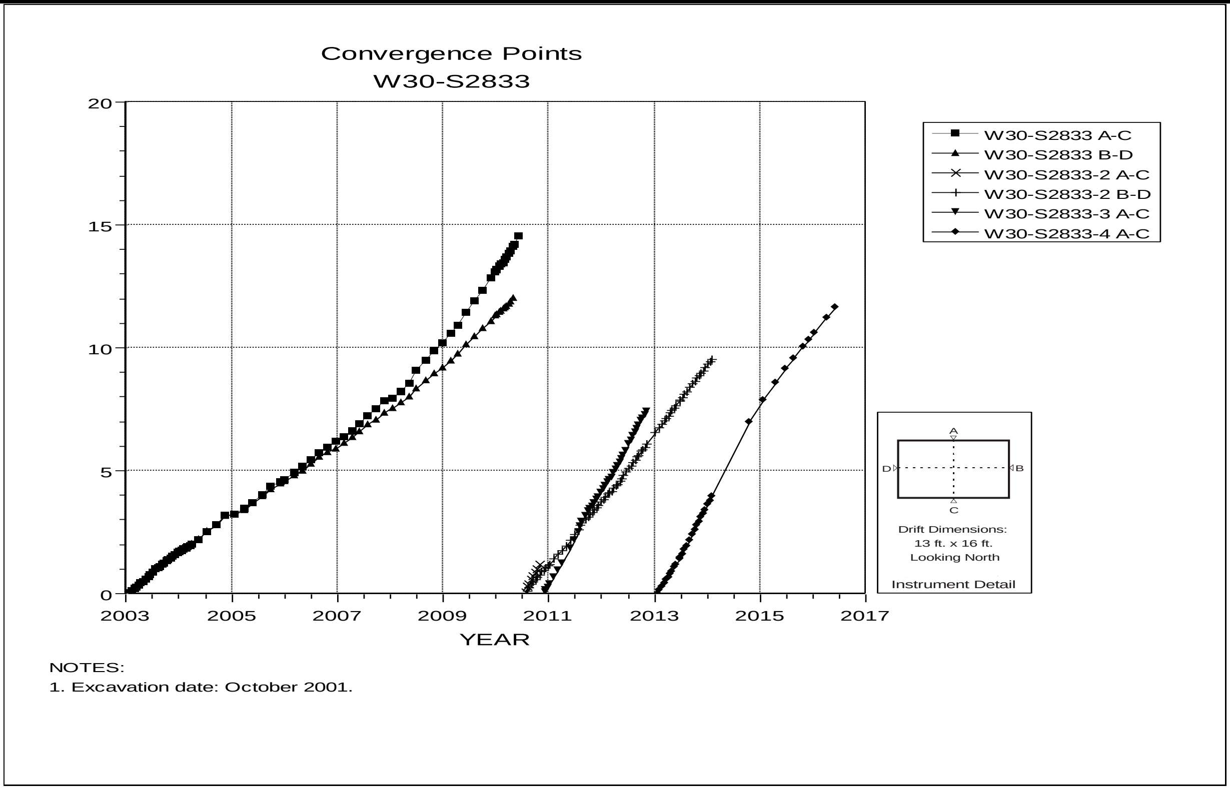

Figure 4-201 Convergence Point Array –
W30 S2833 – All Chords

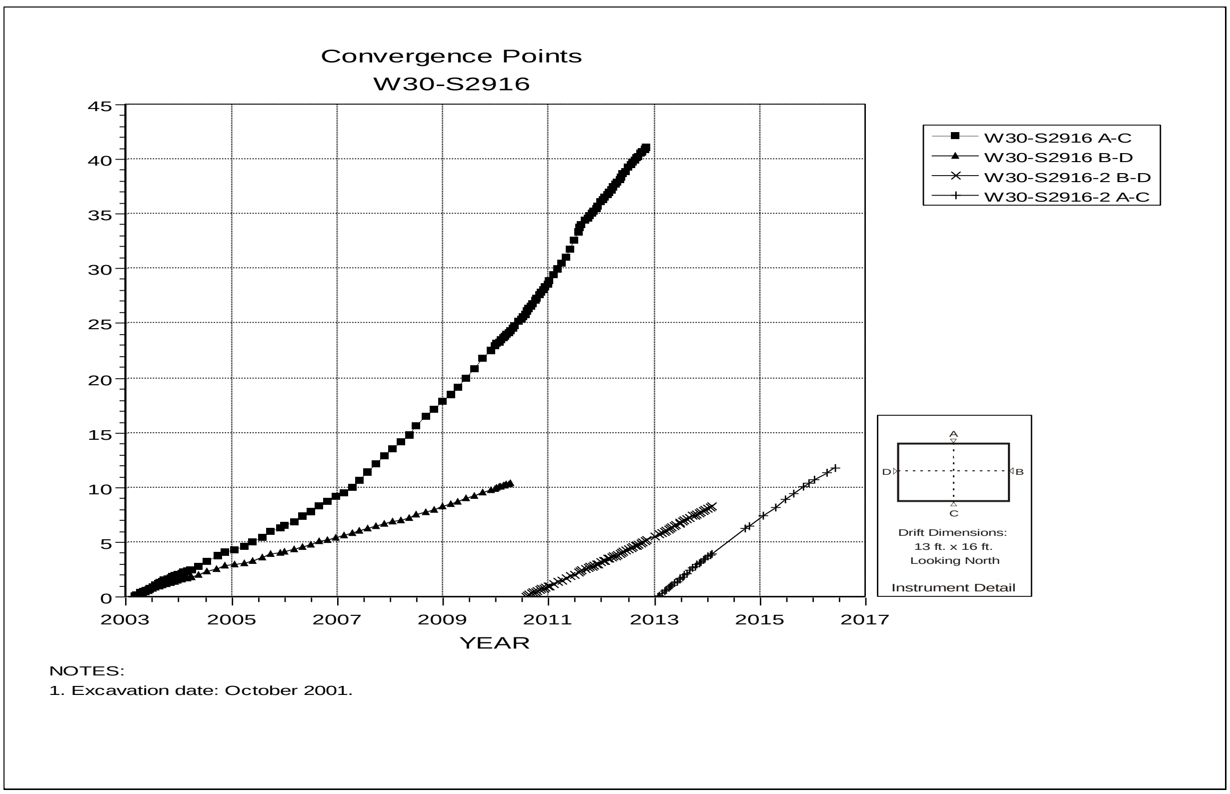

Figure 4-202 Convergence Point Array –
W30 S2916 – All Chords

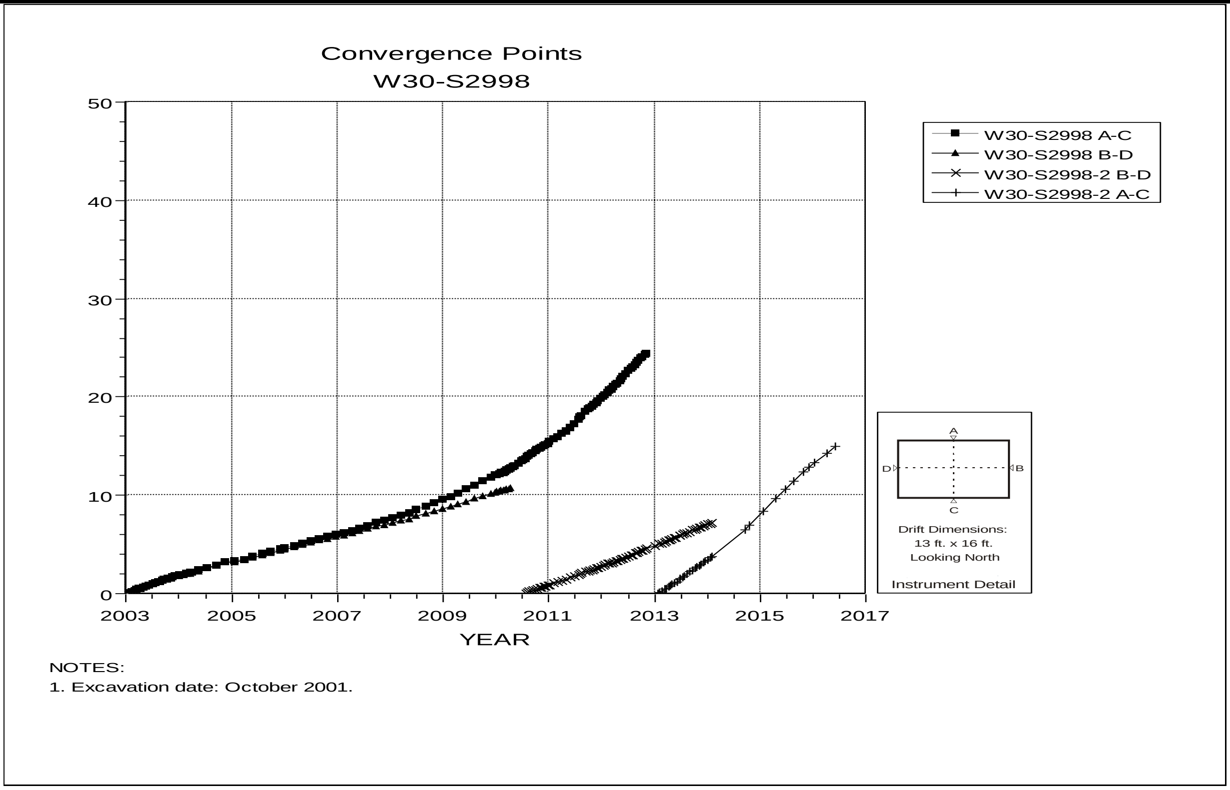

Figure 4-203 Convergence Point Array –
W30 S2998 – All Chords

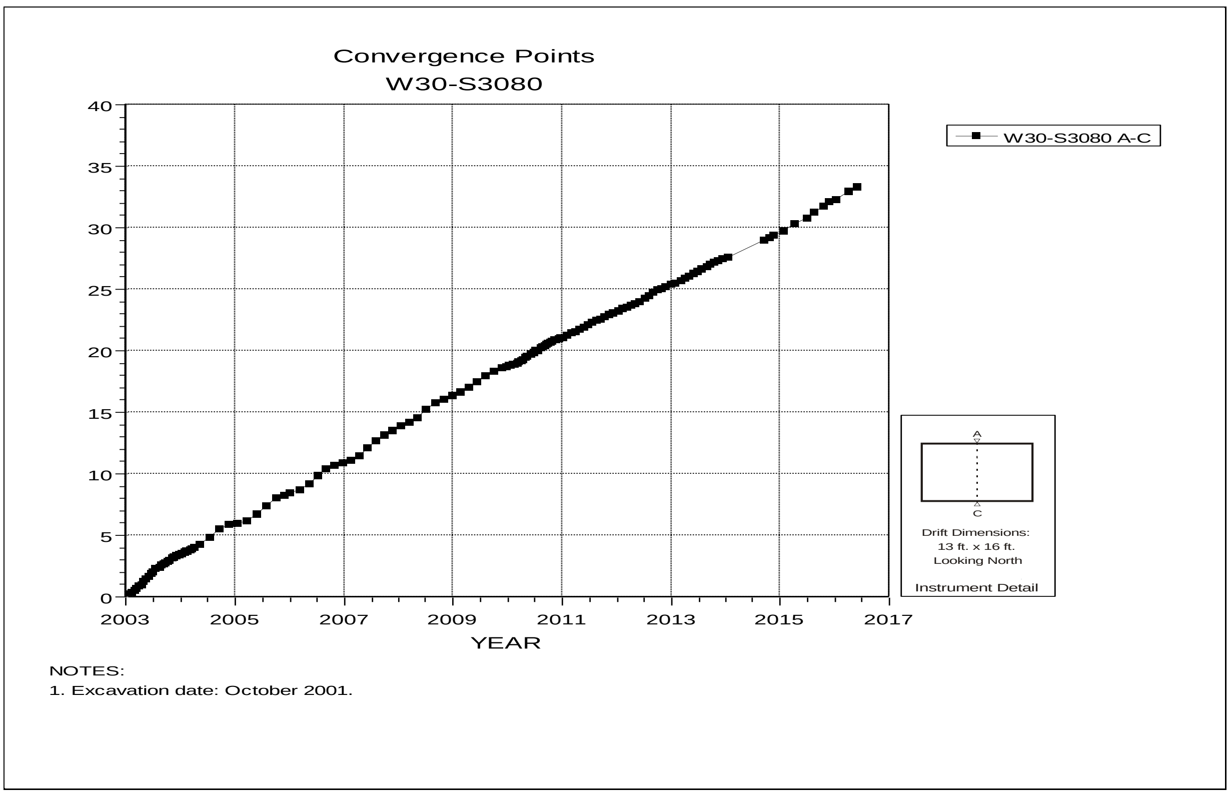

Figure 4-204 Convergence Point Array –
W30 S3080 – Roof to Floor

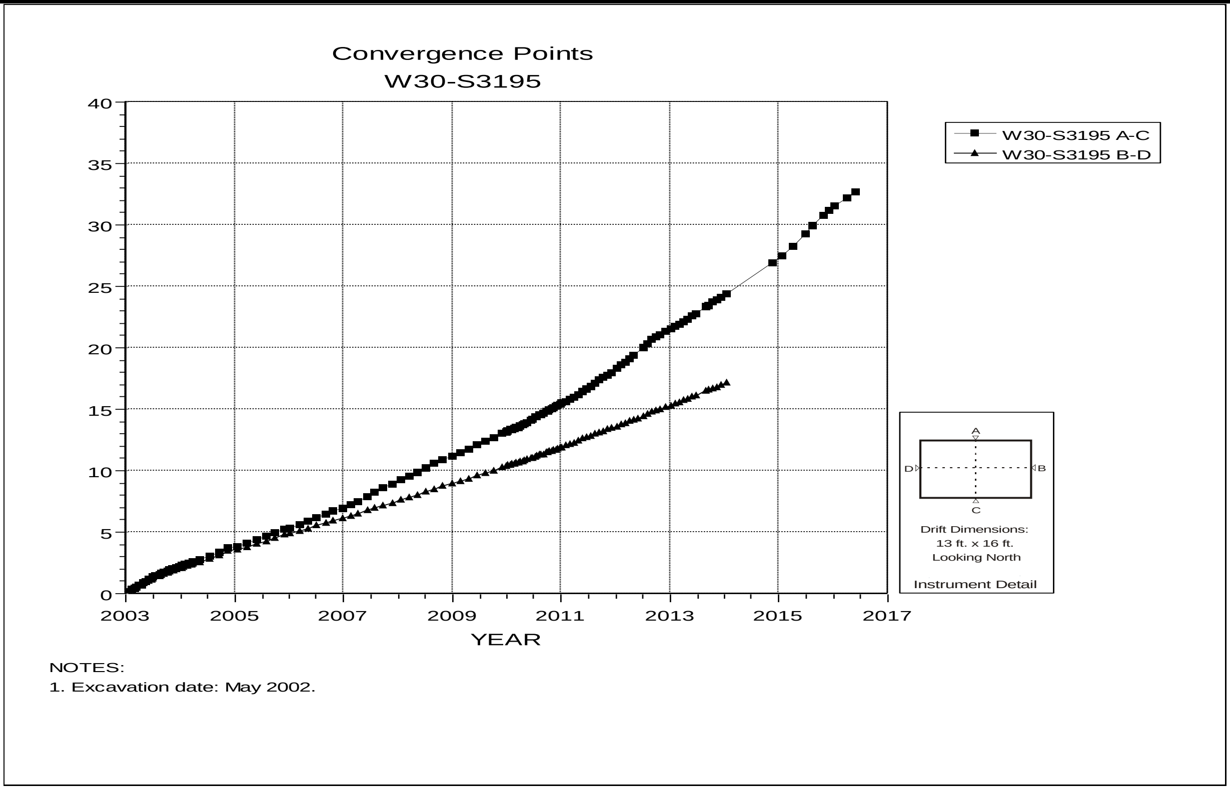

Figure 4-205 Convergence Point Array –
W30 S3195 – All Chords

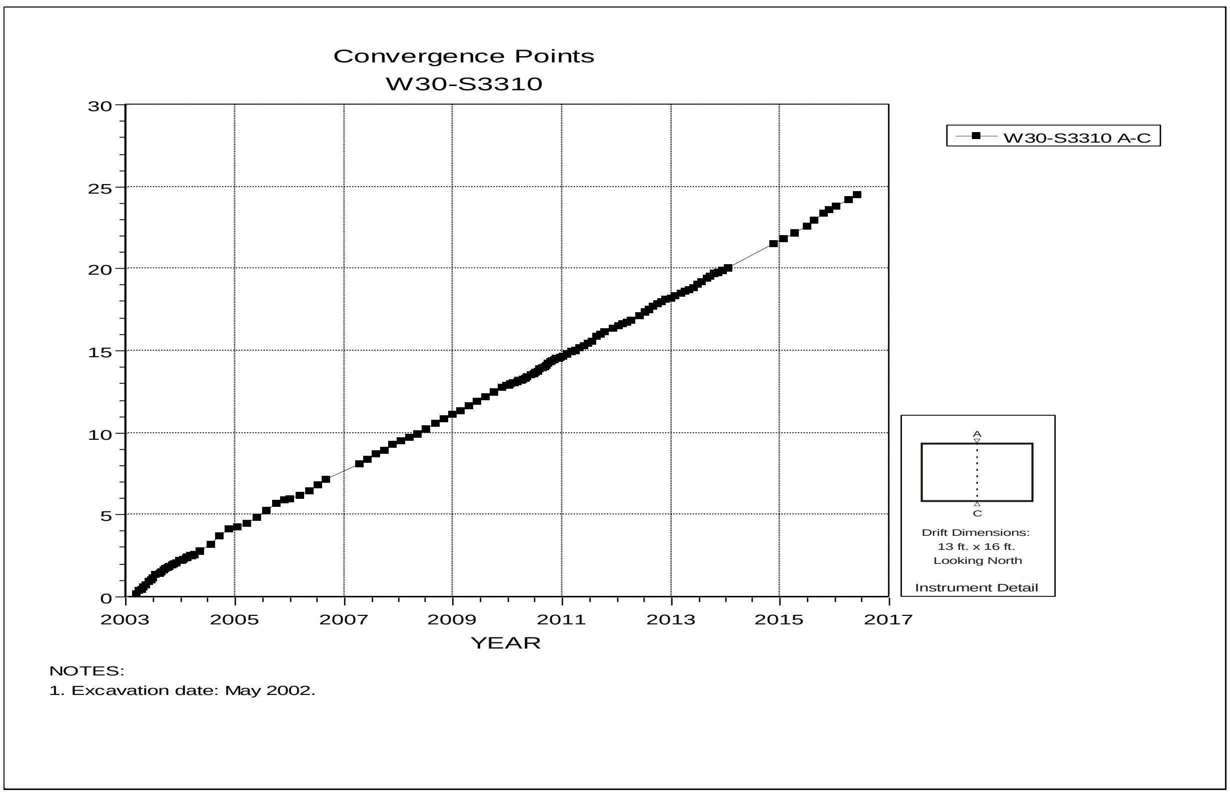

Figure 4-206 Convergence Point Array –
W30 S3310 – Roof to Floor

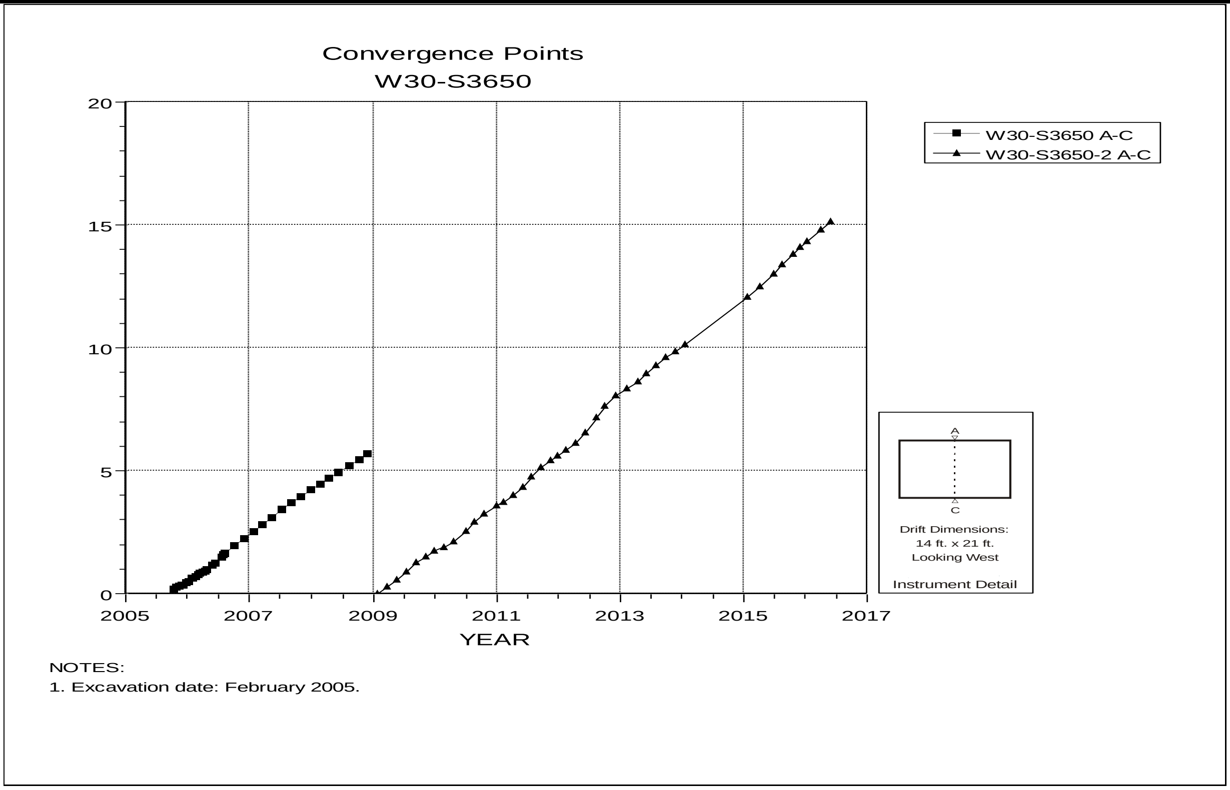

Figure 4-207 Convergence Point Array –
W30 S3650 – Roof to Floor

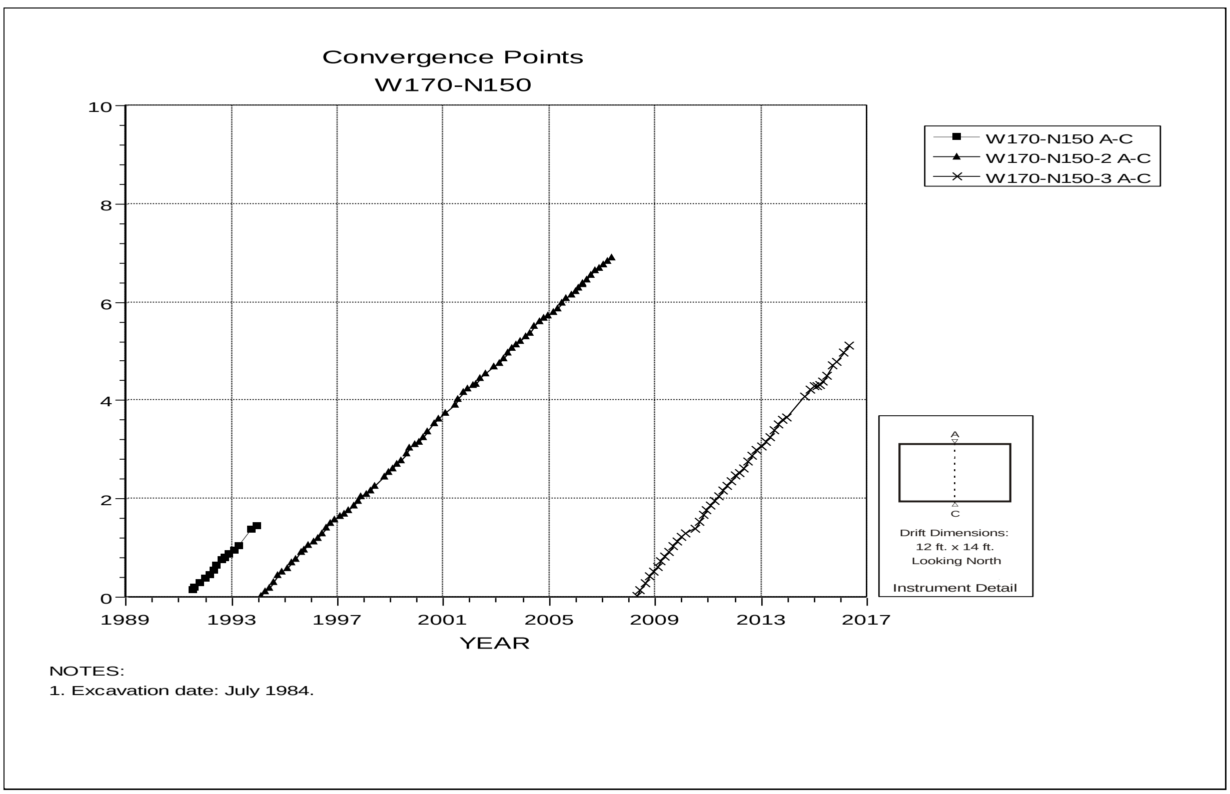

Figure 4-208 Convergence Point Array –
W170 N150 – Roof to Floor

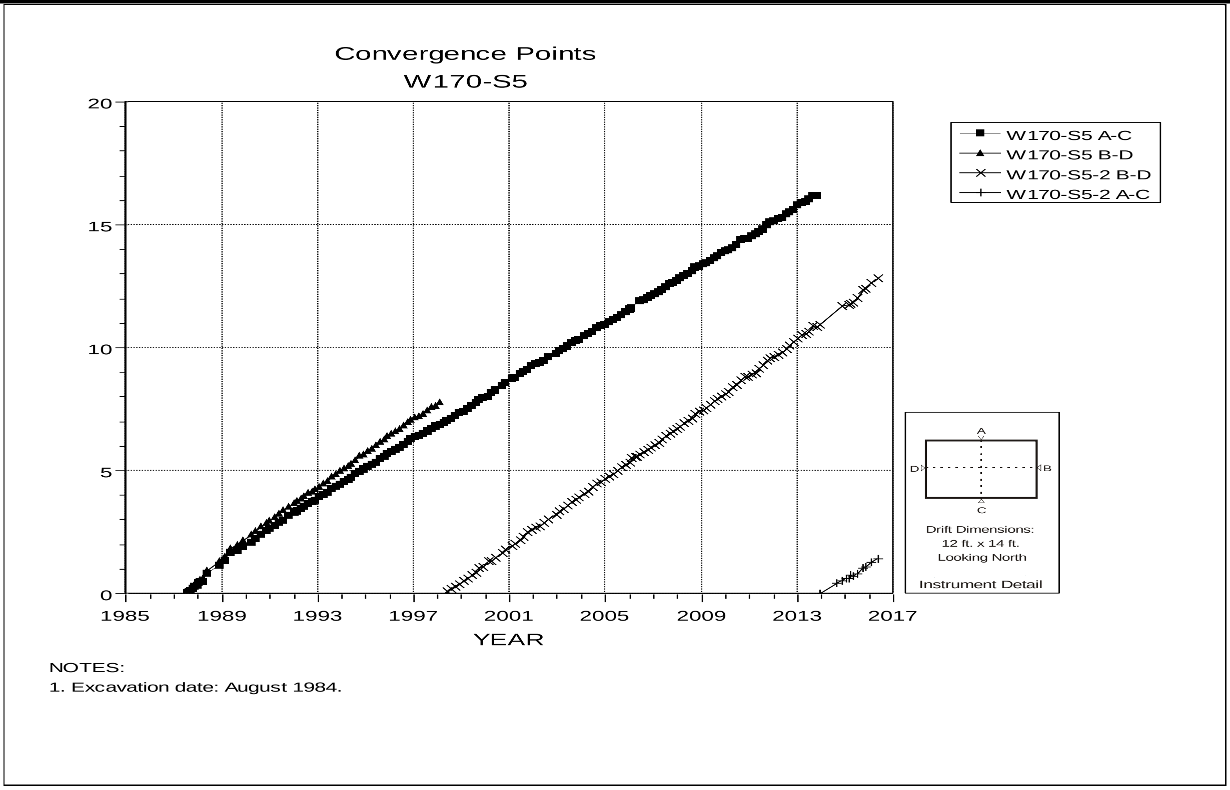

Figure 4-209 Convergence Point Array –
W170 S5 – All Chords

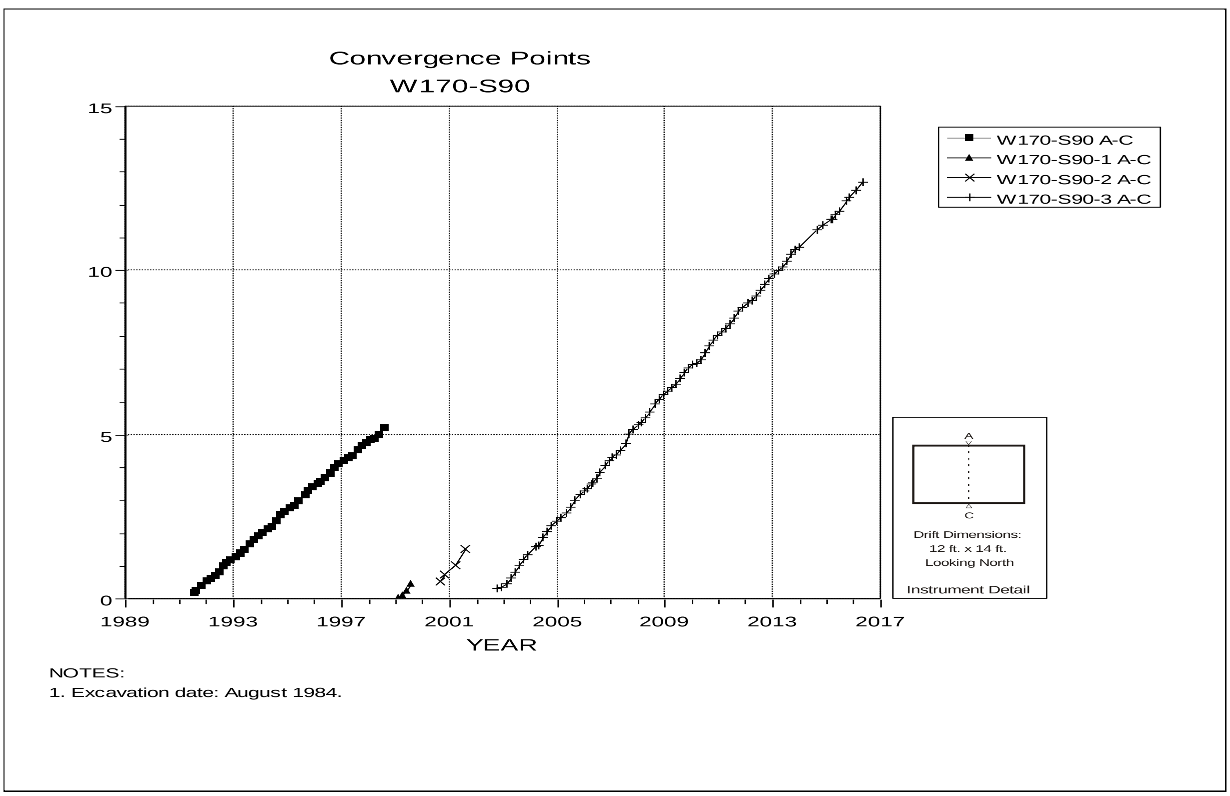

Figure 4-210 Convergence Point Array –
W170 S90 – Roof to Floor

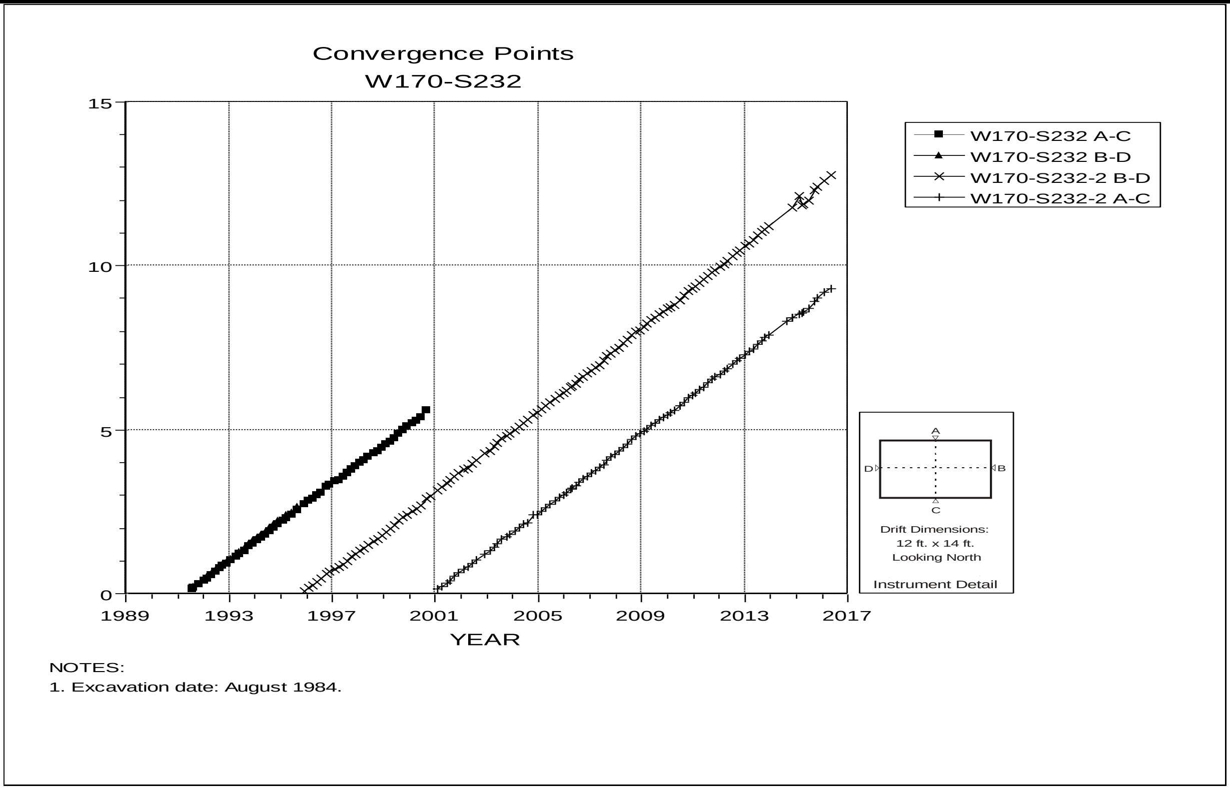

Figure 4-211 Convergence Point Array –
W170 S232 – All Chords

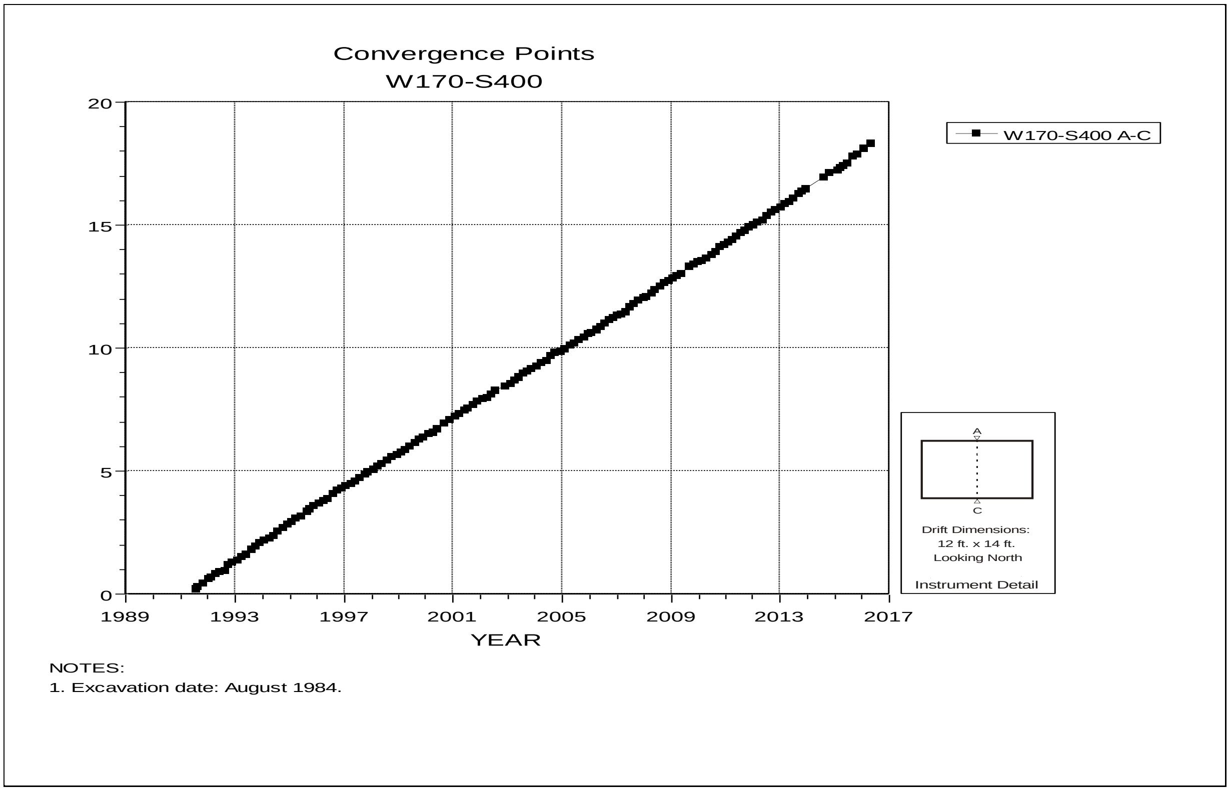

Figure 4-212 Convergence Point Array –
W170 S400 – Roof to Floor

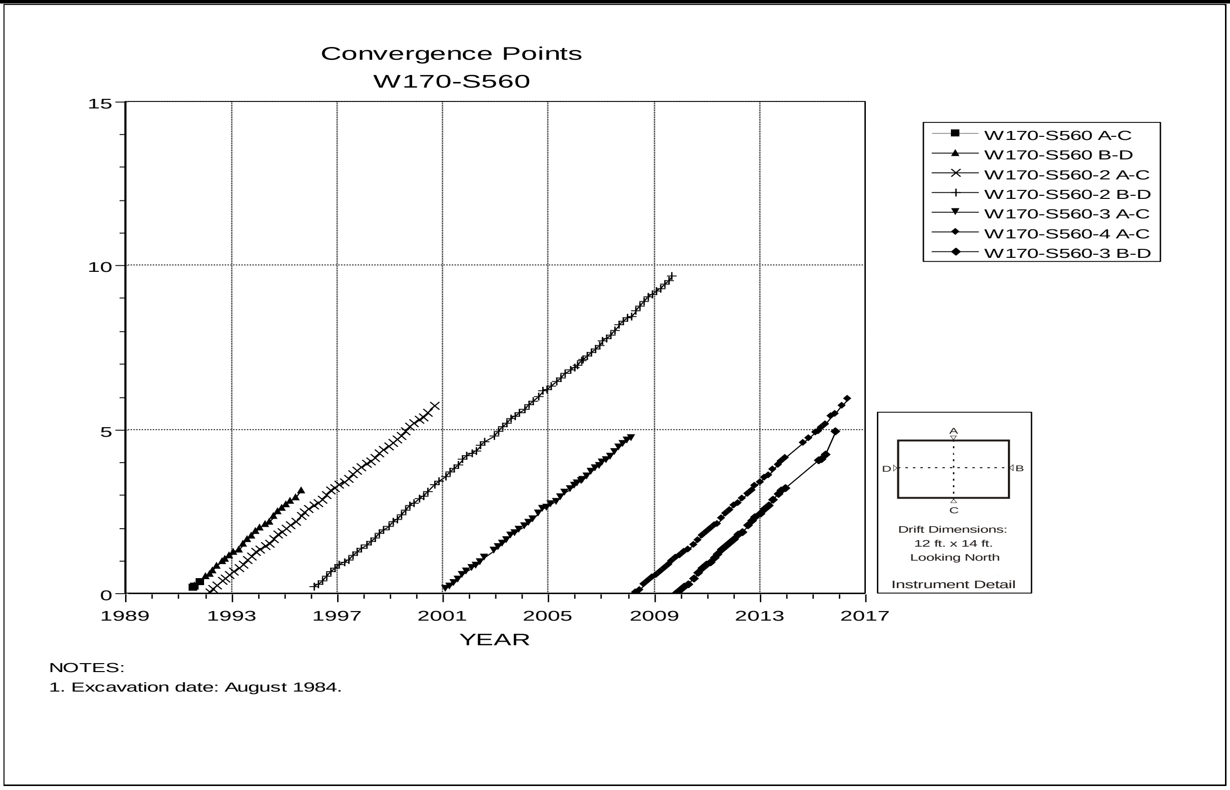

Figure 4-213 Convergence Point Array –
W170 S560 – All Chords

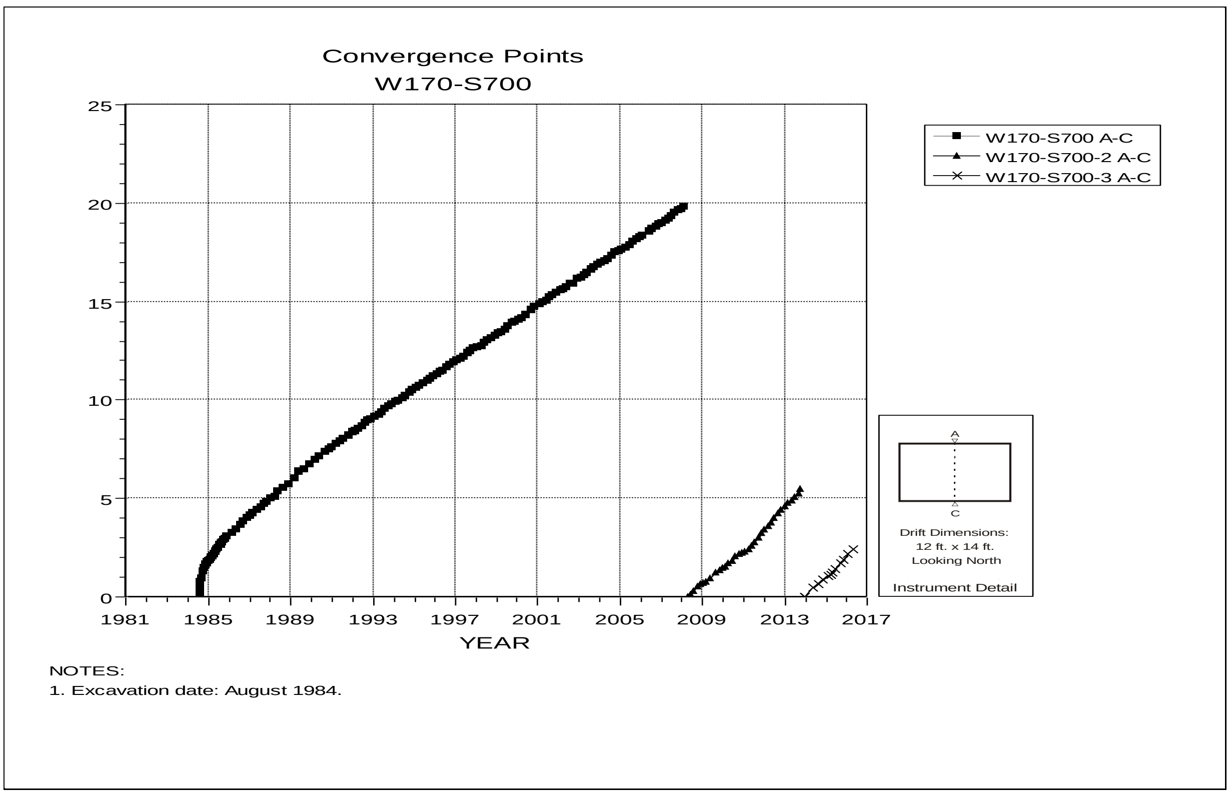

Figure 4-214 Convergence Point Array –
W170 S700 – Roof to Floor

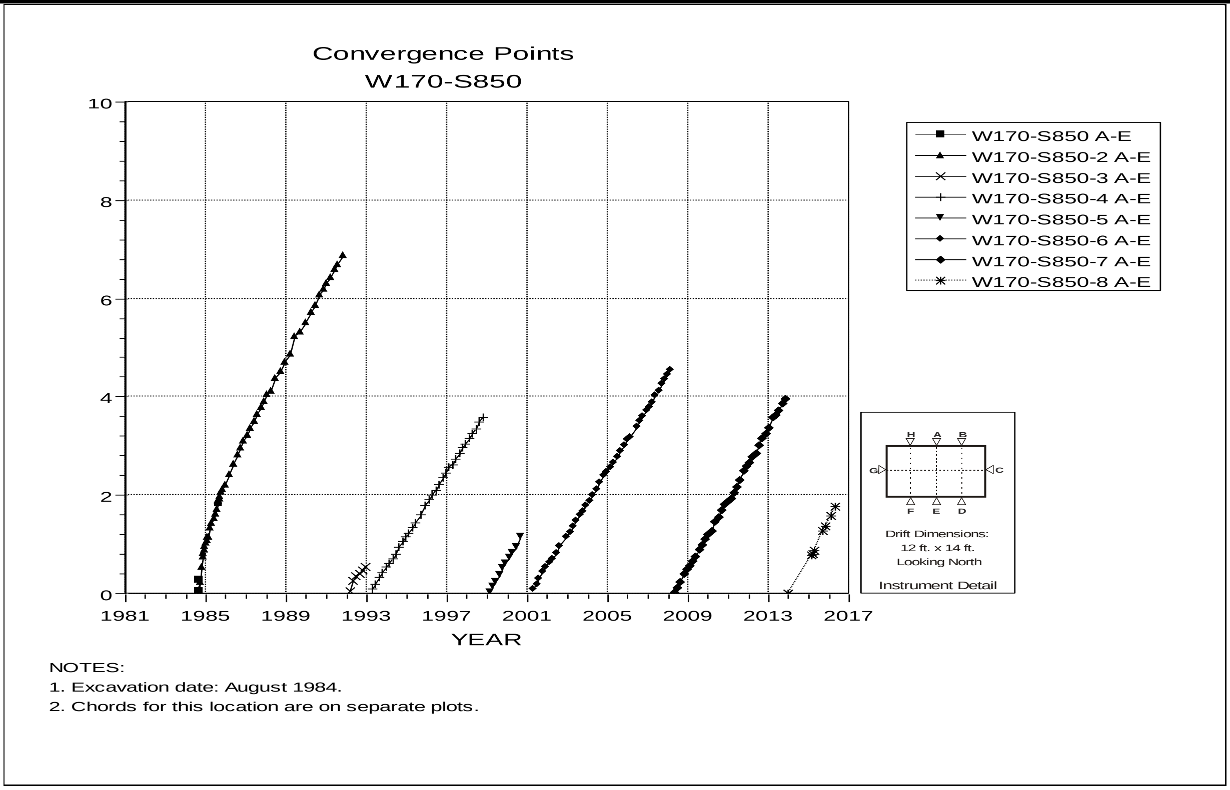

Figure 4-215 Convergence Point Array –
W170 S850 – Roof to Floor – Centerline

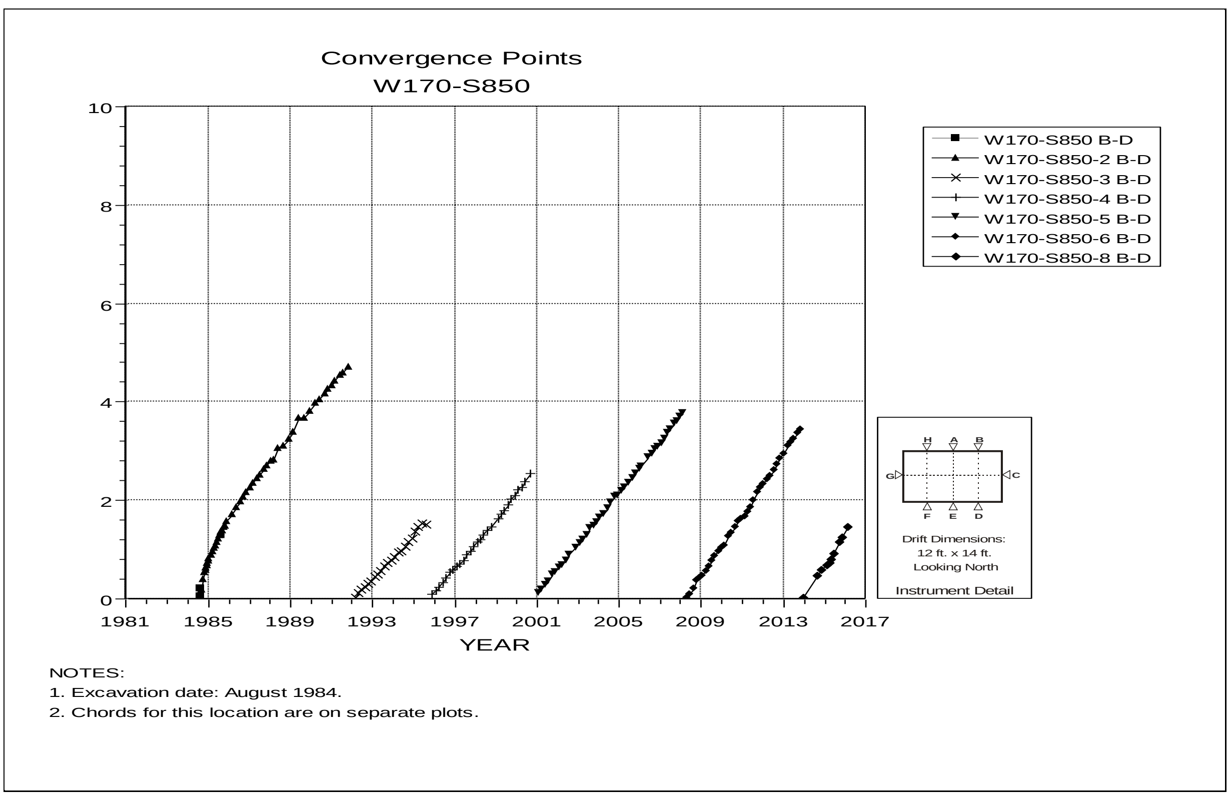

Figure 4-216 Convergence Point Array –
W170 S850 – Roof to Floor – East Quarter Point

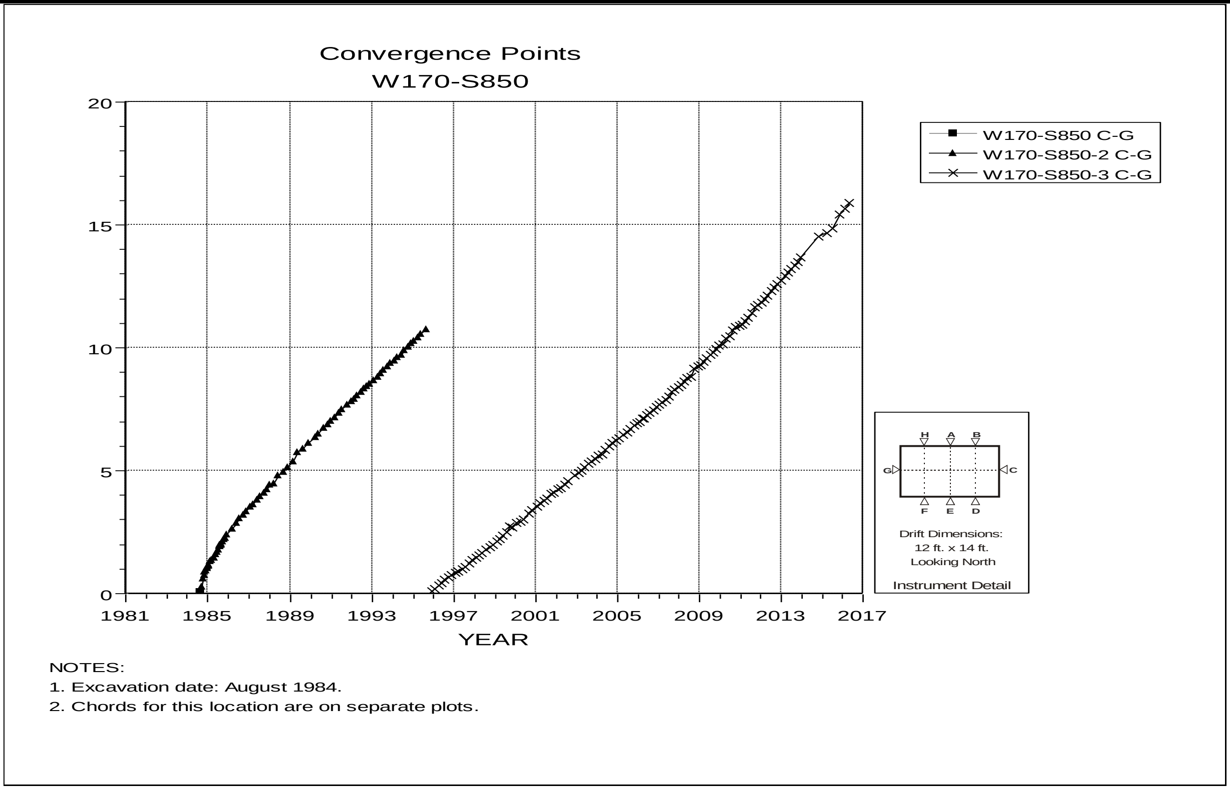

Figure 4-217 Convergence Point Array –
W170 S850 – Rib to Rib

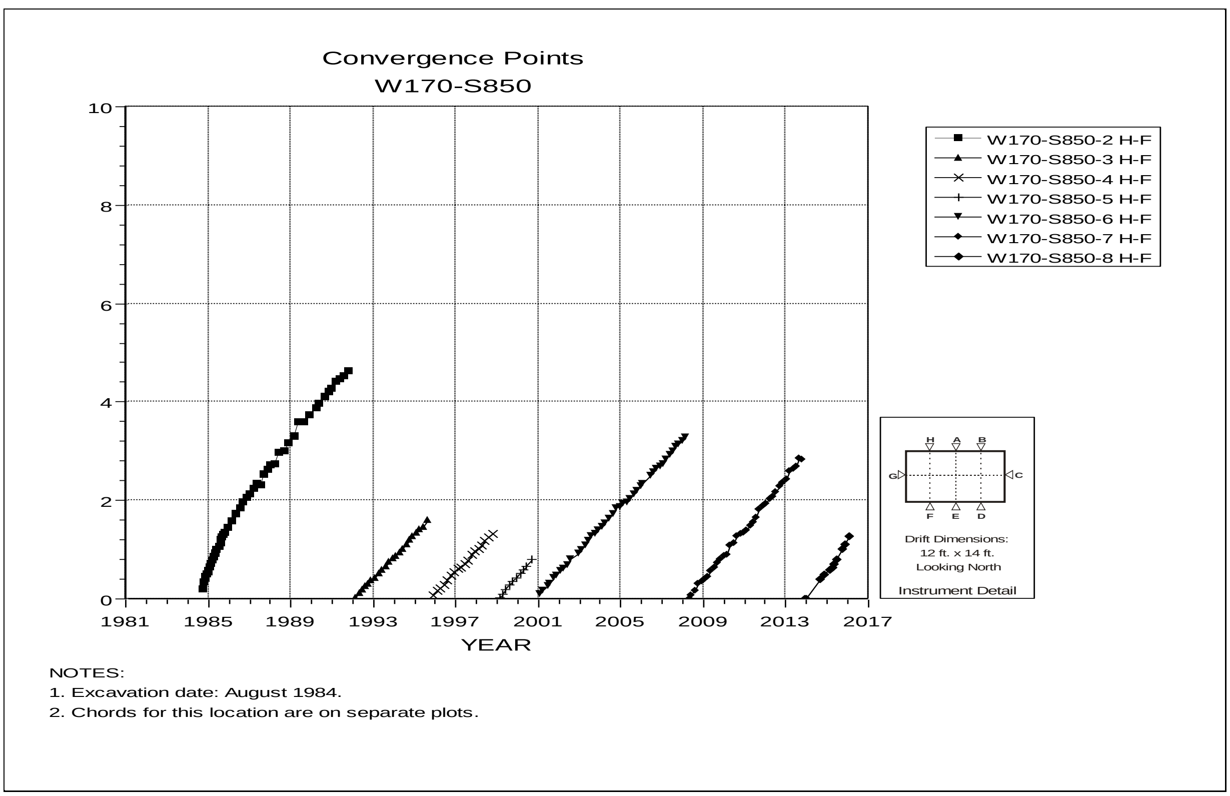

Figure 4-218 Convergence Point Array –
W170 S850 – Roof to Floor – West Quarter Point

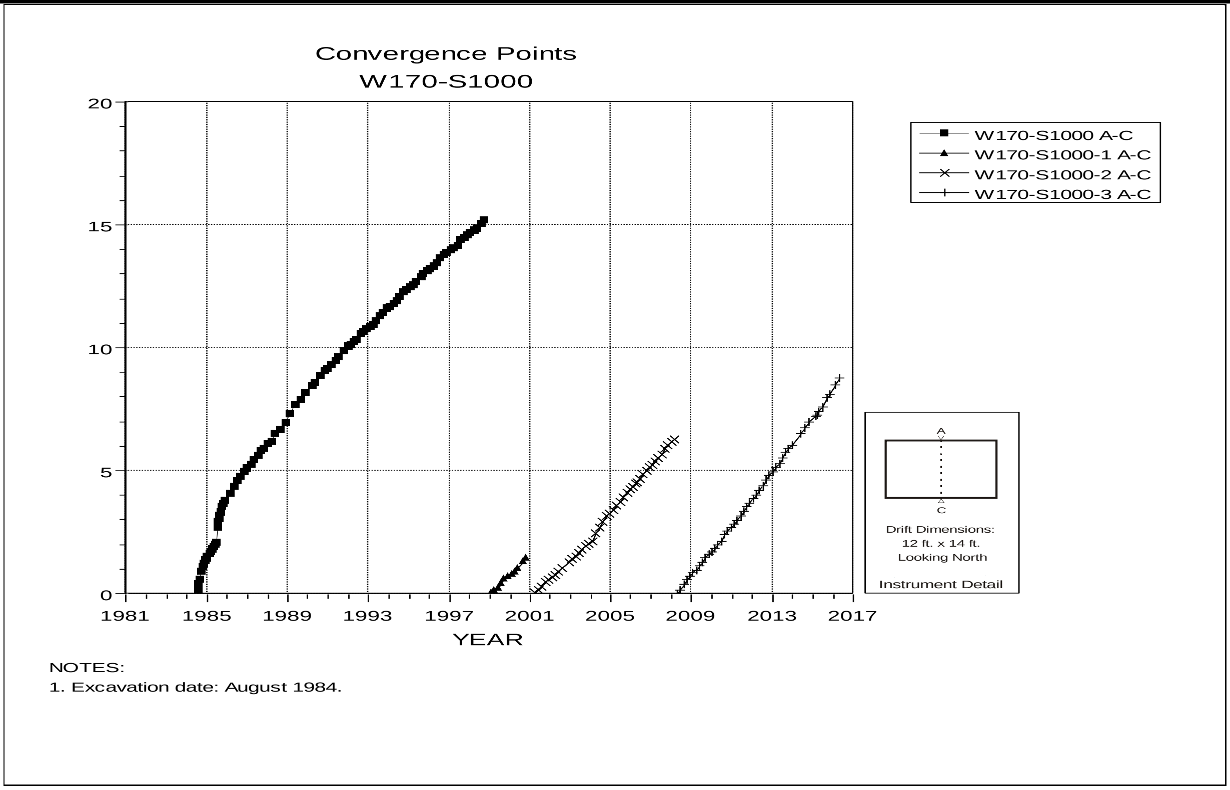

Figure 4-219 Convergence Point Array –
W170 S1000 – Roof to Floor

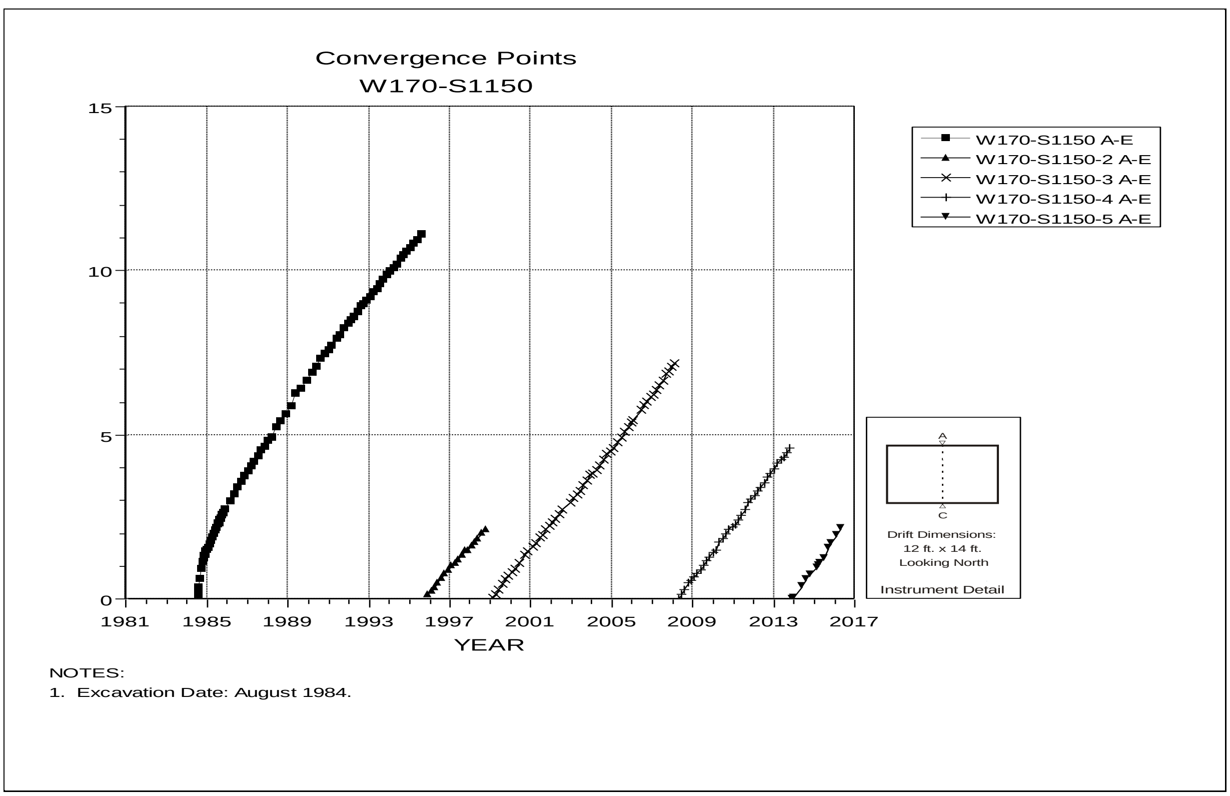

Figure 4-220 Convergence Point Array –
W170 S1150 – Roof to Floor – Centerline

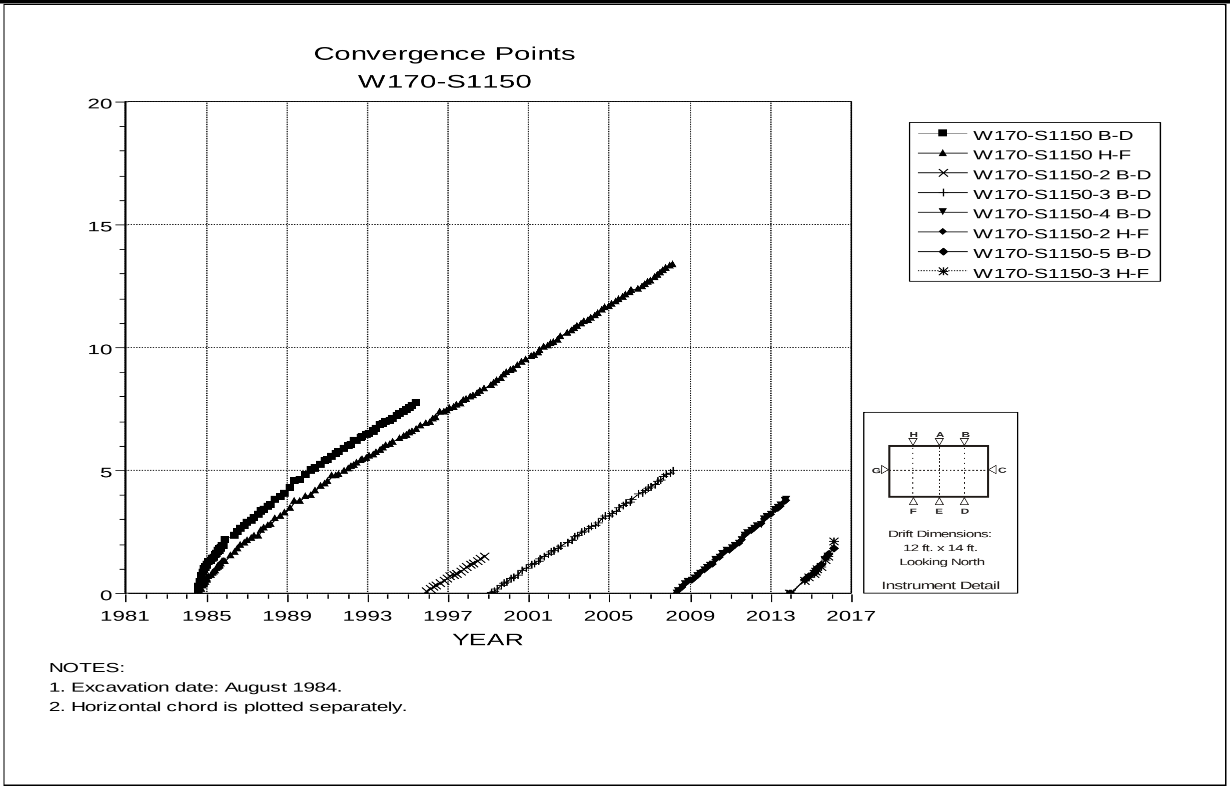

Figure 4-221 Convergence Point Array –
W170 S1150 – Roof to Floor – East Quarter Point

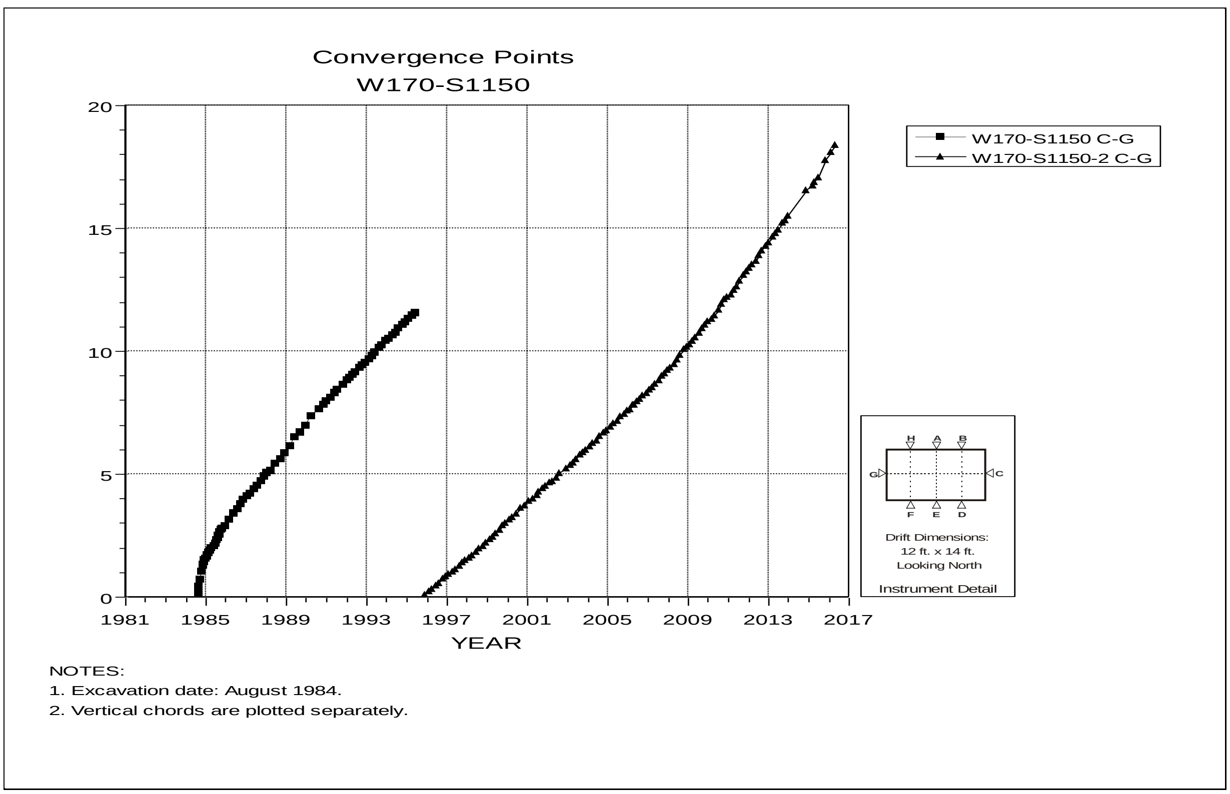

Figure 4-222 Convergence Point Array –
W170 S1150 – Rib to Rib

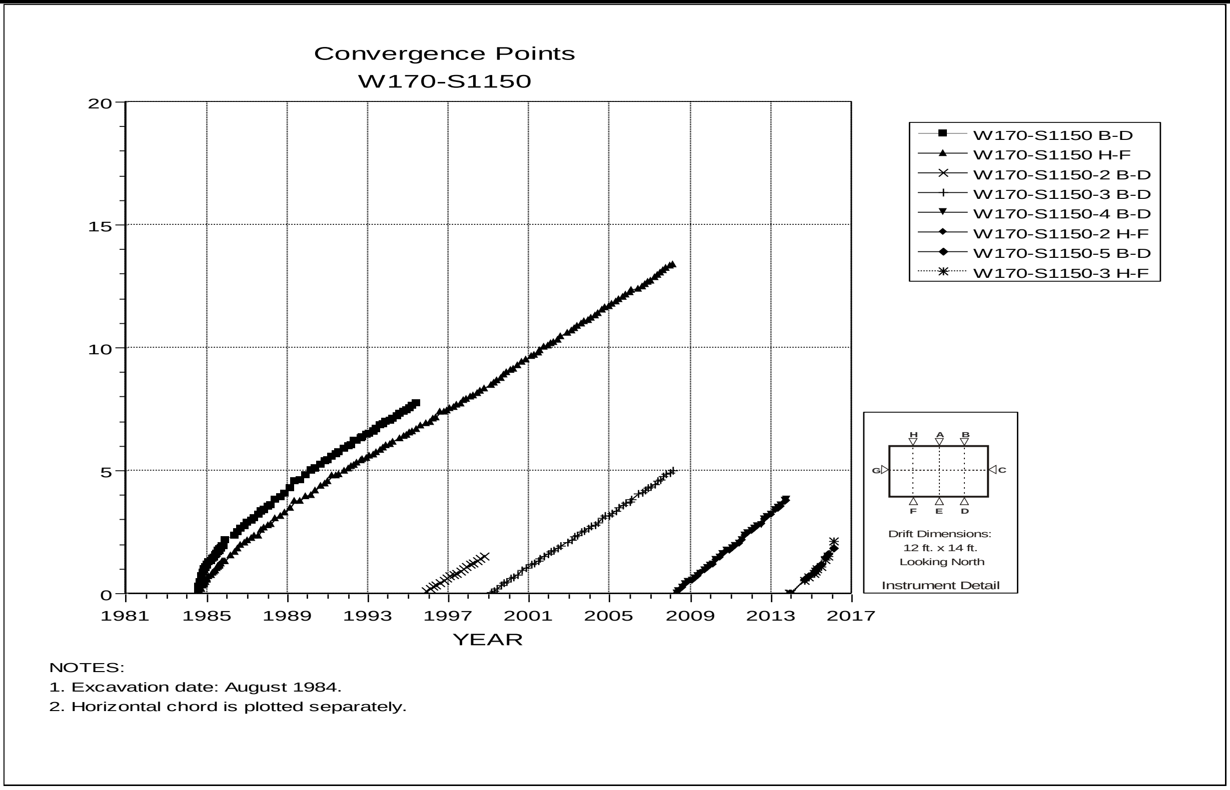

Figure 4-223 Convergence Point Array –
W170 S1150 – Roof to Floor – West Quarter Point

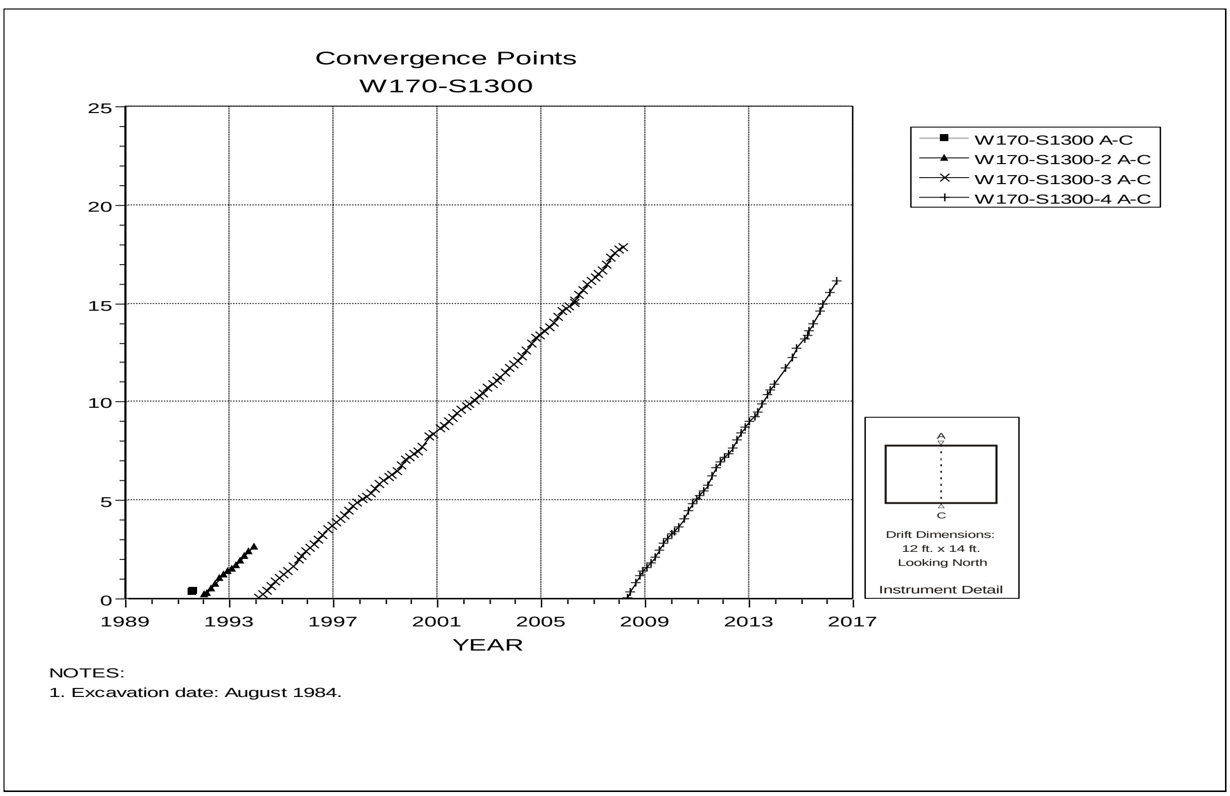

Figure 4-224 Convergence Point Array –
W170 S1300 – Roof to Floor

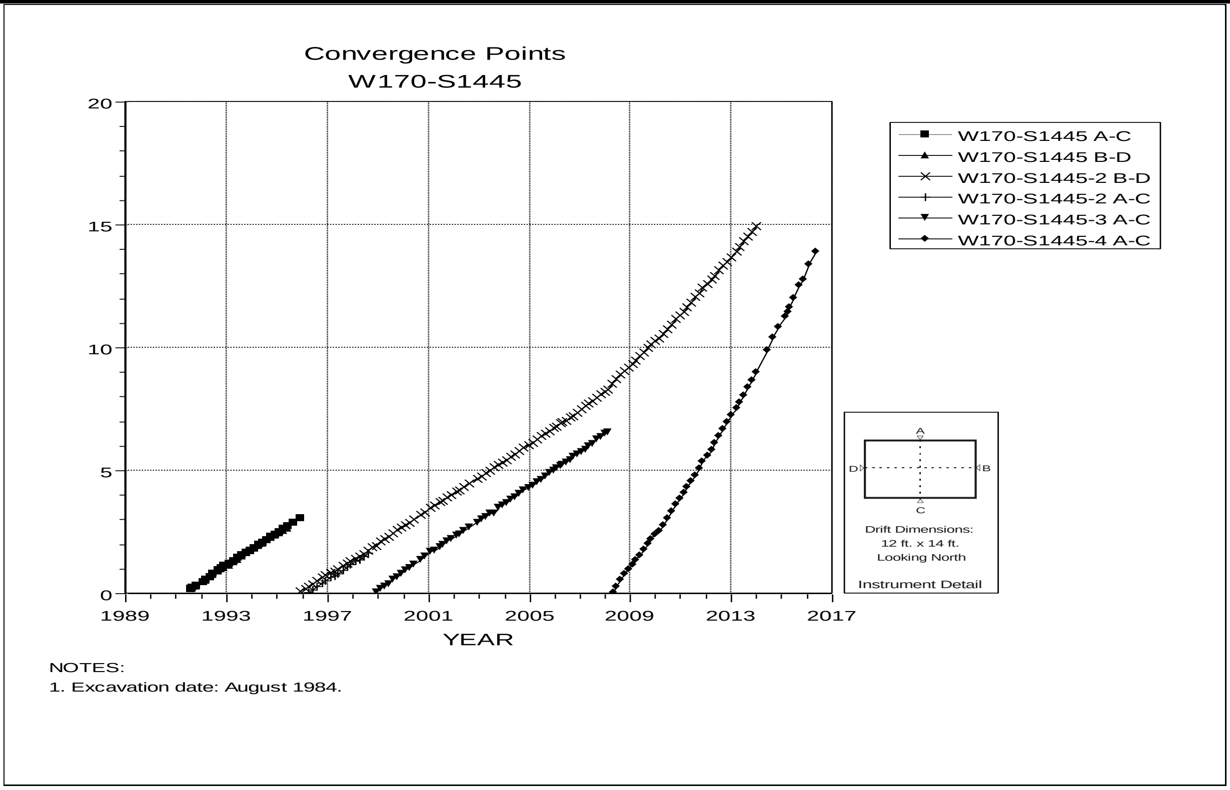

Figure 4-225 Convergence Point Array –
W170 S1445 – All Chords

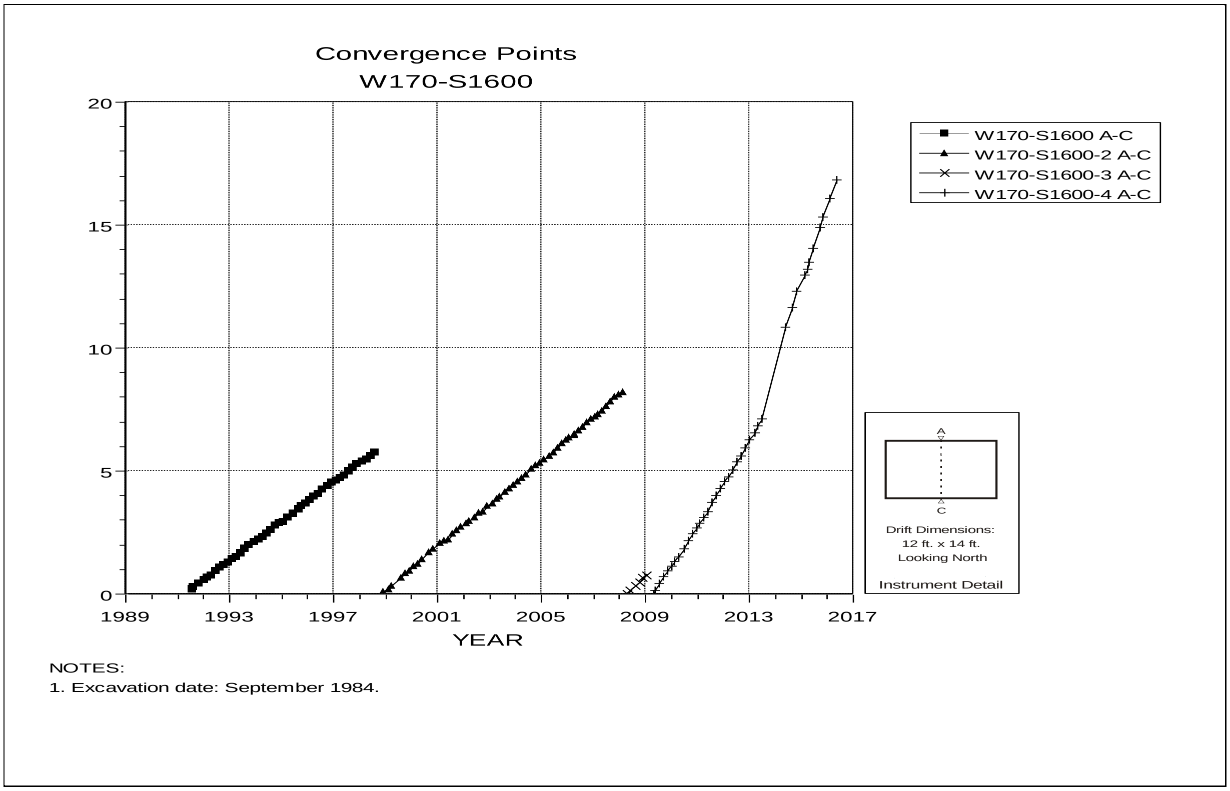

Figure 4-226 Convergence Point Array –
W170 S1600 – Roof to Floor

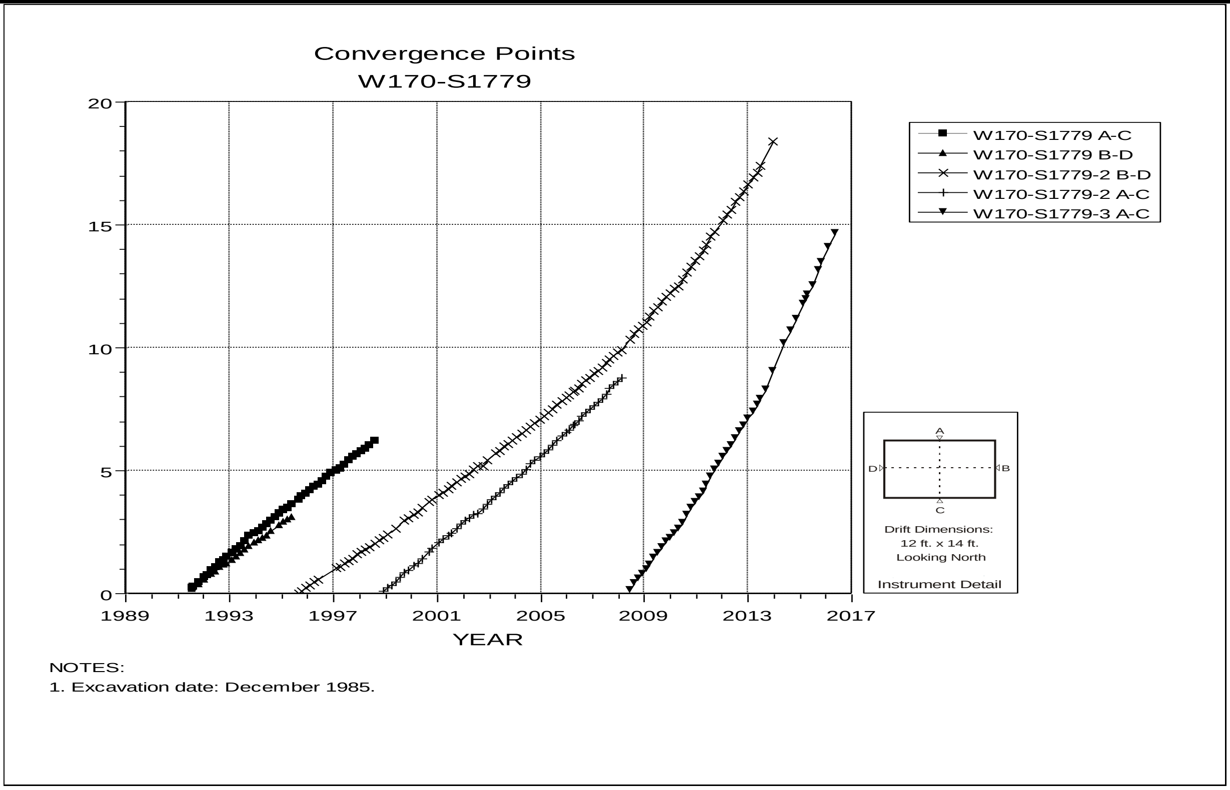

Figure 4-227 Convergence Point Array –
W170 S1779 – All Chords

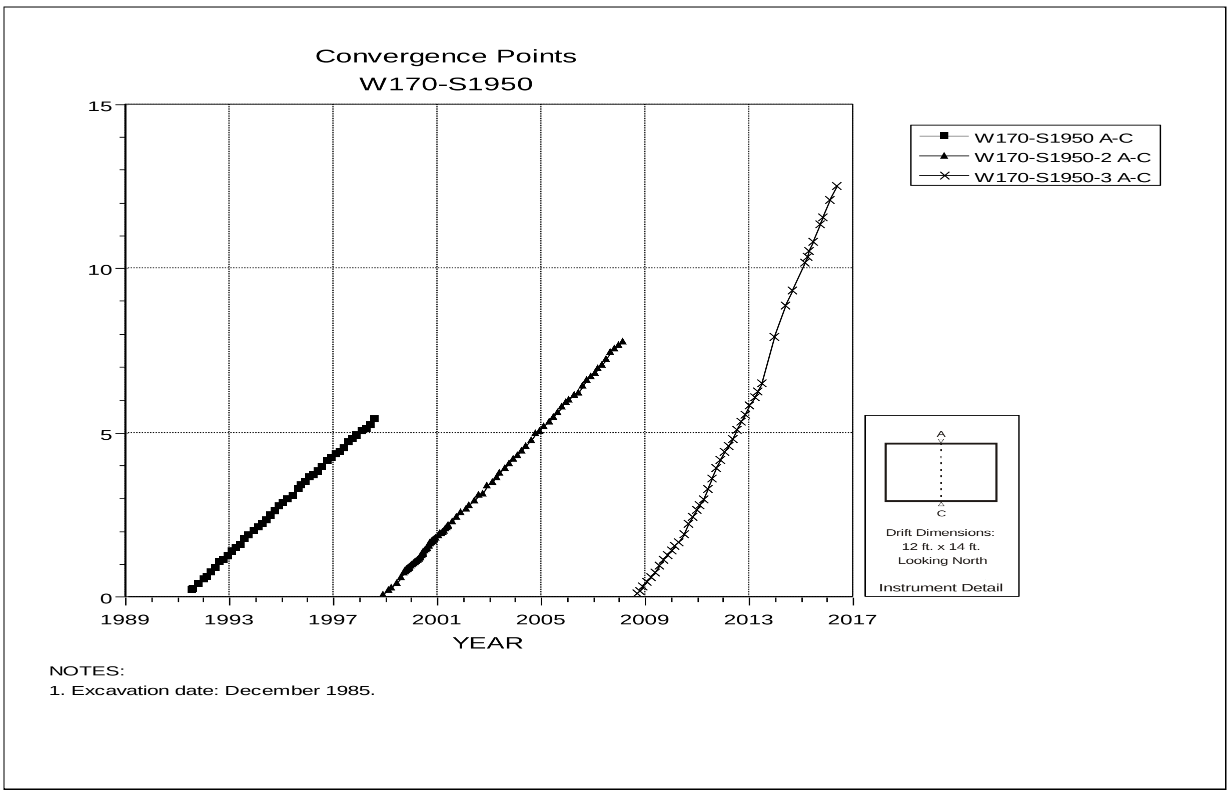

Figure 4-228 Convergence Point Array –
W170 S1950 – Roof to Floor

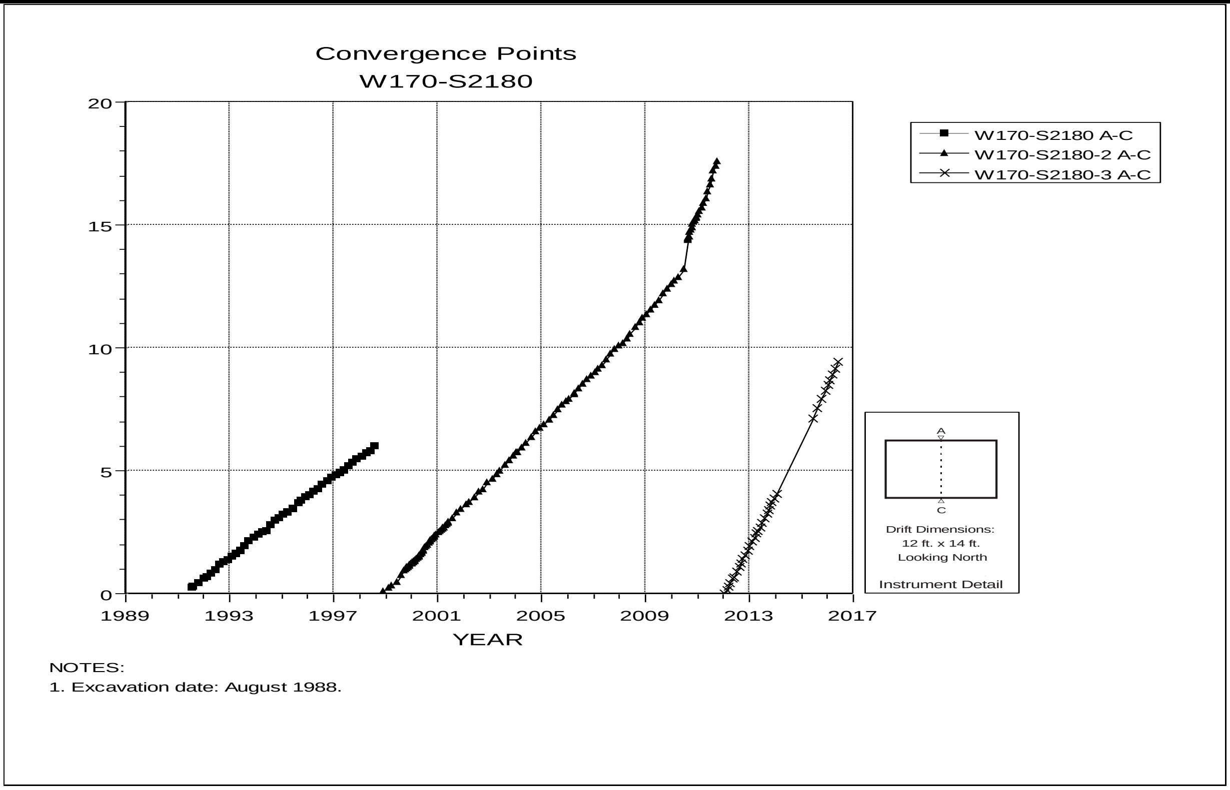

Figure 4-229 Convergence Point Array –
W170 S2180 – Roof to Floor

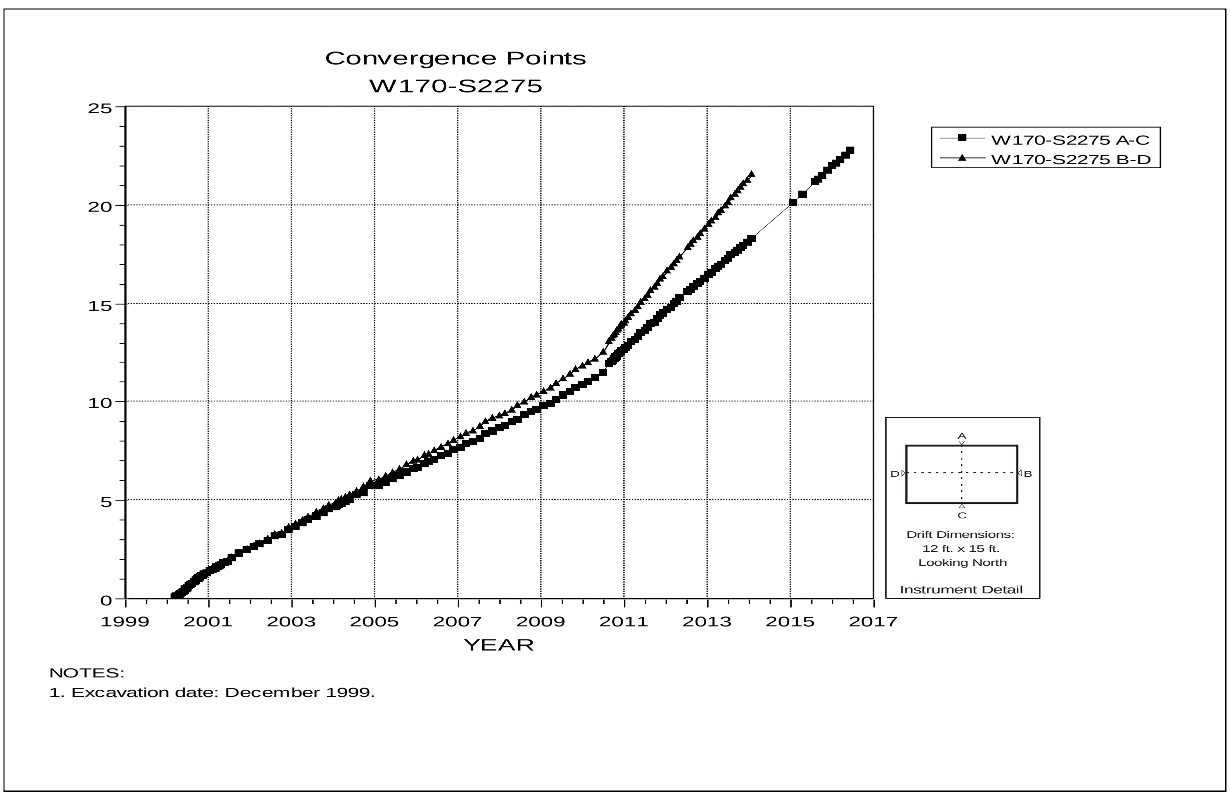

Figure 4-230 Convergence Point Array –
W170 S2275 – All Chords

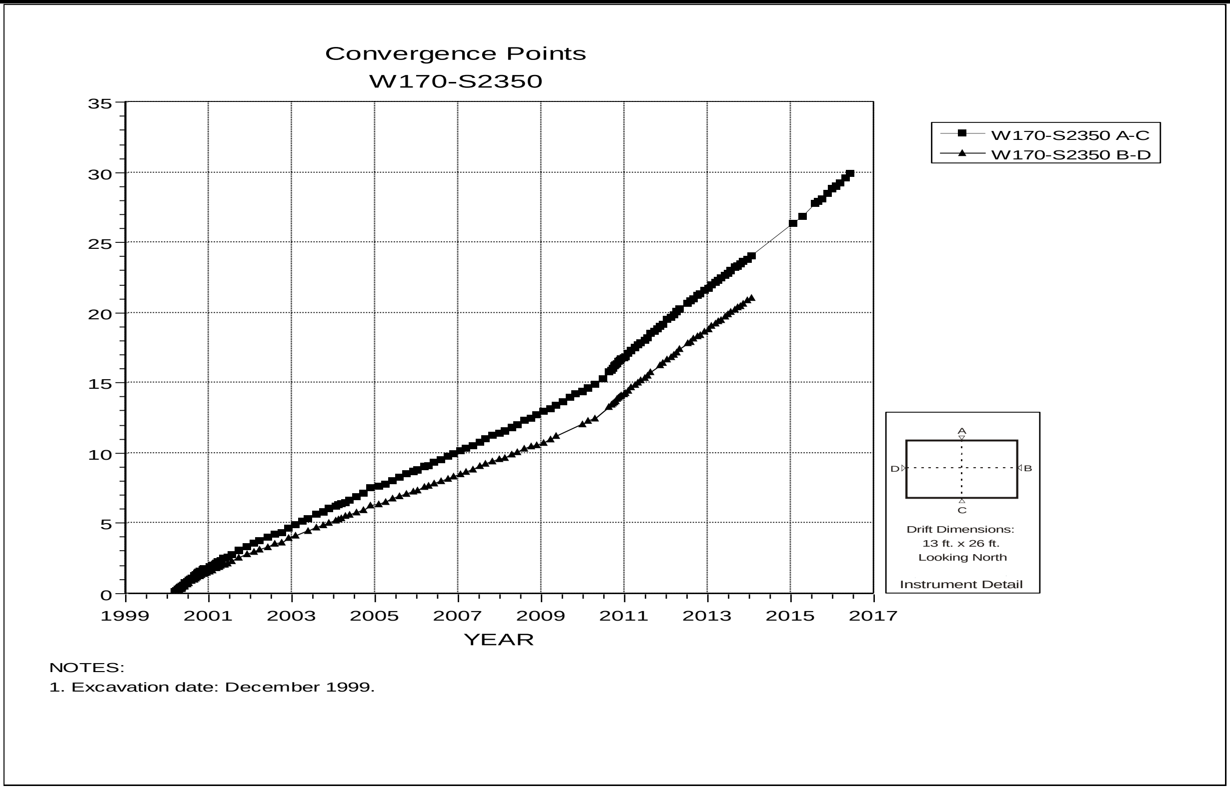

Figure 4-231 Convergence Point Array –
W170 S2350 – All Chords

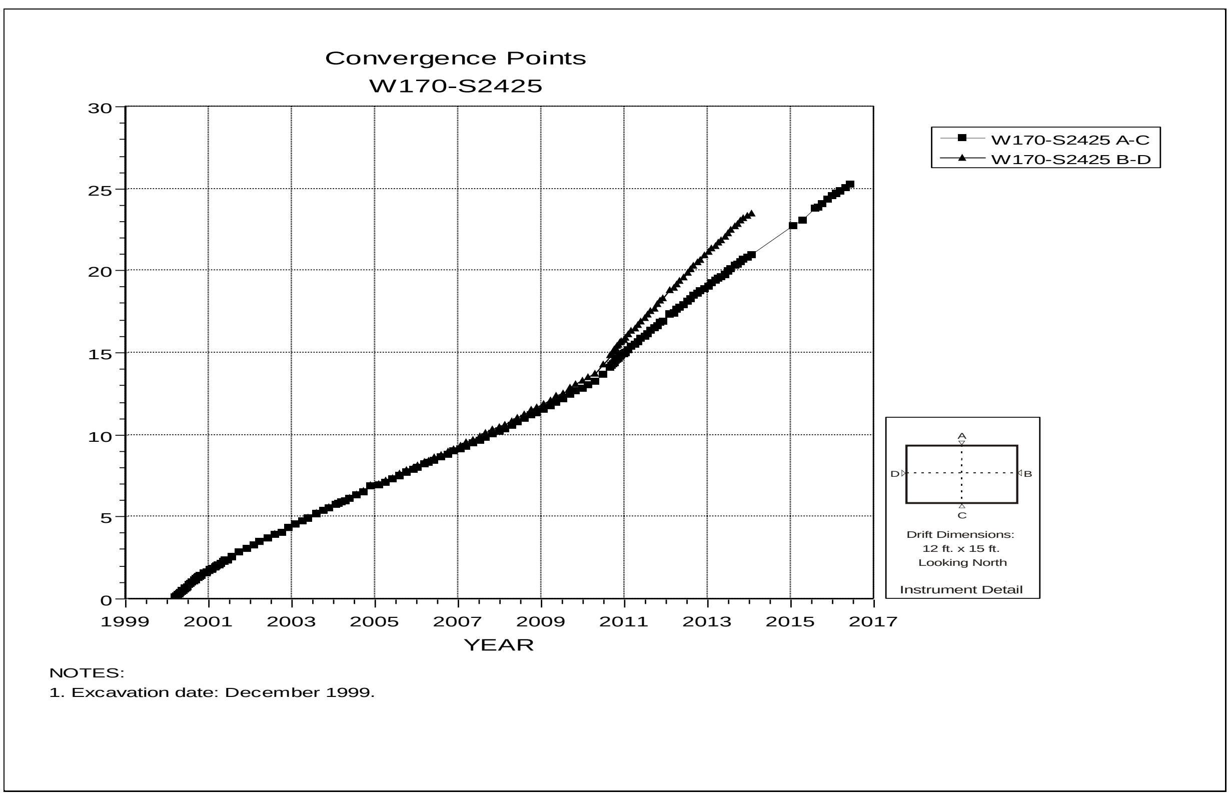

Figure 4-232 Convergence Point Array –
W170 S2425 – All Chords

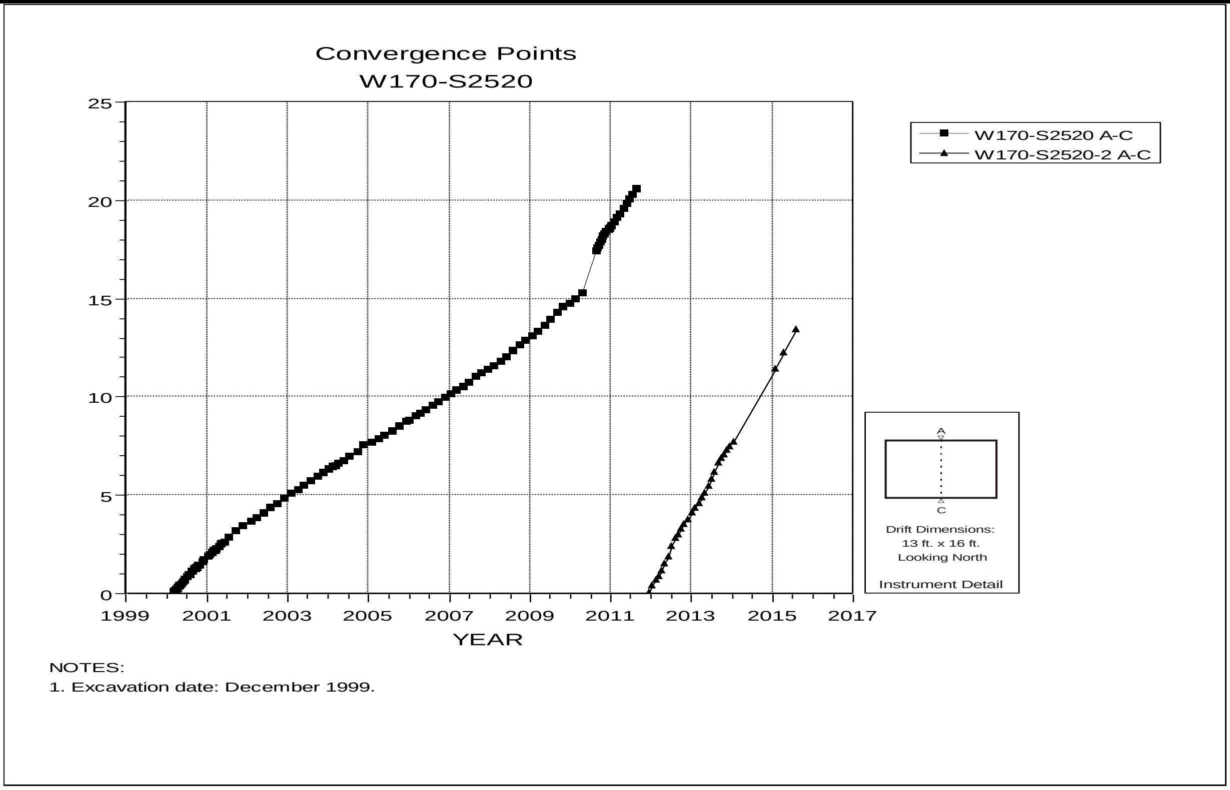

Figure 4-233 Convergence Point Array –
W170 S2520 – Roof to Floor

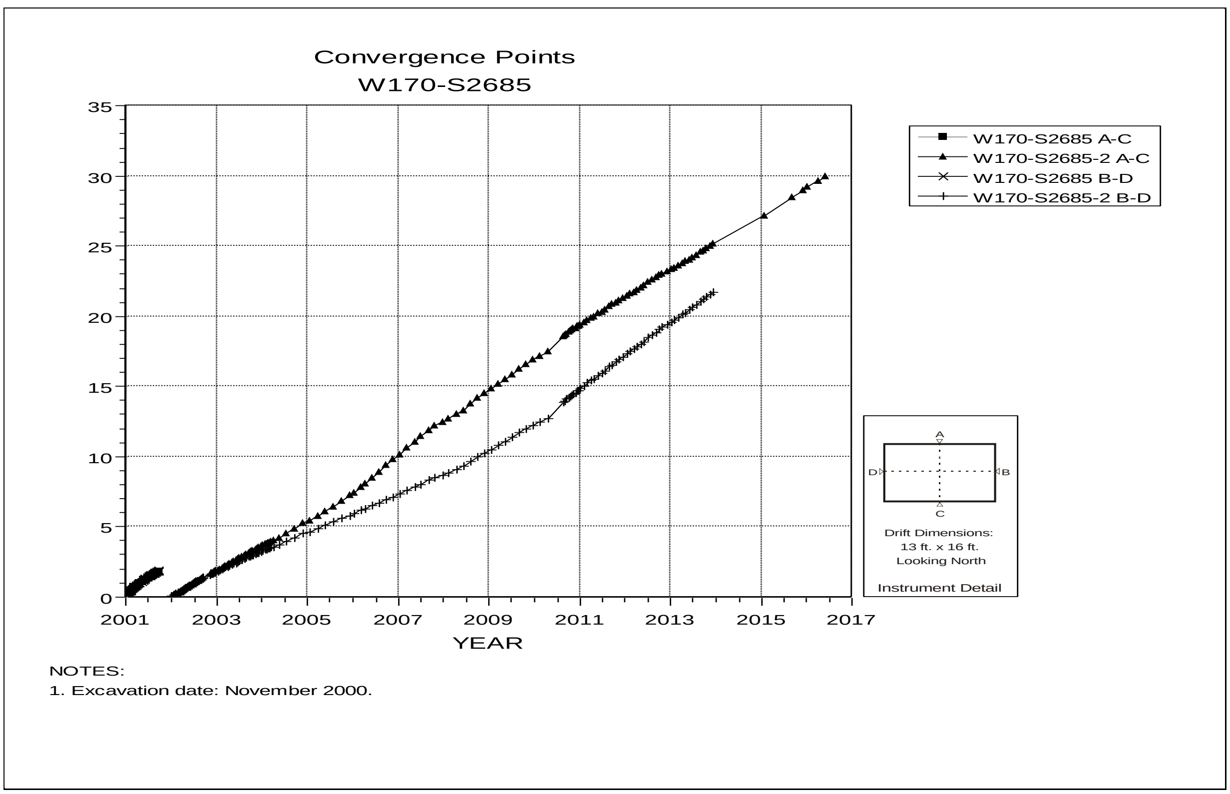

Figure 4-234 Convergence Point Array –
W170 S2685 – All Chords

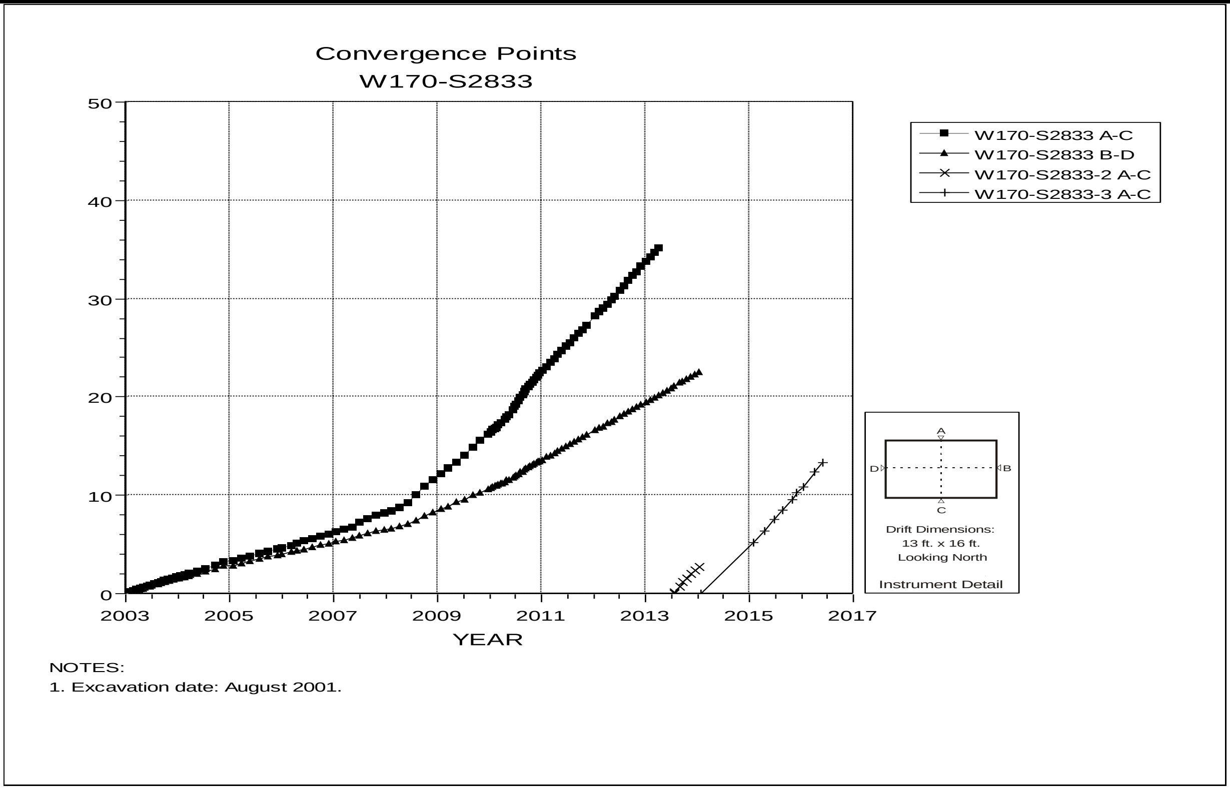

Figure 4-235 Convergence Point Array –
W170 S2833 – All Chords

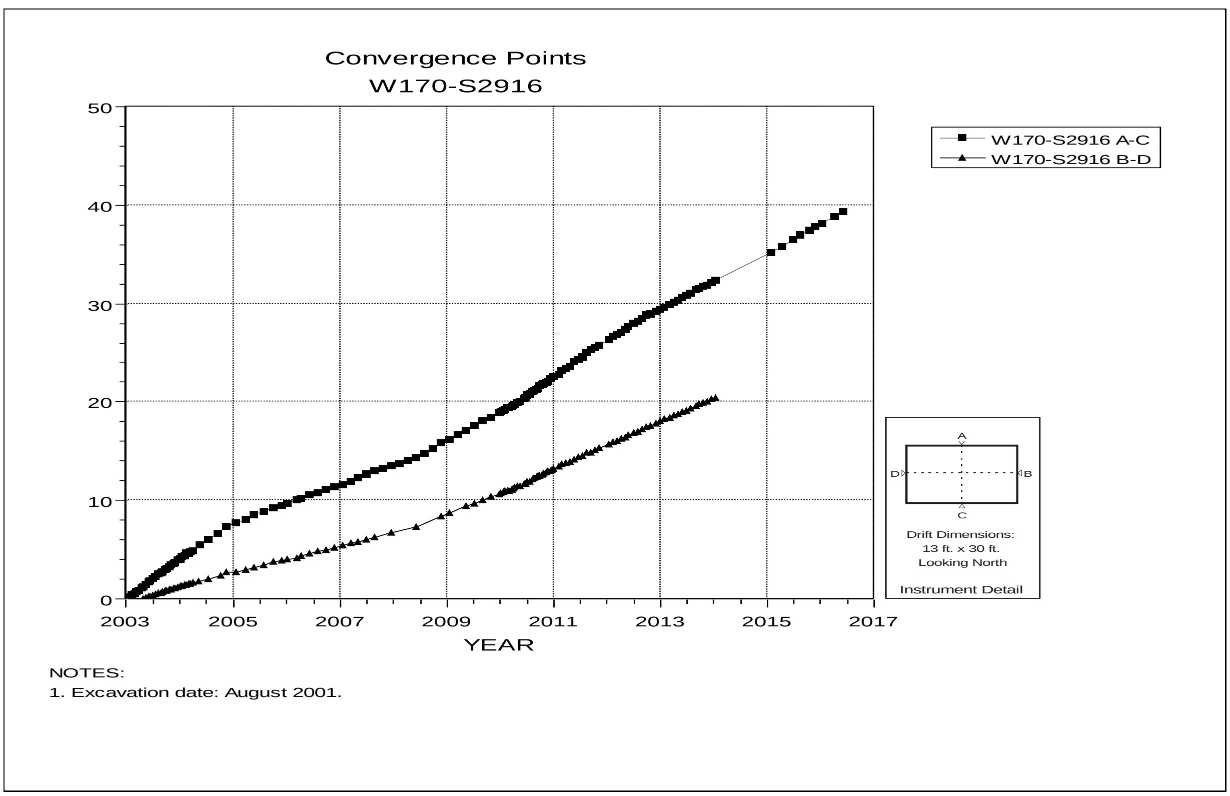

Figure 4-236 Convergence Point Array –
W170 S2916 – All Chords

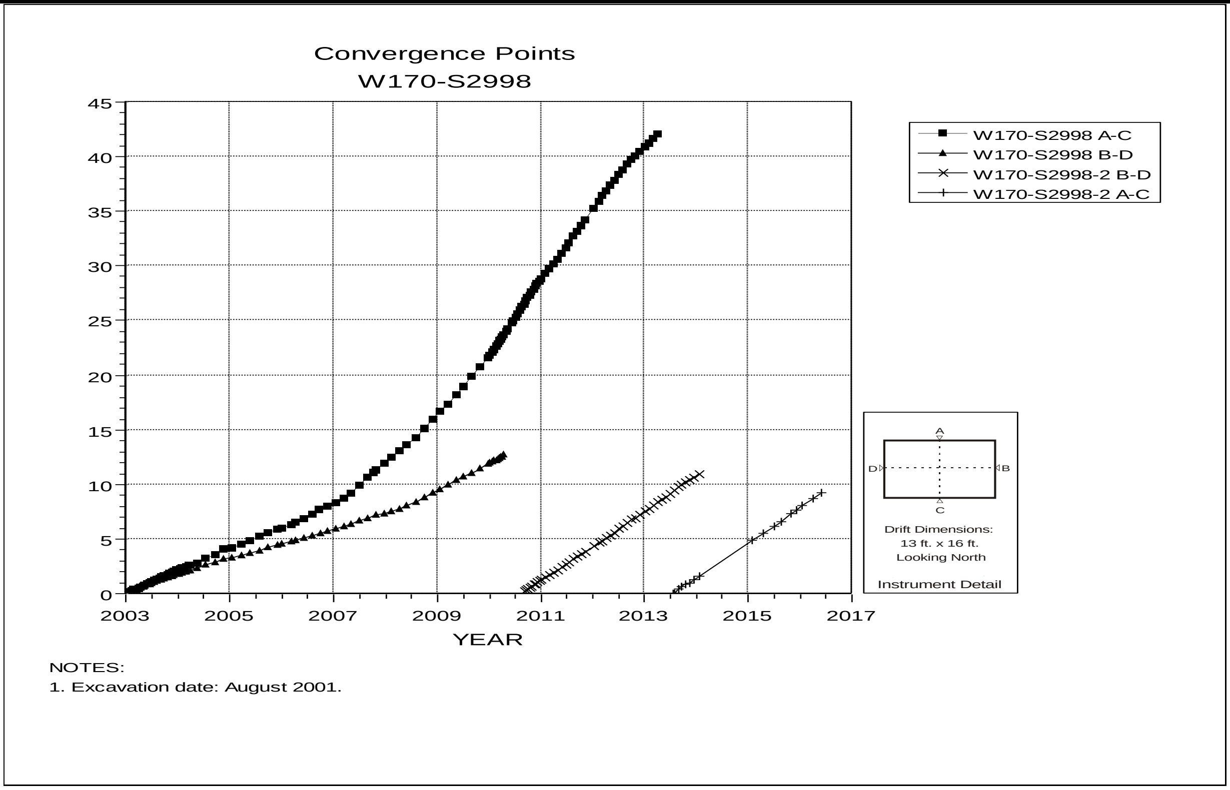

Figure 4-237 Convergence Point Array –
W170 S2998 – All Chords

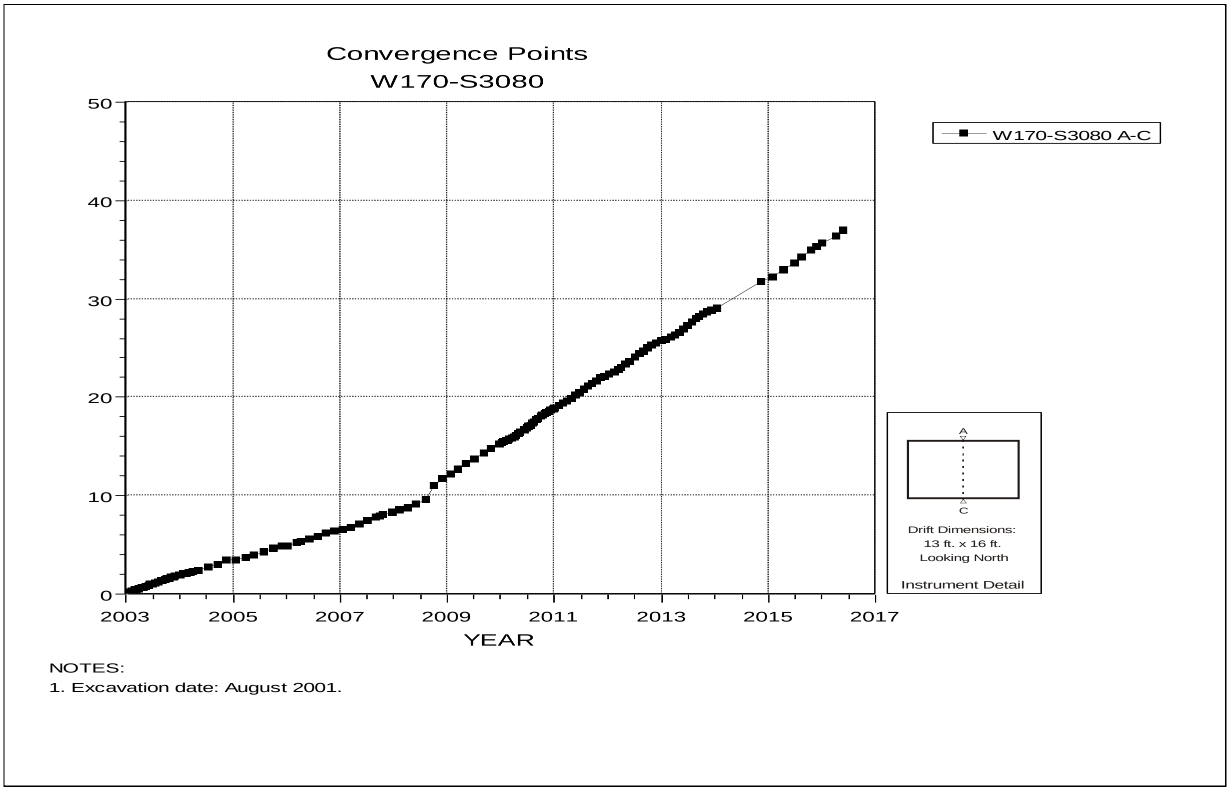

Figure 4-238 Convergence Point Array –
W170 S3080 – Roof to Floor

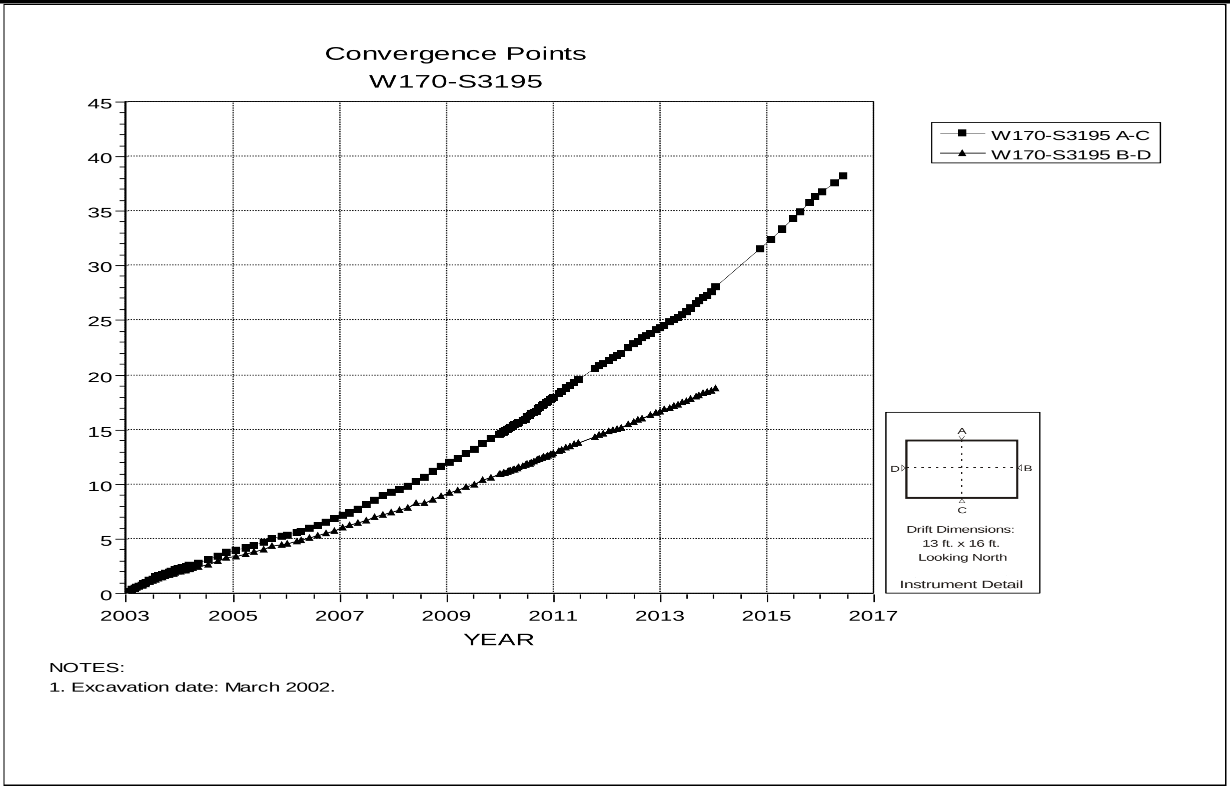

Figure 4-239 Convergence Point Array –
W170 S3195 – All Chords

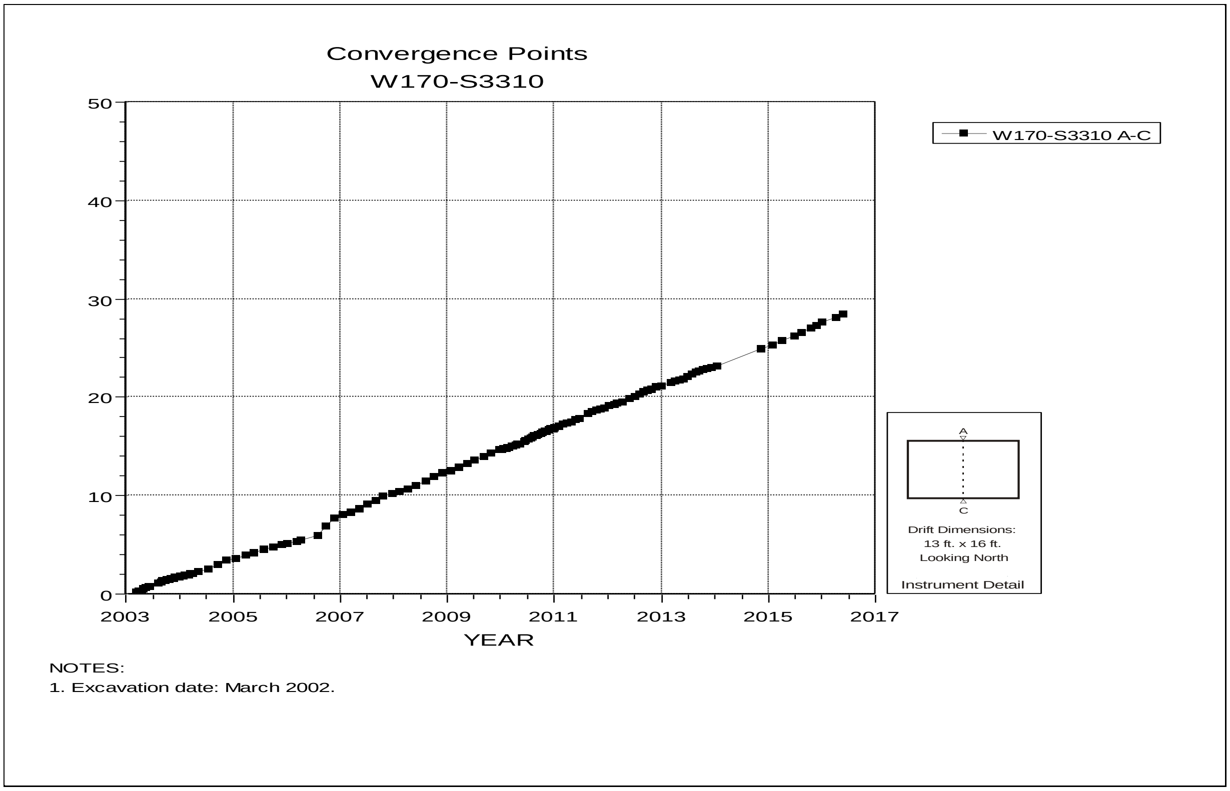

Figure 4-240 Convergence Point Array –
W170 S3310 – Roof to Floor

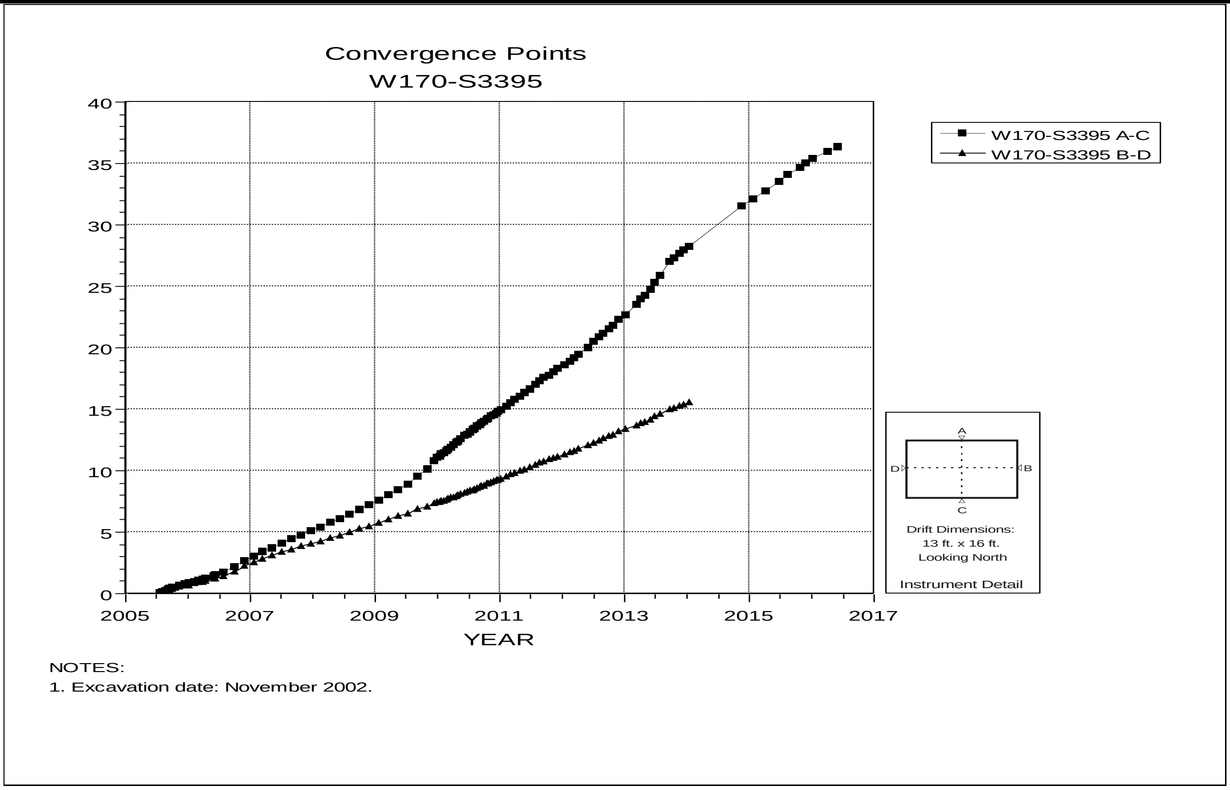

Figure 4-241 Convergence Point Array –
W170 S3395 – All Chords

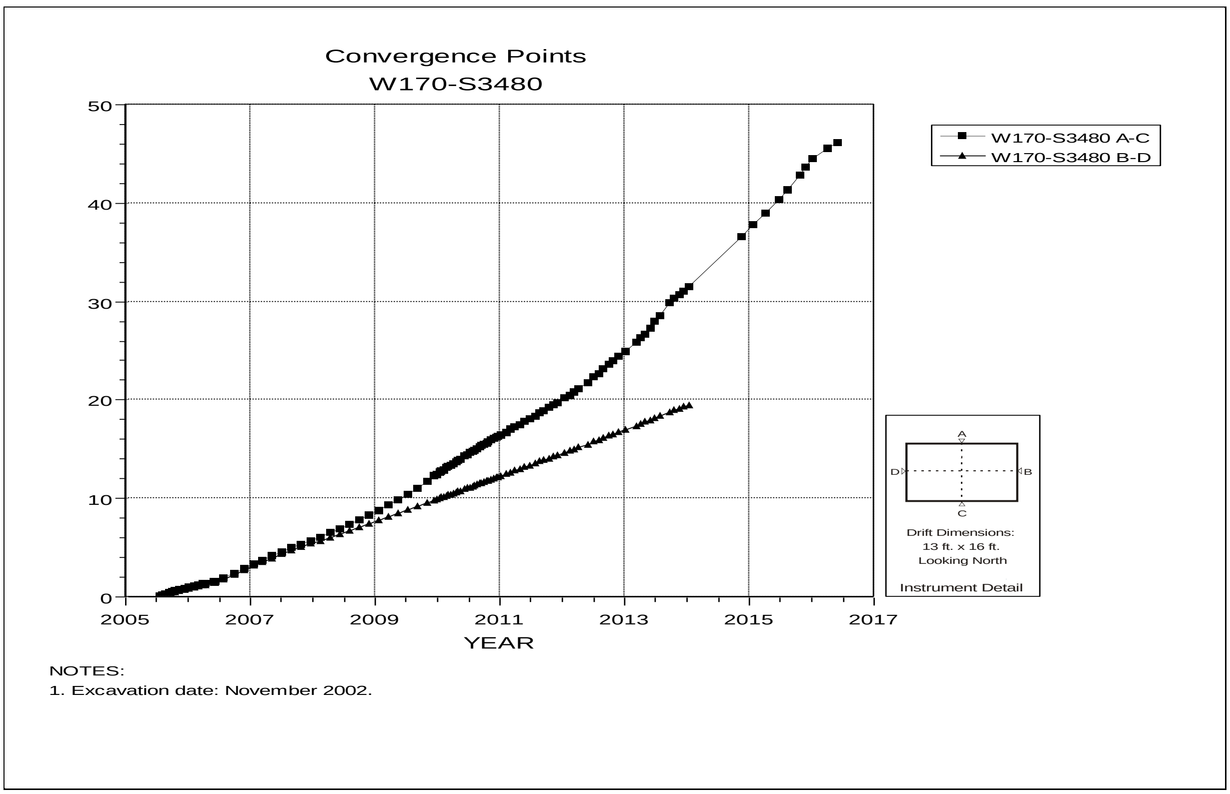

Figure 4-242 Convergence Point Array –
W170 S3480 – All Chords

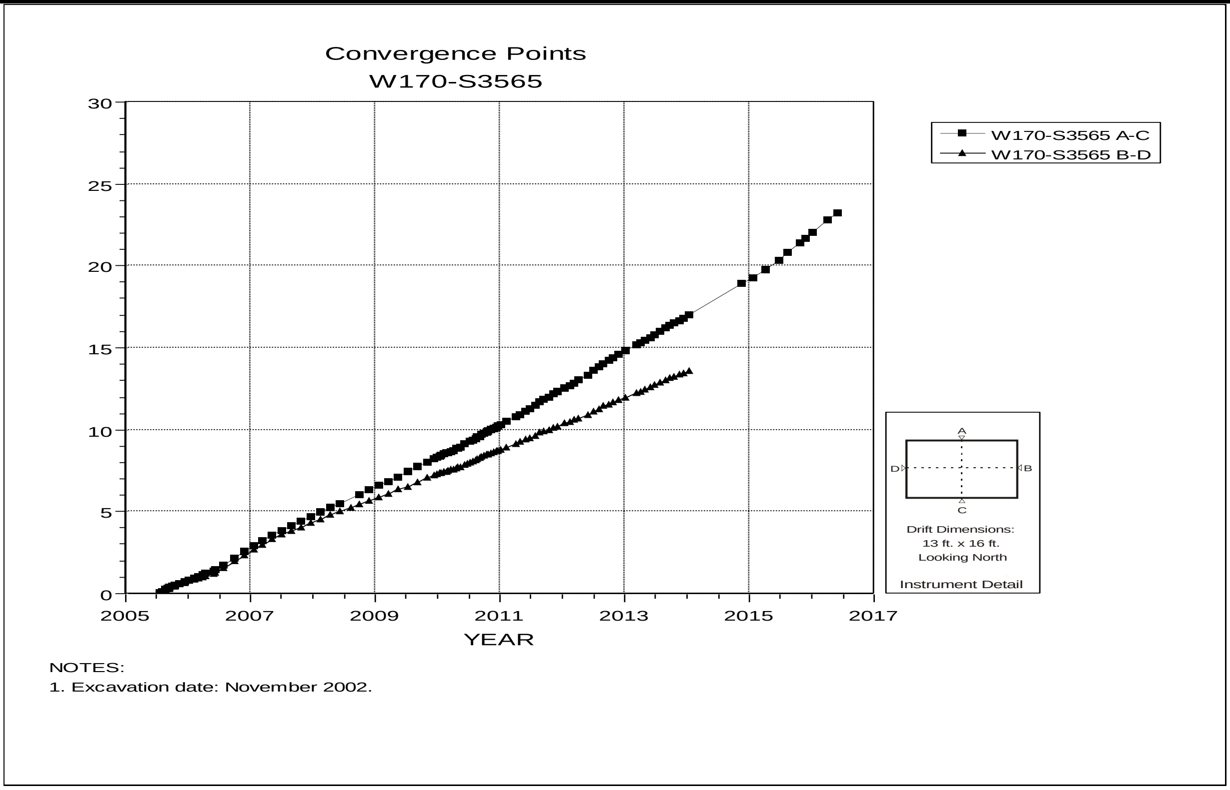

Figure 4-243 Convergence Point Array –
W170 S3565 – All Chords

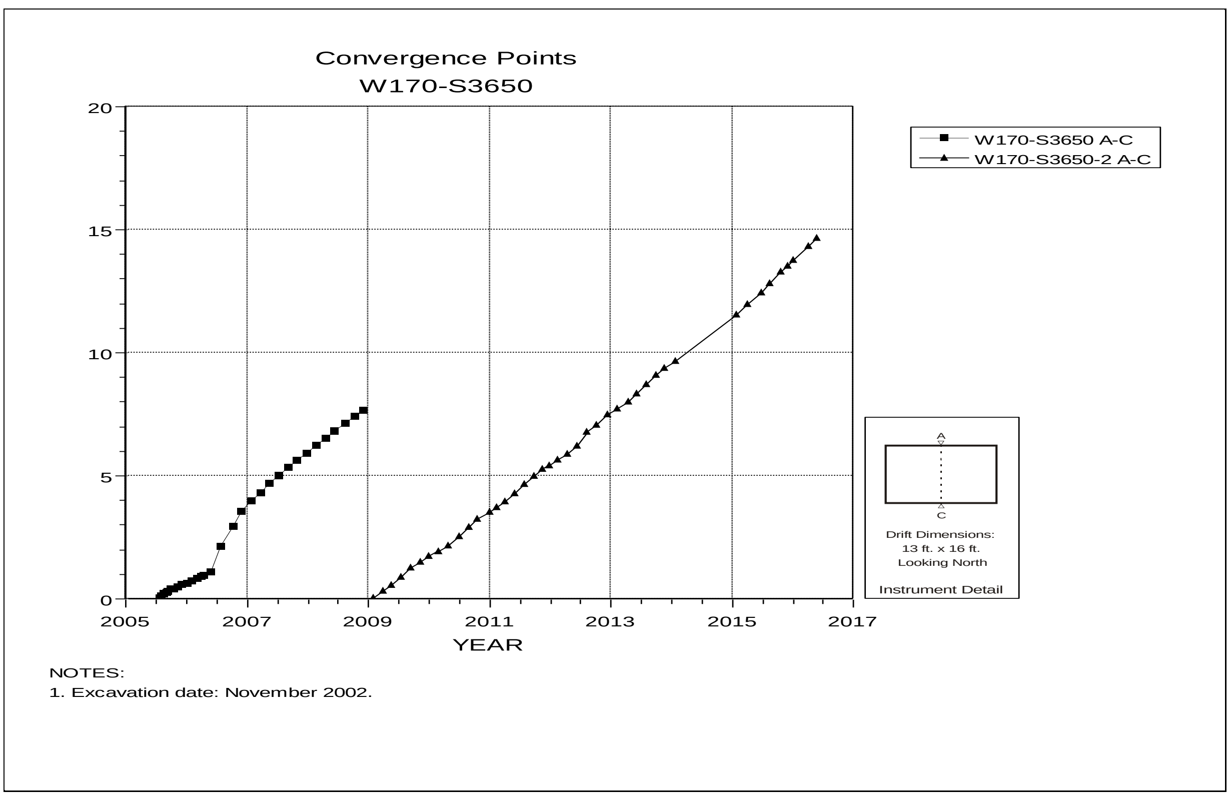

Figure 4-244 Convergence Point Array –
W170 S3650 – Roof to Floor

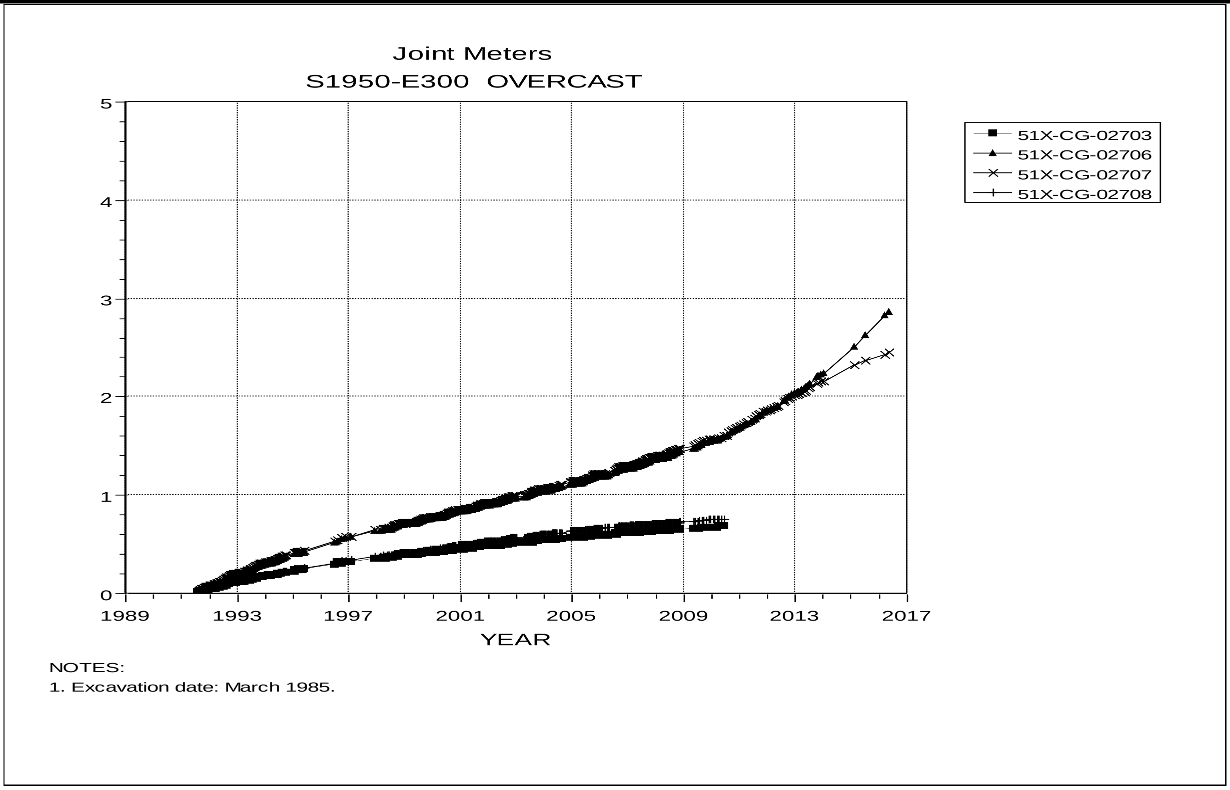

Figure 4-245 Joint Meters –
S1950-E300 Overcast

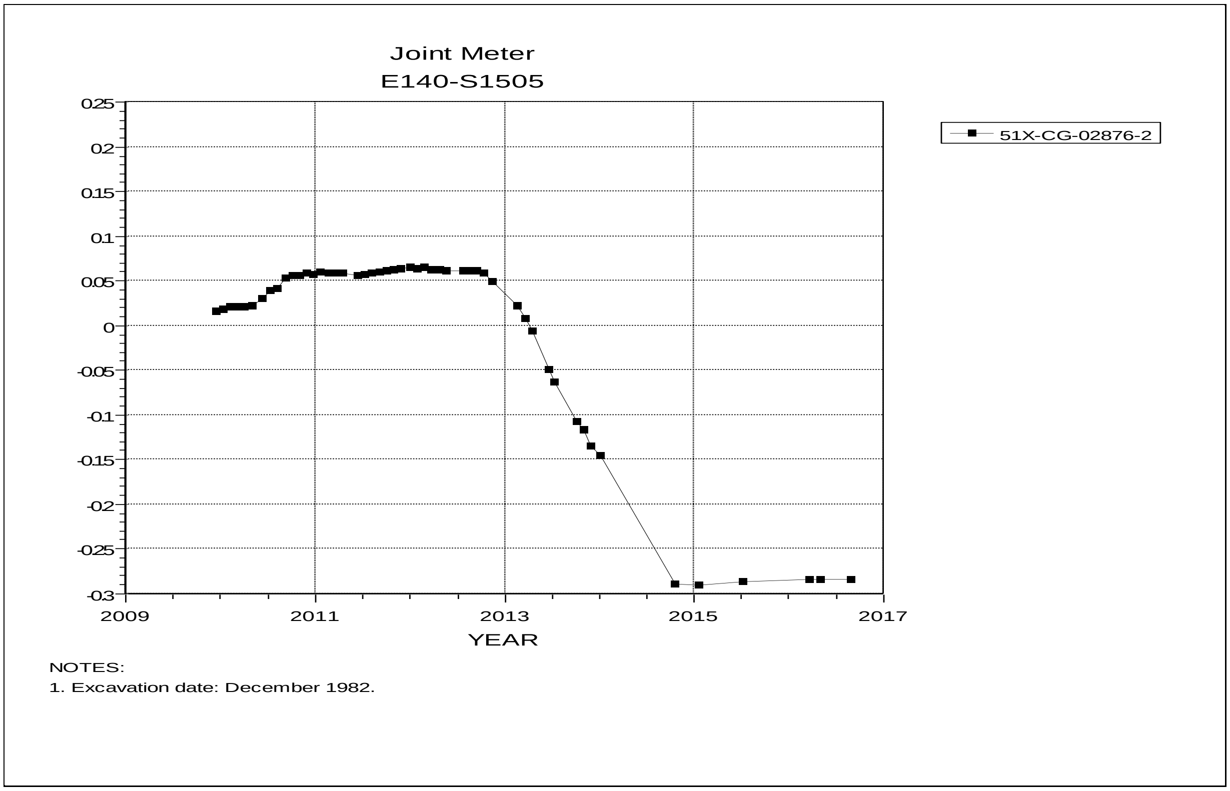

Figure 4-246 Joint Meter –
E140 S1505

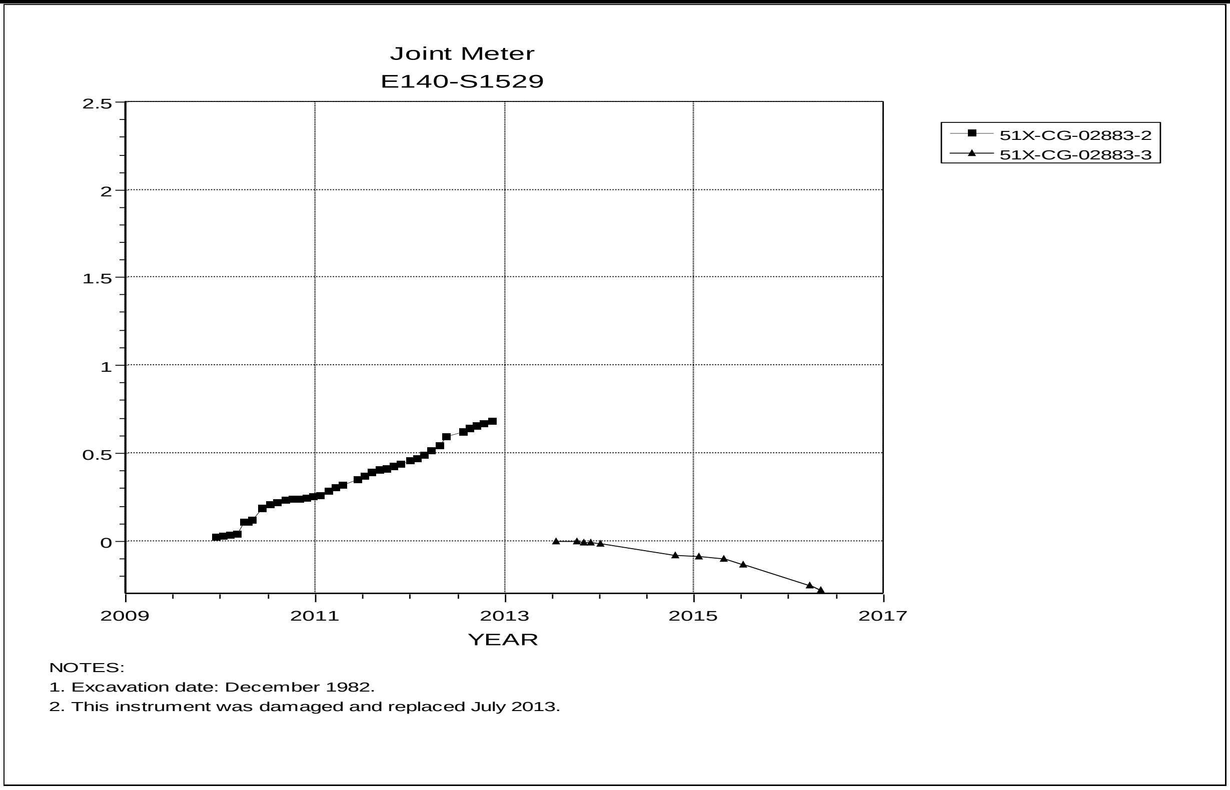

Figure 4-247 Joint Meters –
E140 S1529

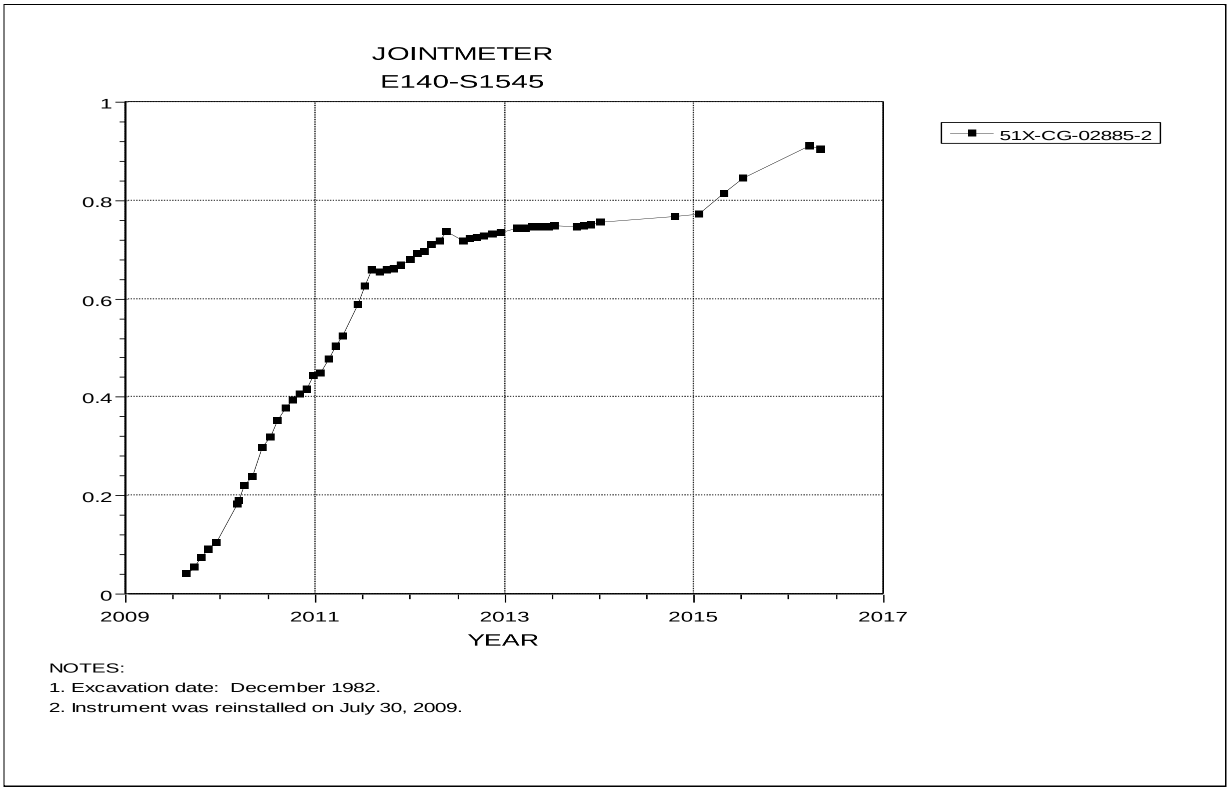

Figure 4-248 Joint Meter –
E140 S1545

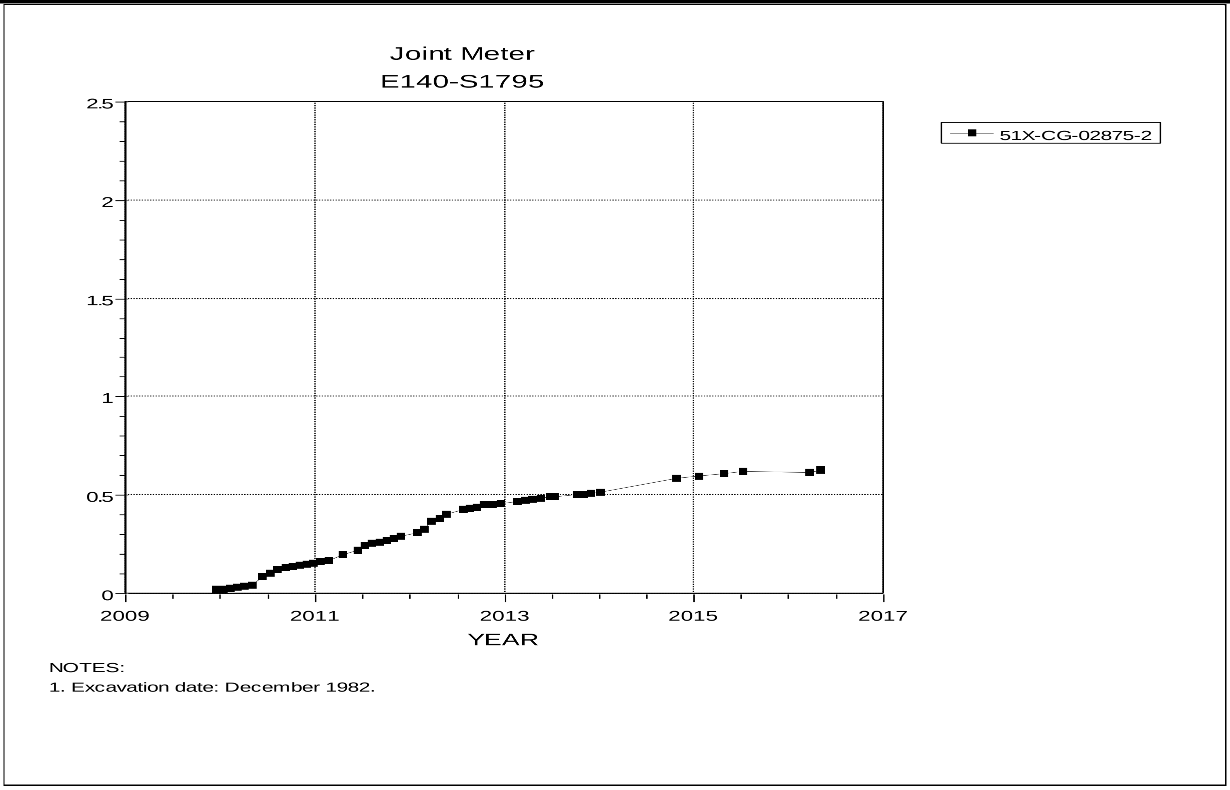

Figure 4-249 Joint Meter –
E140 S1795

5.0 Instrumentation Summary for the Waste Disposal Area

This chapter presents a summary of the data collected from instruments located in the Waste Disposal Area at the WIPP. Table 5-1 presents data and analysis of the access drifts associated with Panel 1. Plots of the instrument data are presented as Figures 5-1 through 5-12.

Table 5-2 presents data and analysis of the access drifts associated with Panel 2. A Plot of the instrument data is presented as Figure 5-12.

Table 5-5 presents data and analysis of Panel 5. Plots of the instrument data are presented as Figures 5-13 and 5-14.

Table 5-6 presents data and analysis of Panel 6. Plots of the instrument data are presented as Figures 5-15 through 5-16.

Table 5-7 presents data and analysis of Panel 7. Plots of the instrument data are presented as Figures 5-17 through 5-68.

Table 5-8 presents data and analysis of Panel 8. Plots of the instrument data are presented as Figures 5-69 through 5-78.

Table 5-1
Panel 1 Access Drifts Data Analysis

Convergence Points

Field Tag	Location	Figure Number	Last Reading 2015 to 2016		Cumulative Displacement (inches)	Closure Rate[4] 2015 to 2016 (in/year)	Closure Rate[4] 2014 to 2015 (in/year)	Rate Change Percent[4]	Comments
			Date	Inches					
S1600-E311-3 A-C	S1600-E311	5-1	05/24/16	2.444	25.891	1.3	1.1	18%	
S1600-E332-4 A-C	S1600-E332	5-2	05/24/16	2.402	24.492	1.1	3.3	-67%	
S1600-E357-3 A-C	S1600-E357	5-3	05/24/16	2.897	28.868	1.3	1.3	0%	
S1600-E382-3 A-C	S1600-E382	5-4	05/24/16	2.835	28.514	1.3	1.2	8%	
S1600-E407-3 A-G	S1600-E407	5-5	05/24/16	3.871	32.322	1.7	1.7	0%	
S1600-E407-3 B-F	S1600-E407	5-5	01/18/16	3.056	29.299	1.7	N/A	N/A	
S1600-E407-3 L-H	S1600-E407	5-5	01/18/16	3.063	3.063	1.6	N/A	N/A	
S1600-E432-3 A-C	S1600-E432	5-6	05/24/16	4.842	38.65	2.1	2.2	-5%	
S1950-E311-7 A-C	S1950-E311	5-7	05/24/16	8.652	38.043	1.6	1.5	7%	
S1950-E332-4 A-C	S1950-E332	5-8	05/24/16	11.382	29.944	1.9	N/A	N/A	
S1950-E357-8 A-C	S1950-E357	5-9	05/24/16	5.674	55.214	2.5	2.3	9%	
S1950-E382-5 A-C	S1950-E382	5-10	05/24/16	41.564	60.199	2.6	2.7	-4%	
S1950-E407-4 A-G	S1950-E407	5-11	05/24/16	40.32	62.144	2.5	N/A	N/A	
S1950-E407-3 H-L	S1950-E407	5-11	01/18/16	38.89	59.622	2.7	N/A	N/A	
S1950-E432-4 A-C	S1950-E432	5-12	05/24/16	5.612	61.156	2.4	2.5	-4%	

[4] N/A – Insufficient data available to perform the calculation. This is usually due to the inability to read the instruments because of activities such as the removal of an instrument due to floor, rib or back trimming; locations blocked by equipment or waste disposal; installation timing, access issues, etc.

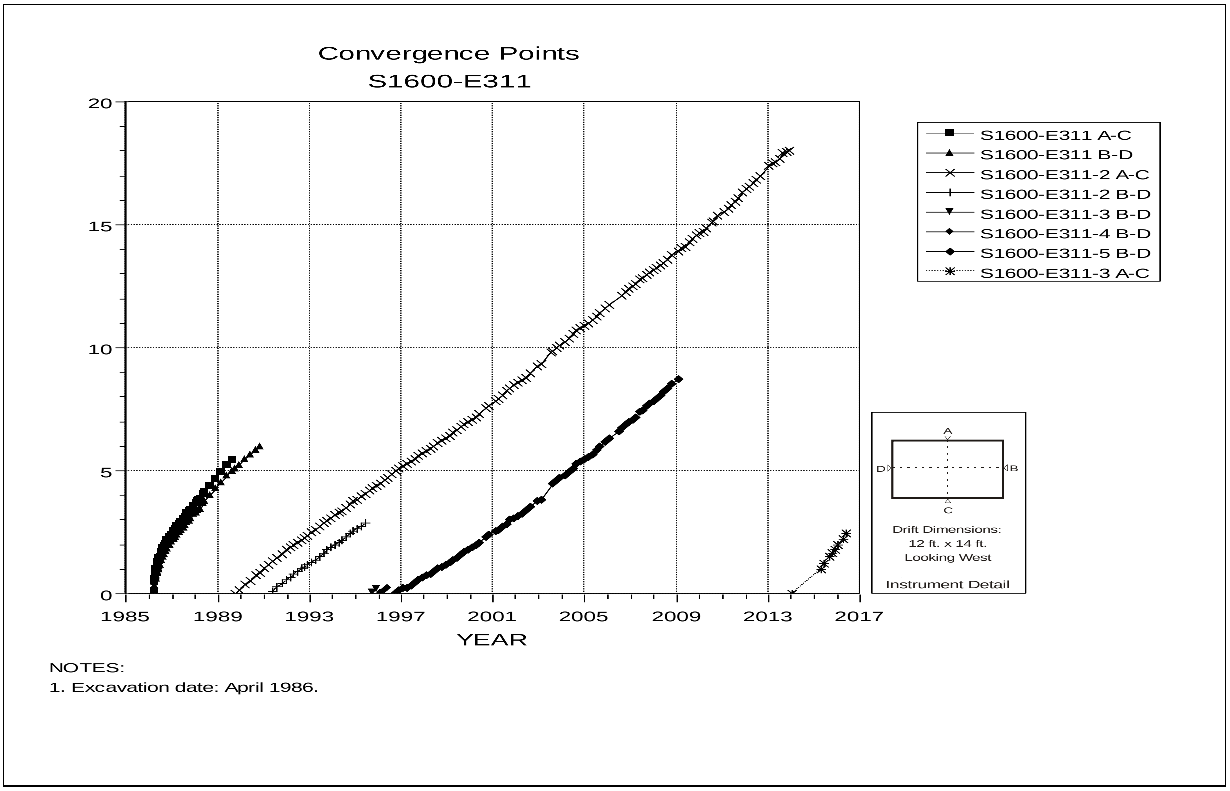

Figure 5-1 Convergence Point Array –
S1600 E311 – All Chords

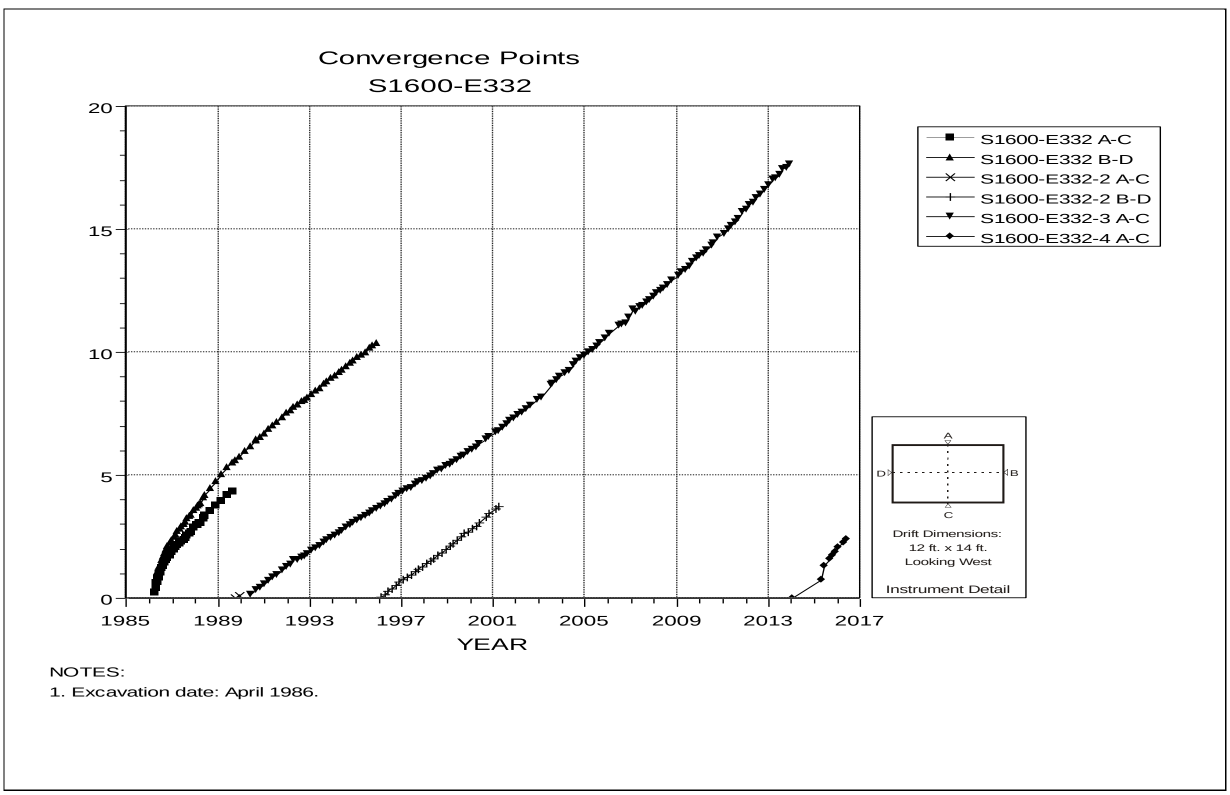

Figure 5-2 Convergence Point Array –
S1600 E332 – All Chords

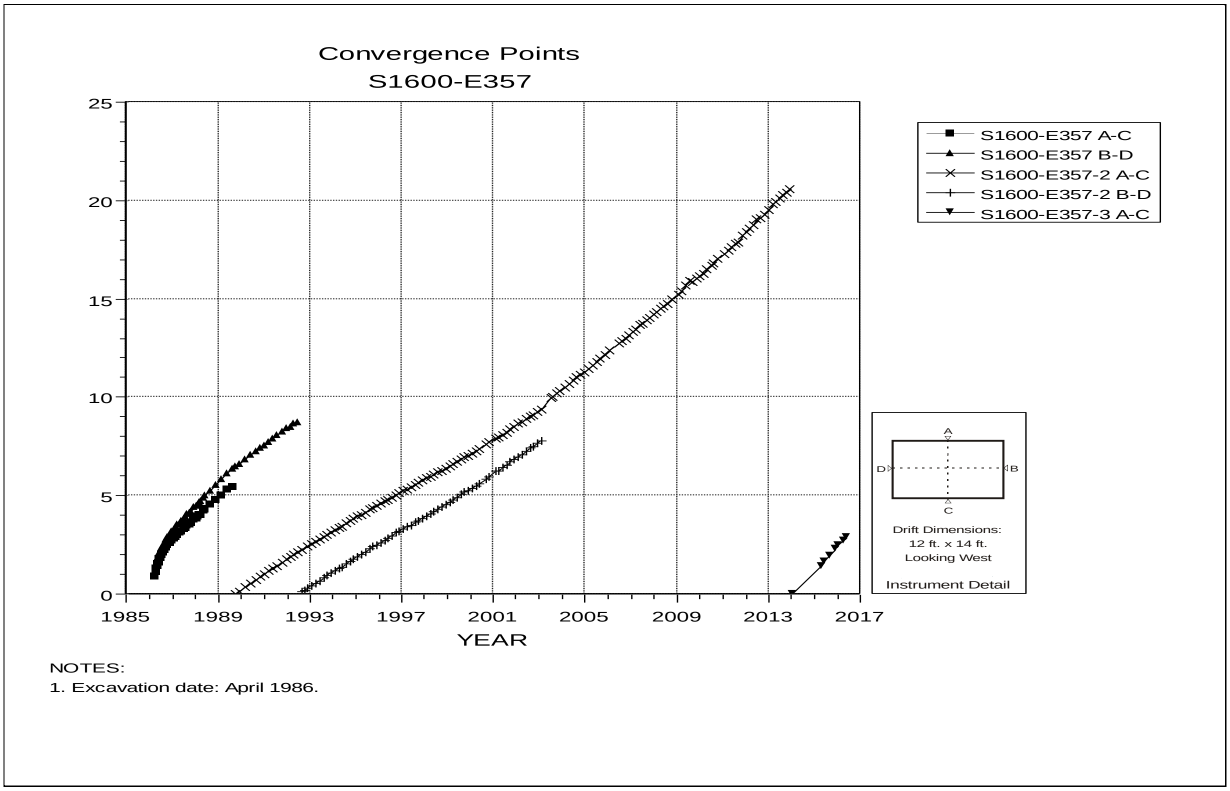

Figure 5-3 Convergence Point Array –
S1600 E357 – All Chords

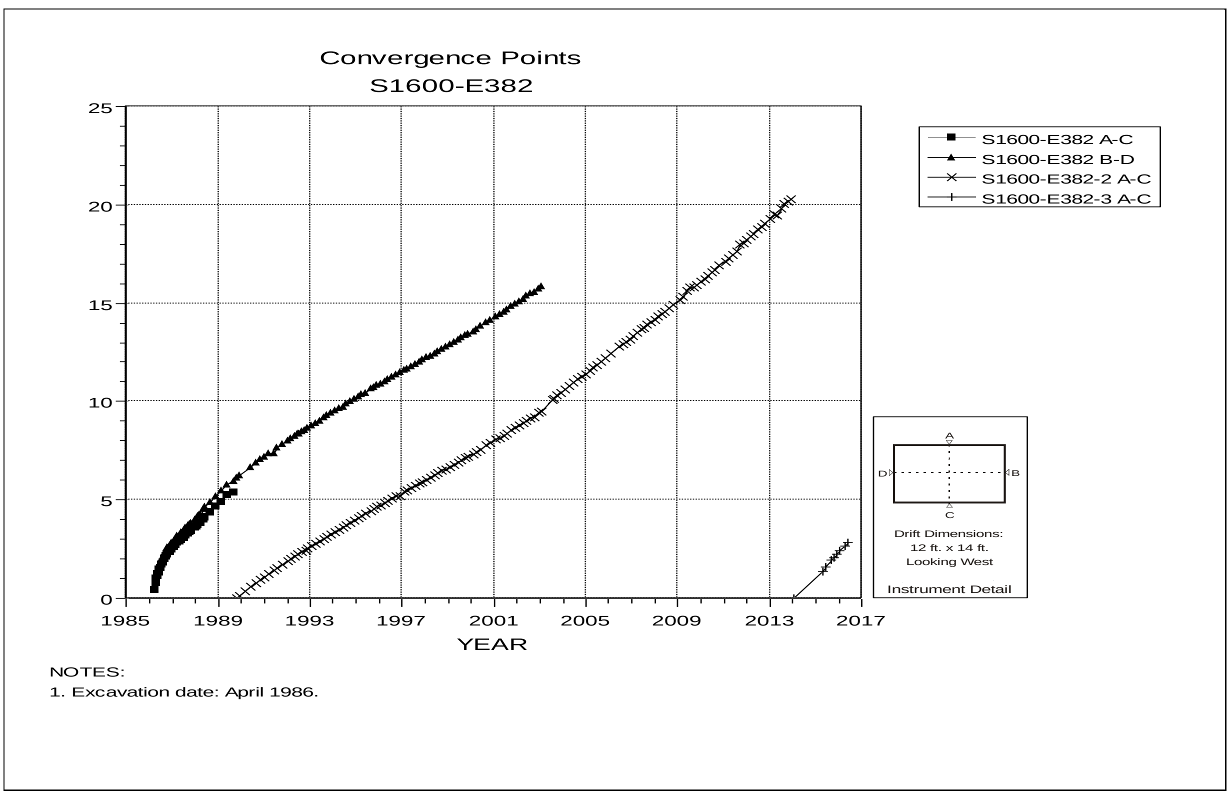

Figure 5-4 Convergence Point Array –
S1600 E382 – All Chords

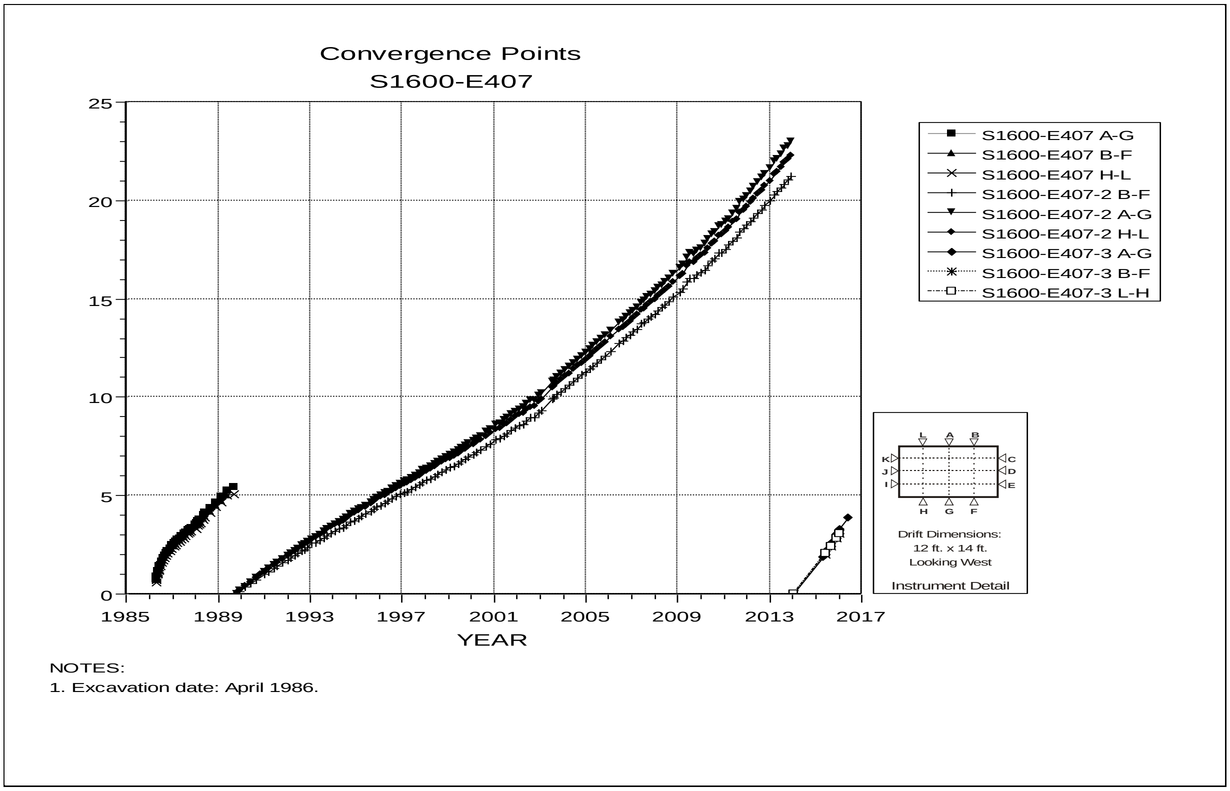

Figure 5-5 Convergence Point Array –
S1600 E407 – All Chords

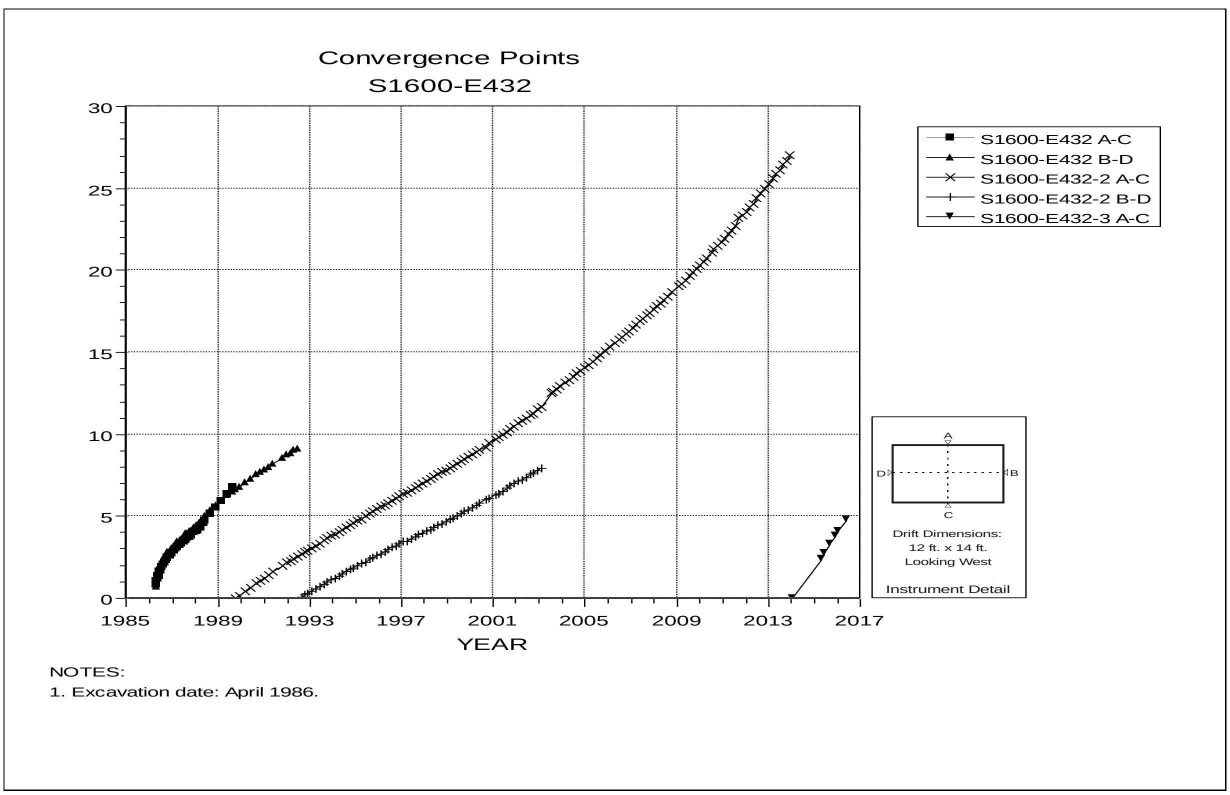

Figure 5-6 Convergence Point Array –
S1600 E432 – All Chords

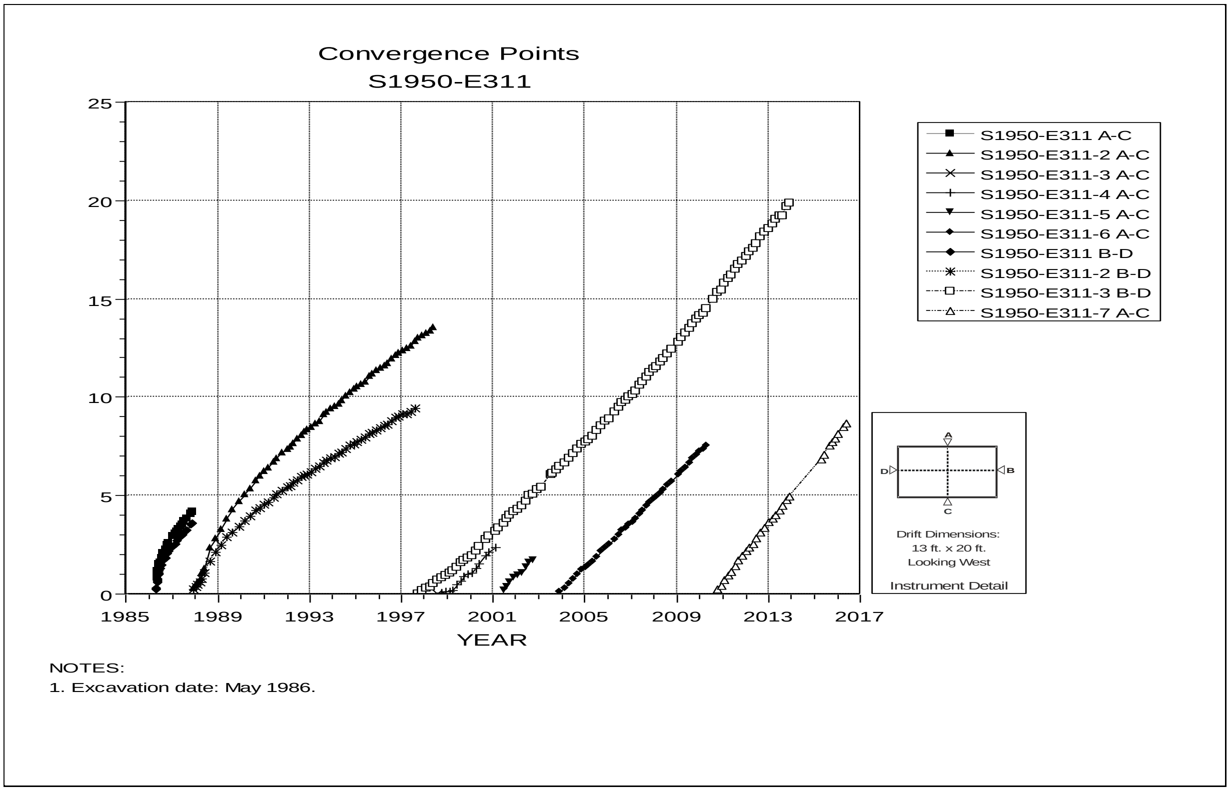

Figure 5-7 Convergence Point Array –
S1950 E311 – Roof to Floor

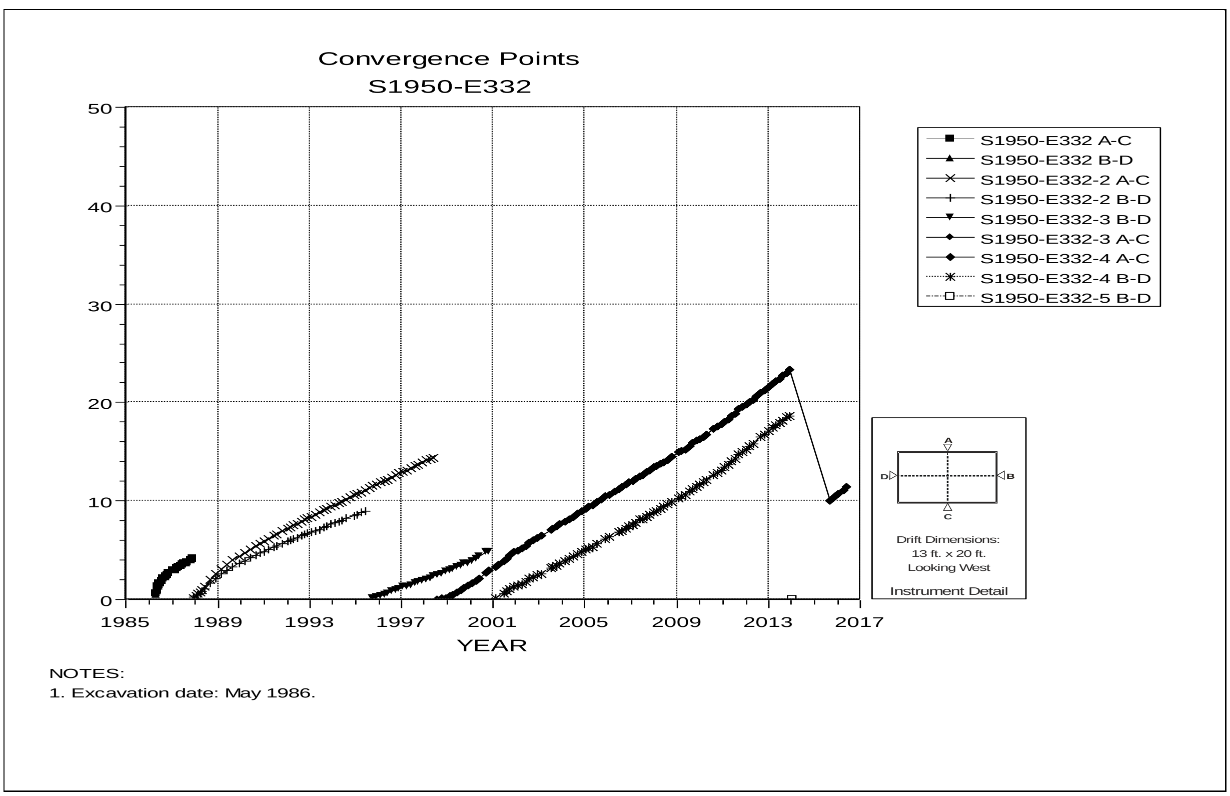

Figure 5-8 Convergence Point Array –
S1950 E332 – Roof to Floor

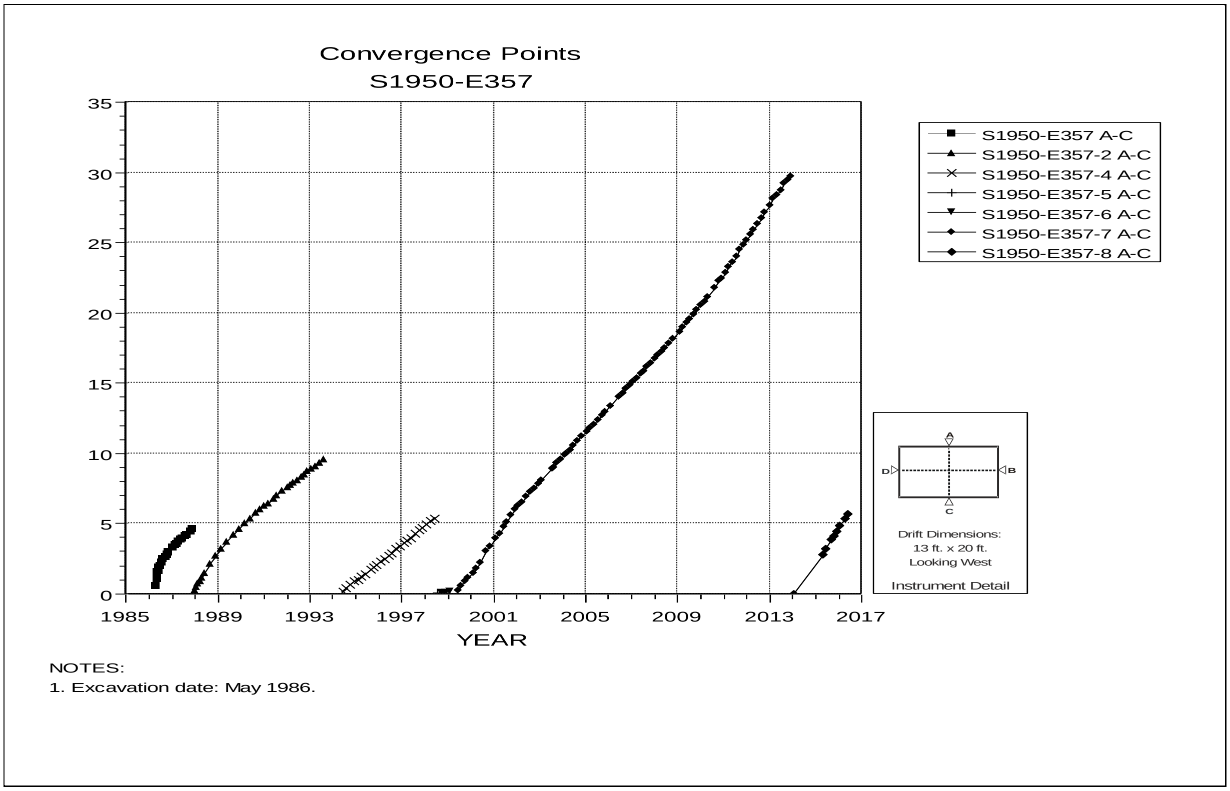

Figure 5-9 Convergence Point Array –
S1950 E357 – Roof to Floor

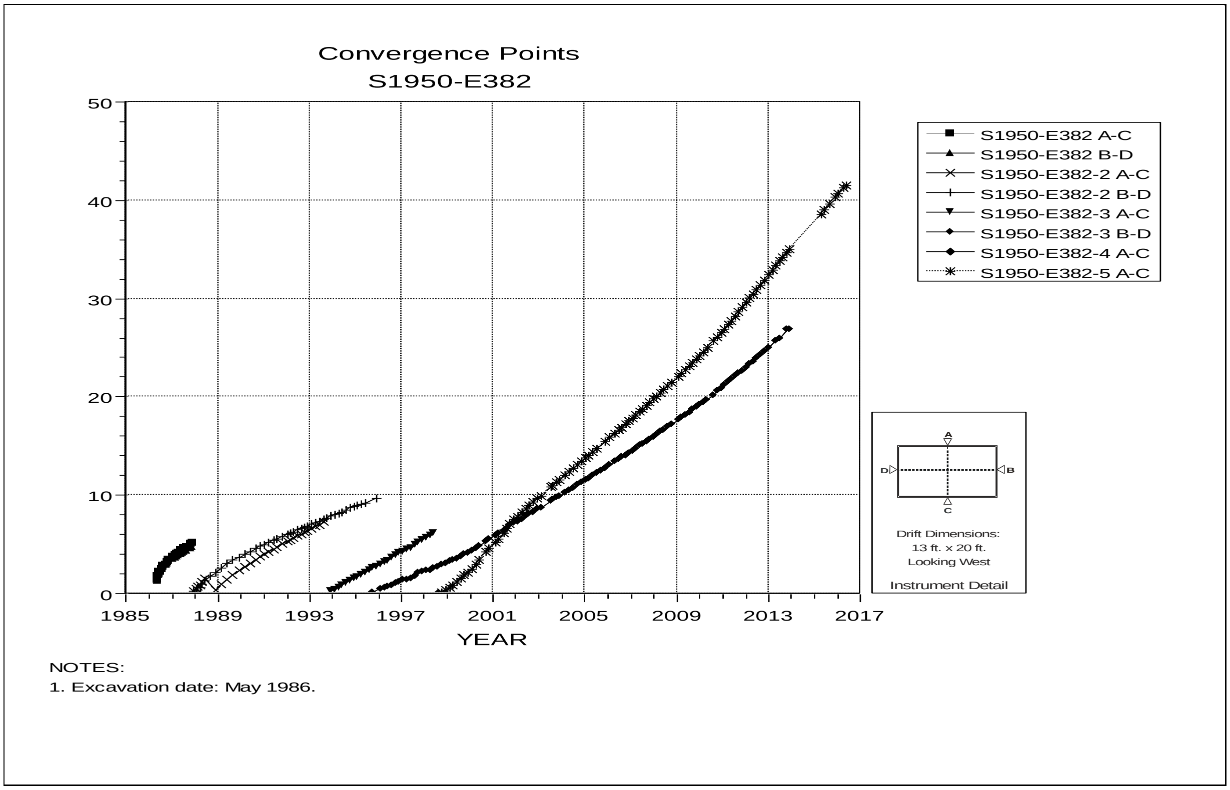

Figure 5-10 Convergence Point Array –
S1950 E382 – Roof to Floor

ISSUED

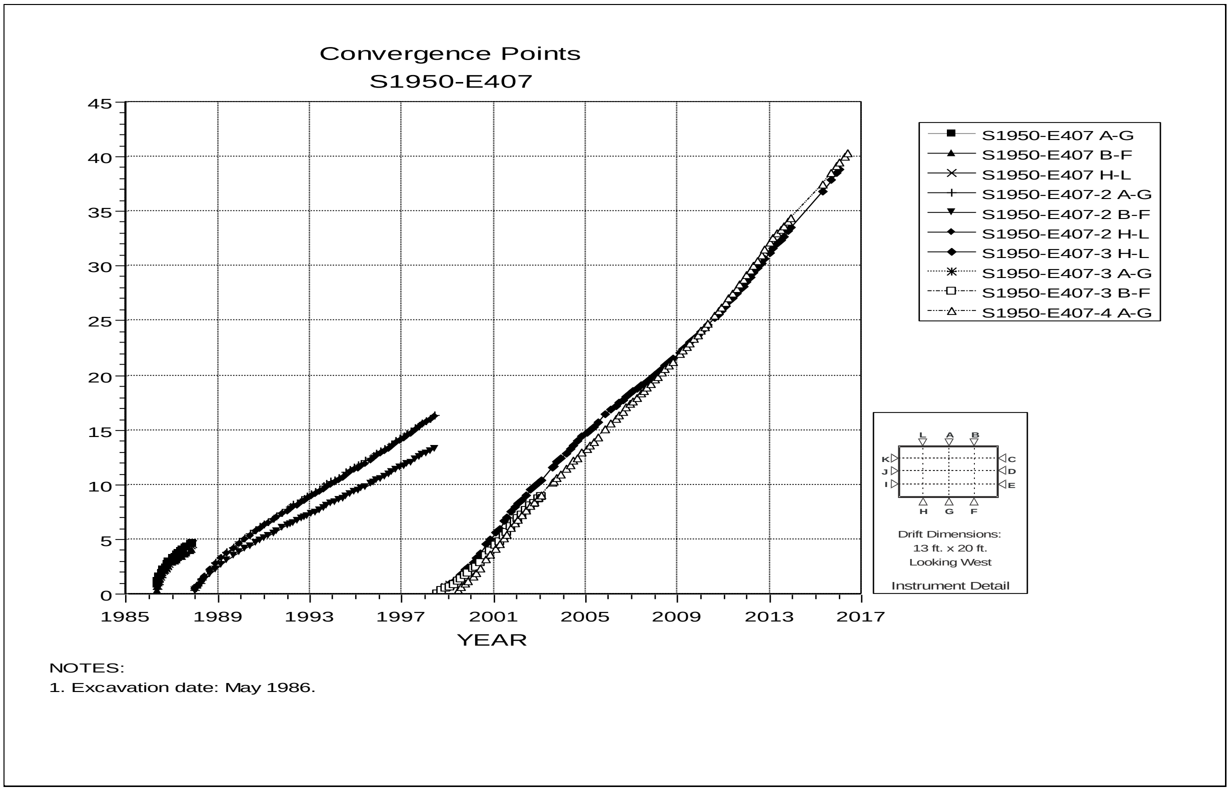

Figure 5-11 Convergence Point Array –
S1950 E407 – All Vertical Chords

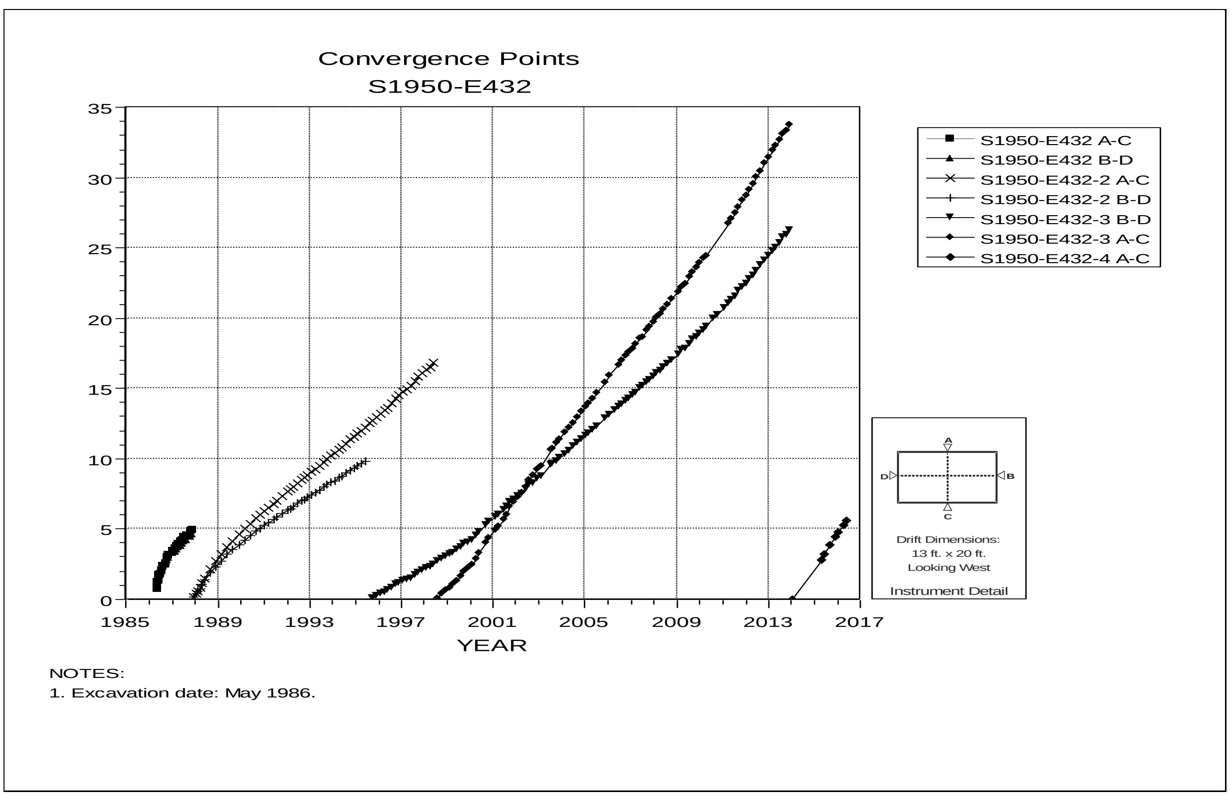

Figure 5-12 Convergence Point Array –
S1950 E432 – All Chords

Table 5-2
Panel 2 Access Drift Data Analysis

Convergence Points

Field Tag	Location	Figure Number	Last Reading 2015 to 2016		Cumulative Displacement (inches)	Closure Rate 2015 to 2016 (in/year)	Closure Rate 2014 to 2015 (in/year)	Rate Change Percent	Comments
			Date	Inches					
S2180-E410-2 A-C	S2180-E410	5-12	04/05/16	17.179	21.976	1.9	1.9	0%	

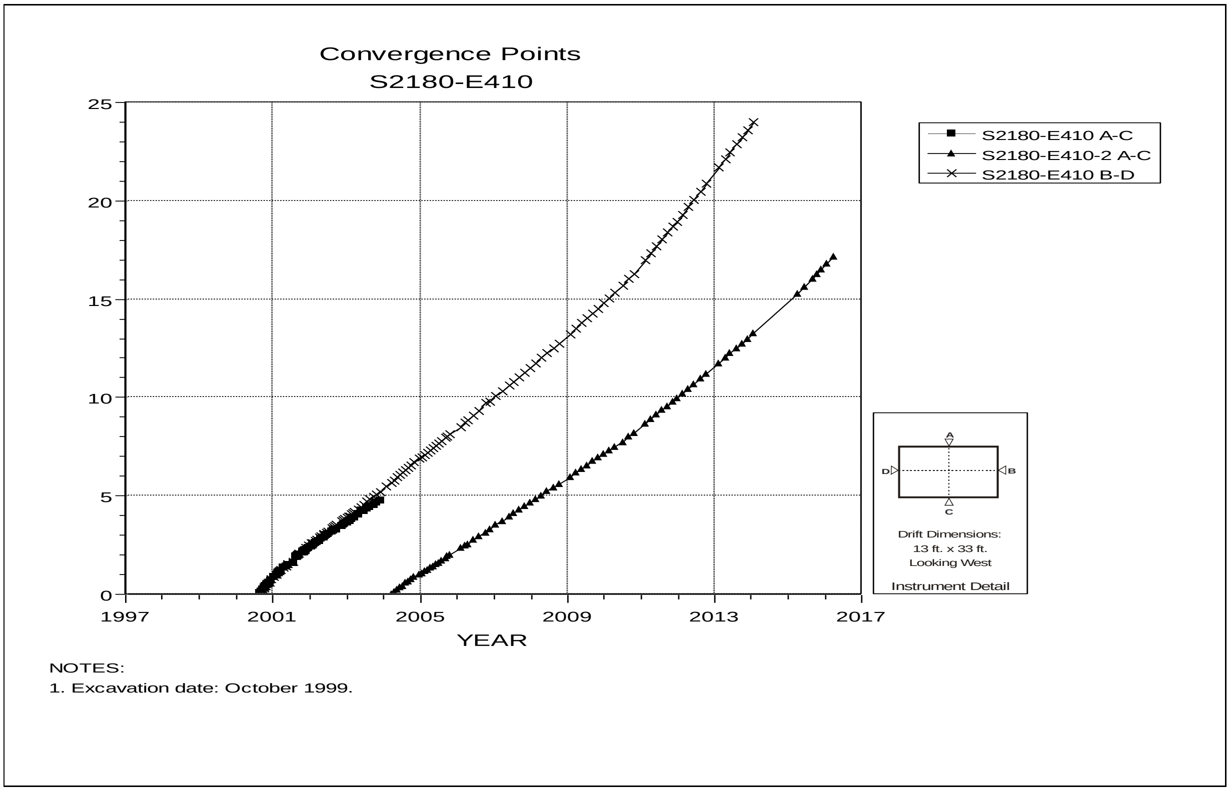

Figure 5-12 Convergence Point Array –
S2180 E410 – Roof to Floor

Table 5-5
Panel 5 Access Data Analysis

Convergence Points

Field Tag	Location	Figure Number	Last Reading 2015 to 2016		Cumulative Displacement (inches)	Closure Rate 2015 to 2016 (in/year)	Closure Rate 2014 to 2015 (in/year)	Rate Change Percent	Comments
			Date	Inches					
S3310-W285 A-C	S3310-W285	5-13	01/12/16	21.297	21.297	3.0	2.6	15%	
S3650-W285-2 A-C	S3650-W285	5-14	01/12/16	27.372	29.813	7.0	5.2	35%	

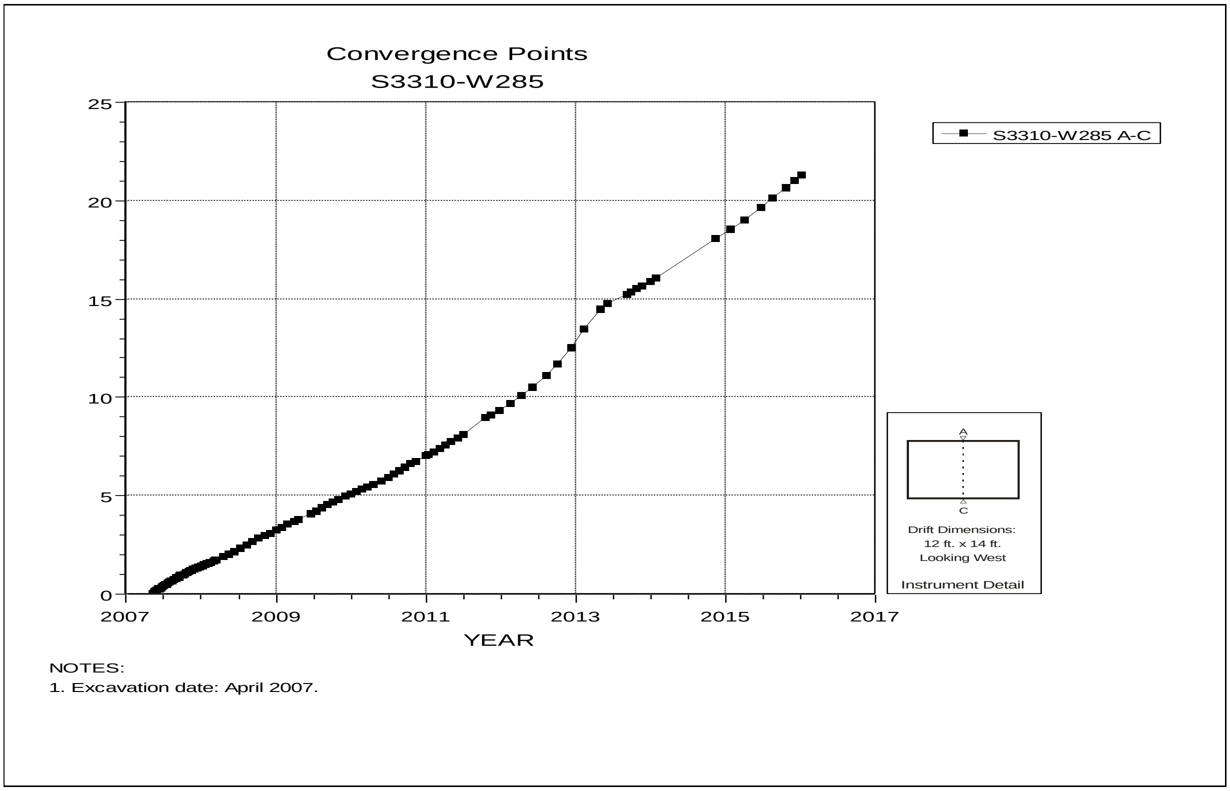

Figure 5-13 Convergence Point Array –
S3310 W285 – Roof to Floor

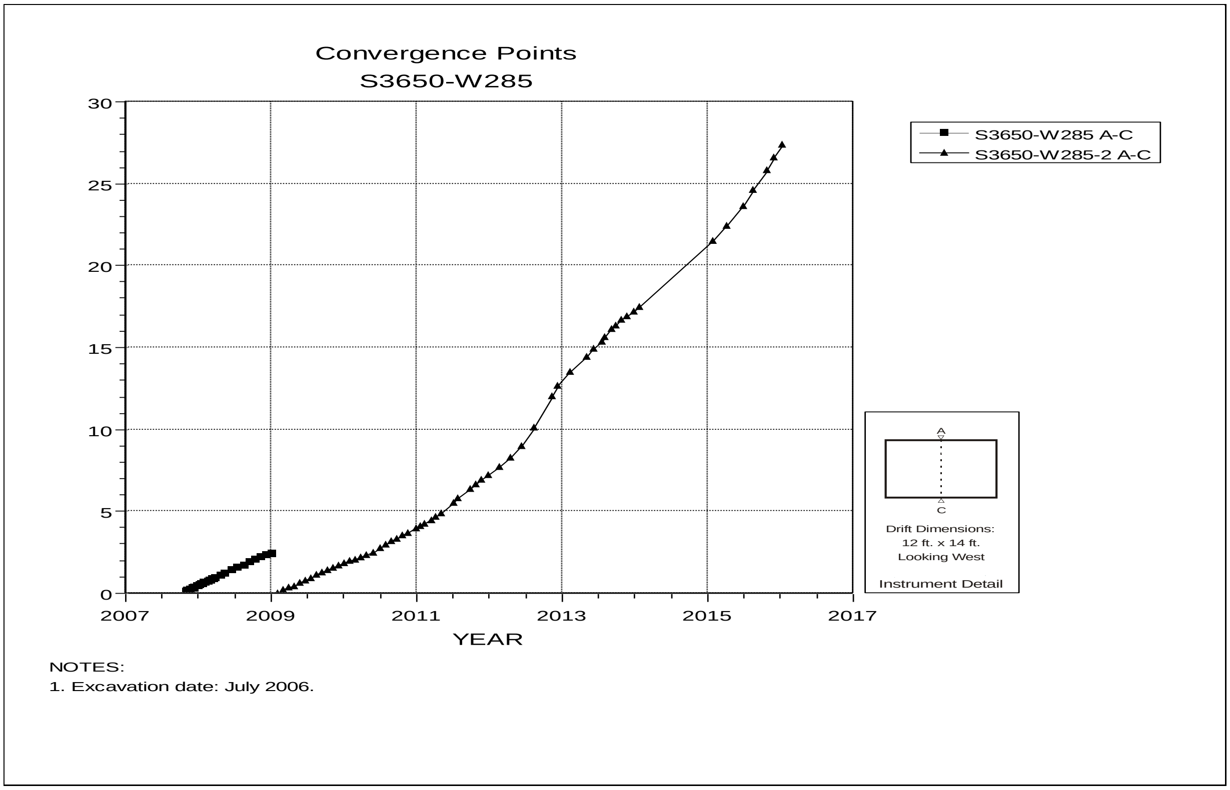

Figure 5-14 Convergence Point Array –
S3650 W285 – Roof to Floor

Table 5-6
Panel 6 Data Analysis

Convergence Points

Field Tag	Location	Figure Number	Last Reading 2015 to 2016		Cumulative Displacement (inches)	Closure Rate 2015 to 2016 (in/year)	Closure Rate 2014 to 2015 (in/year)	Rate Change Percent	Comments
			Date	Inches					
S2750-W285-2 A-C	S2750-W285	5-15	01/12/16	38.47	43.151	4.5	5.5	-18%	
S3080-W285-2 A-C	S3080-W285	5-16	01/12/16	17.363	21.33	4.0	3.3	21%	

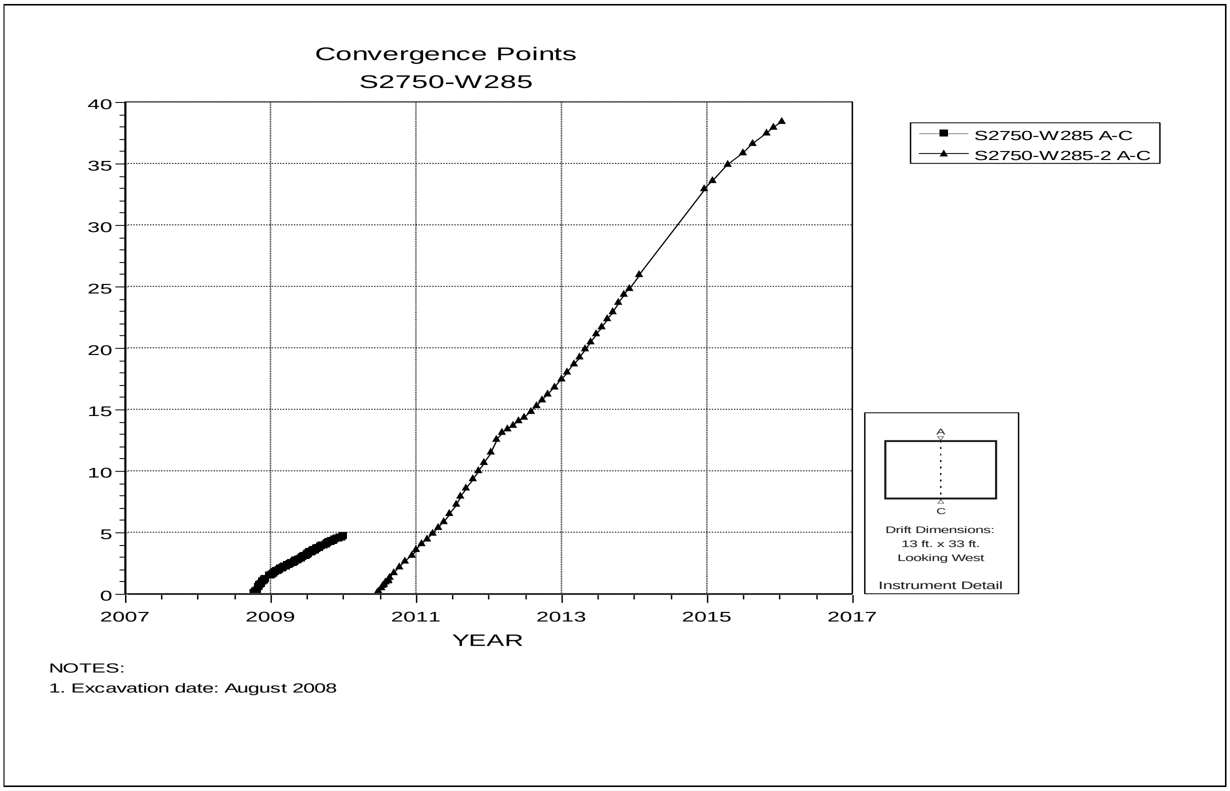

Figure 5-15 Convergence Point Array –
S2750 W285 – Roof to Floor

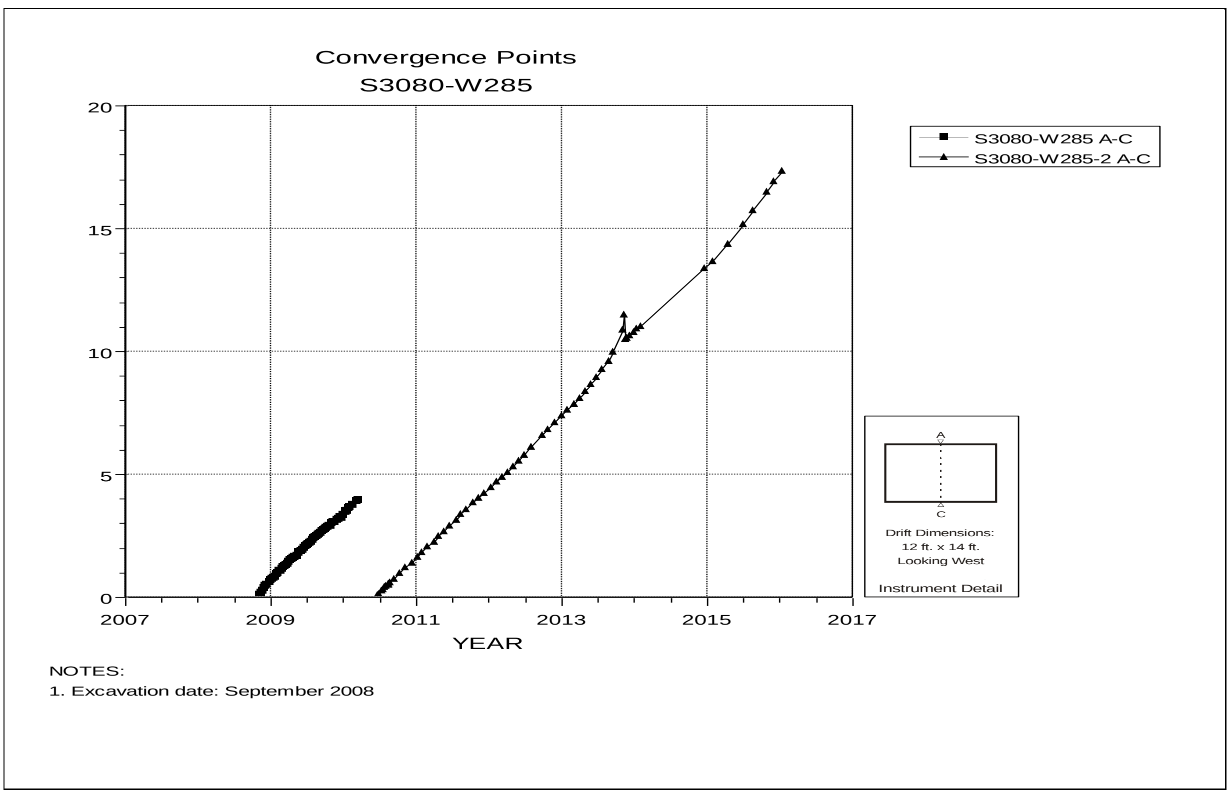

Figure 5-16 Convergence Point Array –
S3080 W285 – Roof to Floor

Table 5-7
Panel 7 Data Analysis

Extensometers

Field Tag	Location	Figure Number	Date of Last Reading	Collar Displacement Relative to Deepest Anchor (inches)	Displacement Rate 2015 to 2016 (in/year)	Displacement Rate 2014 to 2015 (in/year)	Rate Change Percent	Comments
51X-GE-00416	S2180-W585	5-17	06/23/16	7.861	2.5	1.7	47%	
51X-GE-00417	S2180-W985	5-18	11/23/15	10.409	4.9	3.8	29%	
51X-GE-00425	W390-S2350	5-19	11/23/15	4.925	2.6	1.1	136%	
51X-GE-00426	W520-S2350	5-20	06/21/16	6.54	2.0	1.3	54%	
51X-GE-00418	W660-S2350	5-21	06/21/16	11.528	5.5	2.2	150%	
51X-GE-00419	W790-S2350	5-22	06/23/16	8.355	2.8	2.2	27%	
51X-GE-00420	W920-S2350	5-23	06/23/16	12.388	7.1	3.2	122%	
51X-GE-00421	W1050- S2350	5-24	11/23/15	6.192	2.9	1.6	81%	
51X-GE-00423	S2520-W585	5-25	06/21/16	6.98	2.0	1.4	43%	
51X-GE-00424	S2520-W985	5-26	11/23/15	7.014	2.5	2.1	19%	

Table 5-7
Panel 7 Data Analysis (continued)

Convergence Points

Field Tag	Location	Figure Number	Last Reading 2015 to 2016		Cumulative Displacement (inches)	Closure Rate[4] 2015 to 2016 (in/year)	Closure Rate 2014 to 2015 (in/year)	Rate Change Percent[4]	Comments
			Date	Inches					
S2180-W285-2 A-C	S2180-W285	5-27	06/09/16	8.279	8.725	1.5	N/A	N/A	
S2180-W390-3 A-C	S2180-W390	5-28	06/09/16	15.556	21.256	4.6	N/A	N/A	
S2180-W460-3 A-C	S2180-W460	5-29	06/09/16	18.321	26.545	5.9	N/A	N/A	
S2180-W520-3 A-C	S2180-W520	5-30	06/09/16	22.923	33.833	8.0	N/A	N/A	
S2180-W585-4 A-C	S2180-W585	5-31	06/09/16	19.019	28.996	6.0	N/A	N/A	
S2180-W660-4 A-C	S2180-W660	5-32	06/09/16	16.781	26.19	5.4	N/A	N/A	
S2180-W725-4 A-C	S2180-W725	5-33	06/09/16	18.557	25.976	5.0	N/A	N/A	
S2180-W790-3 A-C	S2180-W790	5-34	06/09/16	17.31	27.882	5.9	N/A	N/A	
S2180-W855-3 A-C	S2180-W855	5-35	06/09/16	16.538	26.912	5.8	N/A	N/A	
S2180-W920-3 A-C	S2180-W920	5-36	06/09/16	14.93	24.811	5.8	N/A	N/A	
S2180-W985-4 A-C	S2180-W985	5-37	06/09/16	15.175	31.221	5.9	N/A	N/A	
S2180-W1050-2 A-C	S2180-W1050	5-38	06/09/16	12.529	21.102	4.6	N/A	N/A	
W390-S2275-3 A-C	W390-S2275	5-39	04/28/16	18.887	26.821	4.2	4.4	-5%	
W390-S2350-3 A-C	W390-S2350	5-40	04/28/16	13.684	20.248	0.8	5.2	-85%	
W390-S2425-3 A-C	W390-S2425	5-41	04/28/16	12.989	23.056	3.7	3.3	12%	
W520-S2275-3 A-C	W520-S2275	5-42	06/09/16	21.718	30.17	4.6	6.5	-29%	
W520-S2350-3 A-C	W520-S2350	5-43	06/09/16	18.054	30.923	4.6	5.7	-19%	
W520-S2425-3 A-C	W520-S2425	5-44	04/28/16	21.584	30.866	6.5	6.9	-6%	
W660-S2275-3 A-C	W660-S2275	5-45	06/09/16	16.52	25.536	4.9	3.8	29%	
W660-S2350-3 A-C	W660-S2350	5-46	06/09/16	17.681	34.41	3.6	6.8	-47%	
W660-S2425-3 A-C	W660-S2425	5-47	06/09/16	17.459	30.013	3.4	6.9	-51%	
W790-S2275-3 A-C	W790-S2275	5-48	06/09/16	14.463	19.067	4.4	4.3	2%	
W790-S2350-3 A-C	W790-S2350	5-49	06/09/16	18.322	22.613	6.5	6.5	0%	
W790-S2425-2 A-C	W790-S2425	5-50	06/09/16	16.98	19.279	6.5	5.5	18%	
W920-S2275-3 A-C	W920-S2275	5-51	06/09/16	13.147	16.215	4.8	4.3	12%	
W920-S2425-3 A-C	W920-S2425	5-52	06/09/16	18.876	21.719	6.6	6.7	-1%	

Table 5-7
Panel 7 Data Analysis (continued)

Convergence Points (continued)

Field Tag	Location	Figure Number	Last Reading 2015 to 2016 Date	Last Reading 2015 to 2016 Inches	Cumulative Displacement (inches)	Closure Rate 2015 to 2016 (in/year)	Closure Rate 2014 to 2015 (in/year)	Rate Change Percent	Comments
W920-S2350-3 A-C	W920-S2350	5-53	06/09/16	20.221	23.237	8.7	6.9	26%	
W1050-S2275-3 A-C	W1050-S2275	5-54	06/09/16	12.264	21.893	4.7	3.9	21%	
W1050-S2350-3 A-C	W1050-S2350	5-55	06/09/16	12.338	21.489	4.4	3.9	13%	
W1050-S2425-3 A-C	W1050-S2425	5-56	06/09/16	10.42	19.941	3.6	3.2	13%	
S2520-W285-4 A-C	S2520-W285	5-57	04/28/16	18.014	22.989	4.6	4.8	-4%	
S2520-W390-3 A-C	S2520-W390	5-58	04/28/16	15.321	22.604	4.0	4.2	-5%	
S2520-W455-3 A-C	S2520-W455	5-59	04/28/16	15.783	23.473	4.5	4.5	0%	
S2520-W520-3 A-C	S2520-W520	5-60	06/09/16	16.969	29.747	5.3	5.1	4%	
S2520-W585-4 A-C	S2520-W585	5-61	06/09/16	12.223	19.889	4.1	3.6	14%	
S2520-W660-3 A-C	S2520-W660	5-62	06/09/16	15.853	29.287	5.5	4.7	17%	
S2520-W725-5 A-C	S2520-W725	5-63	06/09/16	16.716	25.667	4.9	5.6	-13%	
S2520-W790-3 A-C	S2520-W790	5-64	06/09/16	15.981	24.082	6.0	5.3	13%	
S2520-W855-3 A-C	S2520-W855	5-65	06/09/16	17.434	31.367	4.4	5.7	-23%	
S2520-W920-4 A-C	S2520-W920	5-66	06/09/16	13.174	22.543	4.7	4.0	18%	
S2520-W985-3 A-C	S2520-W985	5-67	06/09/16	13.836	24.05	4.3	4.6	-7%	
S2520-W1050-4 A-C	S2520-W1050	5-68	06/09/16	11.506	20.019	4.0	3.5	14%	

[4] N/A – Insufficient data available to perform the calculation. This is usually due to the inability to read the instruments because of activities such as the removal of an instrument due to floor, rib or back trimming; locations blocked by equipment or waste disposal; installation timing, access issues, etc.

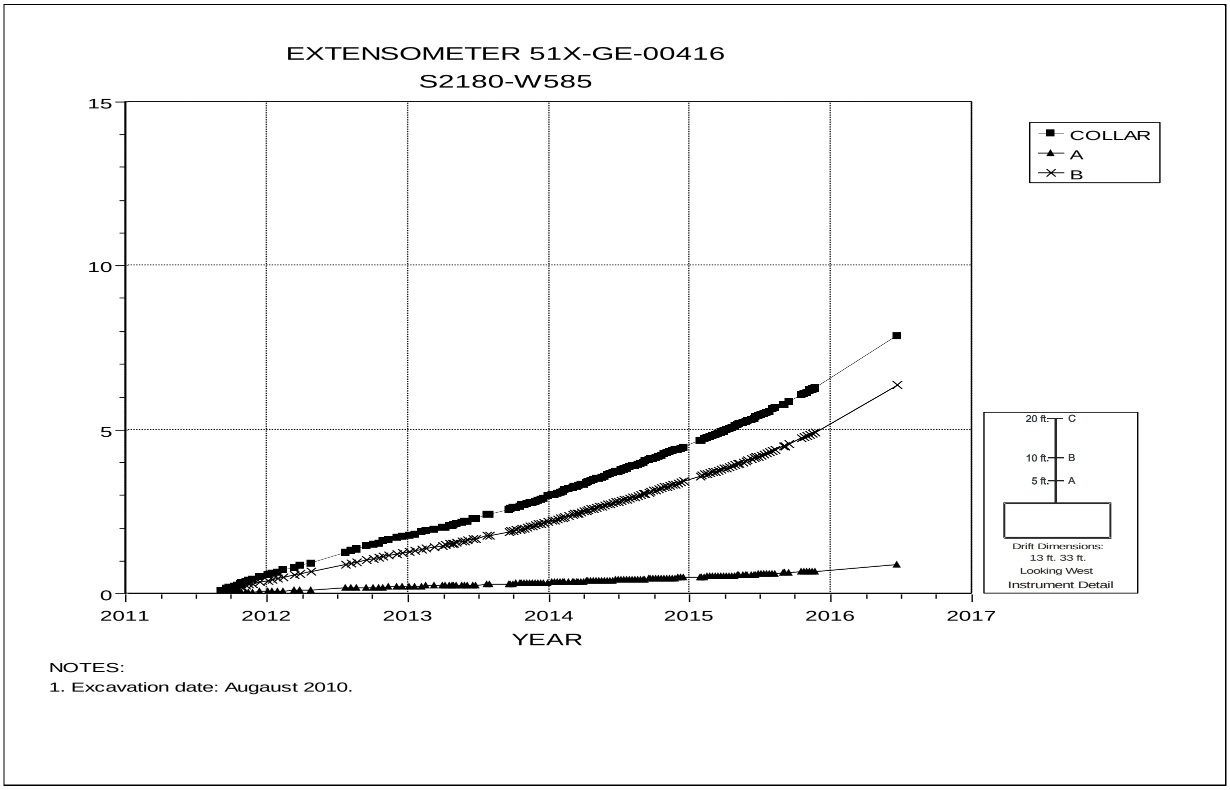

Figure 5-17 Extensometer 51X-GE-00416 –
Panel 7 Exhaust Drift at S2180 W585 – Roof

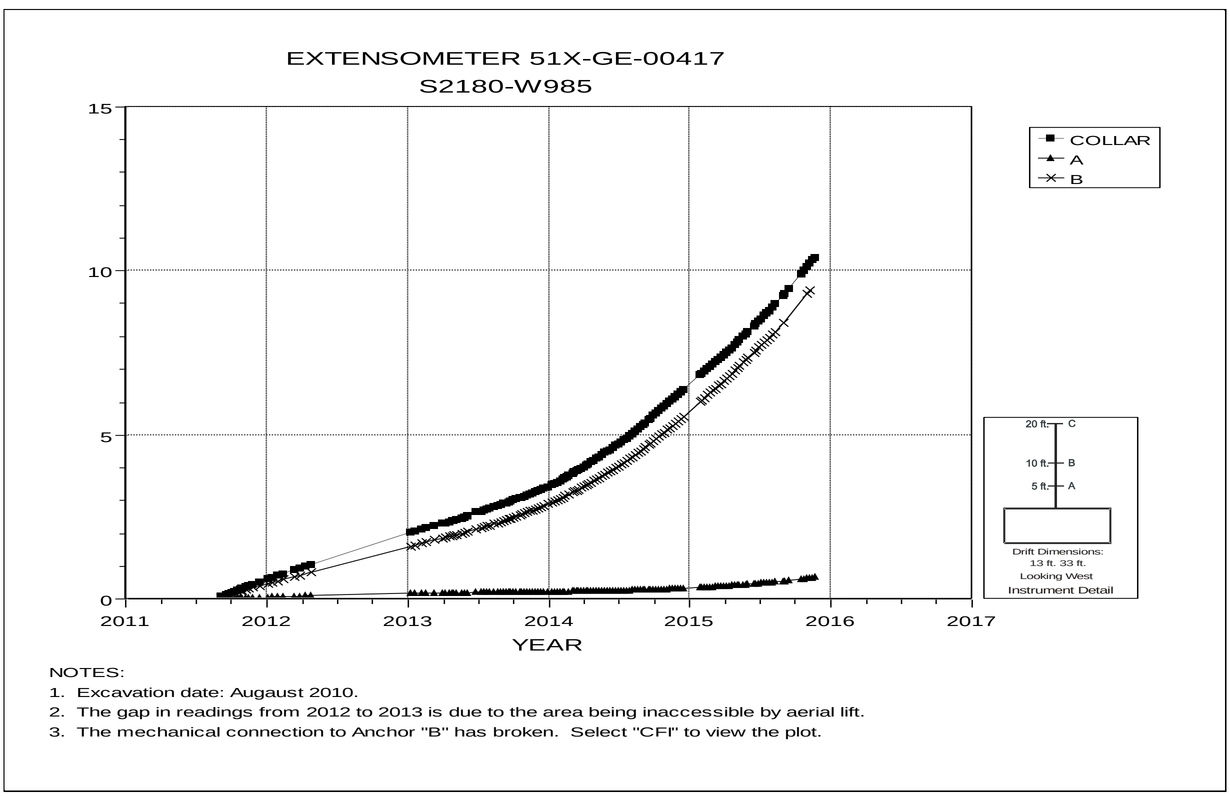

Figure 5-18 Extensometer 51X-GE-00417 –
Panel 7 Exhaust Drift at S2180 W985 – Roof

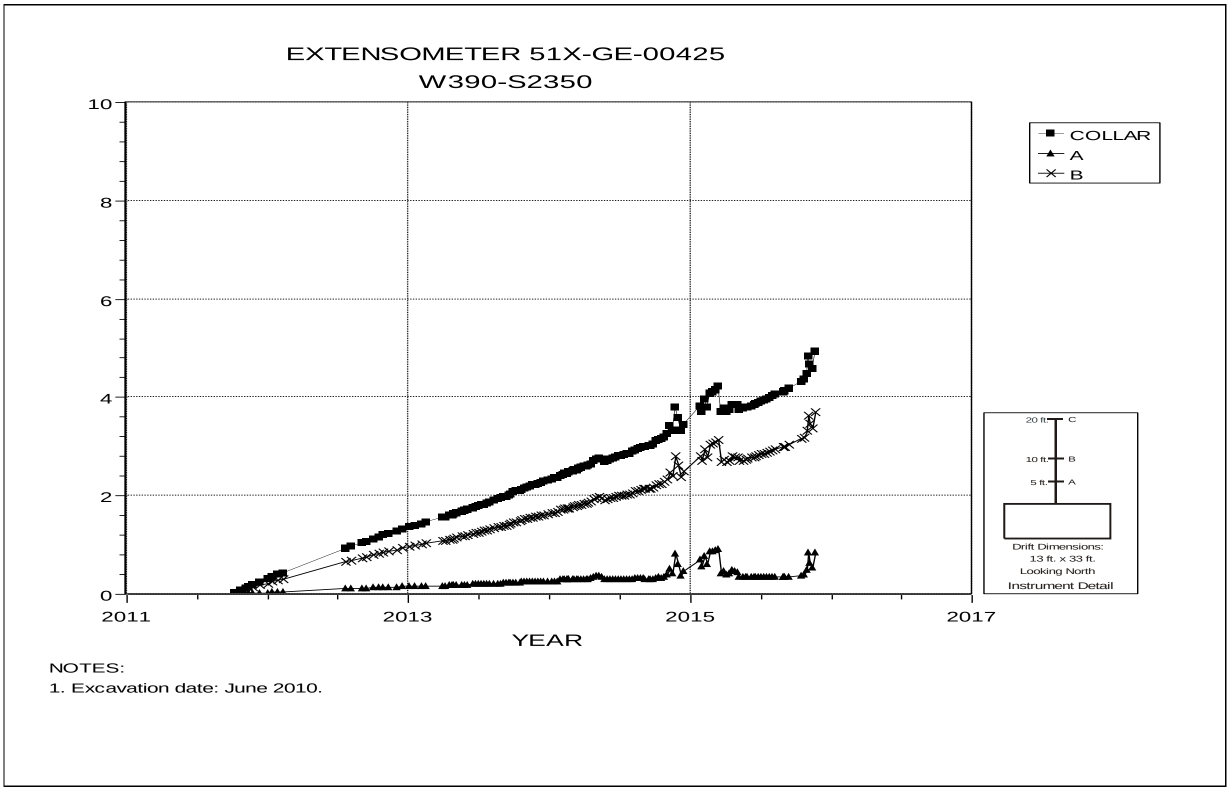

Figure 5-19 Extensometer 51X-GE-00425 –
Room 1 Panel 7 at W390 S2350 – Roof

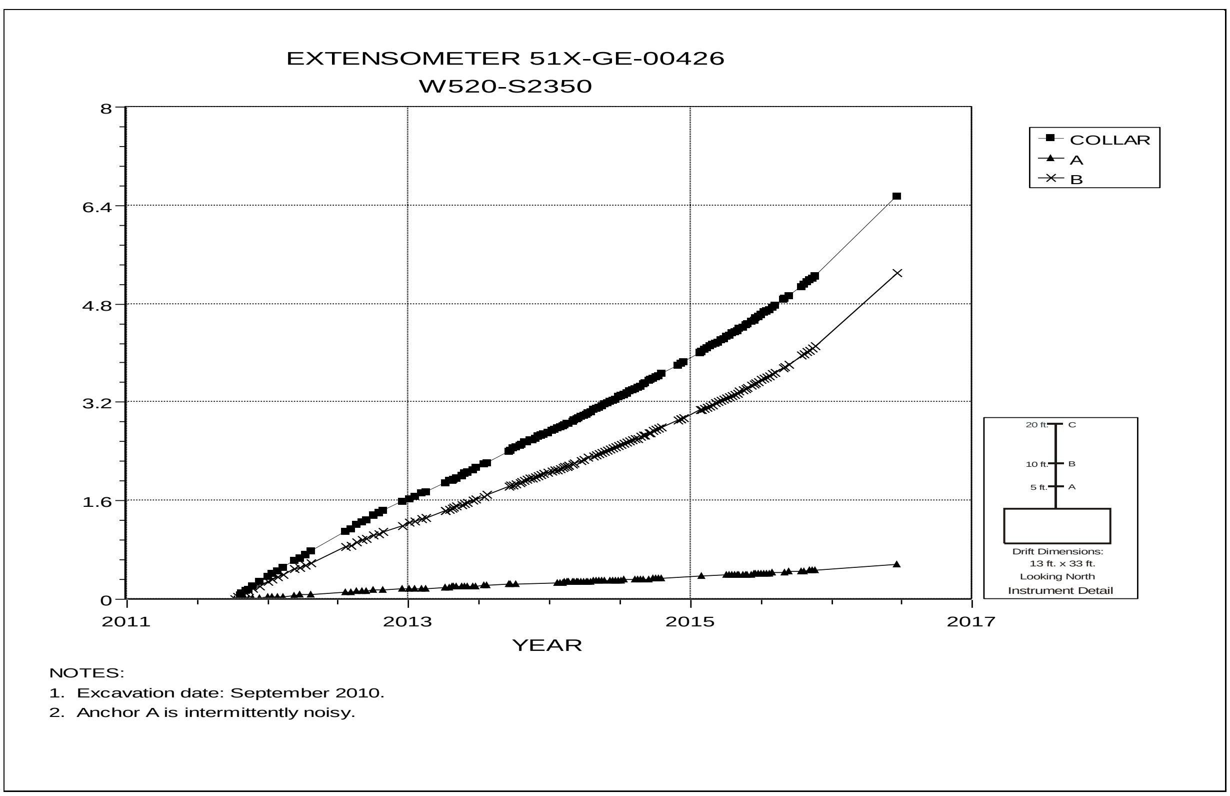

Figure 5-20 Extensometer 51X-GE-00426 –
Room 2 Panel 7 at W520 S2350 – Roof

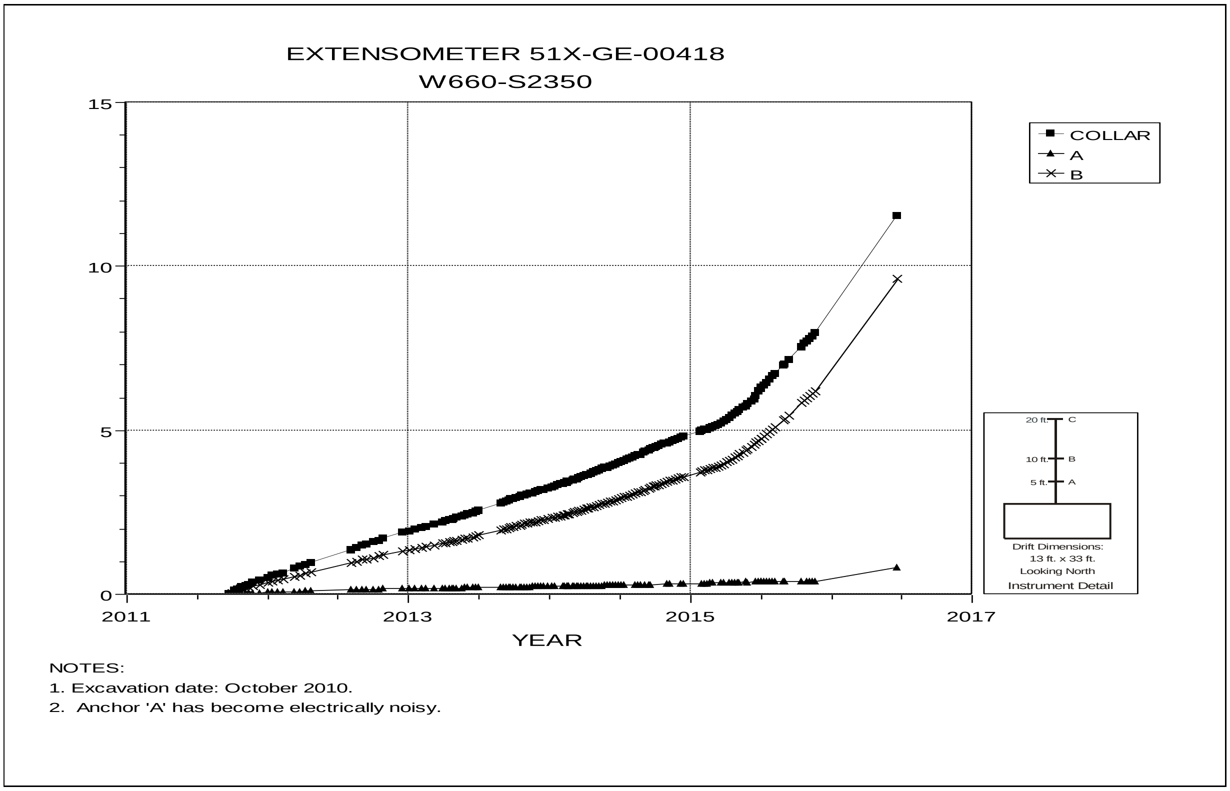

Figure 5-21 Extensometer 51X-GE-00418 –
Room 3 Panel 7 at W660 S2350 – Roof

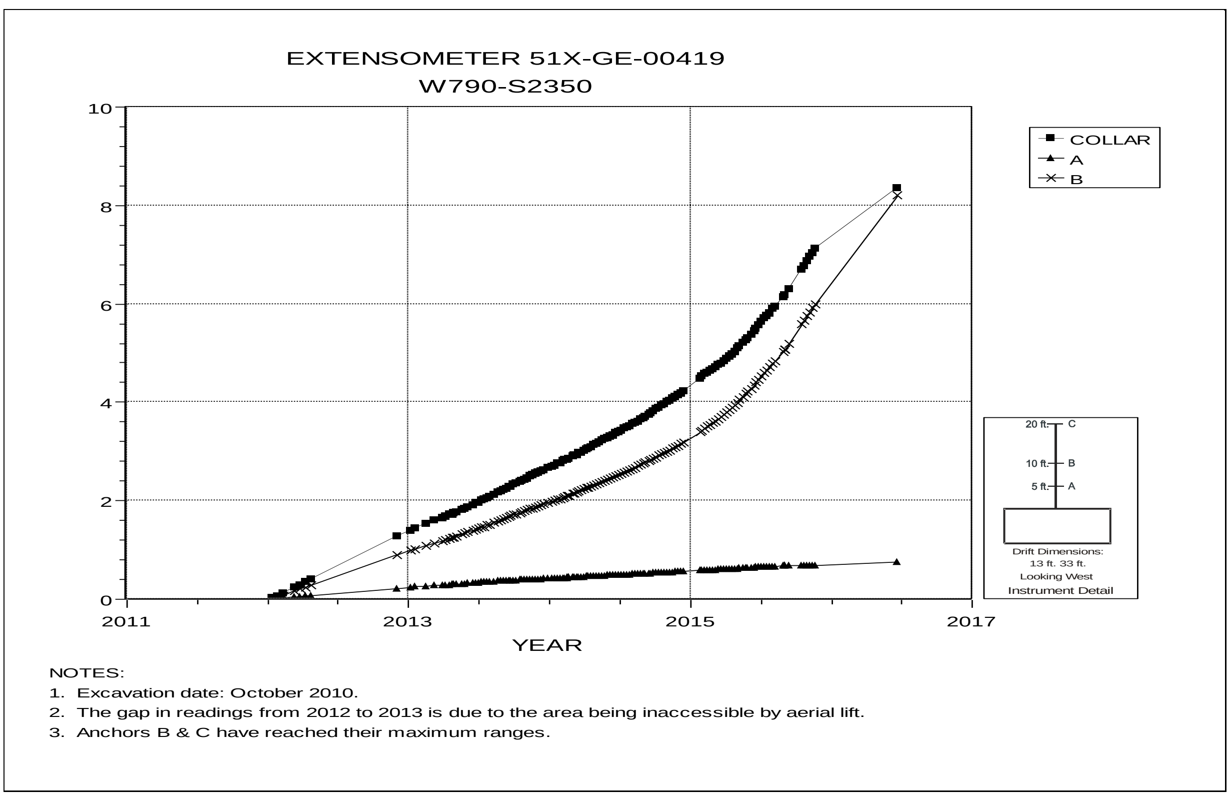

Figure 5-22 Extensometer 51X-GE-00419 –
Room 4 Panel 7 at W790 S2350 – Roof

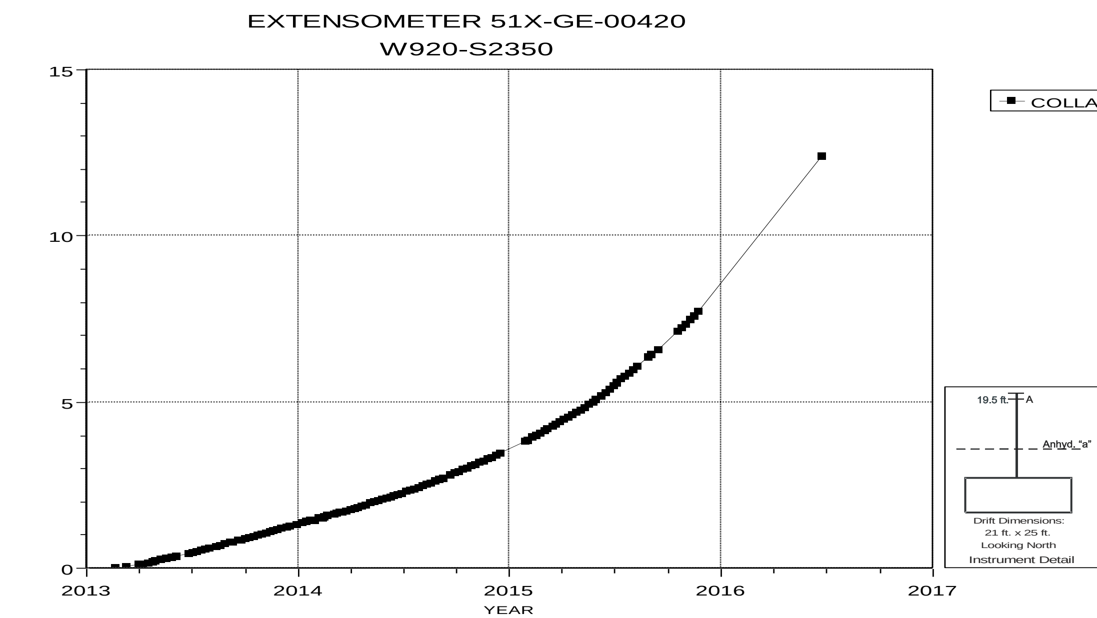

NOTES:
1. Excavation date: November 2010.
2. The instrument's maximum range has been exceeded and the instrument has failed.

Figure 5-23 Extensometer 51X-GE-00420 –
Room 5 Panel 7 at W920 S2350 – Roof

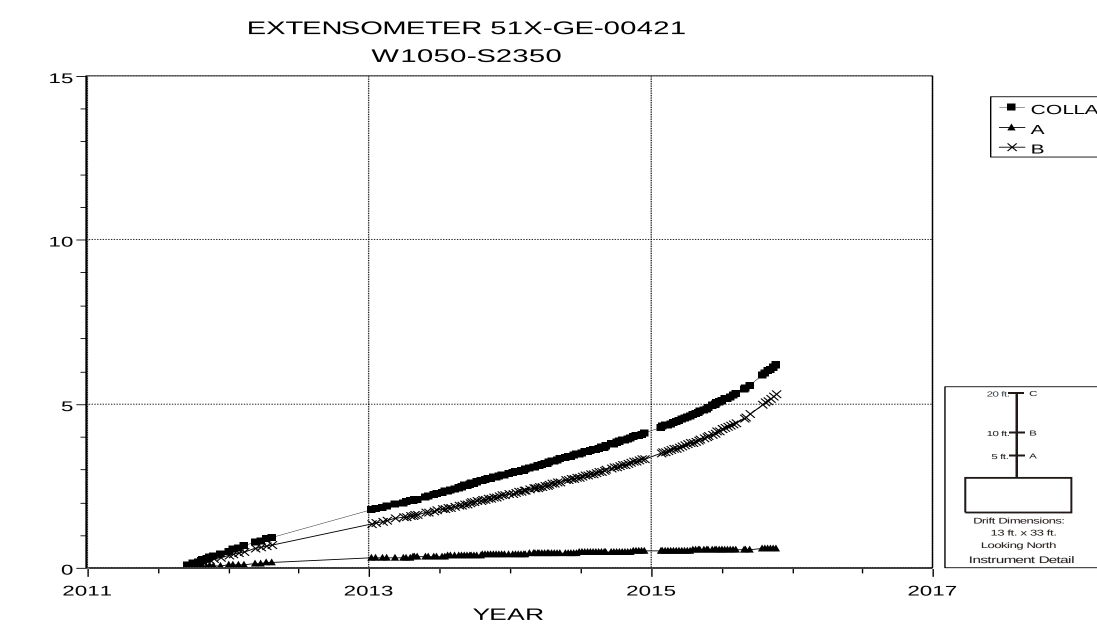

NOTES:
1. Excavation date: November 2010.
2. The gap in readings from 2012 to 2013 is due to the area being inaccessible by aerial lift.

Figure 5-24 Extensometer 51X-GE-00421 –
Room 6 Panel 7 at W1050 S2350 – Roof

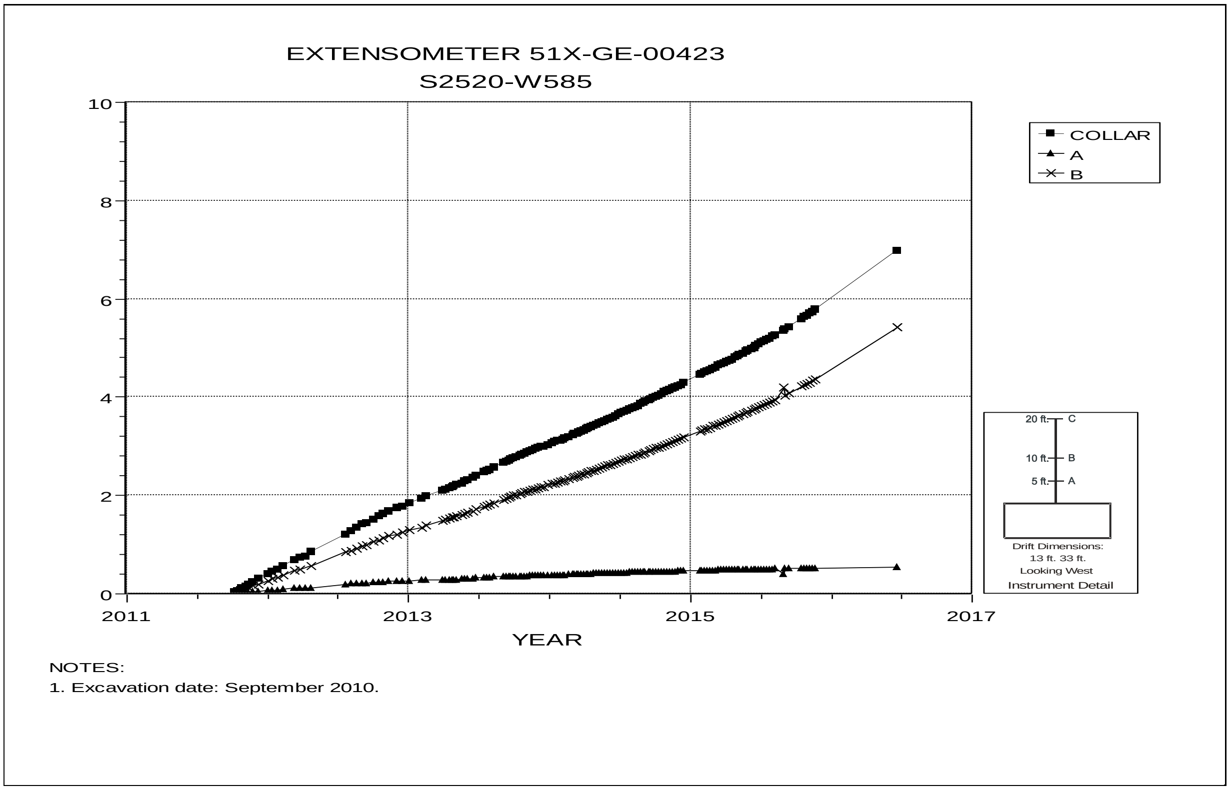

Figure 5-25 Extensometer 51X-GE-00423 –
Panel 7 Intake Drift at S2520 W585 – Roof

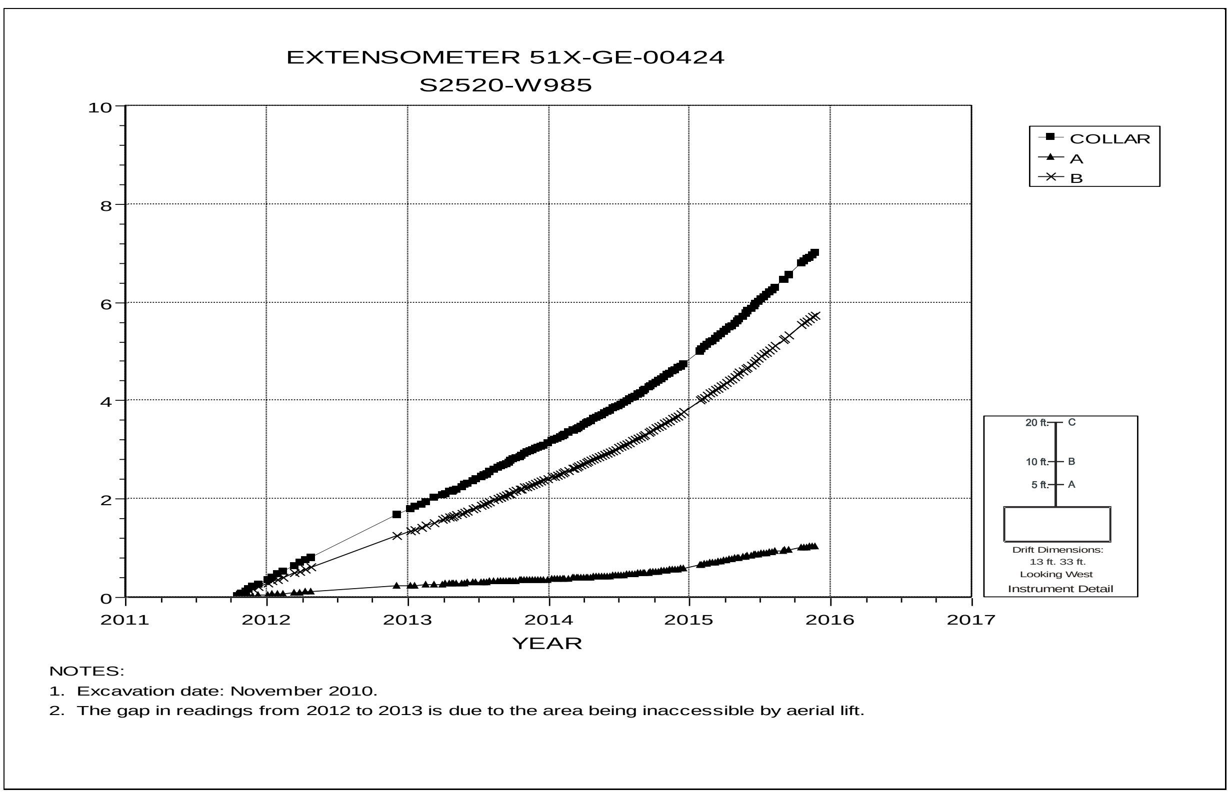

Figure 5-26 Extensometer 51X-GE-00424 –
Panel 7 Intake Drift at S2520 W985 – Roof

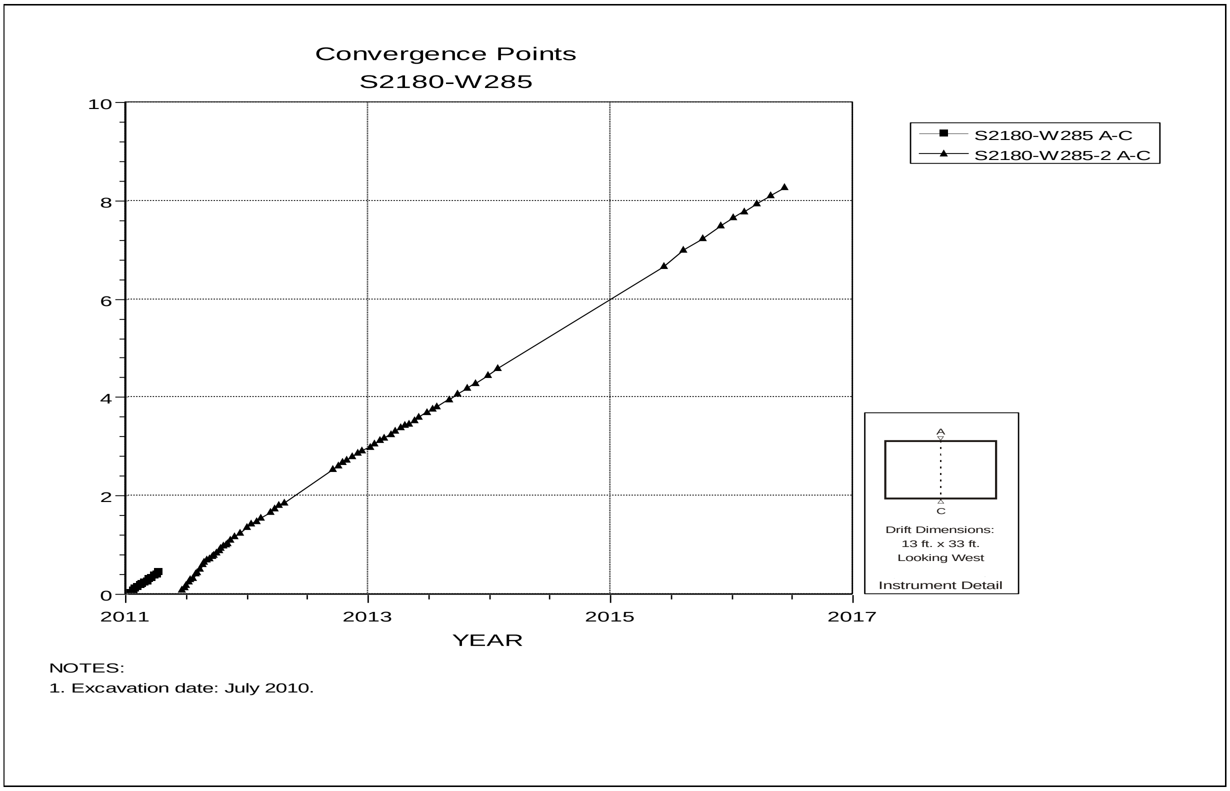

Figure 5-27 Convergence Point Array –
Panel 7 Exhaust Drift at S2180 W285 – Roof to Floor

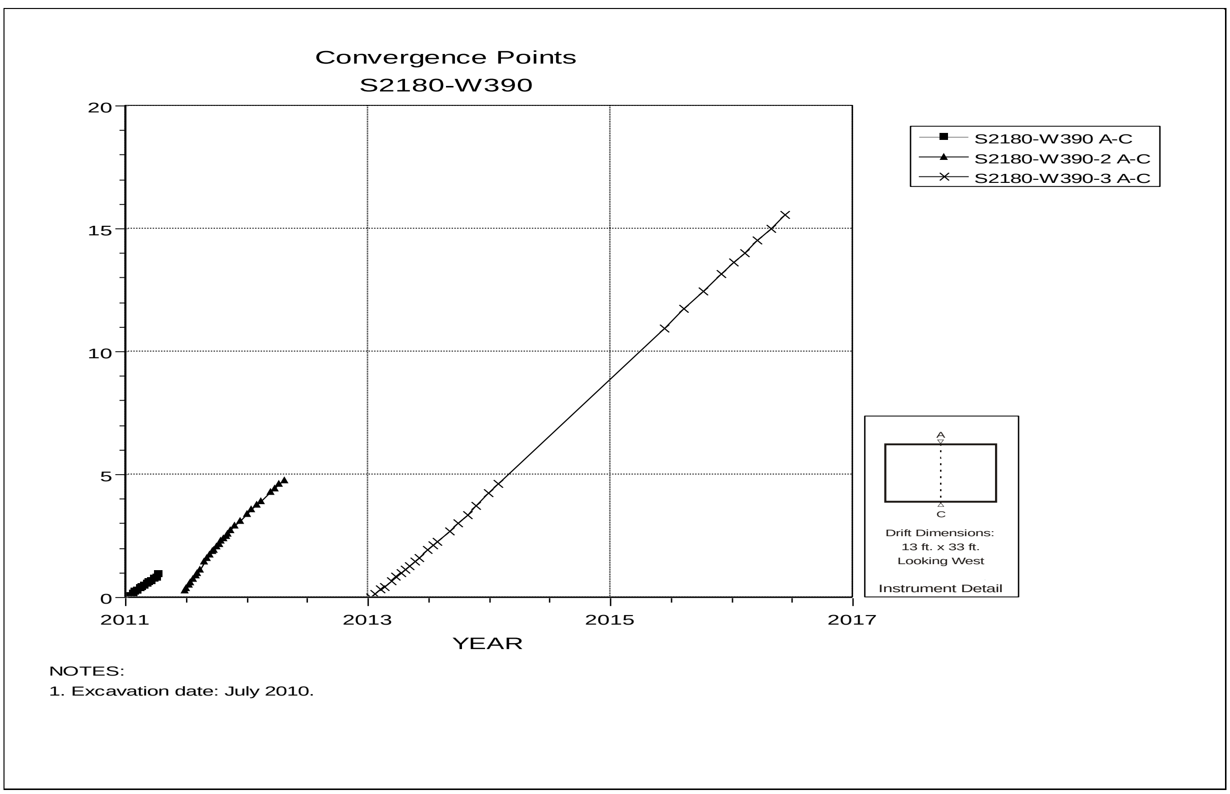

Figure 5-28 Convergence Point Array –
Panel 7 Exhaust Drift at S2180 W390 – Roof to Floor

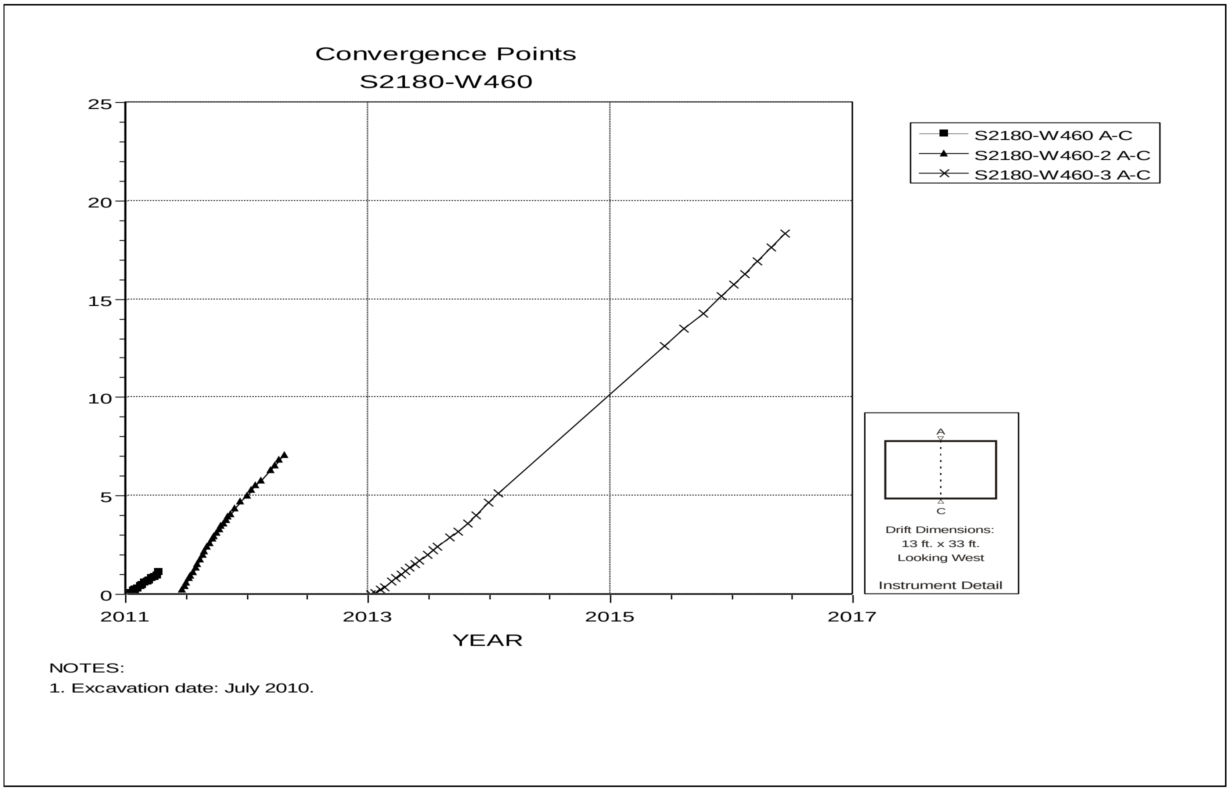

Figure 5-29 Convergence Point Array –
Panel 7 Exhaust Drift at S2180 W460 – Roof to Floor

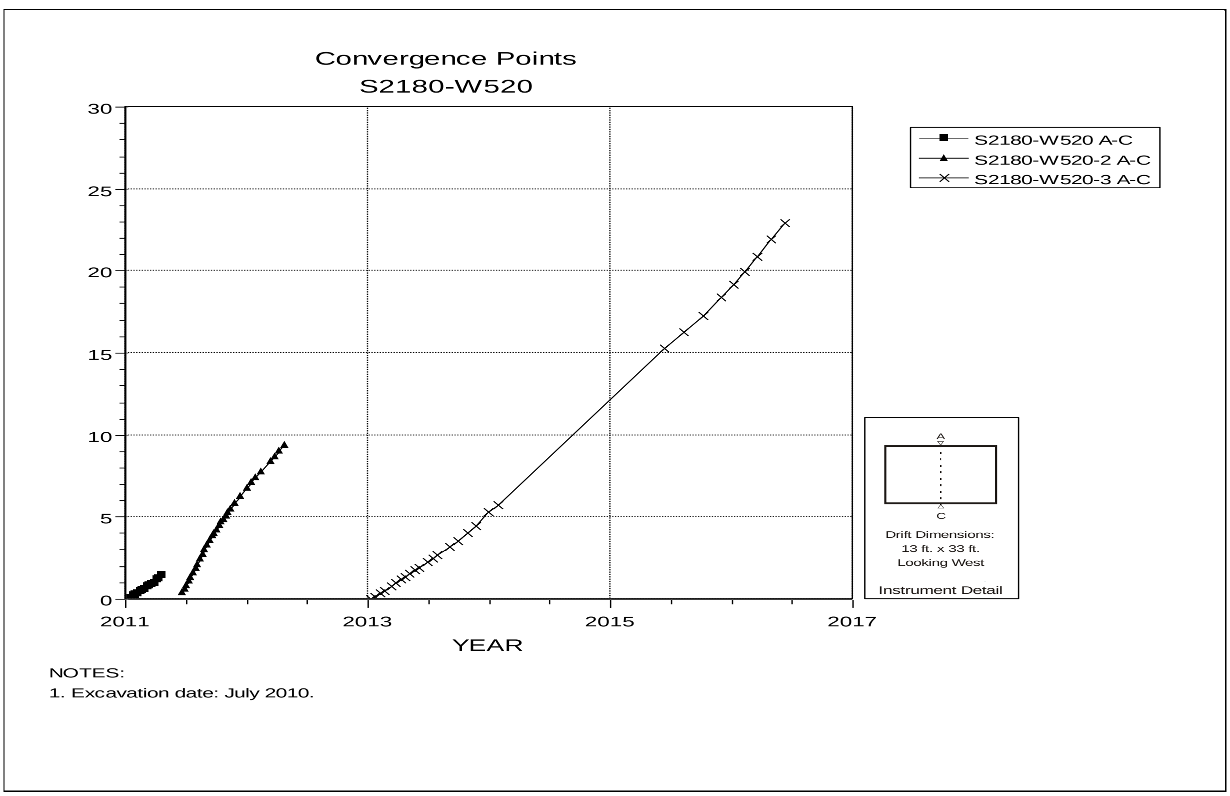

Figure 5-30 Convergence Point Array –
Panel 7 Exhaust Drift at S2180 W520 – Roof to Floor

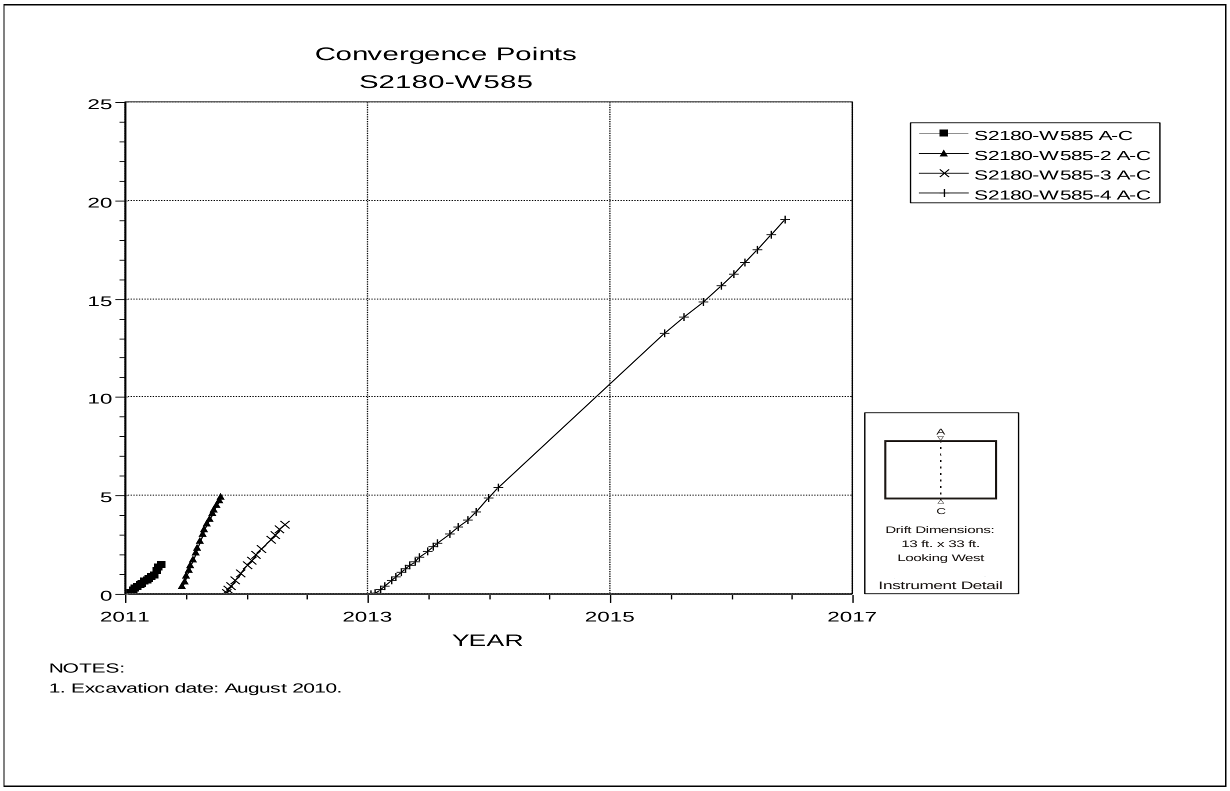

Figure 5-31 Convergence Point Array –
Panel 7 Exhaust Drift at S2180 W585 – Roof to Floor

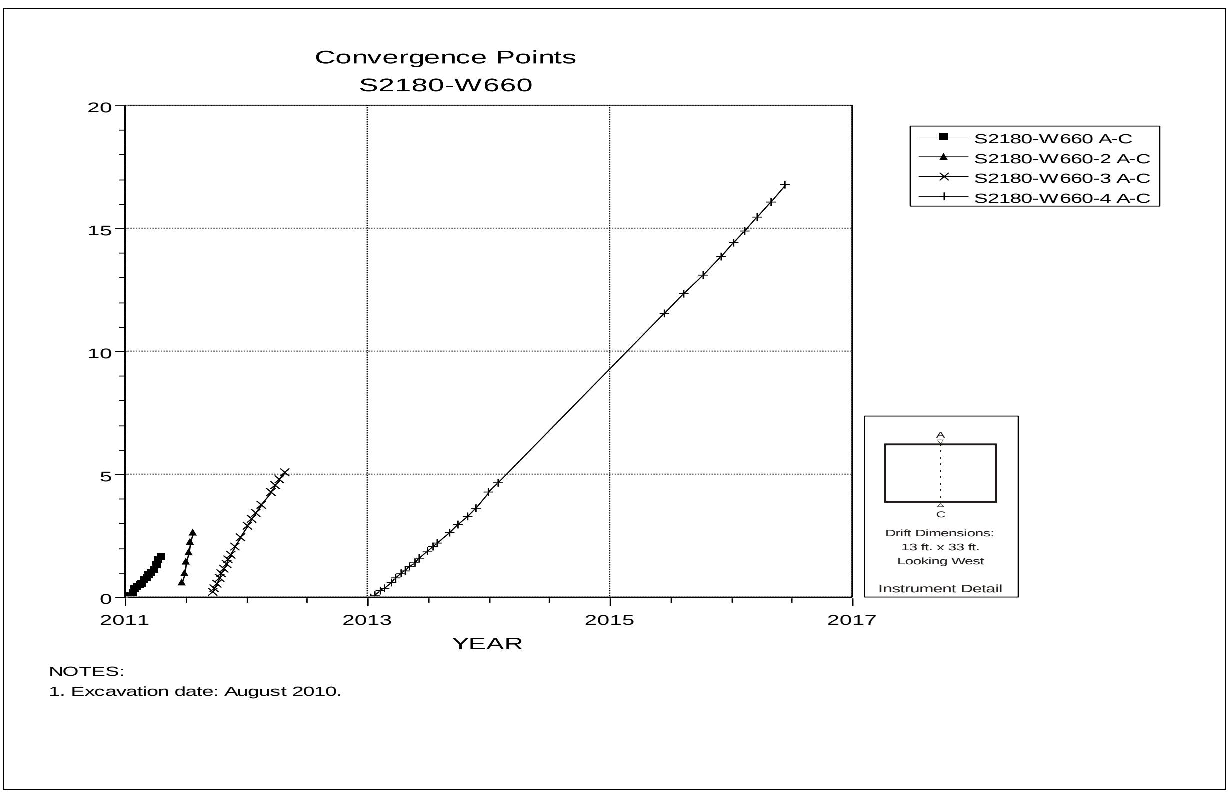

Figure 5-32 Convergence Point Array –
Panel 7 Exhaust Drift at S2180 W660 – Roof to Floor

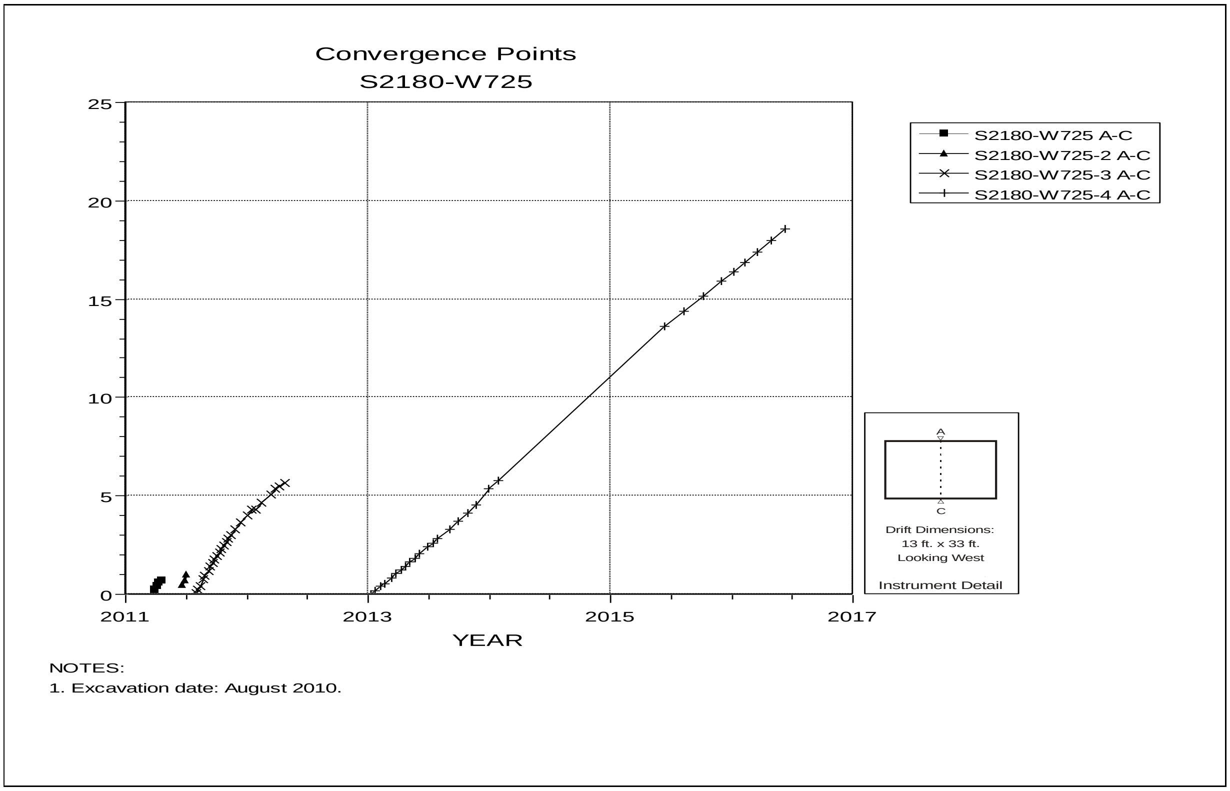

Figure 5-33 Convergence Point Array –
Panel 7 Exhaust Drift at S2180 W725 – Roof to Floor

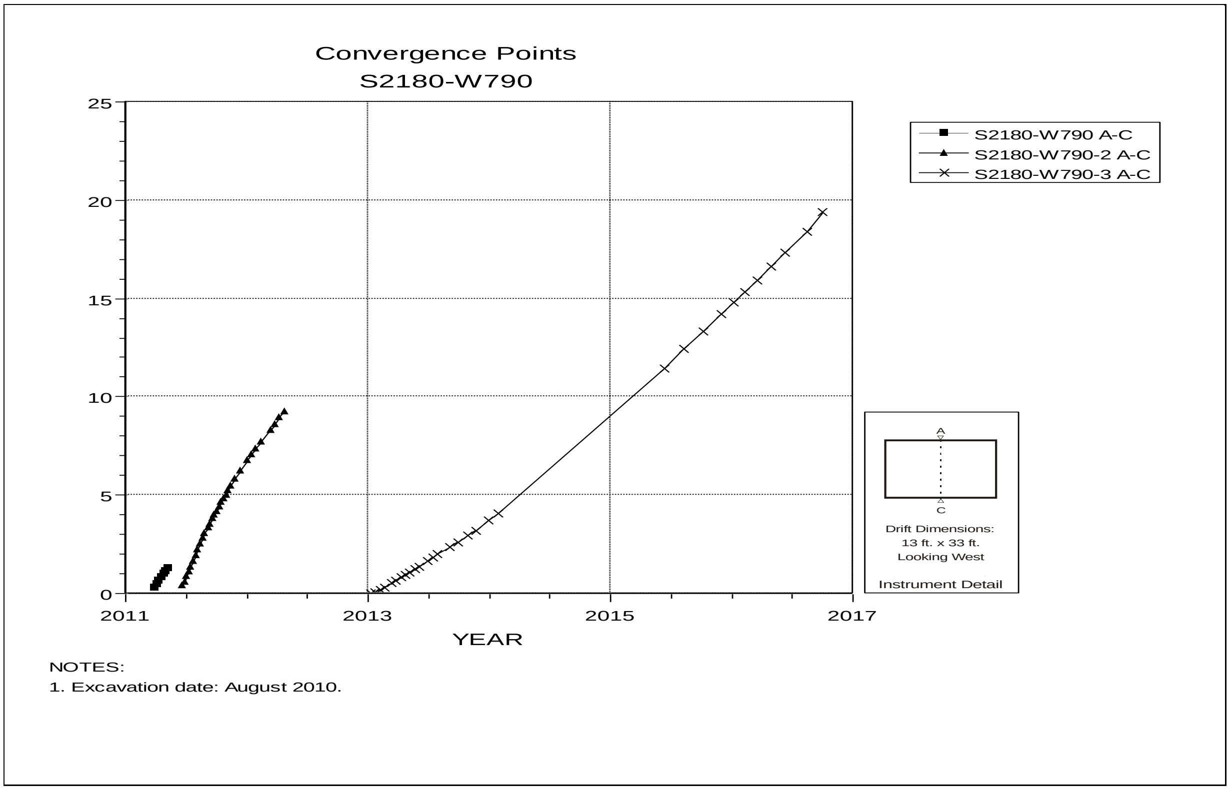

Figure 5-34 Convergence Point Array –
Panel 7 Exhaust Drift at S2180 W790 – Roof to Floor

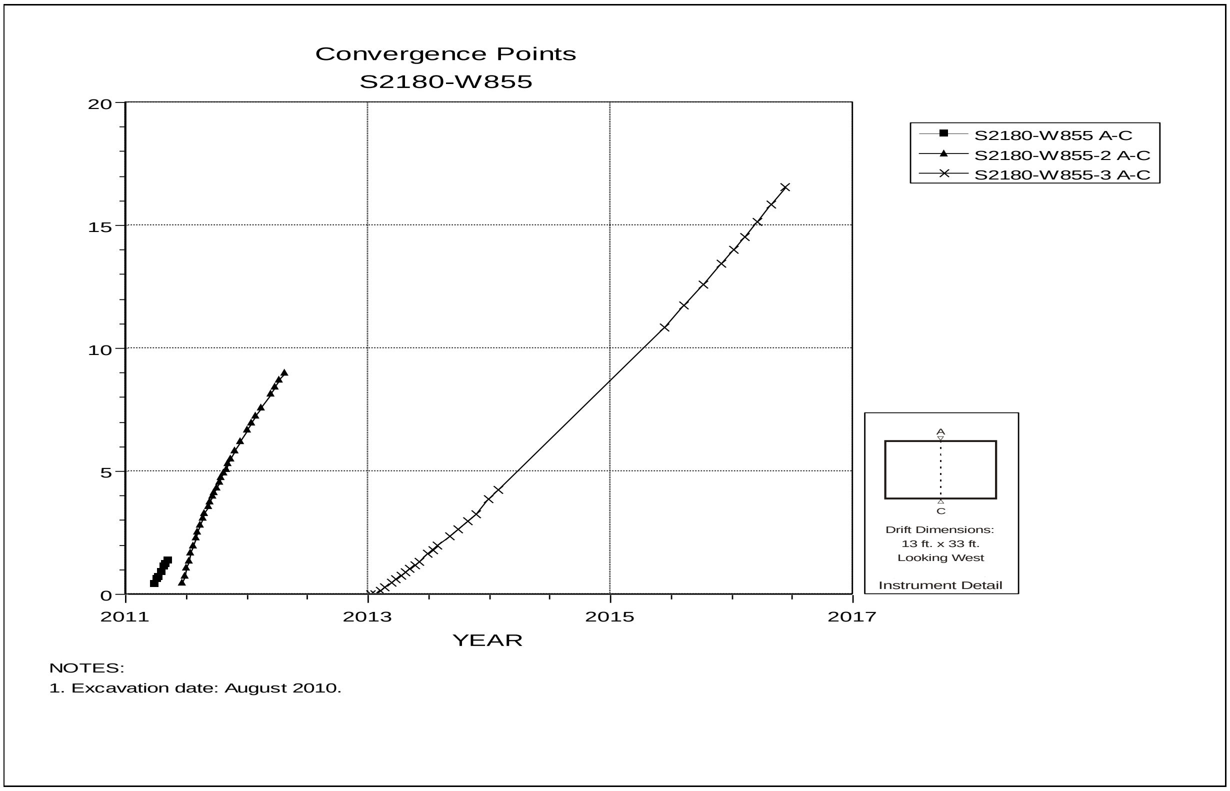

Figure 5-35 Convergence Point Array –
Panel 7 Exhaust Drift at S2180 W855 – Roof to Floor

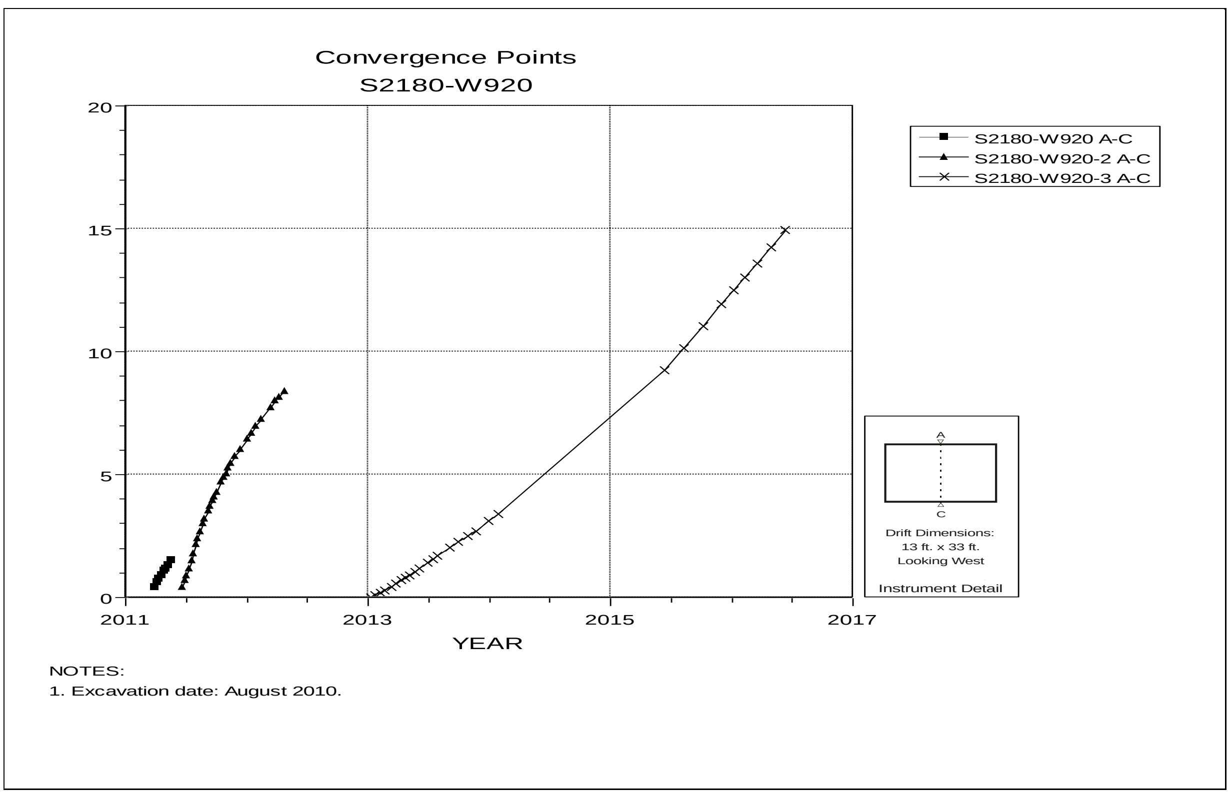

Figure 5-36 Convergence Point Array –
Panel 7 Exhaust Drift at S2180 W920 – Roof to Floor

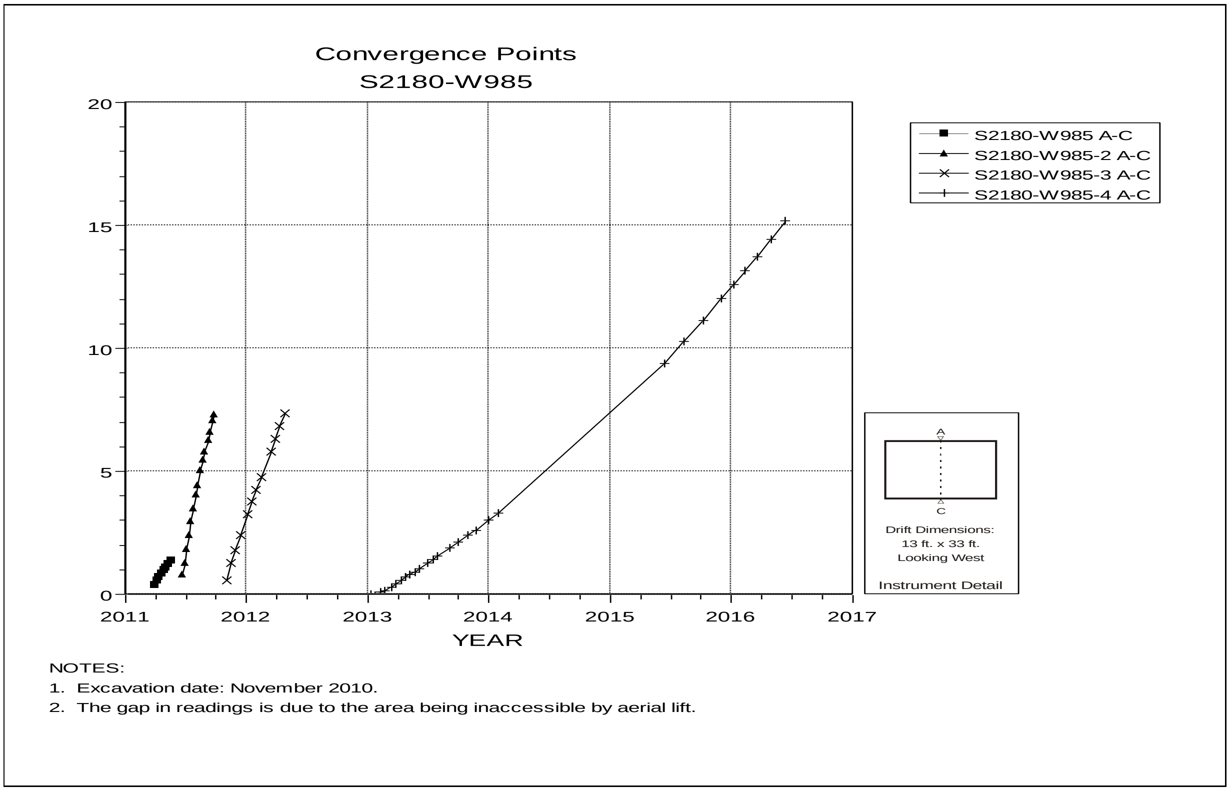

Figure 5-37 Convergence Point Array –
Panel 7 Exhaust Drift at S2180 W985 – Roof to Floor

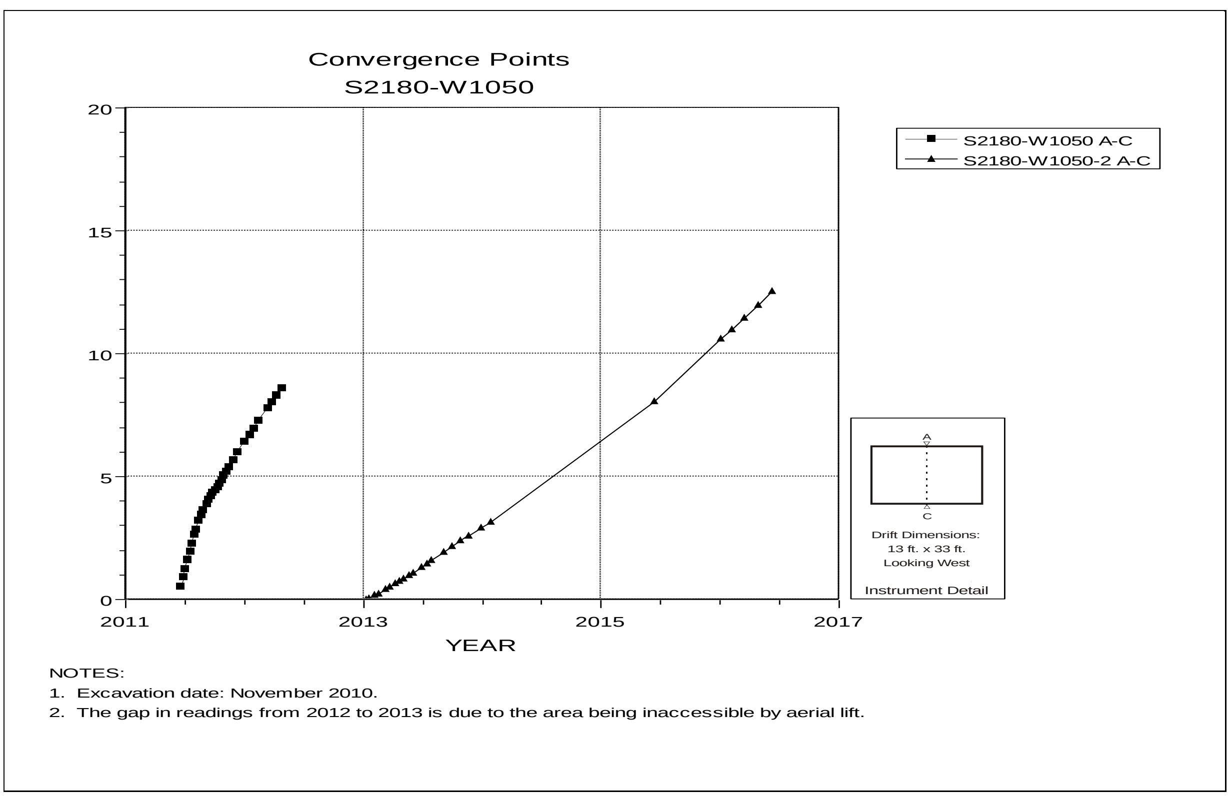

Figure 5-38 Convergence Point Array –
Panel 7 Exhaust Drift at S2180 W1050 – Roof to Floor

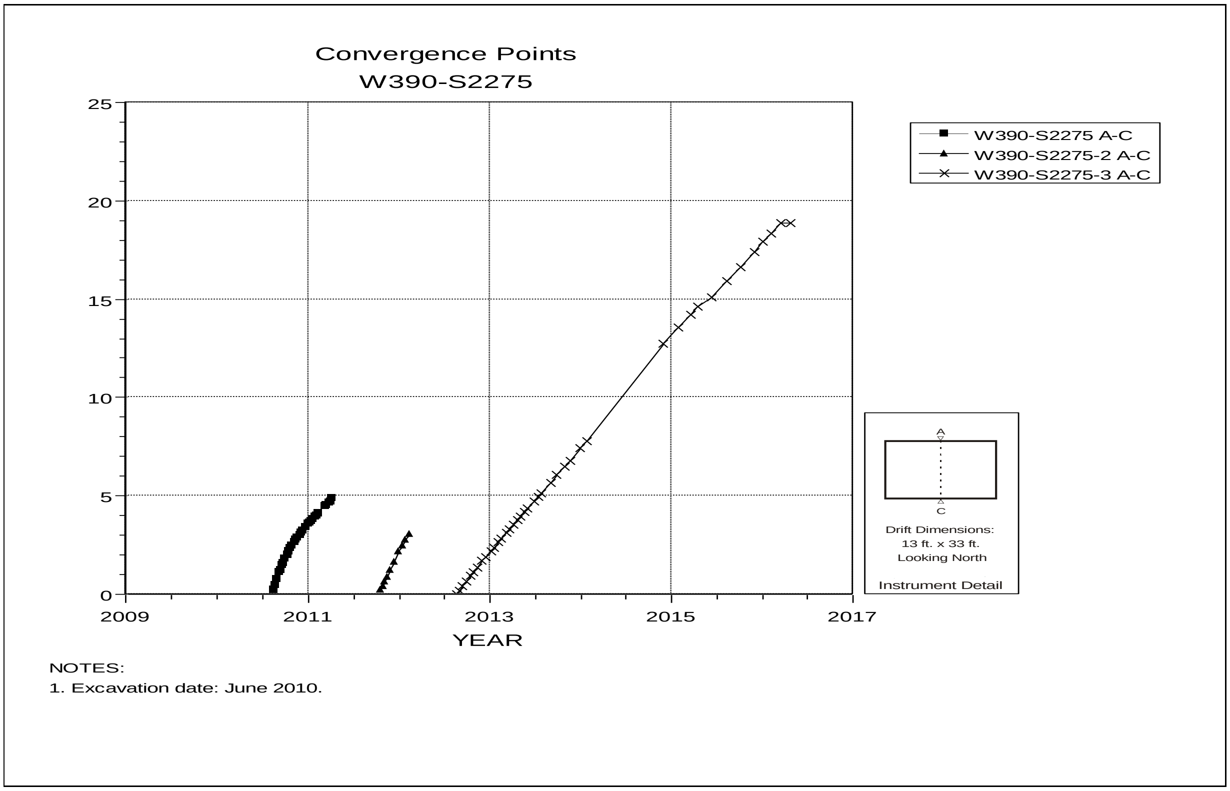

Figure 5-39 Convergence Point Array –
Room 1 Panel 7 at W390 S2275 – Roof to Floor

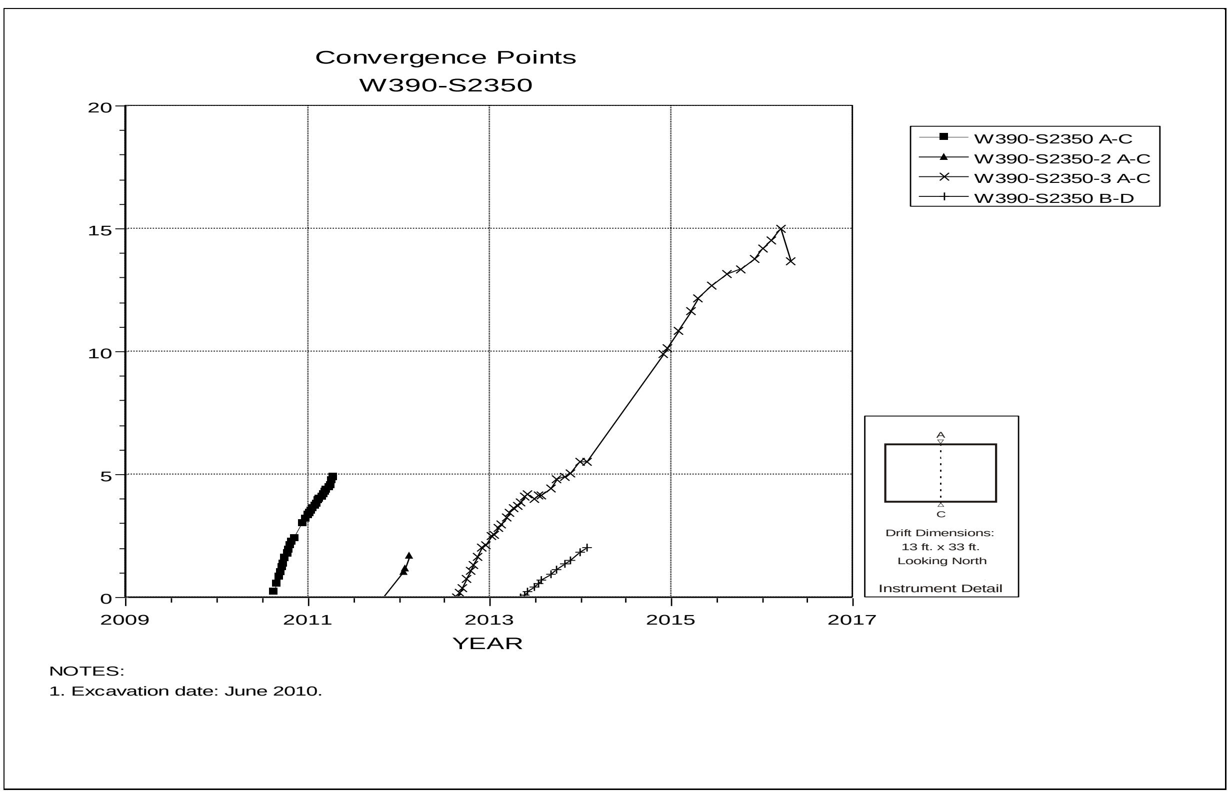

Figure 5-40 Convergence Point Array –
Room 1 Panel 7 at W390 S2350 – All Chords

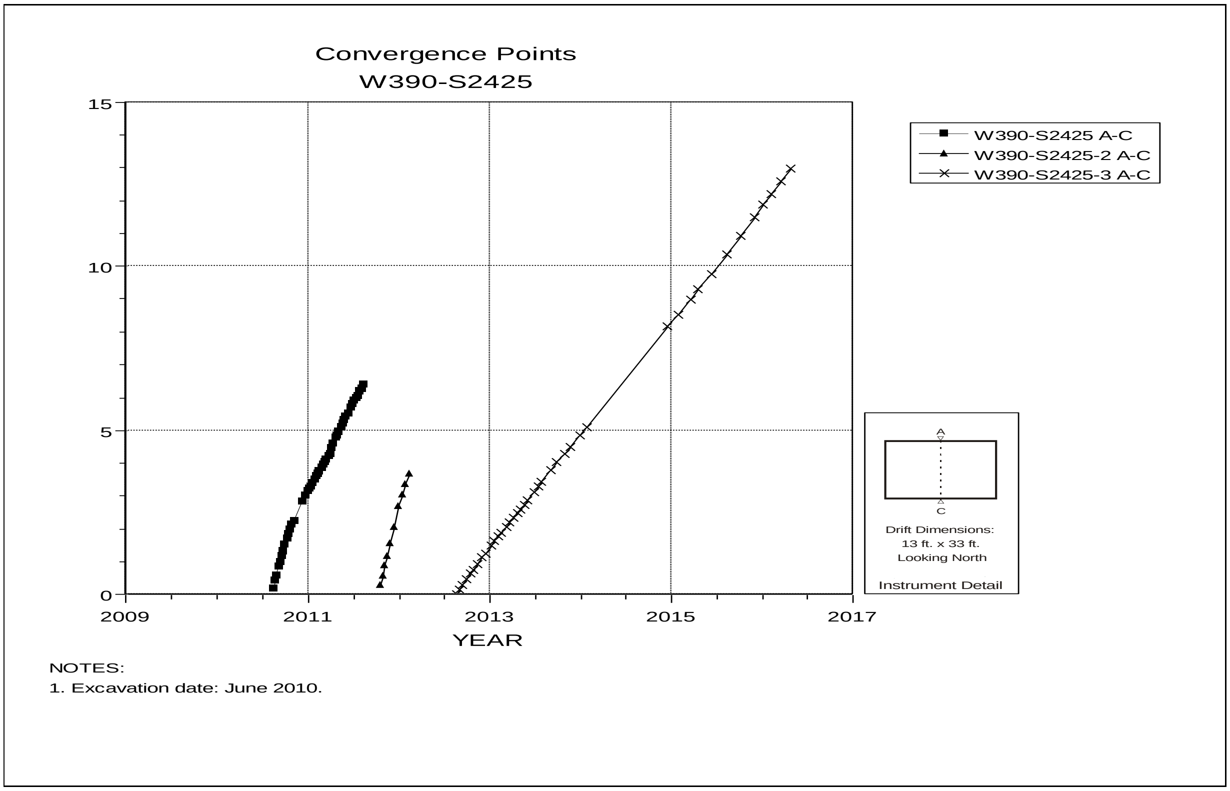

Figure 5-41 Convergence Point Array –
Room 1 Panel 7 at W390 S2425 – Roof to Floor

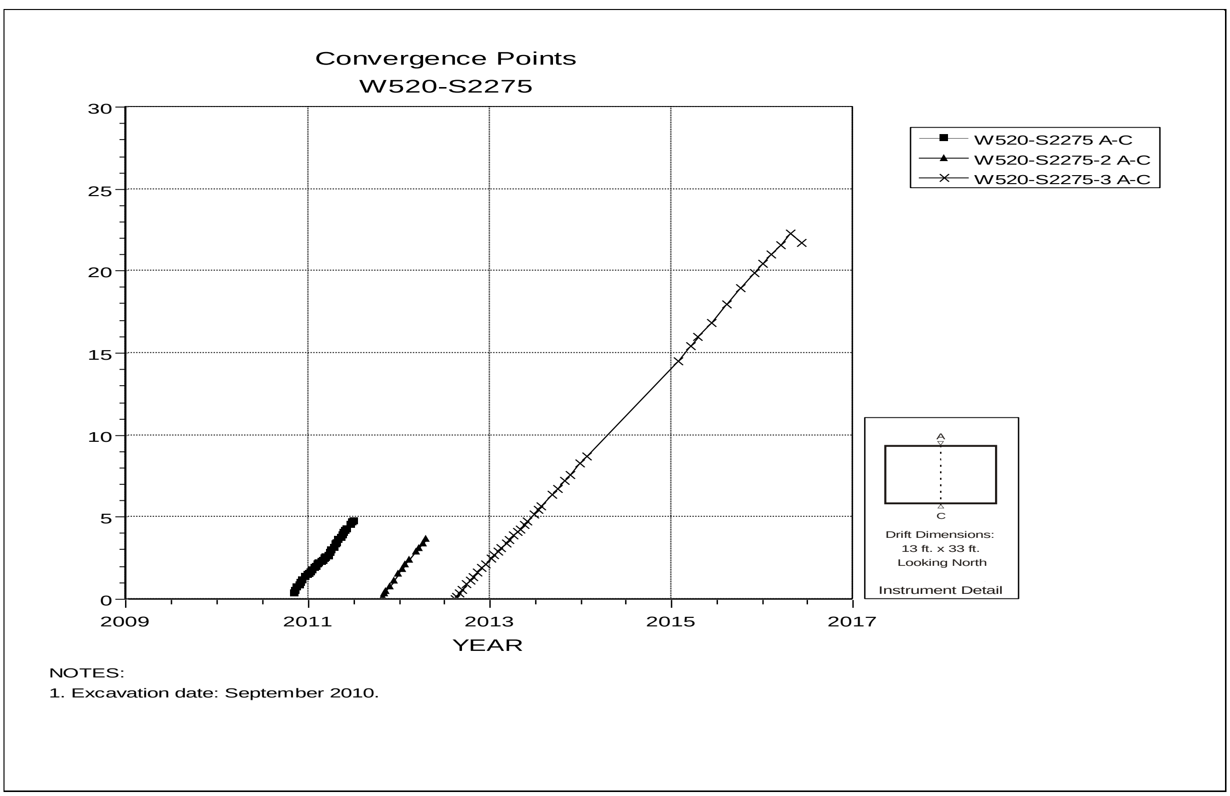

Figure 5-42 Convergence Point Array –
Room 2 Panel 7 at W520 S2275 – Roof to Floor

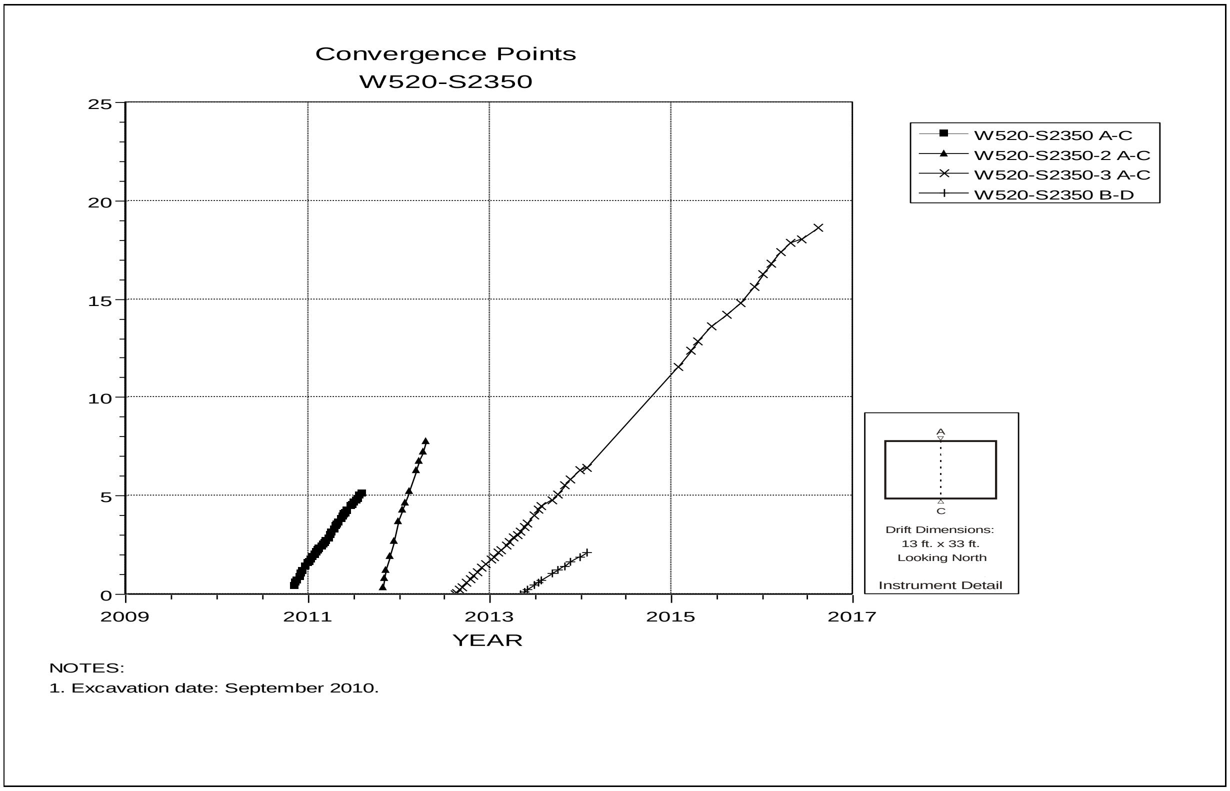

Figure 5-43 Convergence Point Array –
Room 2 Panel 7 at W520 S2350 – All Chords

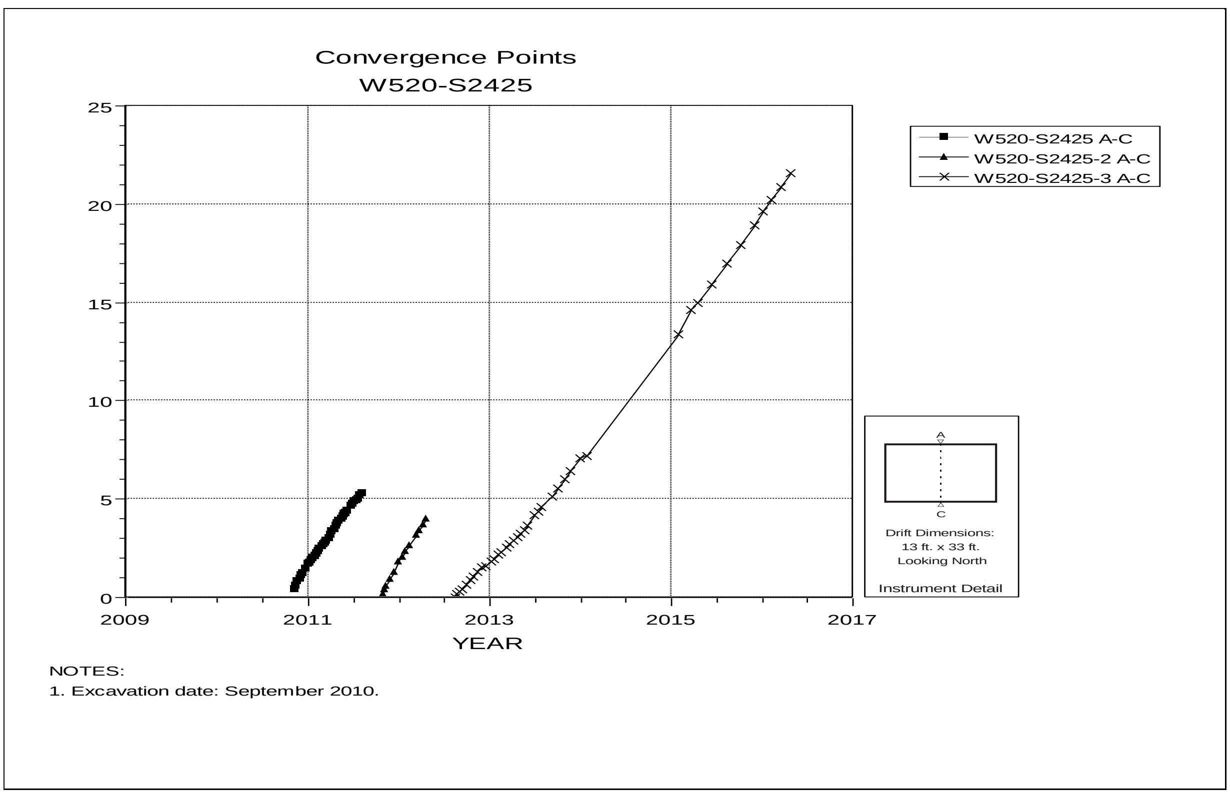

Figure 5-44 Convergence Point Array –
Room 2 Panel 7 at W520 S2425 – Roof to Floor

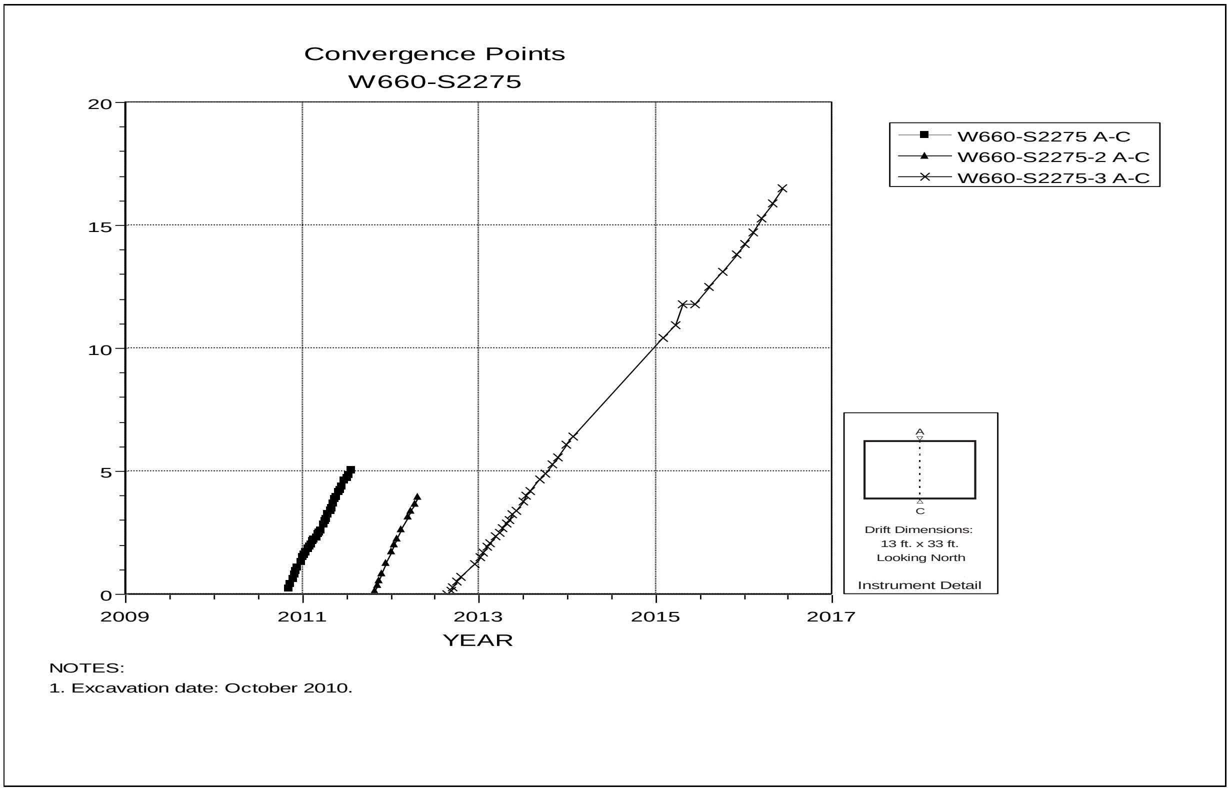

Figure 5-45 Convergence Point Array –
Room 3 Panel 7 W660 S2275 – Roof to Floor

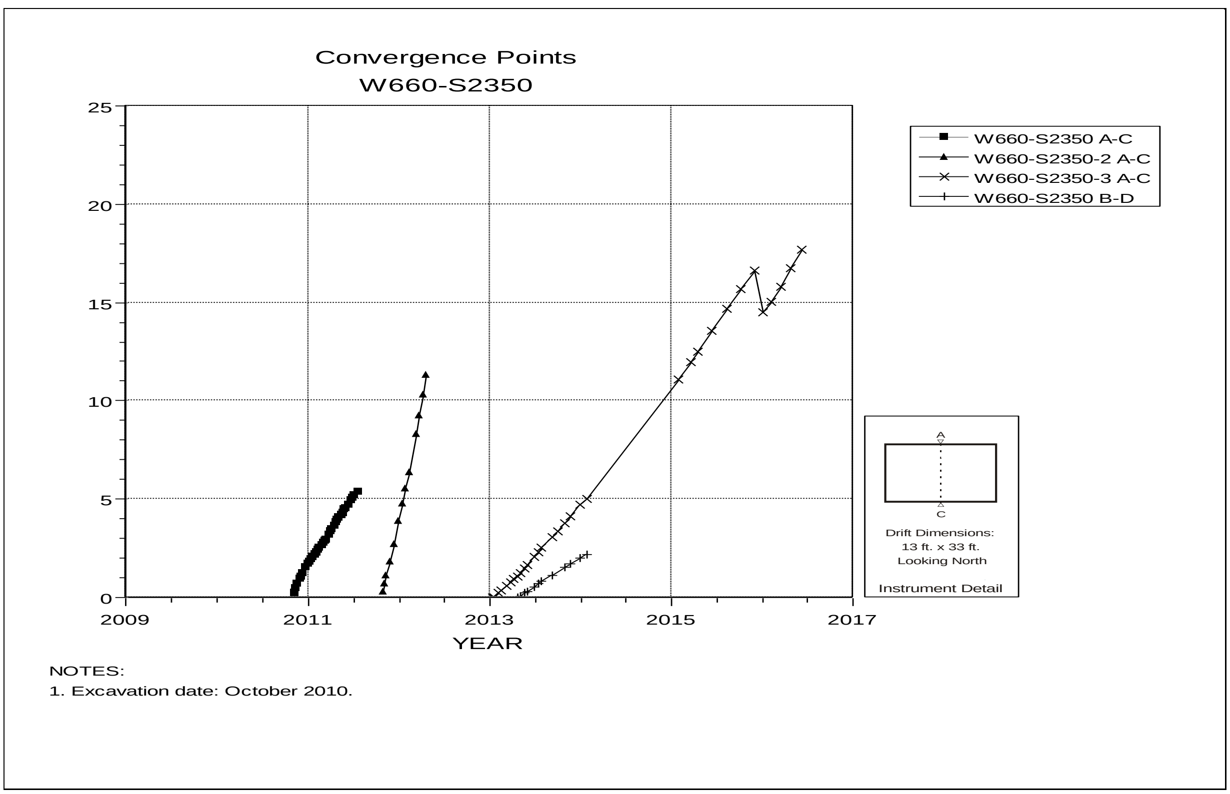

Figure 5-46 Convergence Point Array –
Room 3 Panel 7 at W660 S2350 – All Chords

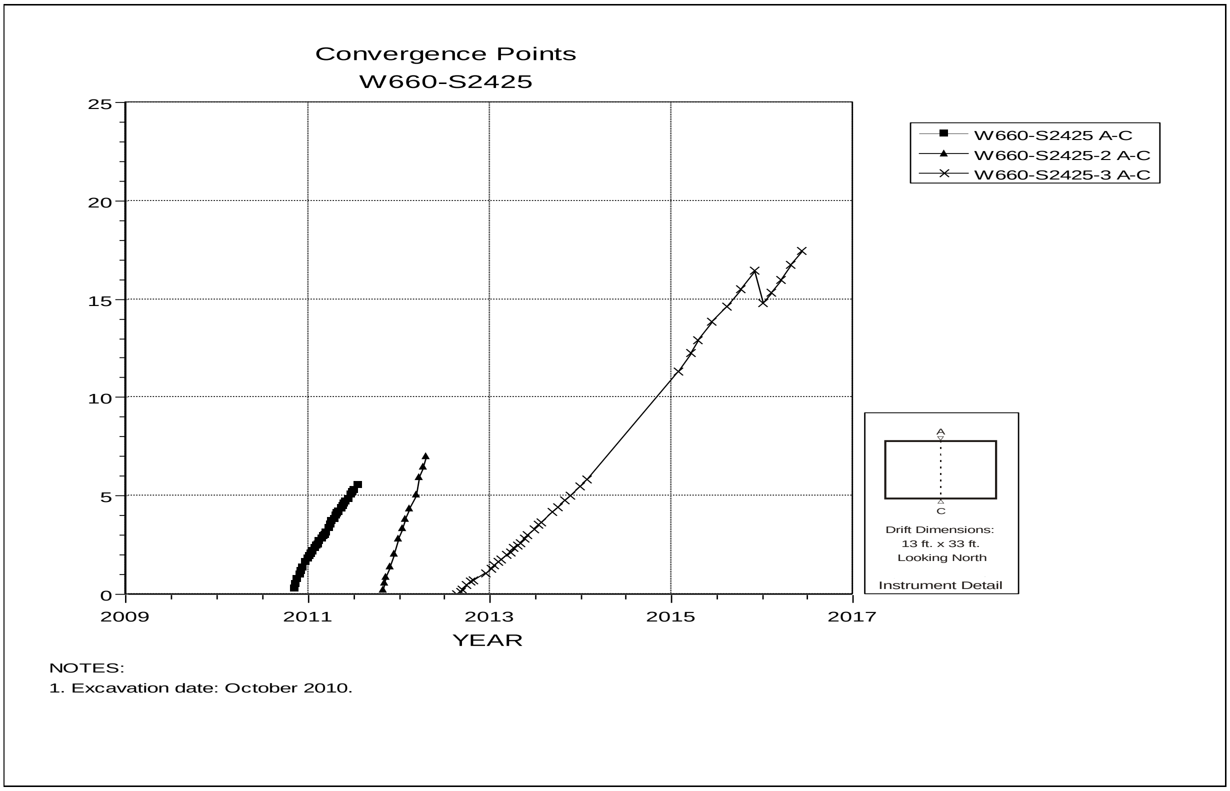

Figure 5-47 Convergence Point Array –
Room 3 Panel 7 at W660 S2425 – Roof to Floor

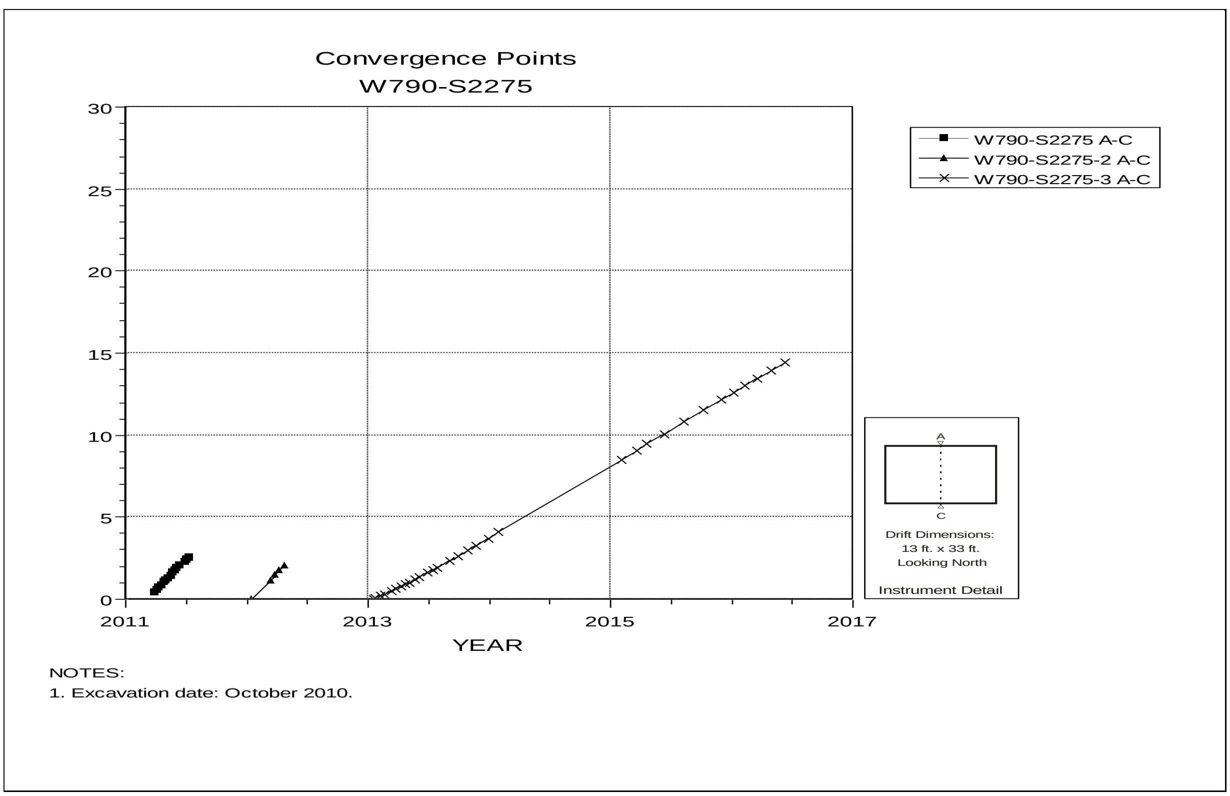

Figure 5-48 Convergence Point Array –
Room 4 Panel 7 at W790 S2275– Roof to Floor

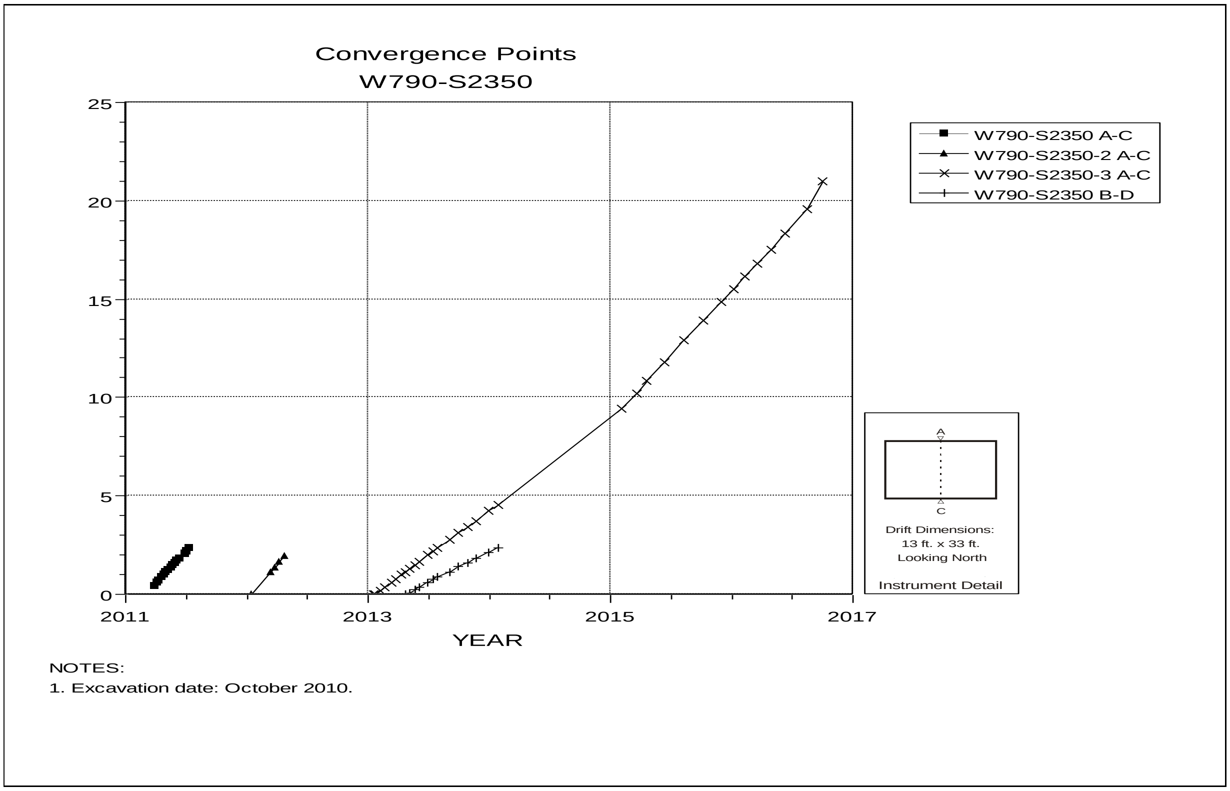

Figure 5-49 Convergence Point Array –
Room 4 Panel 7 at W790 S2350 – All Chords

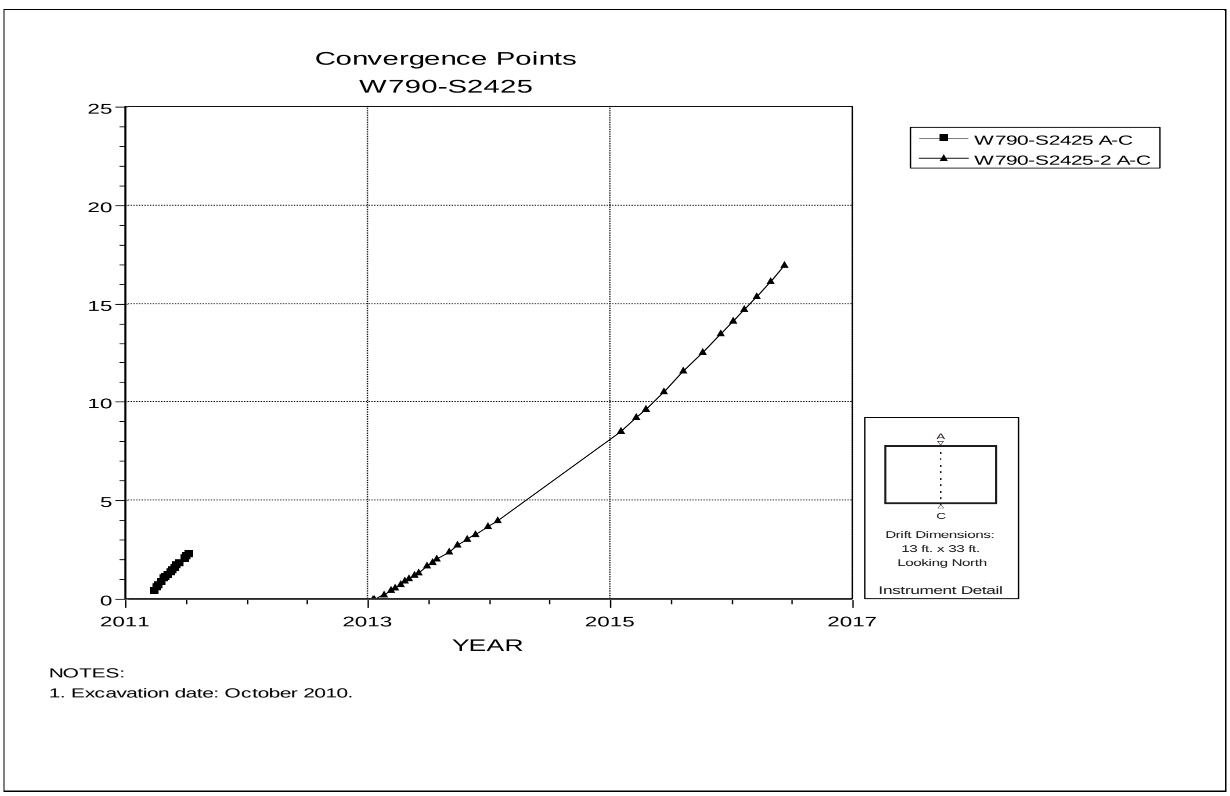

Figure 5-50 Convergence Point Array –
Room 4 Panel 7 at W790 S2425 – Roof to Floor

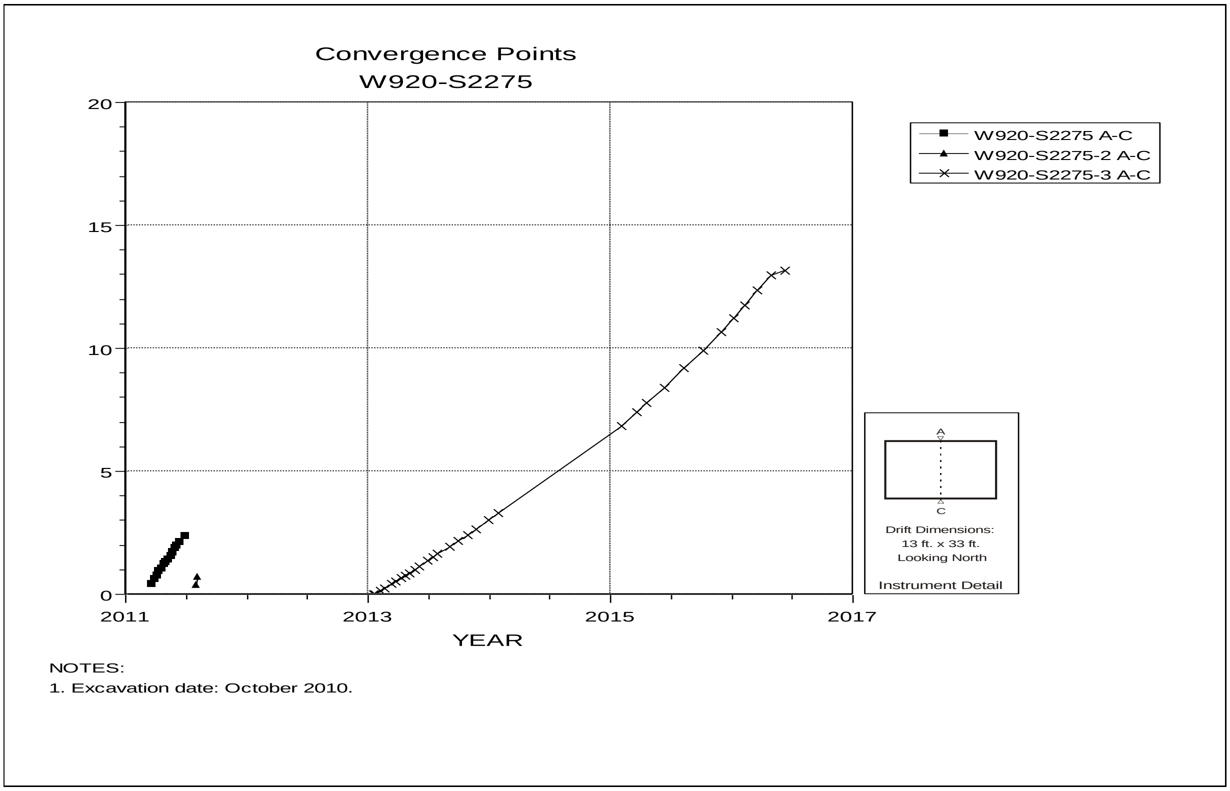

Figure 5-51 Convergence Point Array –
Room 5 Panel 7 at W920 S2275 – Roof to Floor

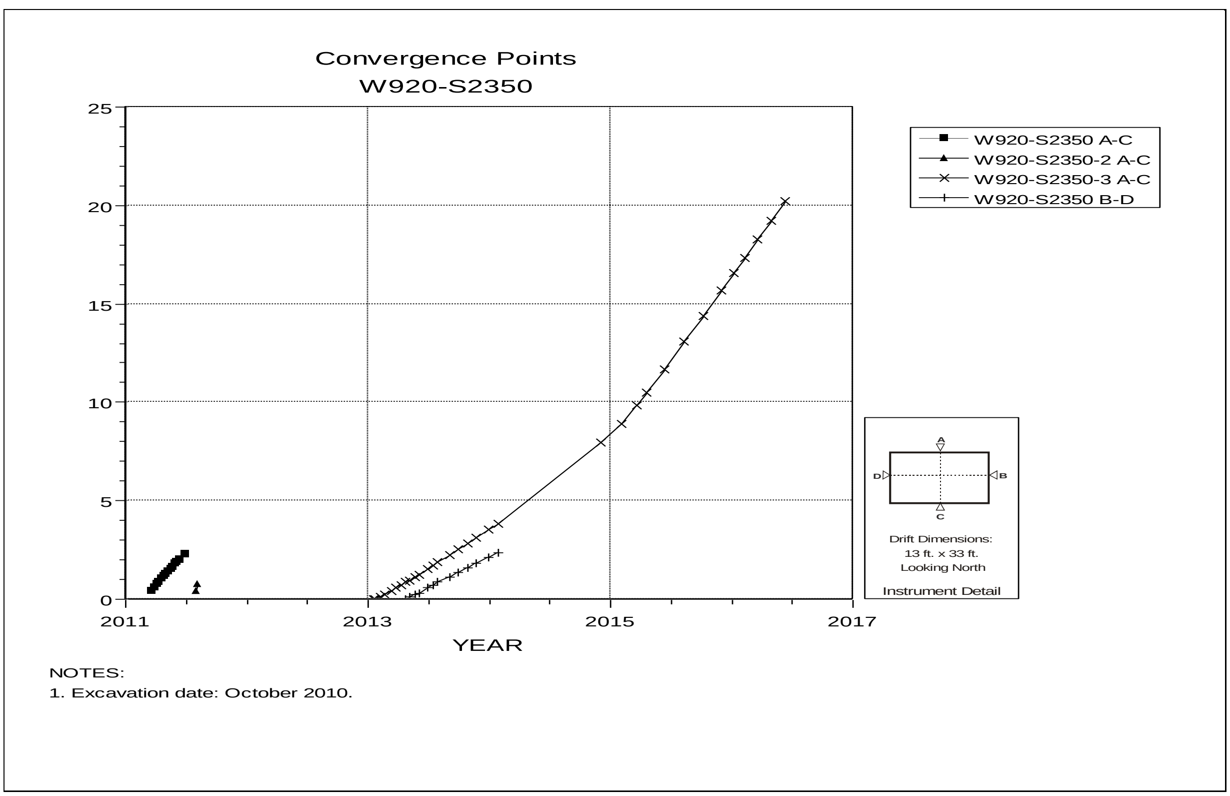

Figure 5-52 Convergence Point Array –
Room 5 Panel 7 at W920 S2350 – All Chords

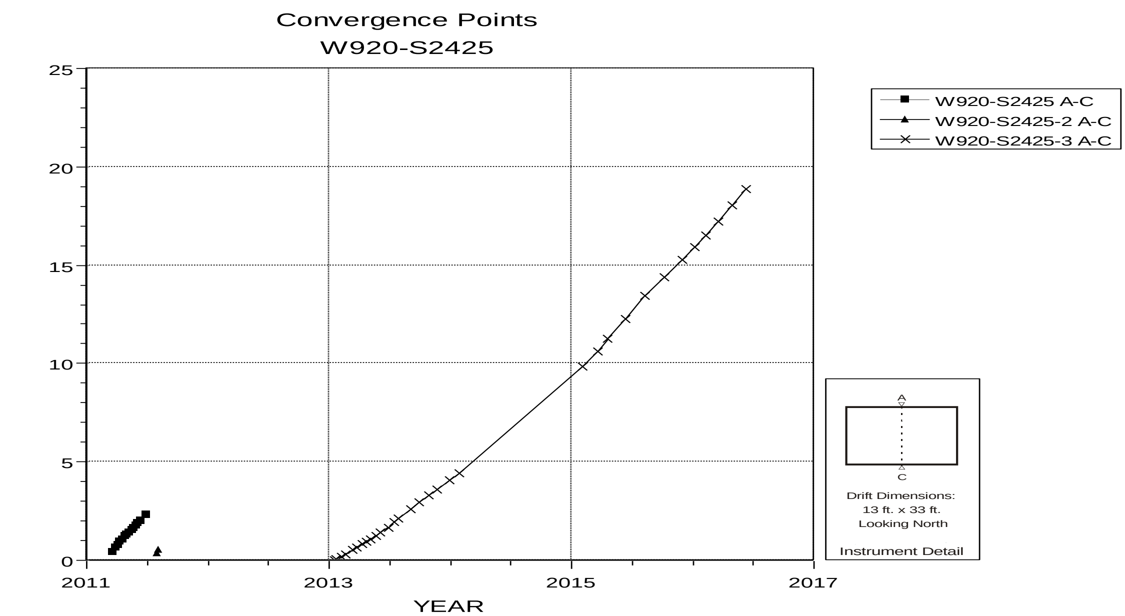

NOTES:
1. Excavation date: October 2010.

Figure 5-53 Convergence Point Array –
Room 5 Panel 7 at W920 S2425 – Roof to Floor

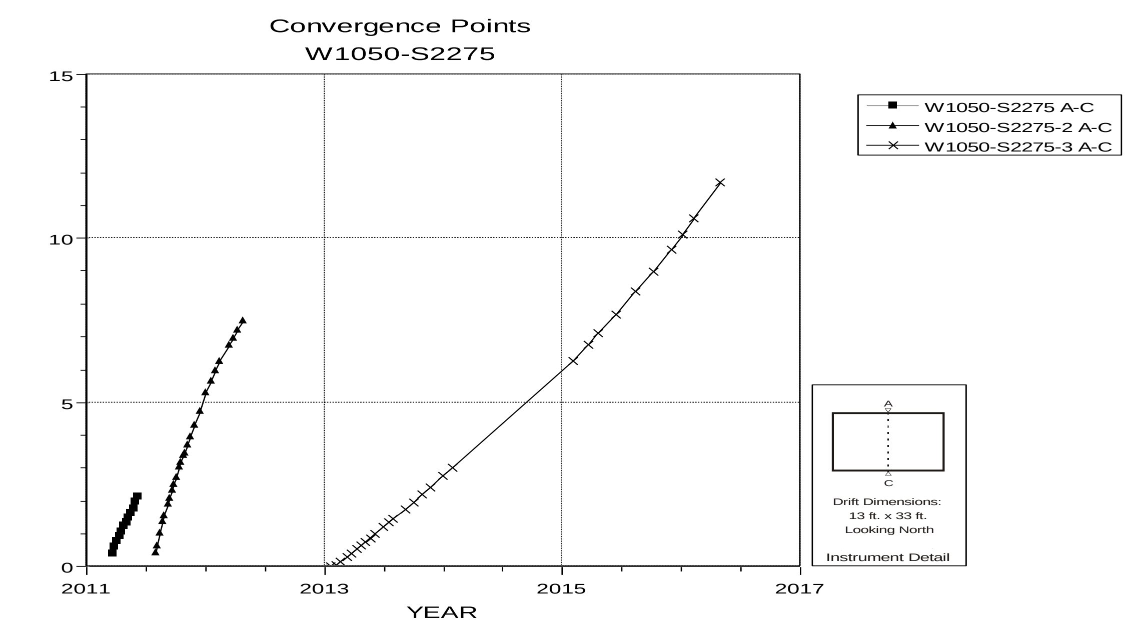

NOTES:
1. Excavation date: November 2010.
2. The gap in readings is due to the area being inaccessible by aerial lift.

Figure 5-54 Convergence Point Array –
Room 6 Panel 7 at W1050 S2275 – Roof to Floor

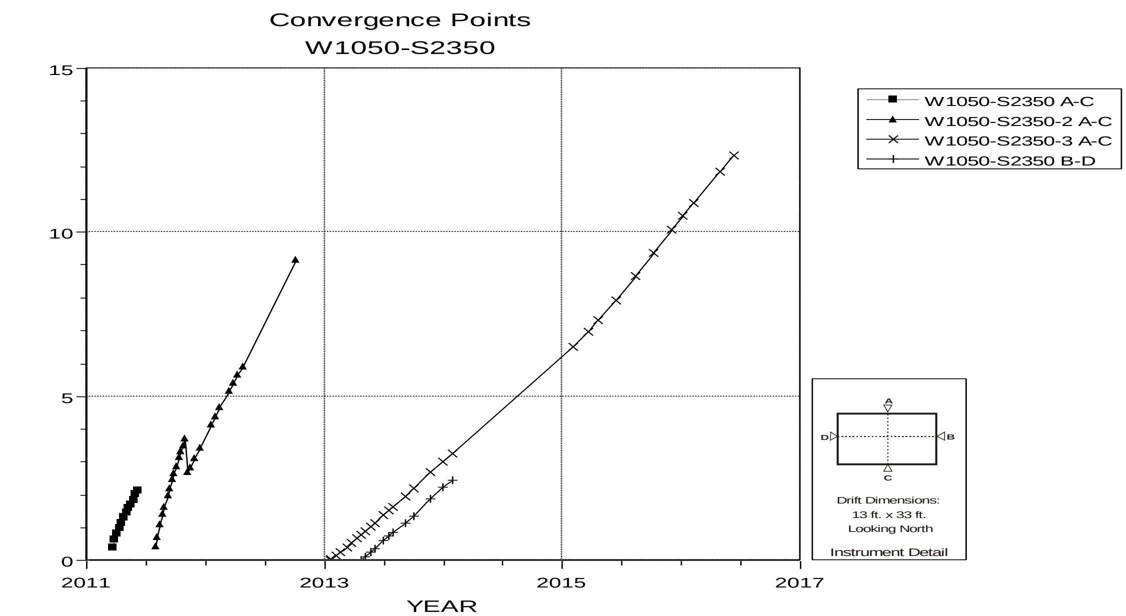

NOTES:
1. Excavation date: November 2010.
2. The gap in readings is due to the area being inaccessible by aerial lift.
3. The negative offset in 4Q of 2011 is most likely due to anchor slippage.

Figure 5-55 Convergence Point Array –
Room 6 Panel 7 at W1050 S2350 – All Chords

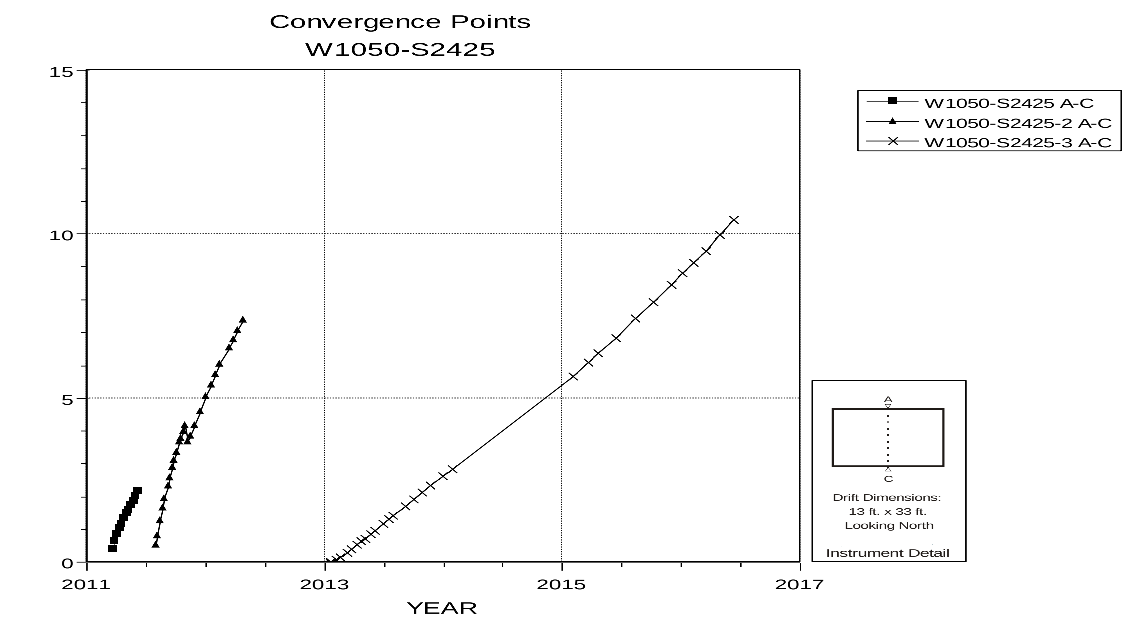

NOTES:
1. Excavation date: November 2010.
2. The gap in readings is due to the area being inaccessible by aerial lift.
3. The negative offset in Q4 of 2011 is most likely due to anchor slippage.

Figure 5-56 Convergence Point Array –
Room 6 Panel 7 at W1050 S2425 – Roof to Floor

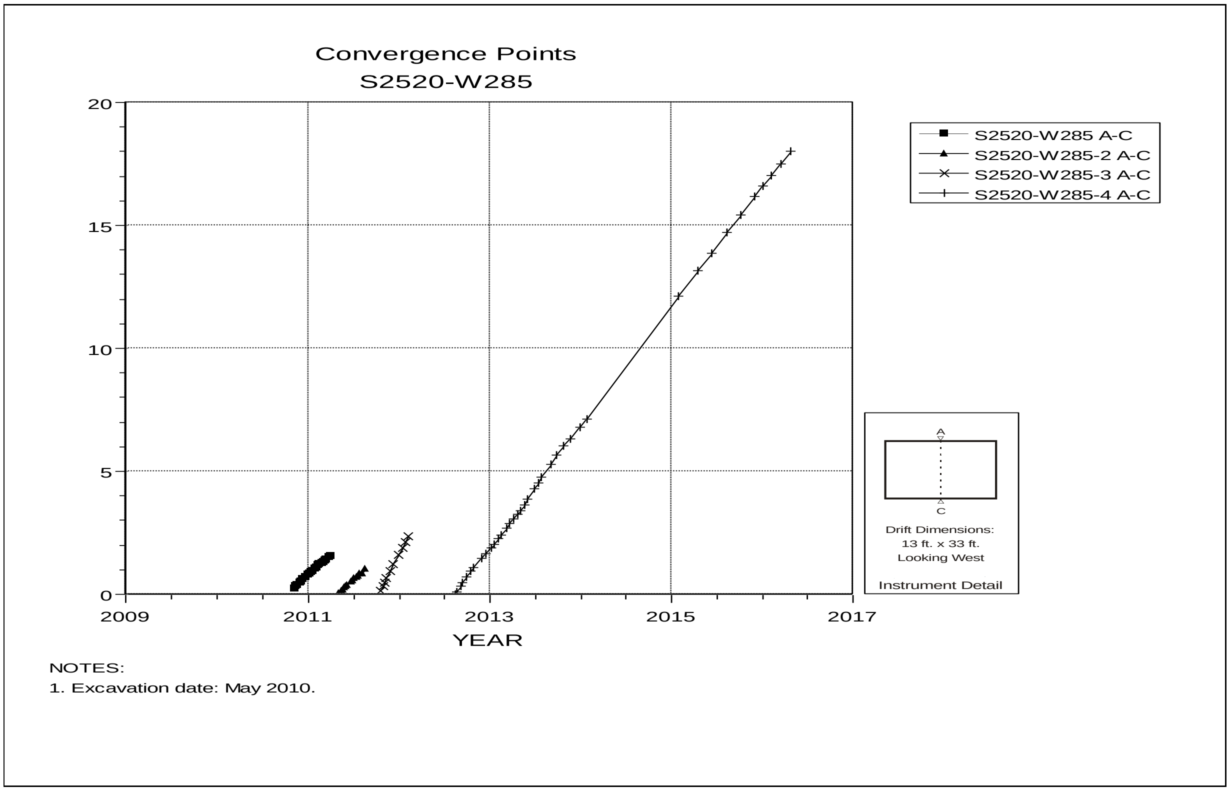

Figure 5-57 Convergence Point Array –
Panel 7 Intake Drift at S2520 W285 – Roof to Floor

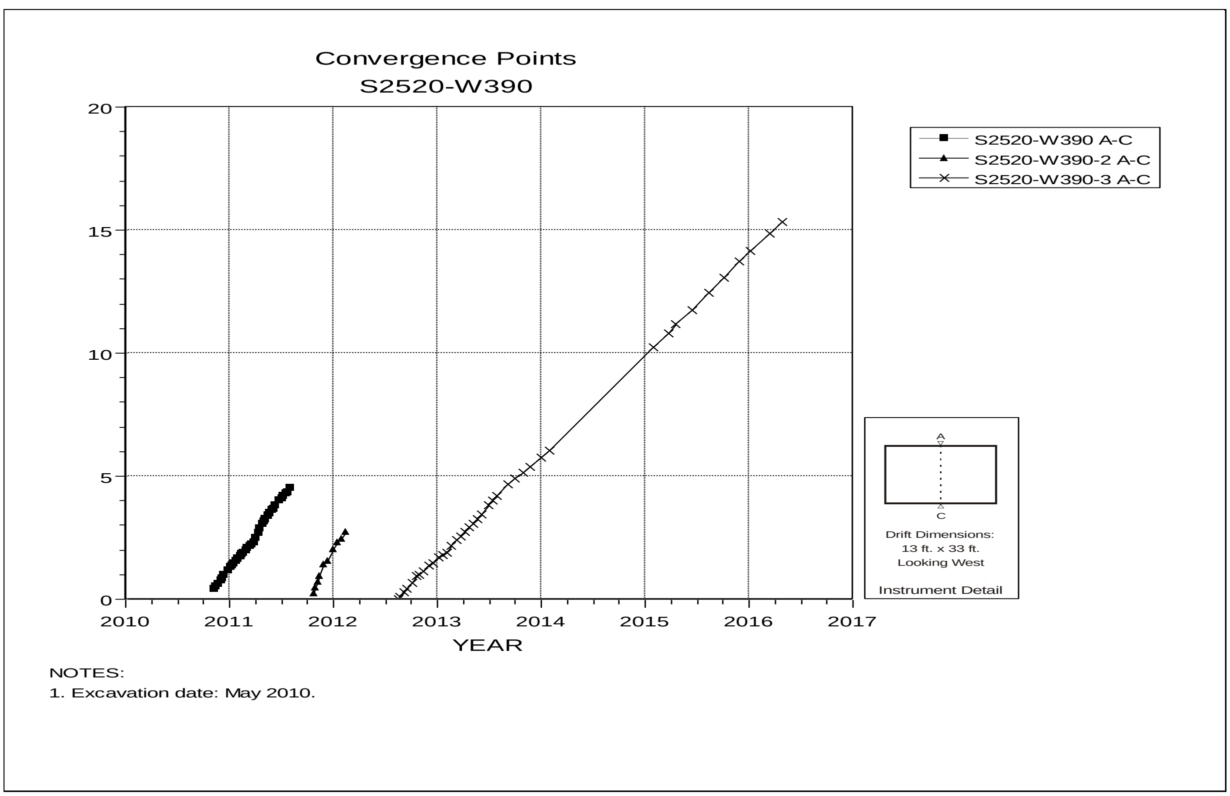

Figure 5-58 Convergence Point Array –
Panel 7 Intake Drift at S2520 W390 – Roof to Floor

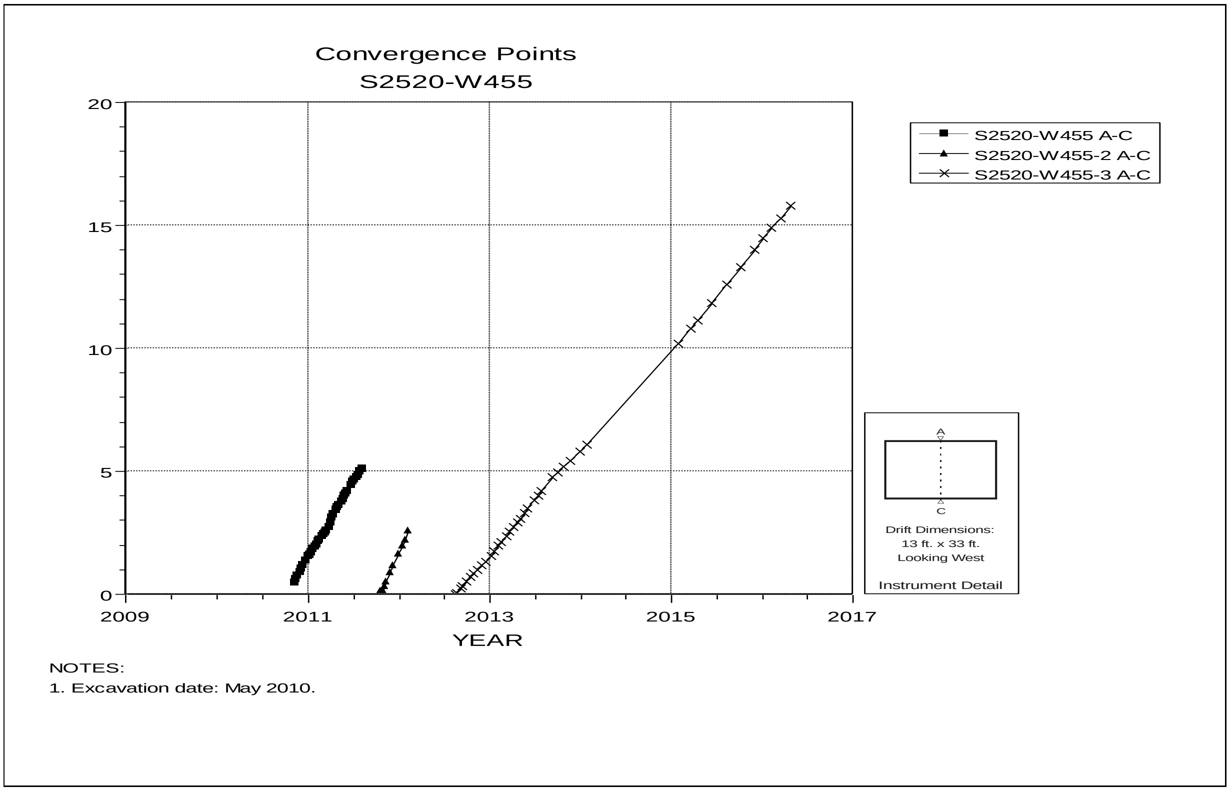

Figure 5-59 Convergence Point Array –
Panel 7 Intake Drift at S2520 W455 – Roof to Floor

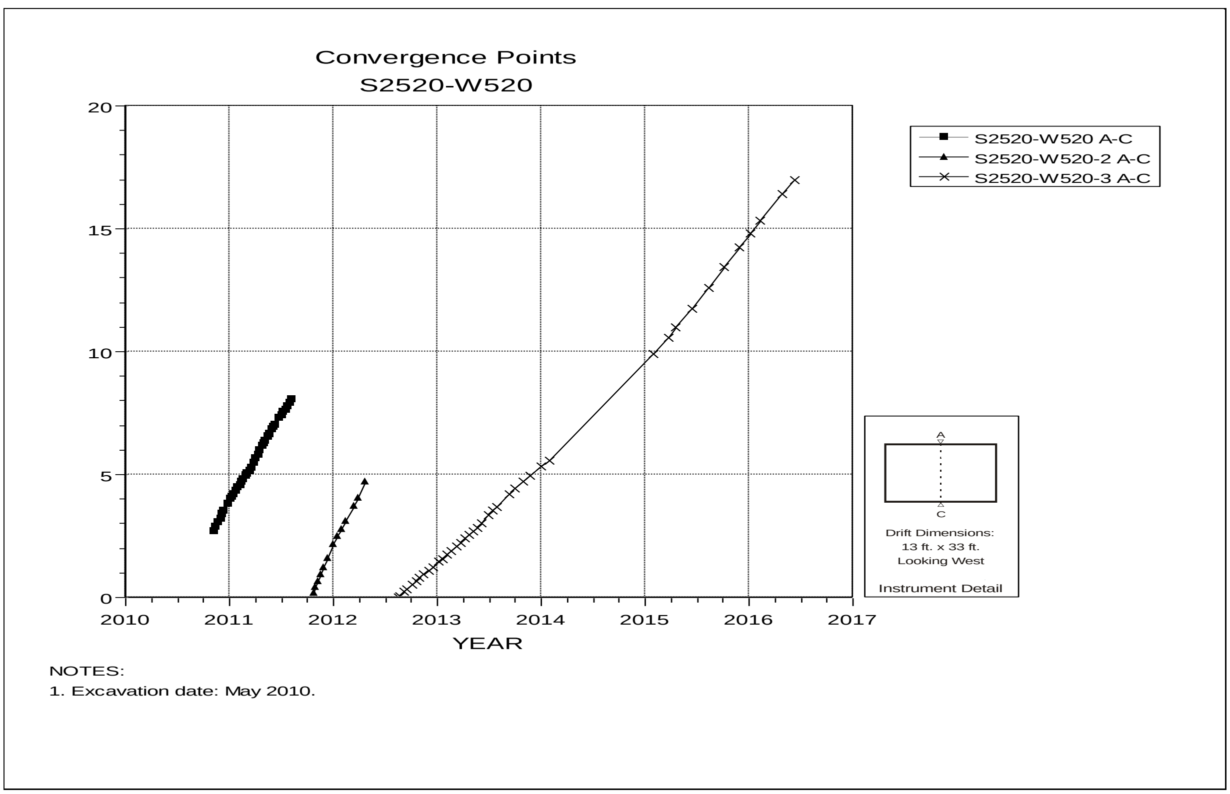

Figure 5-60 Convergence Point Array –
Panel 7 Intake Drift at S2520 W520 – Roof to Floor

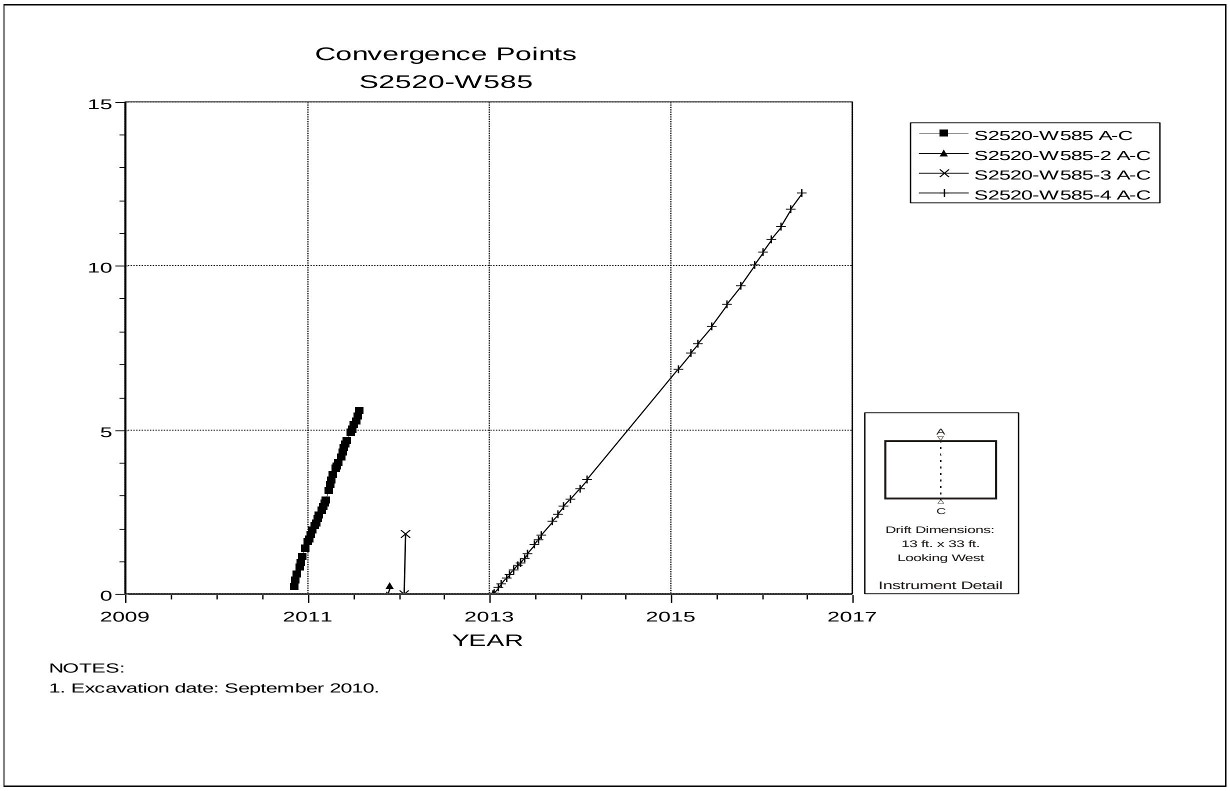

Figure 5-61 Convergence Point Array –
Panel 7 Intake Drift at S2520 W585 – Roof to Floor

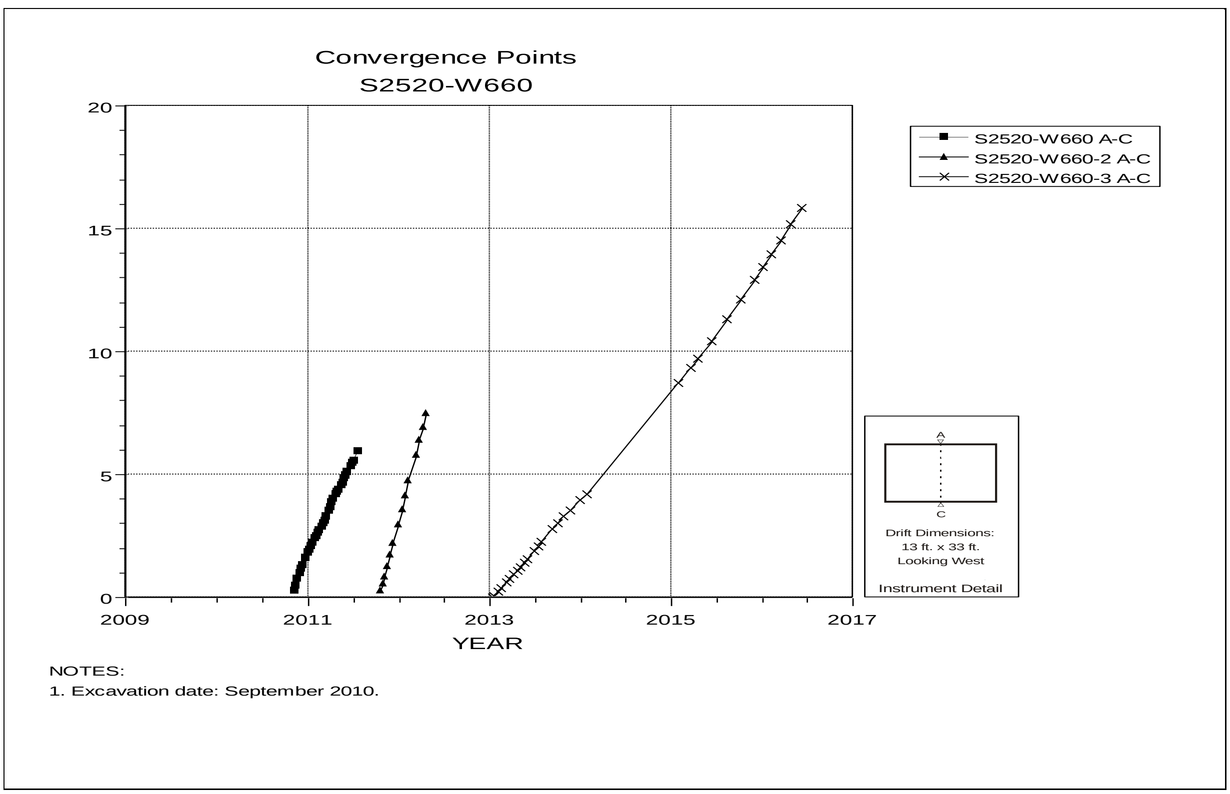

Figure 5-62 Convergence Point Array –
Panel 7 Intake Drift at S2520 W660 – Roof to Floor

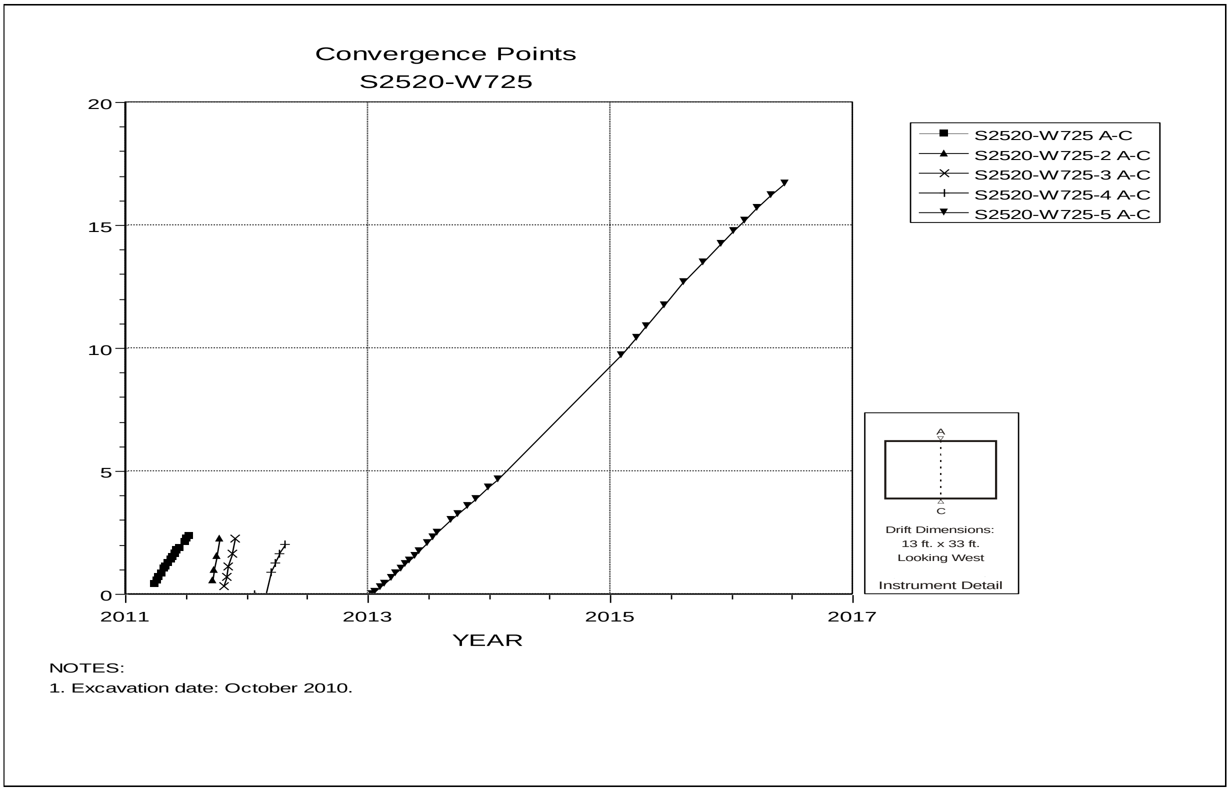

Figure 5-63 Convergence Point Array –
Panel 7 Intake Drift at S2520 W725 – Roof to Floor

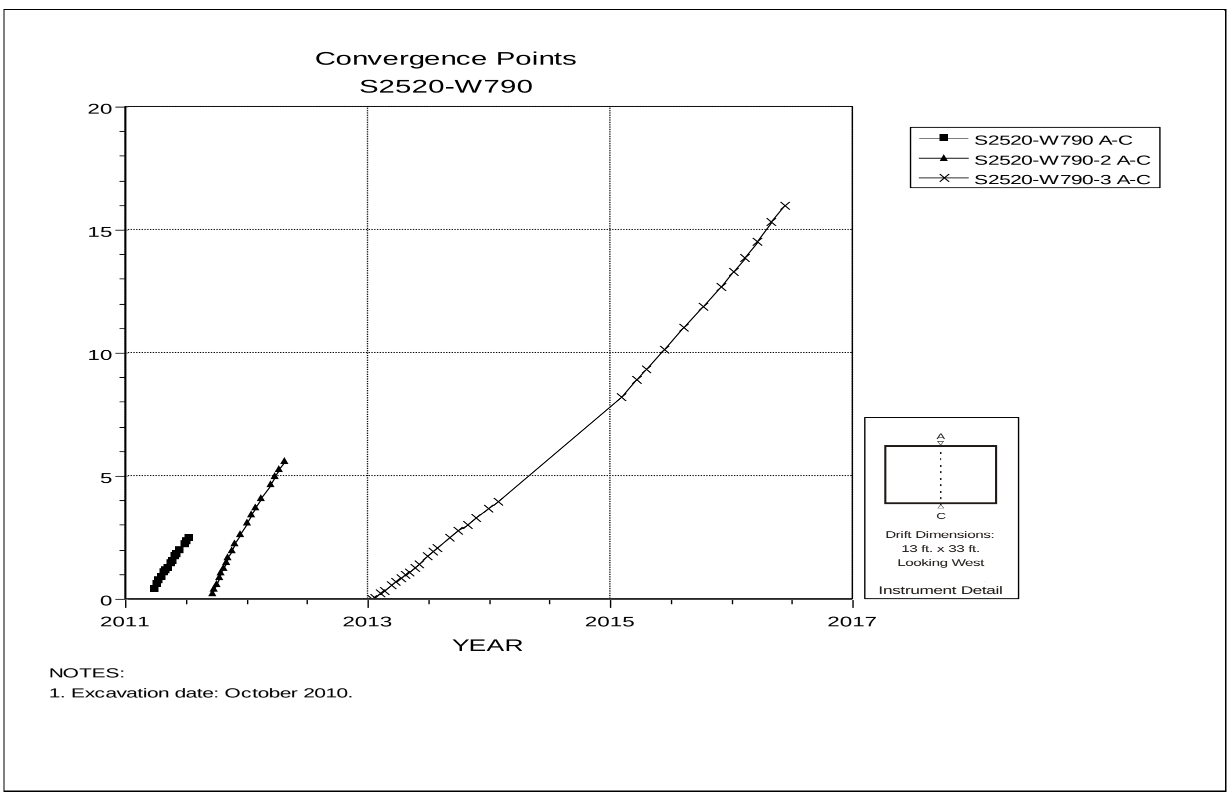

Figure 5-64 Convergence Point Array –
Panel 7 Intake Drift at S2520 W790 – Roof to Floor

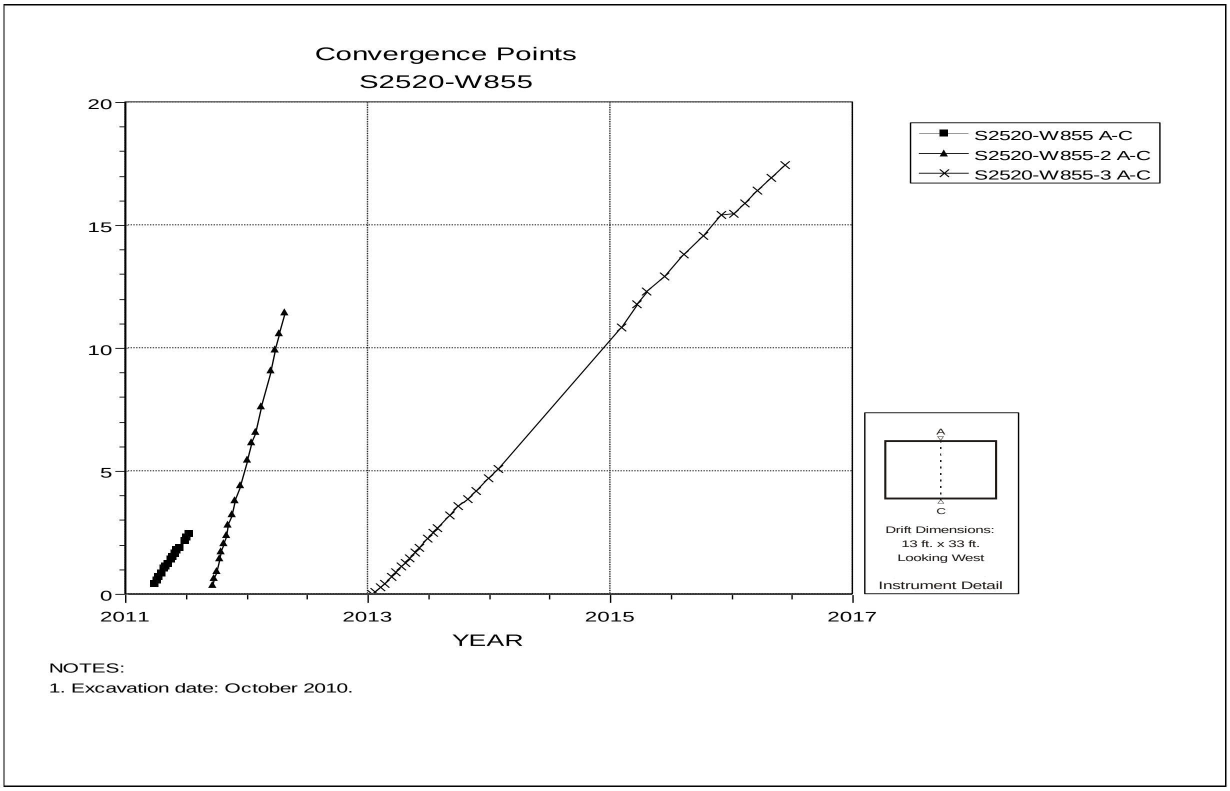

Figure 5-65 Convergence Point Array –
Panel 7 Intake Drift at S2520 W855 – Roof to Floor

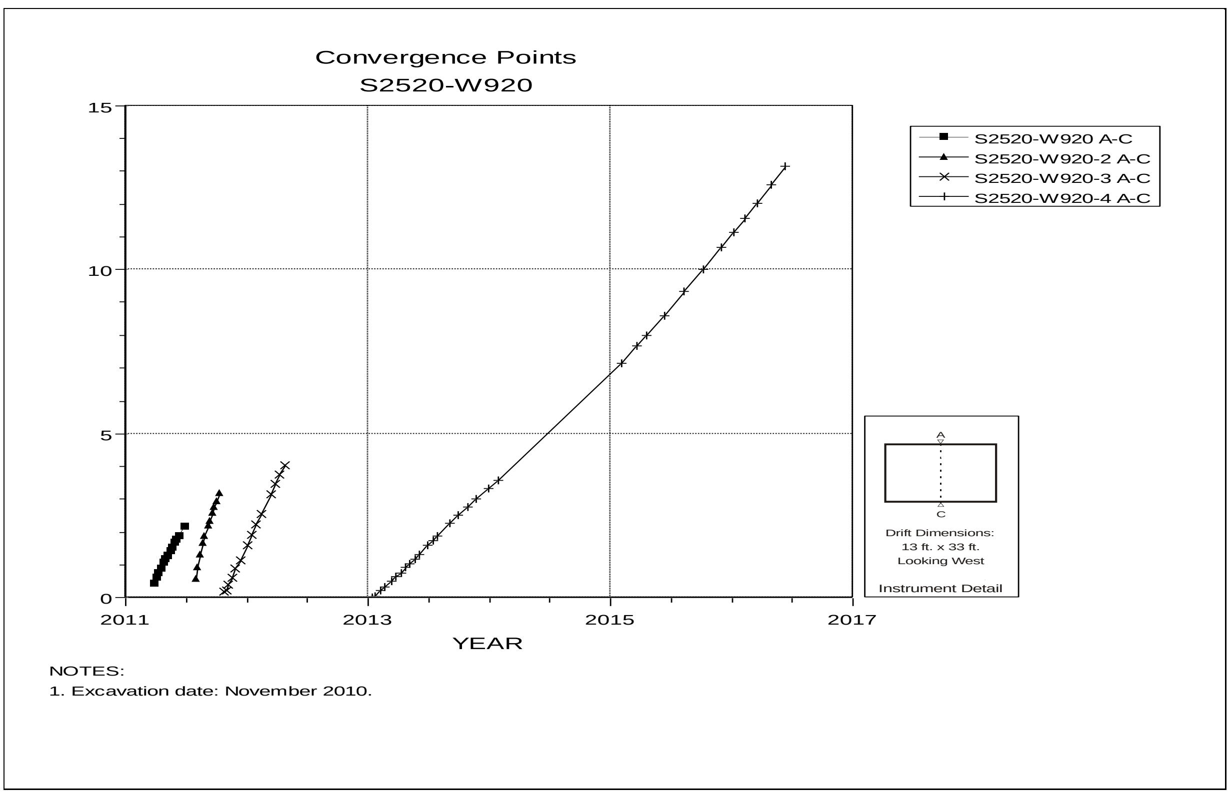

Figure 5-66 Convergence Point Array –
Panel 7 Intake Drift at S2520 W920 – Roof to Floor

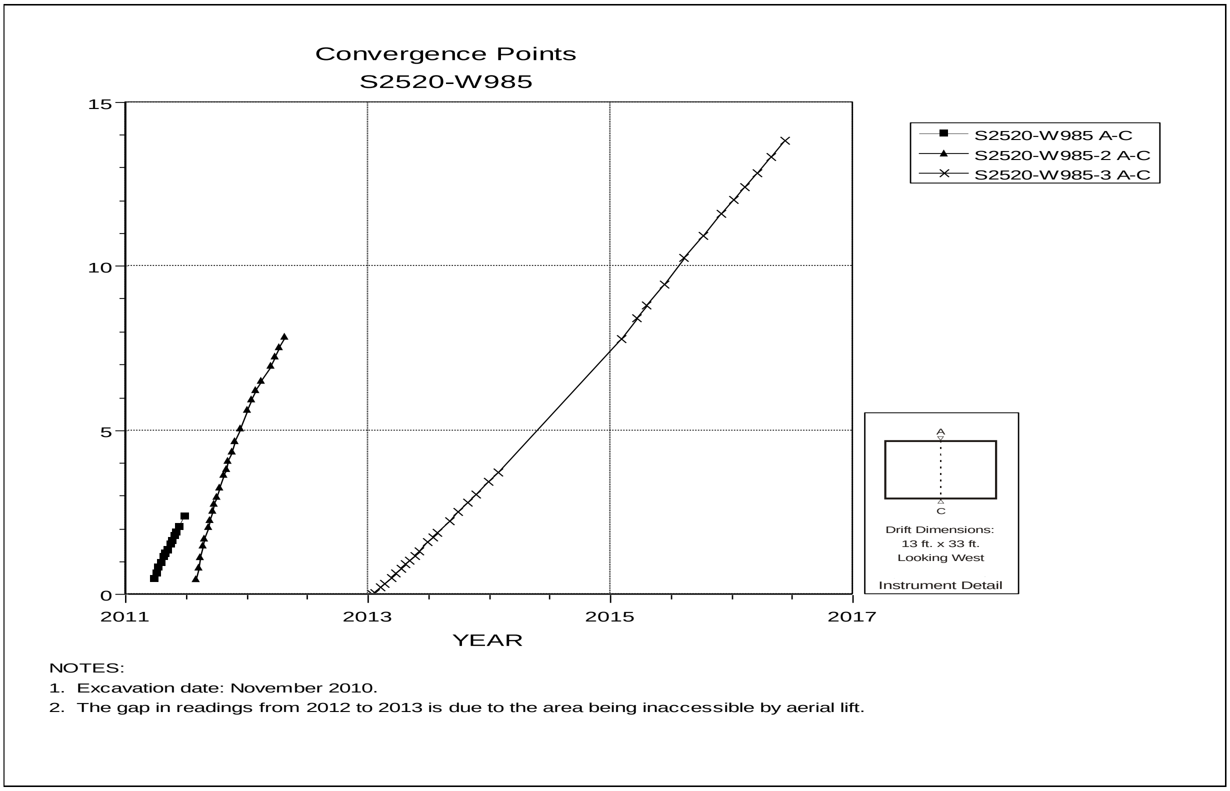

Figure 5-67 Convergence Point Array –
Panel 7 Intake Drift at S2520 W985 – Roof to Floor

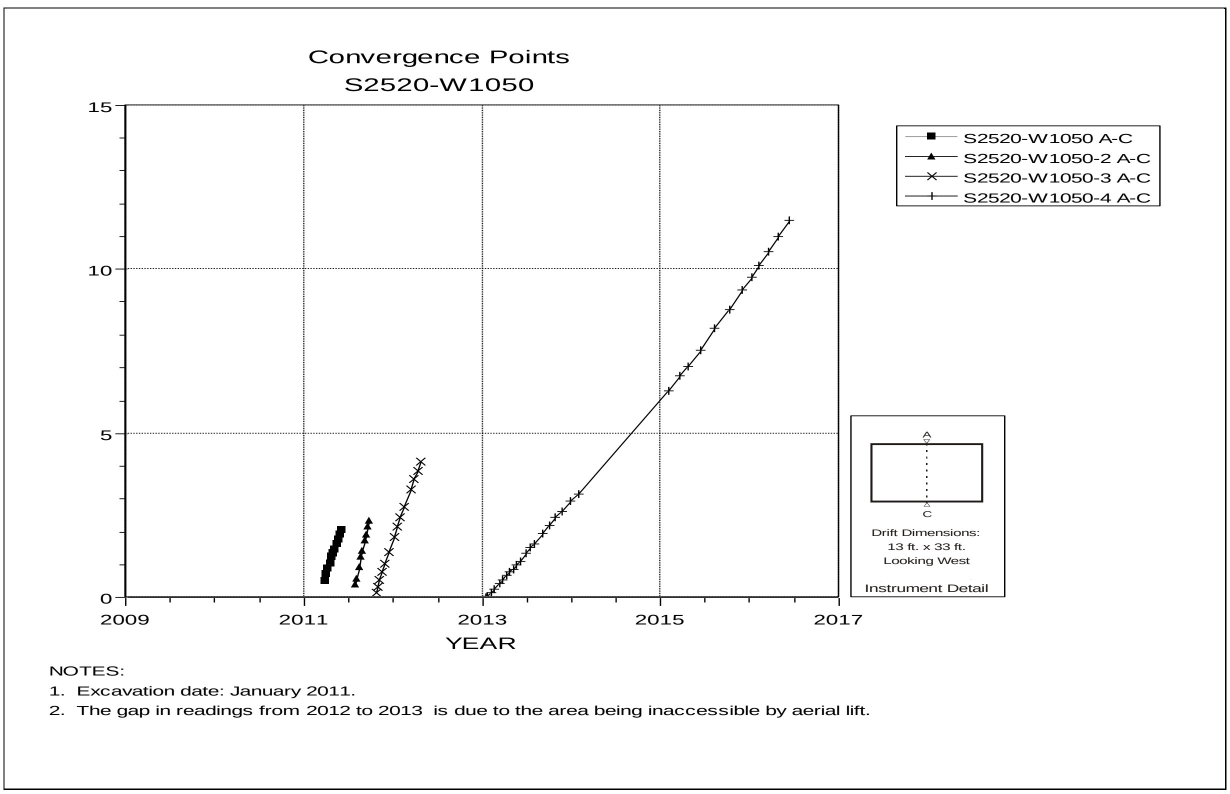

Figure 5-68 Convergence Point Array –
Panel 7 Intake Drift at S2520 W1050 – Roof to Floor

Table 5-8
Panel 8 Data Analysis

Convergence Points

Field Tag	Location	Figure Number	Last Reading 2015 to 2016		Cumulative Displacement (inches)	Closure Rate 2015 to 2016 (in/year)	Closure Rate[4] 2014 to 2015 (in/year)	Rate Change Percent[4]	Comments
			Date	Inches					
S1600-W285 A-C	S1600-W285	5-69	05/26/16	5.456	5.456	2.1	1.8	17%	
S1600-W390 A-C	S1600-W390	5-70	05/26/16	9.407	9.407	3.3	3.2	3%	
S1600-W455 A-C	S1600-W455	5-71	05/26/16	10.91	10.91	3.7	3.5	6%	
S1600-W520 A-C	S1600-W520	5-72	05/26/16	13.554	13.554	4.0	4.5	-11%	
W390-S1682 A-C	W390-S1682	5-73	05/26/16	10.169	10.169	3.5	3.4	3%	
W390-S1765 A-C	W390-S1765	5-74	05/26/16	11.652	11.652	4.0	2.5	60%	
W390-S1846 A-C	W390-S1846	5-75	05/26/16	9.742	9.742	3.3	3.3	0%	
W520-S1682 A-C	W520-S1682	5-76	05/26/16	8.762	8.762	2.9	3.0	-3%	
W520-S1765 A-C	W520-S1765	5-77	05/26/16	10.017	10.017	3.4	3.5	-3%	
W520-S1846 A-C	W520-S1846	5-78	05/26/16	9.678	9.678	3.4	3.5	-3%	

[4] N/A – Insufficient data available to perform the calculation. This is usually due to the inability to read the instruments because of activities such as the removal of an instrument due to floor, rib or back trimming; locations blocked by equipment or waste disposal; installation timing, access issues, etc.

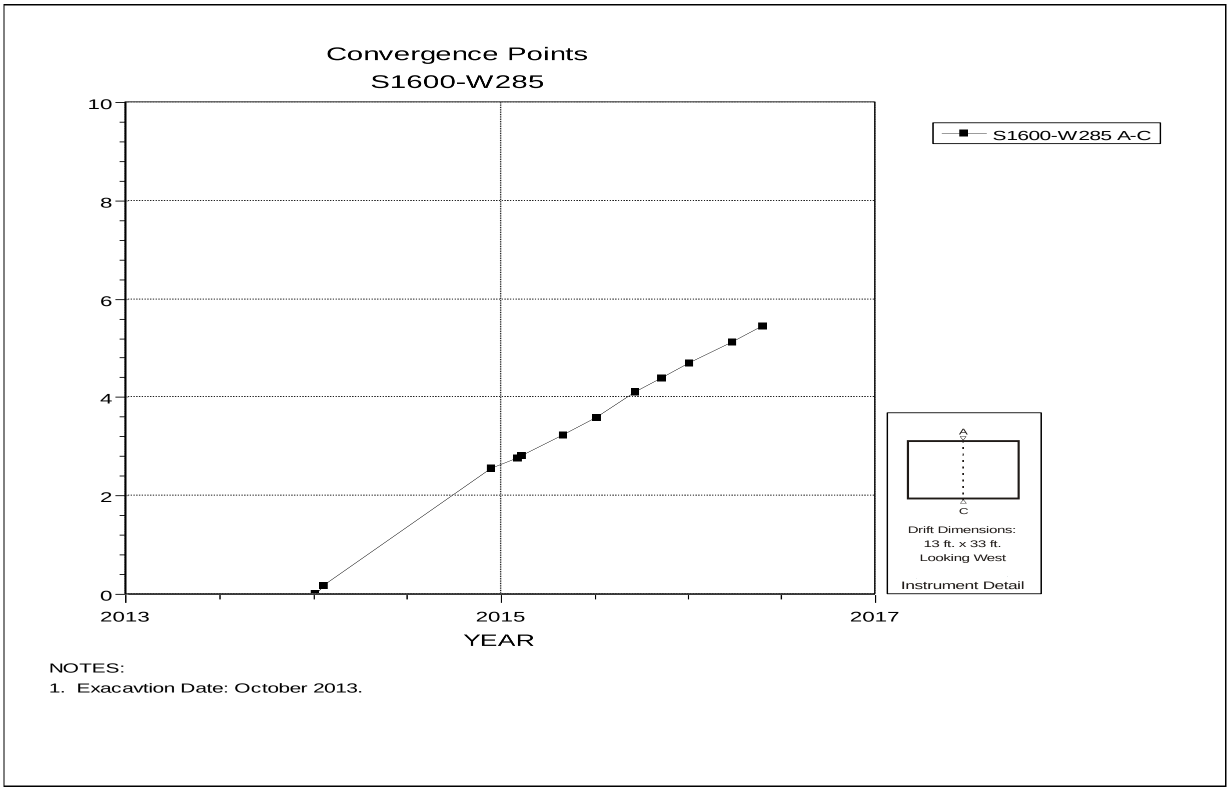

Figure 5-69 Convergence Point Array –
Panel 8 Intake Drift at S1600 W285 – Roof to Floor

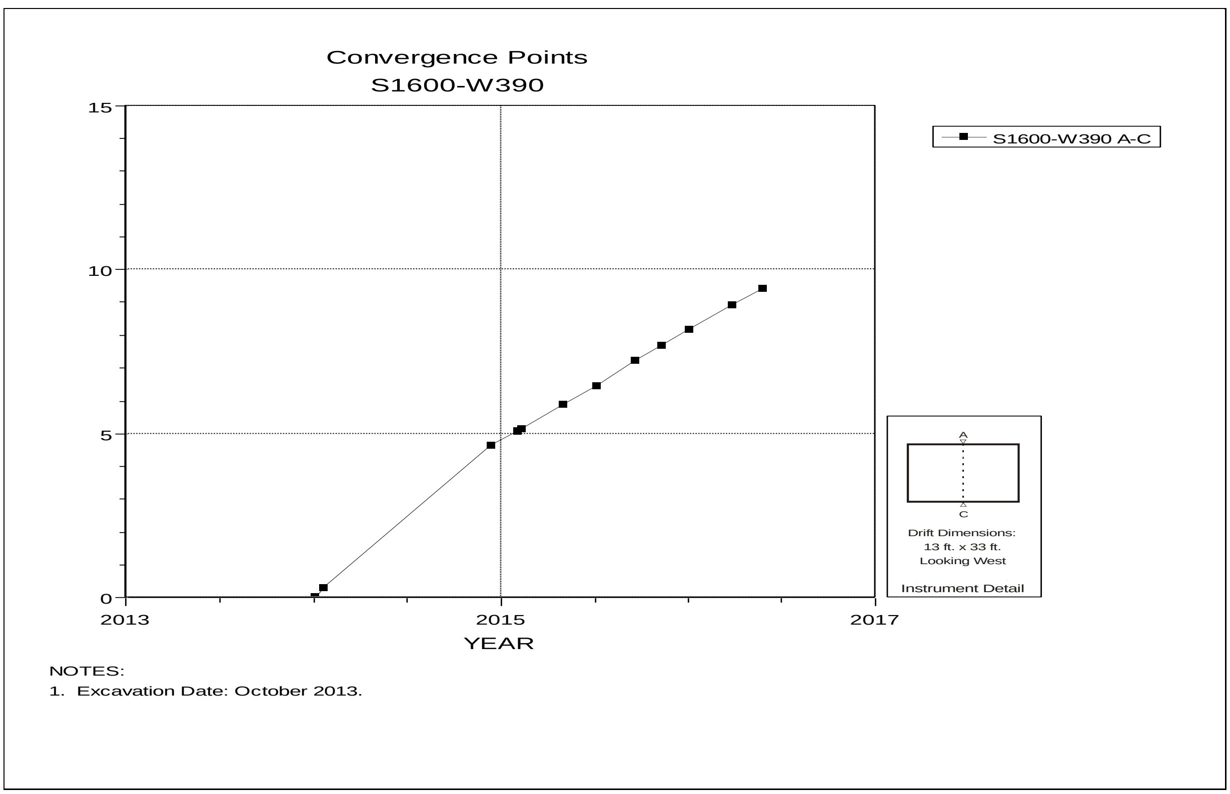

Figure 5-70 Convergence Point Array –
Panel 8 Intake Drift at S1600 W390 – Roof to Floor

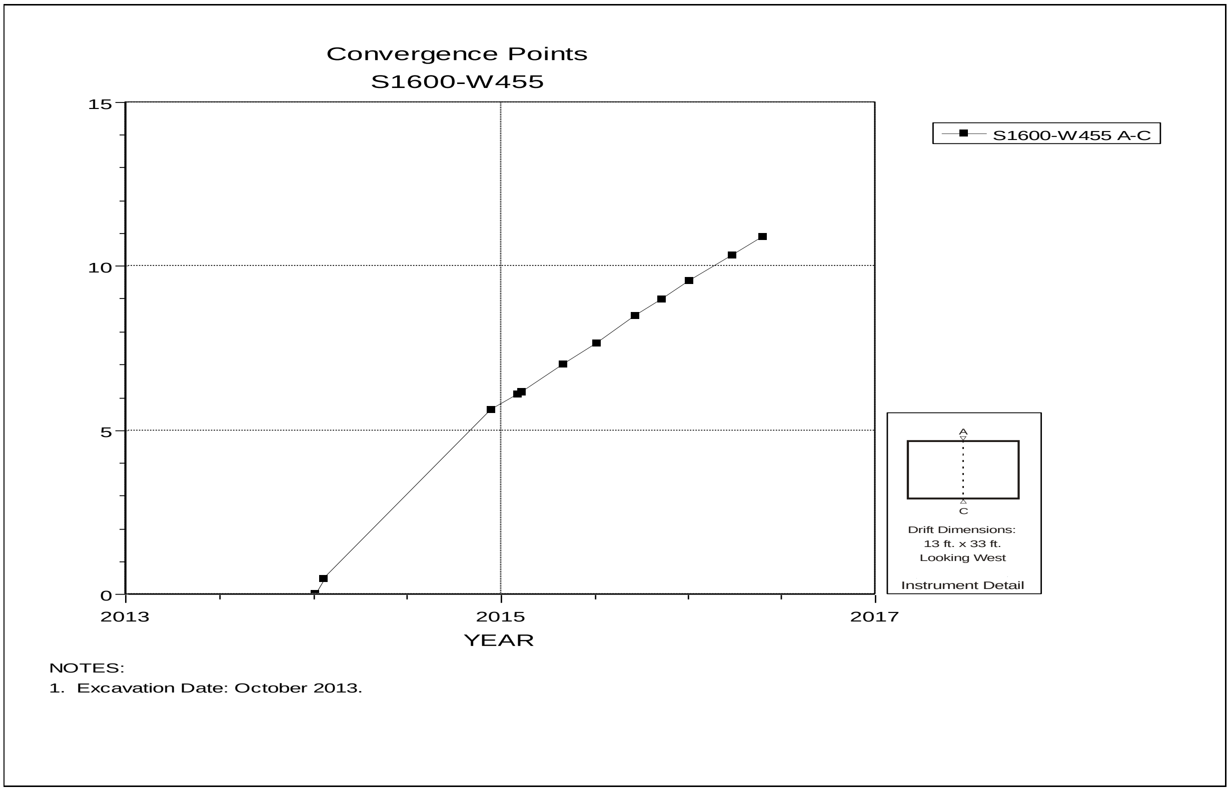

Figure 5-71 Convergence Point Array –
Panel 8 Intake Drift at S1600 W455 – Roof to Floor

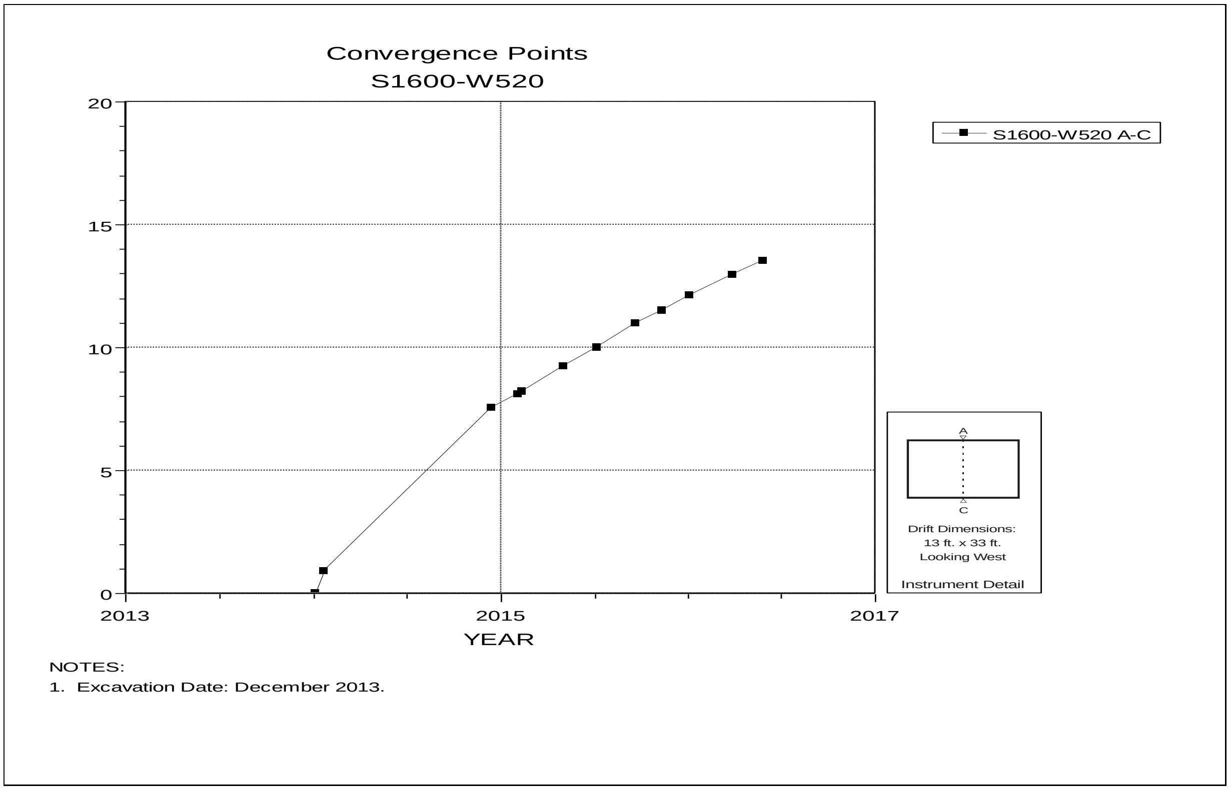

Figure 5-72 Convergence Point Array –
Panel 8 Intake Drift at S1600 W520 – Roof to Floor

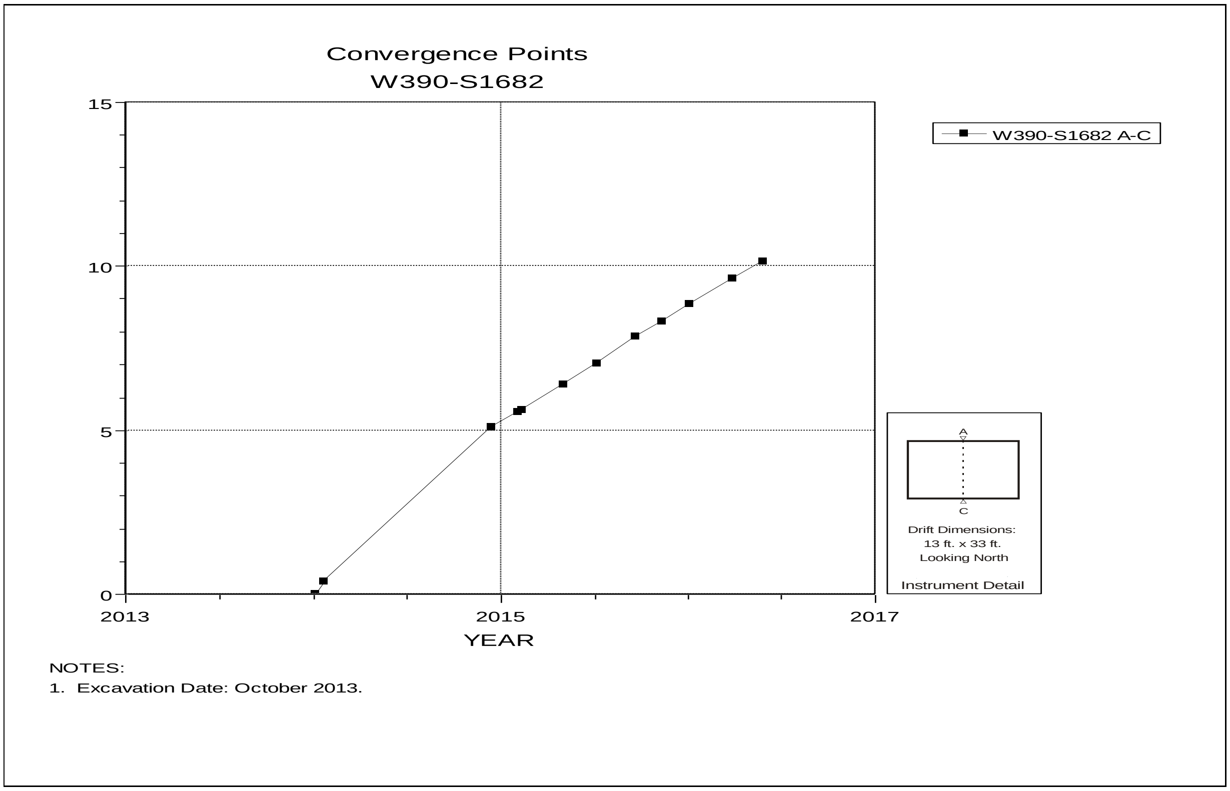

Figure 5-73 Convergence Point Array –
Room 1 Panel 8 at W390 S1682 – Roof to Floor

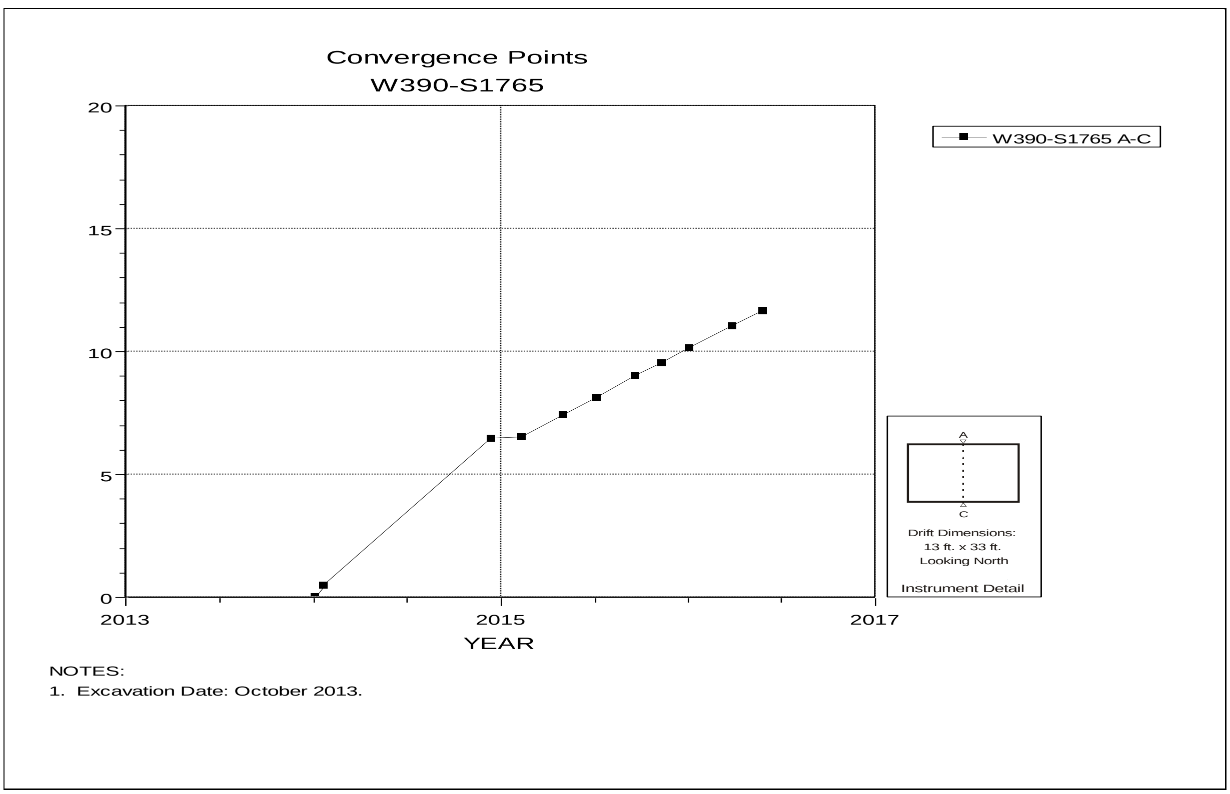

Figure 5-74 Convergence Point Array –
Room 1 Panel 8 at W390 S1765 – Roof to Floor

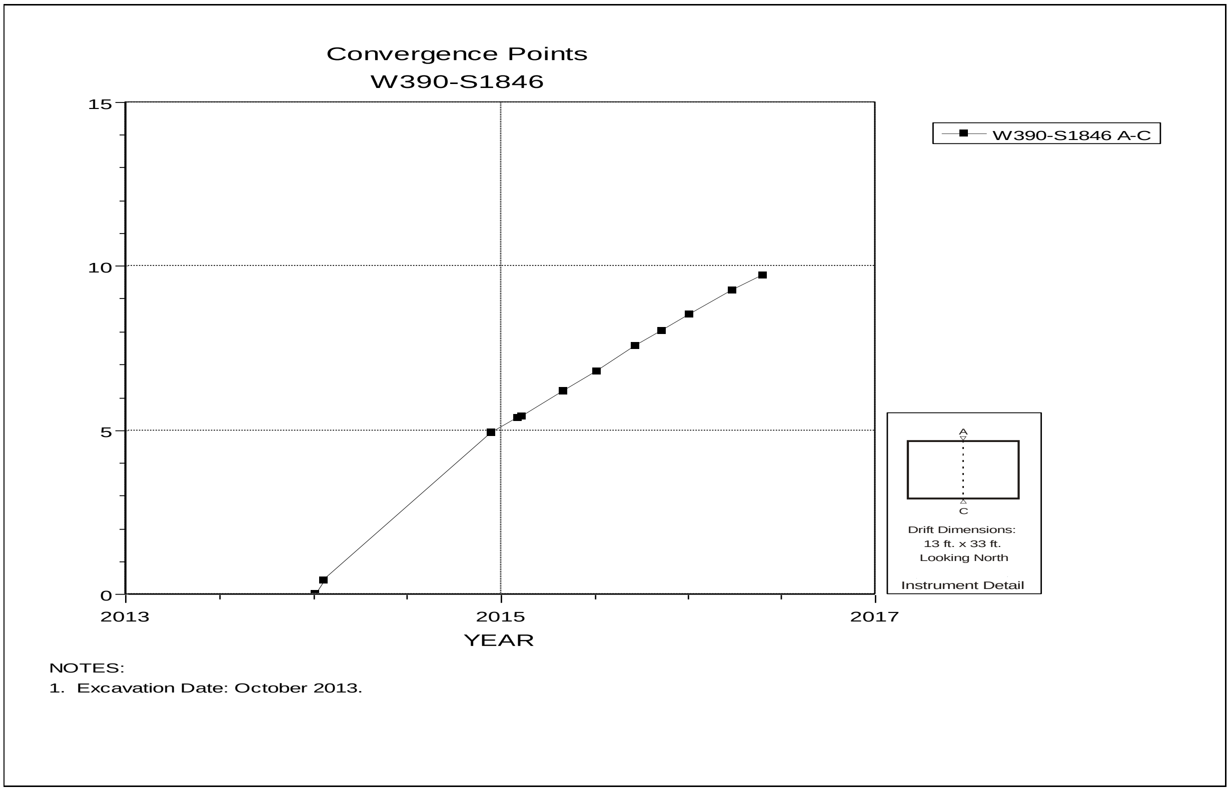

Figure 5-75 Convergence Point Array –
Room 1 Panel 8 at W390 S1846 – Roof to Floor

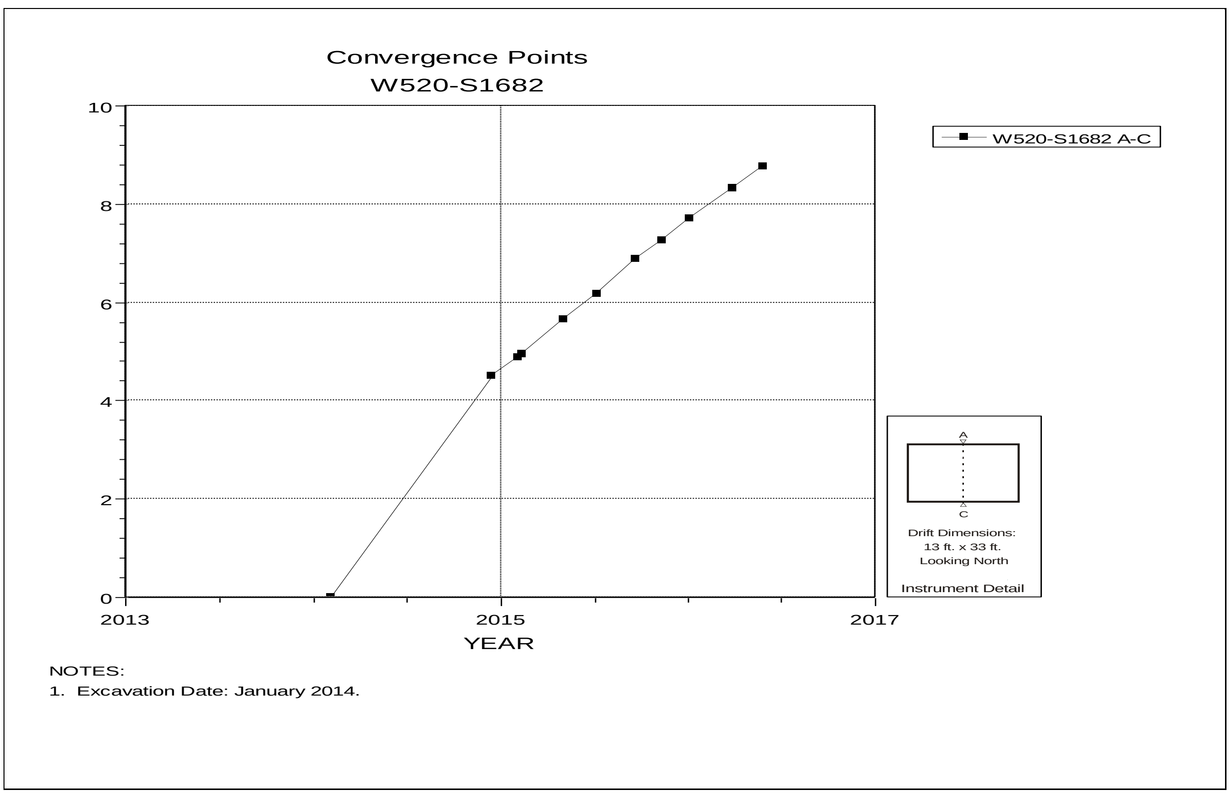

Figure 5-76 Convergence Point Array –
Room 2 Panel 8 at W520 S1682 – Roof to Floor

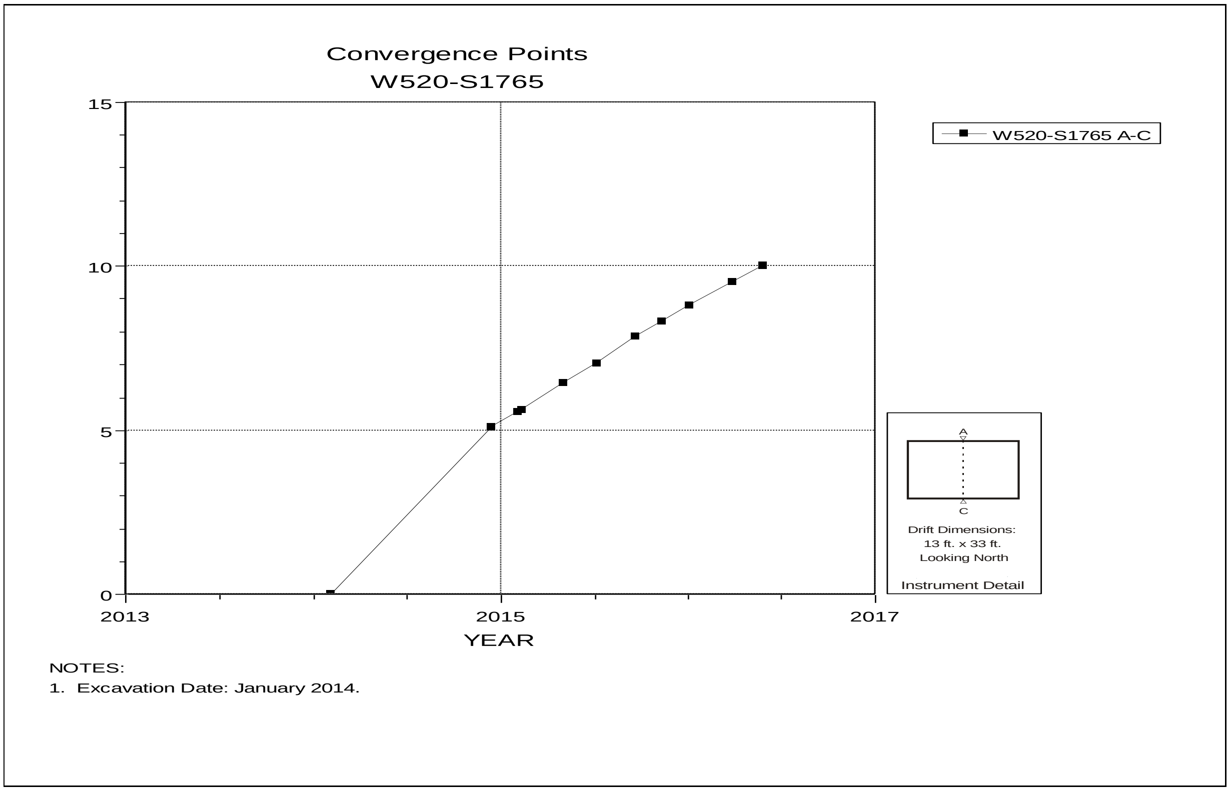

Figure 5-77 Convergence Point Array –
Room 2 Panel 8 at W520 S1765 – Roof to Floor

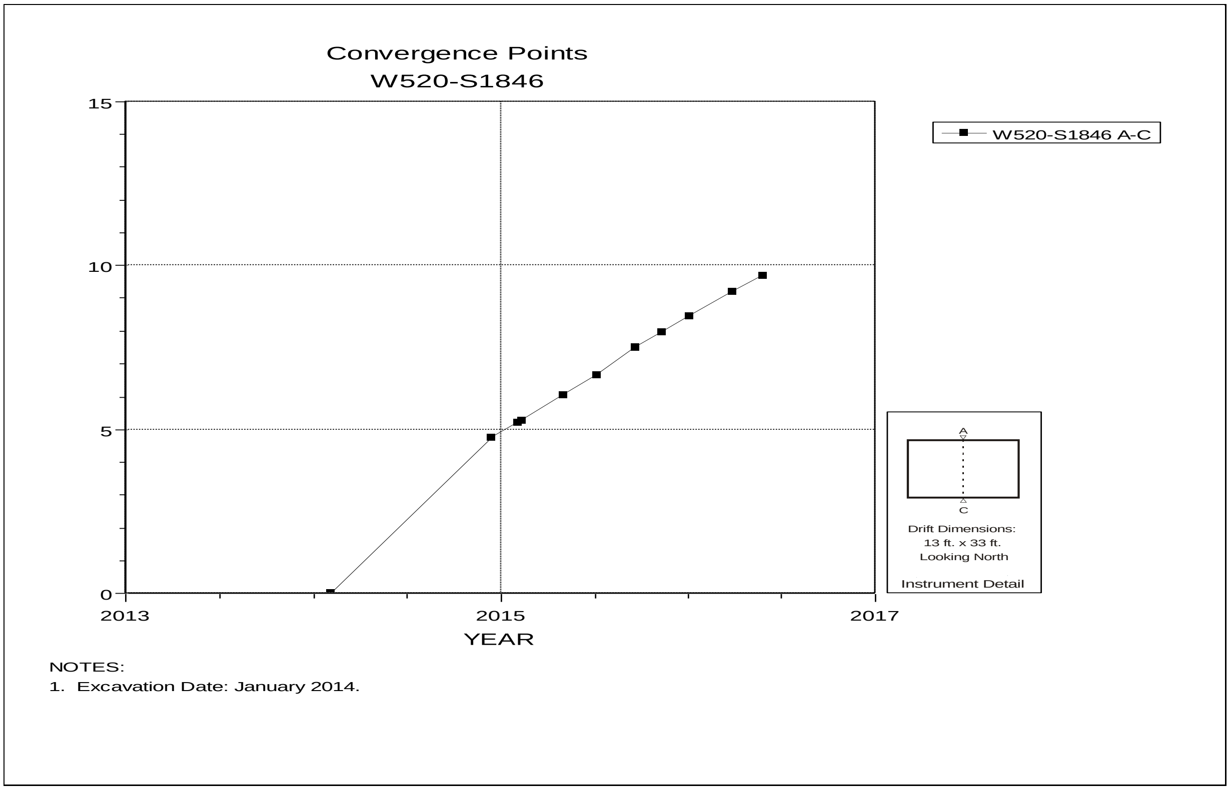

Figure 5-78 Convergence Point Array –
Room 2 Panel 8 at W520 S1846 – Roof to Floor

This page was intentionally left blank.

6.0 Instrumentation Summary for the SDI Area

This chapter presents a summary of the data collected from radial convergence points located in the Storage Disposal Investigations (SDI) area at the WIPP. Table 6-1 presents data and analysis of the access drifts associated with the SDI area. Plots of the instrument data are presented as Figures 6-1 through 6-57.

Table 6-1
SDI Data Analysis

Convergence Points

Field Tag	Location	Figure Number	Last Reading 2015 to 2015 Date	Last Reading 2015 to 2015 Inches	Cumulative Displacement (inches)	Closure Rate 2014 to 2015 (in/year)	Closure Rate 2013 to 2014 (in/year)	Rate Change Percent	Comments
E540-N55 A-C	E540-N55	6-1	06/13/16	5.258	5.258	1.3	1.4	-7%	
E540-N128 A-C	E540-N128	6-2	06/13/16	5.753	5.753	1.4	1.5	-7%	
E540-N200 A-C	E540-N200	6-3	06/13/16	6.214	6.214	1.6	1.6	0%	
E540-N275 A-C	E540-N275	6-4	06/13/16	5.964	5.964	1.5	1.6	-6%	
E540-N350-2 A-C	E540-N350	6-5	06/13/16	6.074	6.074	1.6	1.6	0%	
E540-N425 A-C	E540-N425	6-6	06/13/16	6.273	6.273	1.6	1.6	0%	
E540-N500-2 A-C	E540-N500	6-7	06/13/16	6.539	6.539	1.7	1.7	0%	
E540-N570 A-C	E540-N570	6-8	06/13/16	6.868	6.868	1.8	1.8	0%	
E540-N640-2 A-C	E540-N640	6-9	06/13/16	7.027	8.242	1.8	1.8	0%	
E540-N710 A-C	E540-N710	6-10	06/13/16	6.055	6.055	1.5	1.5	0%	
E540-N860 A-C	E540-N860	6-11	06/13/16	5.922	5.922	1.5	1.4	7%	
E540-S17 A-C	E540-S17	6-12	06/13/16	4.43	4.43	1.1	1.1	0%	
E540-S90 A-C	E540-S90	6-13	06/13/16	6.261	6.261	1.6	1.6	0%	
E690-N55-2 A-C	E690-N55	6-14	06/13/16	5.387	5.387	1.4	1.4	0%	
E690-N128-2 A-C	E690-N128	6-15	06/13/16	5.764	6.543	1.5	1.4	7%	
E690-N200-2 A-C	E690-N200	6-16	06/13/16	8.042	9.158	2.1	2.2	-5%	
E690-N275-2 A-C	E690-N275	6-17	06/13/16	6.62	7.492	1.7	1.7	0%	
E690-N350-2 A-C	E690-N350	6-18	06/13/16	9.165	10.332	2.3	2.4	-4%	
E690-N425-2 A-C	E690-N425	6-19	06/13/16	6.931	7.754	1.7	1.8	-6%	
E690-N500-2 A-C	E690-N500	6-20	06/13/16	9.33	10.32	2.3	2.5	-8%	
E690-N570 A-C	E690-N570	6-21	06/13/16	6.088	6.088	1.8	1.8	0%	
E690-N640-2 A-C	E690-N640	6-22	06/13/16	6.134	8.07	1.8	1.8	0%	
E690-N710 A-C	E690-N710	6-23	06/13/16	5.435	5.435	1.5	1.6	-3%	
E690-S17-2 A-C	E690-S17	6-24	06/13/16	5.379	5.379	1.4	1.4	0%	
E690-S90 A-C	E690-S90	6-25	06/13/16	5.734	5.734	1.5	1.5	0%	

Table 6-1, (continued)
SDI Data Analysis

Convergence Points, (continued)

Field Tag	Location	Figure Number	Last Reading 2015 to 2016		Cumulative Displacement (inches)	Closure Rate[4] 2015 to 2016 (in/year)	Closure Rate 2014 to 2015 (in/year)	Rate Change Percent[4]	Comments
			Date	Inches					
N780-E220-4 A-C	N780-E220	6-26	06/13/16	9.662	23.088	2.9	2.9	0%	
N780-E300-3 A-C	N780-E300	6-27	06/13/16	7.086	9.715	2.0	1.8	11%	
N780-E420-2 A-C	N780-E420	6-28	06/13/16	6.343	10.169	1.6	1.5	7%	
N780-E540-2 A-C	N780-E540	6-29	06/13/16	8.574	12.994	2.1	2.1	0%	
N780-E615-2 A-C	N780-E615	6-30	06/13/16	6.492	9.71	1.7	1.7	0%	
N780-E690-2 A-C	N780-E690	6-31	06/13/16	8.807	14.157	2.1	2.2	-5%	
N780-E768 A-C	N780-E768	6-32	06/13/16	7.863	7.863	1.7	1.7	0%	
N780-E845 A-C	N780-E845	6-33	06/13/16	8.736	8.736	1.9	2.0	-5%	
N780-E922 A-C	N780-E922	6-34	06/13/16	9.026	9.026	1.8	2.0	-10%	
N780-E1050 A-C	N780-E1050	6-35	06/13/16	9.055	9.055	1.7	1.9	-11%	
N780-E1100 A-C	N780-E1100	6-36	06/13/16	9.358	9.358	1.7	1.9	-11%	
N780-E1150 A-C	N780-E1150	6-37	06/13/16	8.303	8.303	1.6	1.7	-6%	
N780-E1200 A-C	N780-E1200	6-38	06/13/16	8.302	8.302	1.6	1.7	-6%	
N780-E1250 A-C	N780-E1250	6-39	06/13/16	6.761	6.761	1.3	1.4	-7%	
N780-E1300 A-C	N780-E1300	6-40	06/13/16	3.62	3.62	1.1	1.1	0%	
N940-E220-2 A-C	N940-E220	6-41	06/13/16	3.722	5.157	1.1	0.9	22%	
N940-E300-2 A-C	N940-E300	6-42	06/13/16	4.496	6.262	1.3	1.1	18%	
N940-E540-2 A-C	N940-E540	6-43	06/13/16	6.784	9.735	1.8	N/A	N/A	
N940-E615-2 A-C	N940-E615	6-44	06/13/16	6.953	9.778	1.7	1.5	13%	
N940-E690-3 A-C	N940-E690	6-45	06/13/16	10.619	12.987	2.4	N/A	N/A	
N940-E768-2 A-C	N940-E768	6-46	06/13/16	6.305	7.14	1.9	N/A	N/A	
N940-E845-2 A-C	N940-E845	6-47	06/13/16	5.796	6.719	1.7	1.6	6%	
N940-E922-2 A-C	N940-E922	6-48	06/13/16	6.092	7.315	1.7	1.7	0%	
N940-E1000 A-C	N940-E1000	6-49	06/13/16	7	7	2.0	1.9	5%	
N940-E1050-2 A-C	N940-E1050	6-50	06/13/16	5.598	7.115	1.6	1.7	-6%	
N940-E1100 A-C	N940-E1100	6-51	06/13/16	7.056	7.056	2.1	2.3	-9%	
N940-E1150 A-C	N940-E1150	6-52	06/13/16	5.67	5.67	1.7	1.8	-6%	
N940-E1200 A-C	N940-E1200	6-53	06/13/16	5.993	5.993	1.8	1.9	-5%	

Convergence Points, (continued)

Field Tag	Location	Figure Number	Last Reading 2015 to 2016 Date	Last Reading 2015 to 2016 Inches	Cumulative Displacement (inches)	Closure Rate[4] 2015 to 2016 (in/year)	Closure Rate 2014 to 2015 (in/year)	Rate Change Percent[4]	Comments
N940-E1250 A-C	N940-E1250	6-54	06/13/16	4.519	4.519	1.4	N/A	N/A	
N940-E1300 A-C	N940-E1300	6-55	06/13/16	5.127	5.127	1.5	1.6	-6%	
E1300-N860 A-C	E1300-N860	6-56	06/13/16	4.067	4.067	1.1	1.2	-8%	
S90-E615 A-C	S90-E615	6-57	06/13/16	5.062	5.062	1.3	1.3	0%	

[4] N/A – Insufficient data available to perform the calculation. This is usually due to the inability to read the instruments because of activities such as the removal of an instrument due to floor, rib or back trimming; locations blocked by equipment or waste disposal; installation timing, access issues, etc.

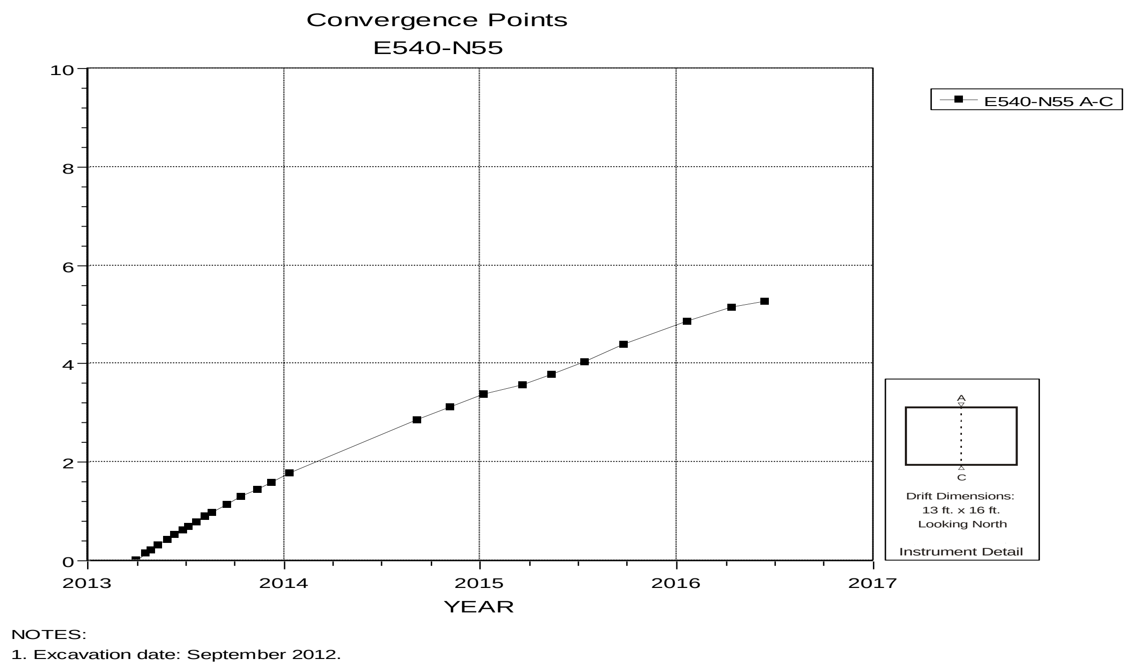

Figure 6-1 Convergence Point Array –
E540 N55 – Roof to Floor

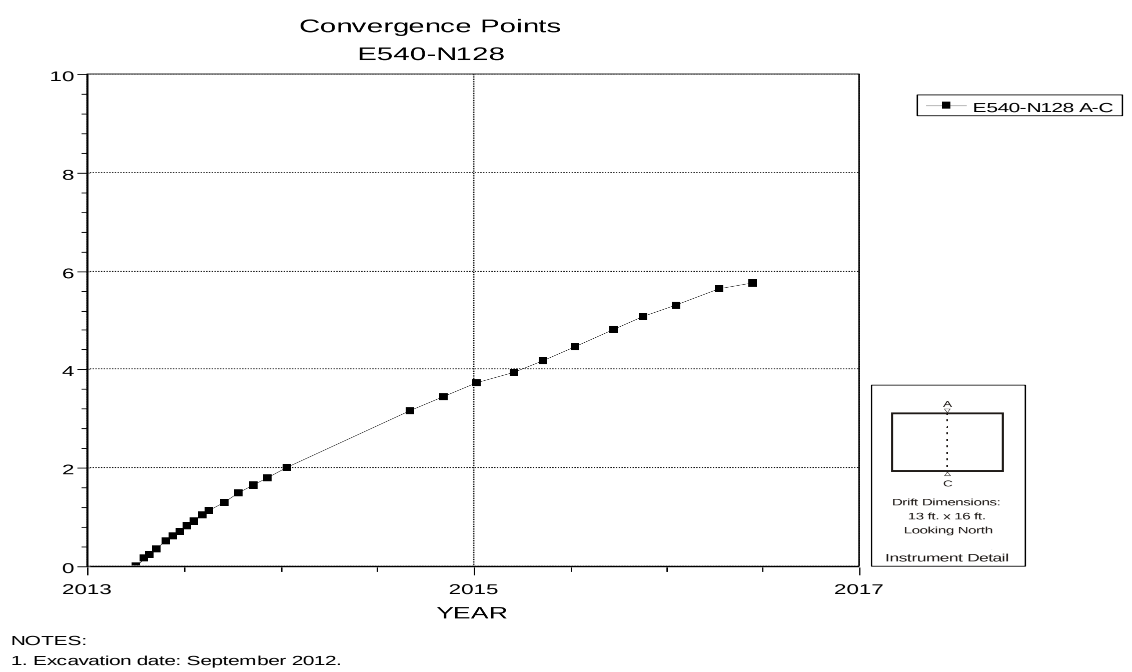

Figure 6-2 Convergence Point Array –
E540 N128 – Roof to Floor

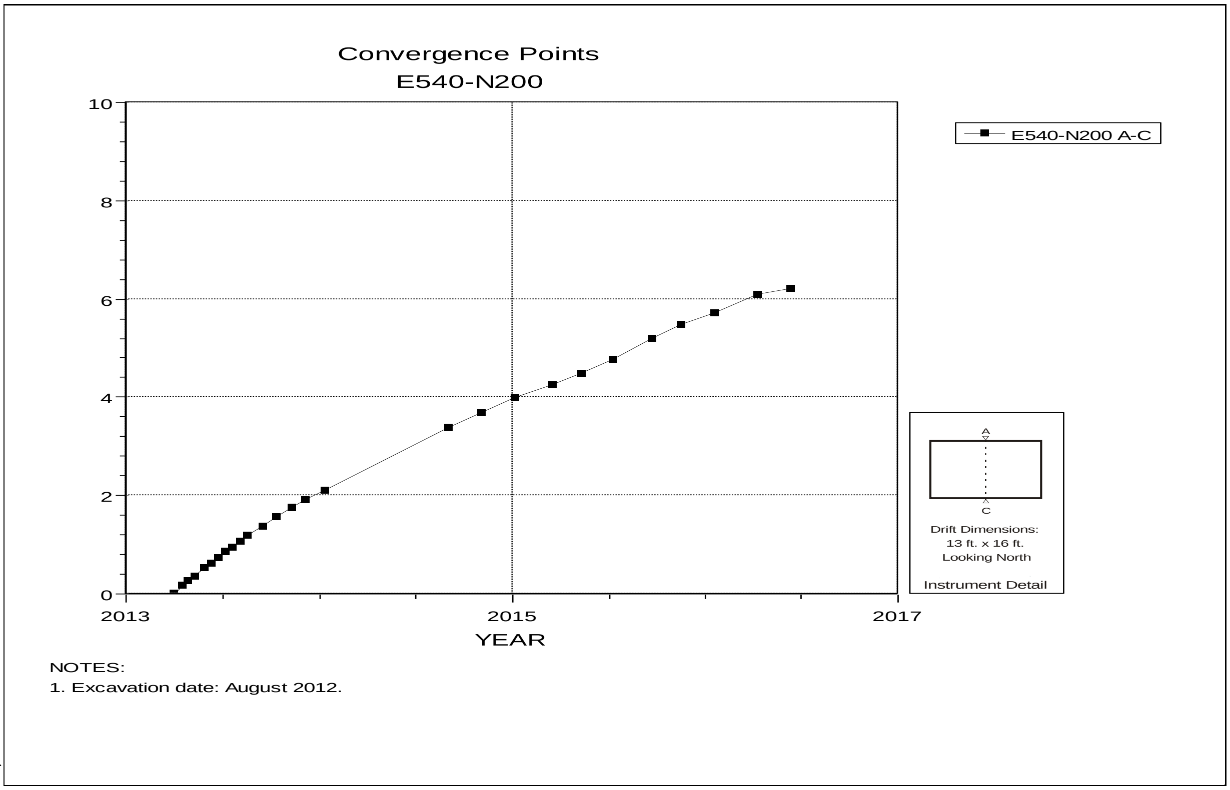

Figure 6-3 Convergence Point Array –
E540 N200 – Roof to Floor

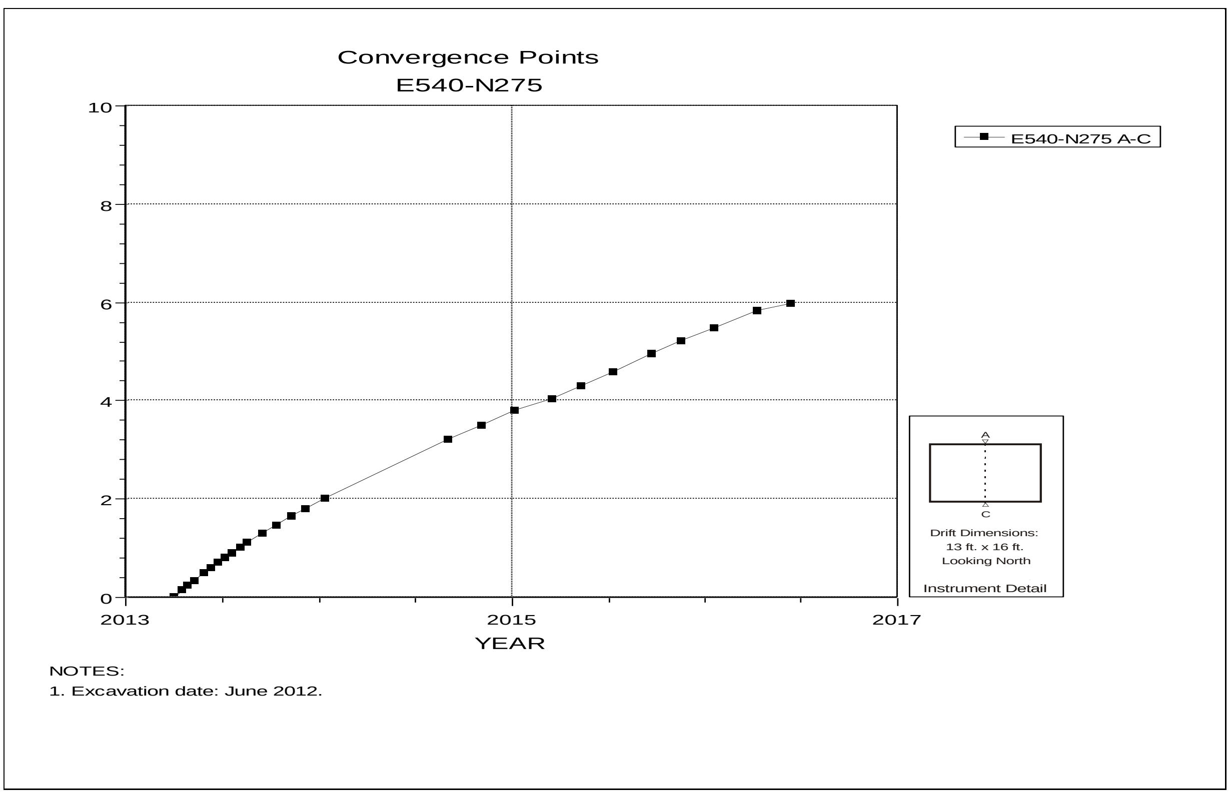

Figure 6-4 Convergence Point Array –
E540 N275 – Roof to Floor

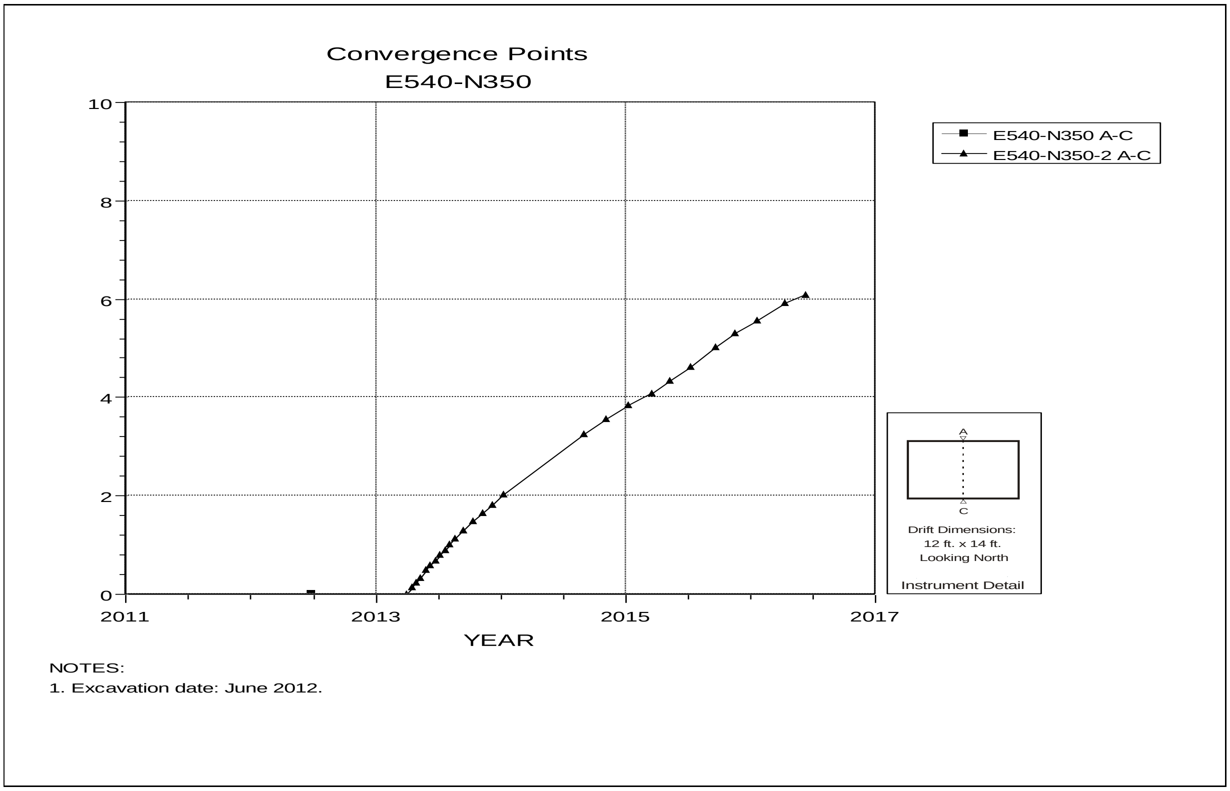

Figure 6-5 Convergence Point Array –
E540 N350 – Roof to Floor

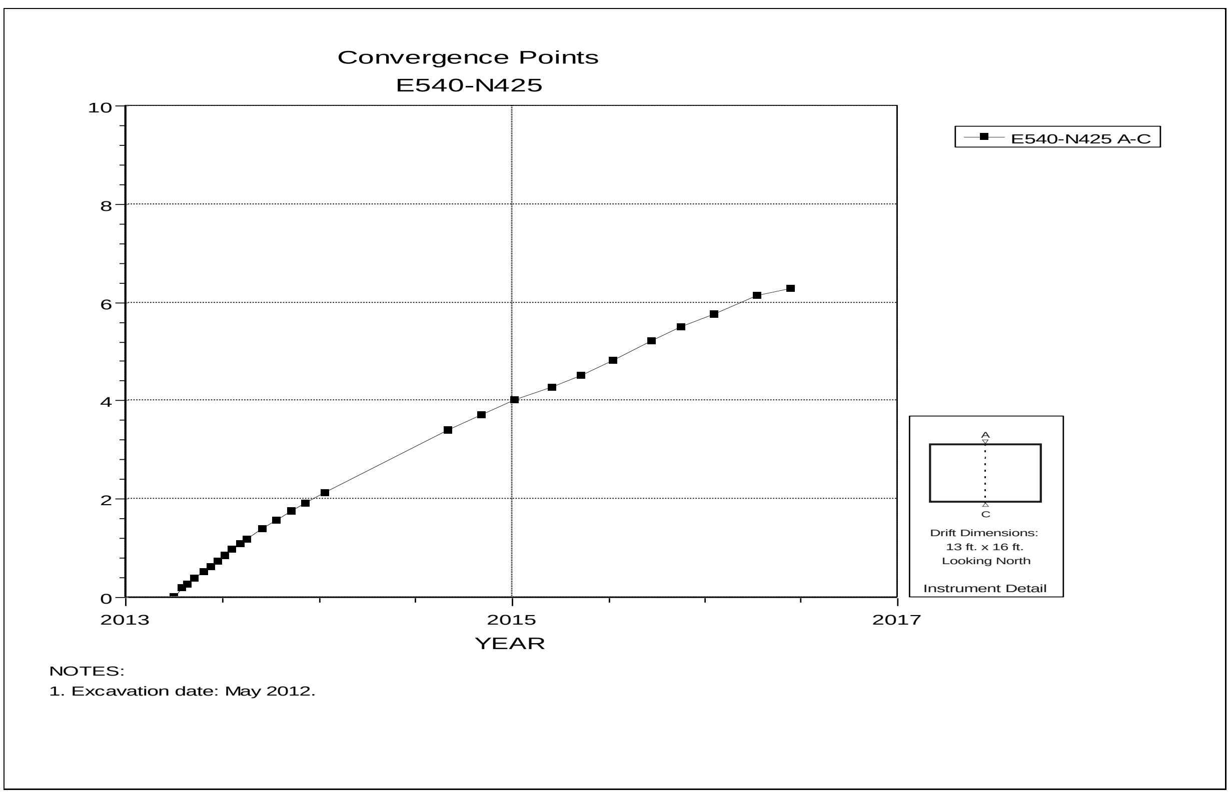

Figure 6-6 Convergence Point Array –
E540 N425 – Roof to Floor

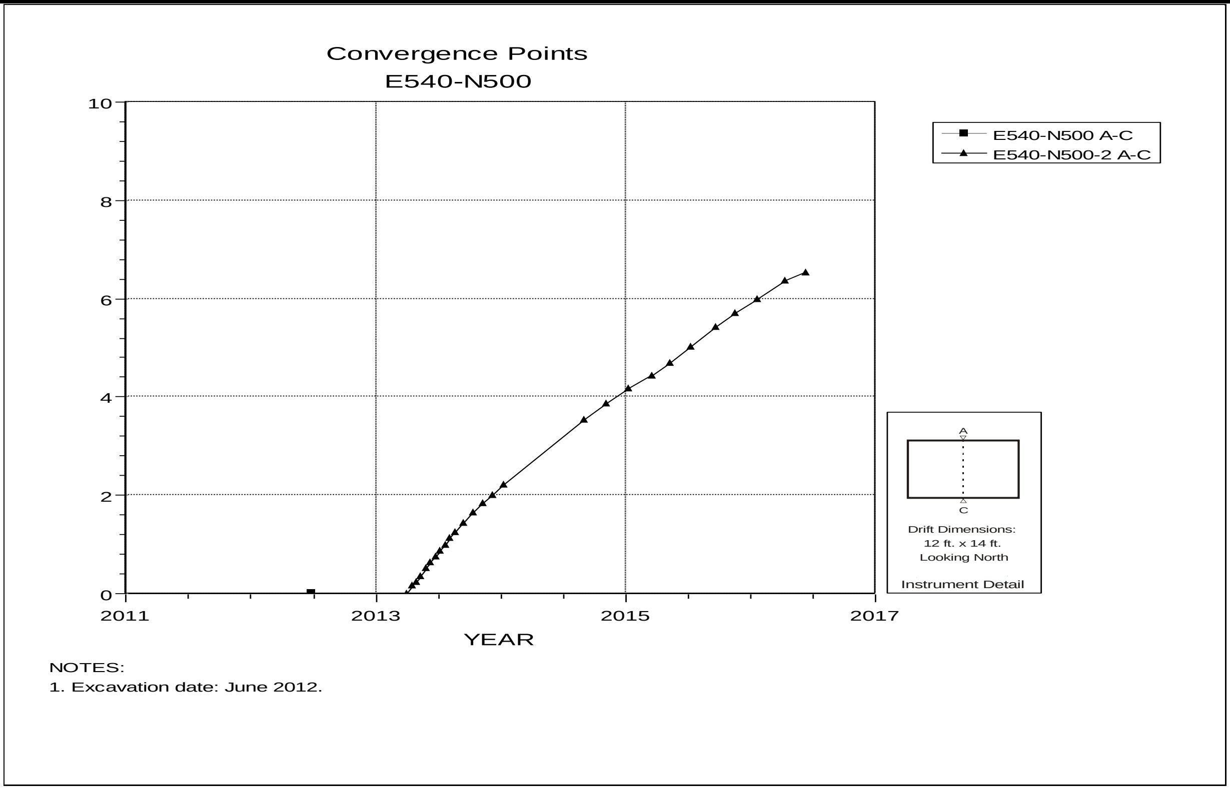

Figure 6-7 Convergence Point Array –
E540 N500 – Roof to Floor

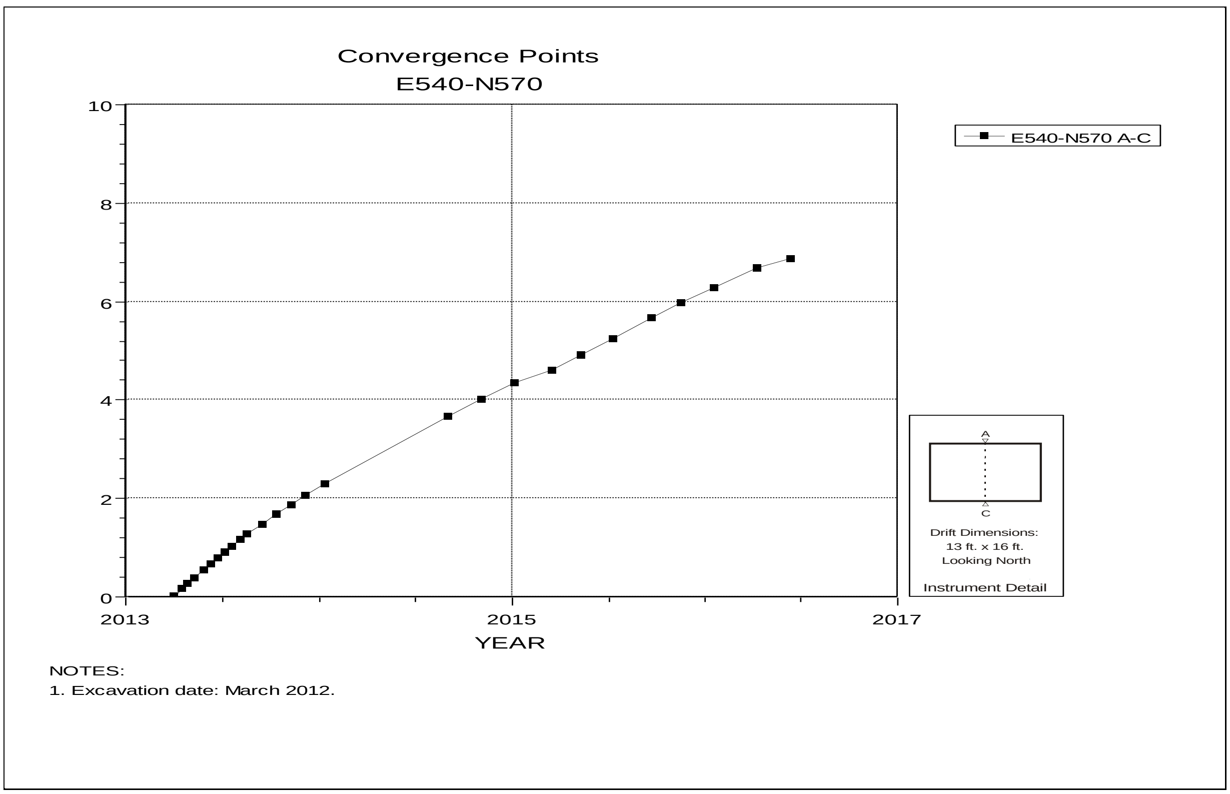

Figure 6-8 Convergence Point Array –
E540 N570 – Roof to Floor

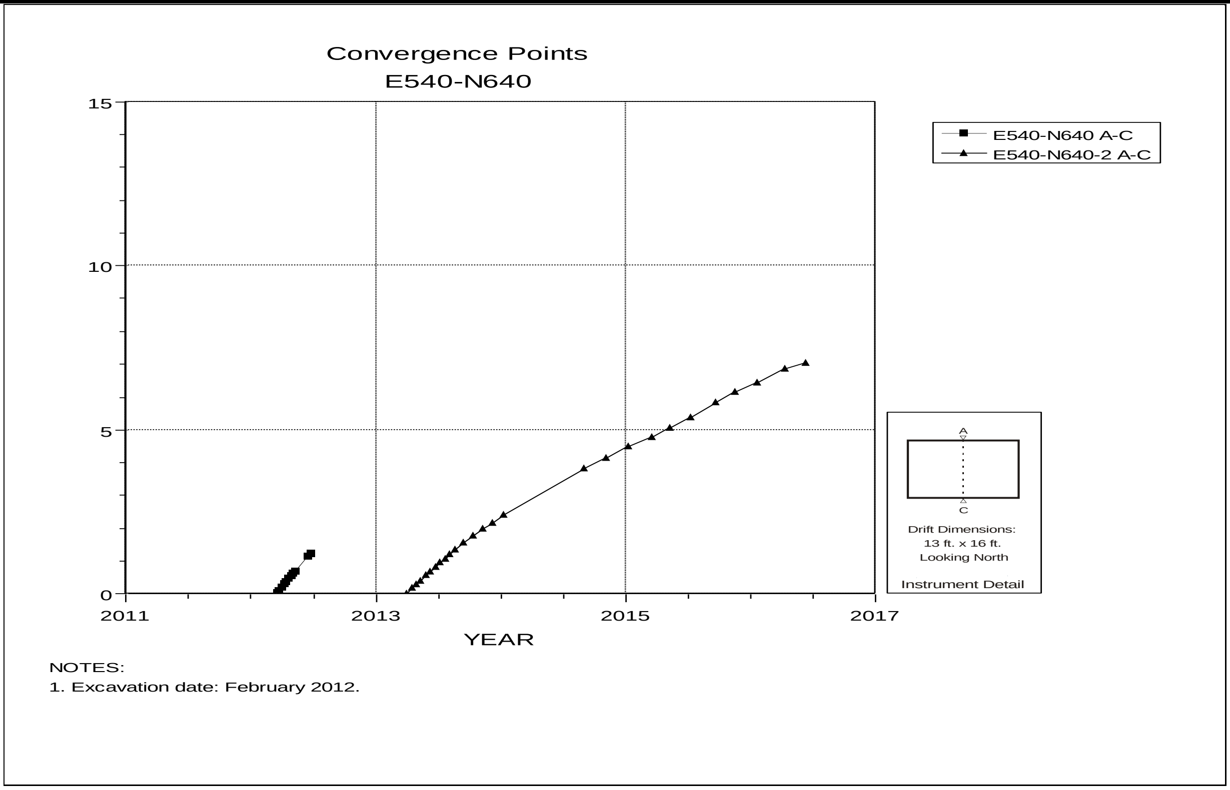

Figure 6-9 Convergence Point Array –
E540 N640 – Roof to Floor

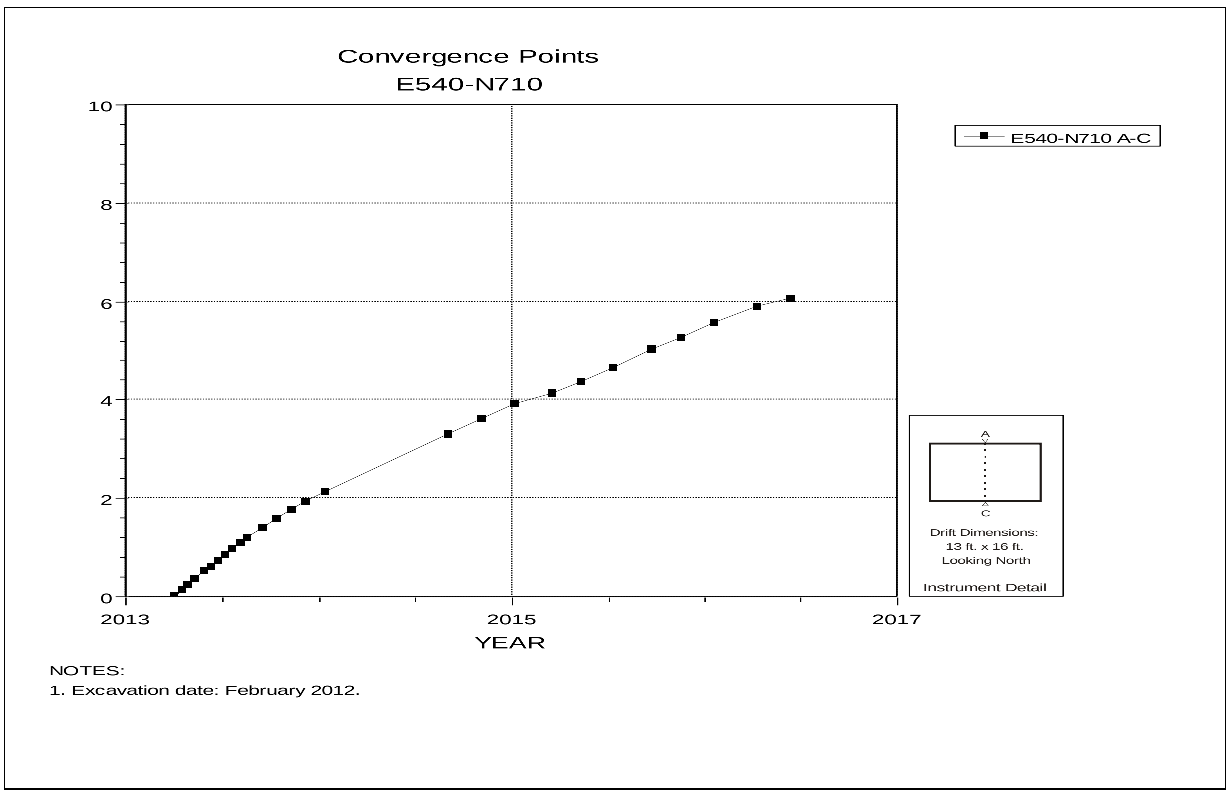

Figure 6-10 Convergence Point Array –
E540 N710 – Roof to Floor

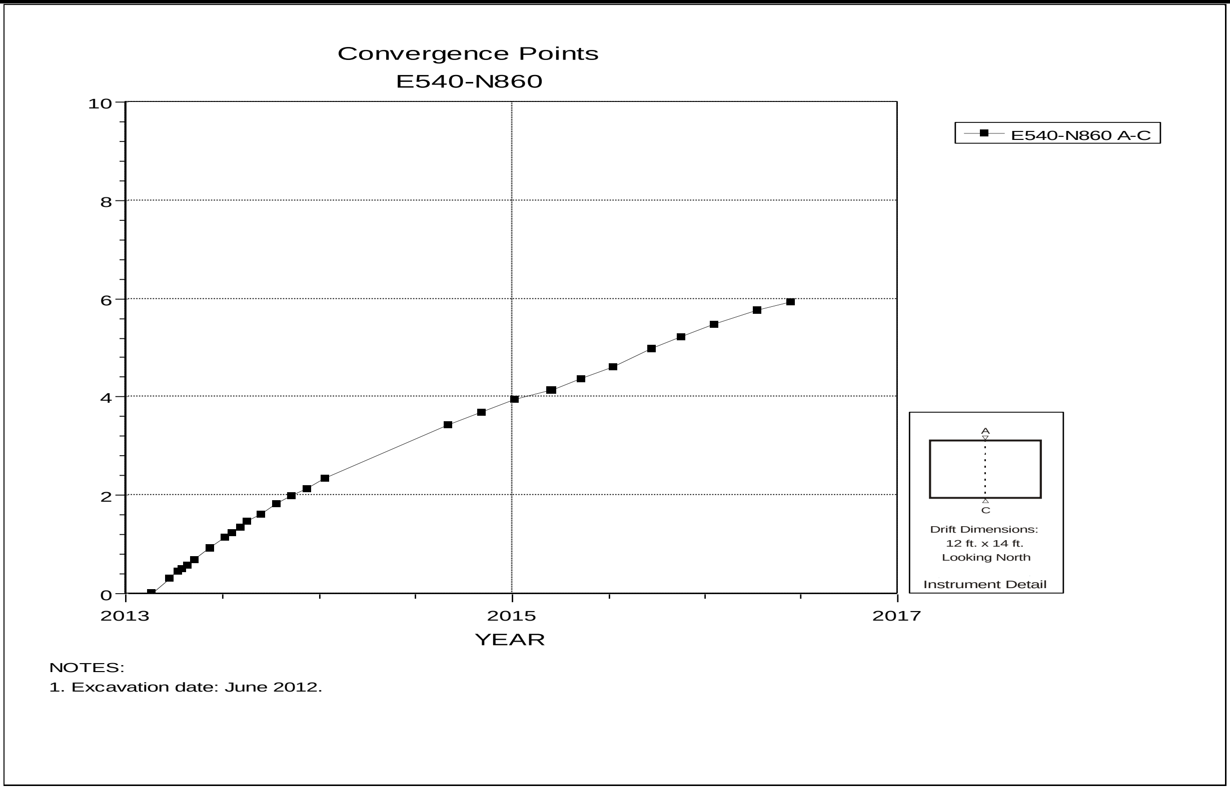

Figure 6-11 Convergence Point Array –
E540 N860 – Roof to Floor

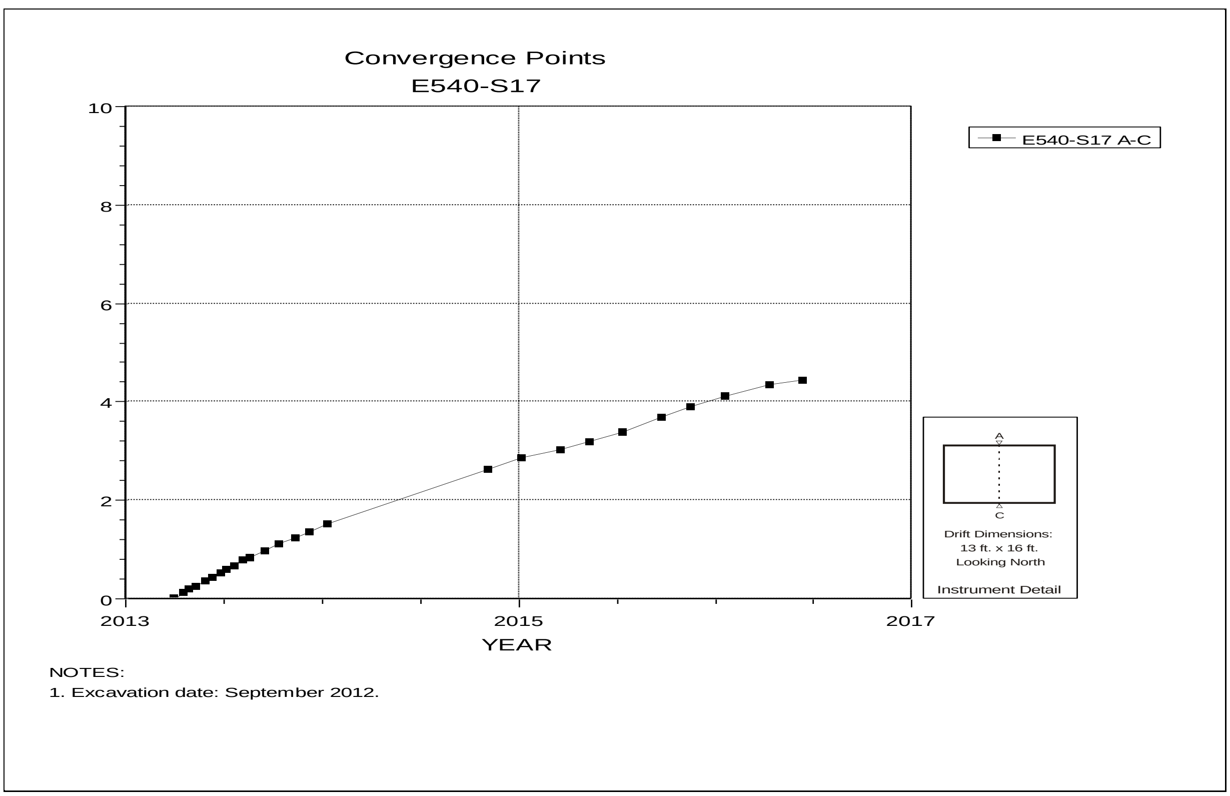

Figure 6-12 Convergence Point Array –
E540 S17 – Roof to Floor

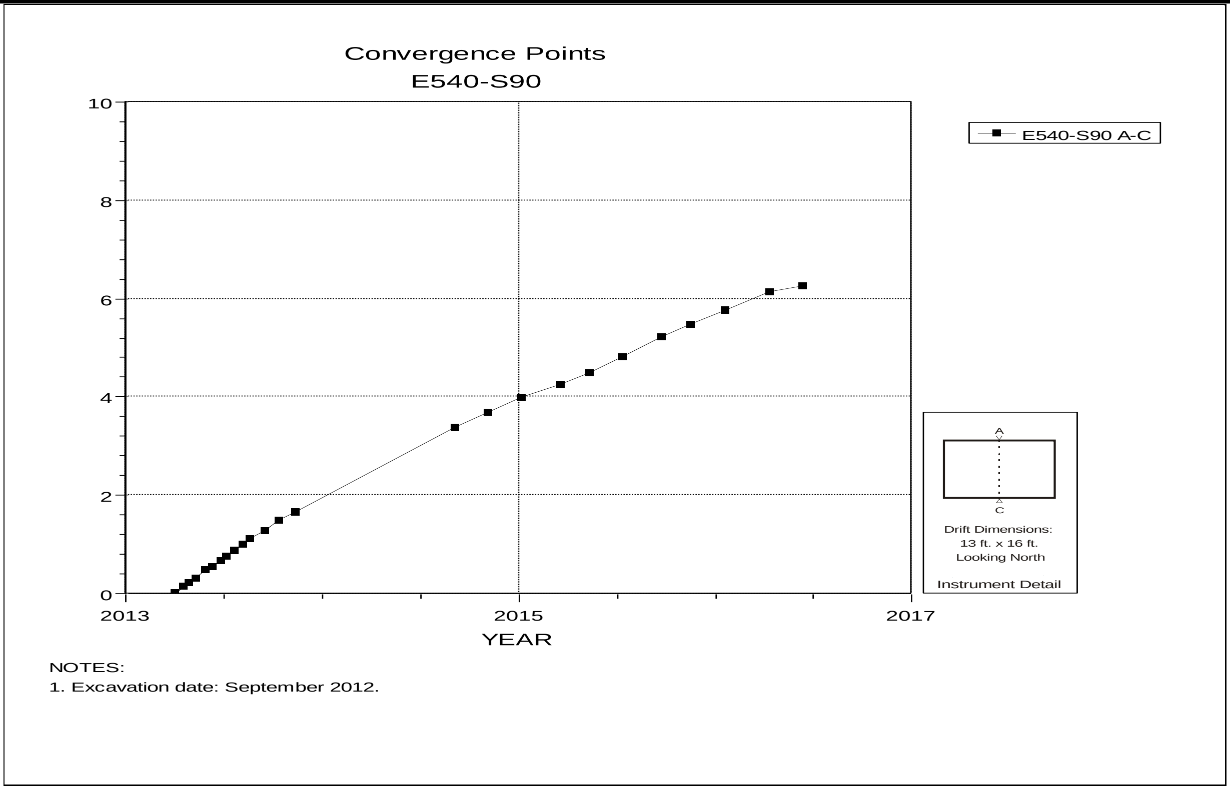

Figure 6-13 Convergence Point Array –
E540 S90 – Roof to Floor

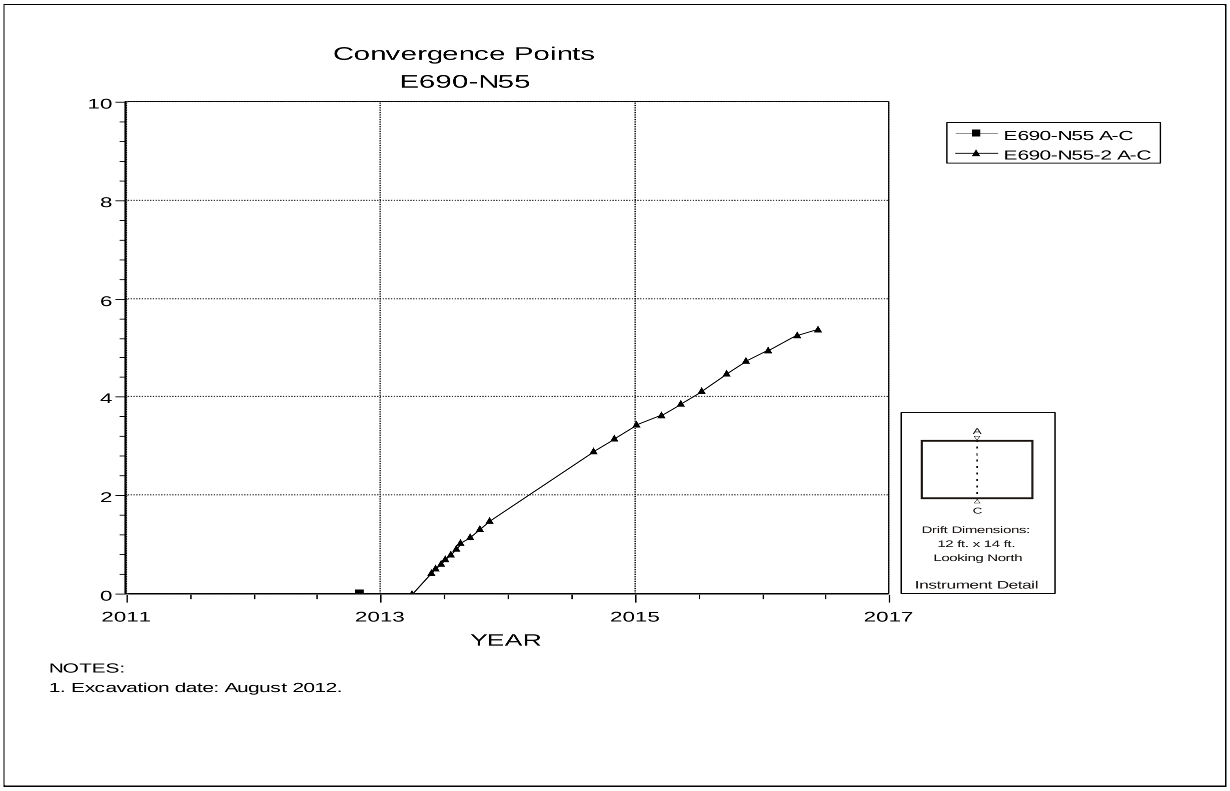

Figure 6-14 Convergence Point Array –
E690 N55 – Roof to Floor

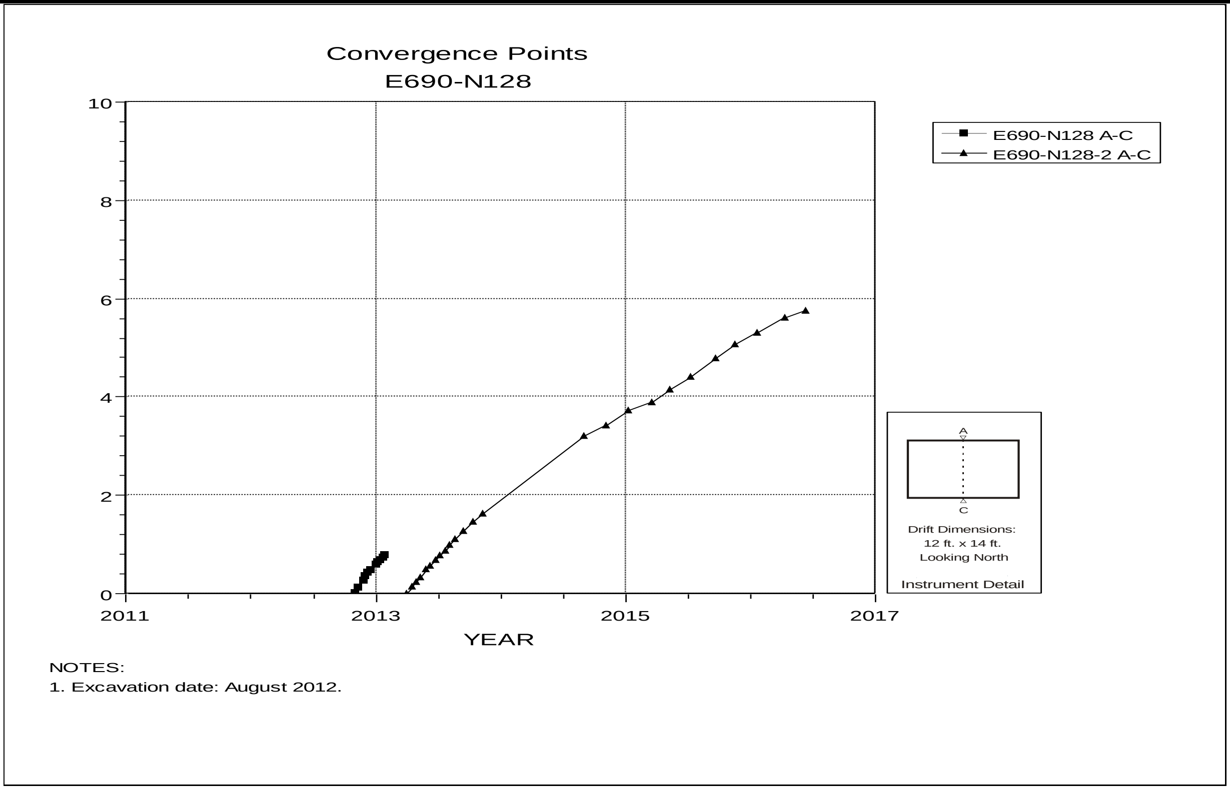

Figure 6-15 Convergence Point Array –
E690 N128 – Roof to Floor

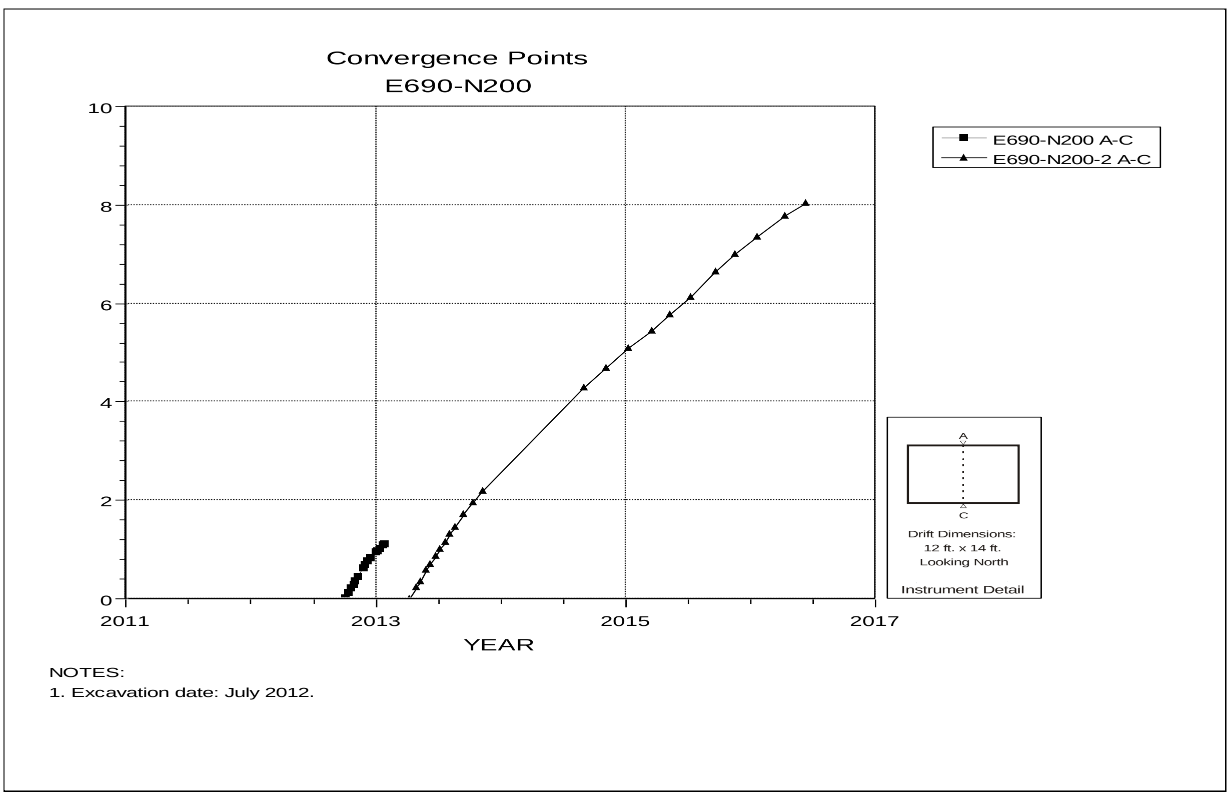

Figure 6-16 Convergence Point Array –
E690 N200 – Roof to Floor

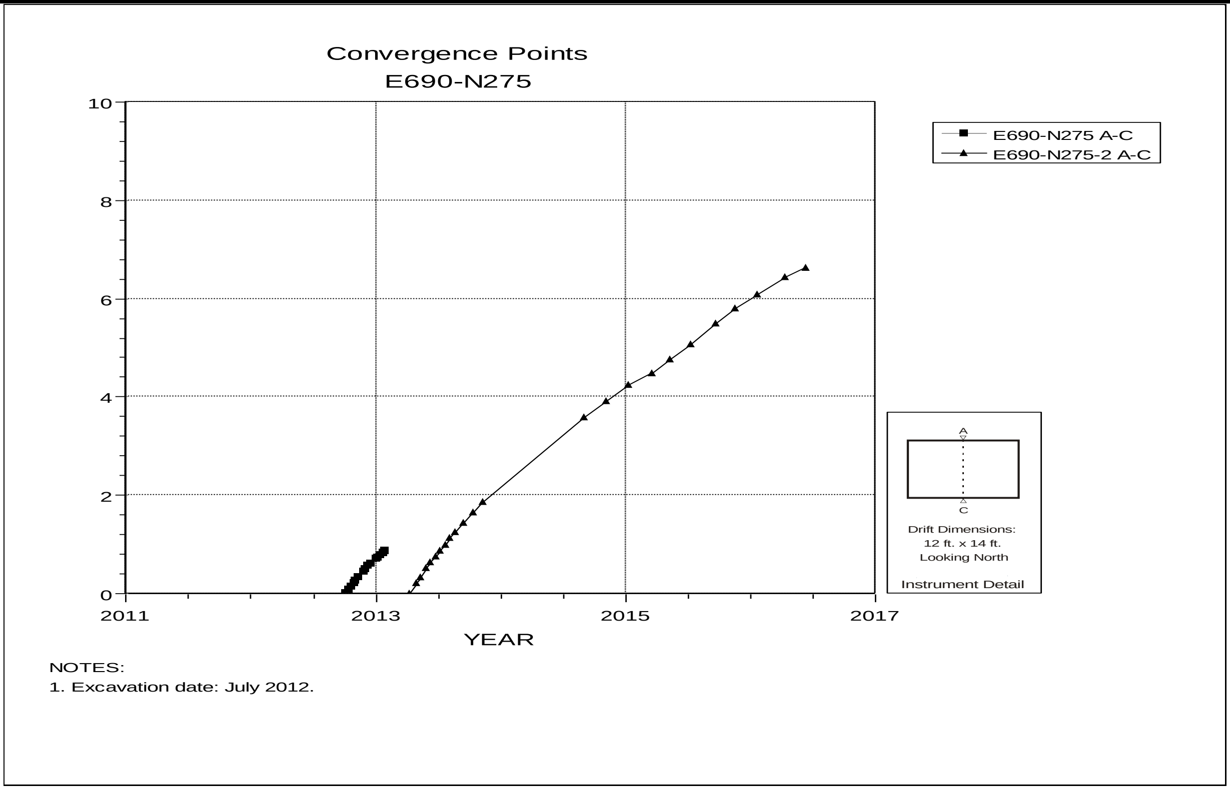

Figure 6-17 Convergence Point Array –
E690 N275 – Roof to Floor

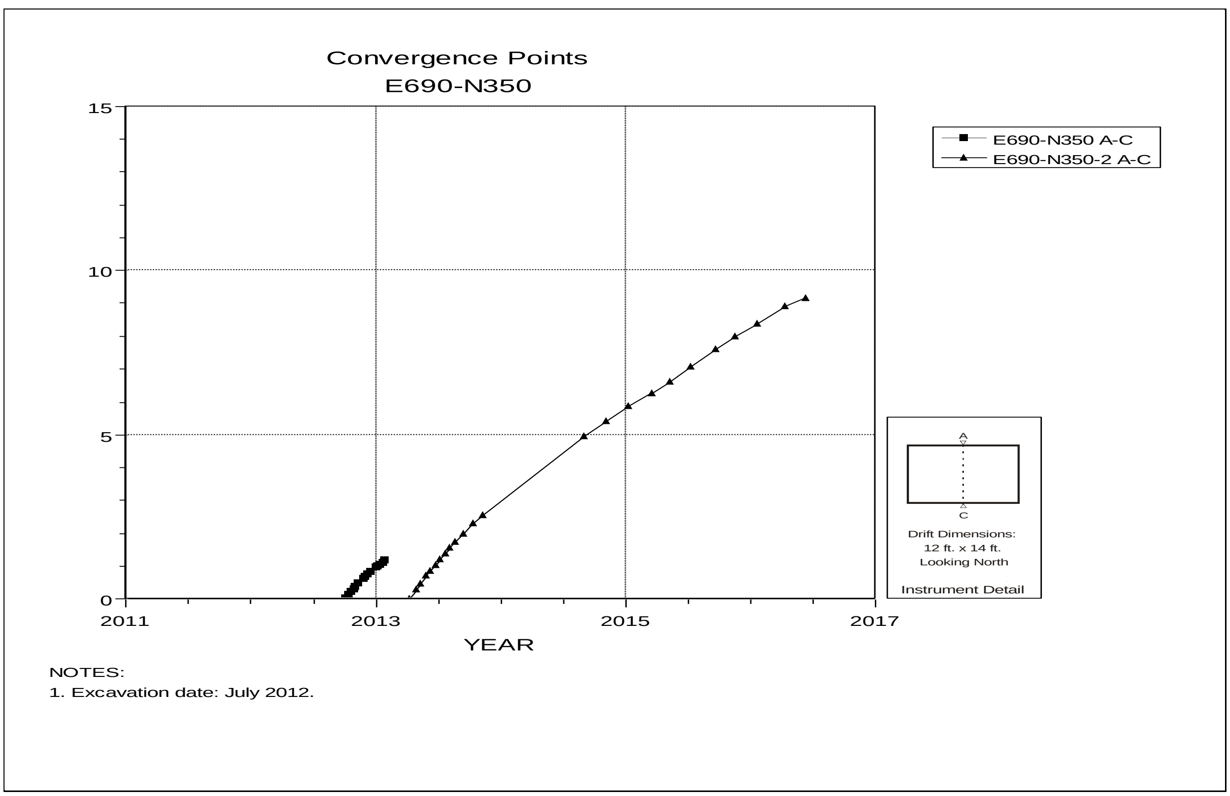

Figure 6-18 Convergence Point Array –
E690 N350 – Roof to Floor

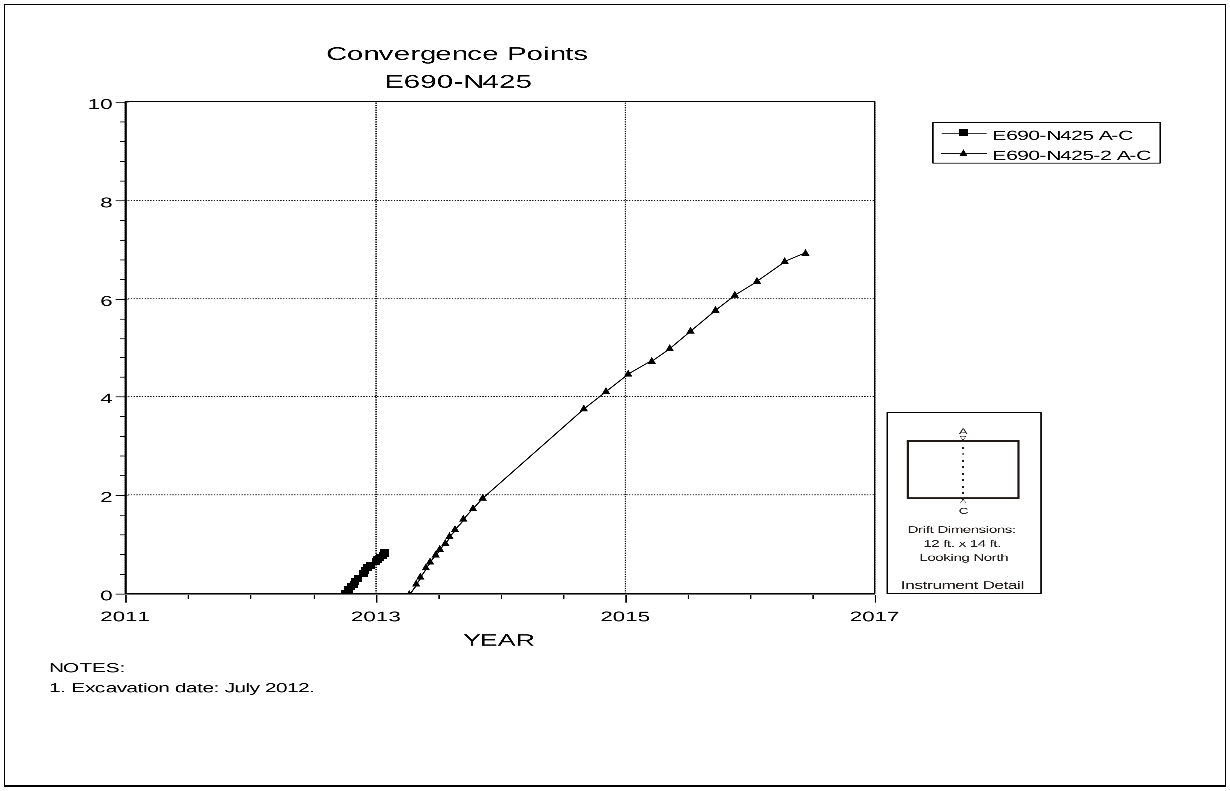

Figure 6-19 Convergence Point Array
E690 N425 – Roof to Floor

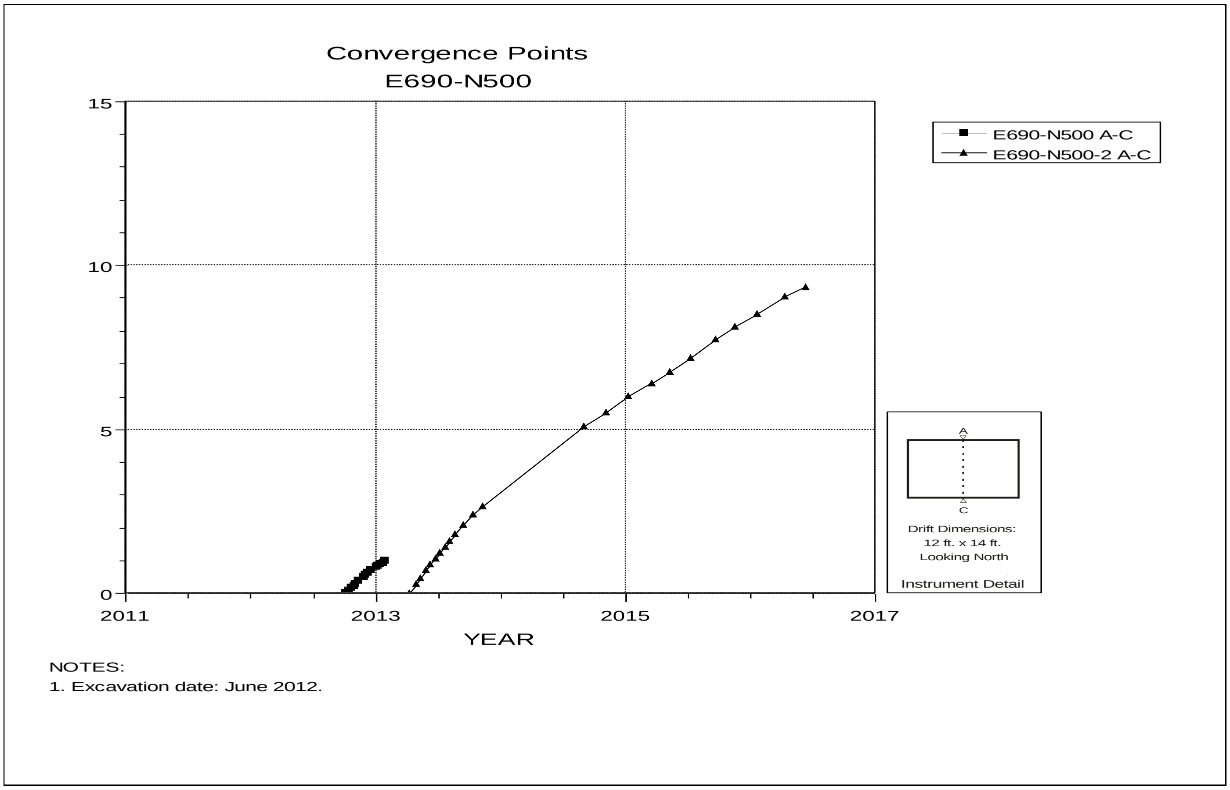

Figure 6-20 Convergence Point Array –
E690 N500 – Roof to Floor

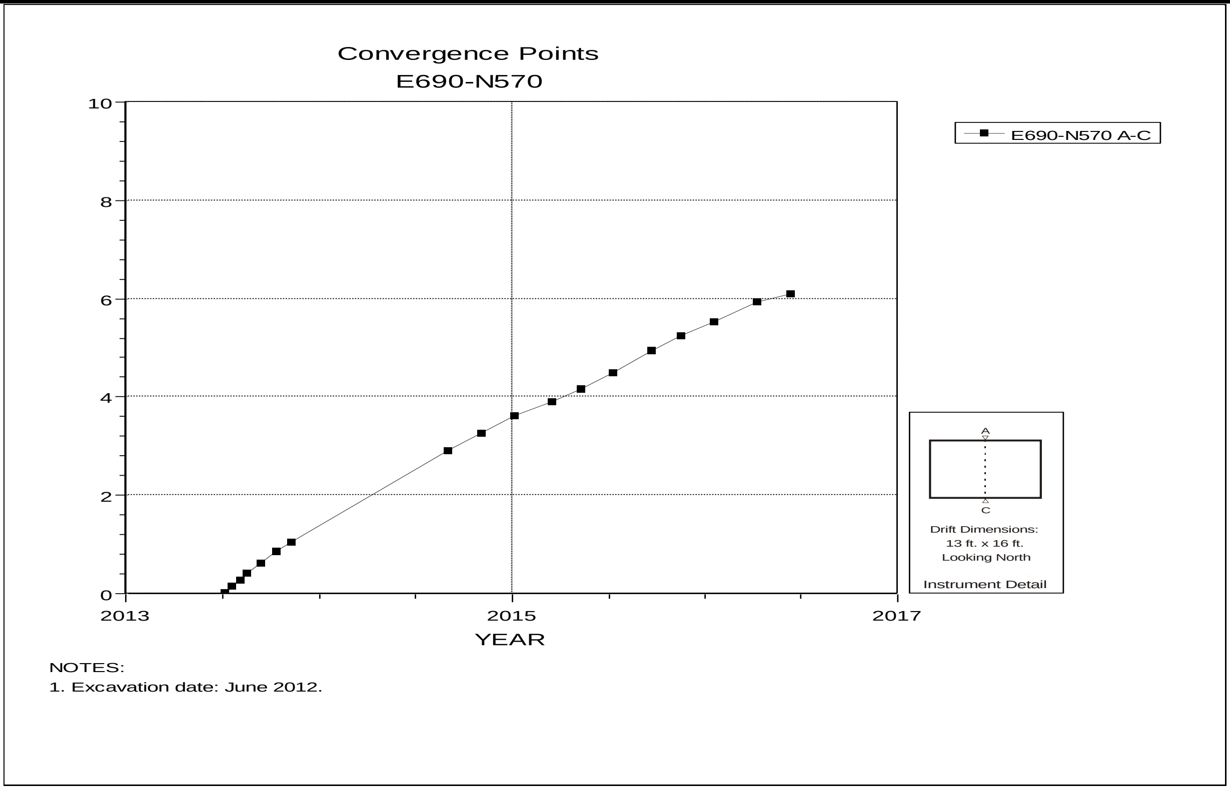

Figure 6-21 Convergence Point Array –
E690 N570 – Roof to Floor

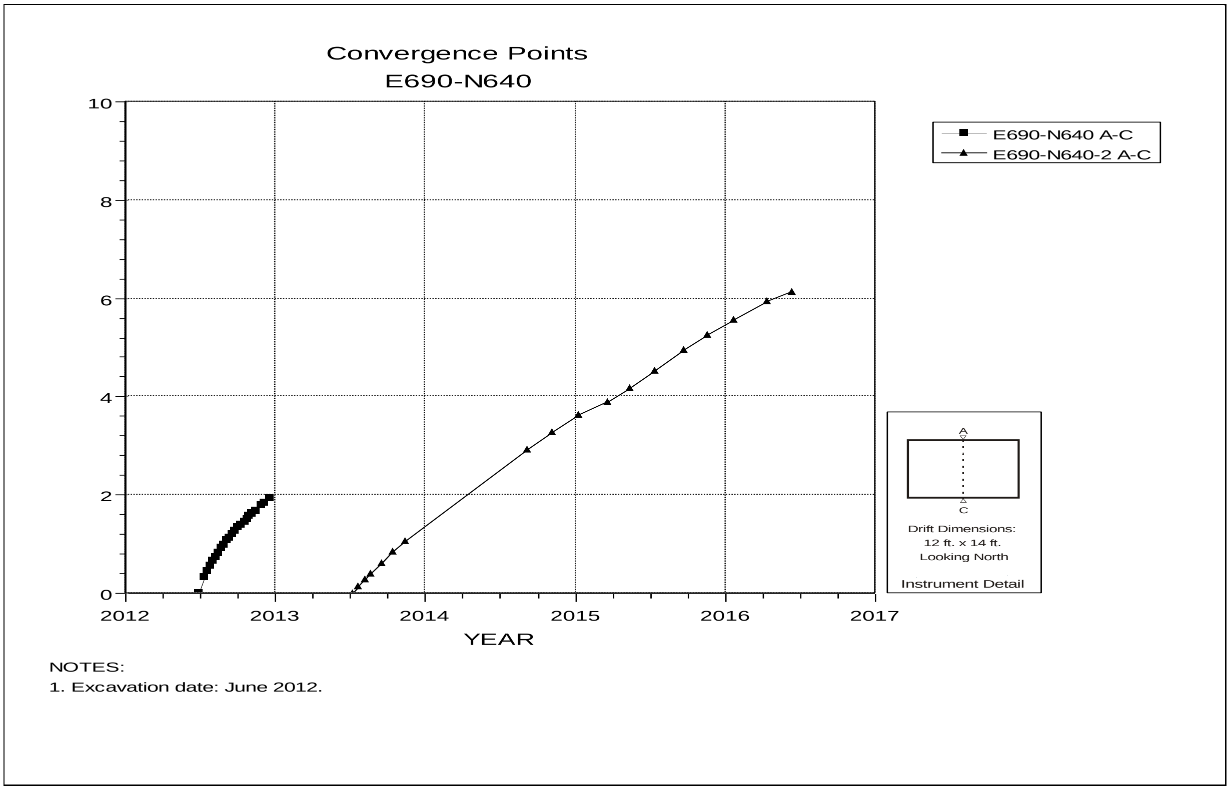

Figure 6-22 Convergence Point Array –
E690 N640 – Roof to Floor

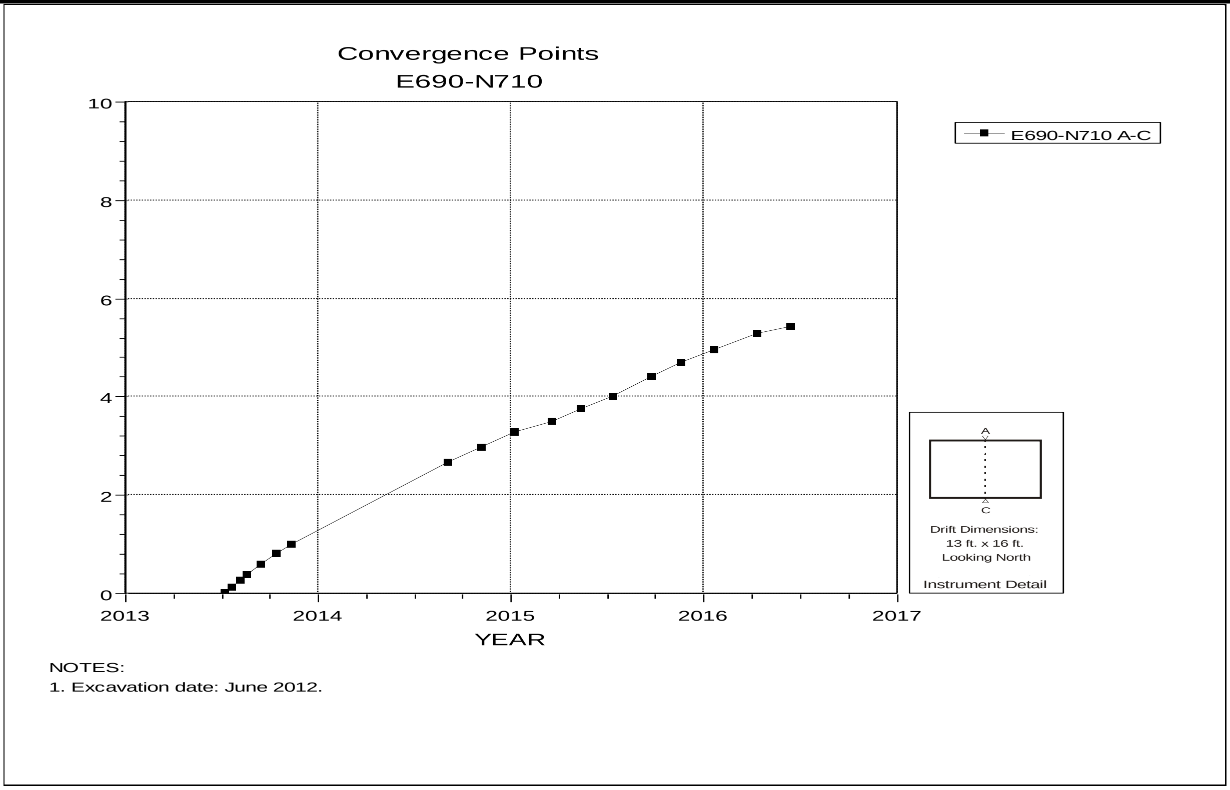

Figure 6-23 Convergence Point Array –
E690 N710 – Roof to Floor

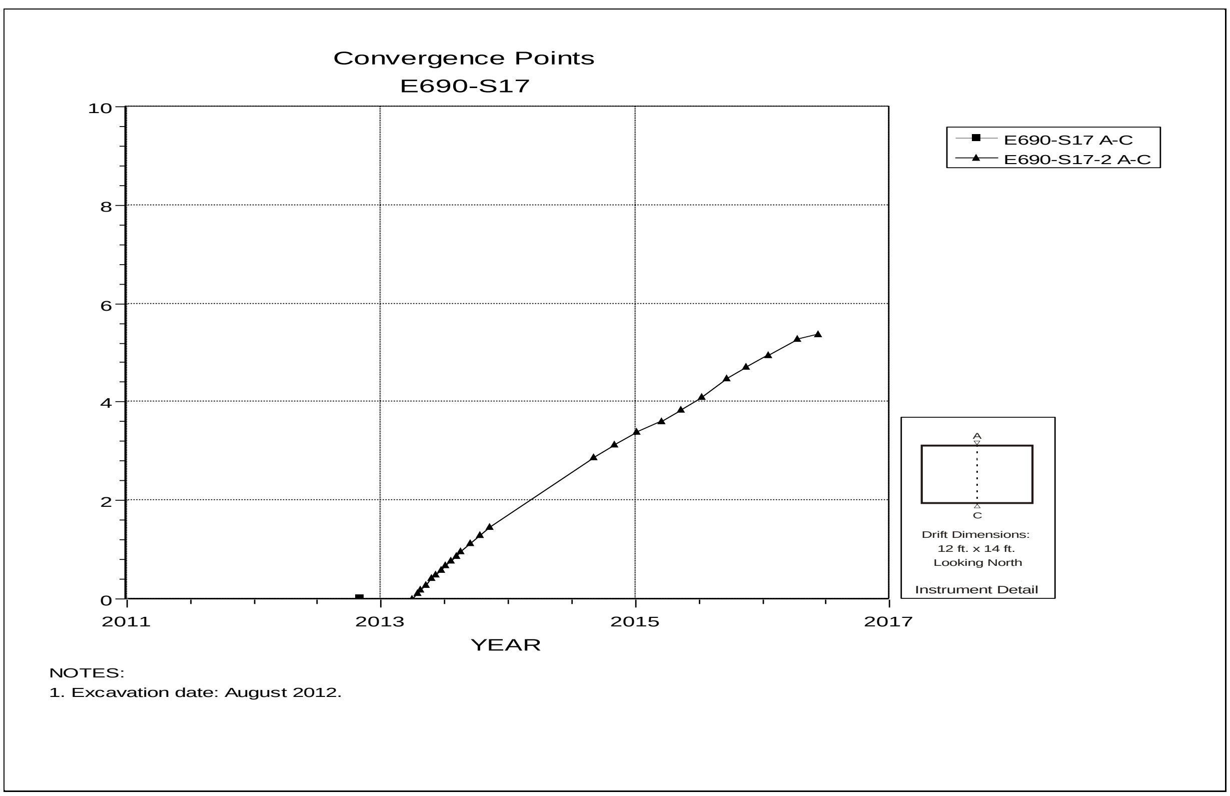

Figure 6-24 Convergence Point Array –
E690 S17 – Roof to Floor

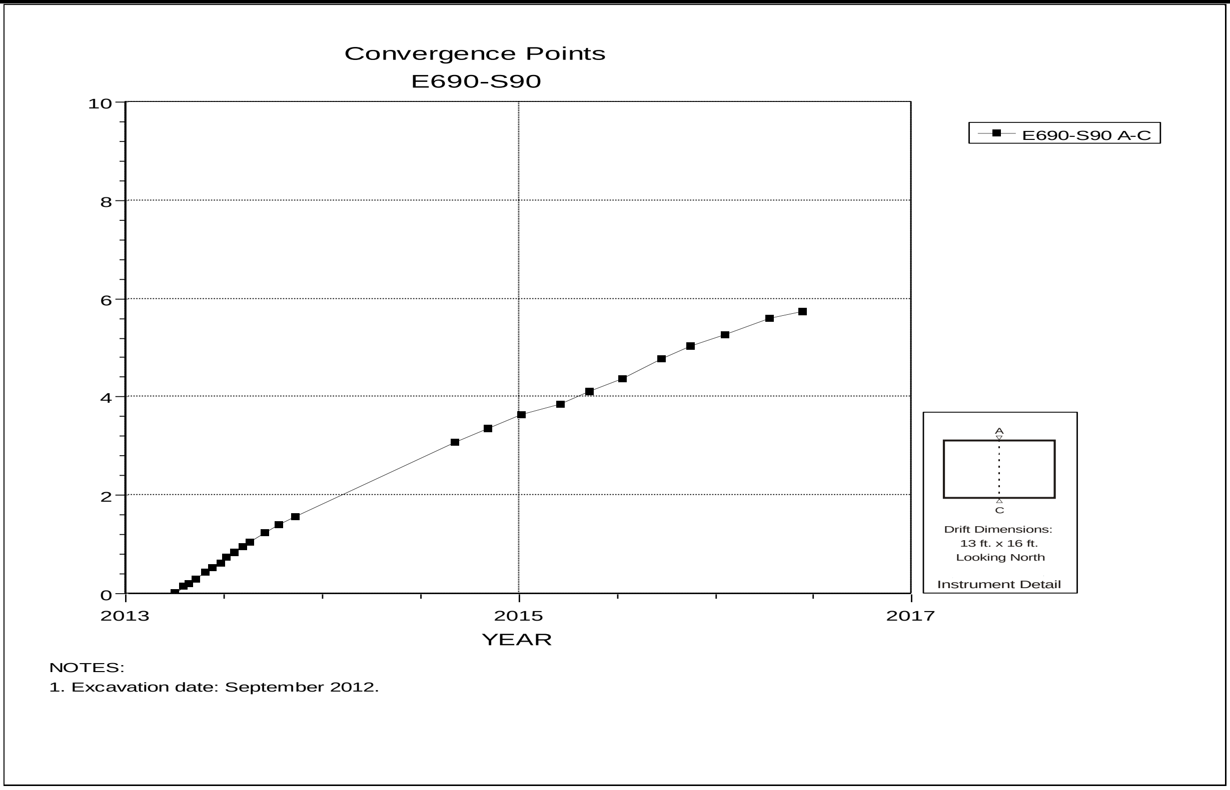

Figure 6-25 Convergence Point Array –
E690 S90 – Roof to Floor

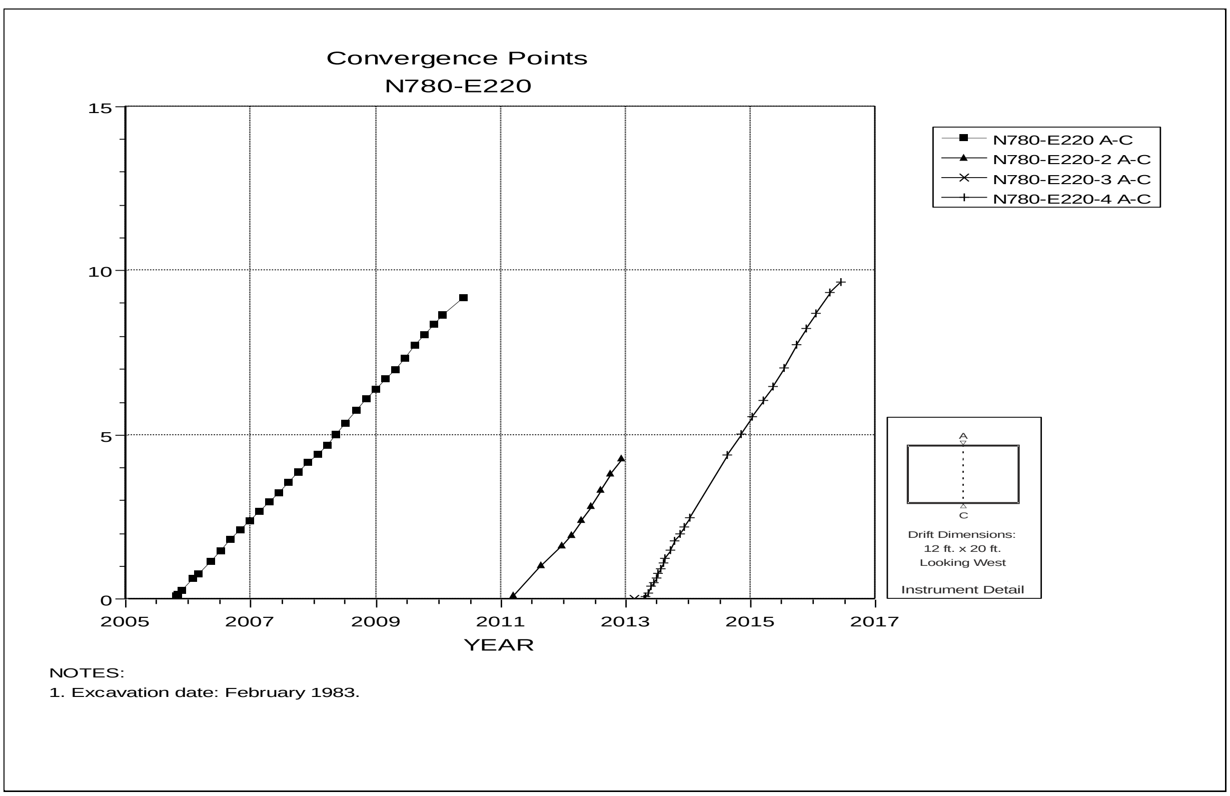

Figure 6-26 Convergence Point Array –
N780 E220 – Roof to Floor

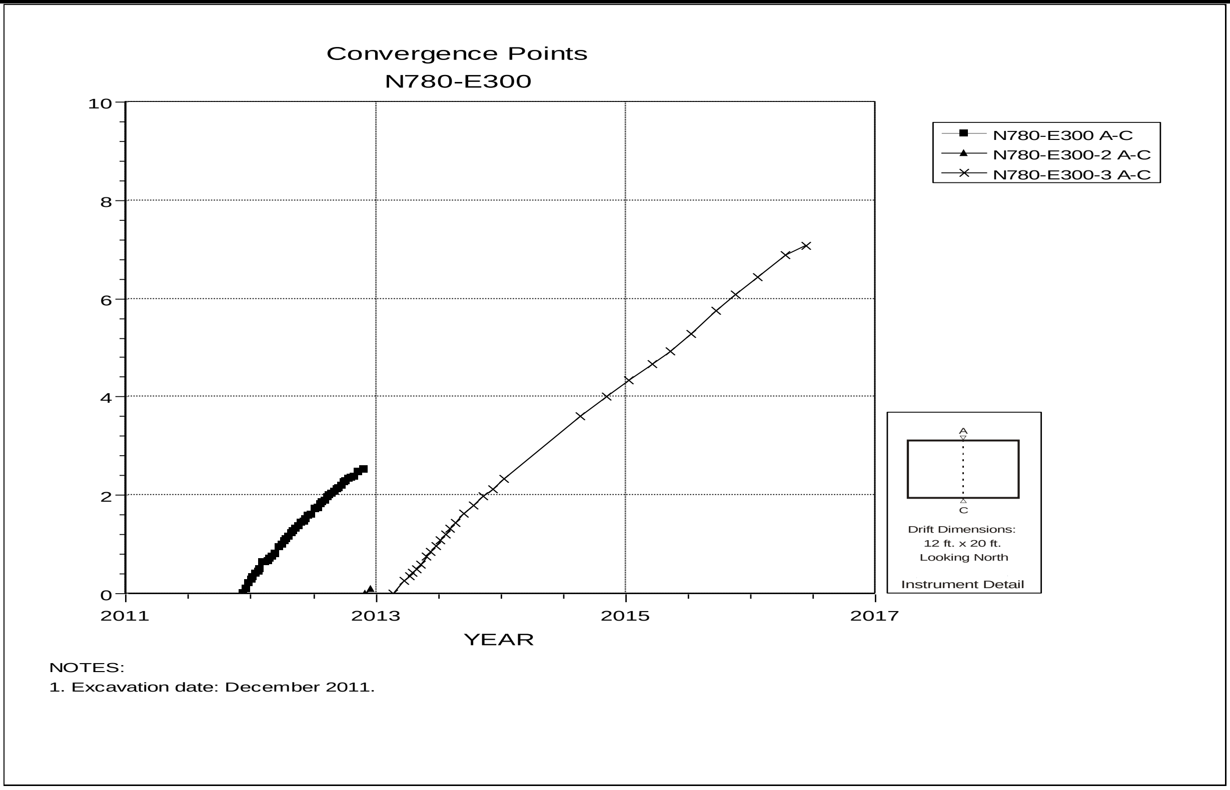

Figure 6-27 Convergence Point Array –
N780 E300 – Roof to Floor

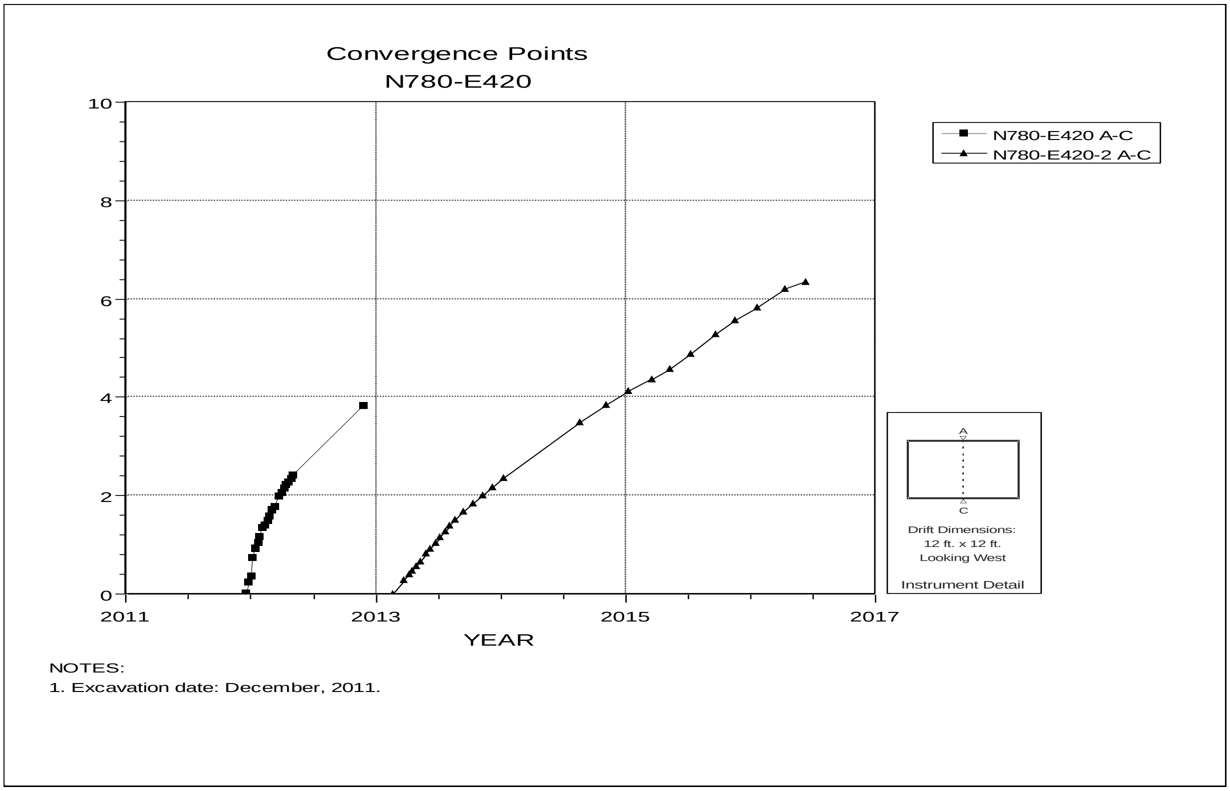

Figure 6-28 Convergence Point Array –
N780 E420 – Roof to Floor

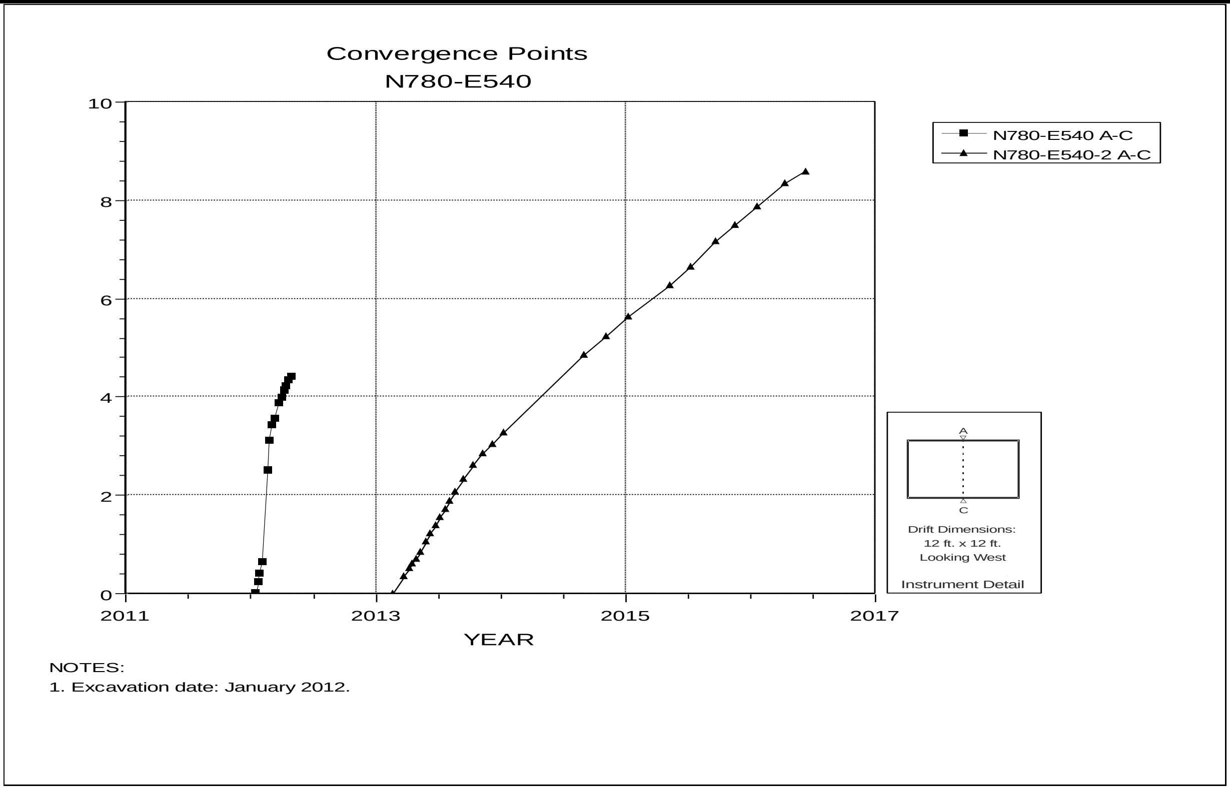

Figure 6-29 Convergence Point Array –
N780 E540 – Roof to Floor

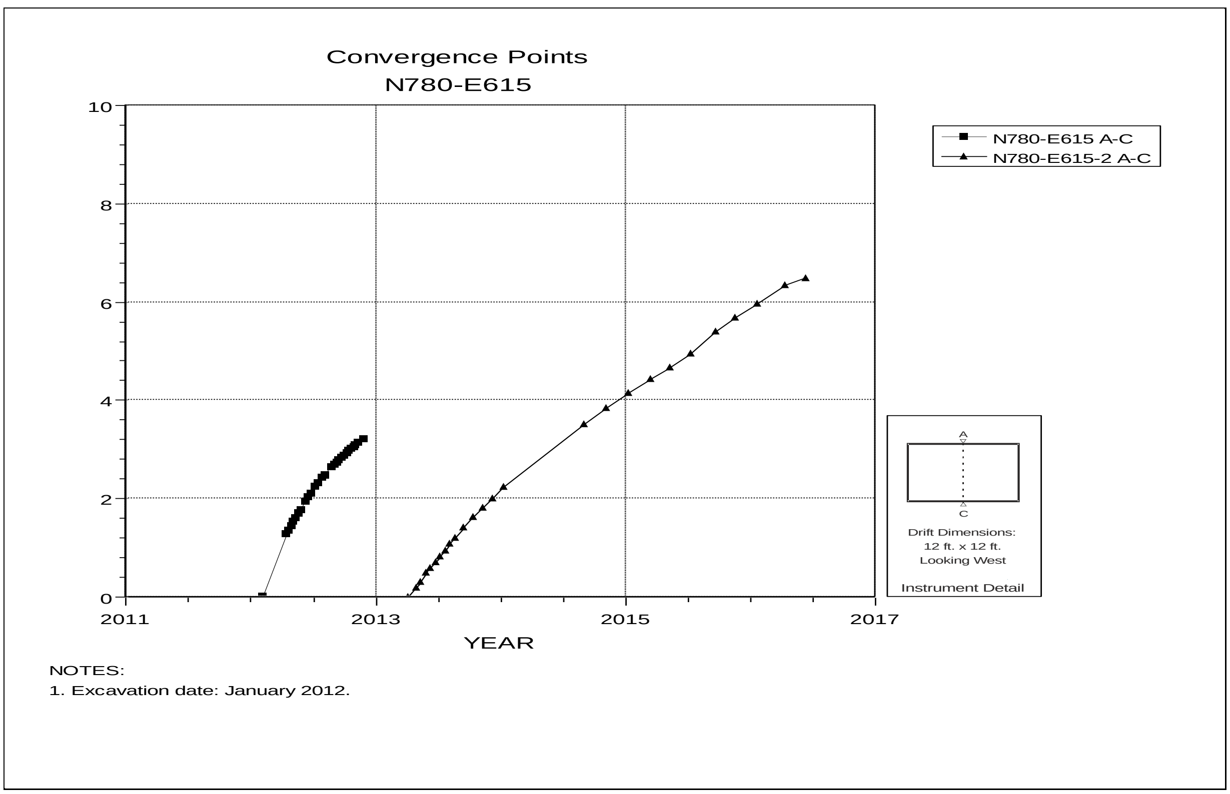

Figure 6-30 Convergence Point Array
N780 E615 – Roof to Floor

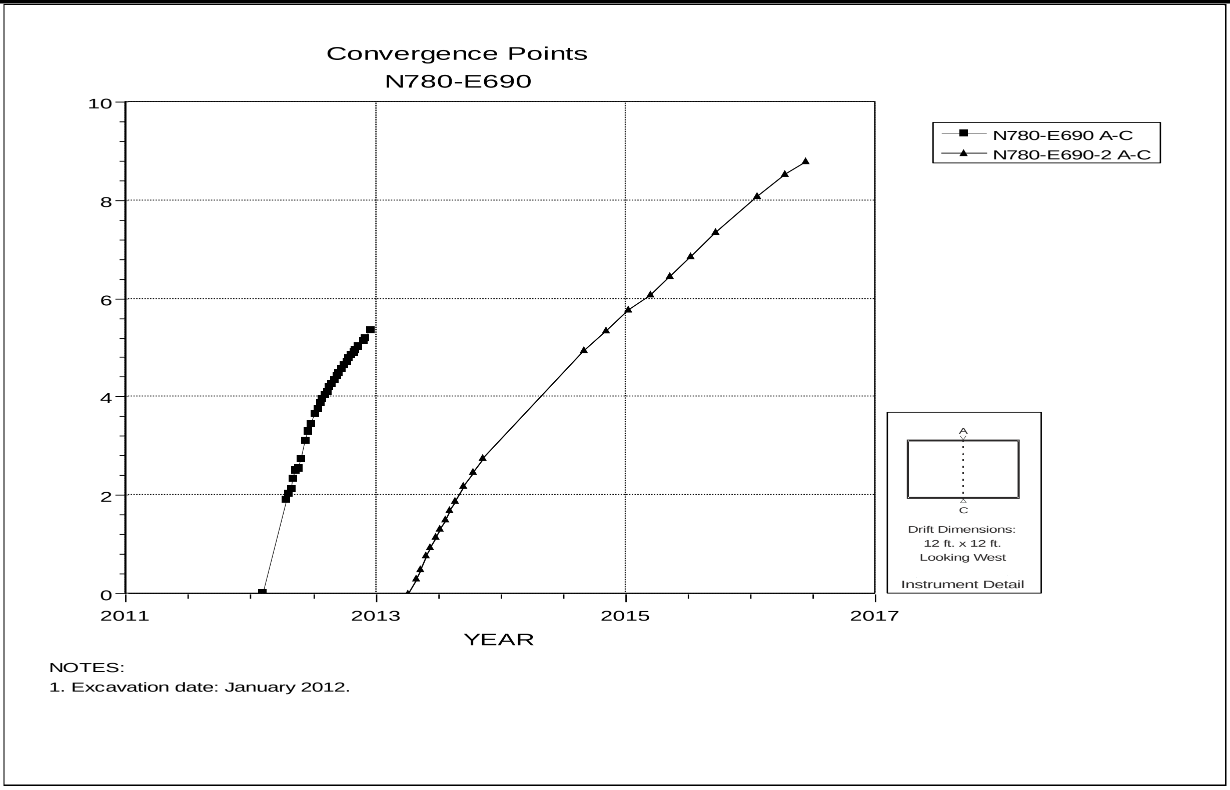

Figure 6-31 Convergence Point Array –
N780 E690 – Roof to Floor

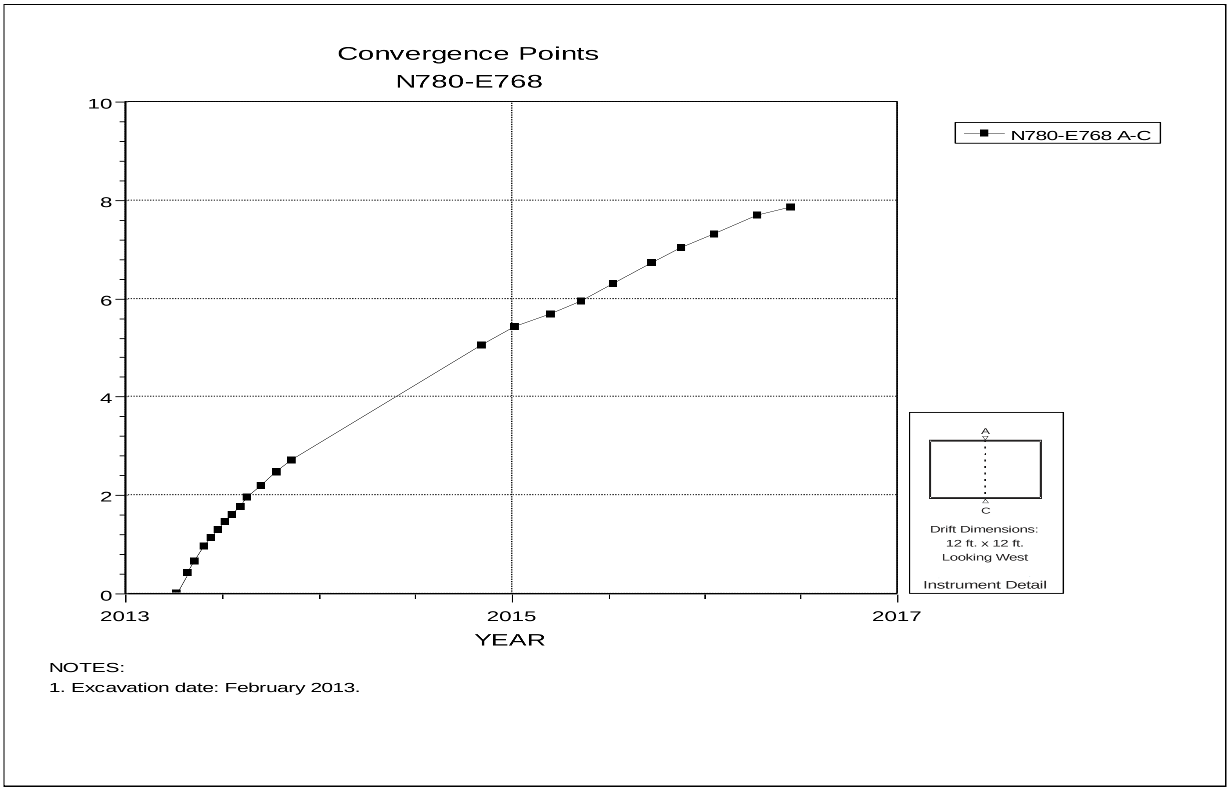

Figure 6-32 Convergence Point Array –
N780 E768 – Roof to Floor

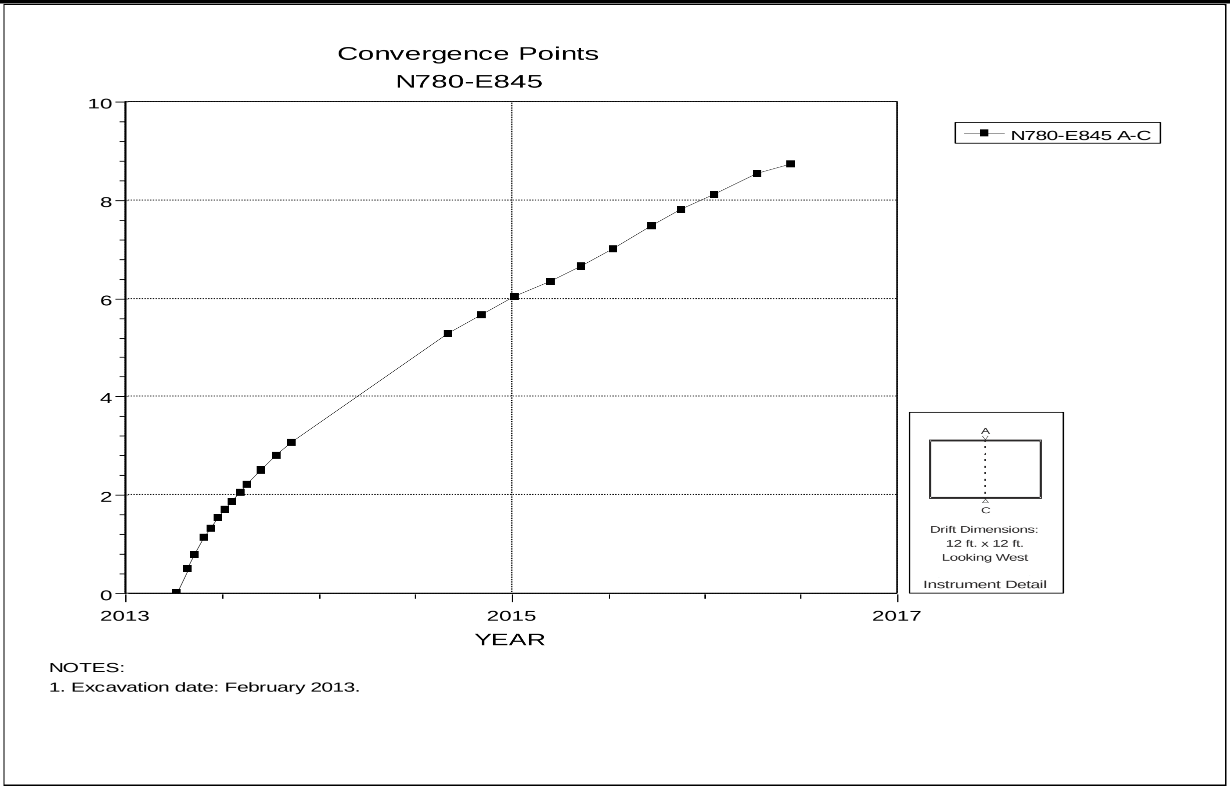

Figure 6-33 Convergence Point Array –
N780 E845 – Roof to Floor

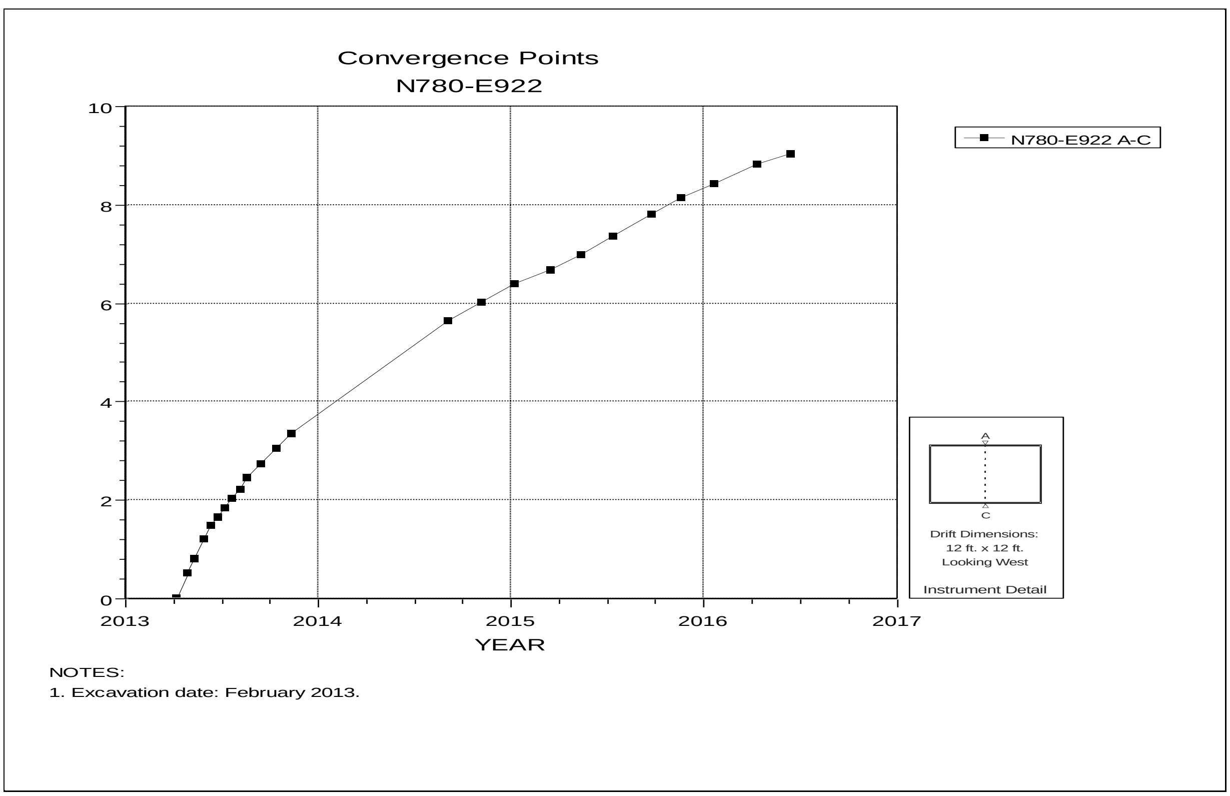

Figure 6-34 Convergence Point Array –
N780 E922 – Roof to Floor

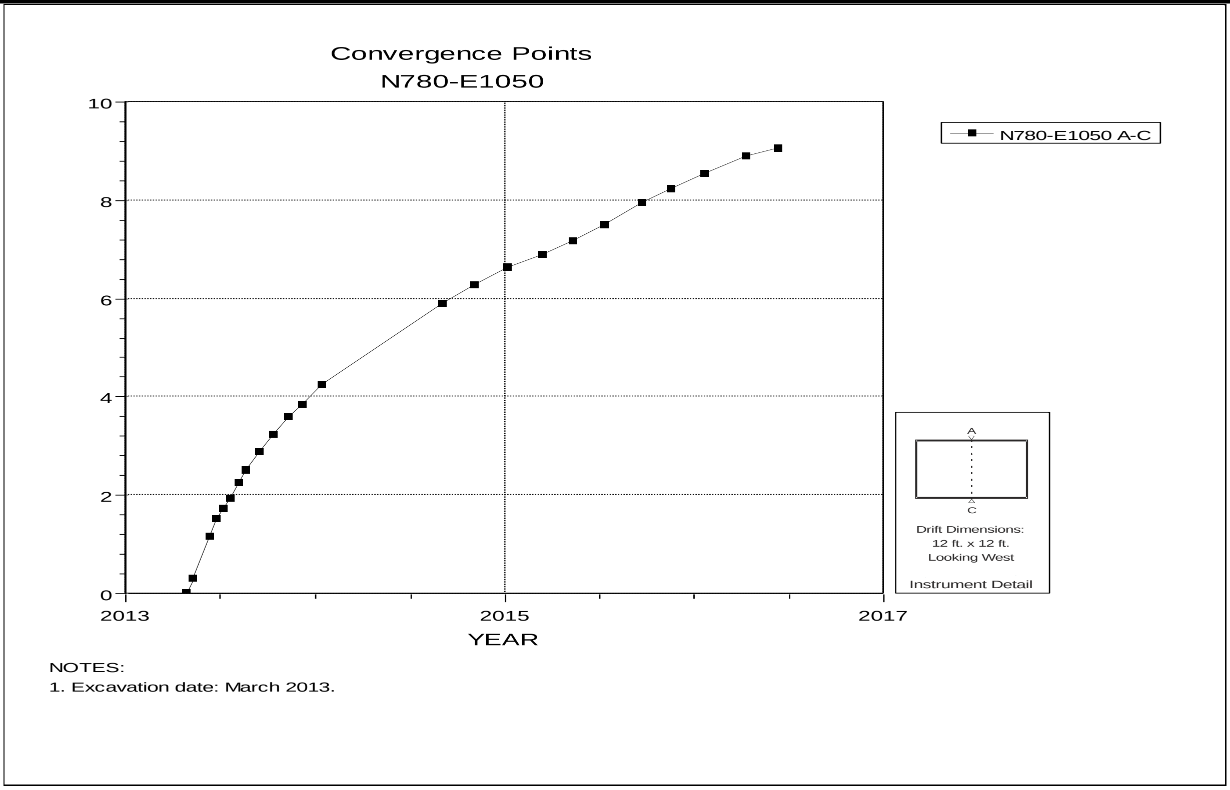

Figure 6-35 Convergence Point Array –
N780 E1050 – Roof to Floor

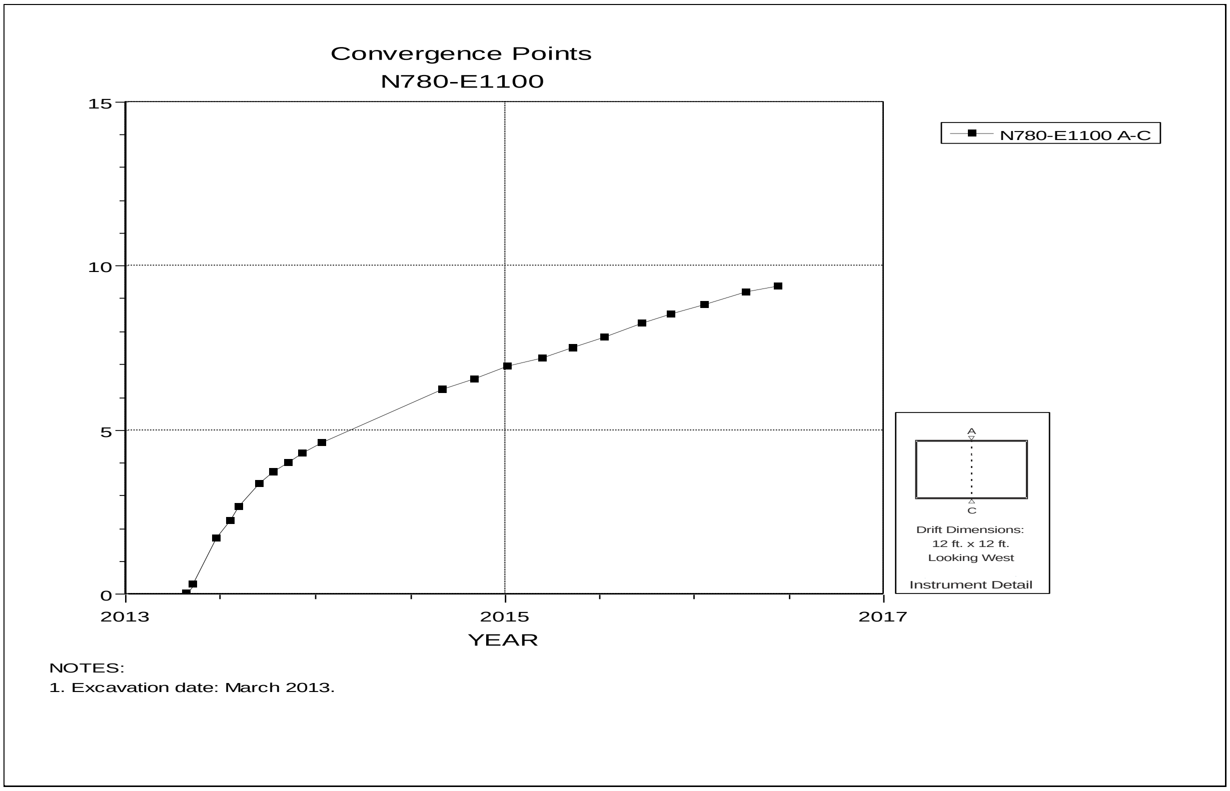

Figure 6-36 Convergence Point Array –
N780 E1100 – Roof to Floor

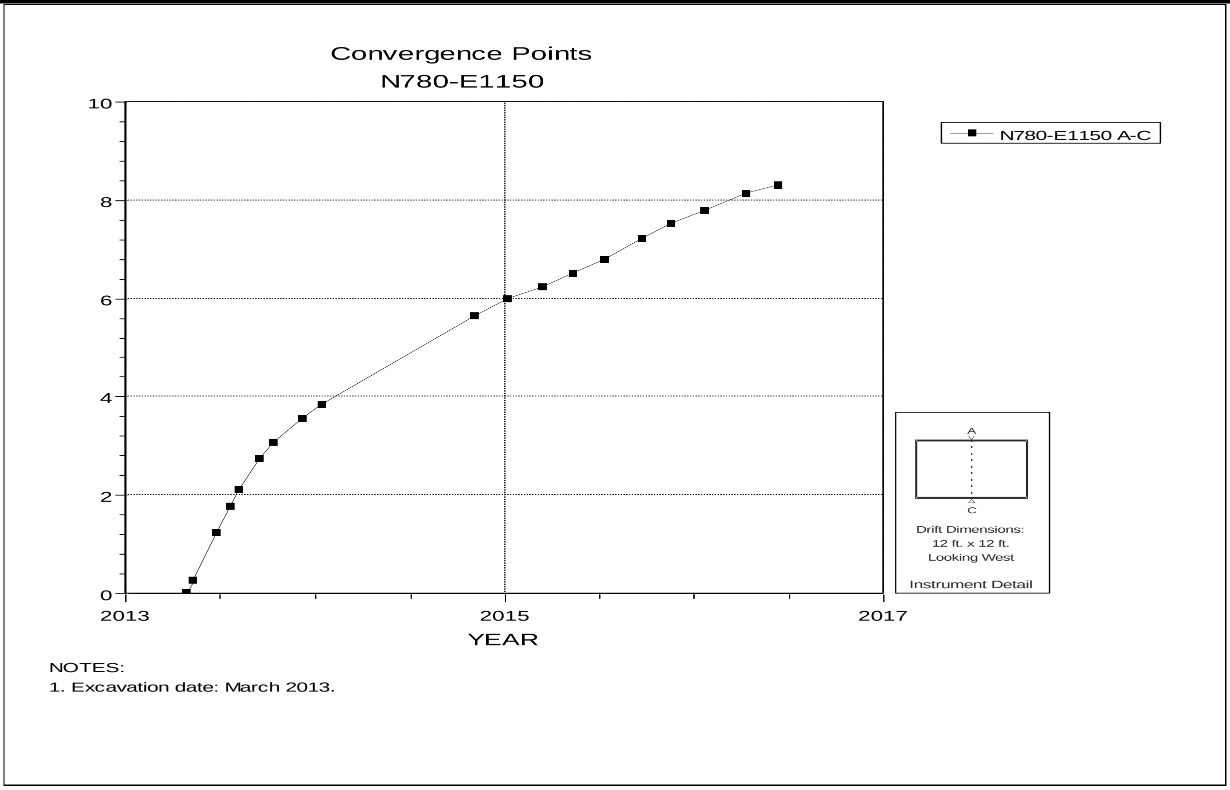

Figure 6-37 Convergence Point Array –
N780 E1150 – Roof to Floor

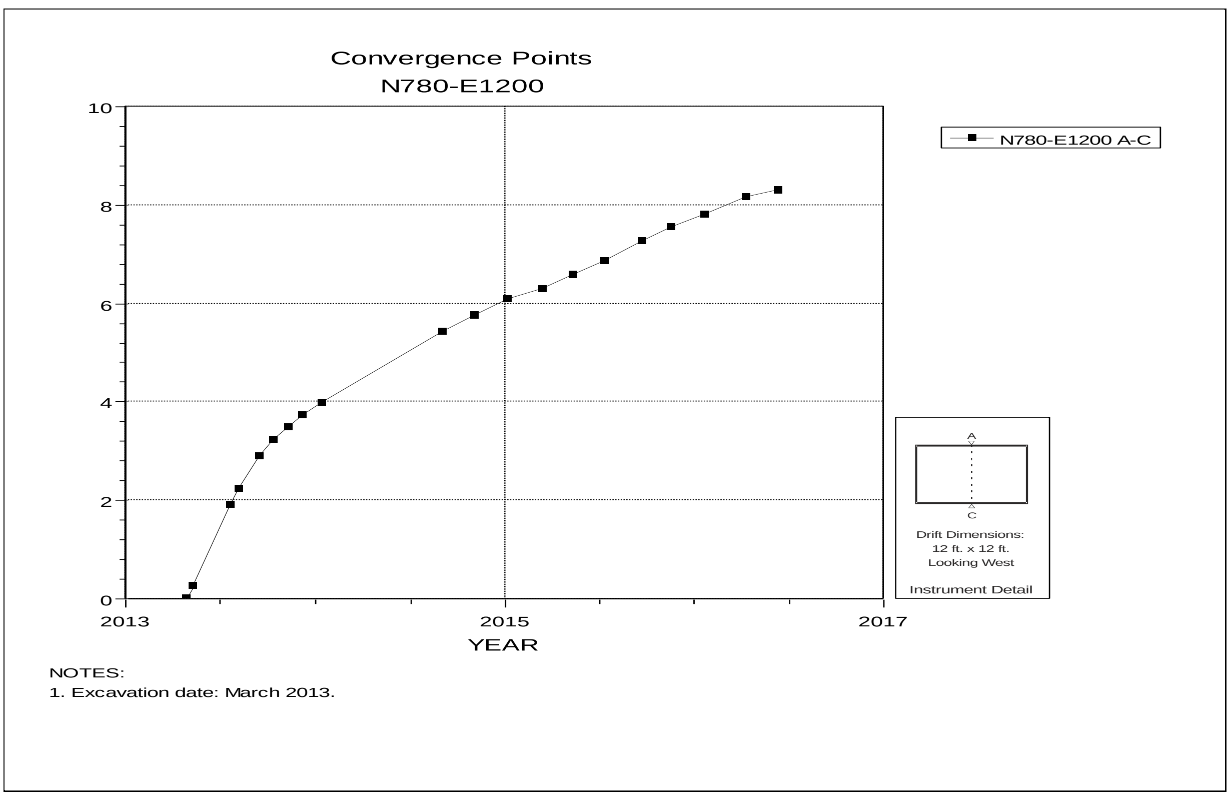

Figure 6-38 Convergence Point Array –
N780 E1200 – Roof to Floor

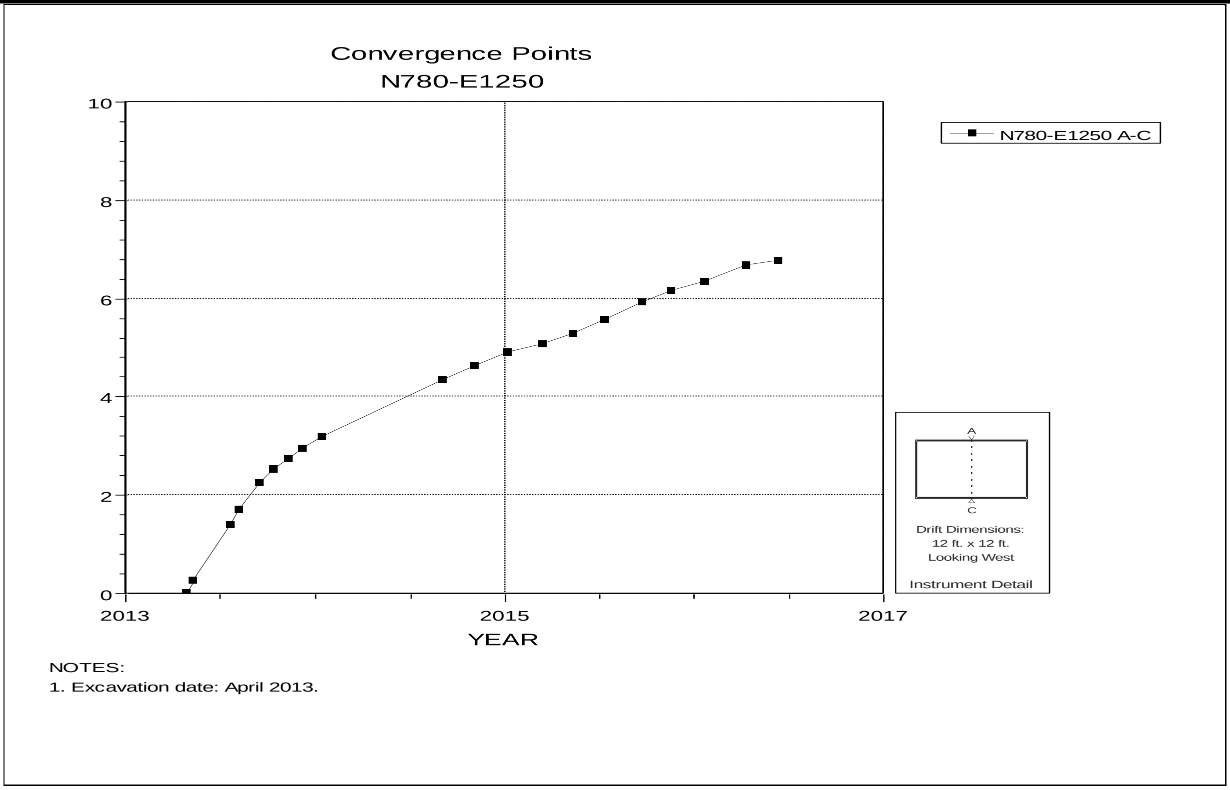

Figure 6-39 Convergence Point Array –
N780 E1250 – Roof to Floor

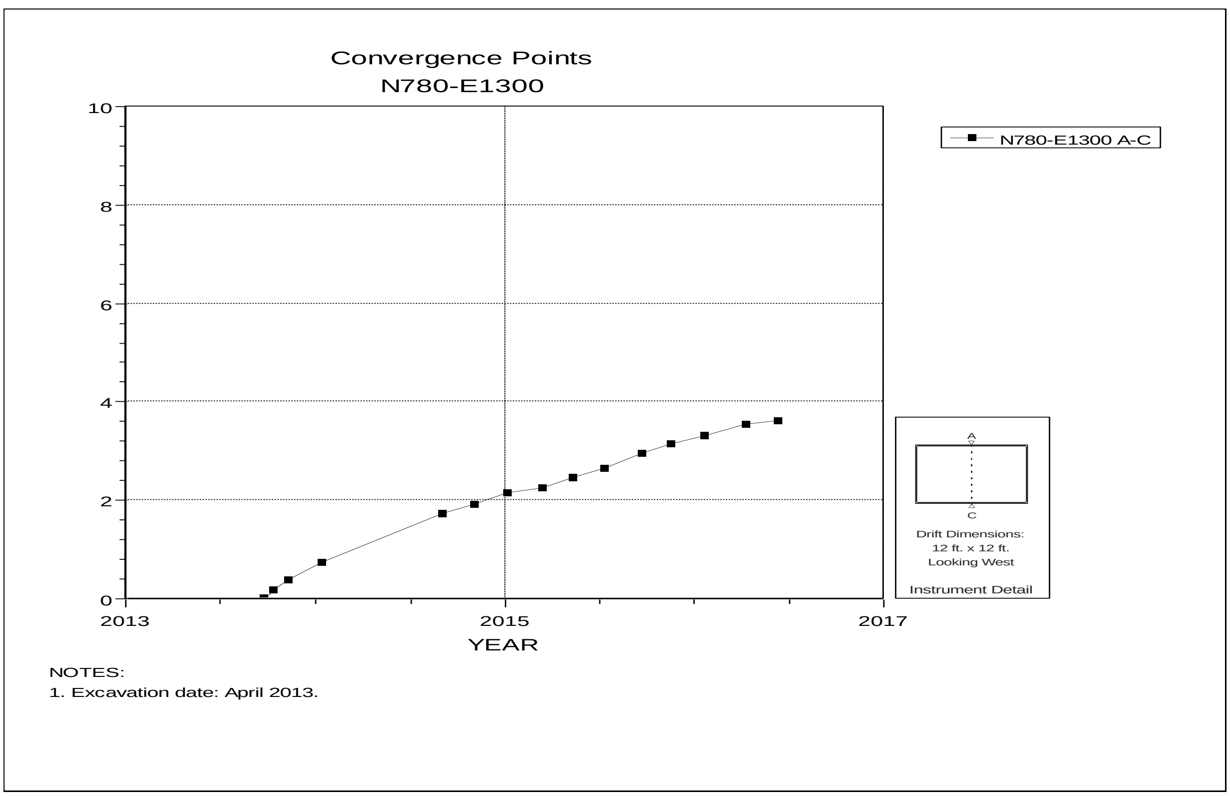

Figure 6-40 Convergence Point Array –
N780 E1300 – Roof to Floor

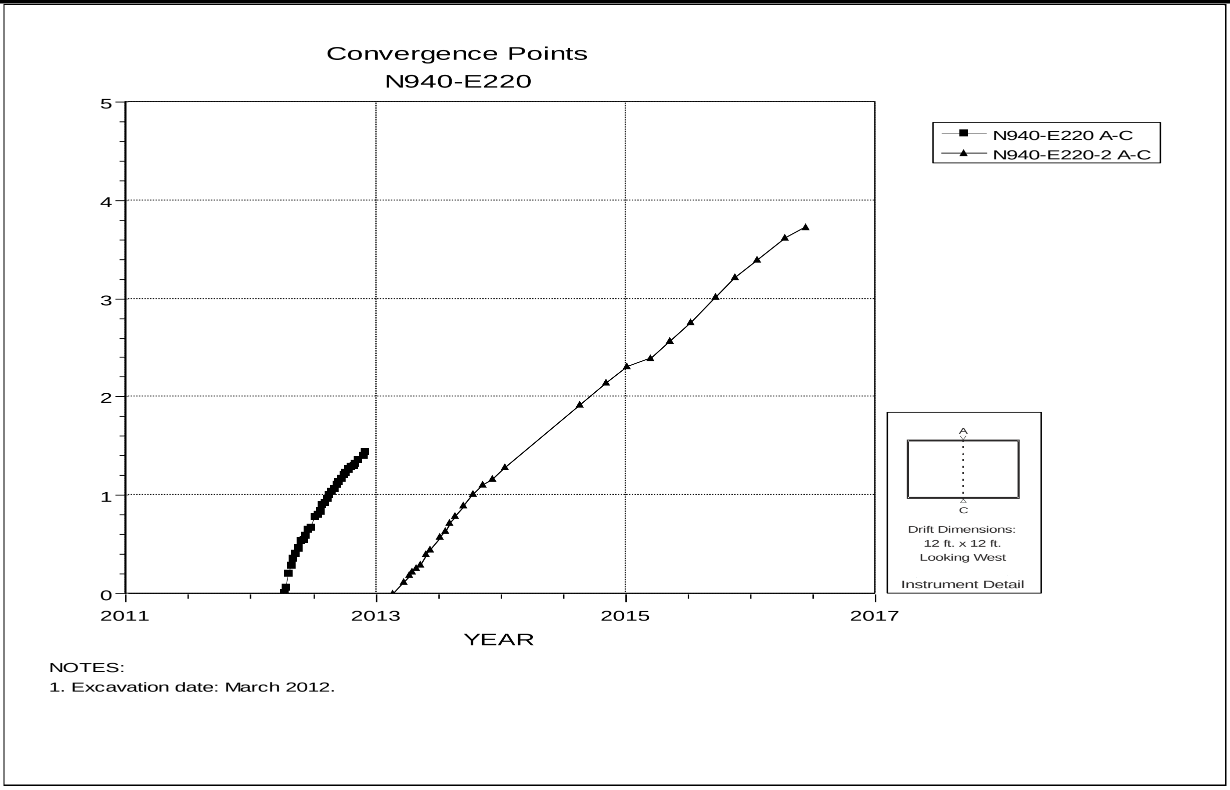

Figure 6-41 Convergence Point Array –
N940 E220 – Roof to Floor

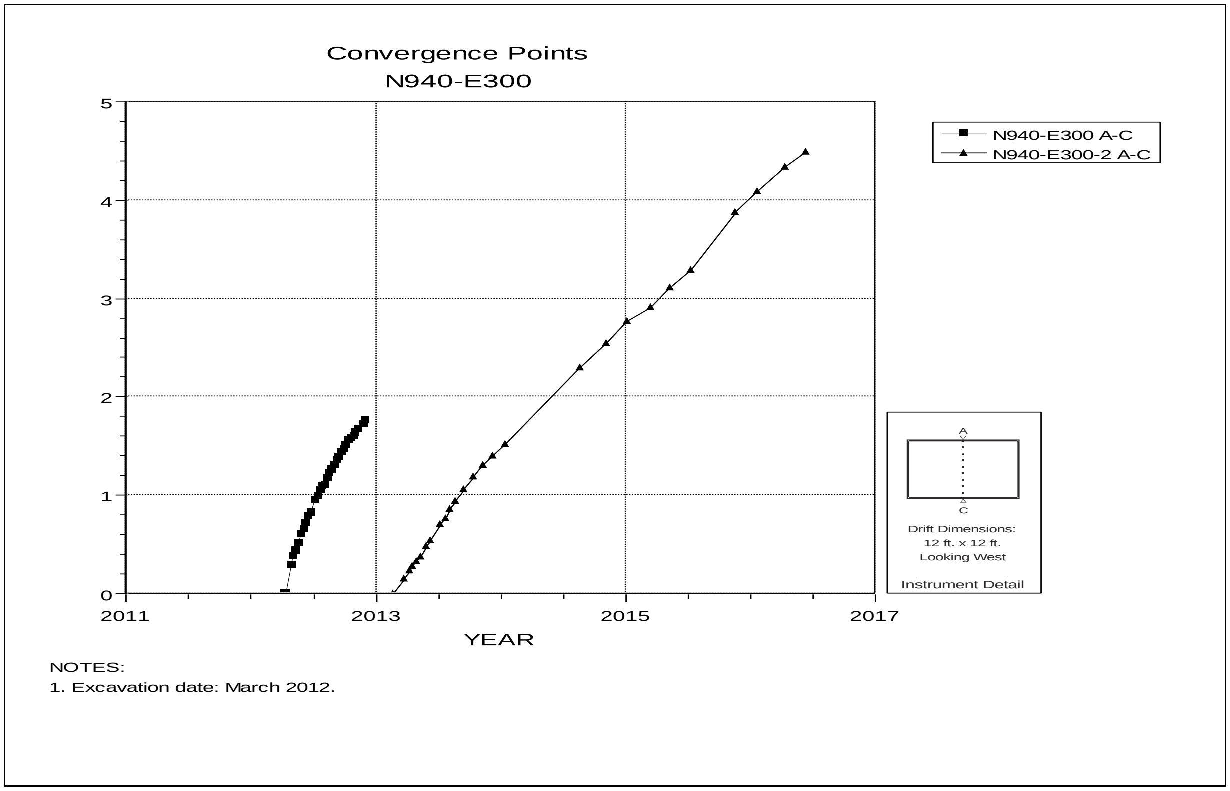

Figure 6-42 Convergence Point Array –
N940 E300 – Roof to Floor

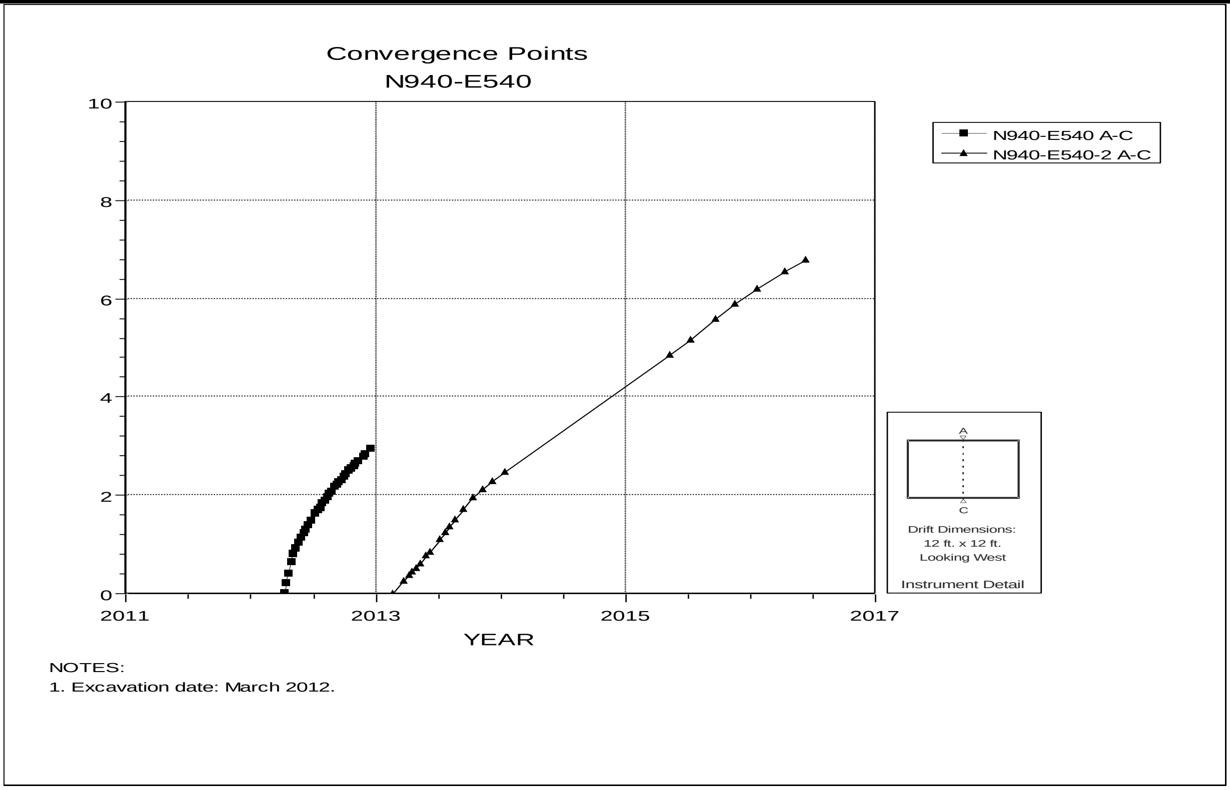

Figure 6-43 Convergence Point Array –
N940 E540 – Roof to Floor

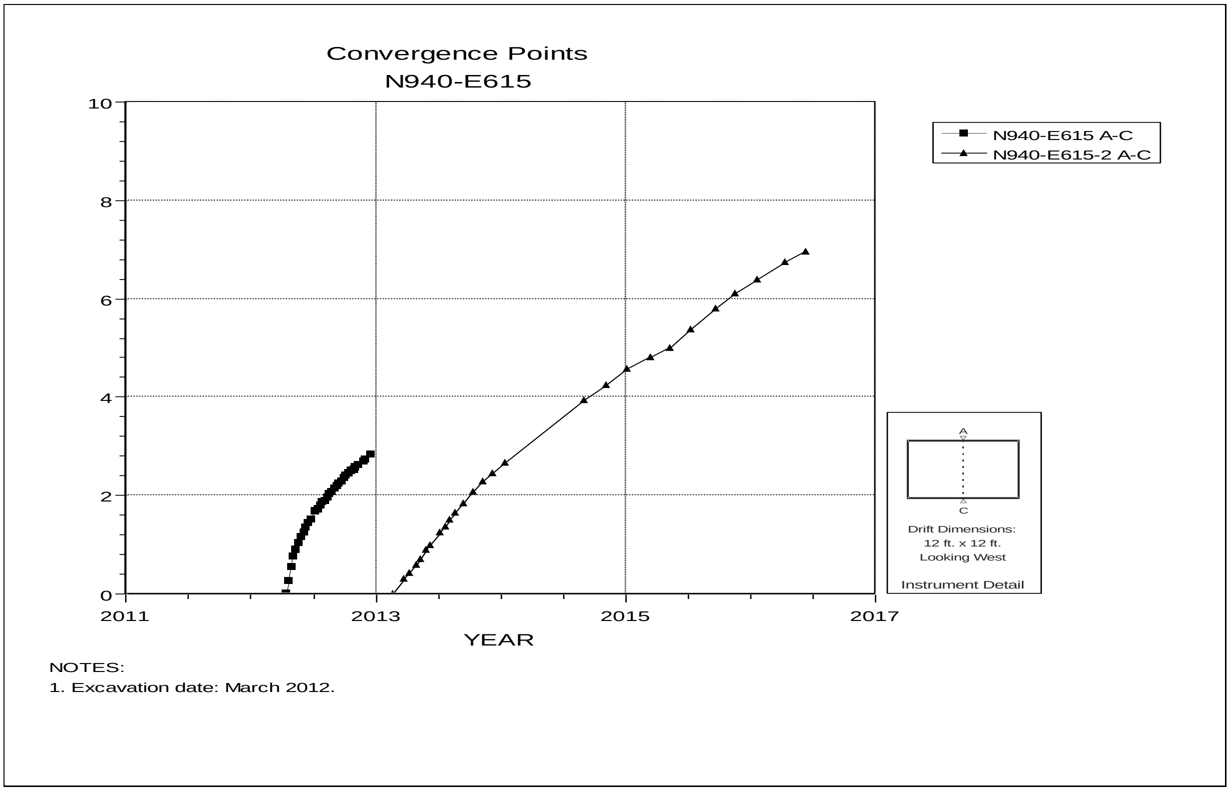

Figure 6-44 Convergence Point Array –
N940 E615 – Roof to Floor

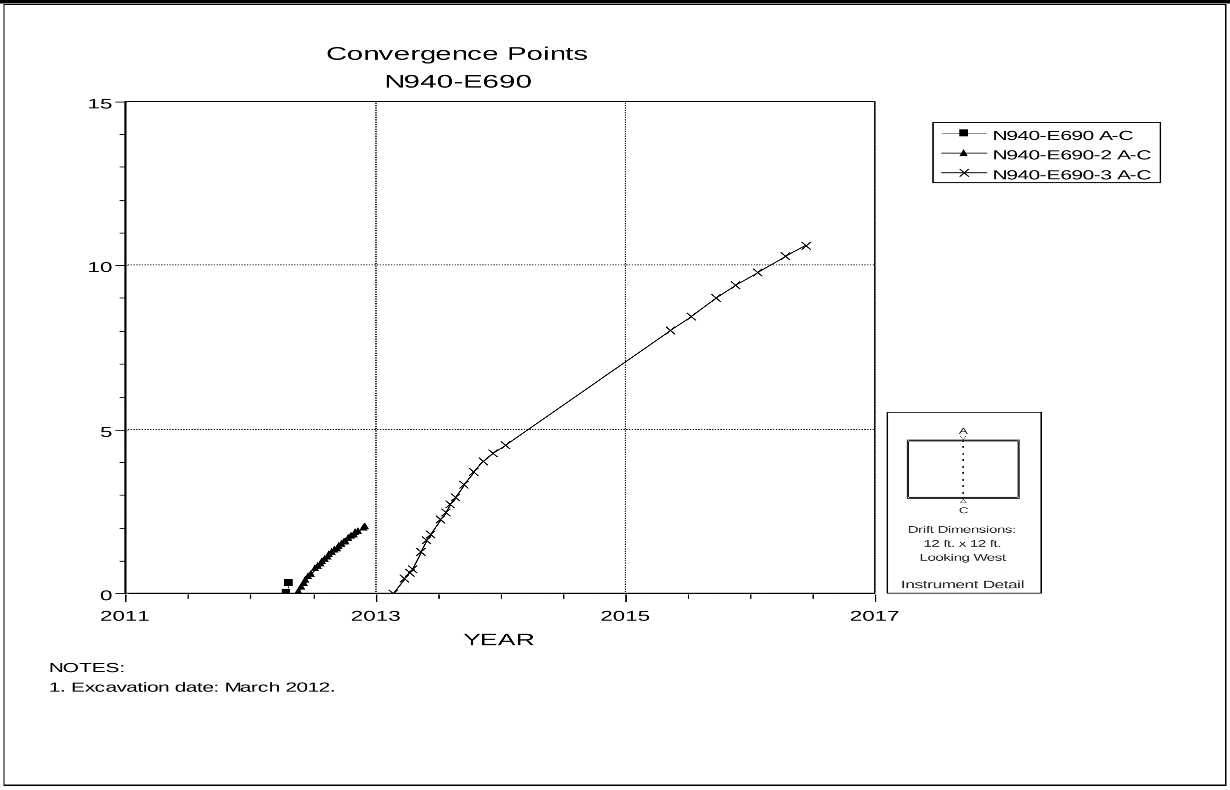

Figure 6-45 Convergence Point Array –
N940 E690 – Roof to Floor

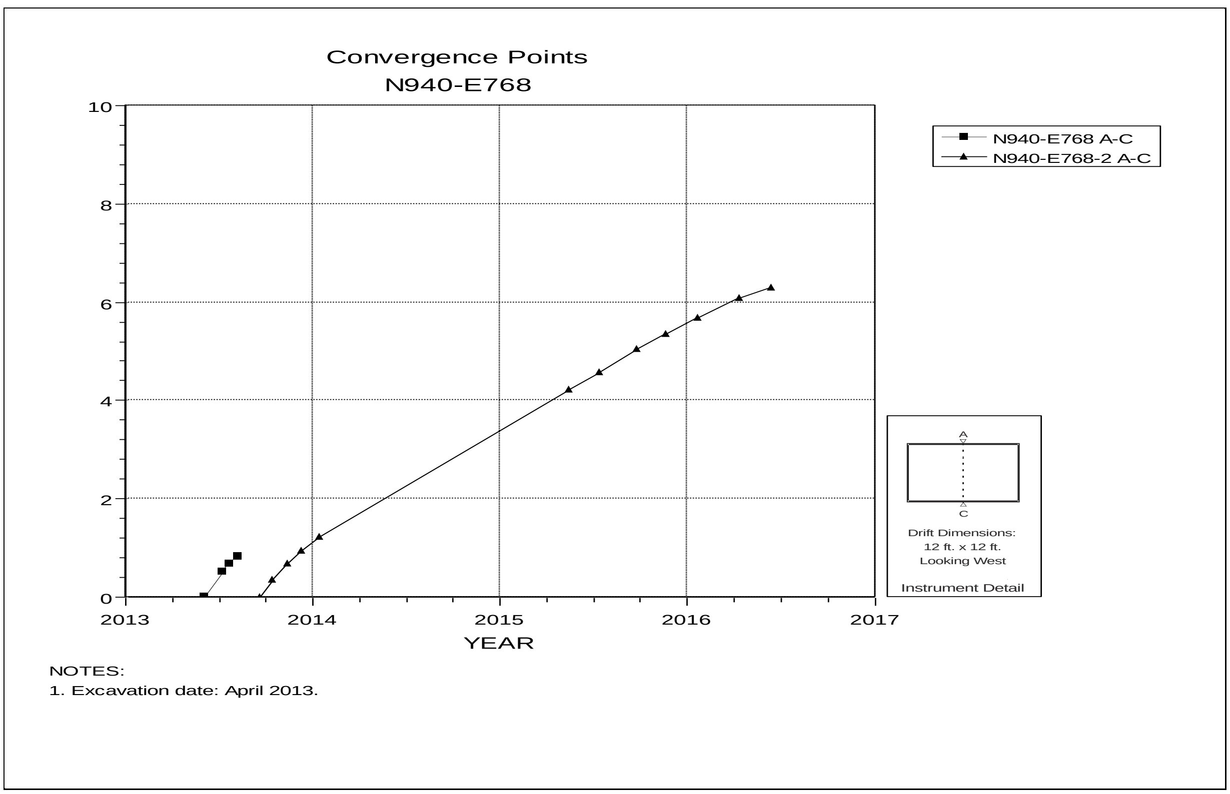

Figure 6-46 Convergence Point Array –
N940 E768 – Roof to Floor

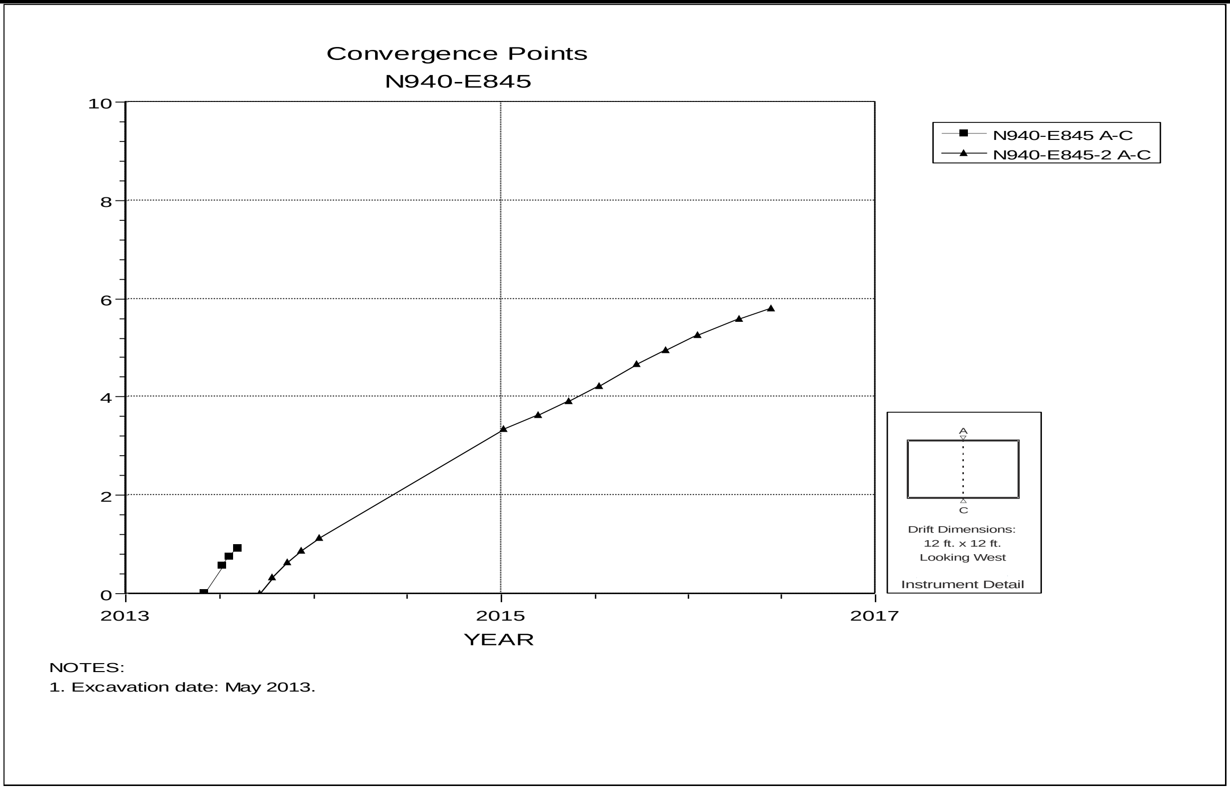

Figure 6-47 Convergence Point Array –
N940 E845 – Roof to Floor

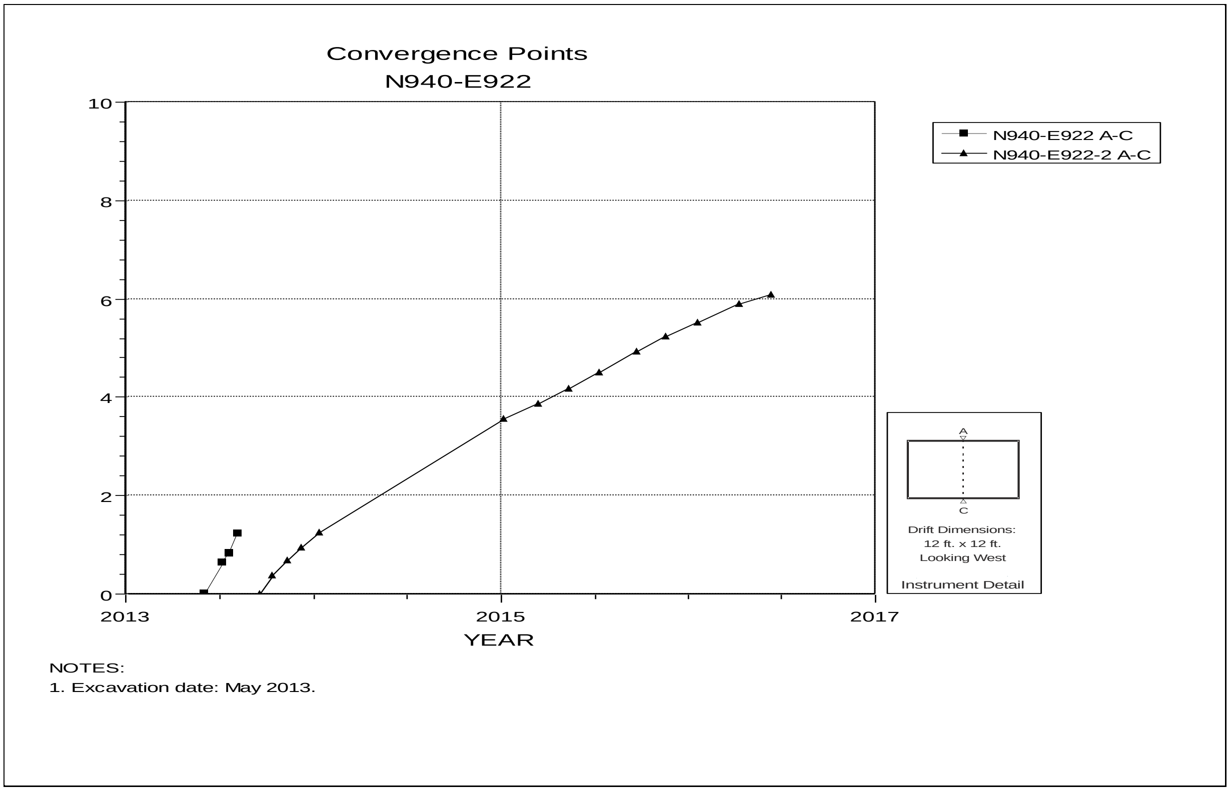

Figure 6-48 Convergence Point Array –
N940 E922 – Roof to Floor

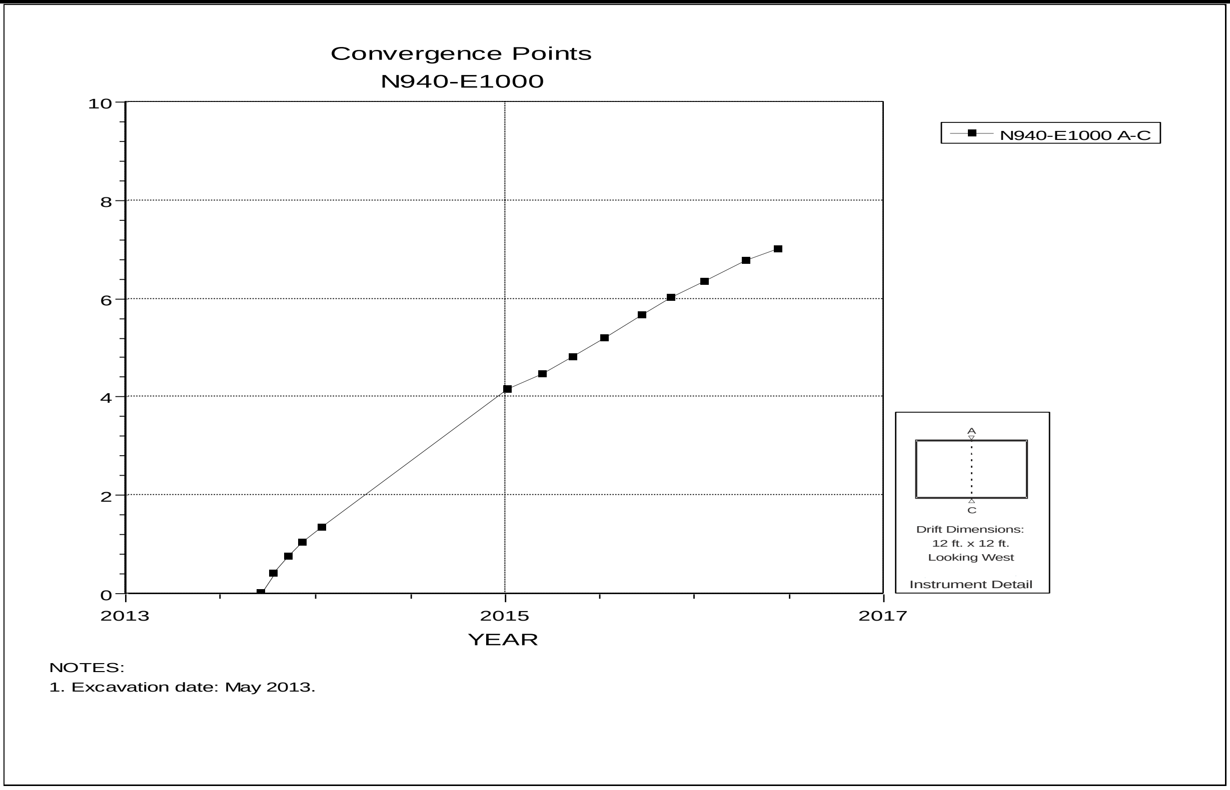

Figure 6-49 Convergence Point Array –
N940 E1000 – Roof to Floor

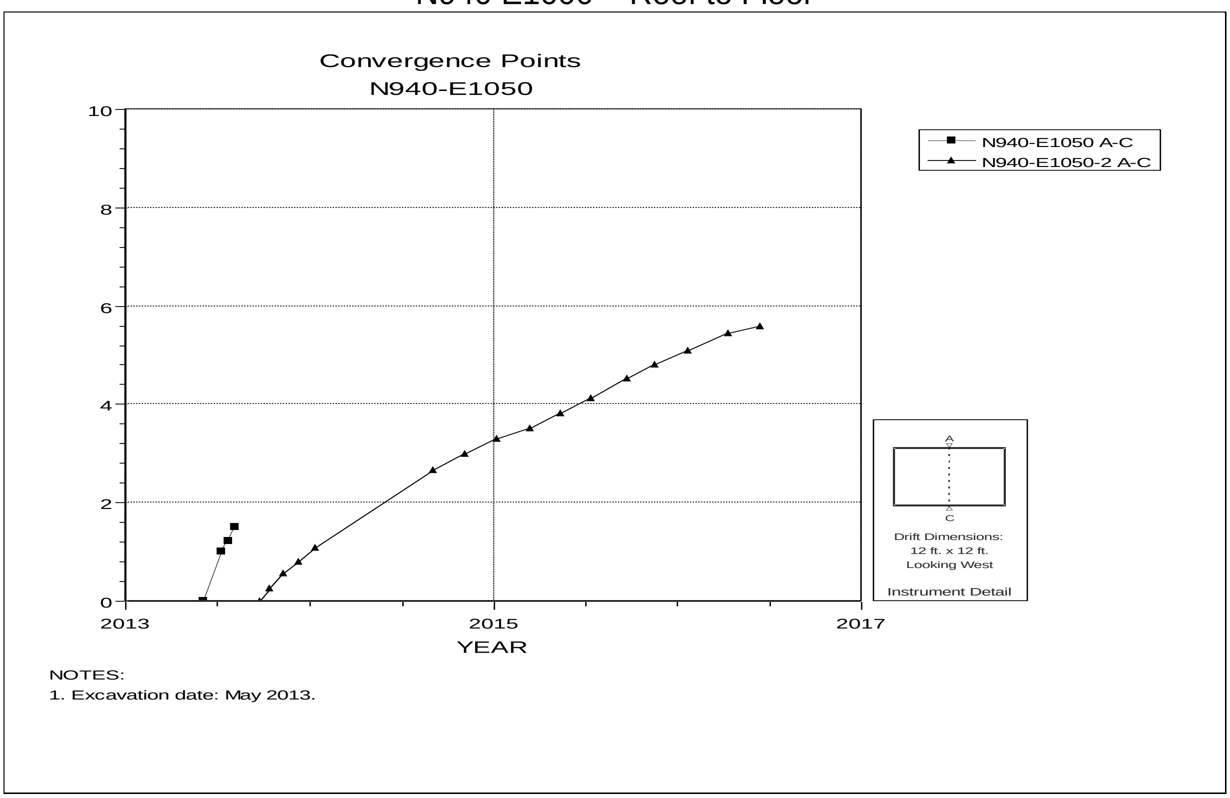

Figure 6-50 Convergence Point Array –
N940 E1050 – Roof to Floor

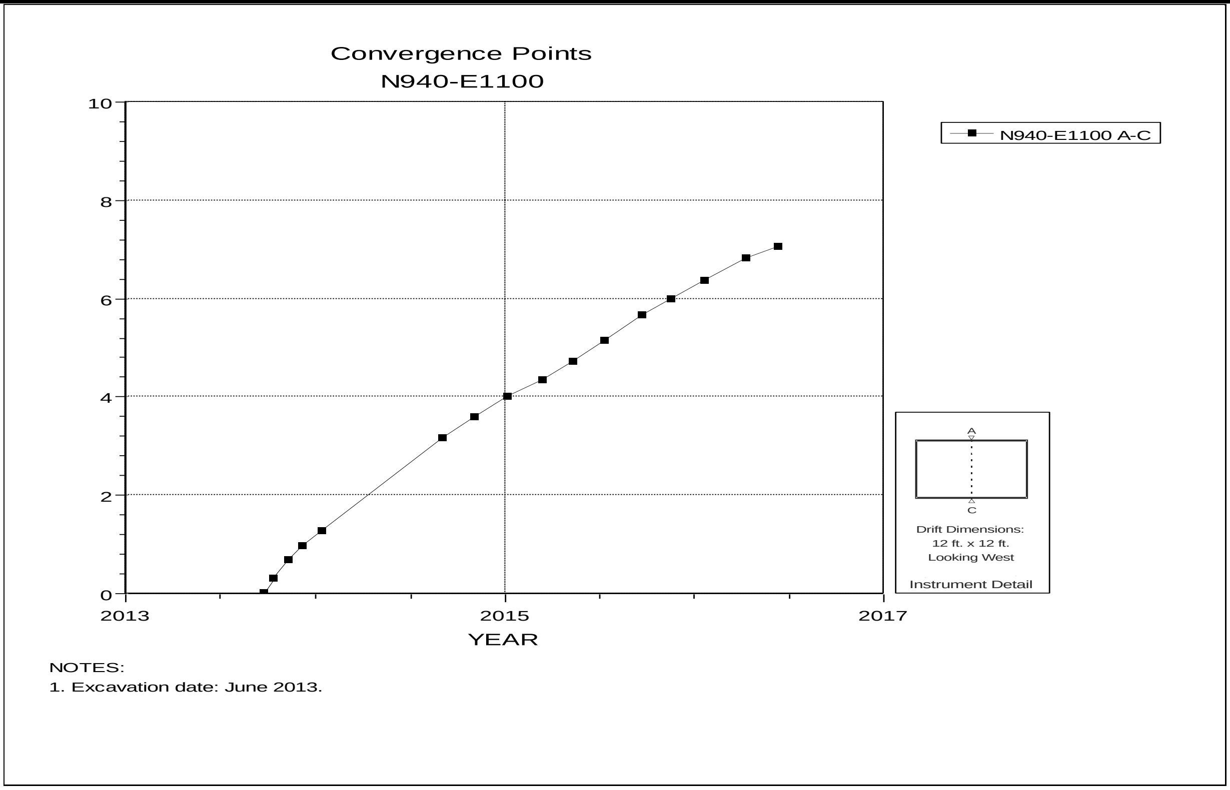

Figure 6-51 Convergence Point Array –
N940 E1100 – Roof to Floor

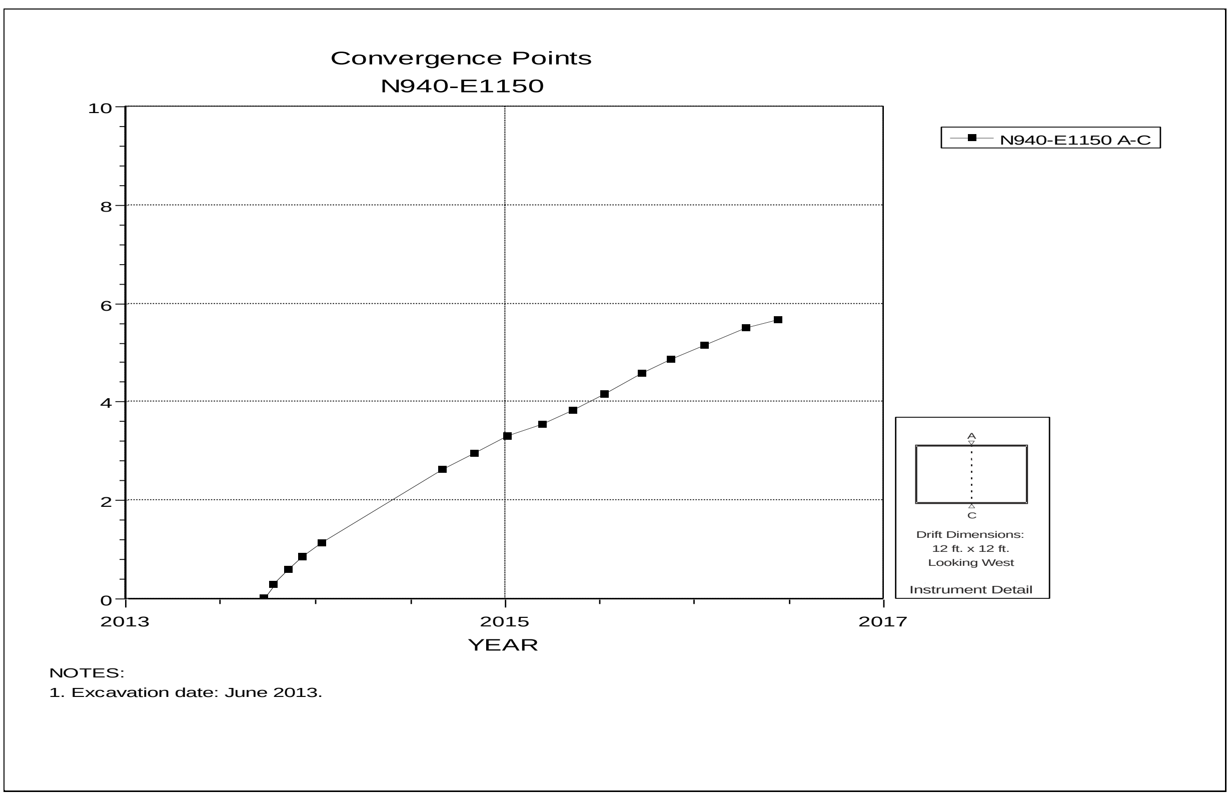

Figure 6-52 Convergence Point Array –
N940 E1150 – Roof to Floor

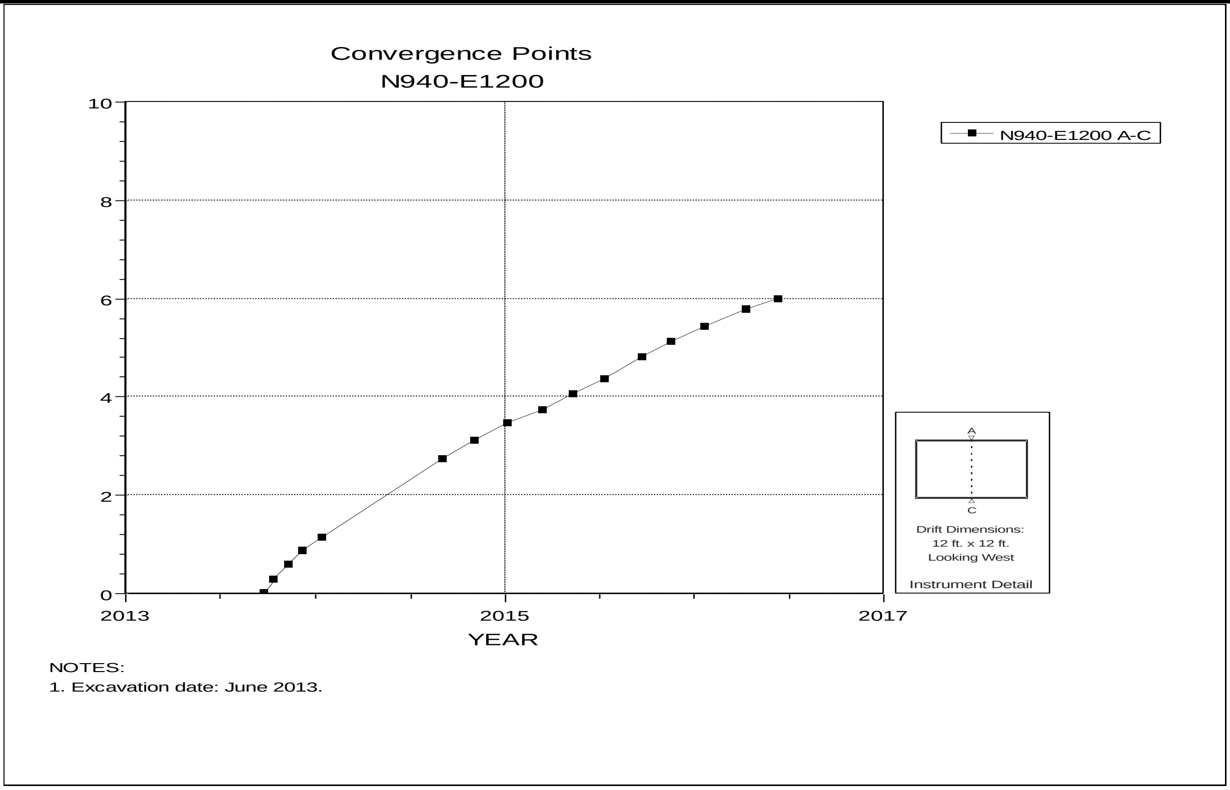

Figure 6-53 Convergence Point Array –
N940 E1200 – Roof to Floor

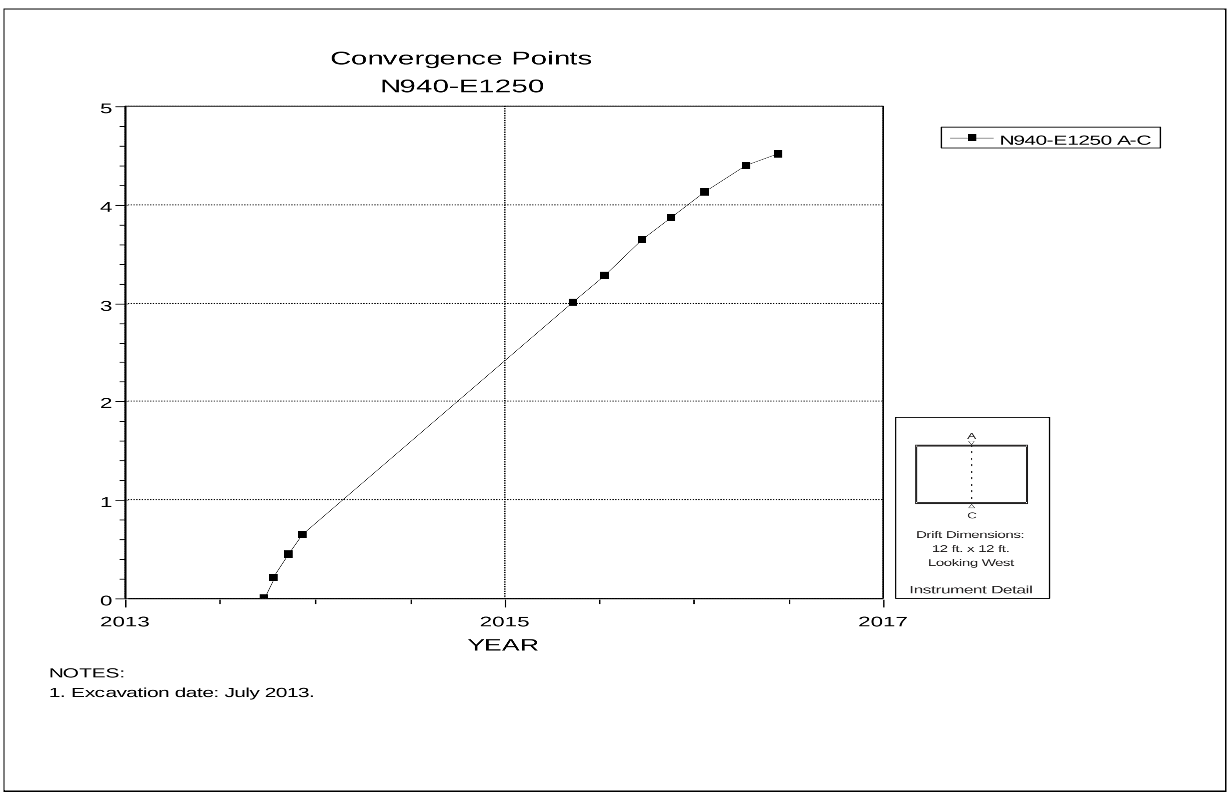

Figure 6-54 Convergence Point Array –
N940 E1250 – Roof to Floor

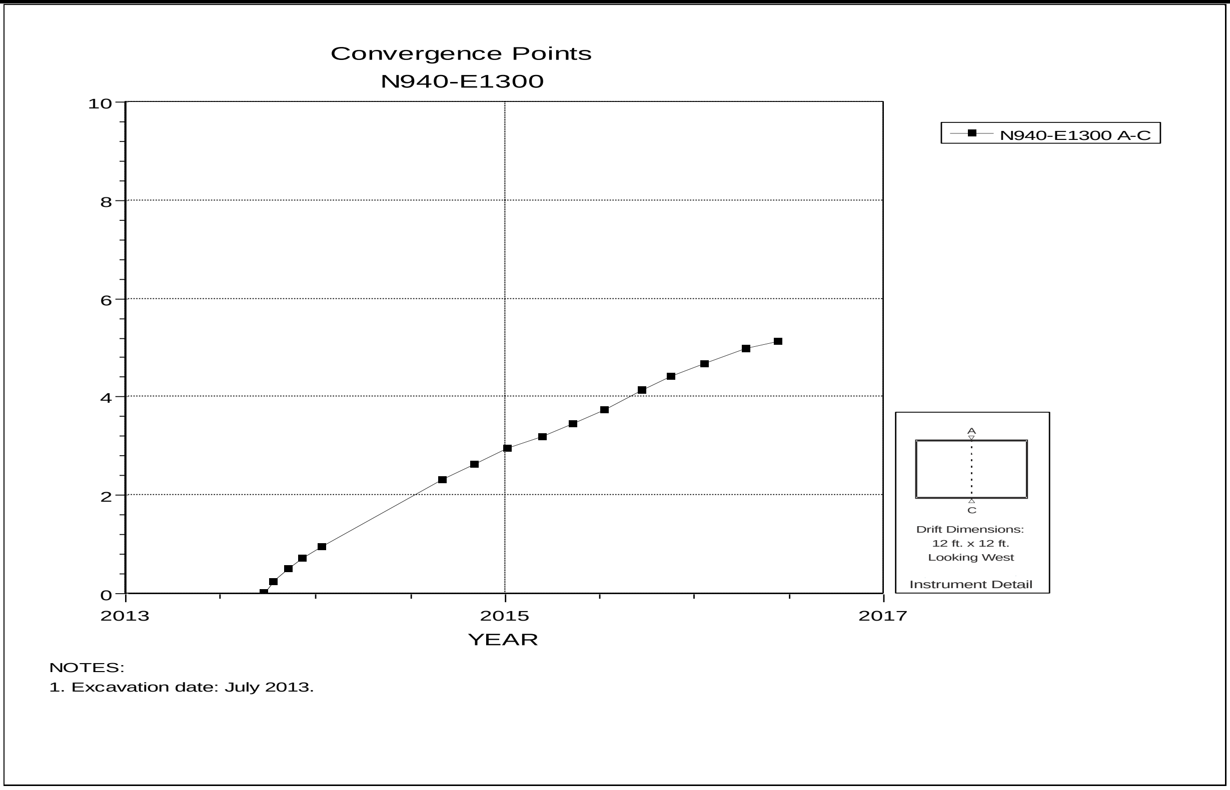

Figure 6-55 Convergence Point Array –
N940 E1300– Roof to Floor

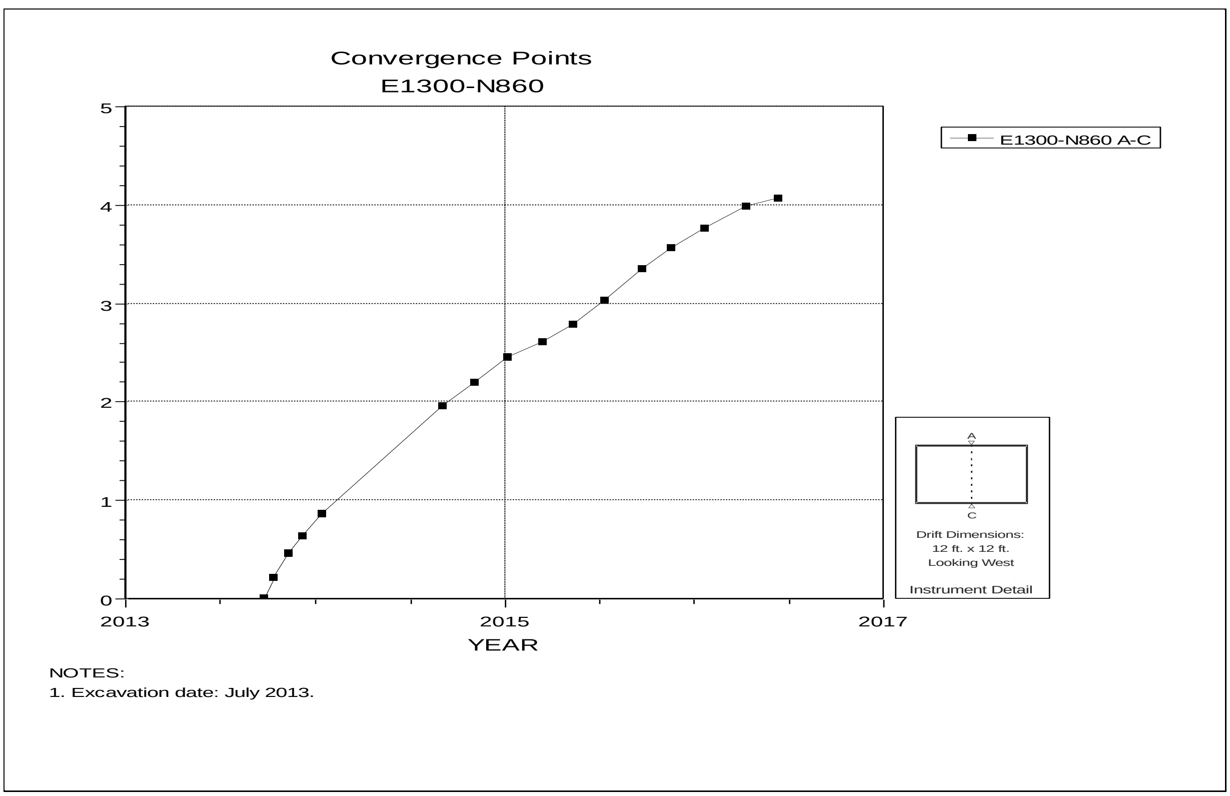

Figure 6-56 Convergence Point Array –
N1300 N860– Roof to Floor

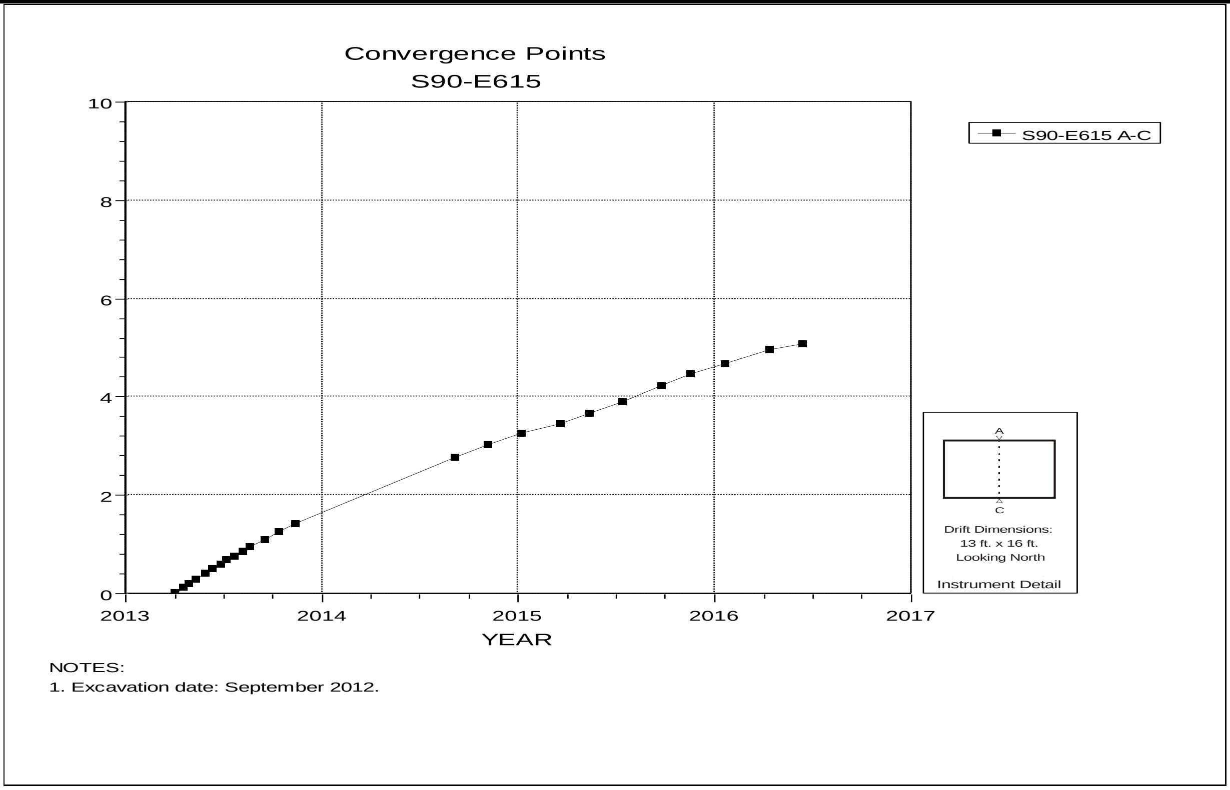

Figure 6-57 Convergence Point Array –
S90 E615 – Roof to Floor

This page was intentionally left blank.

7.0 Geoscience Summary for the Waste Disposal Area

This chapter typically presents supporting data acquired as part of the Geoscience Program including observations of clay seam displacements and other features in vertical observation holes, fracture maps of excavation surfaces as well as stratigraphic mapping. The resulting reduction in ventilation following the radiological event has significantly curtailed the use of man-lifting vehicles in the underground. Consequently, no fracture mapping or stratigraphic mapping was performed in the Panel 7 area.

Table 7-1
Observation Borehole Fractures and Offset Data Summary

Hole	Location	Initial Inspection Date	Recent Inspection Date	FR[1]	FZ[2]	Beam Height (ft)	Feature	Fracture Density (BH/FR[1])	Feature Depth (ft)	Separation (in)	Offset (in)	Compass	Hole closure (%)	Offset Rate (in/yr)
OH620-1	E140-S700	5/5/2016	5/5/2016				Separation		4	0.19	0	-	0	-
		5/5/2016	5/5/2016	1		5.7	Separation	5.7	5.7	1.50	0	-	0	-
		5/5/2016	5/5/2016				Separation		6.1	0.13	0	-	0	-
		5/5/2016	5/5/2016				Clay Seam		14.1	-	0	-	0	-
		5/5/2016	5/5/2016				BOH		20.1					
OH750-2	E140-S773	5/5/2016	5/5/2016				Separation		3.3	3.50	0	-	0	-
		5/5/2016	5/5/2016				Separation		6.8	0.13	0	-	0	-
		5/5/2016	5/5/2016				BOH		20.1					
OH874-3	E140-S840	5/5/2016	5/5/2016				Separation		2.6	0.25	0	-	0	-
		5/5/2016	5/5/2016				Separation		2.8	0.13	0	-	0	-
		5/5/2016	5/5/2016				Separation		5.8	0.13	0	-	0	-
		5/5/2016	5/5/2016				Rough Spot		6.9		0		0	
		5/5/2016	5/5/2016				BOH		19.9					
OH751-2	E140-S940	5/5/2016	5/5/2016				Separation		1.8	0.13	0	-	0	-
		5/5/2016	5/5/2016				Separation		3.1	0.13	0	-	0	-
		5/5/2016	5/5/2016				Separation		3.5	2.13	0	-	0	-
		5/5/2016	5/5/2016				Separation		3.8	0.13	0	-	0	-
		5/5/2016	5/5/2016				Separation		6.1	0.13	0	-	0	-
		5/5/2016	5/5/2016				Rough Spot		6.9		0		0	
		5/5/2016	5/5/2016	5		8.4	Separation	1.68	8.4	0.13	0	-	0	-
		5/5/2016	5/5/2016				BOH		19.9					

[1] Number of fractures (FR) in immediate roof beam
[2] Number of fracture zones (FZ) in the immediate roof beam
[3] Fracture Density = (FR + 2 FZ)/Beam Height

Table 7-1
Observation Borehole Fractures and Offset Data Summary

Hole	Location	Initial Inspection Date	Recent Inspection Date	FR[1]	FZ[2]	Beam Height (ft)	Feature	Fracture Density (BH/FR[1])	Feature Depth (ft)	Separation (in)	Offset (in)	Compass	Hole closure (%)	Offset Rate (in/yr)
OH575-2	E140-S1000	5/5/2016	5/5/2016				Separation		4.3	0.25	0	-	0	-
		5/5/2016	5/5/2016				Separation		6	0.125	0	-	0	-
		5/5/2016	5/5/2016				Separation		6.3	0.125	0	-	0	-
		5/5/2016	5/5/2016				Rough Spot		7.0		0		0	
		5/5/2016	5/5/2016				BOH		20.1					
OH577-2	E140-S1070	5/5/2016	5/5/2016				Separation		2.4	0.125	0.00	-	0	-
		5/5/2016	5/5/2016				Separation		3.8	0.125	0.00	-	0	-
		5/5/2016	5/5/2016				Separation		4.6	0.125	0.00	-	0	-
		5/5/2016	5/5/2016				Separation		4.8	0.125	0.00	-	0	-
		5/5/2016	5/5/2016	4		5.1	Separation	1.28	5.1	0.375	0.00	-	0	-
		5/5/2016	5/5/2016				Separation		6.6	0.125	0.00	-	0	-
		5/5/2016	5/5/2016				BOH		20.1					

[1] Number of fractures (FR) in immediate roof beam

[2] Number of fracture zones (FZ) in the immediate roof beam

[3] Fracture Density = (FR + 2 FZ)/Beam Height

Table 7-1
Observation Borehole Fractures and Offset Data Summary

Hole	Location	Initial Inspection Date	Recent Inspection Date	FR[1]	FZ[2]	Beam Height (ft)	Feature	Fracture Density (BH/FR[1])	Feature Depth (ft)	Separation (in)	Offset (in)	Compass	Hole closure (%)	Offset Rate (in/yr)
OH873-3	E140-S1158	5/5/2016	5/5/2016				Separation		1.6	0.13	0	-	0	-
		5/5/2016	5/5/2016				Separation		1.7	0.13	0	-	0	-
		5/5/2016	5/5/2016				Separation		1.8	0.13	0	-	0	-
		5/5/2016	5/5/2016				Separation		2.2	0.13	0	-	0	-
		5/5/2016	5/5/2016				Separation		2.5	2.00	0	-	0	-
		5/5/2016	5/5/2016				Separation		3.2	0.13	0	-	0	-
		5/5/2016	5/5/2016				Separation		3.7	7.00	0	-	0	-
		5/5/2016	5/5/2016	7		5.3	Separation	1.32	5.3	1.00	0	-	0	-
		5/5/2016	5/5/2016				Separation		5.8	1.00	0	-	0	-
		5/5/2016	5/5/2016				Separation		6.1	0.13	0	-	0	-
		5/5/2016	5/5/2016				Separation		6.6	0.25	0	-	0	-
		5/5/2016	5/5/2016				Rubble		7.0	1.50	0	-	0	-
		5/5/2016	5/5/2016				BOH		20					

[1] Number of fractures (FR) in immediate roof beam

[2] Number of fracture zones (FZ) in the immediate roof beam

[3] Fracture Density = (FR + 2 FZ)/Beam Height

Table 7-1
Observation Borehole Fractures and Offset Data Summary

Hole	Location	Initial Inspection Date	Recent Inspection Date	FR[1]	FZ[2]	Beam Height (ft)	Feature	Fracture Density (BH/FR[1])	Feature Depth (ft)	Separation (in)	Offset (in)	Compass	Hole closure (%)	Offset Rate (in/yr)
OH753-2	E140-S1226	5/5/2016	5/5/2016				Separation		1.3	0.38	0	-	0	-
		5/5/2016	5/5/2016				Separation		2.7	0.38	0	-	0	-
		5/5/2016	5/5/2016				Separation		5.2	0.38	0	-	0	-
		5/5/2016	5/5/2016				Separation		5.4	0.25	0	-	0	-
		5/5/2016	5/5/2016	4		5.5	Separation	1.35	5.5	7.00	0	-	0	-
		5/5/2016	5/5/2016				Separation		6.1	0.13	0	-	0	-
		5/5/2016	5/5/2016				Separation		6.4	0.25	0	-	0	-
		5/5/2016	5/5/2016				Separation		7.1	0.13	0	-	0	-
		5/5/2016	5/5/2016				Separation		7.5	0.13	0	-	0	-
		5/5/2016	5/5/2016				BOH		16.7					
OH578-1	E140-S1300	5/5/2016	5/5/2016	1		7.3	Rough Spot	7.30	7.3		0	-	0	-
		5/5/2016	5/5/2016				Separation		0.6	0.06	0	-	0	-
		5/5/2016	5/5/2016				BOH		20.2					

[1] Number of fractures (FR) in immediate roof beam

[2] Number of fracture zones (FZ) in the immediate roof beam

[3] Fracture Density = (FR + 2 FZ)/Beam Height

Table 7-1
Observation Borehole Fractures and Offset Data Summary

Hole	Location	Initial Inspection Date	Recent Inspection Date	FR[1]	FZ[2]	Beam Height (ft)	Feature	Fracture Density (BH/FR[1])	Feature Depth (ft)	Separation (in)	Offset (in)	Compass	Hole closure (%)	Offset Rate (in/yr)
OH872-3	E140-S1390	5/5/2016	5/5/2016				Separation		1.5	0.13	0	-	0	-
		5/5/2016	5/5/2016				Separation		2	0.13	0	-	0	-
		5/5/2016	5/5/2016				Separation		3	0.25	0	-	0	-
		5/5/2016	5/5/2016				Separation		4.2	0.13	0	-	0	-
		5/5/2016	5/5/2016	4		5.4	Separation	1.35	5.4	5.00	0	-	0	-
		5/5/2016	5/5/2016				Separation		6.9	0.13	0	-	0	-
		5/5/2016	5/5/2016				Separation		7.2	0.13	0	-	0	-
		5/5/2016	5/5/2016				Separation		7.4	0.50	0	-	0	-
		5/5/2016	5/5/2016				Separation		7.7	0.13	0	-	0	-
		5/5/2016	5/5/2016				BOH		20.3					

[1] Number of fractures (FR) in immediate roof beam

[2] Number of fracture zones (FZ) in the immediate roof beam

[3] Fracture Density = (FR + 2 FZ)/Beam Height

This page was intentionally left blank.